

David L. Hetrick

# Dynamics of Nuclear Reactors

The University of Chicago Press  
Chicago and London

## Contents

<b>Preface</b>	<b>ix</b>
<b>1. Elementary Derivation of the Dynamic Equations</b>	<b>1</b>
1-1. Basic Concepts	1
1-2. Dynamic Equations	3
1-3. Simplified Neutron Cycle	9
1-4. Delayed Neutrons	10
Problems	15
<b>2. Constant Reactivity and Reactivity Steps</b>	<b>17</b>
2-1. Equilibrium and Criticality	17
2-2. The Inhour Equation	20
2-3. One-Group Representations	27
2-4. Step-Input Response	30
2-5. Time-dependent Sources	38
2-6. Frequency Response and Transfer Functions	44
Problems	50
<b>3. Time-dependent Reactivity</b>	<b>55</b>
3-1. Approximate Dynamic Equations	56
3-2. Reactivity Oscillations	66
3-3. Ramp-Input Response: Hypergeometric Functions	78
3-4. Ramp-Input Response: Integral Representations	88
3-5. Reactor Startup	96
3-6. Some Methods for Arbitrary Reactivity Variation	102
Problems	108

<b>4. Integral Equations and Numerical Computations</b>	111
4-1. An Integrating Factor	111
4-2. Keppin's Integral Equation	113
4-3. An Integro-differential Equation	117
4-4. Numerical Methods	119
4-5. The Method of Adler and Cohen	123
4-6. A Weighted-residual Method	126
4-7. Hansen's Method	128
4-8. A Numerical Experiment	130
4-9. The Inverse Problem	137
Problems	139
<b>5. Reactivity Feedback and Reactor Excursions</b>	141
5-1. Homogeneous Thermal Reactors	141
5-2. Heterogeneous Thermal Reactors	148
5-3. Fast Reactors	155
5-4. The Linear Feedback Kernel	159
5-5. The Nordheim-Fuchs Model	164
5-6. Small Reactivity Excursions	174
5-7. Excursions near Prompt Critical	184
5-8. The Fuchs Ramp-Input Model	198
5-9. Complex Shutdown Mechanisms: Thermal Reactors	210
5-10. Complex Shutdown Mechanisms: Fast Reactors	221
Problems	230
<b>6. Linear System Stability</b>	235
6-1. Linear Systems with Feedback	236
6-2. The Routh Criterion	239
6-3. Representations for Frequency Response	246
6-4. The Nyquist Criterion	260
6-5. The Root-Locus Method	275
6-6. Stability of Simple Reactor Systems	284
6-7. Two-Path Feedback: Effective-Lifetime Model	299
6-8. Two-Path Feedback: Delayed Neutrons	306
6-9. Stability of Fast Reactors	317
6-10. Boiling-Water Reactors	328
6-11. Nuclear Rocket Reactors	332
Problems	335

<b>7. Nonlinear System Stability</b>	341
7-1. Equilibrium Points	343
7-2. Geometry of the Phase Plane	354
7-3. Some Simple Reactor Systems	360
7-4. Definitions of Stability	369
7-5. The Direct Method of Liapunov	373
7-6. Application to Reactor Systems	388
7-7. Boundedness and Lagrange Stability	405
7-8. Frequency-Domain Stability Criteria	415
7-9. Nonlinear Oscillations	423
Problems	436
<b>8. Space-dependent Neutron Dynamics</b>	441
8-1. The Transport Equation	441
8-2. Multimode Dynamics Equations	449
8-3. Calculation Methods	457
8-4. Some Numerical Results	463
8-5. Pulsed Sources	472
8-6. Neutron Waves	482
Problems	488
<b>Bibliography</b>	491
<b>Author Index</b>	529
<b>Subject Index</b>	535

## Preface

The purpose of this book is to present a systematic exposition of nuclear reactor dynamics, suitable as an introduction to the subject for senior or graduate students of science and engineering. Most of the material was assembled for lectures in a graduate course given in the Department of Nuclear Engineering at the University of Arizona. The chief prerequisite is an introductory course in nuclear reactor theory.

Primary attention is focused on lumped-parameter dynamic equations (the so-called point-reactor model), though careful attention is paid to the derivation of this model from neutron diffusion and transport theory, and an attempt has been made to bring the reader up to date in the highly important field of space-dependent effects. The dynamics of large reactors, pulsed neutron techniques, and a brief introduction to neutron waves are included as examples of space-dependent phenomena.

One unique feature of this book is that it attempts to bridge the gap between the viewpoint of the reactor physicist and that of the control engineer; it is hoped that the student will emerge from this course with the ability to communicate in the language of either persuasion. Another unique feature is the discussion of the numerous methods that have been developed for casting the differential equations of reactor dynamics in forms suitable for digital computer solution. In addition, special attention is given to the difficult and important problem of computing dynamic reactivity coefficients from basic reactor data.

It is assumed that the reader's mathematical background includes differential equations, Laplace transforms, and an elementary acquaintance with matrices. More sophisticated concepts and methods are introduced as needed. Occasionally, as for example in the treatment of nonlinear stability, mathematical theorems are quoted without proof.

## **1 Elementary Derivation of the Dynamic Equations**

Nuclear fission reactors are described, in the first approximation, by the same basic dynamic principles, whether they are thermal reactors or fast reactors, and whether the nuclear fuel is  $\text{U}^{235}$ ,  $\text{Pu}^{239}$ , or  $\text{U}^{233}$ . The essential phenomenon is of course neutron-induced fission of these isotopes, with the accompanying release of other neutrons (usually two or three per fission event), thus making a self-sustaining neutron chain reaction possible.

In this approximation, the most important difference between fast and thermal reactors is the time scale for neutron reproduction. The major difference among the various fuels is that with each fuel a different fraction of neutrons is delayed (not produced immediately in fission).

### **1-1. Basic Concepts**

The basic concepts of reactor dynamics, common to all types of fission reactors, are reactivity, neutron generation time, and delayed neutrons.

Reactivity is the relative departure of the neutron reproduction factor  $k$  from unity. When properly defined, it is an integral property of the entire reactor. Measured values are usually deduced from observation of dynamic behavior, although static measurements of the reproduction factor are possible. The lumped-parameter (point-reactor) model is satisfactory only when  $k$  is very near to unity (when the reactor is not very far from "critical"), which fortunately includes a wide variety of important practical cases.

The reactivity depends on the size of the reactor, the relative amounts and densities of various materials, and the neutron cross-sections for scattering, absorption, and fission. Since all of these are affected by temperature, pressure, and other effects of fission (arising primarily

### *Elementary Derivation of the Dynamic Equations*

from the dissipation of kinetic energy of the fission fragments), the reactivity depends on the power history of the reactor. The computation of this reactivity "feedback" is one of the central problems of reactor dynamics. Further, since the dynamic equations contain the product of reactivity and instantaneous power, the equations are generally nonlinear.

The neutron generation time is the mean time for neutron reproduction in a multiplying assembly. It also is an integral property of the entire reactor. It may be as short as  $10^{-8}$  sec for a fast reactor, in which fissions are produced by fast neutrons, or as long as  $10^{-3}$  sec for a thermal reactor, in which neutrons slow down considerably and subsequently diffuse at "thermal" energies before causing fission. The generation time depends primarily on the number of scattering collisions that a typical neutron undergoes before it escapes from the reactor (leakage) or disappears in a nuclear reaction (absorption).

Delayed neutrons, although representing less than one percent of the neutron production in fission, are extremely important in determining the time scales in reactor dynamics. These neutrons are released in certain nuclear transitions that occur in a few types of highly excited fission fragments, and the relevant processes have half-lives of the order of a few seconds.

When the reproduction factor is sufficiently large that the neutron chain reaction would be self-sustaining with only the prompt neutrons (neutrons released immediately in fission), the neutron generation time is dominant in determining the time scale. When the reactor is not too far above critical, in the regime where prompt neutrons alone would be insufficient to sustain a chain reaction, the relatively large delay times of the delayed neutrons are dominant, even though the delayed-neutron fraction is small. If all neutrons were prompt, it would be extremely difficult to control a reactor by conventional mechanical means such as movement of fuel, neutron absorbers, or neutron reflectors because of the high frequency response required to compensate for the short neutron generation time. Control of a fast reactor would indeed be impossible.

Problems in reactor dynamics may be roughly classified according to time scale:

1. Fast transients (microsec-sec)
  - a. Nuclear explosives
  - b. Pulsed reactors
  - c. Reactor accidents
2. Short-term operating transients (min.-hrs)
  - a. Reactor startup

- b. Power level-reactivity effects
- c. Fluctuations of power demand
- d. Fission-product poisons
- 3. Long-term operating transients (days-months)
  - a. Fuel burnup
  - b. Buildup of heavy isotopes
  - c. Breeding and conversion
  - d. Effects of radiation on materials

This book is concerned with the first two of these time regimes.

The remainder of chapter 1 is concerned with (1) an elementary derivation of the dynamic equations from time-dependent diffusion theory, (2) an interpretation of the dynamic equations in terms of a simplified neutron cycle, and (3) a discussion of delayed neutrons. Neutron transport and multigroup theory are deferred until later, where they serve to introduce the discussions of space-dependent effects and the limitations of the point-reactor model. Before proceeding, the advanced reader may wish to study the derivation of the dynamic equations from transport theory in chapter 8. Other readers who are willing to accept the dynamic equations as postulated may proceed directly to chapter 2.

For further background, the reader is referred to texts in reactor theory<sup>1</sup> (Bell and Glasstone 1970; Galanin 1960; Glasstone and Edlund 1952; Isbin 1963; Kramerov and Shevelev 1964; Larmorsh 1966; Meghrebian and Holmes 1960; Weinberg and Wigner 1958); reactor dynamics (Akcasu, Lellouche, and Shotkin, forthcoming; Ash 1965; Keepin 1965; Smets 1962; Stacey 1969a; Weaver 1968); linearized reactor systems and control (Harrer 1963; Hitchcock 1960; Schultz 1961; Weaver 1963); reactor noise analysis (Pacilio 1969; Thie 1963); and neutron transport theory (Case and Zweifel 1967; Davison 1957; Osborn and Yip 1967; Tait 1964). Several important handbooks may also be cited (Argonne National Laboratory 1963a; Etherington 1958; Radkowsky 1964; Soodak 1962; Thompson and Beckerley 1964), as well as books on mathematical methods (Clark and Hansen 1964; Greenspan, Kelber, and Okrent 1968; Wachpress 1966a).

## 1-2. Dynamic Equations

The time-dependent diffusion of neutrons in a reactor may be described by

$$\frac{\partial N}{\partial t} = Dv\nabla^2 N - \Sigma_a v N + S, \quad (1-1)$$

<sup>1</sup>. Citations refer to the bibliography at the end of the book, where the authors' names are arranged alphabetically with each author's works listed chronologically.

### 1 Elementary Derivation of the Dynamic Equations

where

- $N(\mathbf{r}, t) dV$  = number of neutrons in a volume element  $dV$  at a point  $\mathbf{r}$  at time  $t$ ;
- $Dv\nabla^2 N dV$  = number of neutrons diffusing into  $dV$  per unit time at time  $t$ ;
- $\Sigma_a v N dV$  = number of neutrons absorbed in  $dV$  per unit time at time  $t$ ;
- $S(\mathbf{r}, t) dV$  = number of neutrons produced in  $dV$  per unit time at time  $t$ .

The coefficients  $D$ ,  $v$ , and  $\Sigma_a$  are respectively the diffusion constant, the neutron speed, and the macroscopic neutron absorption cross-section (absorption probability per unit path length).

An important assumption in this theory is that the neutron current density is given by Fick's law,  $\mathbf{j} = -Dv\nabla N$ . It is further assumed that all the coefficients are independent of position, and that their numerical values represent suitable averages over the neutron velocity distribution.

Eq. (1-1) may be taken as a first approximation for the dynamic behavior of many types of reactors. Often  $N$  represents only the neutrons in the energy range where most of the fissions occur (for example, thermal neutrons in a thermal reactor), and the source term  $S$  includes the neutrons slowing down from higher energies. A simple example results if all processes are considered as occurring at one neutron energy, with neutrons of all speeds counted in the density  $N$ .

In this approximation, the production of neutrons in a steady state is written as  $k_\infty \Sigma_a v N$ , where  $k_\infty$  is the number of neutrons produced per neutron absorbed (often called the infinite-medium reproduction factor). In the time-dependent case, prompt and delayed neutrons must be treated separately. If  $\beta$  is the delayed-neutron fraction, the prompt-neutron contribution to the source is  $(1 - \beta)k_\infty \Sigma_a v N$ . Delayed neutrons are produced by radioactive decay of certain fission fragments (delayed-neutron precursors); let  $\lambda_i$  be the decay constant and  $C_i(\mathbf{r}, t)$  the density of the  $i$ th type of precursor so that the contribution to the neutron source is the sum  $\sum_i \lambda_i C_i$ . Including sources of neutrons extraneous to the fission process as a term  $S_0(\mathbf{r}, t)$ ,

$$S = (1 - \beta)k_\infty \Sigma_a v N + \sum_i \lambda_i C_i + S_0, \quad (1-2)$$

and the diffusion equation becomes

$$\frac{\partial N}{\partial t} = Dv\nabla^2 N - \Sigma_a v N + (1 - \beta)k_\infty \Sigma_a v N + \sum_i \lambda_i C_i + S_0. \quad (1-3)$$

Let  $\beta_i$  be the delayed-neutron fraction for the  $i$ th emitter such that  $\beta = \sum_i \beta_i$  and assume that the fission fragments do not migrate appre-

ciable distances. (This is invalid for a circulating-fuel reactor.) Then

$$\frac{\partial C_i}{\partial t} = \beta_i k_{\infty} \Sigma_a v N - \lambda_i C_i. \quad (1-4)$$

Eqs. (1-3) and (1-4) constitute an approximate system of dynamic equations, with the understanding that any or all of the coefficients may be time dependent because of changes in the reactor arising from external causes or from internal effects of power transients.

In this approximate treatment, it is next assumed that  $N$  and  $C_i$  are separable in space and time. It will later become clear that this is equivalent to rejecting all but the lowest mode in an eigenfunction expansion, a procedure that is valid only if the reactor is very near the critical state and if there are no large localized perturbations. For now, assume that

$$N(\mathbf{r}, t) = f(\mathbf{r})n(t); \quad C_i(\mathbf{r}, t) = g_i(\mathbf{r})c_i(t). \quad (1-5)$$

Eq. (1-4) becomes

$$\frac{dc_i}{dt} = \beta_i k_{\infty} \Sigma_a v \frac{f(\mathbf{r})}{g_i(\mathbf{r})} n(t) - \lambda_i c_i(t) \quad (1-6)$$

Note that  $f/g_i$  is independent of time. Further, if eq. (1-6) is to be independent of position, it is necessary to assume the same shape for the functions  $f$  and  $g_i$ . (An alternative procedure is to integrate eqs. (1-3) and (1-4) over the reactor volume, but this introduces additional considerations beyond the scope of this chapter.)

It will be convenient to assume  $f/g_i = 1$ , and rewrite eq. (1-6) as

$$\frac{dc_i}{dt} = \beta_i k_{\infty} \Sigma_a v n - \lambda_i c_i. \quad (1-7)$$

Substituting eq. (1-5) into eq. (1-3) yields

$$\begin{aligned} \frac{dn}{dt} &= Dv \frac{\nabla^2 f}{f} n(t) - \Sigma_a v n(t) + (1 - \beta) k_{\infty} \Sigma_a v n(t) \\ &\quad + \Sigma_i \lambda_i \frac{g_i}{f} c_i(t) + \frac{S_0}{f}. \end{aligned} \quad (1-8)$$

Here, in addition to setting  $g_i = f$ , the removal of space dependence requires that  $\nabla^2 f/f$  and  $S_0/f$  be independent of position. The former is equivalent to assuming that  $f(\mathbf{r})$  satisfies a Helmholtz equation

$$\nabla^2 f + B^2 f = 0$$

where  $B^2$  is the so-called fundamental-mode buckling. The requirement that  $S_0/f$  be space independent is a peculiarity of this method of

## 6 Elementary Derivation of the Dynamic Equations

derivation, as will be seen in chapter 8. Assuming for now that  $S_0$  has the same spatial dependence as  $f$ , let  $q(t) = S_0(\mathbf{r}, t)/f(\mathbf{r})$ .

Two further symbols may be introduced, the absorption lifetime  $\ell_\infty$  and the diffusion length  $L$ :

$$= 1/\nu\Sigma_a; \quad L^2 = D/\Sigma_a.$$

The characteristic time  $\ell_\infty$  may also be called the infinite-medium neutron lifetime, and  $L^2$  may be interpreted as a "diffusion area" or "migration area." Eq. (1-8) may now be rewritten as

$$\frac{dn}{dt} = \frac{(1 - \beta)k_\infty + (1 + L^2B^2)}{\ell_\infty} n + \sum_i \lambda_i c_i + q. \quad (1-9)$$

At this point the effective reproduction factor  $k$  and the neutron lifetime  $\ell_0$  are introduced:

$$k = \frac{k_\infty}{1 + L^2B^2}; \quad \ell_0 = \frac{\ell_\infty}{1 + L^2B^2}.$$

The symbols  $k_{\text{eff}}$  and  $\ell^*$  are often encountered in the older literature; more recent practice is to abandon them as too cumbersome. Eq. (1-9) is rewritten as

$$\frac{dn}{dt} = \frac{k - 1 - \beta k}{\ell_0} n + \sum_i \lambda_i c_i + q. \quad (1-10)$$

In this notation eq. (1-7) becomes

$$\frac{dc_i}{dt} = \frac{\beta k}{\ell_0} n - \lambda_i c_i \quad (1-11)$$

Eqs. (1-10) and (1-11) represent the point-reactor model in terms of the neutron lifetime  $\ell_0$ . Note the term  $-n/\ell_0$  in eq. (1-10); it represents the decay rate of the neutron density in the absence of all sources, whence the name "neutron lifetime".

An alternative formulation in terms of the "neutron generation time" may be constructed; this terminology is suggested by the production term  $kn/\ell_0$  in eq. (1-10). Defining the generation time by  $\ell = \ell_0/k$  and the reactivity by<sup>2</sup>

$$\rho = \frac{k - 1}{k}, \quad (1-12)$$

eqs. (1-10) and (1-11) become

$$\frac{dn}{dt} = \frac{\rho - \beta}{\ell} n + \sum_i \lambda_i c_i + q \quad (1-13)$$

2. The symbol  $k_{\text{ex}}$  for  $k - 1$  ("excess  $k$ ") is not used in this book, nor is the redundant terminology "excess reactivity." The symbol  $\delta k$  (for either  $k - 1$  or  $\rho$ ) is also avoided.

and

$$\frac{dc_i}{dt} = \frac{\beta_i}{\ell} n - \lambda_i c_i. \quad (1-14)$$

This is the formulation of the point-reactor model used in this book.

A distinction is sometimes made between these two alternative formulations of the point-reactor model on the grounds that sometimes  $\ell_0$  varies more than  $\ell$ , or vice versa, depending on the physical mechanisms causing reactivity changes. Actually, the only parameter having sensitive time dependence in this model is  $k = 1$ , or  $\rho$ . Neglecting time dependence in all other coefficients, including  $k$  in eq. (1-11), can hardly introduce errors greater than those incurred by employing the model in the first place; for example, significant variations in lifetime would imply large departures from criticality that would invalidate the model.

Consistency therefore suggests setting  $k = 1$  in eqs. (1-10) and (1-11), except of course in the small difference  $k = 1$ , and the result is essentially eqs. (1-13) and (1-14). Moreover, as will become clear later, the physically significant parameters of this model are the time constants  $\ell/\beta$ ,  $\ell/\beta_b$ , and  $1/\lambda_b$ , together with the ratio  $\rho/\beta$  (the reactivity in "dollars"); this further suggests that  $k$  need not be retained as an explicit parameter. For further discussions of neutron lifetime and generation time, the reader is referred to the literature (Keepin 1965; Lewis 1960a).

Note that  $n(t)$  may have any units, as long as the units of  $n$  and  $c$  are the same, and provided that  $q$  (properly normalized) has the units of  $dn/dt$ . Since the neutron density is assumed to have a fixed spatial distribution,  $n$  may be regarded as any integral or volume-averaged property that is proportional to the instantaneous neutron density at some point in the reactor, such as total number of neutrons, fission rate, power, or average power density. In much that follows, the terms power and neutron density are used interchangeably. However, as we shall see in chapter 8, this highly simplified view can be misleading.

Details of structure in a heterogeneous reactor, in which fuel and moderator are fully or partially separated, are quite outside the scope of the point-reactor model. Of course, such details affect the computation of parameters used in the model, but these parameters are necessarily integral properties of the entire reactor.

Neutron energy effects, which can be extremely complicated, are also outside the scope of this model. Some corrections are possible. For example, if  $N$  in eq. (1-1) is regarded as the density of thermal neutrons in a thermal reactor, then each term in eq. (1-2) can be multiplied by correction factors to account for leakage and absorption above thermal energies. These factors may be computed from Fermi age theory, two-energy-group theory, or more complex theories (Glasstone and Edlund 1952; Lamarsh 1966; Weinberg and Wigner 1958). Ordinarily,

each term in eq. (1-2) requires different correction factors because prompt neutrons, delayed neutrons, and extraneous-source neutrons are produced at different energies.

Since delayed neutrons are born at lower energies than prompt neutrons, they are on the average subjected to less epithermal leakage and capture. This is recognized by using effective delayed-neutron fractions, often written as  $\gamma\beta_i$  and  $\gamma\beta$ , where  $\gamma$  can be as large as 1.3 for a small water-moderated thermal reactor (deHoffman 1944). A detailed discussion is presented by Keepin (1965), with emphasis on fast assemblies; notable is the unreflected  $\text{Pu}^{239}$  assembly where  $\gamma < 1$  because of a dip in the fission cross-section near 0.5 Mev.

Further refinement recognizes that each delayed-neutron emitter has a different neutron-emission spectrum, requiring a different correction factor for each  $\beta_i$ . In the point-reactor model as used here, the symbol  $\beta$  is to be interpreted as the effective fraction, different for each reactor, and the ratios  $\beta_i/\beta$  are assumed fixed for each nuclear fuel.

The neutron energy spectrum in a reactor may shift during a transient, and this would be reflected as variations in parameters computed as spectrum-weighted averages. Actually, the spectral shift is but one component in a complex interrelation involving changes in density, temperature, etc., all of which are of primary importance in computing reactivity, but the effect on the other parameters of the point-reactor model is generally neglected.

The presence of a mixture of several types of fuel, each having its own delayed-neutron emission characteristics, introduces complications that will be mentioned only in passing, except to note that fast-neutron fission in  $\text{U}^{238}$  yields some additional delayed neutrons in any uranium-fueled reactor. This effect, which depends on the neutron spectrum and the degree of uranium enrichment, is small and will not be considered further here. A similar effect, which depends on the fuel-cycle history of a uranium reactor, arises from fission of  $\text{Pu}^{239}$  that is produced by radiative neutron capture in  $\text{U}^{238}$ .

The chief limitation of the point-reactor model is its inability to describe spatially dependent dynamic effects. These effects are often described as changes in the spatial distribution (flux tilting) during transients. They can be regarded as arising from time lags in propagating the effects of localized perturbations, and it is not surprising that these effects are often highly important in large reactors. Even in small reactors, the point-reactor model is inadequate for large departures from criticality. Further discussion of these problems is postponed until later.

Finally, it must be mentioned that neutron diffusion and nuclear fission are discrete processes, ultimately requiring statistical treatment.

The point-reactor model, diffusion theory, and transport theory, which deal with continuous distributions, are approximate descriptions of the underlying stochastic processes. This is dramatically illustrated in experimental measurements of dynamic parameters using intrinsic "reactor noise" (Thie 1963), and by observed fluctuations in the time of occurrence of neutron bursts in pulsed fast assemblies (Keepin 1965). The point-reactor model may be derived from a simple stochastic description (Soodak 1961). There has been much recent study of the theoretical fundamentals; however, these phenomena are not treated in this book. (References are cited at the end of chapter 6.)

### 1-3. Simplified Neutron Cycle

In this section the point-reactor model is interpreted in terms of a simplified dynamic neutron cycle, shown in fig. 1-1. The symbols used are those of the previous section. Some material is repeated so that this section could stand alone as an alternative derivation of the dynamic equations, provided the reader is willing to accept the concept of the neutron lifetime without a definition in terms of neutron diffusion parameters.

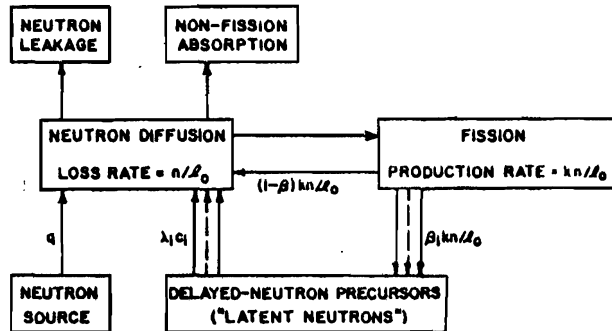


Fig. 1-1. Simplified neutron cycle.

Let  $n(t)$  be the number of neutrons in the system at time  $t$ , and let  $\tau_0$  be a characteristic time (the neutron lifetime) such that the total loss rate is  $n/\tau_0$ . Define  $k$  as the "total" number of neutrons, whether prompt or latent (delayed-neutron precursors), produced per neutron lost. The corresponding production rate is then  $kn/\tau_0$ .

Prompt neutrons are "back in circulation" immediately, and latent neutrons are "in the bank" for various mean times  $1/\lambda_i$ . The  $i$ th species of delayed-neutron precursor (delayed-neutron fraction  $\beta_i$ ) is produced at a rate  $\beta_i kn/\tau_0$ . The prompt-neutron production rate is  $(1 - \beta)kn/\tau_0$ , where  $\beta = \sum_i \beta_i$ . If  $c_i$  is the number of precursors of the  $i$ th type, the

## 10 Elementary Derivation of the Dynamic Equations

delayed-neutron production rate is  $\sum_i \lambda_i c_i$ . Then, if  $q$  is the number of neutrons per second produced by extraneous sources, the balance equation is

$$\frac{dn}{dt} = (1 - \beta)k \frac{n}{\ell_0} + \sum_i \lambda_i c_i + q - \frac{n}{\ell_0},$$

which may be rearranged as

$$\frac{dn}{dt} = \frac{k - 1 - \beta k}{\ell_0} n + \sum_i \lambda_i c_i + q$$

This is eq. (1-10) of the previous section.

The balance equation for delayed-neutron emitters is eq. (1-11):

$$\frac{dc_i}{dt} = \frac{\beta k}{\ell_0} n - \lambda_i c_i.$$

The definitions of neutron generation time,  $\ell = \ell_0/k$ , and reactivity,  $\rho = (k - 1)/k$ , yield eqs. (1-13) and (1-14):

$$\frac{dn}{dt} = \frac{\rho - \beta}{\ell} n + \sum_i \lambda_i c_i + q$$

and

$$\frac{dc_i}{dt} = \frac{\beta_i}{\ell} n - \lambda_i c_i$$

### 1-4. Delayed Neutrons

Six distinct groups of delayed-neutron emitters are generally recognized in reactor dynamics studies. There are grounds, both experimental and theoretical, for recognizing the presence of others, but existing neutron-irradiation data are satisfactorily interpreted by assuming six decay constants (Keepin 1965). It was indeed observed that "six exponential periods were found necessary and sufficient for optimum least-squares fit to the data" (Keepin, Wimett, and Zeigler 1957).

Significant variation was observed among the sets of six half-lives and abundances obtained for different isotopes and incident neutron energies; it is therefore recommended that separate data be used for each fissile species and each neutron spectrum. Thermal-fission data are summarized in table 1-1, and fast-fission data are in table 1-2.

Limits of error are not reproduced here. The uncertainties in half-lives (Keepin 1965) range from approximately 2 percent for the longer half-lives to roughly 10 percent for the shorter ones. In a few cases the

uncertainties for the two shortest half-lives approach 20 percent, but for the four longest-lived groups the half-life is generally known within a few percentage points. For the total delayed-neutron yield, the result  $0.0158 \pm 0.0005$  neutrons per fission for thermal fission in  $\text{U}^{235}$  is typical.

Table 1-1. Delayed Neutrons from Thermal Fission

Fuel	Isotopic Purity (%)	Group No. (i)	Half-life ( $\tau_{1/2}$ , sec)	Decay Constant ( $\lambda_i$ , sec $^{-1}$ )	Relative Yield ( $\beta_i/\beta$ )	Yield (Neutrons per Fission)
$\text{U}^{235}$	99.9	1	55.72	0.0124	0.033	0.00052
		2	22.72	0.0305	0.219	0.00346
		3	6.22	0.111	0.196	0.00310
		4	2.30	0.301	0.395	0.00624
		5	0.610	1.14	0.115	0.00182
		6	0.230	3.01	0.042	0.00066
	Total				1.000	0.0158
$\text{Pu}^{239}$	99.8	1	54.28	0.0128	0.035	0.00021
		2	23.04	0.0301	0.298	0.00182
		3	5.60	0.124	0.211	0.00129
		4	2.13	0.325	0.326	0.00199
		5	0.618	1.12	0.086	0.00052
		6	0.257	2.69	0.044	0.00027
	Total				1.000	0.0061
$\text{U}^{233}$	100	1	55.00	0.0126	0.086	0.00057
		2	20.57	0.0337	0.299	0.00197
		3	5.00	0.139	0.252	0.00166
		4	2.13	0.325	0.278	0.00184
		5	0.615	1.13	0.051	0.00034
		6	0.277	2.50	0.034	0.00022
	Total				1.000	0.0066

SOURCE: Physics of Nuclear Kinetics, by G. R. Keepin (Reading, Mass.: Addison-Wesley Publishing Co., 1965). © 1965 by Addison-Wesley Publishing Co.

Table 1-2. Delayed Neutrons from Fast Fission

Fuel	Isotopic Purity (%)	Group No. (i)	Half-life ( $\tau_{1/2}$ , sec $^{-1}$ )	Decay Constant ( $\lambda_i$ , sec $^{-1}$ )	Relative Yield ( $\beta_i/\beta$ )	Yield (Neutrons per Fission)
$\text{U}^{235}$	99.9	1	54.51	0.0127	0.038	0.00063
		2	21.84	0.0317	0.213	0.00351
		3	6.00	0.115	0.188	0.00310
		4	2.23	0.311	0.407	0.00672
		5	0.496	1.40	0.128	0.00211
		6	0.179	3.87	0.026	0.00043
	Total				1.000	0.0165
$\text{Pu}^{239}$	99.8	1	53.75	0.0129	0.038	0.00024
		2	22.29	0.0311	0.280	0.00176
		3	5.19	0.134	0.216	0.00136

12 Elementary Derivation of the Dynamic Equations

Table 1-2--Continued

Fuel	Isotopic Purity (%)	Group No. (i)	Half-life ( $\tau_{1/2}$ , sec)	Decay Constant ( $\lambda_i$ , sec $^{-1}$ )	Relative Yield ( $\beta_i/\beta$ )	Yield (Neutrons per Fission)
$U^{235}$	100	4	2.09	0.331	0.328	0.00207
		5	0.549	1.26	0.103	0.00065
		6	0.216	3.21	0.035	0.00022
		Total			1.000	0.0063
		1	55.11	0.0126	0.086	0.00060
		2	20.74	0.0334	0.274	0.00192
		3	5.30	0.131	0.227	0.00159
		4	2.29	0.302	0.317	0.00222
		5	0.546	1.27	0.073	0.00051
		6	0.221	3.13	0.023	0.00016
		Total			1.000	0.0070

SOURCE: Physics of Nuclear Kinetics, by G. R. Keepin (Reading, Mass.: Addison-Wesley Publishing Co., 1965). © 1965 by Addison-Wesley Publishing Co.

Table 1-3. Delayed-neutron Fractions and Weighted Mean Decay Constants

Effective Neutron Energy	Fuel	Yield (Delayed Neutrons per Fission)	$v$ (Neutrons per Fission)	$\beta$ (Delayed-neutron fraction)	$\lambda$ $\left( \frac{1}{\beta} \sum_i \frac{\beta_i}{\lambda_i} \right)^{-1}$ (sec $^{-1}$ )	$\lambda'$ $\frac{1}{\beta} \sum_i \beta_i \lambda_i$ (sec $^{-1}$ )
Thermal	$U^{235}$	0.0158	2.432	0.00650	0.0767	0.405
	$Pu^{239}$	0.0061	2.874	0.00212	0.0648	0.356
	$U^{233}$	0.0066	2.482	0.00266	0.0543	0.279
1.15 Mev	$U^{235}$	0.0165	2.57	0.00642	0.0784	0.435
	$Pu^{239}$	0.0063	3.09	0.00204	0.0683	0.389
	$U^{233}$	0.0070	2.62	0.00267	0.0559	0.300

Table 1-3 includes the neutron number  $v$  (mean number of neutrons per fission) and the values of the delayed-neutron fraction  $\beta$  derived by dividing  $v$  into the total yields from tables 1-1 and 1-2. Values of  $v$  were obtained from empirical correlations for  $v$ , as a function of neutron energy, using computed effective neutron energies for Los Alamos fast-fission data (Keepin 1965). Note that the resulting delayed-neutron fraction for thermal fission in  $U^{235}$ , 0.00650, is significantly smaller than the earlier accepted value of 0.00755 (Hughes et al. 1948). The lower value is consistent with various measurements of effective delayed-neutron fractions, as corrected by computed effectiveness factors (Keepin 1965). Note also that  $\beta$  is not greatly dependent on incident neutron energy; both  $v$  and the absolute yield increase with energy in approximately the same manner.

Also included in table 1-3 are composite decay constants for delayed-neutron emission, obtained by two different weighting schemes. The

number  $1/\lambda = (1/\beta)\sum_i(\beta_i/\lambda_i)$  is the abundance-weighted mean decay time, and  $\lambda' = (1/\beta)\sum_i\beta_i\lambda_i$  is the abundance-weighted mean decay constant. It is shown in chapter 2 that  $\lambda$  and  $\lambda'$  are the effective decay constants for two of the possible representations of delayed neutrons as a single group,  $\lambda$  being appropriate for very slowly varying neutron densities and  $\lambda'$  being suitable during very rapid changes. Note that  $\lambda$  and  $\lambda'$  are independent of the absolute yields; they are determined directly from the  $\lambda_i$  and the relative yields  $\beta_i/\beta$  in tables 1-1 and 1-2.

The individual  $\beta_i$  are not included in the tables. They may be calculated by multiplying the appropriate set of relative yields by the corresponding value of  $\beta$ , but they have minor significance. As pointed out in sec. 1-2, the important dynamic parameters are  $\ell/\beta$ ,  $\ell/\beta_i$ ,  $\lambda_i$ , and  $\rho/\beta$ . Given  $\ell/\beta$  from a dynamic measurement, eq. (1-14) is completely specified by some  $\lambda_i$  and its corresponding ratio  $\beta_i/\beta$ . Further, as mentioned in sec. 1-2, the effective value of  $\beta$  is different for different reactor types using the same fuel because of the different epithermal leakage and capture probabilities for prompt and delayed neutrons, while the additional refinement of slightly different effectiveness for each delayed-neutron group is a much smaller effect that is generally ignored.

Delayed neutron emitters are fission fragments that are highly unstable because of excess neutrons. The usual mode of decay in such cases is beta emission, often in chains of four or five successive events. Occasionally, a branch is followed that leads to an unusually highly excited nucleus; the result is the immediate ejection of a neutron, leaving a stable nuclide. An example is  $\text{Br}^{87}$ , shown in fig. 1-2, which probably accounts for the delayed-neutron group  $i = 1$ .

Note that the lifetime for neutron emission is controlled by the beta-decay half-life of the parent nuclide. Note also that only a fraction of the

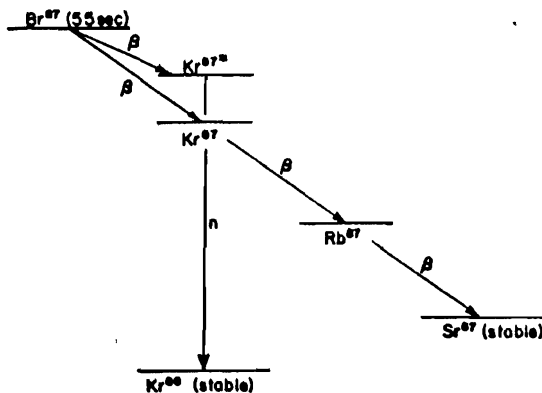


Fig. 1-2. Origin of delayed neutrons from  $\text{Br}^{87}$  (Weinberg and Wigner 1958).

## 14 Elementary Derivation of the Dynamic Equations

$\text{Br}^{87}$  formed in fission leads to a delayed neutron; when counting precursors or "latent neutrons" as in sec. 1-3, one includes only that fraction of the  $\text{Br}^{87}$  which decays to  $\text{Kr}^{87*}$ .

Similarly, the group  $i = 2$  is probably due (at least in part) to the fission fragment  $\text{I}^{137}$ , as depicted in fig. 1-3. Other groups are not easily identifiable, because each of the "six groups" is probably the combined result of two or more neutron emitters with half-lives too close together to permit resolution in neutron-irradiation experiments. In fact, seven neutron-emitting halogens have been identified radiochemically, with half-lives ranging from 1.6 to 54.5 sec, while some theoretical considerations suggest the possibility of more than fifty emitters (Keepin 1965).

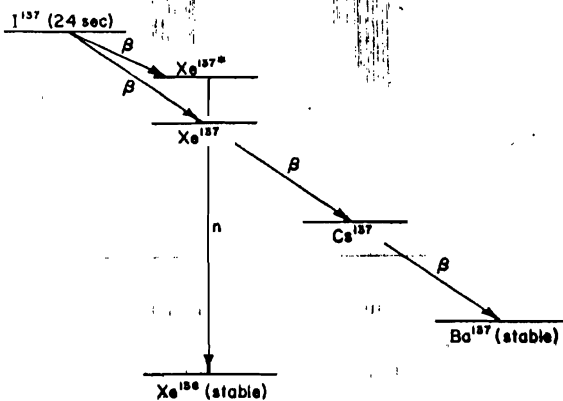


Fig. 1-3. Origin of delayed neutrons from  $\text{I}^{137}$  (Weinberg and Wigner 1958).

On the other hand, many of the important phenomena of reactor dynamics are well described by combining all the emitters into one effective group, or, at most, two or three effective groups, and the question of the exact number of neutron-emitting nuclides becomes rather academic.

Special situations require refinements, depending on reactor type and degree of rigor desired. The circulating-fuel reactor is a notable example, because a significant number of delayed neutrons may be emitted while the fuel is in an external loop (Ergen 1954; Keepin 1965; MacPhee 1958). The problem can be further complicated by continuous fission-product extraction, which causes further depletion of the longer-lived emitters. Loss of emitters by high-temperature diffusion may also be important, as in a nuclear rocket engine. All these effects result in a decrease in the effective delayed-neutron yield, leading to more stringent control requirements.

The presence of more than one fissile isotope can be described approximately by using a weighted-average set of delayed-neutron yields. Also, the buildup of heavier fissile isotopes in long-lived cores will cause a slight shift in effective yields. Finally, in reactors containing beryllium or heavy water, photoneutrons are produced outside the fuel by both prompt and delayed gamma rays; some of this photoproduction is due to very long-lived fission-product decays, resulting in significant neutron background after reactor shutdown even though the change in the total effective yield is very small (Bernstein et al. 1947, 1956; Keepin 1965).

It is often difficult to predict the importance of these special effects. In many cases, the point-reactor model will be adequate if suitably corrected parameters are used. In other cases, the special phenomena must be carefully analyzed and properly related to the nuclear dynamics. In all cases, cautious judgment is indicated, lest the analyst be led astray by an injudicious application of the point-reactor model.

### Problems

- 1-1. Estimate the neutron lifetime in infinite graphite. Use  $\sigma_a = 5 \times 10^{-3}$  barn, density =  $1.6 \text{ gm/cm}^3$ , atomic weight = 12, Avogadro's number =  $6 \times 10^{23}$ , and a characteristic thermal-neutron speed of 2,200 mps.
- 1-2. Disperse one atom of  $\text{U}^{235}$  in graphite for every 10,000 carbon atoms. Use  $\sigma_a = 650$  barns (fission included). Calculate the infinite-medium lifetime for thermal neutrons.
- 1-3. Estimate the infinite-medium lifetime for 0.25-Mev neutrons in  $\text{U}^{235}$ . Use  $\sigma_a = 1.6$  barns and a density of  $19 \text{ gm/cm}^3$ . Obtain the speed from the fact that 2,200 mps corresponds to 0.025 ev.
- 1-4. Assume that the result of prob. 1-3 may be applied to neutrons having the energy spectrum found in a critical sphere of  $\text{U}^{235}$ . If the measured neutron lifetime for the sphere is  $6 \times 10^{-9}$  sec, calculate the fraction of neutrons that leak out.
- 1-5. A free neutron decays to a proton and a beta particle with a half-life of 11 min. What effect does this have in a reactor? What effect would it have if the half-life were 0.01 sec?



## 2 Constant Reactivity and Reactivity Steps

In this chapter the solutions of the point-reactor equations for constant reactivity are explored. These include the response of the reactor to so-called step inputs of reactivity, step changes in neutron-source strength, and neutron bursts represented as impulse (delta-function) sources.

The use of step functions or impulse functions to simulate real perturbations or sources is particularly fruitful in reactor dynamics because of the presence of one time constant that is frequently much shorter than all the other time constants of the system. The result is that in many problems the spurious part of the response that arises from such simulation dies out quickly. For example, the response to a change in control-rod position may often be closely simulated by the response to a step input of reactivity within a very short time after the new reactivity level is achieved.

A more important reason for studying the constant-reactivity solutions is their simplicity. They are linear combinations of exponential functions whose properties are easily understood, and they serve as a useful departure point for the study of more complex problems. Of course, such solutions become meaningless once the reactor power and temperature are high enough to produce reactivity feedback (reactivity changes caused by changes in the material densities and the neutron spectrum); this topic is treated in chapter 5.

### 2-1. Equilibrium and Criticality

Eqs. (1-13) and (1-14), the point-reactor equations, are repeated here:

$$\frac{dn}{dt} = \frac{\rho - \beta}{\ell} n + \sum_i \lambda_i c_i + q \quad (2-1)$$

and

$$\frac{dc_i}{dt} = \frac{\beta_i}{\ell} n - \lambda_i c_i, \quad (2-2)$$

where, as before,

$n$  = neutron density (or power, etc.);

$c_i$  = precursor density ("latent-neutron" density or latent power, etc.; same units as  $n$ );

$t$  = time;

$\rho$  = reactivity,  $(k - 1)/k$ , the fractional change in neutron reproduction factor;

$\beta$  = delayed-neutron fraction ( $\sum \beta_i$ );

$\ell$  = neutron generation time;

$\lambda_i$  = decay constant for precursor decay;

$q$  = effective source strength (same units as  $dn/dt$ ).

The summation in eq. (2-1) extends from  $i = 1$  to  $m$ , where  $m$  is the number of delayed-neutron groups; the  $m$  will be omitted unless needed for clarity. The parameters  $\beta_i$ ,  $\lambda_i$ , and  $\ell$  are assumed constant. The point-reactor model thus consists of  $m + 1$  coupled first-order differential equations, together with the specification of the functions  $\rho(t)$  and  $q(t)$ . In general,  $\rho$  is a functional of  $n$ , and the system is nonlinear (see chapter 5); in the absence of reactivity feedback,  $\rho(t)$  is an explicit function of time and the system is linear.

Consider first the equilibrium state of the system (steady state) defined by the vanishing of all time derivatives. Summing eqs. (2-2) over  $i$  and adding to eq. (2-1) yields

$$\frac{d}{dt} (n + \sum_i c_i) = \frac{\rho}{\ell} n + q. \quad (2-3)$$

Equilibrium implies

$$\rho = -\frac{\ell q}{n}. \quad (2-4)$$

This could be satisfied in the presence of a time-dependent source, with constant  $n = n_0$ , if  $\rho(t)$  and  $q(t)$  were precisely proportional; complete equilibrium requires, however, that  $q$  and  $\rho$  be constants  $q_0$  and  $\rho_0$ . In this case

$$\rho_0 = -\frac{\ell q_0}{n_0}, \quad (2-5)$$

and the reactor is said to be in subcritical equilibrium ( $\rho_0 < 0, k < 1$ ).

The "shutdown power level" is then

$$n_0 = -\frac{\ell q_0}{\rho_0} = \frac{\ell q_0}{|\rho_0|}. \quad (2-6)$$

Note that the equilibrium precursor density, by eq. (2-2), is

$$c_{10} = \frac{\beta_1 n_0}{\lambda_1 \ell}. \quad (2-7)$$

Criticality, defined as  $k = 1$  ( $\rho = 0$ ) is, strictly speaking, a non-equilibrium situation; in the presence of a source the critical reactor is divergent, as shown by eq. (2-3). A neutron source, inserted prior to reactor startup to provide adequate detector readings, may be withdrawn as criticality is approached; nevertheless, neutrons from spontaneous fission and cosmic rays will always represent sources. In consequence, an operating reactor at steady power is always slightly subcritical, though the reactivity as expressed in eq. (2-5) is usually undetectably small. This will be the case when  $n_0/\ell$  is large, and if the magnitude of the reactivity at power is very much smaller than the magnitude of the shutdown reactivity, then the source may be neglected in further calculations.

When the reactor is highly subcritical and the source is important, the concept of neutron multiplication is useful. From eq. (2-5),

$$\frac{n_0}{\ell} = -\frac{q_0}{\rho_0}.$$

When  $\rho_0 = (k - 1)/k$  and  $\ell_0 = k\ell$  (see sec. 1-2) are used, this may be written in terms of the reproduction factor  $k$  and the neutron lifetime  $\ell_0$ :

$$\frac{n_0}{\ell_0} = \frac{q_0}{1 - k} = M q_0, \quad (2-8)$$

where  $M$  is the neutron multiplication. Since  $k < 1$ ,

$$M = \frac{1}{1 - k} = 1 + k + k^2 + \dots, \quad (2-9)$$

which lends itself to the interpretation that a subcritical multiplying system "multiplies" a source neutron  $k$  times during the lifetime of an average neutron,  $M$  being the ratio of neutron-loss rate  $n_0/\ell_0$  to source strength  $q_0$ .

During the loading of fuel in a new reactor, the approach to criticality is monitored by means of a neutron source and neutron detectors; as  $k \rightarrow 1$  the reciprocal of the detector counting rate, which is inversely proportional to  $n_0$  in eq. (2-8), approaches zero. Extrapolation to zero

### 2.1 Constant Reactivity and Reactivity Steps

of a curve of reciprocal counting rate vs. number of fuel elements then serves as a rough prediction of the amount of fuel needed for criticality, though the procedure is highly dependent on spatial effects (spatial variation of source, detector, and fuel effectiveness) that are not contained in the point-reactor model.

On the other hand, at high power when sources are negligible, the model is described by eqs. (2-1) and (2-2) with  $q = 0$ . This mathematical model, as seen from eq. (2-3), is in equilibrium at arbitrary power  $n_0$  provided the precursors satisfy eq. (2-7). This model is generally satisfactory unless the power becomes extremely small.

In nonlinear stability studies, this model often yields a nonphysical zero-power equilibrium state, which by eq. (2-1) corresponds to arbitrary reactivity (unless the equilibrium states for the feedback equations specify some unique equilibrium reactivity); this situation is nonphysical because sooner or later a stray neutron appears which starts a chain that does not die out. Nevertheless, this concept is a useful one because stability conclusions are generally the same whether negative reactivity means an asymptotic approach to zero power or to a very small source-dominated shutdown power. This is possible because of an important property of the source-free model: once positive, as in any physically meaningful case,  $n$  and  $c_i$  cannot change sign.

This property is easily demonstrated. If  $q = 0$  in eq. (2-1), and if  $n \rightarrow 0$  through positive values,

$$\frac{dn}{dt} \cong \sum_i \lambda_i c_i,$$

which is positive if all  $c_i > 0$ . Similarly, from eq. (2-2), small  $c_i$  implies

$$\frac{dc_i}{dt} \cong \frac{\beta_i}{\ell} n,$$

which is positive if  $n > 0$ ; hence the dependent variables always remain positive. This property of the source-free model is needed for the nonlinear stability studies of chapter 7.

#### 2-2. The Inhour Equation

The solutions of eqs. (2-1) and (2-2) for constant reactivity, in the absence of a source, are linear combinations of  $m + 1$  exponentials  $e^{\omega_j t}$ . The  $\omega_j$  depend upon the reactivity through the characteristic equation, which is called the inhour equation. The name originated in the early days of reactor technology, one inhour being defined as the amount of positive reactivity which corresponds to an asymptotic power rise having a time constant (period) of one hour (reciprocal period of one "inverse hour").

We proceed to seek the solution  $n(t)$  of the source-free equations with  $\rho$  unspecified for  $t < 0$  and  $\rho = \rho_0$ , a constant, for  $t \geq 0$ . More detailed specifications for  $t < 0$  will be needed to complete the solution, but the characteristic equation is independent of them. The characteristic equation is also unaffected by the presence of a source; the source merely generates additional terms which are added to the solution of the homogeneous (source-free) equations.

Introduce the Laplace transforms

$$N(s) = \int_0^\infty n(t)e^{-st} dt;$$

$$\Gamma_i(s) = \int_0^\infty c_i(t)e^{-st} dt.$$

Eqs. (2-1) and (2-2) are transformed into

$$sN - n(0) = \frac{\rho_0 - \beta}{\ell} N + \sum_i \lambda_i \Gamma_i; \quad (2-10)$$

$$s\Gamma_i - c_i(0) = \frac{\beta_i}{\ell} N - \lambda_i \Gamma_i. \quad (2-11)$$

From eq. (2-11),

$$\Gamma_i = \frac{(\beta_i/\ell)N + c_i(0)}{s + \lambda_i}. \quad (2-12)$$

Substituting into eq. (2-10) and solving for  $N$  gives

$$N(s) = \frac{\ell \left[ n(0) + \sum_i \frac{\lambda_i c_i(0)}{s + \lambda_i} \right]}{\ell s + \beta - \rho_0 - \sum_i \frac{\beta_i \lambda_i}{s + \lambda_i}}. \quad (2-13)$$

Eq. (2-13) may be written as the ratio of two polynomials in  $s$ ; the degrees of the numerator and denominator respectively are  $m$  and  $m + 1$ . It can be shown that the denominator has  $m + 1$  distinct real roots, whence  $N(s)$  has  $m + 1$  simple poles on the real  $s$ -axis. The inverse transform is

$$n(t) = \sum_{j=1}^{m+1} A_j e^{\omega_j t}, \quad (2-14)$$

where the  $\omega_j$  are the  $m + 1$  roots  $s = \omega_j$  of the denominator of  $N(s)$ .

### Constant Reactivity and Reactivity Steps

In other words, each  $\omega_j$  satisfies the equation

$$\rho_0 = \beta + \ell\omega + \sum_i \frac{\beta_i \lambda_i}{\omega + \lambda_i}, \quad (2-15)$$

or, since  $\beta = \Sigma_i \beta_i$ ,

$$\rho_0 = \ell\omega + \sum_i \frac{\beta_i \omega}{\omega + \lambda_i}. \quad (2-16)$$

Eqs. (2-15) and (2-16) are two forms of the inhour equation, which, regarded as an algebraic equation of degree  $m + 1$  in  $\omega$ , can be shown to have  $m$  negative real roots and one real root of the same sign as  $\rho_0$ . For large  $t$ , one term in eq. (2-14) will eventually dominate, and  $n \rightarrow A_1 e^{\omega_1 t}$  where  $\omega_1$  is the algebraically greatest  $\omega_j$ . For positive  $\rho_0$  the dominant term is a growing exponential, and the characteristic time  $T = 1/\omega_1$  is called the "reactor period" or "asymptotic period" (also known as "stable period" and "e-folding time").

For very large  $\omega$ , either positive or negative, eq. (2-15) has the asymptote

$$\rho_0 = \beta + \ell\omega, \quad (2-17)$$

from which

$$\omega = \frac{\rho_0 - \beta}{\ell}. \quad (2-18)$$

For small  $\omega$  ( $|\omega| \ll \min. \lambda_i$ ), eq. (2-16) becomes

$$\rho_0 \cong \left( \ell + \sum_i \frac{\beta_i}{\lambda_i} \right) \omega. \quad (2-19)$$

Since this  $\omega$  changes sign with  $\rho_0$ , it is the root  $\omega_1$  which corresponds to the asymptotic period. Further, it is seen from either eq. (2-15) or (2-16) that  $\rho_0 \rightarrow \pm \infty$  as  $\omega \rightarrow -\lambda_i$ ; this means that there is a set of  $m$  asymptotes  $\omega = -\lambda_i$ , and it may be shown that  $m - 1$  branches of the inhour curve are bounded by adjacent asymptotes  $-\lambda_i$  and  $-\lambda_{i+1}$ . These observations are summarized in fig. 2-1, which is a qualitative plot of  $\omega$  vs.  $\rho_0$  showing the seven branches for six groups of delayed neutrons.

If there were no delayed neutrons, the inhour equation would reduce to  $\rho_0 = \ell\omega$  and the neutron density would be simply

$$n = n(0)e^{\rho_0/\ell t}$$

For small reactivity, eq. (2-19) may be used in the form  $\rho_0 = \ell'\omega$ , where

$$\ell' = \ell + \sum_i \frac{\beta_i}{\lambda_i}. \quad (2-20)$$

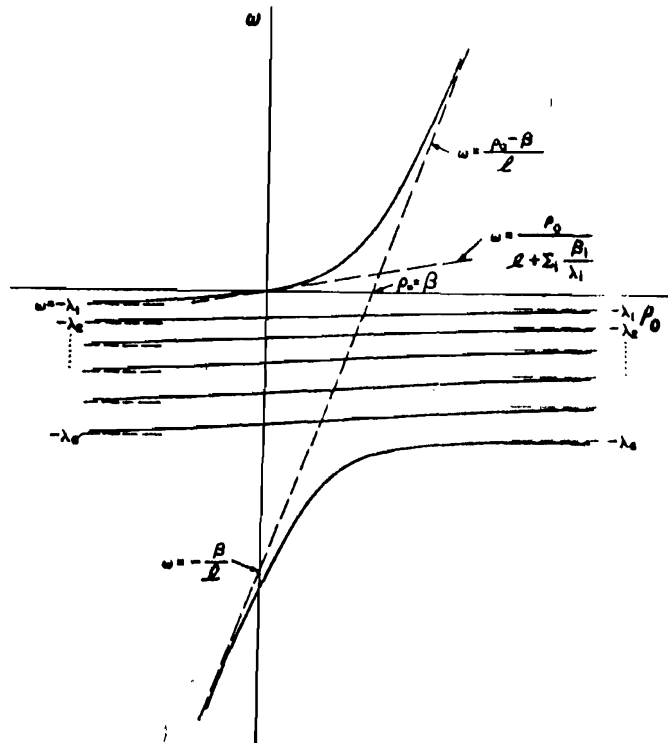


Fig. 2-1. Qualitative plot of the inhour equation for six groups of delayed neutrons. In practice,  $\beta/\ell \gg \lambda_6$ , and the asymptote for large  $\omega$  has a much steeper slope than shown.

The dominant term in the solution would then be approximately

$$A_1 e^{(\rho_0/\ell') t}$$

Since  $\ell' > \ell$ , it is clear that delayed neutrons have a slowing influence; just how much is made clear upon comparing the magnitudes of  $\ell$  and  $\Sigma_i (\beta_i/\lambda_i)$ . The generation time  $\ell$  ranges from about  $10^{-8}$  sec (unreflected fast metal assembly) to about  $10^{-3}$  sec (large thermal reactor), while values of  $\Sigma_i (\beta_i/\lambda_i) = \beta/\lambda$ , derived from table 1-3, are presented in table 2-1; these are all greater than 0.03. Hence  $\ell'$  is quite unimportant in eq. (2-20), and the effective lifetime is

$$\ell' \cong \sum_i \frac{\beta_i}{\lambda_i} = \frac{\beta}{\lambda}. \quad (2-21)$$

The inhour equation for the asymptotic period is then

$$\rho_0 \cong \ell' \omega \cong \sum_i \frac{\beta_i}{\lambda_i} \omega = \frac{\beta}{\lambda} \omega; \quad (2-22)$$

## 24 Constant Reactivity and Reactivity Steps

Table 2-1. Effective Lifetimes  $\beta/\lambda = \sum_i(\beta_i/\lambda_i)$  Derived from Table 1-3

Effective Neutron Energy	Fuel	Effective Lifetime (sec)
Thermal	U <sup>235</sup>	0.0847
	Pu <sup>239</sup>	0.0327
	U <sup>233</sup>	0.0490
1.45 Mev	U <sup>235</sup>	0.0819
	Pu <sup>239</sup>	0.0299
	U <sup>233</sup>	0.0477

and the asymptotic response for a small reactivity input is therefore dominated by the delayed neutrons. The consequences of this for reactor stability are discussed in chapters 6 and 7.

Note how these considerations affect the graph in fig. 2-1. The scale is vastly distorted because of the smallness of  $\ell$ , and the asymptote  $\omega = (\rho_0 - \beta)/\ell$  should indeed be almost vertical. As  $\rho_0$  increases from zero, the positive root increases very slowly according to eq. (2-19), but once  $\rho_0$  increases past  $\beta$  the slowing effect of delayed neutrons is lost. The crossover  $\rho_0 = \beta$  is called prompt critical because at this point the chain reaction is self-sustaining on prompt neutrons alone.

The smallness of  $\ell$  suggests the use of an important approximation obtained by letting  $\ell \rightarrow 0$ . From eqs. (2-15) and (2-16),

$$\rho_0 \cong \beta - \sum_i \frac{\beta_i \lambda_i}{\omega + \lambda_i} = \sum_i \frac{\beta_i \omega}{\omega + \lambda_i}. \quad (2-23)$$

This approximation is much better than eq. (2-22) in most of the range  $\rho_0 < \beta$ , though clearly it fails as  $\rho_0 \rightarrow \beta$ . Eq. (2-23) is the inhour equation for the "prompt-jump" approximation, which is widely used in this book. Eq. (2-23) is also a good approximation for all the negative roots except the most highly negative one which is lost by setting  $\ell = 0$ .

The smallness of  $\ell$  also permits a simple approximate formula to express values of  $\omega$  near prompt critical. For  $|\omega| \gg \max_i \lambda_i$ , eq. (2-15) becomes

$$\rho_0 \cong \beta + \ell \omega - \sum_i \frac{\beta_i \lambda_i}{\omega}. \quad (2-24)$$

At prompt critical, this yields

$$\omega^2 \cong \frac{1}{\ell} \sum_i \beta_i \lambda_i = \frac{\beta \lambda'}{\ell}, \quad (2-25)$$

where  $\lambda' = (1/\beta) \sum_i \beta_i \lambda_i$  (see table 1-3 for numerical values). The two

solutions of eq. (2-25) represent the algebraically largest and smallest values of  $\omega$  at prompt critical; the positive root is more closely approximated by this formula.

Because of the wide range of numerical values, the positive root is often displayed in a log-log plot, variations of which are sketched in fig. 2-2. The straight lines of unit slope for small  $\omega$  and large  $\omega$  are respectively eq. (2-19) and the limit  $\rho_0 \rightarrow \ell\omega$  of eq. (2-18). Between these extremes is the transition through prompt critical where a small change in reactivity corresponds to a large change in  $\omega$ .

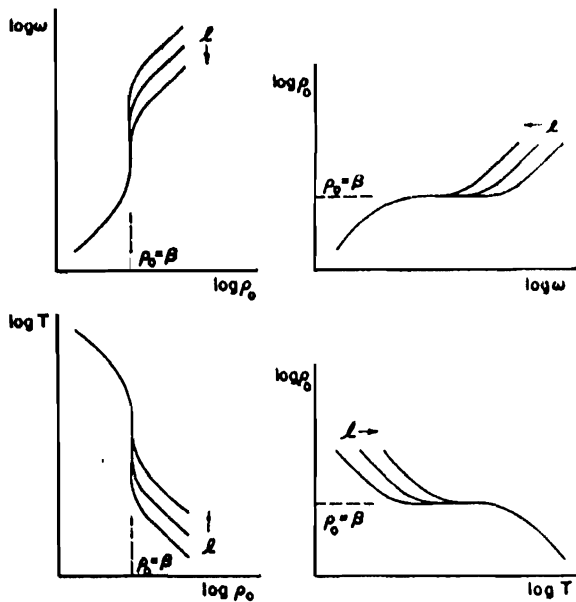


Fig. 2-2. Logarithmic representation for the positive branch of the inhour equation ( $T = 1/\omega$ ). Arrows indicate the effect of increasing  $\Lambda$ .

Although reactivity is nondimensional, there are different ways of expressing it numerically. The numerical value of the fraction  $(k - 1)/k$  is commonly used. The numerical value of  $\rho/\beta$ , called "dollars", is more practical because  $\ell/\beta$  is usually better known than either  $\ell$  or  $\beta$  separately, and the inhour equation is consequently better suited for predicting  $\rho/\beta$  than  $\rho$  itself from dynamic observations. Prompt critical is thus a reactivity of one dollar, and it is often convenient to express reactivity in cents (at the usual rate of 100 to the dollar). The inhour (the reactivity for which the stable period is 3,600 sec) is no longer widely used. Small reactivities are sometimes expressed as "percent reactivity."

$100(k - 1)/k$ . Other units are based on the name "re" for the number  $(k - 1)/k$ , whence the name "millire" for  $10^3(k - 1)/k$  and "microre" for  $10^6(k - 1)/k$ .

A quantitative semilog graph of the roots of the inhour equation for thermal fission in  $U^{235}$  is shown in fig. 2-3 (Keepin 1965). The ordinates are reciprocals of the  $\omega_j$  (stable period and transient periods). These curves were computed using the neutron lifetime instead of the generation time (see chapter 1), but the difference is undetectable in the figure. Note that the period at prompt critical (one dollar) ranges from about one sec for a thermal reactor down to the millisecond range for a fast reactor.

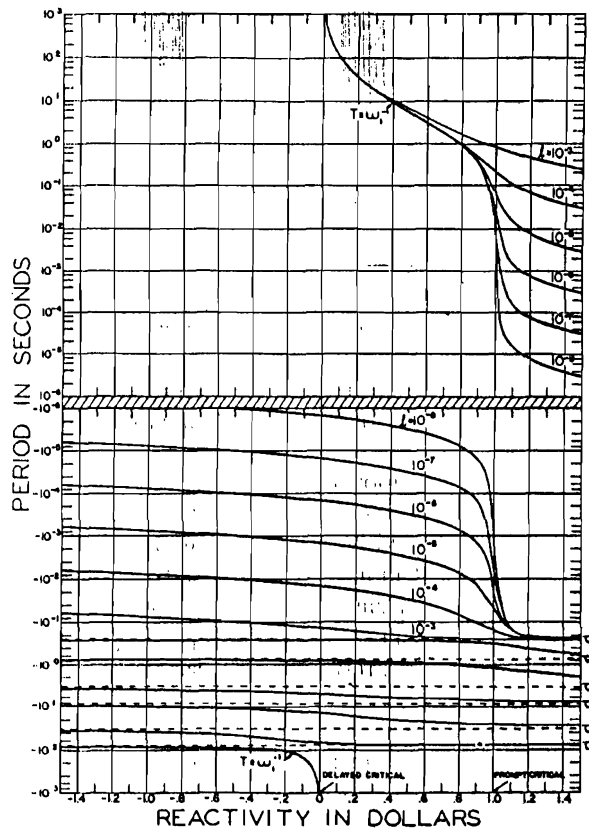


Fig. 2-3. Reactor "stable" and "transient" periods vs. reactivity for  $U^{235}$  delayed-neutron data. Dotted lines,  $\tau_1, \dots, \tau_6, (1/\lambda_1, \dots, 1/\lambda_6)$ , are the six delayed-neutron mean lives for  $U^{235}$ . Parameter  $\beta$  is neutron generation time;  $\beta = 0.0064$  (from *Physics of Nuclear Kinetics* by G. R. Keepin. © 1965 by Addison-Wesley Publishing Co., Reading, Mass.).

### 2-3. One-Group Representations

It is often convenient (and sometimes satisfactory) to simplify the dynamic equations by representing all the delayed neutrons as though they had a single mean lifetime. In this section we explore the consequences of this for the inhour equation, discuss some of the limitations, and mention briefly the useful compromises obtained with two- and three-group models.

The usual procedure is to construct a model which has the same period-reactivity relationship for small  $\omega$ . For one group ( $\sum_i \beta_i \rightarrow \beta$ ) eq. (2-19) would be

$$\rho_0 \cong \left( \ell + \frac{\beta}{\lambda} \right) \omega \cong \frac{\beta}{\lambda} \omega. \quad (2-26)$$

Comparing eqs. (2-19) and (2-26) shows that these match if  $\lambda$  satisfies

$$\frac{1}{\lambda} = \frac{1}{\beta} \sum_i \frac{\beta_i}{\lambda_i}. \quad (2-27)$$

For thermal fission in  $U^{235}$ ,  $\lambda = 0.0767 \text{ sec}^{-1}$ . This and other values are given in table 1-3.

From eq. (2-16) the inhour relation for one group is

$$\rho_0 = \ell \omega + \frac{\beta \omega}{\omega + \lambda}. \quad (2-28)$$

This may be regarded as a quadratic in  $\omega$ :

$$\ell \omega^2 + (\beta - \rho_0 + \lambda') \omega - \lambda \rho_0 = 0. \quad (2-29)$$

It is easily shown that for realistic ranges of the parameters this quadratic has two real roots, one always negative and the other with the same sign as  $\rho_0$ . A sketch is shown in fig. 2-4.

Comparison with fig. 2-1 shows that the one- and six-group curves match at very small  $\omega$  and again at very large  $\omega$ . The error in the intermediate range may be quite large. An alternative procedure is to attempt a matching near prompt critical. From eq. (2-24) with one group,

$$\rho_0 \cong \beta + \ell \omega - \frac{\beta \lambda'}{\omega}. \quad (2-30)$$

Comparison yields

$$\lambda' = \frac{1}{\beta} \sum_i \beta_i \lambda_i. \quad (2-31)$$

For thermal fission in  $U^{235}$ ,  $\lambda' = 0.405$ ; see table 1-3.

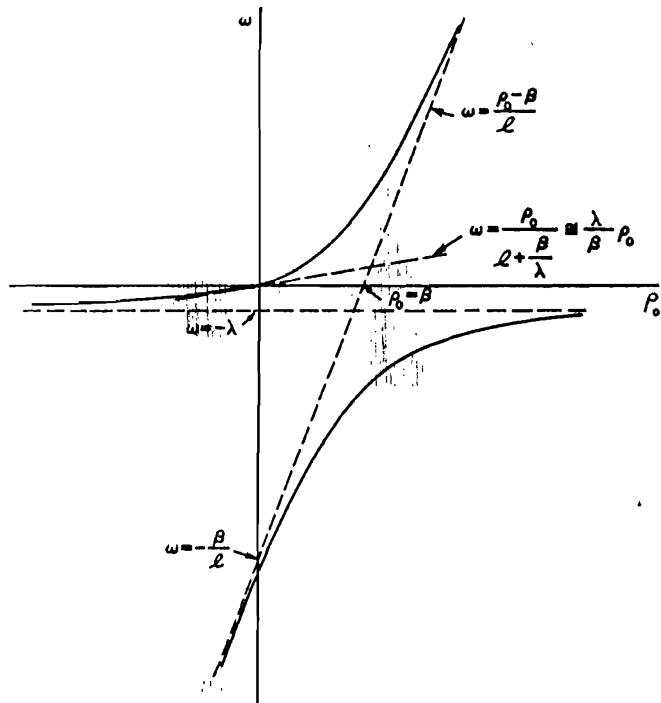


Fig. 2-4. Qualitative plot of the inhour equation for one group of delayed neutrons.

A quantitative comparison is shown in fig. 2-5, which is a sample calculation for  $\beta = 0.0079$  and  $\ell = 10^{-4}$  sec, nominal values for a TRIGA reactor (General Atomic 1958). The greatest relative error between the six-group reactivity and the one-group reactivity for  $\lambda = 0.077$  is about 40 percent, occurring at  $\omega = 0.1 \text{ sec}^{-1}$ . The one-group reactivity for  $\lambda' = 0.40$  is actually closer to the six-group value over a wide range, though it is always an underestimate that becomes quite useless for very small reactivities.

Another difficulty appears for small and intermediate positive reactivities. The one-group  $n(t)$  has one rising exponential and one rapidly decaying exponential term. The absence of the intermediate branches of the inhour curve (the more slowly decaying terms) means that the one-group model underestimates the elapsed time after a reactivity step before the asymptotic term is dominant. This can be misleading when discussing measurements of period-reactivity data by means of observing asymptotic responses to small reactivity steps.

For large negative reactivities, these one-group models are useless. Here all terms in  $n(t)$  are decaying exponentials, and the term having

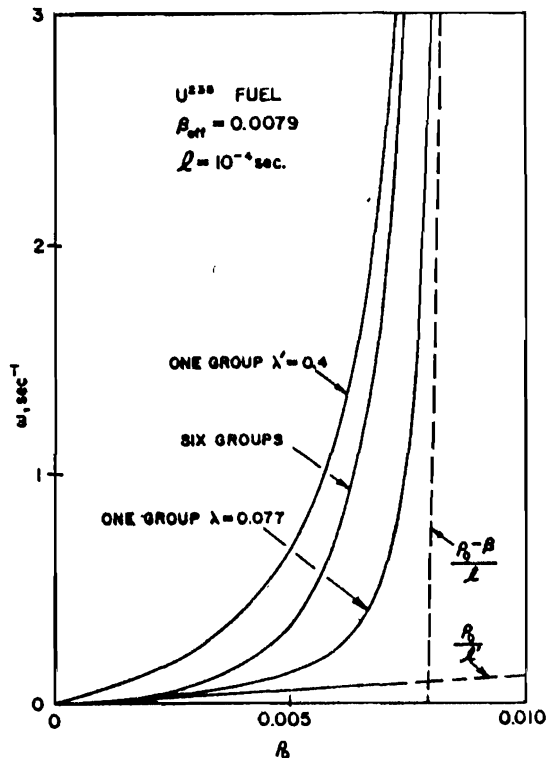


Fig. 2-5. Comparison of one- and six-group calculations for the positive branch of the inhour curve.

the  $\omega_i$  of smallest magnitude will eventually dominate. Comparison of figs. 2-1 and 2-4 shows that the one-group model predicts an asymptotic decay that is much too rapid. A better result might be predicted in some cases by using  $\lambda_1$  instead of  $\lambda$ , but the error for small reactivity would then be very great.

One way to improve the situation for negative reactivity without greatly increasing the mathematical complexity would be to use a two-group model, with one group defined as the first group (longest-lived group) of the complete set of six, and the other group being a suitable average of the remaining five. The inhour equation would then be a cubic in  $\omega$ .

Skinner and Cohen (1959) studied other few-group representations. For a two-group model they selected one which matched simultaneously the four quantities  $\Sigma_i \beta_i$ ,  $\Sigma_i (\beta_i / \lambda_i)$ ,  $\Sigma_i \beta_i \lambda_i$ , and  $\Sigma_i (\beta_i / \lambda_i^2)$ . Matching the first three of these quantities guarantees conformity with the six-group inhour equation, both for small  $\omega$  and for the neighborhood of prompt

### 30 Constant Reactivity and Reactivity Steps

critical. The fourth quantity arises in the frequency response (see chapter 3); matching  $\sum_i(\beta_i/\lambda_i^2)$  guarantees that the phase of the frequency response, as well as its amplitude, is the same for both two- and six-group models at zero frequency. The four conditions are sufficient to determine the two effective decay constants and yields. Numerical values for this two-group model for thermal fission in  $U^{235}$  are reproduced in table 2-2.

Table 2-2. Few Group Representations for Thermal Fission in  $U^{235}$

<i>m</i>	<i>i</i>	$\lambda_i (\text{sec}^{-1})$	$\beta_i/\beta$
1	1	0.0767	1.000
	2	0.0252	0.297
3	1	0.566	0.703
	2	0.0124	0.033
	3	0.0369	0.346
		0.632	0.621

SOURCE: Skinner and Cohen 1959.

This two-group model is still unsatisfactory for large negative reactivities. This is improved by using a three-group model of Skinner and Cohen (1959), which identifies one group with the longest-lived group of the complete set of six. The other two effective groups are defined by matching the four quantities cited above, so that this model has all the features of their two-group model and, in addition, represents fairly well the asymptotic shutdown behavior.

This three-group model, as applied to thermal fission in  $U^{235}$ , is also presented in table 2-2. Other models are tabulated by Skinner and Cohen (1959). These two- and three-group models have been widely used in practice for yielding reasonable accuracy over a wide range under conditions of limited computer capacity or running time.

#### 2-4. Step-Input Response

Before solving for the response  $n(t)$ , we note that a reactivity step implies a jump in  $dn/dt$ . This may be seen as follows: Assume for the moment that  $n(t)$  and  $c_i(t)$  are continuous functions of time. Then  $dc_i/dt$  is continuous by eq. (2-2). If  $q$  also happens to be continuous, then, from eq. (2-3) for a jump in  $\rho$  at  $t = 0$ ,

$$\frac{dn}{dt} \Big|_{t=+0} - \frac{dn}{dt} \Big|_{t=-0} = [\rho(+0) - \rho(-0)] \frac{n(0)}{\epsilon}. \quad (2-32)$$

This formula does not hold in the presence of artificial discontinuities in

$n$ ,  $c_i$ , or  $q$ , which are used later in special approximations, but it will be useful in this section.

We consider now the special case of a source-free equilibrium followed by a step input of reactivity at  $t = 0$ . Hence  $q = 0$  for all  $t$ ,  $\rho = 0$  for  $t < 0$ , and  $\rho = \rho_0$  for  $t \geq 0$ . Let  $n = n_0$  for  $t \leq 0$ , whence by eq. (2-7)

$$c_i(t) = \frac{\beta_i n_0}{\lambda_i}, \quad t \leq 0.$$

By eq. (2-13) the Laplace transform of  $n(t)$  is

$$N(s) = n_0 \frac{\ell + \sum_i \frac{\beta_i}{s + \lambda_i}}{\ell s + \beta - \rho_0 - \sum_i \frac{\beta_i \lambda_i}{s + \lambda_i}}. \quad (2-33)$$

Rewrite eq. (2-33) as the ratio of two polynomials

$$\frac{N(s)}{n_0} = \frac{P(s)}{D(s)}, \quad (2-34)$$

where

$$P(s) = \left( \ell + \sum_i \frac{\beta_i}{s + \lambda_i} \right) \prod_i (s + \lambda_i), \quad (2-35)$$

$$D(s) = \left( \ell s + \beta - \rho_0 - \sum_i \frac{\beta_i \lambda_i}{s + \lambda_i} \right) \prod_i (s + \lambda_i), \quad (2-36)$$

and where the product  $\prod_i$  extends from  $i = 1$  to  $m$ . The function  $N(s)$  is analytic except at  $m + 1$  simple poles  $s = \omega_j$  (the  $m + 1$  distinct real roots of the inhour equation). There are no poles at  $s = -\lambda_i$  since the right-hand side of eq. (2-33) has a finite limit.

The degree of  $D(s)$  is one higher than the degree of  $P(s)$ ; hence the inverse transform is simply the sum of the residues of  $N(s)e^{st}$  at the poles  $s = \omega_j$ . Write eq. (2-36) as

$$D(s) = (s - \omega_1)(s - \omega_2) \dots (s - \omega_{m+1}).$$

The residues each have the form

$$n_0 \lim_{s \rightarrow \omega_j} (s - \omega_j) \frac{P(s)}{D(s)} e^{st}.$$

To evaluate the limit we need

$$\lim_{s \rightarrow \omega_j} \frac{s - \omega_j}{D(s)} = \lim_{s \rightarrow \omega_j} \frac{1}{D'(s)}$$

## 32 Constant Reactivity and Reactivity Steps

where the derivative  $D'(s)$  may be written

$$\begin{aligned} D'(s) &= (s - \omega_2)(s - \omega_3) \dots (s - \omega_{m+1}) \\ &\quad + (s - \omega_1)(s - \omega_3) \dots (s - \omega_{m+1}) \\ &\quad + \dots + (s - \omega_1)(s - \omega_2) \dots (s - \omega_m). \end{aligned}$$

All terms in  $D'(\omega_j)$  vanish except one which does not contain the factor  $s - \omega_j$ ; therefore the limit exists and is simply

$$\lim_{s \rightarrow \omega_j} \frac{s - \omega_j}{D(s)} = \frac{1}{D'(\omega_j)}.$$

The inverse transform is

$$n(t) = n_0 \sum_{j=1}^{m+1} \frac{P(\omega_j)}{D'(\omega_j)} e^{\omega_j t}. \quad (2-37)$$

From eq. (2-36),

$$D'(s) = \left[ \ell + \sum_i \frac{\beta_i \lambda_i}{(s + \lambda_i)^2} \right] \prod_i (s + \lambda_i) + \dots,$$

where the dots indicate terms which vanish at  $s = \omega_j$  because of the inhour equation. Hence

$$D'(\omega_j) = \left[ \ell + \sum_i \frac{\beta_i \lambda_i}{(\omega_j + \lambda_i)^2} \right] \prod_i (\omega_j + \lambda_i).$$

When eq. (2-35) is used to evaluate  $P(\omega_j)$ , eq. (2-37) becomes

$$n(t) = n_0 \sum_{j=1}^{m+1} \frac{\ell + \sum_i \frac{\beta_i}{\omega_j + \lambda_i}}{\ell + \sum_i \frac{\beta_i \lambda_i}{(\omega_j + \lambda_i)^2}} e^{\omega_j t}. \quad (2-38)$$

By eq. (2-16) this may also be written

$$n(t) = n_0 \rho_0 \sum_{j=1}^{m+1} \frac{e^{\omega_j t}}{\omega_j \left[ \ell + \sum_i \frac{\beta_i \lambda_i}{(\omega_j + \lambda_i)^2} \right]}. \quad (2-39)$$

Eq. (2-39) is a convenient representation for the step-input response. Note that, for positive  $\rho_0$ , each coefficient  $A_j$  has the same sign as its corresponding  $\omega_j$ . Also, for negative  $\rho_0$ , the  $\omega_j$  are all negative and the  $A_j$  all positive.

Sample calculations of the response to positive reactivity steps starting from equilibrium are shown in fig. 2-6. Note that a single rising exponential eventually dominates, producing a straight line in the semilog graph. Here the reactivity is expressed in cents, one cent having the meaning  $\rho_0/\beta = 0.01$  (see sec. 2-2). Graphs of the coefficients in eq. (2-38) as functions of  $\omega_j$  in the limit  $\ell \rightarrow 0$  are given by Soodak (1962); these are useful whenever the reactivity is small enough that the periods are independent of the neutron generation time. Other graphs are given by Schultz (1961).

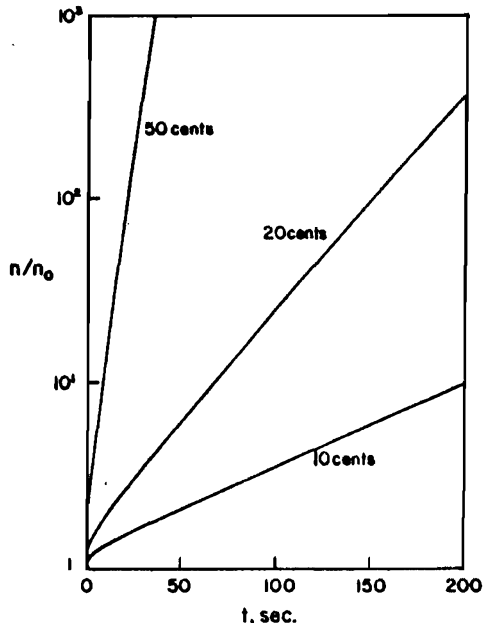


Fig. 2-6. Relative neutron density  $n/n_0$  as a function of time for a step input of reactivity  
 $\{$   
 $(U^{233} \text{ thermal reactor}, \ell = 10^{-4} \text{ sec}, \beta_{\text{eff}} = 0.0079)$

For one group of delayed neutrons, eq. (2-39) reduces to

$$n(t) = n_0 \rho_0 \left\{ \frac{e^{\omega_1 t}}{\omega_1 \left[ \ell + \frac{\beta \lambda}{(\omega_1 + \lambda)^2} \right]} + \frac{e^{\omega_2 t}}{\omega_2 \left[ \ell + \frac{\beta \lambda}{(\omega_2 + \lambda)^2} \right]} \right\}. \quad (2-40)$$

With the aid of eq. (2-28) this may be rewritten as

$$n(t) = \frac{n_0}{\omega_1 - \omega_2} \left[ \left( \frac{\rho_0}{\ell} - \omega_2 \right) e^{\omega_1 t} + \left( \omega_1 - \frac{\rho_0}{\ell} \right) e^{\omega_2 t} \right]. \quad (2-41)$$

### 34 Constant Reactivity and Reactivity Steps

Eq. (2-41) may also be obtained directly from the two equations

$$\frac{dn}{dt} = \frac{\rho - \beta}{\ell} n + \lambda c \quad (2-42)$$

and

$$\frac{dc}{dt} = \frac{\beta}{\ell} n - \lambda c \quad (2-43)$$

using the conditions of equilibrium at  $n = n_0$  for  $t < 0$ , followed by a step input at  $t = 0$ . The demonstration of the equivalence of eqs. (2-40) and (2-41) is left as a problem.

Eq. (2-41) is easily interpreted. For  $\rho_0$  positive,  $\omega_1 > 0$  and  $\omega_2 < 0$ . Hence the coefficient of the rising term  $e^{\omega_1 t}$  is positive, as expected. Further, as seen from fig. 2-4, when  $\rho_0 > 0$ ,

$$\frac{\rho_0 - \beta}{\ell} < \omega_1 < \frac{\rho_0}{\ell},$$

and so the coefficient of the decaying exponential is negative. A sketch of  $n(t)$  and the two exponentials which comprise it is shown in fig. 2-7.

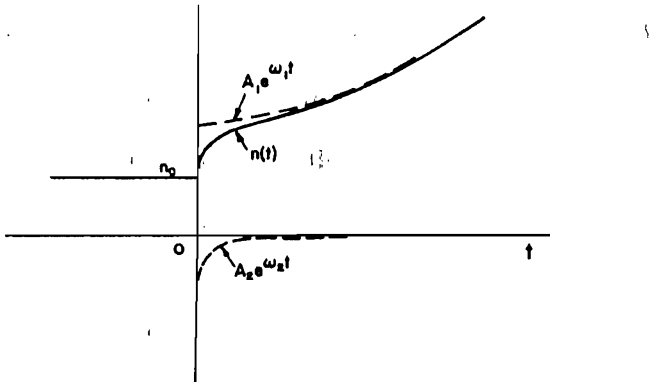


Fig. 2-7. Neutron density as a function of time for a step input of reactivity (one group of delayed neutrons). The dashed lines are the individual terms of eq. (2-41).

The rapid initial rise, called the "prompt jump," is due to the fact that the delayed neutrons depend on the past history of  $n(t)$ . For a short time, delayed neutrons are still being produced at a rate determined essentially by  $n_0$ , and this rate is initially sufficient to sustain a rapid rise in  $n(t)$ . The initial slope is  $\rho_0 n_0 / \ell$ , as seen from eq. (2-32), just as though all neutrons were prompt. But when  $n(t)$  has risen appreciably, the delayed neutron production cannot keep pace. The chain reaction adjusts itself until both  $n(t)$  and  $c(t)$  are rising with the same exponential

time dependence, and the rate is slower (the asymptotic period is larger) than it would be if all neutrons were prompt.

For large reactivity this effect, while still present, is not so marked. As seen from fig. 2-4,  $\omega_1$  increases rapidly with  $\rho_0$ , and  $|\omega_2|$  decreases. Hence the second term decays slowly relative to the rate of rise, and the breaks in the curves of  $n(t)$  would be much less pronounced than indicated in fig. 2-7.

For a negative reactivity step,

$$\omega_2 < \frac{\rho_0}{\ell} < \omega_1 < 0,$$

and both coefficients in eq. (2-41) are positive. The solution consists of two superposed decaying exponentials, with  $e^{\omega_2 t}$  always a more rapid decay (the "prompt drop").

We consider next some limiting cases. For one group of delayed neutrons, the inhour equation is a quadratic in  $\omega$ , eq. (2-29). The sum of the roots is

$$\omega_1 + \omega_2 = -\frac{\beta - \rho_0 + \lambda\ell}{\ell}.$$

For  $\rho_0$  not too near  $\beta$ ,  $\lambda\ell \ll \beta - \rho_0$ . For  $\rho_0$  sufficiently small,  $\omega_1 \ll |\omega_2|$ , and

$$\omega_2 \cong -\frac{\beta - \rho_0}{\ell}. \quad (2-44)$$

This is of course just the asymptote of figs. 2-1 and 2-4.

From eq. (2-29) the product of the roots is

$$\omega_1 \omega_2 = -\frac{\lambda\rho_0}{\ell},$$

hence from eq. (2-44)

$$\omega_1 \cong \frac{\lambda\rho_0}{\beta - \rho_0}. \quad (2-45)$$

This could also have been obtained from eq. (2-28) with  $\ell \rightarrow 0$ . To the same approximation,

$$\omega_1 - \omega_2 \cong \frac{\beta - \rho_0}{\ell},$$

$$\frac{\rho_0}{\ell} - \omega_2 \cong \frac{\beta}{\ell},$$

$$\omega_1 - \frac{\rho_0}{\ell} \cong -\frac{\rho_0}{\ell},$$

and eq. (2-41) becomes

$$n(t) \cong \frac{n_0}{\beta - \rho_0} \left[ \beta \exp \left( \frac{\lambda \rho_0}{\beta - \rho_0} t \right) - \rho_0 \exp \left( -\frac{\beta - \rho_0}{\ell} t \right) \right]. \quad (2-46)$$

Eq. (2-46) is a useful approximation for small  $\rho_0$ , and it readily displays two important properties:

1. The "prompt jump" in  $n/n_0$  (or "prompt drop" if  $\rho_0 < 0$ ) is approximately from one to  $\beta/(\beta + \rho_0)$ .
2. The duration of the rapidly decaying transient is of the order of  $\ell/(\beta - \rho_0)$  sec.

Eq. (2-46) also serves to suggest the form of the step response in the "prompt-jump approximation" ( $\ell \rightarrow 0$ ), mentioned earlier in connection with eq. (2-23). When

$$\frac{\beta - \rho_0}{\ell} t \gg 1,$$

eq. (2-46) becomes

$$n(t) \cong n_0 \frac{\beta}{\beta - \rho_0} \exp \left( \frac{\lambda \rho_0}{\beta - \rho_0} t \right), \quad (2-47)$$

which is later shown to be the one-delay-group step response in the prompt-jump approximation. It implies that  $n(t)$  may be approximately described as a function having discontinuities in response to step changes in reactivity (see fig. 2-8). This approximation is discussed in detail in chapter 3.

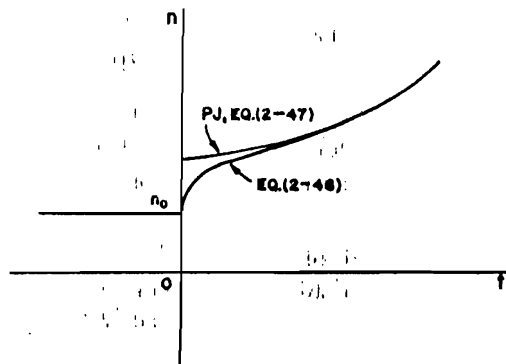


Fig. 2-8. Response to reactivity step: comparison of prompt-jump approximation (PJ) with approximate one-delay-group calculation ( $0 < \rho_0 < \beta$ ).

For large reactivity steps such that  $\omega_1 \gg |\omega_2|$ , a process similar to that used in obtaining eq. (2-46) yields

$$n(t) \cong \frac{n_0}{\rho_0 - \beta} \left[ \rho_0 \exp \left( \frac{\rho_0 - \beta}{\ell} t \right) - \beta \exp \left( -\frac{\lambda \rho_0}{\rho_0 - \beta} t \right) \right]. \quad (2-48)$$

Note that eq. (2-48) is merely eq. (2-46) rearranged. For times sufficiently short that  $\lambda t \ll 1$ , this becomes

$$n(t) \cong \frac{n_0}{\rho_0 - \beta} \left[ \rho_0 \exp \left( \frac{\rho_0 - \beta}{\ell} t \right) - \beta \right]. \quad (2-49)$$

It is interesting to note that eq. (2-49) satisfies eq. (2-42) with  $\lambda c(t)$  replaced by its initial equilibrium value  $\beta n_0 / \ell$ , as might be expected if  $t \ll 1/\lambda$ . This means that eq. (2-49) is valid for any size step  $\rho_0$ , provided  $0 < t \ll 1/\lambda$ , and its behavior for small reactivity is more easily seen if it is rewritten as

$$n(t) \cong \frac{n_0}{\beta - \rho_0} \left[ \beta - \rho_0 \exp \left( -\frac{\beta - \rho_0}{\ell} t \right) \right]. \quad (2-50)$$

This equation describes the initial prompt-jump portion for small reactivity with a curve that levels off at  $n/n_0 = \beta/(\beta - \rho_0)$ ; see fig. 2-9.

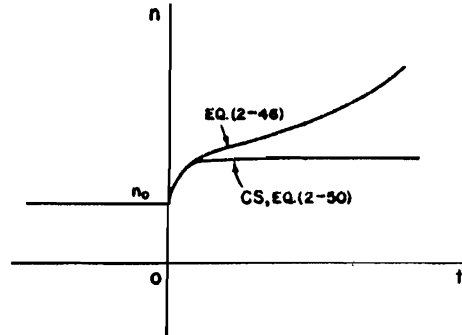


Fig. 2-9. Response to reactivity step: comparison of constant-source approximation (CS) with approximate one-delay-group calculation ( $0 < \rho_0 < \beta$ ).

Since this limiting case of the step response may be derived by setting the source of delayed neutrons  $\lambda c(t)$  equal to a constant, the approximation is often called the "constant source approximation." For step changes in reactivity, its use is restricted to small time intervals. In chapter 3 we discuss this approximation in connection with large rates of reactivity change; its use in such cases has led to the name "rapid-rate approximation" (Soodak 1962).

## 38 Constant Reactivity and Reactivity Steps

Finally, we note the possibility of solving for  $n(t)$  in the presence of a number of successive step changes in reactivity. The essential feature is the step change in  $dn/dt$  that accompanies each reactivity step; see eq. (2-32). One of the problems at the end of this chapter illustrates the response to a step input of reactivity followed by subsequent step changes of varying amounts. Other problems consider the "dragon" (a fast assembly that is made superprompt critical for a very short time) and a periodically pulsed fast reactor (repetitive dragon) of the type described by Bondarenko and Stavisskii (1961), by Larrimore (1967), and by Blaesser and Larrimore (1969).

### 2-5. Time-dependent Sources

Before leaving the subject of linear differential equations with constant coefficients, it is appropriate to consider some simple problems involving time-dependent neutron sources. The simplest of these is the impulse response (or Green's function), which may be used for representing the response to an arbitrary time-dependent source. In this section we derive the point-reactor response for an arbitrary source and use it to discuss the impulse response and the response to a step change in a steady source. In the following section we develop the concept of frequency response and consider the steady-state response to an oscillating source.

To derive the response to a source, retain  $q(t)$  in eqs. (2-1) and (2-2) and introduce the additional Laplace transform

$$Q(s) = \int_0^\infty q(t)e^{-st} dt.$$

As in sec. 2-2, set  $\rho = \rho_0$ , and solve the transformed equations for  $N(s)$ , the Laplace transform of  $n(t)$ . The result is

$$N(s) = \frac{\ell \left[ n(0) + \sum_i \frac{\lambda_i c_i(0)}{s + \lambda_i} + Q(s) \right]}{\ell s + \beta - \rho_0 - \sum_i \frac{\beta_i \lambda_i}{s + \lambda_i}}. \quad (2-51)$$

This is just eq. (2-13) with a term  $\ell Q(s)$  added to the numerator, as expected from the fact that eq. (2-13) represents the solution of the homogeneous (source-free) system.

Here we choose the viewpoint that  $\rho_0$  is some constant reactivity and  $q(t)$  is a source inserted at  $t = 0$ . The solution of the homogeneous system with arbitrary  $n(0)$  and  $c_i(0)$  may be carried through by the procedure of sec. 2-4; therefore, we restrict the discussion to the

inhomogeneous part

$$N_i(s) = I(s)Q(s), \quad (2-52)$$

where

$$I(s) = \frac{\ell}{\ell s + \beta - \rho_0 - \sum_i \frac{\beta_i \lambda_i}{s + \lambda_i}}. \quad (2-53)$$

Note that the inhour equation may be written

$$\frac{1}{I(\omega_j)} = 0. \quad (2-54)$$

The inverse transform of eq. (2-52) is

$$n_i(t) = \int_0^t i(t-t')q(t') dt', \quad (2-55)$$

where  $i(t)$  is the inverse transform of  $I(s)$ . To interpret  $i(t)$ , consider a source

$$q(t) = Q_0 \delta(t), \quad (2-56)$$

where  $\delta(t)$  is the impulse function (Dirac delta function). Eq. (2-56) is an idealized representation of a very short pulse of  $Q_0$  neutrons injected into the reactor by a pulsed neutron generator. Since the transform of the impulse source is  $Q_0$ , eqs. (2-52) and (2-55) become respectively

$$N_i(s) = Q_0 I(s) \quad (2-57)$$

and

$$n_i(t) = Q_0 i(t), \quad (2-58)$$

and we interpret  $i(t)$ , the impulse response, as the reactor response to the injection of one neutron at  $t = 0$  provided  $n(0) = c_i(0) = 0$ . Eq. (2-55) shows how the response to any arbitrary source may be expressed in terms of  $i(t)$ .

For a critical reactor, eq. (2-53) becomes

$$I(s) = \frac{\ell}{\ell s + \beta - \sum_i \frac{\beta_i \lambda_i}{s + \lambda_i}}. \quad (2-59)$$

The impulse response of a critical reactor is therefore

$$i(t) = \sum_{j=1}^{m+1} B_j e^{\omega_j t} = \ell \sum_{j=1}^{m+1} \frac{e^{\omega_j t}}{\ell + \sum_i \frac{\beta_i \lambda_i}{(\omega_j + \lambda_i)^2}}, \quad (2-60)$$

#### 4.0 Constant Reactivity and Reactivity Steps

where the  $B_j$  are determined from the residues of the inversion integral at  $s = \omega_j$  (in this case, the roots of the inhour equation for  $\rho_0 = 0$ ). By the initial-value theorem

$$\lim_{s \rightarrow \infty} sI(s) = \lim_{t \rightarrow 0} i(t)$$

it is quickly seen that  $i(0) = 1$ . Since  $\omega_1 = 0$  for a critical reactor, the first term in eq. (2-60) represents the asymptotic value

$$\lim_{t \rightarrow \infty} i(t) = \frac{\ell}{\ell + \sum_i \beta_i / \lambda_i}. \quad (2-61)$$

This may be verified by rewriting eq. (2-59) as

$$I(s) = \frac{\ell}{\ell s + \sum_i \frac{\beta_i s}{s + \lambda_i}} \quad (2-62)$$

and using the final-value theorem

$$\lim_{s \rightarrow 0} sI(s) = \lim_{t \rightarrow \infty} i(t).$$

For one group of delayed neutrons, the roots are  $\omega_1 = 0$ ,  $\omega_2 = -(\lambda + \beta/\ell)$ . Eq. (2-60) reduces to

$$i(t) = \frac{1}{\beta + \lambda\ell} [\lambda\ell + \beta e^{-(\lambda + \beta/\ell)t}]. \quad (2-63)$$

The characteristic roots  $\omega_j$  and the coefficients  $B_j$  for the impulse response of a thermal reactor ( $\ell = 10^{-4}$  sec,  $\beta_{eff} = 0.0079$ ) are listed in table 2-3 for both the one-group and six-group cases. The resulting two curves are compared in fig. 2-10, using the one-group constant  $\lambda = 0.0767$  sec $^{-1}$ . Note that the one-group response approaches the final steady-state value 0.00097 much more rapidly than the more realistic six-group curve; in fact the six-group response is 0.00153 at  $t = 10$  sec and 0.00099 at  $t = 100$ . This illustrates one of the major limitations of a one-group representation. (The use of another one-group model with the mean decay constant  $\lambda' = 0.405$  sec $^{-1}$  is discussed in the problem set.)

Note how the smallness of the neutron generation time produces an extremely rapid decay, followed by the slowly decreasing "delayed-neutron tail." This effect is extremely pronounced for a fast reactor. Since the prompt decay is easily separated from the delayed-neutron tail, the possibility of using this effect in experiments is readily apparent.

From sec. 2-2, the largest negative root is very nearly  $-\beta/\ell$ . One uses a pulsed source capable of injecting a sufficient number of neutrons in a

Table 2-3. Characteristic Roots and Coefficients in Impulse Response  
for a Critical Thermal Reactor ( $\ell = 10^{-4}$  sec,  $\beta_{\text{eff}} = 0.0079$ )

$m$	$j$	$\omega_j$	$B_j$
1	1	0	0.000 970
	2	-79.077	0.999 030
6	1	0	0.000 970
	2	-0.01433	0.000 091
	3	-0.0682	0.000 664
	4	-0.1947	0.000 901
	5	-1.023	0.001 282
	6	-2.896	0.001 292
	7	-79.4	0.994 8

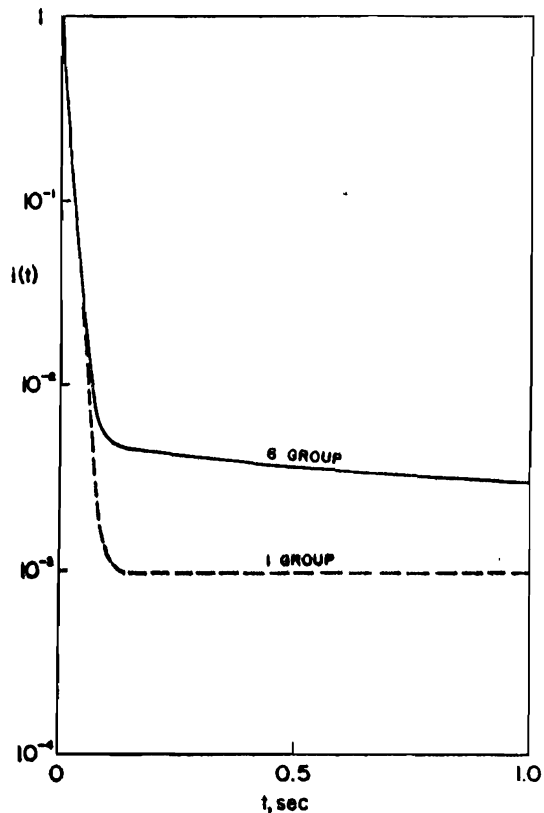


Fig. 2-10. Typical impulse response for a critical reactor ( $U^{235}$  thermal reactor,  $\ell = 10^{-4}$  sec,  $\beta_{\text{eff}} = 0.0079$ ).

## 1.2 Constant Reactivity and Reactivity Steps

time short compared to  $\ell/\beta$ . The exponential decay as observed by a fast detector system is readily analyzed to yield a value for  $\beta/\ell$ .

Further, if one retains  $\rho_0$  in eq. (2-53), the impulse response for a subcritical reactor is easily obtained in the same form as eq. (2-60). By sec. 2-2, the largest negative root is approximately  $(\rho_0 - \beta)/\ell$ . Comparison of the prompt decay in the critical and subcritical cases yields a measure of the shutdown reactivity  $\rho_0$ . This is the essential idea behind the well-known method of pulsed-neutron reactivity measurements, which is discussed in more detail in chapter 8 (Sjostrand 1956; Gozani 1962; Garels and Russell 1963; Becker and Quisenberry 1966).

We note also the possibility of pulsing a supercritical reactor, augmenting by neutron multiplication the pulse from a neutron generator. This system (called a "booster") is an effective high-yield pulsed-neutron source (Poole and Wiblin 1958; Beyster and Russell 1965; Larrimore 1967). The booster is discussed further in the problems at the end of the chapter.

The response of the reactor to a sudden insertion of a steady neutron source is easily derived from eq. (2-55). If it is assumed that  $q = 0$  for  $t < 0$  and  $q = q_0$  for  $t > 0$ ,

$$n_i(t) = q_0 \int_0^t i(t-t') dt' = q_0 \int_0^t i(t') dt'. \quad (2-64)$$

For a critical reactor, eq. (2-60) yields

$$n_i(t) = q_0 \left\{ \frac{\ell t}{\ell + \sum_i \beta_i/\lambda_i} + \ell \sum_{j=2}^{m+1} \frac{e^{\omega_j t} - 1}{\omega_j \left[ \ell + \sum_i \frac{\beta_i \lambda_i}{(\omega_j + \lambda_i)^2} \right]} \right\}. \quad (2-65)$$

Since the  $\omega_j$  appearing in eq. (2-65) are all negative, the response is a linear function, plus a sum of terms of which each is initially zero and eventually builds up to a saturation value. This is illustrated more clearly by the one-delay-group case, for which eq. (2-65) becomes

$$n_i(t) = \frac{\ell q_0}{\beta + \lambda \ell} \left\{ \lambda t + \frac{\beta}{\beta + \lambda \ell} [1 - e^{-(\lambda + \beta/\ell)t}] \right\}. \quad (2-66)$$

If the reactor is initially at equilibrium with  $n = n_0$ , the solution is the superposition of  $n_0$  and  $n_i(t)$ . A sketch is shown in fig. 2-11. Note that the final asymptotic rate of rise is greatly reduced from the value  $q_0$  that would obtain in the absence of delayed neutrons.

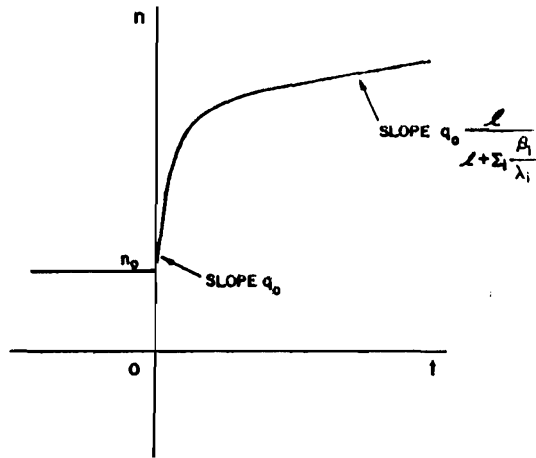


Fig. 2-11. Qualitative sketch of neutron density as a function of time for a sudden insertion of a steady neutron source at  $t = 0$ .

As a final example of step changes in neutron source strength, consider a reactor that is subcritical ( $\rho = \rho_0 < 0$ ) in equilibrium ( $n = n_0$ ) with a fairly strong steady source  $q_0$ . The rate of production of delayed neutrons is

$$\sum_i \lambda_i c_{i0} = \beta n_0 / \ell.$$

If the source is suddenly removed, the delayed-neutron production rate remains near its equilibrium value for a short time (constant-source approximation), and the neutron density may be described by

$$\frac{dn}{dt} = \frac{\rho_0 - \beta}{\ell} n + \frac{\beta}{\ell} n_0, \quad (2-67)$$

where we assume that the source itself has negligible absorption so that the reactivity remains at the value  $\rho_0$ . The neutron density undergoes a “prompt drop” in a time of the order of  $\ell / (\beta - \rho_0)$  to a quasistatic level  $n_1$ , given by

$$0 = \frac{\rho_0 - \beta}{\ell} n_1 + \frac{\beta}{\ell} n_0. \quad (2-68)$$

Therefore

$$\rho_0 = -\beta \frac{n_0 - n_1}{n_1}. \quad (2-69)$$

---

#### 4.4 Constant Reactivity and Reactivity Steps

The neutron density is sketched in fig. 2-12, showing the prompt drop to the level  $n_1$  at the beginning of the delayed-neutron tail. This is the essence of the "source-jerk" method for determining subcritical reactivity by observing  $n_0$  and  $n_1$ . (Exactly the same equations may be used to describe a "rod-drop" experiment in which a reactor, initially critical with a negligible source, is suddenly made subcritical by a step reactivity change from  $\rho = 0$  to  $\rho = \rho_0$ .)

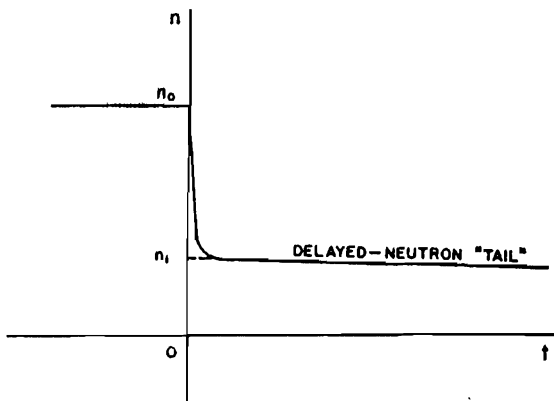


Fig. 2-12. Qualitative sketch of neutron density as a function of time illustrating either a "source-jerk" or "rod-drop" measurement of reactivity.

#### 2-6. Frequency Response and Transfer Functions

Consider a subcritical reactor ( $\rho = \rho_0$ ) in equilibrium with a steady source  $q_0$ . By eq. (2-6), the neutron level is

$$n_0 = -\frac{\ell q_0}{\rho_0} \quad (2-70)$$

If a sinusoidal fluctuation in source strength is introduced such that  $q_0$  is the time-average source, and if  $\rho_0$  remains constant, then  $n(t)$  will fluctuate about its time average  $n_0$ . This is true for the oscillating source because the system of differential equations is linear with constant coefficients, and the principle of superposition may be applied. (We consider oscillating reactivity in chapter 3.)

The response to the oscillating source could be computed by substituting the source into eq. (2-55) and integrating. Instead, we note from eq. (2-52) that the Laplace transforms of the source and of the inhomogeneous part of the solution have a simple relationship. This suggests a source-to-response relation, which may be generalized in terms of an input and an output related by a transfer function.

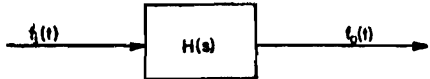


Fig. 2-13. Block diagram for a system whose transfer function is  $H(s)$ .

Fig. 2-13 shows a block diagram, where  $f_i(t)$  represents the input (stimulus) and  $f_o(t)$  represents the output (response). The "black box" labeled  $H(s)$  represents the system that is "acted on" by the input function. We define the transfer function as the ratio of Laplace transforms of output and input:

$$H(s) = \frac{F_o(s)}{F_i(s)} \quad (2-71)$$

with the system initially at rest. Eq. (2-71) may be regarded as a basic property of linear systems, and  $f_o(t)$  is the particular solution of the inhomogeneous linear equation such that  $f_o$  and its derivatives vanish at  $t = 0$ .

Next we postulate a sinusoidal input of angular frequency  $\omega_0$ :

$$f_i(t) = \sin \omega_0 t \quad (2-72)$$

for  $t > 0$  and  $f_i(t) = 0$  for  $t < 0$ . The Laplace transform of the input is

$$F_i(s) = \frac{\omega_0}{s^2 + \omega_0^2}. \quad (2-73)$$

From eq. (2-71) the Laplace transform of the output is

$$F_o(s) = \frac{\omega_0}{s^2 + \omega_0^2} H(s). \quad (2-74)$$

The objective is to compute the inverse transform  $f_o(t)$ , which contains the frequency response, and to identify the role of the function  $H(s)$  together with any conditions on  $H(s)$  that may be needed to carry out the computation.

The inverse transform is

$$f_o(t) = \frac{1}{2\pi j} \int_C \frac{\omega_0}{s^2 + \omega_0^2} H(s) e^{st} ds, \quad (2-75)$$

where the contour of integration in the complex  $s$ -plane is to the right of all singularities of the integrand. Assume that the singularities of  $H(s)$  are in the left half-plane, so that their contributions to  $f_o(t)$  are decaying transients. (For example, if all the singularities are poles in the left half-plane, then each term arising from them contains the time factor  $e^{-pt}$ , where  $p$  is real and positive.) We lump the transients together as a term  $T(t)$  in the output.

### (b) Constant Reactivity and Reactivity Steps

The rest of  $f_o(t)$  will be simply the sum of the residues at the two poles at  $s = \pm j\omega_0$ :

$$\begin{aligned}\Sigma(\text{residues}) &= \lim_{s \rightarrow j\omega_0} \left[ \frac{(s - j\omega_0)\omega_0}{s^2 + \omega_0^2} H(s)e^{st} \right] \\ &\quad + \lim_{s \rightarrow -j\omega_0} \left[ \frac{(s + j\omega_0)\omega_0}{s^2 + \omega_0^2} H(s)e^{st} \right].\end{aligned}$$

Since the singularities of  $H(s)$  are assumed to be away from the imaginary axis, this becomes

$$\begin{aligned}\left. \frac{\omega_0}{s + j\omega_0} H(s)e^{st} \right|_{s=j\omega_0} + \left. \frac{\omega_0}{s - j\omega_0} H(s)e^{st} \right|_{s=-j\omega_0} \\ = \frac{\omega_0}{2j\omega_0} H(j\omega_0)e^{j\omega_0 t} + \frac{\omega_0}{-2j\omega_0} H(-j\omega_0)e^{-j\omega_0 t}.\end{aligned}$$

To proceed further, assume that  $H(-j\omega_0)$  is the complex conjugate of  $H(j\omega_0)$ . The two residues may then be identified as the complex conjugates of each other, and the sum is twice the real part of either:

$$\operatorname{Re}\{-jH(j\omega_0)e^{j\omega_0 t}\} = \operatorname{Re}\{-j|H(j\omega_0)|e^{j(\omega_0 t + \theta)}\},$$

where we have written  $H(j\omega_0)$  in polar form

$$H(j\omega_0) = |H(j\omega_0)|e^{j\theta}; \quad (2-76)$$

Finally, note that

$$\operatorname{Re}\{-je^{j(\omega_0 t + \theta)}\} = \sin(\omega_0 t + \theta).$$

The complete output function is therefore

$$f_o(t) = |H(j\omega_0)| \sin(\omega_0 t + \theta) + T(t), \quad (2-77)$$

where  $T(t)$  is the sum of decaying transients.

We now compare eqs. (2-72) and (2-77) under the conditions imposed by the assumptions:

1. The singularities of  $H(s)$  are in the left half-plane.
2. The complex conjugate of  $H(j\omega_0)$  is  $H(-j\omega_0)$ .

If these conditions are satisfied, then we conclude that a pure sinusoidal input produces a sinusoidal output of the same frequency, with a relative amplitude given by the absolute value of  $H(j\omega_0)$  and a phase shift given by the phase  $\theta$  of  $H(j\omega_0)$  in eq. (2-76). Superimposed on this sinusoidal output are the so-called starting transients, represented by  $T(t)$ , which decay to negligible values in a finite time. Therefore, the frequency response (the sustained or steady-state oscillation) is completely

characterized by the magnitude and phase of  $H(j\omega_0)$ , where  $H(s)$  is the system transfer function. In fact, the term "frequency response" is usually understood to mean this magnitude and phase, rather than the sustained oscillation itself.

Note that an arbitrary periodic input can be represented as a Fourier series. If the principle of superposition applies, each harmonic component is transformed independently into a corresponding component of the output, and the frequency response can be used to construct the response to any input waveform.

The restrictions imposed by the assumptions are important. If Assumption No. 1 is not satisfied, then at least part of the function  $T(t)$  represents a diverging response that eventually dominates. Assumption No. 1 corresponds to the requirement that the system represented by  $H(s)$  be stable, as defined and discussed in chapter 6. If the singularities are poles, and if any are in the right half-plane, then the response will be dominated by a growing exponential; the time constant will be determined by the coordinate of the pole (or by the real part of the coordinates for a pair of poles) that is furthest to the right in the  $s$ -plane. Note that the calculation can still proceed in this case, providing Assumption No. 2 is not violated, yielding eq. (2-77) but with  $T(t)$  containing one or more diverging terms.

Assumption No. 2 guarantees that the output  $f_o(t)$  is real. The most important special cases that we will consider will be functions  $H(s)$  expressible as a ratio of two polynomials of finite degree.

For example, consider a system represented by a linear differential equation of order  $n$  with constant coefficients:

$$A_n \frac{d^n f_o}{dt^n} + A_{n-1} \frac{d^{n-1} f_o}{dt^{n-1}} + \cdots + A_1 \frac{df_o}{dt} + A_0 f_o = f_i(t). \quad (2-78)$$

Let  $Z\left(\frac{d}{dt}\right)$  be the differential operator

$$Z\left(\frac{d}{dt}\right) = A_n \frac{d^n}{dt^n} + A_{n-1} \frac{d^{n-1}}{dt^{n-1}} + \cdots + A_1 \frac{d}{dt} + A_0. \quad (2-79)$$

Eq. (2-78) may be written symbolically as

$$Zf_o = f_i. \quad (2-80)$$

If we take the Laplace transform of eq. (2-78) and assume that all initial conditions are zero, we find

$$Z(s)F_o(s) = F_i(s), \quad (2-81)$$

and the transfer function of the system represented by eq. (2-78) is,

### 15. Constant Reactivity and Reactivity Steps

from eq. (2-71),

$$H(s) = \frac{1}{Z(s)} \quad (2-82)$$

where  $Z(s)$  is an  $n$ th degree polynomial in  $s$ . The roots of the polynomial  $Z(s)$  locate the poles of the transfer function. For this example, the black box of fig. 2-13 is recognized as a symbolic way of representing the inverse differential operator that transforms the signal  $f_i$  into  $f_o$ .

If initial conditions are retained, then eq. (2-81) is replaced by

$$Z(s)F_o(s) = F_i(s) + P(s),$$

where  $P(s)$  is a polynomial whose degree can be no higher than  $n - 1$ . The transform of the output is

$$F_o(s) = \frac{F_i(s) + P(s)}{Z(s)}. \quad (2-83)$$

If the input function  $f_i(t)$  is such that  $F_i(s)$  does not diverge for  $s \rightarrow \infty$ , then  $F_o(s)$  will behave for large  $s$  as the ratio of two polynomials, the denominator being of degree at least one higher than the numerator. Hence for large  $s$ ,  $F_o(s) \rightarrow 0$  as  $1/s^r$  where  $r \geq 1$ .

By eq. (2-83) the solution of the homogeneous equation  $Zf_o = 0$  is the inverse transform of

$$F_o(s) = \frac{P(s)}{Z(s)}$$

and it will yield the familiar linear combination of exponentials  $e^{st}$ . These arise from the poles of  $H(s)$ , which are of course the zeros of  $Z(s)$ , so that the familiar characteristic equation is just

$$Z(s) = 0. \quad (2-84)$$

The characteristic equation also applies to the transients in eq. (2-77). Since the same time functions are involved, it is possible by a suitable choice of initial conditions to construct a particular solution of the complete equation in which the transients vanish identically.

Finally, we may set  $F_i(s) = 1$  in eq. (2-71) and observe that the impulse response satisfies

$$I(s) = H(s). \quad (2-85)$$

The transfer function is therefore the Laplace transform of the impulse response. Similarly, a unit step input, for which  $F_i(s) = 1/s$ , produces a response whose Laplace transform is

$$C(s) = \frac{H(s)}{s}. \quad (2-86)$$

We complete this chapter on constant-reactivity problems by formulating the point-reactor response to an oscillating source, as described in the beginning of this section. Let

$$\begin{aligned} n &= n_0 + \delta n, \\ c_i &= c_{i0} + \delta c_i, \\ q &= q_0 + \delta q, \\ \rho &= \rho_0. \end{aligned}$$

By eqs. (2-7) and (2-70), the equilibrium conditions are

$$c_{i0} = \frac{\beta_i n_0}{\lambda_i \ell} \quad \text{and} \quad n_0 = -\frac{\ell q_0}{\rho_0}.$$

Substituting into eqs. (2-1 and 2-2) yields

$$\frac{d}{dt} \delta n = \frac{\rho_0 - \beta}{\ell} \delta n + \sum_i \lambda_i \delta c_i + \delta q; \quad (2-87)$$

$$\frac{d}{dt} \delta c_i = \frac{\beta_i}{\ell} \delta n - \lambda_i \delta c_i. \quad (2-88)$$

These equations expressing the fluctuations about average values are identical in form to the equations for the corresponding total quantities  $n$ ,  $c_i$ , and  $q$ . Proceeding as in the beginning of section 2-5, but using instead the transforms

$$\delta N(s) = \int_0^\infty \delta n(t) e^{-st} dt,$$

$$\delta \Gamma_i(s) = \int_0^\infty \delta c_i(t) e^{-st} dt,$$

and

$$\delta Q(s) = \int_0^\infty \delta q(t) e^{-st} dt,$$

one finds as in eq. (2-51)

$$\delta N(s) = \frac{\ell \left[ \delta n(0) + \sum_i \frac{\lambda_i \delta c_i(0)}{s + \lambda_i} + \delta Q(s) \right]}{\ell s + \beta - \rho_0 - \sum_i \frac{\beta_i \lambda_i}{s + \lambda_i}}. \quad (2-89)$$

The steady-state portion of the response corresponds to

$$\delta N(s) = \frac{\ell \delta Q(s)}{\ell s + \beta - \rho_0 - \sum_i \frac{\beta_i \lambda_i}{s + \lambda_i}}. \quad (2-90)$$

By comparison with eq. (2-53), the so-called source transfer function is

$$\frac{\delta N(s)}{\delta Q(s)} = I(s) = \frac{\ell}{\ell s + \beta - \rho_0 - \sum_i \frac{\beta_i \lambda_i}{s + \lambda_i}}, \quad (2-91)$$

i.e., the Laplace transform of the impulse response. The frequency response for a fluctuation  $\delta n$  in response to  $\delta q = \sin \omega t$  is therefore given by the magnitude and phase of  $I(j\omega)$ .

It is noteworthy that eq. (2-91) was derived from the basic point-reactor model without any restriction to small fluctuations. In chapter 3 we obtain the reactivity transfer function in exactly the same form, but it is valid only for small fluctuations. This is because an oscillating reactivity appears as a time-dependent coefficient instead of as a source. Physically, a real source may be oscillated mechanically such that its output varies independently of the neutron flux, whereas an oscillating absorber has an absorption rate proportional to the product of neutron flux and absorption cross-section.

Further consideration of the frequency response is deferred until chapter 3, where it is treated in much greater detail as an example of time-dependent reactivity.

### Problems

- 2-1. Verify  $N(s)$  as given by eq. (2-13).
- 2-2. Show that the two forms of the inhour equation, eqs. (2-15) and (2-16), are equivalent.
- 2-3. Show that the roots of the one-delay-group inhour equation, eq. (2-29), are always real, and that one root is always negative while the other root has the sign of  $\rho_0$ .
- 2-4. Verify from  $n(t)$ , eq. (2-38) or (2-39), that the initial derivative is  $\rho_0 n_0 / \ell$ .
- 2-5. Derive a formula for  $c_i(t)$  to accompany eq. (2-38).
- 2-6. Derive a generalization of eq. (2-38) with a constant source  $q_0$  included and with the reactor in subcritical equilibrium for  $t < 0$ .
- 2-7. Show that eqs. (2-40) and (2-41) for  $n(t)$  with one delay group are equivalent.
- 2-8. Derive eq. (2-41) directly from the differential equations for one delay group.
- 2-9. With more than one delayed-neutron group, the step-input response contains a number of slowly decaying transient terms.

This results in some time lag in establishing the asymptotic exponential period. Discuss the errors that could arise from this in calibrating control rods by measuring asymptotic periods.

- 2-10. The prompt-jump approximation corresponds to the replacement of the most rapidly decaying transient term by a jump discontinuity in  $n(t)$ . For six delay groups, the step-input response in this approximation has six terms, each with  $\ell \rightarrow 0$ . Select a value of  $\rho_0$  and verify numerically that

$$n(+0) \cong n(-0)\beta/(\beta - \rho_0).$$

- 2-11. Derive eq. (2-48) by approximating the roots of the inhour equation for large reactivity steps.  
 2-12. Derive eq. (2-49) for  $n(t)$  in the constant-source approximation by solving directly a first-order differential equation.  
 2-13. Discuss the step-input response in the constant-source approximation in the special case  $\rho_0 = \beta$ .  
 2-14. Calculate and plot  $n(t)$  for the one-delay-group model (negligible source) if

$$\rho = \begin{cases} 0 & \text{for } t < 0, \\ 0.5\beta & \text{for } 0 < t < 10 \text{ sec}, \\ \rho' & \text{for } t > 10 \text{ sec}, \end{cases}$$

for five cases:  $\rho' = 0.75\beta, 0.5\beta, 0.25\beta, 0$ , and  $-0.25\beta$ . Assume the initial condition is a steady state at  $n_0 = 1$ . Let  $\beta/\ell = 10 \text{ sec}^{-1}$  and  $\lambda = 0.1 \text{ sec}^{-1}$ .

- 2-15. A dragon is a subcritical assembly that is suddenly made superprompt critical for a very short time (e.g., one piece of fuel falling past another by gravity). Use reactivity steps to simulate the system:  $\rho = \rho_1$  for  $t < 0$  and  $t > t_0$ , and  $\rho = \rho_0$  for  $0 < t < t_0$  where  $\rho_1 < 0$  and  $\rho_0 > \beta$ . Assume initial subcritical equilibrium and use the constant-source approximation. Find  $n(t)$  for the rising ( $t < t_0$ ) and falling ( $t > t_0$ ) portions and calculate the energy in the prompt burst. Regard this energy as an impulse to find  $c(t)$  for one delay group when  $t \gg t_0$ ; then use the prompt-jump approximation to find  $n(t)$  for  $t \gg t_0$  (the delayed-neutron "tail" following the fast burst). Show that the ratio of energy in the tail to the energy in the burst is  $\beta/(\beta - \rho_1)$ .  
 2-16. A periodically pulsed fast reactor may be regarded as a repetitive dragon in which a piece of fuel or reflector material is placed on the rim of a wheel. The reactor is superprompt critical for a tiny

fraction of each cycle. The cycle is short enough that the precursors are steady, but long enough that  $n(t)$  decays to a constant  $n_{\min}$  after each burst. Using the step-input notation of prob. 2-15, except that the cycle repeats every  $t_1$  sec where  $t_0 \ll t_1 \ll 1/\lambda$ , derive the following approximate relations:

$$n_{\min} = \frac{\beta \bar{n}}{\beta - \rho_1}$$

$$\frac{\ell \bar{n}}{(\rho_0 - \beta)t_1 \bar{n}} + \frac{\beta}{\beta - \rho_1} = 1,$$

where  $\bar{n}$  is the peak power and  $\bar{n}$  is the time-average power. Discuss the optimization of a design to maximize  $\bar{n}$  and minimize  $\bar{n}$ . A typical system might have  $\rho_1 = -18\beta$ ,  $t_1 = 0.02$  sec,  $\bar{n} = 340$  megawatts, and  $\bar{n} = 1$  megawatt (Larrimore 1967).

- 2-17. Compute and plot the one-delay-group impulse response as in fig. 2-10, using  $\lambda' = 0.405$  sec $^{-1}$  in place of  $\lambda$ . Compare with the six-group curve.
- 2-18. What is the impulse response in the prompt-jump approximation? Consider the limit of  $i(t)/\ell$  as  $\ell \rightarrow 0$ .
- 2-19. Derive the impulse response for a subcritical reactor.
- 2-20. The booster is a reactor that is briefly made supercritical ( $0 < \rho_0 < \beta$ ) and pulsed by a neutron generator. The system is then quickly made subcritical (reactivity  $\rho_1 < 0$ ). Show that the ratio of energy in the tail to the energy in the burst is  $\beta/(\beta - \rho_1)$ .
- 2-21. The repetitive booster is operated as in prob. 2-20 except that the cycle is continually repeated. The cycle is short enough that the precursors are steady, but long enough so that the subcritical reactor power decays to a constant  $n_{\min}$  after each burst. Show that

$$n_{\min} = \frac{\beta \bar{n}}{\beta - \rho_1},$$

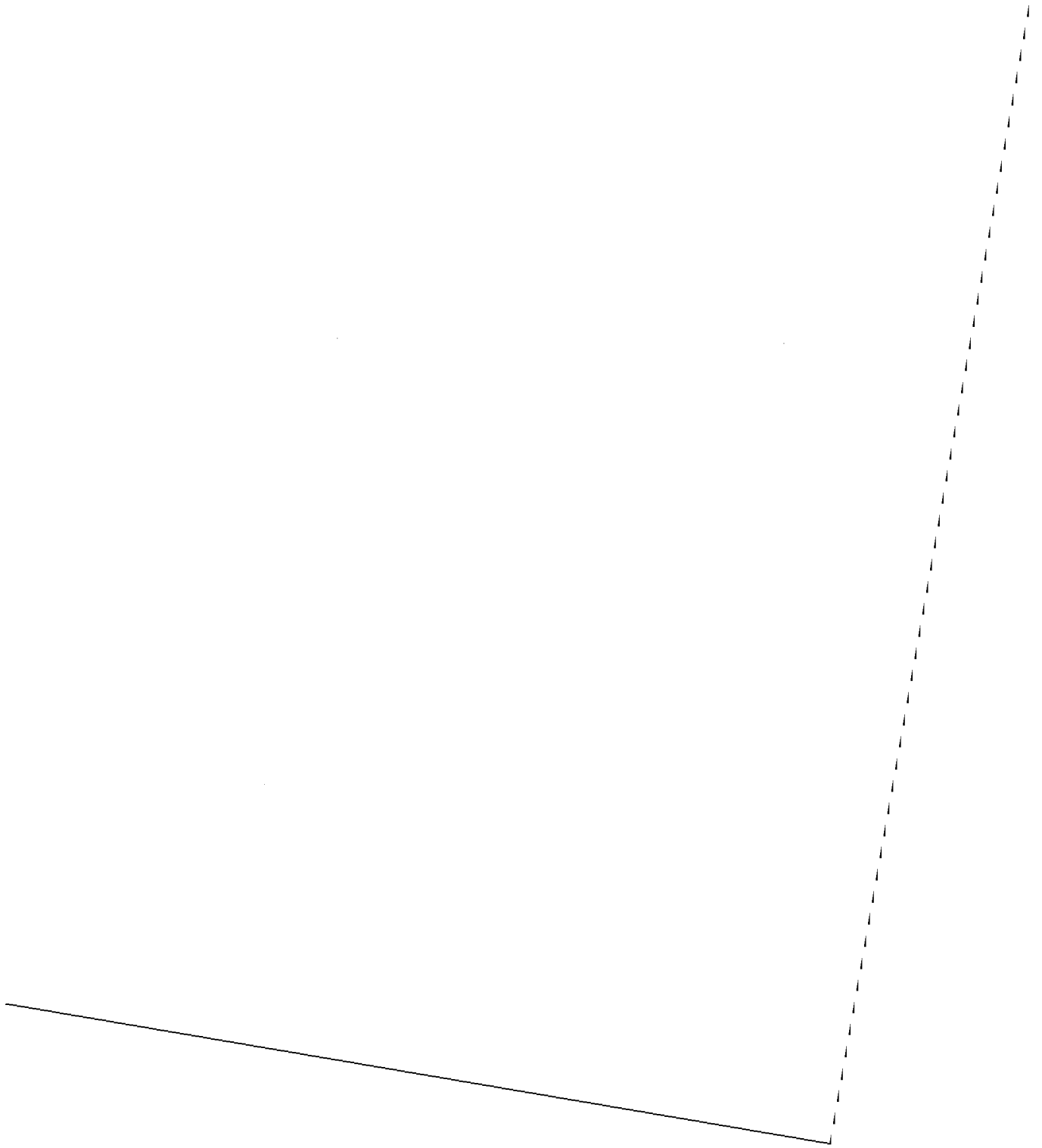
where  $\bar{n}$  is the time-average power.

- 2-22. Show that eq. (2-69) applies to a rod-drop experiment in which a reactor, initially critical with a negligible source, is suddenly made subcritical ( $\rho_0 = \rho_1 < 0$ ).
- 2-23. Show how the impulse response may also be obtained as the solution of a homogeneous differential equation with suitably chosen initial conditions.
- 2-24. Derive the frequency response by substituting an oscillating source into eq. (2-55).

- 2-25. Show that the Laplace transform  $F(s)$  of a real time function  $f(t)$  satisfies

$$F(s^*) = F^*(s).$$

- 2-26. The polynomial  $Z(s)$  in eq. (2-81) arises from the differential operator in eq. (2-78). The resulting transfer function, eq. (2-82), has  $n$  poles but no zeros. Discuss a generalization of eq. (2-78) in which  $f_i(t)$  is preceded by a differential operator.



### **3 Time-dependent Reactivity**

Solutions of the differential equations of reactor dynamics for various prescribed time-dependent reactivities are studied in this chapter. The distinguishing feature of these problems is that, although they are linear in the strict mathematical sense, the differential equations have time-dependent coefficients.

We consider first some simplifying approximations, some of which have been foreshadowed in chapter 2. These frequently lead to analytical solutions that help to set limits on the exact solutions (usually obtainable only by analog or digital computers), thereby providing insights not readily available otherwise. Some of these approximations also have immediate practical interest, and we therefore consider carefully their limitations and ranges of validity.

The next topic is reactivity oscillations. The reactivity transfer function (sometimes called the zero-power reactor transfer function) is derived for both the critical and subcritical reactor, and the relationship between oscillating reactivity and oscillating sources is discussed. The various approximations to the dynamic equations are interpreted in terms of their ability to represent the frequency response in different ranges, and approximate methods are used to study the effect of large oscillations.

The exact solution of the "ramp-input" problem (reactivity a linear function of time) is treated next. Solutions are obtained in terms of hypergeometric-type functions and also as integral representations. Application is made to reactor-accident calculations and to reactor startup problems, and the relationship between exact and approximate solutions is discussed.

Finally we consider several additional schemes for obtaining approximate solutions to the differential equations with arbitrary time-

### 3.6 Time-dependent Reactivity

dependent reactivities. The important topics of integral equations and numerical calculations are reserved for detailed treatment in chapter 4.

#### 3-1. Approximate Dynamic Equations

The first approximation method treated in this section is the “prompt-jump approximation” (abbreviated PJ) or, as it is sometimes called, the “zero-lifetime approximation” (Bethe 1956; Cohen 1958; Soodak 1962). It was introduced in sec. 2-2, where eq. (2-23) was identified as the inhour equation in the limit  $\ell \rightarrow 0$ . Later, in sec. 2-4, it was observed that eq. (2-47) is the one-delay-group step-input response in this approximation.

Another viewpoint is suggested by the differential equations of the point-reactor model. We write eqs. (2-1) and (2-2) as

$$\frac{dn}{dt} = \frac{\rho(t) - \beta}{\ell} n + \sum_i \lambda_i c_i + q(t) \quad (3-1)$$

and

$$\frac{dc_i}{dt} = \frac{\beta_i}{\ell} n - \lambda_i c_i \quad (3-2)$$

When  $\ell$  is small and  $\rho < \beta$ , the right-hand side of eq. (3-1) contains a large negative term  $(\rho - \beta)n/\ell$ . In such cases the derivative  $dn/dt$  is often a very small difference between a large negative number  $(\rho - \beta)n/\ell$  and a large positive number  $\sum_i \lambda_i c_i + q$ . This suggests that a useful approximation might be obtained by neglecting  $dn/dt$  in eq. (3-1), retaining eq. (3-2) as is.

More formally, we attempt an expansion of the neutron density in powers of the small parameter  $\ell$ . Postulate

$$n = n_1 + \ell n_2 + \dots \quad (3-3)$$

and

$$\frac{dn}{dt} = \frac{dn_1}{dt} + \ell \frac{dn_2}{dt} + \dots \quad (3-4)$$

Substitution into eq. (3-1) yields

$$\frac{dn_1}{dt} + \ell \frac{dn_2}{dt} = \frac{\rho - \beta}{\ell} n_1 + (\rho - \beta)n_2 + \sum_i \lambda_i c_i + q + \dots \quad (3-5)$$

From eqs. (2-6) and (2-7), we note that in equilibrium  $c_i$  and  $q$  are of order  $1/\ell$  with respect to  $n$ , and we infer that this remains true during a

slow transient. Assuming that the time derivatives are small, and equating terms of order  $1/\ell$  in eq. (3-5), we have

$$0 = \frac{\rho - \beta}{\ell} n_1 + \sum_i \lambda_i c_i + q,$$

whence

$$n_1 = \frac{\sum_i \lambda_i \ell c_i + \ell q}{\beta - \rho}. \quad (3-6)$$

This function  $n_1$ , which satisfies eq. (3-1) whenever  $dn_1/dt$  is sufficiently small to be ignored, is identified as the neutron density in the prompt-jump approximation.

Note that  $n_1$  satisfies a system of differential equations whose order has been reduced by one. This procedure of expansion in powers of a small parameter, yielding a first approximation that satisfies a differential equation of reduced order, is called the method of singular perturbations (Wasow 1944, 1963; Erdélyi 1963).

To continue, return to eq. (3-5) and equate terms of order  $\ell^0$  (i.e., same order as  $n$ ):

$$\frac{dn_1}{dt} = (\rho - \beta)n_2.$$

Therefore

$$n_2 = \frac{1}{\rho - \beta} \frac{dn_1}{dt}. \quad (3-7)$$

Using eq. (3-6) to evaluate the derivative, we obtain

$$n_2 = -\frac{1}{(\beta - \rho)^2} \left( \sum_i \lambda_i \ell \frac{dc_i}{dt} + \ell \frac{dq}{dt} + \frac{\sum_i \lambda_i \ell c_i + \ell q}{\beta - \rho} \frac{d\rho}{dt} \right). \quad (3-8)$$

The series, eq. (3-3), becomes

$$\begin{aligned} n &= \frac{\sum_i \lambda_i \ell c_i + \ell q}{\beta - \rho} - \frac{1}{(\beta - \rho)^2} \left( \sum_i \lambda_i \ell \frac{dc_i}{dt} + \ell \frac{dq}{dt} \right. \\ &\quad \left. + \frac{\sum_i \lambda_i \ell c_i + \ell q}{\beta - \rho} \frac{d\rho}{dt} \right) + O(\ell^2), \end{aligned} \quad (3-9)$$

where we assume that  $\ell c_i$  and  $\ell q$  are the same order as  $n$ . Eq. (3-9) is essentially that obtained by Birkhoff (1966). It is an asymptotic series in powers of  $\ell$  that diverges if  $\rho \rightarrow \beta$  and has for its first term the prompt-jump approximation. This treatment may also be regarded as a special case of a general method for approximating the solutions of

differential equations containing one or more very small time constants (Vasileva 1952; MacMillan 1967; Szeligowski and Hetrick 1967).

Because  $n_1$  as given by eq. (3-6) satisfies a system of differential equations of reduced order, its interpretation as the approximate neutron density satisfying eq. (3-1) with  $dn/dt$  omitted implies that one initial condition has been lost. The proper interpretation is that a fast-decaying transient part of the solution is missing from the approximate neutron density. For example, as observed in sec. 2-4, the approximate step-input response given by eq. (2-47) is discontinuous at  $t = 0$ . In deriving eq. (2-47) the transient term having a time constant  $\gamma/(\beta - \rho_0)$  was replaced by a jump discontinuity in  $n$ .

The "lost initial condition" is replaced in this approximation by a requirement of the continuity of  $(\beta - \rho)n$ . This follows from eq. (3-1) with  $dn/dt$  omitted and with  $q$  continuous if it is noted that, by eq. (3-2), each  $c_i$  is continuous even in the presence of a finite discontinuity in  $n(t)$ . The condition on the approximate neutron density in the presence of a step change in reactivity at  $t = 0$  is therefore

$$n(+0) = \frac{\beta - \rho(-0)}{\beta - \rho(+0)} n(-0). \quad (3-10)$$

By eq. (3-6), the approximate neutron density in the one-delay-group case is

$$n_1 = \frac{\lambda c + \ell q}{\beta - \rho}. \quad (3-11)$$

If we solve for  $c$  and substitute the result into the precursor equation

$$\gamma \frac{dc}{dt} = \beta n - \lambda c, \quad (3-12)$$

we obtain

$$(\beta - \rho) \frac{dn_1}{dt} - \left( \lambda \rho + \frac{d\rho}{dt} \right) n_1 = \lambda c + \ell \frac{dq}{dt}. \quad (3-13)$$

This is the first-order differential equation for the neutron density in the prompt-jump approximation. For a prescribed source, eq. (3-13) may be solved for  $n_1$ , and the precursor density may then be found from eq. (3-11). In practice, one first computes  $\ell q$  and then regards the product as fixed in the limit  $\gamma \rightarrow 0$ . Similarly, one computes the product  $\gamma c$  and then estimates  $c$  from it by using the original value of  $\ell$ .

In the source-free case for a step input of reactivity at equilibrium, the solution that satisfies the continuity condition, eq. (3-10), is eq. (2-47) of sec. 2-4. Fig. 3-1 illustrates how the starting transient is replaced by a

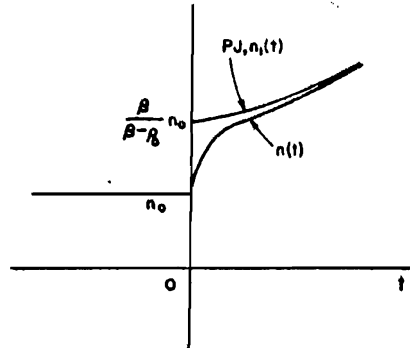


Fig. 3-1. Response to reactivity step: discontinuous prompt-jump approximation (PJ) compared with continuous solution containing a fast transient.

jump discontinuity (see also fig. 2-8). Of course, if  $n(t)$  in fig. 3-1 represents the exact solution, eq. (2-41), rather than eq. (2-46), the two curves eventually diverge because the stable periods are different.

In principle, provided eq. (3-9) holds, the validity of the prompt-jump approximation may be judged by comparing the magnitudes of successive terms in the asymptotic series. A quantitative criterion is easily obtained in the one-delay-group case. With one group of delayed neutrons and no source, eq. (3-9) becomes

$$n = \frac{\lambda c}{\beta - \rho} - \frac{\ell}{(\beta - \rho)^2} \left( \lambda c \frac{dc}{dt} + \frac{\lambda c}{\beta - \rho} \frac{d\rho}{dt} \right) + O(\ell^2). \quad (3-14)$$

Substituting the first term of this series into the precursor equation

$$\frac{dc}{dt} = \frac{\beta}{\ell} n - \lambda c,$$

one obtains an estimate of  $dc/dt$ :

$$\frac{dc}{dt} \approx \frac{\lambda \rho}{\beta - \rho} c.$$

Eq. (3-14) becomes

$$n = \frac{\lambda c}{\beta - \rho} \left[ 1 - \frac{\ell}{(\beta - \rho)^2} \left( \lambda \rho + \frac{d\rho}{dt} \right) + O(\ell^2) \right]. \quad (3-15)$$

We conclude that the prompt-jump approximation in the source-free one-delay-group case, as given by

$$n \approx n_1 = \frac{\lambda c}{\beta - \rho}, \quad (3-16)$$

### (3) Time-dependent Reactivity

is a useful approximation whenever the series, eq. (3-15), is valid and its second term is small. In other words, an approximate criterion of validity for the approximation in this special case is

$$\beta - \rho \gg \sqrt{\left(\ell \left| \lambda \rho + \frac{d\rho}{dt} \right| \right)}. \quad (3-17)$$

Note that the permissible approach to prompt critical may be quite close if  $\ell$  is small.

The criterion stated in eq. (3-17) cannot be used if  $dn/dt$  is very large, as happens during the fast transient following a reactivity step or during a very rapid oscillation. In such situations our basic assumptions about the relative order of magnitude of the terms in eq. (3-5) do not apply, and the resulting asymptotic series are not correctly constructed. The basic criterion for the validity of the prompt-jump approximation, as implied at the beginning of this section, is of course

$$\left| \frac{dn}{dt} \right| \ll \frac{\beta - \rho}{\ell} n. \quad (3-18)$$

It may be noted in passing that eq. (3-18) can be used to derive the criterion stated in eq. (3-17). From eq. (3-13) with  $q = 0$ , the approximate neutron density satisfies

$$(\beta - \rho) \frac{dn}{dt} = \left( \lambda \rho + \frac{d\rho}{dt} \right) n. \quad (3-19)$$

Combining eqs. (3-18) and (3-19) yields eq. (3-17), which in this context might be viewed as answering the question, "For one delay group and no source, and provided eq. (3-18) is satisfied, how close to prompt critical can the prompt-jump approximation be used?"

It must be noted that eq. (3-17) is not meant for use in judging the validity of the one-delay-group prompt-jump approximation as a substitute for the exact six-group model. In a close approach to prompt critical, even if one uses the weighted mean decay constant  $\lambda'$  (see sec. 2-2) in eq. (3-17), one should not expect a good quantitative prediction. One delay group is no substitute for six in the general case of time-dependent reactivity.

Nevertheless, eq. (3-17) may be regarded as a useful rule of thumb for predicting the maximum permissible reactivity that is within the range of validity of the prompt-jump approximation. Since the main concern is the closeness of approach to prompt critical, eq. (3-17) may be replaced by

$$\beta - \rho \gg \sqrt{\left(\ell \left| \lambda \beta + \frac{d\rho}{dt} \right| \right)}. \quad (3-20)$$

For large rates of change of reactivity, this becomes

$$\beta - \rho \gg \sqrt{\left(\ell \left| \frac{d\rho}{dt} \right|\right)}, \quad (3-21)$$

while for slow ramps eq. (3-20) reduces to

$$\beta - \rho \gg \sqrt{(\ell \lambda \beta)}. \quad (3-22)$$

Eq. (3-22) is cited by Cohen (1958) as a criterion for validity of the prompt-jump approximation. Its usefulness is restricted to slow rates of reactivity change.

The criterion for validity of the prompt-jump approximation may be displayed graphically by arbitrarily rewriting eq. (3-20) as

$$\beta - \rho_m = 3 \sqrt{\left(\ell \left| \lambda \beta + \frac{d\rho}{dt} \right|\right)} \quad (3-23)$$

and plotting contours of constant  $\rho_m$  as in fig. 3-2. The coordinate axes are  $\beta/\ell$  and  $(d\rho/dt)/\beta$ , and  $\rho_m$  is the maximum reactivity for which the prompt-jump approximation is valid according to the arbitrary limits set by eq. (3-23). In other words, the approximation is useful in a region to the right of a given contour for reactivities at least as large as that on the contour bounding the region. Note that for small rates of reactivity

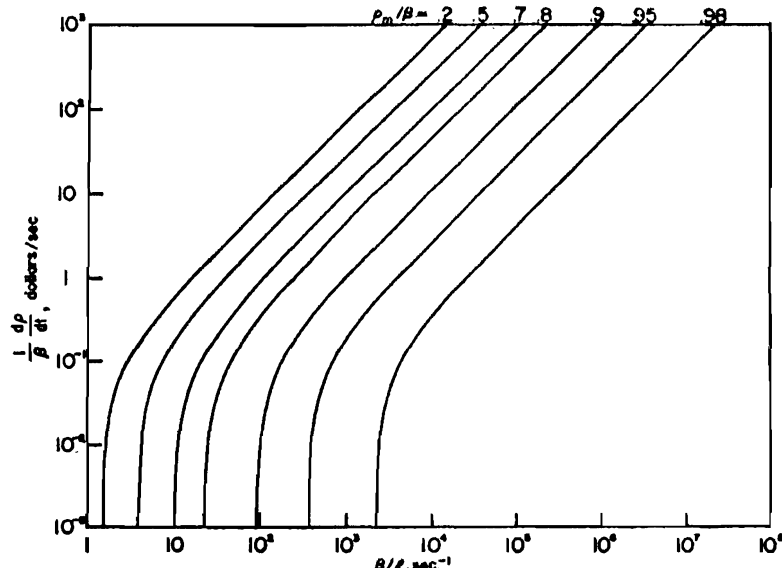


Fig. 3-2. Approximate regions of validity for the prompt-jump approximation (contours of constant limiting reactivity  $\rho_m$ ).

### 6.2 Time-dependent Reactivity

change the limits are independent of the rate, as expected from eq. (3-22), while for larger rates the validity of the approximation requires progressively smaller neutron generation times.

To complete the discussion of the prompt-jump approximation, and to have the equations available for later reference, we next consider the one-delay-group point-reactor model as a second-order differential equation in  $n(t)$ . Eqs. (3-1) and (3-2) become

$$\frac{dn}{dt} = \frac{\rho(t) - \beta}{\ell'} n + \lambda c + q(t) \quad (3-24)$$

and

$$\frac{dc}{dt} = \frac{\beta}{\ell'} n - \lambda c \quad (3-25)$$

The variable  $c(t)$  may be eliminated by solving for it in eq. (3-24) and substituting into eq. (3-25). The result is

$$\gamma' \frac{d^2n}{dt^2} + (\beta + \lambda\ell' - \rho) \frac{dn}{dt} - \left( \lambda\rho + \frac{d\rho}{dt} \right) n = \lambda\ell' q + \ell' \frac{dq}{dt} \quad (3-26)$$

The prompt-jump approximation, eq. (3-13), is seen to be the limit as  $\gamma' \rightarrow 0$  ( $q \neq 0$ ) whenever the second derivative is sufficiently small that  $\gamma' d^2n/dt^2$  may be neglected.

For very small reactivity and small rate of change of reactivity, the prompt-jump approximation reduces to an important special case. If

$$\frac{1}{\lambda} \left| \frac{d\rho}{dt} \right| \ll |\rho| \ll \beta,$$

then eq. (3-19) becomes

$$\frac{dn}{dt} = \frac{\lambda\rho}{\beta} n \approx \frac{\rho}{\ell'} n, \quad (3-27)$$

where  $\ell'$  is the effective lifetime in eq. (2-21). This approximate dynamic equation has the same mathematical form as the point-reactor model for prompt neutrons only, though  $\ell$  is replaced by the much larger effective lifetime  $\ell'$ , reflecting the dominance of delayed neutrons for small reactivity. For  $\rho = \rho_0$ , the characteristic equation corresponding to eq. (3-27) is  $\rho_0 = \omega\ell'$ , in conformity with eqs. (2-19) and (2-20).

This approximation is useful in studies of reactor stability when the qualitative effect of delayed neutrons can be neglected (see chapter 6). We shall use the name “effective lifetime model” or “ $\ell'$ -prime approximation” to distinguish it from the case of no delayed neutrons.

We now turn to the subject of large reactivities and fast excursions. The expansion in powers of  $\ell$ , eq. (3-3), may be used here also, but we make different assumptions about the relative magnitudes of the terms in eq. (3-5). The derivative  $dn_1/dt$  is now taken to be of order  $1/\ell$ , while  $c_i$  and  $q$  are assumed of order  $\ell^0$ .

Equating terms of order  $1/\ell$  in eq. (3-5), we find

$$\frac{dn_1}{dt} = \frac{\rho - \beta}{\ell} n_1, \quad (3-28)$$

which is identified as the Nordheim-Fuchs model for fast excursions (Fuchs 1946; Nordheim 1946). Here  $n_1$  is the approximate neutron density that satisfies eq. (3-1) when the neutron population is growing so rapidly that the sources  $\sum_i \lambda_i c_i$  and  $q$  are negligible.

Equating terms of order  $\ell^0$  in eq. (3-5), we find

$$\ell \frac{dn_2}{dt} = (\rho - \beta)n_2 + \sum_i \lambda_i c_i + q. \quad (3-29)$$

The second term in eq. (3-3) can in principle be evaluated by using  $n_1$ , the solution of eq. (3-28), in eq. (3-2) to estimate the approximate  $c_i$ . Eq. (3-29) may then be solved for  $n_2$ . We can therefore construct a singular perturbation expansion that is valid for large reactivities. Note that once again the first approximation  $n_1$  satisfies a system of differential equations of reduced order. In chapter 5 we use similar expansions in deriving the peak power and energy release in self-limiting power excursions.

The Nordheim-Fuchs approximation, eq. (3-28), may also be regarded as a special case of the "constant-source approximation" discussed in secs. 2-4 and 2-5. Setting  $\sum_i \lambda_i c_i$  equal to a constant in eq. (3-1) and differentiating, we obtain

$$\ell \frac{d^2n}{dt^2} + (\beta - \rho) \frac{dn}{dt} - \frac{d\rho}{dt} n = \ell \frac{dq}{dt}, \quad (3-30)$$

which is apparently the limit of eq. (3-26) as  $\lambda \rightarrow 0$ . It has already been observed in sec. 2-4 that this approximation could be expected to be useful only for short times,  $t \ll 1/\lambda$ , following a step change of reactivity. Comparison of eqs. (3-26) and (3-30) suggests alternative criteria:

$$\left| \frac{d\rho}{dt} \right| \gg \lambda |\rho| \quad (3-31)$$

and

$$\left| \frac{dq}{dt} \right| \gg \lambda q. \quad (3-32)$$

### 6.4 Time-dependent Reactivity

The first of these conditions naturally gives rise to the name “rapid-rate approximation.”

At this point we may observe that the extreme case of very large reactivity, in which delayed neutrons are ignored entirely, is logically obtained from eq. (3-28) if  $|\rho| \gg \beta$ :

$$\frac{dn}{dt} \cong \frac{\rho}{\ell} n. \quad (3-33)$$

For practical reasons this model would be of little interest in reactor theory, except that it is identical in form to the effective-lifetime model, eq. (3-27), which is useful for very small reactivity.

Finally, we note the possibility of using the assumptions of both the prompt-jump approximation and the constant-source model in the same problem. For example, if  $q = 0$  and  $\lambda_i c_i = \lambda_i c_i(0) = \beta_i n_0 / \ell$  in eq. (3-1),

$$\frac{dn}{dt} = \frac{\rho - \beta}{\ell} n + \frac{\beta}{\ell} n_0. \quad (3-34)$$

If the conditions for the prompt-jump approximation should also be satisfied, then

$$n(t) \cong \frac{\beta}{\beta - \rho(t)} n_0. \quad (3-35)$$

If a steady source  $q_0$  is present, corresponding to an initial equilibrium shutdown reactivity  $\rho_0$  given by eq. (2-5), then

$$n(t) \cong \frac{\beta - \rho_0}{\beta - \rho(t)} n_0. \quad (3-36)$$

Note the similarity between eq. (3-36) and the prompt-jump continuity condition eq. (3-10). See also eq. (2-50) and fig. 2-9, where the fast transient in the CS approximation would now be replaced by a jump.

This approximation, which has a very limited range of applicability, satisfies the differential equation

$$(\beta - \rho) \frac{dn}{dt} - \frac{d\rho}{dt} n = 0. \quad (3-37)$$

By comparison with eq. (3-13), with constant  $q$  and with the second derivative omitted, it might be considered the limit as  $\ell \rightarrow 0$  and  $\lambda \rightarrow 0$  simultaneously.

In spite of its obvious limitations, this model can be used for quick estimates in certain practical cases. For example, a ramp input starting from equilibrium (negligible source) may be represented by

$$\rho = t \frac{d\rho}{dt}, \quad (t > 0). \quad (3-38)$$

If we crudely interpret the restriction  $t \ll 1/\lambda$  as  $t < 1/3\lambda$ , the constant-source approximation will not be too greatly in error for reactivities less than some  $\rho_m$  given by

$$\rho_m = \frac{1}{3\lambda} \frac{d\rho}{dt}. \quad (3-39)$$

The combination of approximations represented by eq. (3-35) may now be regarded as limited by the two restrictions eqs. (3-23) and (3-39); i.e., the maximum reactivity for which eq. (3-35) is a useful estimate of a ramp-input response is the smaller of the two values  $\rho_m$  from eqs. (3-23) and (3-39).

A contour plot similar to fig. 3-2 may now be constructed with both these restrictions used. Regions wherein eq. (3-35) is applicable for estimating the ramp response are shown in fig. 3-3 (large  $\beta/\epsilon$  and intermediate ramp rates). The regions of validity of the prompt-jump approximation (fig. 3-2) no longer extend into the range of small ramp rates, where the constant-source approximation fails, if eq. (3-35) is to be meaningful.

In the next section we investigate reactivity oscillations and discuss the approximations to the frequency response. Approximations are compared with an exact solution of a ramp-input problem in sec. 3-3.

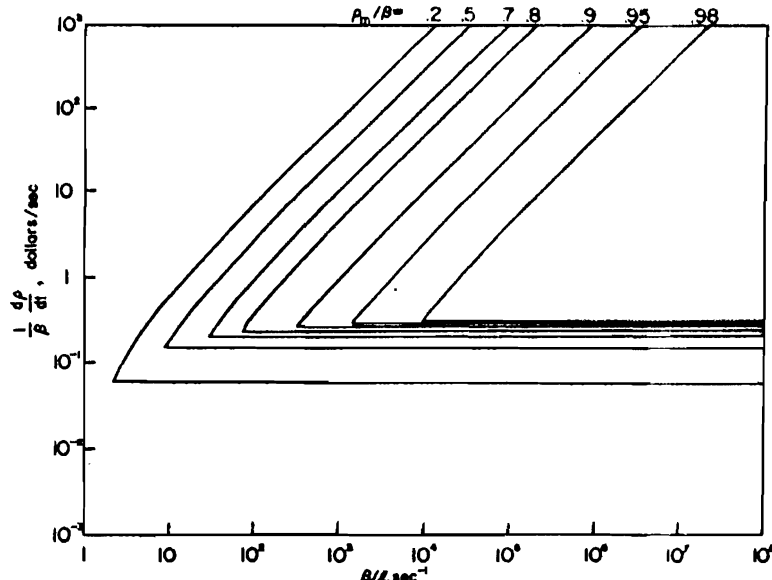


Fig. 3-3. Approximate regions of validity for eq. (3-35),  $n/n_0 \approx \beta/(\beta - \rho)$ , as estimate of ramp-input response (contours of constant limiting reactivity  $\rho_m$ ).

### 3-2. Reactivity Oscillations

In this section we write the point-reactor model for small fluctuations about equilibrium power and obtain, under this restriction, the same frequency response as for the oscillating source of sec. 2-6. Here we study the reactor transfer function in more detail and discuss its limiting forms under the approximations of the previous section. We then find approximate solutions for large-amplitude reactivity oscillations. Reactivity feedback and high-power transfer functions are postponed to later chapters. Space-dependent effects are discussed in chapter 8.

Oscillating neutron absorbers have long been used in measurements of reactor-dynamic parameters and neutron-absorption cross-sections. Basic theory was discussed in many early studies (e.g., Nordheim 1946; Weinberg and Schweinler 1948; Franz 1949). Summaries are given by Corben (1959a) and Sastre (1964). An early pile oscillator, used for neutron cross-section measurements, was built by Langsdorf (1949). The classic reactor transfer-function measurement was made with the Argonne CP-2 reactor (Harrer, Boyar, and Krucoff 1952). A recent review is given by Kerlin (1967).

Proceeding as in section 2-6, let

$$\begin{aligned} n &= n_0 + \delta n, \\ c_i &= c_{i0} + \delta c_i, \\ \rho &= \rho_0 + \delta \rho, \\ q &= q_0, \\ c_{i0} &= \frac{\beta_i n_0}{\lambda_i \ell}, \end{aligned}$$

and

$$q_0 = -\frac{\rho_0 n_0}{\ell},$$

where we have assumed that average values are the same as equilibrium values. (We shall see later that this is not true for large-amplitude oscillations.)

Substituting into eqs. (2-1) and (2-2) yields

$$\frac{d}{dt} \delta n = \frac{\rho_0 - \beta}{\ell} \delta n + \sum_i \lambda_i \delta c_i + \frac{n_0}{\ell} \delta \rho + \frac{1}{\ell} \delta \rho \delta n \quad (3-40)$$

and

$$\frac{d}{dt} \delta c_i = \frac{\beta_i}{\ell} \delta n - \lambda_i \delta c_i. \quad (3-41)$$

These equations are similar to eqs. (2-87) and (2-88) except that the oscillating source  $\delta q$  is now replaced by

$$\frac{n_0}{\ell} \delta\rho + \frac{1}{\ell} \delta\rho\delta n.$$

To proceed further, we assume sufficiently small oscillations that  $|\delta n| \ll n_0$  (i.e., the product  $\delta\rho\delta n$  is at all times negligible). Eqs. (2-87) and (3-40) then have the same form (linear differential equations with constant coefficients).

We use the Laplace transforms

$$\begin{aligned}\delta N(s) &= \int_0^\infty \delta n(t) e^{-st} dt, \\ \delta \Gamma_i(s) &= \int_0^\infty \delta c_i(t) e^{-st} dt,\end{aligned}$$

and

$$\delta R(s) = \int_0^\infty \delta p(t) e^{-st} dt.$$

The Laplace transform of the steady-state portion of the response is given by

$$\delta N(s) = \frac{n_0 \delta R(s)}{\ell s + \beta - \rho_0 - \sum_i \frac{\beta_i \lambda_i}{s + \lambda_i}}. \quad (3-42)$$

By eq. (2-53) or (2-91), the reactivity transfer function is seen to be

$$G(s) = \frac{\delta N(s)}{\delta R(s)} = \frac{n_0}{\ell} I(s) = \frac{n_0}{\ell s + \beta - \rho_0 - \sum_i \frac{\beta_i \lambda_i}{s + \lambda_i}}. \quad (3-43)$$

The reactivity transfer function is therefore  $n_0/\ell$  times the source transfer function (the Laplace transform of the impulse response), provided the resulting power oscillation is small. Note that this system cannot be unstable;  $\rho_0$  is a negative shutdown reactivity, and there can be no pole of  $G(s)$  in the right half-plane.

There is no wide agreement on notation for the reactor transfer function. This function appears in many places in the theory of reactor dynamics; sometimes one normalization is more convenient, sometimes another. We choose the normalization in eq. (3-43), recalling that  $I(s)$  was written so that its inverse Laplace transform, the impulse

63      *Time-dependent Reactivity*

response  $i(t)$ , has the property  $i(0) = 1$ . Of course, whatever the normalization, the inhour equation, eq. (2-15) or (2-54), can be expressed as

$$\frac{1}{G(j\omega_j)} = 0. \quad (3-44)$$

When the results of sec. 2-6 are applied, the frequency response for a fluctuation  $\delta n$  in response to a small reactivity oscillation is given by the magnitude and phase of  $G(j\omega)$ . In other words, if

$$\delta\rho = \epsilon \sin \omega t, \quad (3-45)$$

then

$$\delta n = \epsilon |G(j\omega)| \sin(\omega t + \phi), \quad (3-46)$$

where

$$G(j\omega) = |G(j\omega)| e^{j\phi}. \quad (3-47)$$

Before plotting graphs of the frequency response, we may note some of the properties of  $G(s)$ . Since  $\sum_i \beta_i = \beta$ ,

$$G(s) = \frac{n_0}{\ell s + \beta - \rho_0 - \sum_i \frac{\beta_i \lambda_i}{s + \lambda_i}} = \frac{n_0}{\left(\ell + \sum_i \frac{\beta_i}{s + \lambda_i}\right)s - \rho_0}. \quad (3-48)$$

There are  $m + 1$  poles on the real axis at  $s = \omega_j$ , the  $m + 1$  real roots of the inhour equation. If  $\rho_0 = 0$ , there is a pole at the origin, corresponding to equilibrium operation at arbitrary power level; otherwise, all poles are on the negative real axis. If numerator and denominator are multiplied by  $\Pi_i(s + \lambda_i)$ , then  $G(s)$  becomes a ratio of two polynomials of degree  $m$  and  $m + 1$  respectively, and there are seen to be  $m$  zeros at  $s = -\lambda_i$ .

For very small  $s$ ,

$$G(s) \cong -\frac{n_0}{\rho_0} = \frac{n_0}{|\rho_0|} \quad (3-49)$$

provided  $\rho_0 \neq 0$ ; if  $\rho_0 = 0$ , then for small  $s$

$$G(s) \cong \frac{n_0}{(\ell + \sum_i \beta_i / \lambda_i)s} \cong \frac{n_0}{\ell's}. \quad (3-50)$$

For very large  $s$ ,

$$G(s) \cong \frac{n_0}{\ell s}. \quad (3-51)$$

Since  $\ell$  is very small, there is an intermediate range,  $|s| \gg \max \lambda_i$ , where

$$G(s) \cong \frac{n_0}{\beta - \rho_0}. \quad (3-52)$$

For one group of delayed neutrons,

$$G(s) = \frac{n_0}{\left(\ell + \frac{\beta}{s + \lambda}\right)s - \rho_0}, \quad (3-53)$$

which may be written as

$$G(s) = \frac{n_0(s + \lambda)}{\ell s^2 + (\beta + \lambda\ell - \rho_0)s - \lambda\rho_0}. \quad (3-54)$$

In terms of the two negative roots,  $\omega_1$  and  $\omega_2$ , of the inhour equation, this is

$$G(s) = \frac{n_0(s + \lambda)}{\ell(s - \omega_1)(s - \omega_2)}. \quad (3-55)$$

For a critical reactor,

$$G(s) = \frac{n_0}{\left(\ell + \sum_i \frac{\beta_i}{s + \lambda_i}\right)s}. \quad (3-56)$$

For one group,

$$G(s) = \frac{n_0(s + \lambda)}{\ell s(s + \lambda + \beta/\ell)}. \quad (3-57)$$

This function has poles at  $s = \omega_1 = 0$  and  $s = \omega_2 = -(\lambda + \beta/\ell)$ . Since  $\lambda \ll \beta/\ell$ , it will be an excellent approximation to write

$$G(s) \cong \frac{n_0(s + \lambda)}{\ell s(s + \beta/\ell)}. \quad (3-58)$$

Eqs. (3-48) and (3-56), and their one-delay-group versions eqs. (3-53) and (3-57), are often called the zero-power transfer functions. This is because the equilibrium power  $n_0$  has been assumed sufficiently small that no reactivity feedback effects are significant. The use of  $G(s)$  for a critical reactor ( $\rho_0 = 0$ ) implies at the same time that  $n_0$  is also sufficiently large for the source  $q_0$  to be unimportant.

A typical frequency response for a critical reactor, expressed as magnitude and phase of  $(\beta/n_0)G(j\omega)$ , is shown in fig. 3-4, which compares the one- and six-group models for  $\ell/\beta = 10^{-2}$  sec ( $U^{235}$  thermal delayed-neutron data). As seen from eq. (3-52), this particular normalization gives unit magnitude for intermediate frequencies. This type of

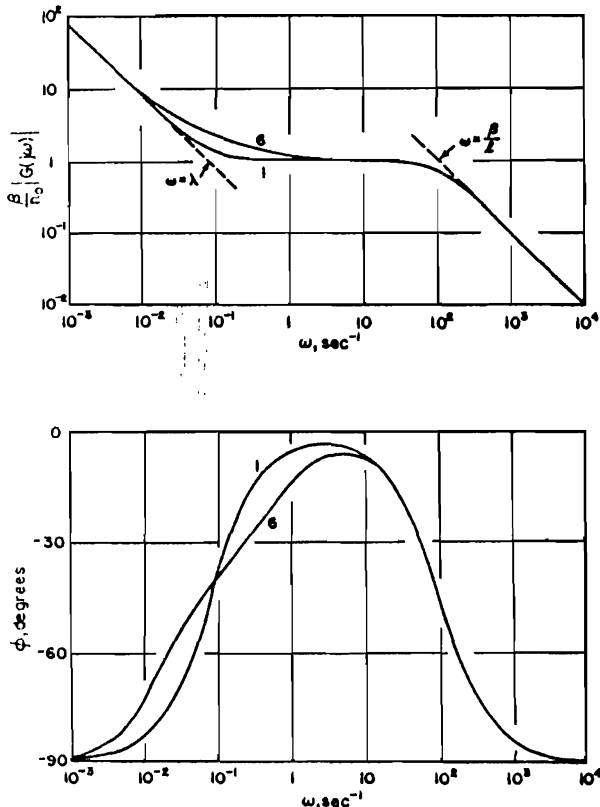


Fig. 3-4. Magnitude and phase of the zero-power reactor transfer function ( $U^{235}$ ,  $\epsilon/\beta = 10^{-2}$  sec) comparing one- and six-group representations.

representation, called a Bode plot, is frequently presented with the magnitude expressed in decibels (db), the number of decibels being twenty times the common logarithm of a relative amplitude. Detailed discussions are presented in many books (e.g., Harrer 1963; Keepin 1965; Schultz 1961; Weaver 1963).

Note that the six-group model does not have as sharp a break in amplitude near  $\omega = \lambda$ . This is a consequence of the closely spaced poles and zeros resulting from the six-group  $\lambda_i$  and  $\omega_j$ . Both models have the same behavior for very low or very high frequencies; this is to be expected from eqs. (3-50) and (3-51), where  $|G(j\omega)|$  varies inversely with  $\omega$  and the phase approaches  $-90^\circ$ .

Another representation that we will need later is the polar plot in the complex  $G(j\omega)$  plane, as shown in fig. 3-5 for the same data as in fig. 3-4. The locus is constructed using  $|G(j\omega)|$  as the radius and  $\phi$  as the angle

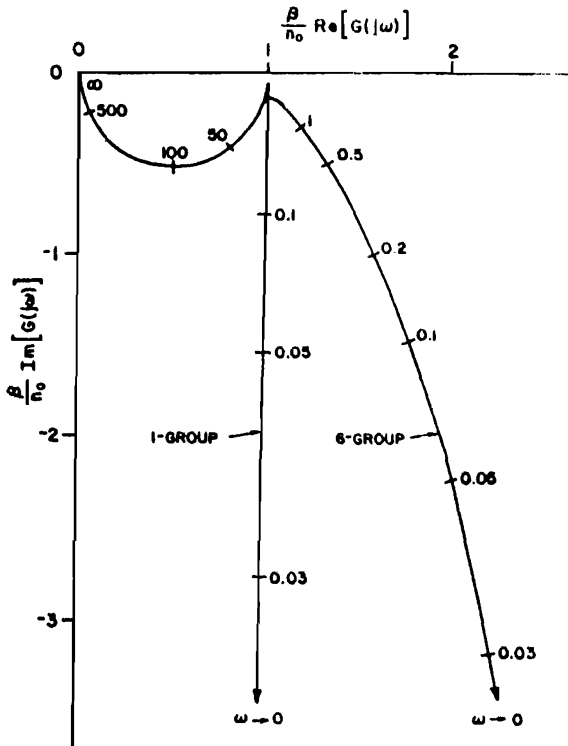


Fig. 3-5. Polar plot of the zero-power reactor transfer function (frequencies as labeled; data from fig. 3-4).

in the conventional sense. Consistent with the convention we use in chapter 6, the locus is regarded as traversed from the origin toward infinity as  $\omega$  varies from  $\infty$  to 0. Note how the polar representation emphasizes the contrast between the one- and six-group models at low frequency.

As may be inferred from eq. (3-51), the effect of decreasing  $\ell$  is to broaden the frequency response at the high end and keep the phase near zero over a wider range. This is illustrated in the six-group amplitude and phase plots for  $U^{235}$  shown in figs. 3-6 and 3-7 (Keepin 1965). Similar graphs for other reactor fuels are also shown by Keepin. Fast-fission delayed-neutron data was used. (Strictly speaking, the curves for larger values of  $\ell$  would be shifted very slightly at low frequencies to reflect the correlation between neutron generation time and mean neutron energy in the reactor. This would hardly be worth the trouble, especially since complete consistency would require a slightly different set of delayed-neutron data for each reactor.)

1.2 Time-dependent Reactivity

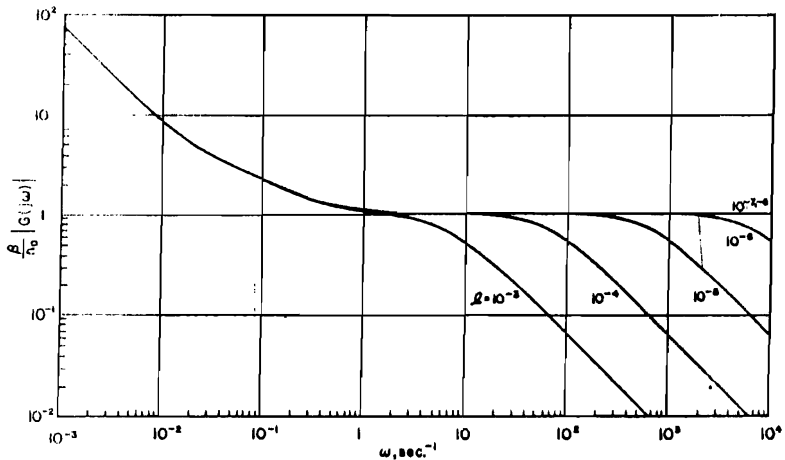


Fig. 3-6. Magnitude of the zero-power reactor transfer function for  $\text{U}^{235}$  for various values of neutron generation time  $\zeta$  (from *Physics of Nuclear Kinetics* by G. R. Keepin. © 1965 by Addison-Wesley Publishing Co., Reading, Mass.).

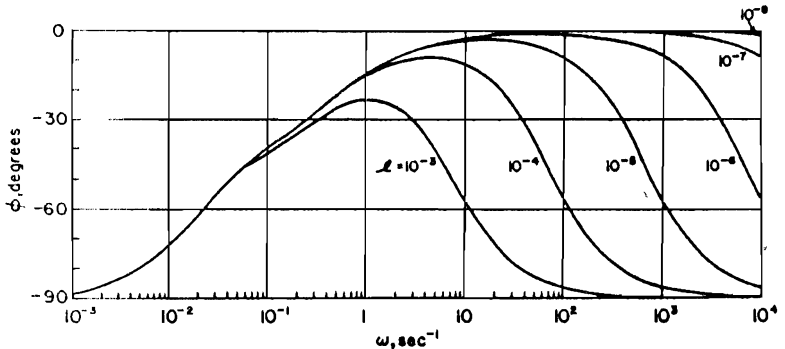


Fig. 3-7. Phase of the zero-power reactor transfer function for  $\text{U}^{235}$  for various values of neutron generation time  $\zeta$  (from *Physics of Nuclear Kinetics* by G. R. Keepin. © 1965 by Addison-Wesley Publishing Co., Reading, Mass.).

Next we consider the frequency response for a critical reactor in each of the approximations discussed in sec. 3-1. We will gain sufficient insight using one group of delayed neutrons; the extension to more groups is not difficult.

First, consider the prompt-jump approximation. In the limit of small  $\zeta$ , eq. (3-58) becomes

$$G(s) \cong \frac{n_0 s + \lambda}{\beta s} \quad (3-59)$$

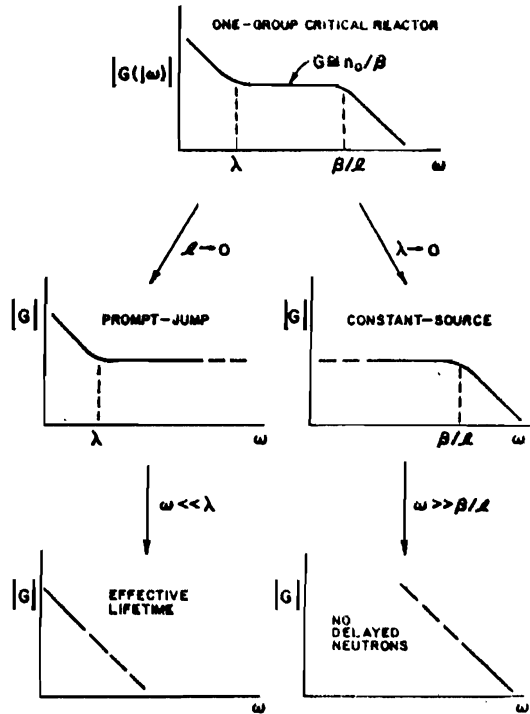


Fig. 3-8. Reactor frequency response,  $\log |G(j\omega)|$  vs.  $\log \omega$ , in various approximations.

This may also be derived from eq. (3-19), which for small oscillations would be

$$\beta \frac{dn}{dt} \cong \left( \lambda \rho + \frac{dp}{dt} \right) n_0. \quad (3-60)$$

We see from eq. (3-59) that the amplitude does not fall off at very high frequencies but remains flat with a limiting value  $n_0/\beta$  (see fig. 3-8). For this reason, the prompt-jump approximation is sometimes known as the "infinite-bandwidth" approximation. Its usefulness in stability studies is not compromised by this unrealistic high-frequency behavior, because the other elements in a realistic system model (reactivity feedbacks, controllers, etc.) would dominate the overall system with their much larger time constants.

For  $|s| \ll \lambda$  (or  $|s| \ll \min \lambda_i$ ), we have

$$G(s) \cong \frac{n_0 \lambda}{\beta s} = \frac{n_0}{\tau' s}. \quad (3-61)$$

74      *Time-dependent Reactivity*

See also eq. (3-50). This is the low-frequency asymptote and is the transfer function for the  $\ell'$  model, eq. (3-27).

For  $|s| \gg \lambda$  (or  $|s| \gg \max \lambda_i$ ), we have the constant-source approximation. From eq. (3-58) with  $\lambda$  neglected,

$$G(s) \cong \frac{n_0}{\ell s + \beta}. \quad (3-62)$$

This may also be derived from eq. (3-28) for small oscillations. In the intermediate range we again have  $G \cong n_0/\beta$ , while for extremely high frequencies

$$G(s) \cong \frac{n_0}{\ell s}. \quad (3-63)$$

This is of course the case of no delayed neutrons, eq. (3-33) for small oscillations, and by eq. (3-51) it plays the role of the high-frequency asymptote.

The relationships among these approximations are illustrated schematically in fig. 3-8. The high-frequency approximations, eqs. (3-62) and (3-63), are of little use in stability studies because of their unrealistic low-frequency behavior.

Finally we note that the overlap region between the prompt-jump and constant-source approximations, the region of flat frequency response where  $G \cong n_0/\beta$ , could have been predicted from eq. (3-52). This flat frequency response might also be regarded as the transfer function obtained from eq. (3-37) for small oscillations; naturally, it also is of little use in stability studies because it represents the intermediate frequency range only. Note that this flat region exists by virtue of the smallness of  $\ell$ . We see from fig. 3-6 that this plateau is very pronounced, even with the six delay groups, for all but the very largest physically reasonable values of  $\ell$ .

The transfer functions in figs. 3-4 through 3-8 are all for critical reactors. In a source-sustained subcritical system the low-frequency behavior is quite different, as seen from eq. (3-49). The amplitude must approach a constant at low frequency, with a corresponding zero phase angle. This is illustrated in figs. 3-9 and 3-10 (Keepin 1965).

If we try to extend these transfer functions into the supercritical range by making  $\rho_0 > 0$  in eq. (3-48), we lose physical meaning because positive  $\rho_0$  would imply a negative source. Instead, we conceive a transfer function for a source-free supercritical system by superimposing an oscillation on an exponential rise with a stable period corresponding to the average reactivity. Postulate

$$\begin{aligned} n &= n_0(1 + \epsilon)e^{\rho t}, \\ c_i &= c_{i0}(1 + \epsilon_i)e^{\rho t}, \end{aligned}$$

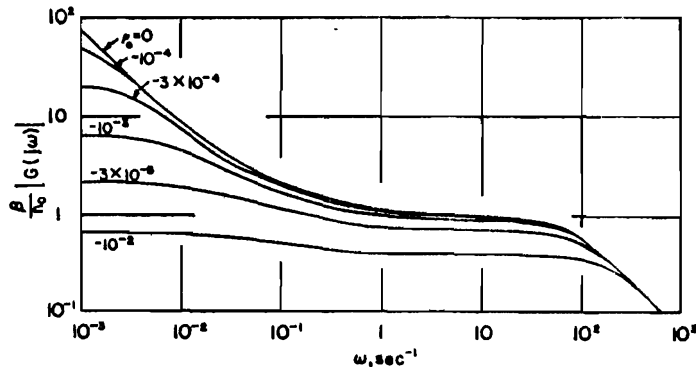


Fig. 3-9. Magnitude of the reactor transfer function ( $\nu = 10^{-4} \text{ sec}$ ) for various degrees of subcriticality (from *Physics of Nuclear Kinetics* by G. R. Keepin. © 1965 by Addison-Wesley Publishing Co., Reading, Mass.).

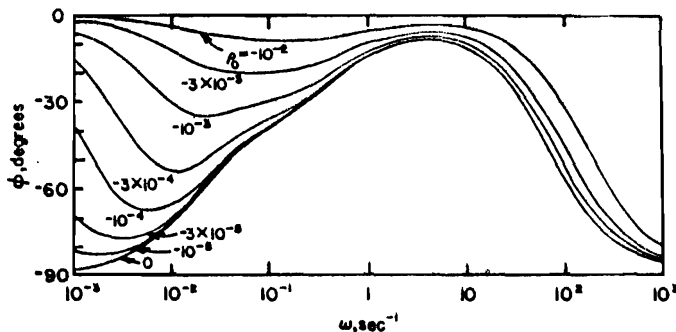


Fig. 3-10. Phase of the reactor transfer function ( $\nu = 10^{-4} \text{ sec}$ ) for various degrees of subcriticality (from *Physics of Nuclear Kinetics* by G. R. Keepin. © 1965 by Addison-Wesley Publishing Co., Reading, Mass.).

and

$$\rho = \rho_0 + \delta\rho,$$

where  $\epsilon$ ,  $\epsilon_i$  and  $\delta\rho$  are small fluctuations, and where  $p$  is the positive root of the inhour equation for reactivity  $\rho_0$ .

Substituting into the point-reactor equations, neglecting the product  $\epsilon\delta\rho$ , and using Laplace transforms we find

$$\frac{\bar{\epsilon}(s)}{\delta R(s)} = \frac{1}{\ell(s+p) + \beta - \rho_0 - \sum_i \frac{\beta_i \lambda_i}{s+p+\lambda_i}}, \quad (3-64)$$

where  $\zeta$  and  $\delta R$  are Laplace transforms of  $\epsilon$  and  $\delta\rho$ . This result is illustrated in figs. 3-11 and 3-12 (Keepin 1965), where  $G$  is  $n_0$  times the above transfer function and  $T$  is the stable period  $1/p$ .

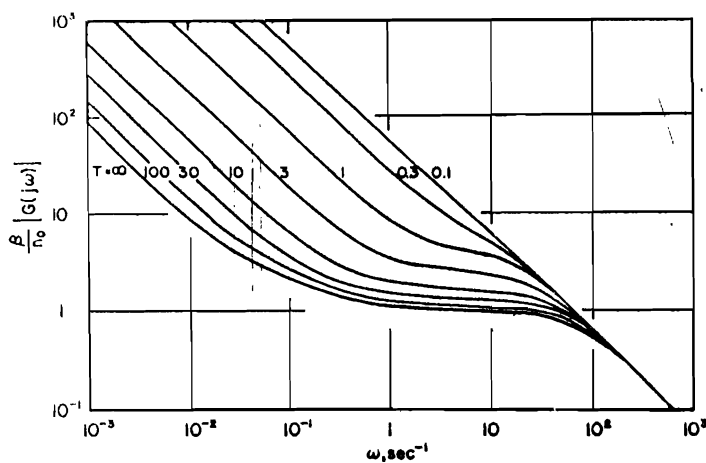


Fig. 3-11. Magnitude of the reactor transfer function ( $\zeta = 10^{-4}$  sec) for various degrees of supercriticality; oscillation superimposed on stable period  $T$  (from *Physics of Nuclear Kinetics* by G. R. Keepin. © 1965 by Addison-Wesley Publishing Co., Reading, Mass.).

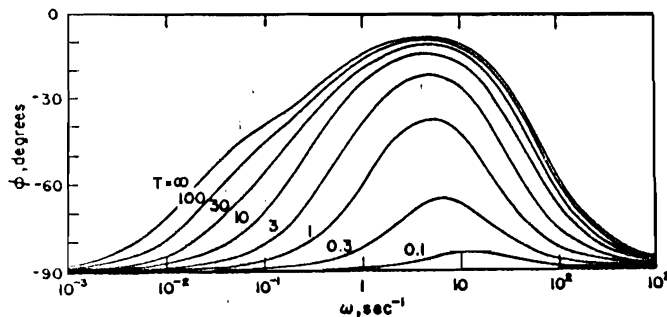


Fig. 3-12. Phase of the reactor transfer function ( $\zeta = 10^{-4}$  sec) for various degrees of supercriticality; oscillation superimposed on stable period  $T$  (from *Physics of Nuclear Kinetics* by G. R. Keepin. © 1965 by Addison-Wesley Publishing Co., Reading, Mass.).

This parametric excitation during a transient, or "transfer-function period effect," is discussed in detail by Carter, Sparks, and Tessier (1964). The importance of this effect has been observed in nuclear rocket prototypes (Singer 1962), where it was found that reactor control systems designed for equilibrium operation developed unstable oscillations during a short-period programmed startup.

We complete this section on reactivity oscillations with a brief treatment of large-amplitude variations. The most striking feature is that a steady oscillation about zero reactivity causes a diverging power; see fig. 3-13 (Akcasu 1958).

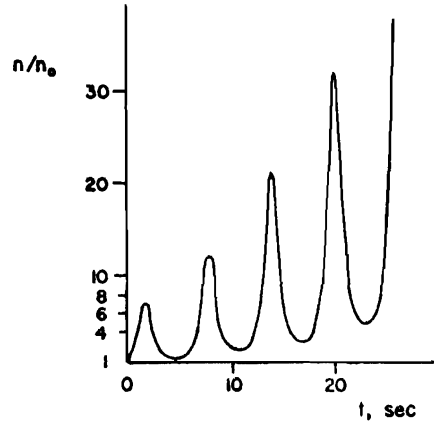


Fig. 3-13. Response to reactivity input  $\rho/\beta = 0.7 \sin t$  dollars (Akcasu 1958).

Here we treat the problem by using a model for which an analytical solution is possible, i.e., the prompt-jump approximation with one delay group. We find the large-amplitude response to an oscillating reactivity having a nonzero average value and then obtain an approximate value for the average (negative-bias) reactivity that produces a nondiverging power (Smith 1965).

We solve eq. (3-19):

$$(\beta - \rho) \frac{dn}{dt} = \left( \lambda\rho + \frac{d\rho}{dt} \right) n$$

with

$$\frac{\rho}{\beta} = A + B \sin \omega t, \quad (3-65)$$

using  $n = n_0$  at  $t = 0$ . The integration is standard, with the result

$$\begin{aligned} \log \frac{n}{n_0} &= \log \frac{1 - A}{1 - A - B \sin \omega t} - \lambda t + \frac{\lambda}{\omega \sqrt{[(1 - A)^2 - B^2]}} \\ &\times \left[ \tan^{-1} \frac{B}{\sqrt{[(1 - A)^2 - B^2]}} - \tan^{-1} \frac{B - (1 - A) \tan \frac{1}{2}\omega t}{\sqrt{[(1 - A)^2 - B^2]}} \right]. \end{aligned} \quad (3-66)$$

As  $t$  increases, the inverse tangent functions are equal at one point in each cycle, and the quantity in the brackets in eq. (3-66) increases by  $\pi$  radians each cycle. We can therefore reduce eq. (3-66) to a simpler form that is valid once in each cycle (whenever  $\frac{1}{2}\omega t$  equals an integral multiple of  $\pi$ ) by setting the quantity in brackets equal to  $\frac{1}{2}\omega t$ :

$$\log \frac{n}{n_0} = \log \frac{1 - A}{1 - A - B \sin \omega t} - \lambda t + \frac{\lambda t}{\sqrt{[(1 - A)^2 - B^2]}}. \quad (3-67)$$

The solution will be periodic (nondivergent power) if

$$(1 - A)^2 - B^2 = 1. \quad (3-68)$$

When the reactor is not too far from critical ( $|A| \ll 1$ ), this result may be approximated by

$$A \approx -\frac{1}{2}B^2, \quad (3-69)$$

which gives the amount of negative-bias reactivity,  $A$  dollars, that is needed to maintain a steady power oscillation when the oscillating reactivity has amplitude  $B$ . This result was also obtained by Akcasu (1958), using a different approach that we discuss briefly in sec. 3-6 (see also sec. 7-9).

It is interesting that the solution has an alternative form, obtained by transforming the integrals and using different standard forms:

$$\begin{aligned} \log \frac{n}{n_0} &= \log \frac{1 - A}{1 - A - B \sin \omega t} - \lambda t + \frac{\lambda}{\omega} \frac{1}{\sqrt{[(1 - A)^2 - B^2]}} \\ &\times \left[ \sin^{-1} \frac{B}{1 - A} - \sin^{-1} \frac{B - (1 - A) \sin \omega t}{1 - A - B \sin \omega t} \right]. \end{aligned} \quad (3-70)$$

This time the quantity in brackets increases by  $2\pi$  radians each cycle. Eq. (3-67) follows if one replaces the bracketed quantity by  $\omega t$ .

The mathematical model is too oversimplified to permit detailed comparison with experimental data, but it does give important insight into the qualitative effect of delayed neutrons in large-amplitude oscillations.

### 3-3. Ramp-Input Response: Hypergeometric Functions

As another example of time-dependent reactivity, we consider the case of reactivity a linear function of time (the so-called ramp input):

$$\rho(t) = \rho_0 + \gamma t \quad (3-71)$$

In this section we treat the one-delay-group case as a second-order differential equation whose solution may be expressed in terms of known

functions. The discussion is based in large part on work reported by Coveyou and Mulliken (1948) and by Smets (1958). An alternate treatment using integral representations, which has a simple extension to several delay groups, is discussed in the following section.

We consider eq. (3-26) with  $\rho(t)$  given by eq. (3-71). The constant  $\gamma = d\rho/dt$  is called the ramp rate. The differential equation is

$$\frac{d^2n}{dt^2} + (At + B)\frac{dn}{dt} + (Ct + D)n = \lambda q + \frac{dq}{dt}, \quad (3-72)$$

where

$$\begin{aligned} A &= -\frac{\gamma}{\ell}, & B &= \lambda + \frac{\beta - \rho_0}{\ell}, \\ C &= -\frac{\lambda\gamma}{\ell}, & D &= -\frac{\gamma + \lambda\rho_0}{\ell}. \end{aligned} \quad (3-73)$$

In this section we treat only the homogeneous case ( $q = 0$ ). In principle, a particular integral can be constructed once the solution to the homogeneous equation is known, but its form in this problem is very complicated. (See instead the integral representation constructed in the next section.)

We therefore seek two linearly independent solutions of the differential equation

$$\frac{d^2n}{dt^2} + (At + B)\frac{dn}{dt} + (Ct + D)n = 0, \quad (3-74)$$

with the constants as given by eq. (3-73). We retain the initial reactivity  $\rho_0$  for now, although it must vanish in the source-free case if the initial state is an equilibrium. We state a transformation that leads to Weber's differential equation and permits the exact solution to be expressed either in terms of parabolic cylinder functions of negative order or in terms of the confluent hypergeometric function. It is then shown that simpler forms involving exponentials and error functions result if  $\lambda\beta/\gamma$  is an integer. Finally, we discuss the relationship of these simpler forms to the approximations of sec. 3-1.

We begin by setting

$$n = xy, \quad \frac{dn}{dt} = x \frac{dy}{dt} + y \frac{dx}{dt}. \quad (3-75)$$

Eq. (3-74) becomes

$$x \frac{d^2y}{dt^2} + \left[ \frac{d^2x}{dt^2} + (At + B)\frac{dx}{dt} + (Ct + D)x \right] y = 0, \quad (3-76)$$

### 3.0 Time-dependent Reactivity

where we have eliminated the term in  $dy/dt$  by requiring that  $x$  be a particular solution of

$$2 \frac{dx}{dt} + (At + B)x = 0. \quad (3-77)$$

A convenient form for  $x$  will be

$$x = \exp \left[ -\frac{(At + B)^2}{4A} \right]. \quad (3-78)$$

Using eq. (3-77) or (3-78), we find

$$\begin{aligned} \frac{1}{x} \frac{d^2x}{dt^2} + \frac{At + B}{x} \frac{dx}{dt} + Ct + D &= -\frac{A^2}{4} t^2 \\ &+ \left( C - \frac{AB}{2} \right) t + D - \frac{A}{2} - \frac{B^2}{4}, \end{aligned}$$

so that eq. (3-76) may be written as

$$\frac{d^2y}{dt^2} = (et^2 + ft + g)y, \quad (3-79)$$

where

$$e = \frac{A^2}{4}, \quad f = \frac{AB}{2} - C, \quad g = \frac{B^2}{4} + \frac{A}{2} - D.$$

We next seek a transformation to a new independent variable to remove the linear term  $ft$ . Set

$$t = \alpha_0 \tau + \beta_0 \quad (3-80)$$

and find  $\alpha_0$  and  $\beta_0$  such that eq. (3-79) is transformed to

$$\frac{d^2y}{d\tau^2} = (\tau^2 + h)y, \quad (3-81)$$

where  $h$  is a constant. Comparison of eqs. (3-79) and (3-81) yields

$$\alpha_0^{-4} e = \alpha_0^{-4} A^2/4 = 1.$$

For positive ramp rate  $\gamma$ ,  $A$  is negative by eq. (3-73). Therefore, to make  $\alpha_0$  real, choose  $\alpha_0^{-2} A/2 = -1$ , or

$$\alpha_0 = \pm \sqrt{(-2/A)} = \pm \sqrt{(2\ell/\gamma)}.$$

The case of negative  $\gamma$  is similar and will not be treated here.

Further comparison of eqs. (3-79) and (3-81) yields

$$\beta_0 = \frac{2C - AB}{A^2} = \frac{\ell}{\gamma} \left( \frac{\beta - \rho_0}{\ell} - \lambda \right)$$

and

$$h = \frac{2D}{A} - \frac{2BC}{A^2} + \frac{2C^2}{A^3} - 1 = 1 + \frac{2\lambda\beta}{\gamma},$$

where we have used eq. (3-73) to recover the physical parameters. Eq. (3-81) is therefore

$$\frac{d^2y}{d\tau^2} = \left(\tau^2 + \frac{2\lambda\beta}{\gamma} + 1\right)y, \quad (3-82)$$

where the original independent variable is

$$\tau = \pm \tau \sqrt{\left(\frac{2\ell}{\gamma}\right) + \frac{\ell}{\gamma} \left(\frac{\beta - \rho_0}{\ell} - \lambda\right)}. \quad (3-83)$$

Finally we compare with Weber's differential equation

$$y'' = \left(\frac{x^2}{4} - v - \frac{1}{2}\right)y$$

for the parabolic cylinder functions  $y = D_v(x)$  (Whittaker and Watson 1952) and conclude that the solution of eq. (3-82) is a parabolic cylinder function of negative order  $v = -1 - \lambda\beta/\gamma$ . The complete solution of eq. (3-82) is a linear combination of two linearly independent parabolic cylinder functions or of two confluent hypergeometric functions.

We do not pursue the general case further, but instead we consider the special case when  $v$  is an integer. In this case, the functions  $D_v$  reduce to Hermite functions, which for negative order can be expressed in terms of the error function. We proceed to generate the error-function solutions directly from the differential equation.

We work with an integer  $\mu$ , defined as

$$\mu = \lambda\beta/\gamma, \quad (3-84)$$

and generate solutions of

$$\frac{d^2y}{d\tau^2} = (\tau^2 + 2\mu + 1)y. \quad (3-85)$$

Consider the function  $Y = e^{a\tau^2}$ , which satisfies

$$\frac{d^2Y}{d\tau^2} = (4a^2\tau^2 + 2a)Y$$

and will therefore satisfy eq. (3-85) for  $\mu = 0$  if  $a = \frac{1}{2}$ , or for  $\mu = -1$  if  $a = -\frac{1}{2}$ . Denote these particular solutions as

$$\begin{aligned} Y_0 &= e^{\frac{1}{2}\tau^2}, & \mu &= 0; \\ Y_{-1} &= e^{-\frac{1}{2}\tau^2}, & \mu &= -1. \end{aligned}$$

8.2      *Time-dependent Reactivity*

We are interested in nonnegative  $\mu$ . For  $\mu = 0$ , a second solution  $Y_0^*$  can be found by setting

$$Y_0^* = X_0 e^{\frac{1}{2}\tau^2}.$$

Substituting into

$$\frac{d^2y}{d\tau^2} = (\tau^2 + 1)y$$

yields

$$\frac{d^2X_0}{d\tau^2} + 2\tau \frac{dX_0}{d\tau} = 0,$$

$$\frac{dX_0}{d\tau} = e^{-\tau^2},$$

$$X_0 = \int_0^\tau e^{-\xi^2} d\xi = \frac{\sqrt{\pi}}{2} \operatorname{erf} \tau.$$

Two linearly independent solutions of eq. (3-85) for  $\mu = 0$  are therefore

$$Y_0 = e^{\frac{1}{2}\tau^2}$$

and

$$Y_0^* = e^{\frac{1}{2}\tau^2} \int_0^\tau e^{-\xi^2} d\xi.$$

The complete solution for  $\mu = 0$  may be written

$$y_0 = C_0 Y_0 + C_0^* Y_0^* = e^{\frac{1}{2}\tau^2} \left( C_0 + C_0^* \int_0^\tau e^{-\xi^2} d\xi \right), \quad (3-87)$$

where  $C_0$  and  $C_0^*$  are constants.

For other values of  $\mu$ , consider the functions  $V_\mu$  defined by

$$Y_\mu = e^{-\frac{1}{2}\tau^2} V_\mu. \quad (3-88)$$

Substituting in eq. (3-85), we find that  $V_\mu$  satisfies

$$\frac{d^2V_\mu}{d\tau^2} - 2\tau \frac{dV_\mu}{d\tau} - 2(\mu + 1)V_\mu = 0. \quad (3-89)$$

Differentiating gives

$$\frac{d^3V_\mu}{d\tau^3} - 2\tau \frac{d^2V_\mu}{d\tau^2} - 2(\mu + 2) \frac{dV_\mu}{d\tau} = 0.$$

Compare this result with eq. (3-89) rewritten with  $\mu$  replaced by  $\mu + 1$ :

$$\frac{d^2 V_{\mu+1}}{d\tau^2} - 2\tau \frac{dV_{\mu+1}}{d\tau} - 2(\mu + 2)V_{\mu+1} = 0.$$

We identify

$$\frac{dV_{\mu}}{d\tau} = V_{\mu+1}$$

and

$$\frac{d^2 V_{\mu}}{d\tau^2} = \frac{dV_{\mu+1}}{d\tau} = V_{\mu+2}.$$

When these relations are used, eq. (3-89) becomes a recurrence relation for the functions  $V_{\mu}$ :

$$V_{\mu+2} - 2\tau V_{\mu+1} - 2(\mu + 1)V_{\mu} = 0.$$

By eq. (3-88), the functions  $Y_{\mu}$  satisfy the same relation,

$$Y_{\mu+2} - 2\tau Y_{\mu+1} - 2(\mu + 1)Y_{\mu} = 0; \quad (3-90)$$

therefore, if we know two of the functions in the set  $Y_{\mu}$  we can generate the rest.

Setting  $\mu = -1$  in eq. (3-90) yields

$$Y_1 = 2\tau Y_0 = 2\tau e^{\frac{1}{2}\tau^2}.$$

A second solution  $Y_1^*$  may be found by the procedure employed for finding  $Y_0^*$ . The result is

$$Y_1^* = e^{-\frac{1}{2}\tau^2} + 2\tau e^{\frac{1}{2}\tau^2} \int_0^{\tau} e^{-\xi^2} d\xi.$$

Functions  $V_{\mu}^*$  analogous to  $V_{\mu}$  may be defined and shown to satisfy the same recurrence relation.

To summarize, the solution of eq. (3-85)

$$\frac{d^2 y}{d\tau^2} = (\tau^2 + 2\mu + 1)y$$

for integer values of  $\mu$  is given by

$$y_{\mu} = C_{\mu} Y_{\mu} + C_{\mu}^* Y_{\mu}^*, \quad (3-91)$$

where

$$\begin{aligned} Y_0 &= e^{\frac{1}{2}\tau^2}, \\ Y_0^* &= e^{\frac{1}{2}\tau^2} \int_0^{\tau} e^{-\xi^2} d\xi, \\ Y_1 &= 2\tau e^{\frac{1}{2}\tau^2}, \end{aligned}$$

### + Time-dependent Reactivity

$$Y_1^* = e^{-\frac{1}{4}\tau^2} + 2\tau e^{\frac{1}{4}\tau^2} \int_0^\tau e^{-\xi^2} d\xi,$$

$$Y_{\mu+2} = 2\tau Y_{\mu+1} + 2(\mu+1)Y_\mu,$$

$$Y_{\mu+2}^* = 2\tau Y_{\mu+1}^* + 2(\mu+1)Y_\mu^*.$$

This may be expressed more compactly by noting that

$$V_\mu = \frac{d^\mu}{d\tau^\mu}(V_0) = \frac{d^\mu}{d\tau^\mu}(e^{\tau^2}),$$

and

$$V_\mu^* = \frac{d^\mu}{d\tau^\mu}(V_0^*) = \frac{d^\mu}{d\tau^\mu} \left( e^{\tau^2} \int_0^\tau e^{-\xi^2} d\xi \right),$$

so that eq. (3-91) becomes

$$y_\mu = e^{-\frac{1}{4}\tau^2} \frac{d^\mu}{d\tau^\mu} \left[ e^{\tau^2} \left( C_\mu + C_\mu^* \int_0^\tau e^{-\xi^2} d\xi \right) \right]. \quad (3-92)$$

The solution of eq. (3-72) for integer values of  $\mu$  is  $n = xy_\mu$ , where  $x$  is given by eq. (3-78). In terms of the physical parameters,

$$x = \exp \left[ \frac{\gamma}{4\ell} \left( t - \frac{\beta + \lambda\ell - \rho_0}{\gamma} \right)^2 \right],$$

and if we use the transformation eq. (3-83),

$$e^{-\frac{1}{4}\tau^2} = \exp \left[ -\frac{\gamma}{4\ell} \left( t - \frac{\beta - \lambda\ell - \rho_0}{\gamma} \right)^2 \right].$$

Therefore

$$xe^{-\frac{1}{4}\tau^2} = e^{-\lambda t},$$

and the solution for integer values of  $\mu = \lambda\beta/\gamma$  may finally be expressed as

$$n(t) = e^{-\lambda t} \frac{d^\mu}{d\tau^\mu} \left[ e^{\tau^2} \left( C_\mu + C_\mu^* \int_0^\tau e^{-\xi^2} d\xi \right) \right], \quad (3-93)$$

where  $\tau$  is defined by eq. (3-83).

In particular, for the special cases  $\mu = 0$  and  $\mu = 1$  with  $q = 0$  and  $\rho_0 = 0$ , and with initial equilibrium  $n(0) = n_0$ , we find

$$\begin{aligned} \frac{n}{n_0} &= \left[ 1 + \beta \left( \frac{\pi}{2\gamma\ell} \right)^{1/2} \left( \exp \frac{\beta^2}{2\gamma\ell} \right) \left( \operatorname{erf} \frac{\beta}{\sqrt{2\gamma\ell}} - \operatorname{erf} \frac{\beta - \gamma t}{\sqrt{2\gamma\ell}} \right) \right] \\ &\quad \times \exp \left( \frac{\gamma}{2\ell} t^2 - \frac{\beta}{\ell} t \right), \quad \lambda\beta/\gamma = 0, \quad (3-94) \end{aligned}$$

and

$$\begin{aligned} \frac{n}{n_0} = & \frac{\beta^2}{\gamma\ell} \left\{ e^{-\lambda t} - \frac{\beta - \lambda\ell - \gamma t}{\beta} \exp \left( \frac{\gamma}{2\ell} t^2 - \frac{\beta}{\ell} t \right) \right. \\ & \times \left[ 1 + \beta \left( \frac{\pi}{2\gamma\ell} \right)^{1/2} \exp \frac{(\beta - \lambda\ell)^2}{2\gamma\ell} \right. \\ & \left. \left. \left( \operatorname{erf} \frac{\beta - \lambda\ell}{\sqrt{(2\gamma\ell)}} - \operatorname{erf} \frac{\beta - \lambda\ell - \gamma t}{\sqrt{(2\gamma\ell)}} \right) \right] \right\}, \quad \lambda\beta/\gamma = 1, \quad (3-95) \end{aligned}$$

where

$$\operatorname{erf} \tau = \frac{2}{\sqrt{\pi}} \int_0^\tau e^{-\xi^2} d\xi.$$

It can be verified that eq. (3-94) is the solution of eq. (3-34) with  $\rho = \gamma t$ , and is therefore the ramp-input response in the constant-source approximation (small  $\lambda$ ), or, from another viewpoint, the rapid-rate approximation (large  $\gamma$ ).

From eq. (3-83),

$$\pm\tau = \frac{1}{\sqrt{(2\gamma\ell)}} [\gamma t - (\beta - \lambda\ell - \rho_0)]. \quad (3-96)$$

By eq. (3-71), this vanishes at  $\rho = \beta - \lambda\ell$ , which is slightly below prompt critical. For convenience we choose the negative sign in eq. (3-96). For much of the range below prompt critical,  $\tau$  is sufficiently large that one can use the asymptotic expansion

$$\operatorname{erf} \tau = 1 - \frac{e^{-\tau^2}}{\tau\sqrt{\pi}} \left[ 1 - \frac{1}{2\tau^2} + \frac{1 \cdot 3}{(2\tau^2)^2} - \frac{1 \cdot 3 \cdot 5}{(2\tau^2)^3} + \dots \right].$$

From eqs. (3-94) and (3-95) we find

$$\begin{aligned} \frac{n}{n_0} = & \frac{\beta}{\beta - \gamma t} \left( 1 - \frac{1}{u^2} + \frac{1 \cdot 3}{u^4} - \frac{1 \cdot 3 \cdot 5}{u^6} + \dots \right), \\ \lambda\beta/\gamma = 0, \quad (3-97) \end{aligned}$$

where

$$u = \frac{\beta - \gamma t}{\sqrt{(\gamma\ell)}}$$

and

$$\frac{n}{n_0} = \frac{\beta^2}{\gamma\ell} e^{-\lambda t} \left( \frac{1}{v^2} - \frac{1 \cdot 3}{v^4} + \frac{1 \cdot 3 \cdot 5}{v^6} - \dots \right), \quad \lambda\beta/\gamma = 1, \quad (3-98)$$

where

$$\nu = \frac{\beta - \lambda\ell - \gamma t}{\sqrt{(\gamma\ell)}}.$$

Since eq. (3-94) is identical to the constant-source approximation, and since  $1/u \rightarrow 0$  as  $\ell \rightarrow 0$ , we might expect that the first term of eq. (3-97) ought to be the same as the result of combining the prompt-jump and constant-source approximations. This is verified by consulting eq. (3-35).

Also, since  $1/\nu \rightarrow 0$  as  $\ell \rightarrow 0$ , we might expect that the first term of eq. (3-98) is the ramp-input response for  $\lambda\beta/\gamma = 1$  in the prompt-jump approximation. To verify this, solve eq. (3-19),

$$(\beta - \rho) \frac{dn}{dt} = \left( \lambda\rho + \frac{d\rho}{dt} \right) n,$$

with  $\rho = \gamma t$  and  $n(0) = n_0$ , to find

$$\frac{n}{n_0} = e^{-\lambda t} \left( \frac{\beta}{\beta - \gamma t} \right)^{1 + \lambda\beta/\gamma}. \quad (3-99)$$

Setting  $\lambda\beta/\gamma = 1$  in eq. (3-99) gives the same result as taking the limit in eq. (3-98) for  $\ell \rightarrow 0$ . Note that eq. (3-19) may be solved for the derivative in the form

$$\omega(t) = \frac{1}{n} \frac{dn}{dt} = \frac{1}{\beta - \rho} \left( \lambda\rho + \frac{d\rho}{dt} \right) = \frac{\lambda\rho + \gamma}{\beta - \rho}.$$

The initial value is  $\omega(0) = \gamma/\beta$ , which indicates that the initial derivative is not free to assume arbitrary values. This is of course a consequence of reducing the order of the differential equation and "losing" one initial condition. Here  $n(t)$  is continuous, but the derivative jumps from the true initial value to the value  $\gamma/\beta$ .

The exact solution, eq. (3-95), and the prompt-jump approximation, eq. (3-99), are shown in fig. 3-14 for  $\mu = \lambda\beta/\gamma = 1$ . For comparison, we include the constant-source approximation, eq. (3-94), and the simple formula of eq. (3-35). Numerical values used are  $\lambda = 0.1 \text{ sec}^{-1}$  and  $\beta/\ell = 100 \text{ sec}^{-1}$ ; the ramp rate is 0.1 dollar/sec. It is interesting to study fig. 3-14 with reference to the criteria for validity of the approximations: eq. (3-17) for the prompt-jump approximation and  $t \ll 1/\lambda$  for the constant-source approximation.

As expected from physical grounds, the constant-source approximation, interpreted here as the solution for  $\mu = 0$ , is a lower bound for the set of solutions for  $\mu = 1, 2, \dots$ , etc. Physically, curves for noninteger values of  $\mu$  might be expected to fill in smoothly between those for the integers. That this is true can be deduced from the integral representa-

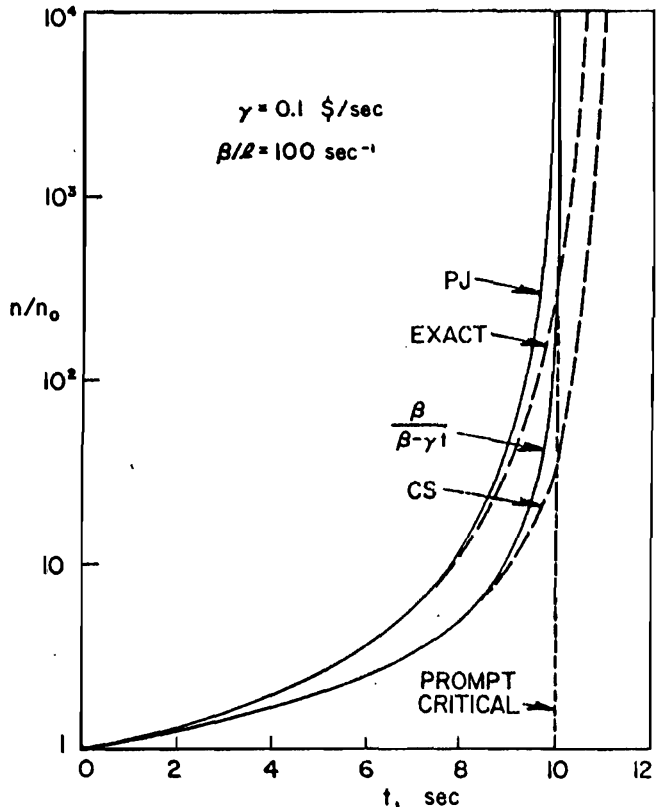


Fig. 3-14. Ramp-input response for one delay group (reactor initially critical;  $\gamma = 0.1$  dollar/sec,  $\beta/\lambda = 100 \text{ sec}^{-1}$  and  $\lambda = 0.1 \text{ sec}^{-1}$ ). The exact solution is eq. (3-95), the prompt-jump approximation is eq. (3-99), and the constant-source approximation is eq. (3-94).

tions derived in the next section; hence the case  $\mu = 0$  is a lower bound for the curves for  $\mu > 0$ , other parameters being the same.

Finally, note that the exact solution is fairly well represented by the prompt-jump approximation until very near prompt critical, where it suddenly diverges. It must be remembered, however, that the simple formula of eq. (3-99) cannot be expected to represent the exact six-delay-group solution nearly as well once the reactivity exceeds a substantial fraction of  $\beta$ . The numerical value of  $\lambda$ , chosen for slow transients, cannot represent the delayed neutrons once the rate of rise becomes large, and unfortunately eq. (3-99) is highly sensitive to the value of  $\lambda$ . This difficulty is avoided if one uses the six-delay-group prompt-jump approximation, which, as discussed in chapter 4, is

### §3. Time-dependent Reactivity

extremely helpful in circumventing numerical difficulties. The one-group prompt-jump approximation has more practical uses in representing reactor startup; this is treated in a later section of this chapter.

In spite of their limitations, the solutions described in this section serve to provide a feeling for the demands on reactor safety systems in the event of accidental reactivity increase. More important, they illustrate dramatically the practical need for safeguards designed to prevent such reactivity increases.

Exact solutions in terms of special functions have been derived for two other cases: reactivity varying inversely with time, and exponentially with time. For details see the paper by Smets (1958).

#### 3-4. Ramp-Input Response: Integral Representations

An alternative approach to the ramp-input problem is afforded by means of integral representations (Wallach 1950; Smets 1958; Wilkins 1959). The appropriate representation is a generalization of the Laplace inversion integral, introduced because the ordinary Laplace transform of the solution for  $\gamma > 0$  does not exist. The solutions obtained in the preceding section are strongly dominated at large  $t$  by the factor

$$\exp\left(\frac{\gamma}{2\ell}t^2 - \frac{\beta}{\ell}t\right),$$

which incidentally is easily recognized as a particular solution for the Nordheim-Fuchs model, eq. (3-28), when  $\rho = \gamma t$ . The treatment here is restricted to  $\gamma > 0$ ; the solution for  $\gamma < 0$ , which is Laplace-transformable, is discussed by Ash (1965).

The integral representations are useful in that they yield simple approximate formulas for the power and period at the time of prompt critical. Also, the error-function formulas of the previous section provide little information about large ramp rates;  $\mu = 1$  corresponds to a ramp rate of the order of ten cents per second, while larger  $\mu$  corresponds to smaller ramp rates and more complicated formulas.

We seek integral representations for the solution of eq. (3-72) with  $q = q_0$ ,

$$\frac{d^2n}{dt^2} + (At + B)\frac{dn}{dt} + (Ct + D)n = \lambda q_0, \quad (3-100)$$

where the constants are defined by eq. (3-73). We postulate a particular solution of the form

$$n(t) = \int_{\Gamma} F(s)e^{st} ds, \quad (3-101)$$

where the integration contour  $\Gamma$  in the complex  $s$ -plane is as yet unknown (except that it cannot be the Laplace inversion contour). Assume that the integrand at the endpoints is independent of time. Then

$$\frac{dn}{dt} = \int_{\Gamma} sF(s)e^{st} ds,$$

and

$$\frac{d^2n}{dt^2} = \int_{\Gamma} s^2F(s)e^{st} ds.$$

By partial integration it is easily found that

$$tn = Fe^{st}\Big|_{\Gamma} - \int_{\Gamma} \frac{dF}{ds} e^{st} ds.$$

Differentiating and solving for  $t$  ( $dn/dt$ ) yields

$$t \frac{dn}{dt} = -n - \int_{\Gamma} s \frac{dF}{ds} e^{st} ds.$$

Substituting into eq. (3-100), we find

$$\begin{aligned} \int_{\Gamma} (s^2 + Bs + D - A)Fe^{st} ds - \int_{\Gamma} (C + As) \frac{dF}{ds} e^{st} ds \\ = \lambda q_0 - CF e^{st}\Big|_{\Gamma}. \end{aligned}$$

If we choose the contour  $\Gamma$  such that

$$\lambda q_0 = CF e^{st}\Big|_{\Gamma},$$

that is, if

$$\gamma F e^{st}\Big|_{\Gamma} + \ell q_0 = 0, \quad (3-102)$$

then  $F$  satisfies the first-order differential equation

$$\frac{dF}{ds} + \frac{A - D - Bs - s^2}{C + As} F = 0. \quad (3-103)$$

Eq. (3-102) is consistent with the assumption that the integrand at the endpoints is independent of  $t$ .

Eq. (3-103) may be written

$$\frac{dF}{ds} + U(s) F(s) = 0, \quad (3-104)$$

(m) *Time-dependent Reactivity*

where

$$U(s) = \frac{A - D - Bs - s^2}{C + As}.$$

Referring to eq. (3-73), we obtain

$$U(s) = \frac{\ell s^2 + (\beta + \lambda\ell - \rho_0)s - \lambda\rho_0}{\gamma(s + \lambda)}.$$

It will prove convenient to rewrite this as

$$U(s) = \frac{1}{\gamma} \left( \ell s + \beta + \rho_0 - \frac{\beta\lambda}{s + \lambda} \right). \quad (3-105)$$

The solution of eq. (3-104) may be written as

$$F(s) = \exp \left[ - \int U(s) ds \right]$$

Using eq. (3-105), we have

$$F(s) = (s + \lambda)^{\lambda\beta/\gamma} \exp \left( -\frac{\ell}{2\gamma} s^2 - \frac{\beta - \rho_0}{\gamma} s \right). \quad (3-106)$$

It remains only to select appropriate integration contours for eq. (3-101). For  $q_0 = 0$ , eq. (3-100) is homogeneous. Eq. (3-102) is satisfied if the integrand vanishes at both endpoints of the contour. By eq. (3-106),  $F e^{st}$  vanishes for  $s = -\lambda$  and  $s \rightarrow \pm\infty$ . Hence, for two linearly independent solutions of the homogeneous equation, we choose for contours the two segments of the real axis:  $-\infty$  to  $-\lambda$  and  $-\lambda$  to  $\infty$ . The complete solution of the homogeneous equation is therefore

$$\begin{aligned} n(t) &= C_1 \int_{-\infty}^{-\lambda} (s + \lambda)^{\lambda\beta/\gamma} \exp \left[ -\frac{\ell}{2\gamma} s^2 - \left( \frac{\beta - \rho_0}{\gamma} - t \right) s \right] ds \\ &\quad + C_2 \int_{-\lambda}^{\infty} (s + \lambda)^{\lambda\beta/\gamma} \exp \left[ -\frac{\ell}{2\gamma} s^2 - \left( \frac{\beta - \rho_0}{\gamma} - t \right) s \right] ds, \\ q_0 &= 0. \end{aligned} \quad (3-107)$$

The complete solution of eq. (3-100) is found by adding to eq. (3-107) a particular integral chosen such that eq. (3-102) is satisfied. A convenient choice of contour is the real axis from 0 to  $\infty$ . The result is

$$\frac{q_0}{\gamma} \int_0^{\infty} \left( \frac{s + \lambda}{\lambda} \right)^{\lambda\beta/\gamma} \exp \left[ -\frac{\ell}{2\gamma} s^2 - \left( \frac{\beta - \rho_0}{\gamma} - t \right) s \right] ds. \quad (3-108)$$

The complete solution is therefore the sum of eqs. (3-107) and (3-108).

The procedure is easily adapted for  $m$  groups of delayed neutrons.

One still obtains a first-order differential equation for  $F$ , with eq. (3-105) replaced by

$$U(s) = \frac{1}{\gamma} \left( \ell s + \beta - \rho_0 - \sum_i \frac{\beta_i \lambda_i}{s + \lambda_i} \right),$$

and with, in eq. (3-106),

$$(s + \lambda)^{\lambda \beta / \gamma} \rightarrow \prod_i (s + \lambda_i)^{\gamma_i \beta_i / \gamma}.$$

The solution of the homogeneous equation has  $m + 1$  terms, obtained by integrating on the real axis from  $-\infty$  to  $-\lambda_m$ ,  $-\lambda_m$  to  $-\lambda_{m-1}, \dots, -\lambda_1$  to  $\infty$ .

Because of the factor  $e^{\ell s}$  in the integrand, the dominant term as  $t$  increases will be the integral with upper limit  $\infty$ . We therefore study the  $C_2$  term in eq. (3-107) to gain information about the source-free ramp-input response for large  $t$ . Let

$$n(t) \cong C_2 I(t), \quad (3-109)$$

where

$$I(t) = \int_{-\lambda}^{\infty} (s + \lambda)^{\mu} \exp \left[ -\frac{\ell}{2\gamma} s^2 - \left( \frac{\beta - \rho_0}{\gamma} - t \right) s \right] ds, \quad (3-110)$$

with  $\mu = \lambda \beta / \gamma$  as in the previous section. The form of eq. (3-110) is suggestive of the gamma function

$$\Gamma(\xi) = \int_0^{\infty} y^{\xi-1} e^{-y} dy \quad (3-111)$$

because of the relationship

$$\int_0^{\infty} z^{\mu} e^{-az^2} dz = \frac{\Gamma\left(\frac{\mu+1}{2}\right)}{2a^{(\mu+1)/2}}. \quad (3-112)$$

Consider the transformation

$$\begin{aligned} z &= \left(\frac{\ell}{2\gamma}\right)^{\frac{1}{2}} (s + \lambda), \\ x &= \left(\frac{2\gamma}{\ell}\right)^{\frac{1}{2}} \left( \frac{\beta - \lambda\ell - \rho_0}{\gamma} - t \right). \end{aligned} \quad (3-113)$$

Note  $z = 0$  at  $s = -\lambda$ , and  $x = 0$  at

$$t = t^* = \frac{\beta - \lambda\ell - \rho_0}{\gamma},$$

12      *Time-independent Reactivity*

where  $t^*$  is a time very slightly before prompt critical when the reactivity is  $\rho = \beta - \lambda\ell$ .

Eq. (3-110) becomes

$$I(t) = \left(\frac{2\gamma}{\ell}\right)^{(\mu+1)/2} \exp\left[\lambda\left(\frac{\ell}{2\gamma}\right)^{\frac{1}{2}} x + \frac{\lambda^2\ell}{2\gamma}\right] \int_0^\infty z^\mu e^{-z^2-xz} dz. \quad (3-114)$$

Near prompt critical, at  $x = 0$  and  $t = t^*$ , we have from eqs. (3-112) and (3-114)

$$I(t^*) = \frac{1}{2} \left(\frac{2\gamma}{\ell}\right)^{(\mu+1)/2} e^{\lambda^2\ell/2\gamma} \Gamma\left(\frac{\mu+1}{2}\right). \quad (3-115)$$

If we write  $n = n_0$  and  $x = x_0$  at  $t = 0$ , we have

$$\frac{n}{n_0} \cong \frac{I(t)}{I(0)} = \exp\left[\lambda\left(\frac{\ell}{2\gamma}\right)^{\frac{1}{2}} (x - x_0)\right] \frac{\int_0^\infty z^\mu e^{-z^2-xz} dz}{\int_0^\infty z^\mu e^{-z^2-x_0z} dz}.$$

From eq. (3-113),

$$x - x_0 = -\left(\frac{2\gamma}{\ell}\right)^{\frac{1}{2}} t,$$

and we find

$$\frac{n}{n_0} \cong e^{-\lambda t} \frac{\int_0^\infty z^\mu e^{-z^2-xz} dz}{\int_0^\infty z^\mu e^{-z^2-x_0z} dz}. \quad (3-116)$$

We can obtain a simple approximation to the integral in the denominator. Since

$$x_0 = \left(\frac{2}{\gamma\ell}\right)^{\frac{1}{2}} (\beta - \lambda\ell - \rho_0) \cong \left(\frac{2}{\gamma\ell}\right)^{\frac{1}{2}} (\beta - \rho_0)$$

is large compared to unity, especially for small  $\ell$ , the factor  $e^{-x_0z}$  will fall off much more rapidly than  $e^{-z^2}$ . For the significant part of the range of integration,  $e^{-z^2} \cong 1$ , and the integral in the denominator of eq. (3-116) is approximately

$$\int_0^\infty z^\mu e^{-x_0z} dz = \frac{\Gamma(\mu+1)}{x_0^{\mu+1}}. \quad (3-117)$$

Near prompt critical ( $t = t^*$ ) we can use eqs. (3-112) and (3-117) to reduce eq. (3-116) to

$$\frac{n(t^*)}{n_0} \cong \frac{1}{2} e^{-\lambda t^*} x_0^{\mu+1} \frac{\Gamma\left(\frac{\mu+1}{2}\right)}{\Gamma(\mu+1)}. \quad (3-118)$$

If  $\rho_0 = 0$ , then  $t^* \cong \beta/\gamma$  and  $x_0 \cong \beta\sqrt{(2/\gamma\ell)}$ . The power at prompt critical is thus

$$\frac{n(t^*)}{n_0} \cong \frac{1}{2} e^{-\mu} \left(\frac{2\beta^2}{\gamma\ell}\right)^{(\mu+1)/2} \frac{\Gamma\left(\frac{\mu+1}{2}\right)}{\Gamma(\mu+1)}. \quad (3-119)$$

For a very fast ramp,  $\mu = \lambda\beta/\gamma \rightarrow 0$ , eq. (3-119) reduces to

$$\frac{n(t^*)}{n_0} \cong \beta \sqrt{\frac{\pi}{2\gamma\ell}}. \quad (3-120)$$

Note that the error-function formula for  $\mu = 0$ , eq. (3-94), yields the same result for  $t = \beta/\gamma$  if  $\ell$  is small.

The inverse period, defined as

$$\omega = \frac{1}{n} \frac{dn}{dt}, \quad (3-121)$$

may also be evaluated at  $t = t^*$ . We take the time derivative in eq. (3-110) and use eqs. (3-112), (3-113), and (3-115) to find

$$\omega(t^*) \cong -\lambda + \left(\frac{2\gamma}{\ell}\right)^{\frac{1}{2}} \frac{\Gamma\left(\frac{\mu+2}{2}\right)}{\Gamma\left(\frac{\mu+1}{2}\right)}. \quad (3-122)$$

The term  $-\lambda$  will generally prove to be negligible. For a fast ramp ( $\mu \ll 1$ ), eq. (3-122) reduces to

$$\omega(t^*) \cong \sqrt{\frac{2\gamma}{\pi\ell}}. \quad (3-123)$$

For a slow ramp ( $\mu \rightarrow \infty$ ) we use the asymptotic form

$$\Gamma(\xi+1) \rightarrow e^{-\xi}\xi^\xi \sqrt{(2\pi\xi)} \quad (3-124)$$

and find that

$$\omega(t^*) \cong \sqrt{\frac{\lambda\beta}{\ell}}. \quad (3-125)$$

### 3.1 Time-dependent Reactivity

Wilkins (1959) treats this problem for  $m$  delay groups and finds, instead of eq. (3-125),

$$\omega(t^*) \cong \sqrt{\frac{\sum_i \lambda_i \beta_i}{\ell}}. \quad (3-126)$$

This confirms the notion that one should use the mean decay constant  $\lambda'$  instead of  $\lambda$  near prompt critical when the rate of rise is large. In fig. 3-15 (Wilkins 1959) we plot  $\sqrt{(\ell/\beta)}$  times the reciprocal period at prompt critical as a function of the ramp rate. This was computed from a generalized form of eq. (3-122) for six delay groups. (A slightly different set of U<sup>235</sup> delayed-neutron data was used.)

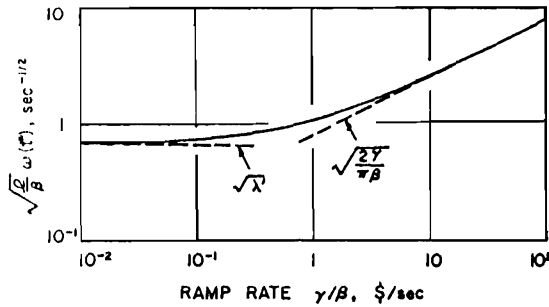


Fig. 3-15. Reciprocal period at prompt critical vs. reactivity insertion rate (Wilkins 1959).

Similar techniques may be employed to verify some of the approximations used elsewhere. If the reactor is not too near prompt critical (i.e., if  $x$  is not too small) we can expand  $e^{-z^2}$  in a power series and integrate term by term in eq. (3-116). We obtain for one integral,

$$\int_0^x z^\mu e^{-z^2 - xz} dz = \frac{\Gamma(\mu + 1)}{x^{\mu+1}} - \frac{\Gamma(\mu + 3)}{x^{\mu+3}} + \frac{\Gamma(\mu + 5)}{2x^{\mu+5}} - \dots,$$

and a similar result for the integral containing  $x_0$ . Treating  $\ell$  as small, we retain only the first term in each series to find

$$\frac{n}{n_0} \cong e^{-\lambda t} \left( \frac{\beta - \rho_0 - \lambda \ell}{\beta - \rho_0 - \lambda \ell - \gamma t} \right)^{\mu+1},$$

which becomes eq. (3-99), the prompt-jump approximation, if  $\rho_0 = 0$  and  $\lambda \ell$  is small.

Finally, we note the result of treating  $\lambda$  as negligibly small in the integral representation for large  $t$ . From eqs. (3-109) and (3-110) with  $\rho_0 = 0$  and  $\lambda \rightarrow 0$ ,

$$n \cong C_2 \int_0^\infty \exp \left[ -\frac{\ell}{2\gamma} s^2 - \left( \frac{\beta}{\gamma} - t \right) s \right] ds. \quad (3-127)$$

This is a standard integral, which yields

$$n \cong C_2 \left( \frac{2\pi\gamma}{\ell} \right)^{\frac{1}{2}} \exp(\beta^2/2\gamma\ell) \cdot \exp\left(\frac{\gamma}{2\ell}t^2 - \frac{\beta}{\ell}t\right). \quad (3-128)$$

Compare with eq. (3-94), which is the limiting form for large ramp rates ( $\mu \rightarrow 0$ ) and which for large  $t$  is approximately

$$n \cong 2n_0\beta \left( \frac{\pi}{2\gamma\ell} \right)^{\frac{1}{2}} \exp(\beta^2/2\gamma\ell) \cdot \exp\left(\frac{\gamma}{2\ell}t^2 - \frac{\beta}{\ell}t\right). \quad (3-129)$$

Here we have used

$$\operatorname{erf}\frac{\beta}{\sqrt{(2\gamma\ell)}} \cong 1$$

and

$$\lim_{t \rightarrow \infty} \operatorname{erf}\frac{\beta - \gamma t}{\sqrt{(2\gamma\ell)}} = -1.$$

From eqs. (3-128) and (3-129) we obtain an estimate of  $C_2$  for fast ramps:

$$C_2 \cong \frac{\beta}{\gamma} n_0. \quad (3-130)$$

As mentioned at the beginning of this section, these asymptotic forms are particular solutions of the Nordheim-Fuchs model, eq. (3-28), for  $\rho = \gamma t$ . For a fast ramp, we can achieve an approximate matching of exact and asymptotic solutions. The asymptotic solution, eq. (3-129), extrapolates back to prompt critical ( $t = \beta/\gamma$ ) with an overestimate of  $n(t^*)$ ,

$$n(t^*) \cong 2n_0\beta \sqrt{\frac{\pi}{2\gamma\ell}}, \quad (3-131)$$

while eq. (3-120), or eq. (3-94) at  $t = \beta/\gamma$ , gives a better estimate:

$$n(t^*) \cong n_0\beta \sqrt{\frac{\pi}{2\gamma\ell}}.$$

We see that the asymptotic solution, eq. (3-129), becomes a good approximation to eq. (3-94) soon after prompt critical is reached, and that the overestimate is only a factor of two at prompt critical. This is sketched in fig. 3-16.

In chapter 5 we will use eq. (3-131) to estimate "initial conditions" for fast self-limiting ramp-induced excursions in which the delayed-neutron production rate is negligible. An indication of this negative-

leedback effect is included in fig. 3-16. Keep in mind, however, that this sketch is for very high ramp rates; slower transients will be self-limiting before prompt critical is reached.

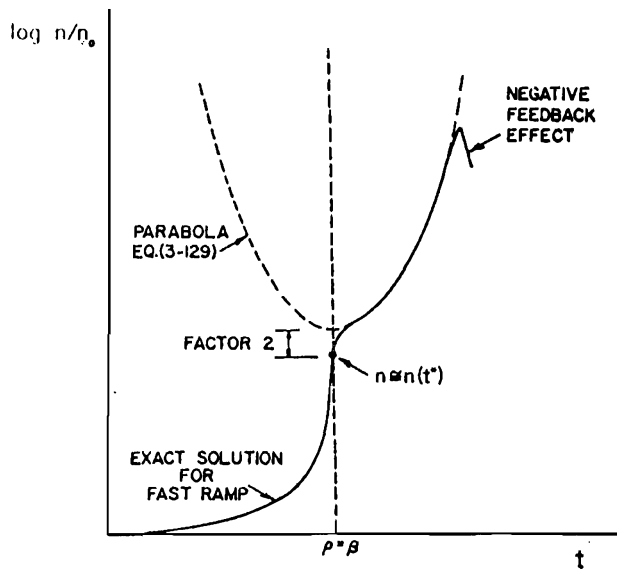


Fig. 3-16. Qualitative comparison of exact and asymptotic ramp-input response for limiting case of fast ramp, eqs. (3-94) and (3-129), including indication of negative feedback effect.

### 3-5. Reactor Startup

Detailed procedures and instrumentation requirements for bringing a reactor from a subcritical source-sustained shutdown level up to operating power are described by many writers (e.g., Harrer 1963; Keppin 1965; Schultz 1961) and will not be repeated here. A major consideration is the wide range of neutron density to be monitored, eight or ten decades not being unusual. Another feature of interest is the possibility that an accident during startup might be more severe than an accident occurring during normal operation; this possibility arises because the reactor could conceivably shoot past its nominal operating level at a high rate of power increase, reducing the time available for the action of automatic safety systems.

In this section we treat an idealized startup accident as a ramp insertion of reactivity starting from a low source-sustained equilibrium and continuing past critical (e.g., failure to halt control-rod withdrawal).

The utility of the prompt-jump approximation for this problem is demonstrated, and simple approximate formulas are obtained for instantaneous power and period at the time the reactor reaches criticality. In particular, it is shown that a larger ramp rate implies a lower power but a higher rate of increase (shorter period) at the instant of zero reactivity.

From eq. (3-13), the neutron density is described by

$$(\beta - \rho) \frac{dn}{dt} - \left( \lambda\rho + \frac{d\rho}{dt} \right) n = \lambda\ell q_0, \quad (3-132)$$

where  $q_0$  is a steady source and where the initial level  $n_0$  is given by eq. (2-6):

$$n_0 = -\frac{\ell q_0}{\rho_0} = \frac{\ell q_0}{|\rho_0|}.$$

Recalling that  $\ell q_0$  remains fixed in the limit of small  $\ell$ , we will find it convenient to introduce an effective source,

$$q' = \lambda\ell q_0 = \lambda|\rho_0|n_0. \quad (3-133)$$

With  $\rho = \rho_0 + \gamma t$ , eq. (3-132) becomes

$$(\beta - \rho_0 - \gamma t) \frac{dn}{dt} - (\gamma + \lambda\rho_0 + \lambda\gamma t)n = q'. \quad (3-134)$$

Using standard methods, we may write the complete solution as

$$\begin{aligned} n &= n_0 e^{-\lambda t} \left( \frac{\beta - \rho_0}{\beta - \rho_0 - \gamma t} \right)^{\mu+1} \\ &\quad + \frac{q' e^{-\lambda t}}{\beta - \rho_0 - \gamma t} \int_0^t \left( \frac{\beta - \rho_0 - \gamma t'}{\beta - \rho_0 - \gamma t} \right)^\mu e^{\lambda t'} dt', \end{aligned} \quad (3-135)$$

where  $\mu = \lambda\beta/\gamma$  as before.

The integral can be expressed in terms of simple functions only if  $\mu$  is an integer. For example, the complete solution for  $\mu = 1$  is

$$\begin{aligned} \frac{n}{n_0} &= \left( \frac{\beta - \rho_0}{\beta - \rho_0 - \gamma t} \right)^2 e^{-\lambda t} \\ &\quad + \frac{|\rho_0|}{(\beta - \rho_0 - \gamma t)^2} \left[ \frac{\gamma}{\lambda} + \beta - \rho_0 - \gamma t - \left( \frac{\gamma}{\lambda} + \beta - \rho_0 \right) e^{-\lambda t} \right], \end{aligned} \quad (3-136)$$

where we have used eq. (3-133) to express  $q'$  in terms of  $|\rho_0|$  and  $n_0$ . For larger integers  $\mu$ , standard integral reduction formulas permit the complete solution to be expressed in terms of exponential functions.

An illustrative case for  $\mu = 1$  is shown in fig. 3-17. For simplicity, the numerical values are  $\lambda = 0.1 \text{ sec}^{-1}$ ,  $\beta = 10^{-2}$ ,  $\gamma = 10^{-3} \text{ sec}^{-1}$  (0.1 dollar/sec), and  $\rho_0 = -\beta$ . Included are points from a digital computer solution (one delay group) with  $\ell/\beta = 10^{-2} \text{ sec}$  (computation by P. A. Secker, University of Arizona, 1964). As in fig. 3-14, the agreement is excellent until very nearly prompt critical, although a six-group case would show an earlier departure.

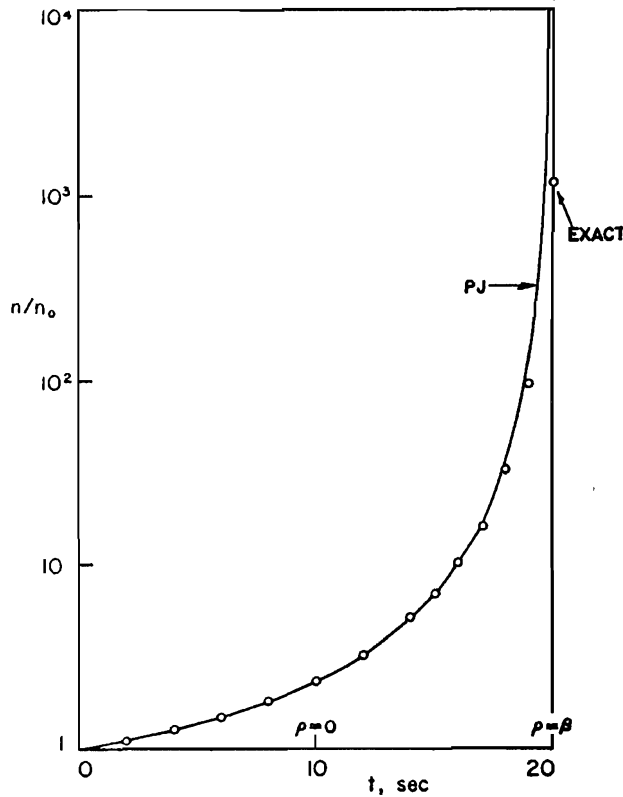


Fig. 3-17. Response to ramp input of 10 cents/sec starting from equilibrium at -1 dollar. One group of delayed neutrons ( $\lambda = 0.1 \text{ sec}^{-1}$ ). Exact solution obtained by digital computer for  $\beta/\ell = 10^{-2} \text{ sec}$ .

The instantaneous reciprocal period in this approximation is, by eqs. (3-132) and (3-133),

$$\omega(t) = \frac{1}{n} \frac{dn}{dt} = \frac{1}{\beta - \rho} \left[ \lambda\rho + \frac{d\rho}{dt} + \lambda|\rho_0| \frac{n_0}{n} \right]. \quad (3-137)$$

Note that the initial value of  $\omega$ ,

$$\omega(0) = \frac{1}{\beta - \rho_0} \frac{d\rho}{dt} = \frac{\gamma}{\beta - \rho_0}, \quad (3-138)$$

cannot correspond to equilibrium in this approximation. The starting transient in  $\omega$ , which dies out in a time of the order of  $\ell/(\beta - \rho_0)$ , has been replaced by a jump from  $\omega = 0$  to the value given by eq. (3-138).

The instantaneous period  $T = 1/\omega$  for the example of fig. 3-17 is plotted in fig. 3-18 as a function of the instantaneous reactivity. Also shown are upper and lower bounds on the instantaneous period. The upper bound

$$T_{\max} = \frac{\ell}{\rho - \beta} \quad (3-139)$$

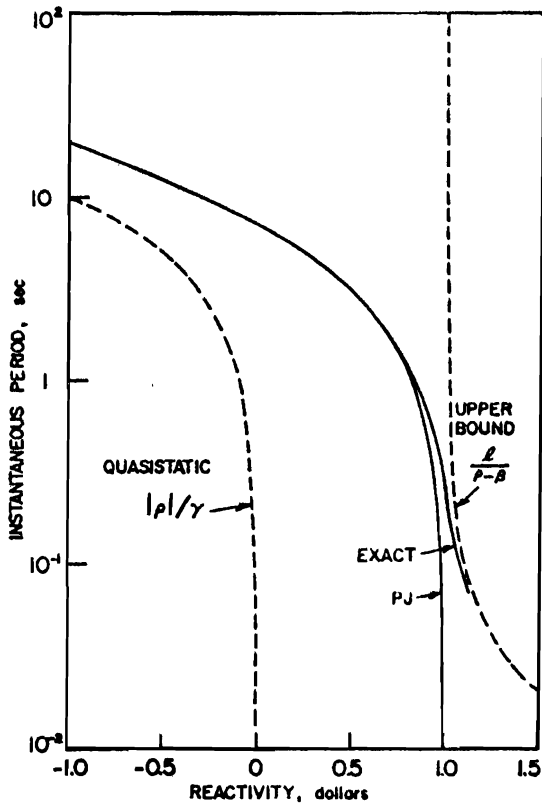


Fig. 3-18. Instantaneous period as a function of instantaneous reactivity for the example of fig. 3-17. Upper and lower bounds are from eqs. (3-139) and (3-141).

may be quickly established from eq. (3-1), while the lower bound is obtained from the quasi-static limit of eq. (2-3):

$$n(t) \cong -\frac{\ell q}{\rho(t)}. \quad (3-140)$$

The proof that the quasi-static period

$$T_{\min} = \frac{|\rho|}{\gamma} \quad (3-141)$$

is a lower bound is left as an exercise.

For  $\mu$  not an integer the problem is more complex. Fortunately, for large  $\mu$  it is possible to derive a highly accurate approximation (Syrett 1954) in terms of the incomplete gamma function

$$\Gamma(a, \xi) = \int_{\xi}^{\infty} y^{a-1} e^{-y} dy. \quad (3-142)$$

It is left for the student to show that for large  $\mu$  (small ramp rate) the complete solution, eq. (3-135), is very well represented by

$$n \cong \frac{q' e^{-\lambda t}}{\beta - \rho_0 - \gamma t} \int_{-\infty}^t \left( \frac{\beta - \rho_0 - \gamma t'}{\beta - \rho_0 - \gamma t} \right)^{\mu} e^{\lambda t'} dt'. \quad (3-143)$$

In terms of reactivity we find

$$n \cong \frac{\lambda |\rho_0| n_0}{\gamma(1 - \rho/\beta)^{\mu+1}} \frac{e^{\mu(1 - \rho/\beta)}}{\mu^{\mu+1}} \Gamma(\mu + 1, \mu(1 - \rho/\beta)). \quad (3-144)$$

The incomplete gamma function is simply related to the probability integral of the chi-squared distribution, as discussed and tabulated by Abramowitz and Stegun (1964) and by others.

Using eq. (3-137), we may write the reciprocal period as

$$\omega = \frac{\gamma}{\beta} \left[ \frac{1 + \mu\rho/\beta}{1 - \rho/\beta} + \frac{\mu^{\mu+1}(1 - \rho/\beta)^{\mu}}{\Gamma(\mu + 1, \mu(1 - \rho/\beta))} e^{-\mu(1 - \rho/\beta)} \right]. \quad (3-145)$$

The great usefulness of this formula is illustrated in fig. 3-19, which shows how eq. (3-145) compares with an exact six-delay-group solution ( $\gamma = 1.2 \times 10^{-4}$  sec $^{-1}$ ,  $\beta = 0.0075$ ,  $\ell = 10^{-4}$  sec) given by Schultz (1961). The agreement is excellent until around fifty cents past critical. Also included are the upper and lower bounds from eqs. (3-139) and (3-141).

Further approximations lead to still simpler results. It can be shown that for large  $\mu$ ,

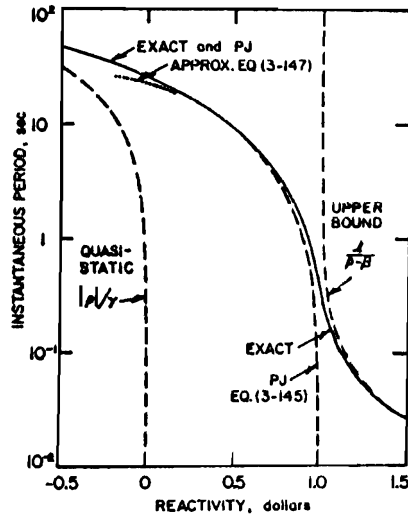


Fig. 3-19. Instantaneous period as a function of instantaneous reactivity comparing an exact six-delay-group solution (Schultz 1961) with the prompt-jump approximation, eq. (3-145), and the error-function estimate, eq. (3-147);  $\gamma = 1.2 \times 10^{-4} \text{ sec}^{-1}$ ,  $\beta = 0.0075$ ,  $\ell = 10^{-4} \text{ sec}$  (from *Control of Nuclear Reactors and Power Plants*, 2d ed., by M. A. Schultz. © 1955, 1961 by McGraw-Hill Book Co. Used with permission of McGraw-Hill Book Co.).

$$\Gamma(\mu + 1, \mu(1 - \rho/\beta)) \cong \left(\frac{\pi}{2\mu}\right)^{\frac{1}{2}} \mu^{\mu+1} e^{-\mu} \left[ 1 + \operatorname{erf}\left(\frac{\mu}{2}\right)^{\frac{1}{2}} \frac{\rho}{\beta} \right].$$

Eq. (3-143) becomes

$$n \cong \frac{\lambda |\rho_0| n_0 e^{-\mu\rho/\beta}}{\gamma(1 - \rho/\beta)^{\mu+1}} \left(\frac{\pi}{2\mu}\right)^{\frac{1}{2}} \left[ 1 + \operatorname{erf}\left(\frac{\mu}{2}\right)^{\frac{1}{2}} \frac{\rho}{\beta} \right]. \quad (3-146)$$

Using this formula together with

$$\left(1 - \frac{\rho}{\beta}\right)^{\mu} e^{\mu\rho/\beta} \cong 1 - \frac{\mu}{2} \left(\frac{\rho}{\beta}\right)^2$$

in eq. (3-137), we find

$$\omega \cong \frac{\gamma}{\beta} \frac{1 + \mu\rho/\beta}{1 - \rho/\beta} + \left(\frac{2\mu}{\pi}\right)^{\frac{1}{2}} \frac{1 - \frac{\mu}{2} \left(\frac{\rho}{\beta}\right)^2}{1 + \operatorname{erf}\left(\frac{\mu}{2}\right)^{\frac{1}{2}} \frac{\rho}{\beta}}. \quad (3-147)$$

This formula, which is confined to a range near critical, is also indicated in fig. 3-19. The error at critical is about 15 percent for this case ( $\mu = 4.794$ ).

## 192 Time-dependent Reactivity

Setting  $\rho = 0$  in eqs. (3-146) and (3-147), we find simple formulas for power and reciprocal period at critical ( $t = t_c$ ):

$$n(t_c) \cong n_0 |\rho_0| \sqrt{\frac{\pi\lambda}{2\gamma\beta}} \quad (3-148)$$

and

$$\omega(t_c) \cong \frac{\gamma}{\beta} + \sqrt{\frac{2\lambda\gamma}{\pi\beta}}. \quad (3-149)$$

These are also reported by Soodak (1962). Graphs are shown in fig. 3-20, where the solid part of each line is a range where the error is less than 10 percent. Note that larger ramp rate means lower power but higher rate of change at critical. Note also that the period curve is more or less dominated by the square-root dependence on ramp rate.

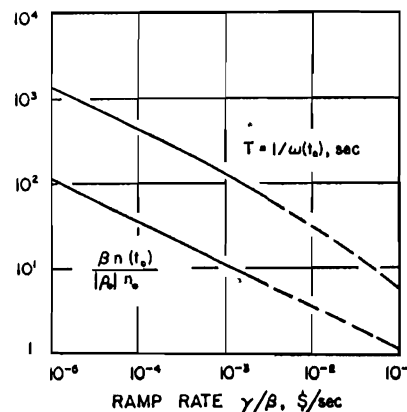


Fig. 3-20. Instantaneous relative power and period at critical as functions of ramp rate from eqs. (3-148) and (3-149);  $\lambda = 0.0767 \text{ sec}^{-1}$ .

Many other numerical examples and applications to safety-system design are in the literature (e.g., Hurwitz 1959; Keepin 1965; MacPhee 1960; Schultz 1961; Syrett 1954).

## 3-6. Some Methods for Arbitrary Reactivity Variation

In this section we outline briefly three methods that have been developed to express approximate analytical solutions of the point-reactor differential equations when the reactivity  $\rho(t)$  is an arbitrary specified function of time. The first of these methods was developed by Hurwitz (1949).

Consider eqs. (3-1) and (3-2) in the source-free case ( $q = 0$ ). The asymptotic solution for constant reactivity is, from sec. 2-2,

$$n = A_1 e^{\omega_1 t}, \quad c_i = \frac{\beta_i n}{\ell(\omega_1 + \lambda_i)},$$

where  $\omega_1$  is the algebraically largest root of the inhour equation. Hurwitz constructed an approximate solution for slowly varying reactivity by assuming the same form with  $A_1$  and  $\omega_1$  replaced by functions of time. Specifically,  $\omega_1$  is replaced by  $p(t)$ , the largest root of the inhour equation with  $\rho_0$  replaced by  $\rho(t)$ :

$$\rho(t) = \beta + \ell p(t) - \sum_i \frac{\beta_i \lambda_i}{p(t) + \lambda_i},$$

which may be written as

$$p = \frac{\rho - \beta}{\ell} + \sum_i \frac{\beta_i \lambda_i}{\ell(p + \lambda_i)}. \quad (3-150)$$

Let

$$n(t) = f(t) \exp \int_0^t p(t') dt' \quad (3-151)$$

and

$$c_i(t) = \left[ \frac{\beta_i f}{\ell(p + \lambda_i)} + \epsilon_i \right] \exp \int_0^t p(t') dt'. \quad (3-152)$$

Substituting into the point-reactor equation, we obtain

$$\frac{df}{dt} + pf = \frac{\rho - \beta}{\ell} f + \sum_i \left[ \frac{\beta_i \lambda_i f}{\ell(p + \lambda_i)} + \lambda_i \epsilon_i \right].$$

Using eq. (3-150), we have

$$\frac{df}{dt} = \sum_i \lambda_i \epsilon_i. \quad (3-153)$$

From eq. (3-152),

$$\frac{dc_i}{dt} = \left\{ \left[ \frac{\beta_i f}{\ell(p + \lambda_i)} + \epsilon_i \right] p + \frac{d}{dt} \left[ \frac{\beta_i f}{\ell(p + \lambda_i)} + \epsilon_i \right] \right\} \exp \int_0^t p(t') dt'.$$

The precursor equation becomes

$$\frac{d\epsilon_i}{dt} + (p + \lambda_i) \epsilon_i = - \frac{d}{dt} \left[ \frac{\beta_i f}{\ell(p + \lambda_i)} \right].$$

3.01 Time-dependent Reactivity

Next, it is assumed that  $\epsilon_i$  changes slowly, so that we may write

$$\epsilon_i = -\frac{1}{p + \lambda_i} \frac{d}{dt} \left[ \frac{\beta_i f}{\ell(p + \lambda_i)} \right].$$

Eq. (3-153) becomes

$$\frac{df}{dt} = -\sum_i \frac{\lambda_i}{p + \lambda_i} \frac{d}{dt} \left[ \frac{\beta_i f}{\ell(p + \lambda_i)} \right],$$

which may be written

$$\frac{1}{f} \frac{df}{dt} = -\frac{\sum_i \frac{\beta_i \lambda_i}{\ell(p + \lambda_i)}}{1 + \sum_i \frac{\beta_i \lambda_i}{\ell(p + \lambda_i)^2}} \frac{d}{dt} \left( \frac{1}{p + \lambda_i} \right). \quad (3-154)$$

If we define

$$D = 1 + \sum_i \frac{\beta_i \lambda_i}{\ell(p + \lambda_i)^2},$$

then eq. (3-154) becomes

$$\frac{1}{f} \frac{df}{dt} = -\frac{1}{2D} \frac{dD}{dt}.$$

This has a solution

$$\frac{f}{f_0} = \sqrt{\frac{D_0}{D}}.$$

Choose  $f_0 = 1$ , and let  $D_0$  be  $D$  evaluated at  $p = 0$ . The result is

$$f = \sqrt{\frac{1 + \frac{1}{\ell} \sum_i \frac{\beta_i}{\lambda_i}}{1 + \frac{1}{\ell} \sum_i \frac{\beta_i \lambda_i}{(p + \lambda_i)^2}}}. \quad (3-155)$$

The solution for  $n(t)$  is then eq. (3-151) with  $f$  given by eq. (3-155) and with  $p(t)$  being the largest root of the inhour equation corresponding to reactivity  $\rho(t)$ . Fig. 3-21 is the example given by Hurwitz (1949), a ramp input  $\rho = 5 \times 10^{-5} t$ .

In a later paper (Hurwitz 1959) there is a graph of  $f$  as a function of  $\rho$  for a  $U^{235}$  reactor with  $\ell = 2 \times 10^{-5}$  sec. This is reproduced in fig. 3-22 as curve A. Also shown are two curves (B and C) derived from the constant-source (rapid-rate) approximation for fast ramp inputs ( $\rho = \gamma t$ ); these may be obtained by computing  $n(t)$  from eq. (3-94) and then solving eq. (3-151) to find functions  $f(t)$ . It appears that eq. (3-151)

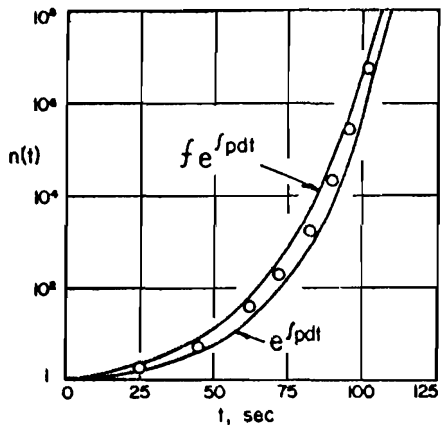


Fig. 3-21. Hurwitz approximation, eq. (3-151), with and without the factor  $f(t)$ ; points from a numerical integration of exact equations (Hurwitz 1949; reprinted by special permission from *Nucleonics*, July 1949; © 1966 by McGraw-Hill, Inc., New York).

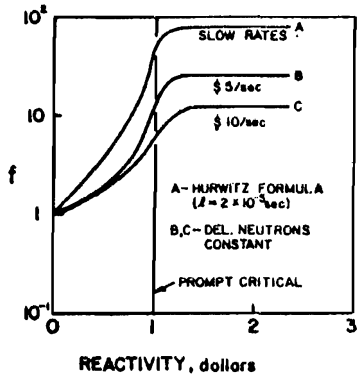


Fig. 3-22. Comparison of Hurwitz approximation with effective  $f$ -factors computed by the constant-source (rapid-rate) approximation (Hurwitz 1959).

is an overestimate of  $n(t)$ , at least for the ramp-input problem, but that a wide range of ramp rates is included in its scope without great error.

The spirit of the Hurwitz method is essentially that of the WKB method (named after Wentzel, Kramers, and Brillouin) for finding approximate solutions of Schrödinger's equation with a varying potential (Morse and Feshbach 1953). The second method we describe is actually closer to the orthodox WKB method in that an approximate solution of the second-order differential equation for  $n(t)$ , eq. (3-26), is put directly into the form of the WKB approximation of quantum mechanics. The application was made by Rodeback (unpublished), as quoted by Cohen (1958).

For one group of delayed neutrons and  $q = 0$ , we have from eq. (3-26),

$$\frac{d^2n}{dt^2} + (\beta + \lambda\ell - \rho) \frac{dn}{dt} - \left( \lambda\rho + \frac{dp}{dt} \right) n = 0. \quad (3-156)$$

This may be written in standard form as

$$\frac{d^2n}{dt^2} + p(t) \frac{dn}{dt} + q(t)n = 0, \quad (3-157)$$

where

$$p = (\beta + \lambda\ell - \rho)/\ell \quad (3-158)$$

and

$$q = -\left( \lambda\rho + \frac{dp}{dt} \right)/\ell. \quad (3-159)$$

The first-derivative term in eq. (3-157) may be removed by making the transformation

$$n = ye^{-\frac{1}{2}\int p dt}, \quad (3-160)$$

which yields

$$\frac{d^2y}{dt^2} + \left( q - \frac{1}{2} \frac{dp}{dt} - \frac{1}{4} p^2 \right) y = 0. \quad (3-161)$$

This is simply the device we used in solving the ramp-input problem (sec. 3-3).

Next, we rewrite eq. (3-161) as

$$\frac{d^2y}{dt^2} - h^2y = 0. \quad (3-162)$$

Postulate

$$y = e^\phi. \quad (3-163)$$

Substitution into eq. (3-162) yields a first-order nonlinear differential equation for  $d\phi/dt$ :

$$\frac{d^2\phi}{dt^2} + \left( \frac{d\phi}{dt} \right)^2 - h^2 = 0. \quad (3-164)$$

If  $d\phi/dt$  is slowly varying, we can seek an iterative solution. The first iteration is

$$\frac{d\phi}{dt} \cong h.$$

The second iteration is

$$\left(\frac{d\phi}{dt}\right)^2 = h^2 - \frac{d^2\phi}{dt^2} \cong h^2 - \frac{dh}{dt}. \quad (3-165)$$

Treating  $dh/dt$  as small, we find

$$\frac{d\phi}{dt} \cong h - \frac{1}{2h} \frac{dh}{dt},$$

$$\phi \cong \int h dt - \frac{1}{2} \log h,$$

$$y \cong \frac{1}{\sqrt{h}} e^{\int h dt}.$$

By eqs. (3-161) and (3-162), we have

$$h^2 = -q + \frac{1}{2} \frac{dp}{dt} + \frac{1}{4} p^2$$

or, using eqs. (3-158) and (3-159),

$$h^2 = \frac{\lambda\rho}{\ell} + \frac{1}{2\ell} \frac{d\rho}{dt} + \left( \frac{\beta + \lambda\ell - \rho}{2\ell} \right)^2. \quad (3-166)$$

We form a complete approximate solution by writing

$$n = \frac{1}{\sqrt{h}} [Ae^{\int h dt} + Be^{-\int h dt}] e^{-\frac{1}{2} \int p dt}, \quad (3-167)$$

where  $A$  and  $B$  are constants and where  $p$  and  $h$  are given by eqs. (3-158) and (3-166) respectively. Clearly, this approximate solution fails if  $h \rightarrow 0$ ; for the procedures used at such "turning points," see Morse and Feshbach (1953). An independent study of the WKB method in reactor dynamics, with a number of applications, is reported in two papers by Tan (1966, 1967).

A third method for obtaining approximate solutions of the differential equations is due to Akcasu (1958). Postulate

$$n(t) = \exp \int_0^t \omega(t') dt' \quad (3-168)$$

and

$$c_i(t) = p_i(t) \exp \int_0^t \omega(t') dt', \quad (3-169)$$

where  $\omega(t)$  and  $p_i(t)$  are to represent power series in a small parameter and where the complete solution for  $n(t)$  is to be a linear combination

of terms like eq. (3-168). We have

$$\frac{dn}{dt} = \omega(t) \exp \int_0^t \omega(t') dt' = \omega(t)n(t)$$

and

$$\frac{dc_i}{dt} = \left( p_i \omega + \frac{dp_i}{dt} \right) \exp \int_0^t \omega(t') dt'.$$

Note that  $\omega$  would be the instantaneous reciprocal period if eq. (3-168) were the complete solution.

The reactivity is written as

$$\rho(t) = \rho_0 + \beta \mu z(t), \quad (3-170)$$

where  $\rho_0$  is a constant and  $\mu$  is a small parameter. Eqs. (3-168) and (3-169) become

$$\omega(t) = \frac{\rho_0}{\ell} + \frac{\beta}{\ell} [\mu z(t) - 1] + \sum_i \lambda_i p_i(t) \quad (3-171)$$

and

$$p_i \omega(t) + \frac{dp_i}{dt} = \frac{\beta_i}{\ell} - \lambda_i p_i. \quad (3-172)$$

Let

$$\omega(t) = \omega_0 + \mu \omega_1(t) + \mu^2 \omega_2(t) + \dots$$

and

$$p_i(t) = p_{0i} + \mu p_{1i}(t) + \mu^2 p_{2i}(t) + \dots,$$

where the time-dependent coefficients are functions to be determined by substituting these series into eqs. (3-171) and (3-172) and equating coefficients of like powers of  $\mu$ .

As expected, the case of constant reactivity reduces to our treatment in chapter 2. For a ramp, this procedure leads to a formula which is limited to describing starting transients in much the same way that a conventional power series solution for  $n(t)$  would be limited. The chief use of this formulation has been the analysis of large-amplitude oscillations, with a result that agrees with our eq. (3-69).

### Problems

- 3-1. Comparing figs. 2-8 and 2-9, we see that eq. (2-46) for the step-input response is well represented for small  $t$  by the constant-source model, and for large  $t$  by the prompt-jump approximation.

Treat this as an example of singular perturbation (i.e., calculate higher terms in the approximate solutions and match the asymptotic solution to the solution for small  $t$ ). Compare the result with the exact one-delay-group step-input response.

- 3-2. Generalize the criterion for validity of the one-group prompt-jump approximation, eq. (3-17), to include a neutron source.
- 3-3. Derive a second-order differential equation for  $c(t)$  to accompany eq. (3-26).
- 3-4. A reactor, initially critical at steady power, is subjected to a ramp input of reactivity of 10 cents/sec. Let  $\beta/\ell = 100 \text{ sec}^{-1}$ . Use the following rough criteria for the validity of approximations:

$$\beta - \rho > 3\sqrt{[\ell(\lambda\beta + d\rho/dt)]} \quad (PJ),$$

$$t < \frac{1}{3\lambda} \quad (\text{constant source}).$$

Find the maximum reactivity for which the solution is satisfactorily represented by (a) the prompt-jump approximation and (b) the formula

$$\frac{n}{n_0} = \frac{\beta}{\beta - \gamma t}.$$

Repeat (a) and (b) for a ramp rate of 1 dollar/sec.

- 3-5. A reactor is initially shut down, with a constant neutron level and a reactivity of  $-2$  dollars. At  $t = 0$  a ramp input of 3 dollars/sec is initiated. Estimate (a) the power at critical (relative to the shutdown level) and (b) the reciprocal period at critical. Justify your approximations.
- 3-6. Derive equations for the real and imaginary parts of the reactor transfer function and investigate the behavior of each at low and high frequencies.
- 3-7. Verify the parameters in the two- and three-group models listed in table 2-2.
- 3-8. Sketch the phase curves corresponding to the amplitude curves in fig. 3-8.
- 3-9. Derive the formula for the transfer-function period effect, eq. (3-64).
- 3-10. Using the oscillating reactivity, eq. (3-65), derive the response to large-amplitude oscillations in the effective-lifetime model. Find the condition for a steady oscillation and sketch a curve of  $n(t)$  for that case.

130      *Time-dependent Reactivity*

- 3-11. Derive the two representations for large-amplitude oscillations in the prompt-jump approximation, eqs. (3-66) and (3-70).
- 3-12. Consider a restricted version of the prompt-jump approximation obtained by neglecting  $\rho$  in the left-hand side of eq. (3-19). Discuss the limitations. What are the consequences for the transfer function and for large-amplitude reactivity oscillations?
- 3-13. Derive the fast-ramp response, eq. (3-94), as the solution of a first-order differential equation.
- 3-14. Derive the exact ramp solutions, eqs. (3-94) and (3-95), as special cases of eq. (3-93).
- 3-15. Derive the asymptotic forms, eqs. (3-97) and (3-98). Explain why these do not yield the exact results at  $t = 0$ .
- 3-16. Derive the ramp-input response, eq. (3-99), as the solution of a first-order differential equation.
- 3-17. Check the criteria for validity of the various approximations by comparing the curves in fig. 3-14.
- 3-18. Derive the generalizations of eqs. (3-105) and (3-106) by considering the integral-representation solution for several groups of delayed neutrons.
- 3-19. Show that eq. (3-120) for the power at prompt critical may be derived from the fast-ramp solution, eq. (3-94), provided  $2\gamma\ell \ll \beta^2$ .
- 3-20. Derive the limiting cases, eqs. (3-123) and (3-125), for the reciprocal period at prompt critical.
- 3-21. Derive the slow-ramp startup formula, eq. (3-135), and integrate the special case to obtain eq. (3-136).
- 3-22. Prove that the quasistatic period, eq. (3-141), is a lower bound for the instantaneous period during startup.
- 3-23. Show that the term containing  $n_0$  in eq. (3-135) is insignificant in a very slow startup.
- 3-24. Compare Keepin's exact ramp solutions (fig. 9-7, p. 298 of *Physics of Nuclear Kinetics* by G. R. Keepin, Addison-Wesley, 1965) with the one-group prompt-jump approximation.
- 3-25. Extend the integral-representation method to the ramp startup with a source.
- 3-26. The dragon (see probs. 2-15 and 2-16) is better represented by a reactivity that is a parabolic function of time, simulating the approach and separation of the two parts of the system. Construct a realistic reactivity function, solve for the power  $n(t)$ , and calculate the width of the burst at half peak power (Kistner 1967).

## 4 Integral Equations and Numerical Computations

In the preceding chapters we have studied some special problems in reactor dynamics as solutions of differential equations. In this chapter we construct several integral-equation formulations for point-reactor dynamics. The integral equations are then used to discuss and compare methods of numerical computation in reactor dynamics.

Included are several computational methods that are practical for cases in which conventional methods fail. For example, slow transients in a fast reactor require the solution of systems of equations containing one very short response time (of order  $\ell/\beta$ ), and the number of time steps in a standard method may become prohibitively large. This limitation may be circumvented by the use of numerical methods, based on integral equations, in which the time-interval size is limited only by the time scale of the overall dynamic process and not by the shortest individual response time in the system.

The integral forms also help to unify concepts introduced previously. In addition, we can gain new insights into the various approximation methods used in chapter 3. Further, some of the integral equations derived here will be found useful in studies of reactor stability (chapters 6 and 7). Finally, we discuss some methods for solving the inverse problem (computing dynamic reactivity from the power history).

### 4-1. An Integrating Factor

We begin with the source-free point-reactor model, eq. (3-1) with  $q = 0$ :

$$\frac{dn}{dt} + \frac{\beta - \rho(t)}{\ell} n = \Sigma_i \lambda_i c_i. \quad (4-1)$$

An integrating factor is  $e^{I(t)}$ , where

$$I(t) = \int_0^t \frac{\beta - \rho(\tau)}{\ell} d\tau. \quad (4-2)$$

A formal integral of eq. (4-1) is

$$n(t) = e^{-I(t)} \left[ n_0 + \sum_i \lambda_i \int_0^t c_i(t') e^{I(t')} dt' \right]. \quad (4-3)$$

The precursor equation is eq. (3-2),

$$\frac{dc_i}{dt} + \lambda_i c_i = \frac{\beta_i}{\ell} n, \quad (4-4)$$

which may be integrated as

$$c_i(t) = e^{-\lambda_i t} \left[ c_{i0} + \frac{\beta_i}{\ell} \int_0^t n(t') e^{\lambda_i t'} dt' \right]. \quad (4-5)$$

In principle, a numerical integration scheme may be constructed that proceeds stepwise in time, alternating between eqs. (4-3) and (4-5); the initial value for each step is the value predicted for the end of the prior step. One disadvantage is that eq. (4-3) contains a double integration. Another disadvantage is that the integrands in eqs. (4-3) and (4-5) may be varying rapidly over time intervals that are sufficiently large to be economically feasible.

From another viewpoint (Belleni-Morante 1963) one can regard eqs. (4-3) and (4-5) as generating successive approximations to the solution at time  $t$ . As the first approximation to  $c_i(t)$ , let

$$c_{i1}(t) = c_{i0} e^{-\lambda_i t}.$$

Use this in eq. (4-3) to generate the first approximation to  $n(t)$ :

$$n_1(t) = e^{-I(t)} \left[ n_0 + \sum_i \lambda_i c_{i0} \int_0^t e^{-\lambda_i t' + I(t')} dt' \right].$$

The  $j$ th approximation is

$$n_j(t) = e^{-I(t)} \left[ n_0 + \sum_i \lambda_i \int_0^t c_{ij}(t') e^{I(t')} dt' \right] \quad (4-6)$$

and

$$c_{ij}(t) = e^{-\lambda_i t} \left[ c_{i0} + \frac{\beta_i}{\ell} \int_0^t n_{j-1}(t') e^{\lambda_i t'} dt' \right]. \quad (4-7)$$

A proof of convergence of the successive approximations is given by Belleni-Morante (1963). Numerical integrations are required for each

successive approximation, and the disadvantages of double integration and limited time-step size are still present. We return to this question later, showing how both disadvantages may be overcome.

## 4-2. Keepin's Integral Equation

Several writers have used integral formulations obtained with the aid of Laplace transforms (Ash 1956; Schmid 1958; Smets 1958; Keepin and Cox 1960; Ash 1965; Keepin 1965). For convenience, we adopt the name "Keepin's equation" for the form used in the RTS code developed at Los Alamos Scientific Laboratory (Keepin and Cox 1960; Keepin 1965).

To derive Keepin's equation, we integrate by parts in eq. (4-5), substitute into eq. (3-1), take Laplace transforms, solve for the transform of  $n(t)$ , and write the Laplace inversion as a convolution. The kernel of the resulting integral equation turns out to be proportional to the impulse response and to the inverse transform of the zero-power transfer function.

After partial integration, eq. (4-5) becomes

$$\begin{aligned} c_i(t) = & \left( c_{i0} - \frac{\beta_i n_0}{\lambda_i \ell} \right) e^{-\lambda_i t} \\ & + \frac{\beta_i}{\lambda_i \ell} \left[ n(t) - \int_0^t \frac{dn(t')}{dt'} e^{-\lambda_i(t-t')} dt' \right]. \end{aligned} \quad (4-8)$$

Substituting into eq. (3-1) yields

$$\begin{aligned} \ell \frac{dn}{dt} = & \rho n - \beta \int_0^t \frac{dn(t')}{dt'} f(t-t') dt' \\ & + \sum_i (\lambda_i \ell c_{i0} - \beta_i n_0) e^{-\lambda_i t} + \ell q, \end{aligned} \quad (4-9)$$

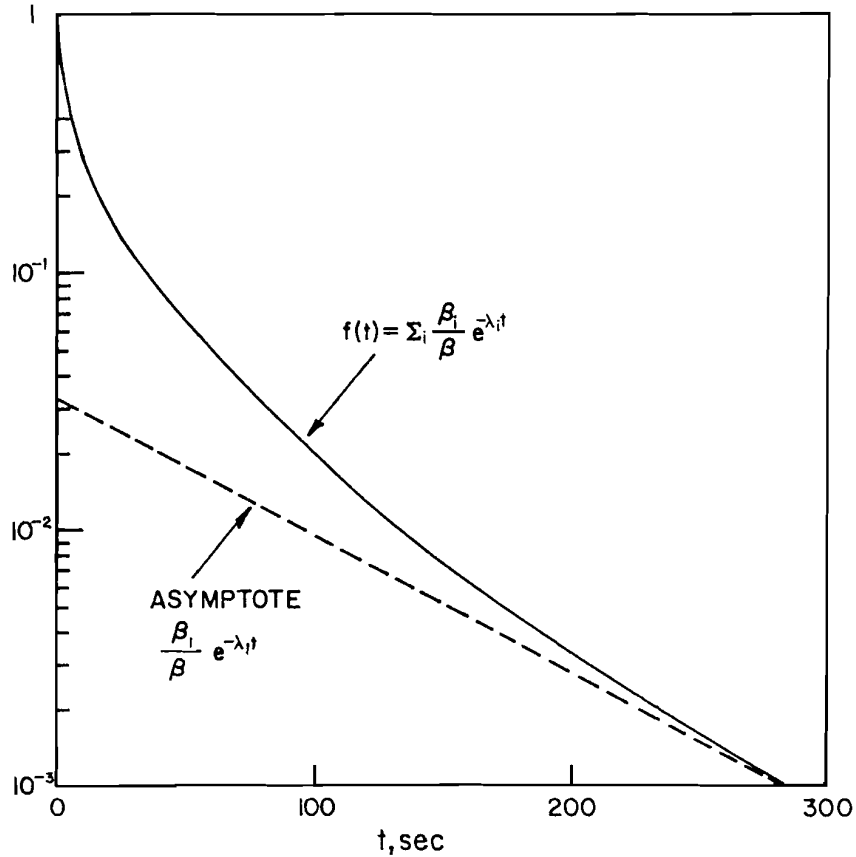
where the kernel in this integro-differential equation is the so-called delayed-neutron decay function

$$f(t) = \sum_i \frac{\beta_i}{\beta} e^{-\lambda_i t}. \quad (4-10)$$

Physically,  $f(t)$  is the probability that a delayed neutron has not yet been emitted at time  $t$  following an impulse of source neutrons at  $t = 0$ . The function  $f(t)$  for thermal fission in  $\text{U}^{235}$  is plotted in fig. 4-1.

The properties of  $f(t)$  may be used to derive the effective-lifetime model directly from eq. (4-9). The details are left as an exercise for the student.

The next step in deriving Keepin's equation is to take Laplace

Fig. 4-1. Delayed-neutron decay function  $f(t)$  for thermal fission in  $U^{235}$ .

transforms in eq. (4-9) and solve for  $N(s)$ ,

$$N(s) = \frac{n_0}{s} + \frac{\mathcal{L}(\rho n) + \sum_i \frac{\lambda_i \ell c_{i0} - \beta_i n_0}{s + \lambda_i} + \ell Q(s)}{s[\ell + \beta F(s)]}, \quad (4-11)$$

where  $N(s)$  and  $Q(s)$  are the transforms of  $n(t)$  and  $q(t)$ , as before, and where  $\mathcal{L}(\rho n)$  and  $F(s)$  are respectively the transforms of  $\rho(t)n(t)$  and  $f(t)$ . Define

$$K(s) = \frac{1}{s[\ell + \beta F(s)]}. \quad (4-12)$$

Since

$$F(s) = \frac{1}{\beta} \sum_i \frac{\beta_i}{s + \lambda_i}, \quad (4-13)$$

we have

$$K(s) = \frac{1}{\ell s + \sum_i \frac{\beta_i s}{s + \lambda_i}} = \frac{I(s)}{\ell} = \frac{G(s)}{n_0}, \quad (4-14)$$

where  $I(s)$  and  $G(s)$  are respectively the source and reactivity zero-power transfer functions for a critical reactor; see eqs. (2-62) and (3-56). Eq. (4-11) may be written

$$N(s) = \frac{n_0}{s} + K(s) \left[ \mathcal{L}(\rho n) + \sum_i \frac{\lambda_i \ell c_{i0} - \beta_i n_0}{s + \lambda_i} + \ell Q(s) \right]. \quad (4-15)$$

Keepin's equation is the inverse transform of eq. (4-15):

$$\begin{aligned} n(t) = n_0 &+ \int_0^t k(t-t') [\rho(t')n(t')] \\ &+ \sum_i (\lambda_i \ell c_{i0} - \beta_i n_0) e^{-\lambda_i t'} + \ell q(t')] dt'. \end{aligned} \quad (4-16)$$

The kernel  $k(t)$  is proportional to the impulse response,

$$k(t) = \frac{i(t)}{\ell} = \frac{g(t)}{n_0}, \quad (4-17)$$

where  $g(t)$  is the inverse transform of  $G(s)$ . A typical function  $i(t) = \ell k(t)$  is plotted in fig. 2-10 for  $\ell = 10^{-4}$  sec. Note that  $k(0) = 1/\ell$  and that

$$\lim_{t \rightarrow \infty} k(t) = \frac{1}{\ell + \sum_i \beta_i / \lambda_i} = \frac{1}{\ell'}, \quad (4-18)$$

where  $\ell'$  is the effective lifetime of sec. 2-2. Therefore  $k(t)$  is a function with an initial spike that is higher and sharper for smaller values of  $\ell$  and that approaches a constant  $1/\ell'$  for large  $t$ . In the limit of  $\ell \rightarrow 0$ ,  $k(t)$  may be represented in terms of a delta function plus a constant; the use of this concept in deriving the prompt-jump approximation is left as an exercise.

By eq. (2-60),  $k(t)$  may be written

$$k(t) = \sum_{j=1}^{m+1} \frac{B_j}{\ell} e^{\omega_j t}. \quad (4-19)$$

Coefficients  $B_j/\ell$  and roots  $\omega_j$  are tabulated by Keepin (1965) and by others. The RTS code is essentially a numerical evaluation of the convolution integral appearing in eq. (4-16). It has proved very useful in fast excursions but is impractical for slow transients with small  $\ell$  because of limitations on time-step size in evaluating the integrals.

It may be remarked that the analogue of eq. (4-16) in the lifetime formulation of reactor dynamics, eqs. (1-10) and (1-11), is considerably more complicated (Smets 1958; Keepin 1965). Extra terms are generated by the time-dependent coefficients in the precursor equations.

Nothing is gained by the extra labor; as noted in sec. 1-2, neither model is correct when the difference between them is large enough to be significant.

Next, we note that eq. (4-15) may be used to derive the inhour equation and the transfer functions. Set  $\rho = \rho_0$  and drop the terms arising from sources and nonequilibrium initial conditions. We have

$$N(s) = \frac{n_0}{s} + \rho_0 K(s)N(s).$$

Solving for  $N(s)$ , we obtain

$$N(s) = \frac{n_0}{s[1 - \rho_0 K(s)]}. \quad (4-20)$$

Because the poles of  $N(s)$  are at  $s = \omega_j$ , the inhour equation may be written as

$$\rho_0 = \frac{1}{K(\omega_j)}. \quad (4-21)$$

This result is not altered if the terms that we dropped are retained. The student should verify that this agrees with eqs. (2-54) and (3-44), which are expressed in terms of  $I(s)$  and  $G(s)$  for a noncritical reactor.

To obtain the source transfer function, let  $n = n_0 + \delta n$ ,  $\rho = \rho_0$ , and  $q = q_0 + \delta q$ . Ignore initial conditions, and eq. (4-15) becomes

$$\frac{n_0}{s} + \delta N(s) = \frac{n_0}{s} + K(s) \left[ \frac{\rho_0 n_0}{s} + \rho_0 \delta N(s) + \frac{\ell q_0}{s} + \ell \delta Q(s) \right].$$

Using eq. (2-70) for the average values, we obtain

$$\delta N(s) = K(s)[\rho_0 \delta N(s) + \ell \delta Q(s)]$$

and

$$\frac{\delta N(s)}{\ell \delta Q(s)} = \frac{K(s)}{1 - \rho_0 K(s)}. \quad (4-22)$$

For the reactivity transfer function, let  $n = n_0 + \delta n$ ,  $\rho = \rho_0 + \delta \rho$ , and  $q = q_0$ . Ignore initial conditions and approximate the product  $\rho n$  by

$$\rho n = (\rho_0 + \delta \rho)(n_0 + \delta n) \cong \rho_0 n_0 + n_0 \delta \rho + \rho_0 \delta n.$$

We find

$$\frac{n_0}{s} + \delta N(s) = \frac{n_0}{s} + K(s) \left[ \frac{\rho_0 n_0}{s} + n_0 \delta R(s) + \rho_0 \delta N(s) + \frac{\ell q_0}{s} \right].$$

Using eq. (2-70), we obtain

$$\delta N(s) = K(s)[n_0 \delta R(s) + \rho_0 \delta N(s)]$$

and

$$\frac{\delta N(s)}{n_0 \delta R(s)} = \frac{K(s)}{1 - \rho_0 K(s)}. \quad (4-23)$$

As expected, we have

$$\frac{I(s)}{\ell} = \frac{G(s)}{n_0},$$

and we shall see in chapter 6 that either of the subcritical reactor transfer functions, written as in eqs. (4-22) and (4-23), may be interpreted as a forward-loop transfer function  $K(s)$  with a constant feedback  $-\rho_0$ .

The student may verify that an alternate form of eq. (4-16), obtained by taking the Laplace transform of the precursor equation and substituting into the transform of eq. (3-1), is

$$n(t) = \ell n_0 k(t) + \int_0^t k(t - t') [\rho(t') n(t') + \sum_i \lambda_i \ell c_{i0} e^{-\lambda_i t'} + \ell q(t')] dt'. \quad (4-24)$$

### 4-3. An Integro-differential Equation

Another integral form, used in stability studies by many writers, is obtained by substituting an integral for  $c_i(t)$  directly into eq. (3-1). Integrating eq. (4-4), we may write

$$c_i(t) = c_i(t_0) e^{-\lambda_i(t-t_0)} + \frac{\beta_i}{\ell} \int_{t_0}^t n(t') e^{-\lambda_i(t-t')} dt'. \quad (4-25)$$

Substitution into eq. (3-1) yields

$$\ell \frac{dn}{dt} = (\rho - \beta)n + \int_{t_0}^t n(t') \sum_i \beta_i \lambda_i e^{-\lambda_i(t-t')} dt' + \ell \sum_i \lambda_i c_i(t_0) e^{-\lambda_i(t-t_0)} + \ell q. \quad (4-26)$$

Define

$$D(t) = \frac{1}{\beta} \sum_i \beta_i \lambda_i e^{-\lambda_i t}, \quad (4-27)$$

which has the property

$$\int_0^t D(t') dt' = 1 - f(t), \quad (4-28)$$

where  $f(t)$  is the delayed-neutron decay function of eq. (4-10). The function  $D(t)$  may be interpreted as a probability density, such that  $D(t) dt$  represents the probability that a delayed neutron will be emitted between  $t$  and  $t + dt$  following an impulse of source neutrons at  $t = 0$ . The function  $D(t)$  for thermal fission in  $\text{U}^{235}$  is plotted in fig. 4-2; note that  $D(0) = \lambda' = 0.405 \text{ sec}^{-1}$ .

Eq. (4-26) becomes

$$\ell \frac{dn}{dt} = (\rho - \beta)n + \beta \int_{t_0}^t n(t') D(t - t') dt' + \ell \sum_i \lambda_i c_i(t_0) e^{-\lambda_i(t-t_0)} + \ell q.$$

Using the properties of the kernel  $D(t)$ , we may write this as

$$\ell \frac{dn}{dt} = \rho n + \beta \int_{t_0}^t [n(t') - n(t)] D(t - t') dt' + \sum_i [\ell \lambda_i c_i(t_0) - \beta_i n(t)] e^{-\lambda_i(t-t_0)} + \ell q. \quad (4-29)$$

This rather complicated form is considerably simplified if we let  $t_0 \rightarrow -\infty$ , provided we make the physically reasonable assumption

$$\lim_{t_0 \rightarrow -\infty} c_i(t_0) e^{\lambda_i t_0} = 0.$$

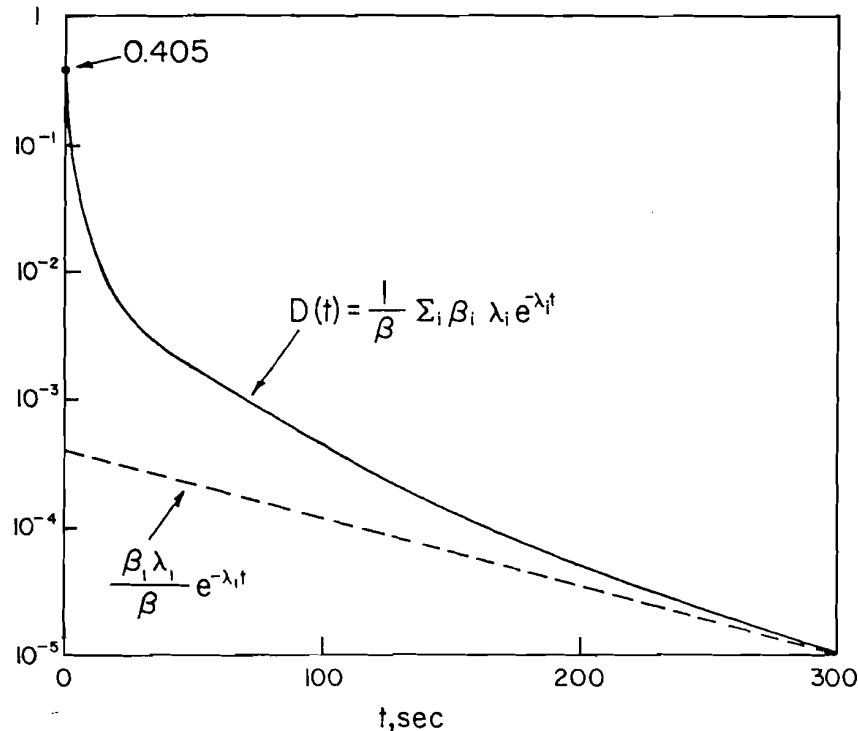


Fig. 4-2. Delayed-neutron probability density function  $D(t)$  for thermal fission in  $\text{U}^{235}$ .

We then have

$$\ell \frac{dn}{dt} = \rho n + \beta \int_{-\infty}^t [n(t') - n(t)] D(t - t') dt' + \ell q. \quad (4-30)$$

Finally, transforming to a new integration variable  $u = t - t'$ , we have

$$\ell \frac{dn}{dt} = \rho n + \beta \int_0^\infty [n(t - u) - n(t)] D(u) du + \ell q. \quad (4-31)$$

This form is inconvenient for numerical computations, but it is useful in stability analyses.

#### 4-4. Numerical Methods

Solution of the differential equations of reactor dynamics by standard numerical methods—e.g., the Adams, Milne, or Runge–Kutta methods as described in standard references such as Abramowitz and Stegun (1964) or Hildebrand (1956)—presents serious difficulties whenever the neutron generation time is very small compared to the time scale of the overall dynamic process. In such cases an enormous number of time steps may be required, resulting in a prohibitively expensive calculation that produces much superfluous information and that may contain large accumulated errors. The difficulty does not arise with very fast transients, and it is usually not a problem in simulating thermal reactors; for these problems, many refinements of standard methods have been developed (e.g., Brown 1957; Auerbach, Mennig, and Sarlos 1968; Vigil 1967), but these methods require switching to the prompt-jump approximation for slow transients in fast reactors.

The purpose of this section is to indicate the source of difficulty and to suggest the basic ideas required to circumvent it. We begin by noting that the source-free point-reactor model, eqs. (3-1) and (3-2) with  $q = 0$ , may be written in matrix notation as

$$\frac{d}{dt} \begin{bmatrix} n \\ c_1 \\ c_2 \\ c_3 \\ \vdots \\ \vdots \end{bmatrix} = \begin{bmatrix} (\rho - \beta)/\ell & \lambda_1 & \lambda_2 & \lambda_3 & \dots \\ \beta_1/\ell & -\lambda_1 & 0 & 0 & \\ \beta_2/\ell & 0 & -\lambda_2 & 0 & \\ \beta_3/\ell & 0 & 0 & -\lambda_3 & \\ \vdots & \vdots & & & \\ \vdots & & & & \end{bmatrix} \begin{bmatrix} n \\ c_1 \\ c_2 \\ c_3 \\ \vdots \\ \vdots \end{bmatrix}.$$

We may illustrate with a simple second-order system having constant coefficients

$$\frac{dx}{dt} = Ax + By$$

and

$$\frac{dy}{dt} = Cx + Dy,$$

which may be written

$$\frac{d}{dt} \begin{bmatrix} x \\ y \end{bmatrix} = \begin{bmatrix} A & B \\ C & D \end{bmatrix} \begin{bmatrix} x \\ y \end{bmatrix}. \quad (4-34)$$

The forward-difference representation is

$$(x_{n+1} - x_n)/h \cong Ax_n + By_n$$

and

$$(y_{n+1} - y_n)/h \cong Cx_n + Dy_n,$$

where  $h$  is the time interval  $t_{n+1} - t_n$ . Solving for  $x_{n+1}$  and  $y_{n+1}$  yields

$$x_{n+1} \cong (1 + Ah)x_n + Bhy_n$$

and

$$y_{n+1} \cong Chx_n + (1 + Dh)y_n,$$

which may be written as

$$\begin{bmatrix} x \\ y \end{bmatrix}_{n+1} \cong \begin{bmatrix} 1 + Ah & Bh \\ Ch & 1 + Dh \end{bmatrix} \begin{bmatrix} x \\ y \end{bmatrix}_n \quad (4-35)$$

On the other hand, the system eq. (4-33) may be integrated in the form

$$x(t) = x(t_0)e^{A(t-t_0)} + B \int_{t_0}^t y(t')e^{A(t-t')} dt' \quad (4-36)$$

and

$$y(t) = y(t_0)e^{D(t-t_0)} + C \int_{t_0}^t x(t')e^{D(t-t')} dt'.$$

For any time interval during which  $x$  and  $y$  do not change greatly (regardless of the values of  $A$  and  $D$ ) we may set  $x(t') \cong x(t_0)$  and

$y(t') \cong y(t_0)$ . The integrals may then be evaluated:

$$x(t) \cong x(t_0)e^{A(t-t_0)} + \frac{By(t_0)}{A} [e^{A(t-t_0)} - 1]$$

and

$$y(t) \cong y(t_0)e^{D(t-t_0)} + \frac{Cx(t_0)}{D} [e^{D(t-t_0)} - 1].$$

Now let  $h = t - t_0$ ,  $x(t) = x_{n+1}$ ,  $x(t_0) = x_n$ , etc.:

$$x_{n+1} \cong e^{Ah}x_n + \frac{B}{A}(e^{Ah} - 1)y_n;$$

$$y_{n+1} \cong \frac{C}{D}(e^{Dh} - 1)x_n + e^{Dh}y_n.$$

In matrix form, we have

$$\begin{bmatrix} x \\ y \end{bmatrix}_{n+1} \cong \begin{bmatrix} e^{Ah} & \frac{B}{A}(e^{Ah} - 1) \\ \frac{C}{D}(e^{Dh} - 1) & e^{Dh} \end{bmatrix} \begin{bmatrix} x \\ y \end{bmatrix}_n. \quad (4-37)$$

It is clear that this reduces to eq. (4-35) only if  $|Ah|$  and  $|Dh|$  are both small compared to unity. We therefore infer that the smallest time constant (larger of  $A$  or  $D$ ) governs the size of the time step used in a finite-difference method, even when the solution itself is very smooth.

In this simple difference method, one is attempting to represent an exponential by a linear approximation. For example, consider

$$\frac{dx}{dt} = Ax, \quad x(t) = x(t_0)e^{A(t-t_0)}.$$

For the interval  $t_n$  to  $t_{n+1}$  this is

$$x_{n+1} = x_n e^{Ah}.$$

With forward differences,

$$(x_{n+1} - x_n)/h \cong Ax_n$$

$$x_{n+1} \cong x_n(1 + Ah).$$

If  $A$  is negative (decaying exponential) this linear representation introduces a sign change at  $h = -1/A$ .

A better representation for a decaying exponential is obtained with backward differences:

$$(x_{n+1} - x_n)/h \cong Ax_{n+1}$$

and

$$x_{n+1} \cong x_n / (1 - Ah).$$

There is no sign change as  $|Ah|$  is increased, and the backward-difference method remains stable as the interval increases. Therefore, backward differences may be preferred when the system is dominated by a large negative coefficient, though the basic time-step limitation caused by truncation error is still present.

In a slow transient, when  $\rho$  is small, the controlling time constant is approximately  $\ell/\beta$ ; see eq. (4-32). This may be of the order of  $10^{-6}$  sec, while the power transient may involve several minutes or more. Physically, this is a manifestation of the prompt transient that is replaced by a jump discontinuity when using the prompt-jump approximation.

Of course, there are numerous methods that are superior to the crude difference method we used here for illustration; some methods may increase the permissible time step by a factor of ten or more. However, reformulation of the problem in terms of integral equations and use of special treatment for the integrals have made it possible in certain cases to augment the allowable time step by many orders of magnitude. In these methods, integrals such as those appearing in eq. (4-36) are evaluated analytically using known functional forms for the slowly varying factors only, and thus gross errors in evaluating the integrals are avoided.

Obviously, the types of problems that require this treatment are generally those problems for which the prompt-jump approximation is highly accurate (small  $\rho$  and small  $\ell$ ). But if  $\rho$  should stray too near  $\beta$  during a power transient, the method of computation must be switched. In contrast, the methods described in the following sections can handle all dynamic situations. If an automatically self-adjusting time interval, controlled only by the rate of change of reactor power, is incorporated, the computer can follow, in near-optimum fashion, a ramp-induced startup accident where the period might vary continuously from many minutes down to a fraction of a millisecond. Another application is the computation of cyclic power variation in a repetitive pulsed reactor that is super prompt critical for a tiny fraction of each cycle; the computer can easily follow the early stages of initiation, the sharp power burst, and the delayed-neutron aftereffect without having to switch computing method.

Before proceeding, we note that these same cases (small  $\ell$  and small  $\rho$ ) are also the cases that produce insurmountable scaling difficulties in analogue computation. Dynamic-range difficulties in fast transients may usually be avoided by working with  $\log n(t)$  instead of  $n(t)$  itself,

but a transient near prompt critical in a fast reactor might have a time scale of several milliseconds and be very sensitive to all the individual response times in the system, ranging from a microsecond up to several seconds. Techniques of analogue computation are not treated in this book; for analogue simulation of reactors and reactor systems see Schultz (1961), Harrer (1963), and Weaver (1963).

#### 4-5. The Method of Adler and Cohen

In Cohen's method (Cohen 1958), which is the basis of the AIREK and AIROS codes developed at Atomics International (Blaine and Berland 1965), the variable part of the differential operator acting on  $n(t)$  is transposed to the inhomogeneous term. This yields a quasi-linear differential equation whose integrating factor does not contain an integral, and thus the double integration appearing in eq. (4-3) is avoided. After formal integration, the slowly varying factor in the integrand is expressed as a power series and the result integrated term by term. The series is truncated after three terms, and the coefficients are determined by an iterative procedure at each time step. The original suggestion of this approach appears to be due to Soodak (Wills et al. 1957).

Specifically, eq. (3-1) may be rewritten as

$$\frac{dn}{dt} + \alpha n = \left( \frac{\rho - \beta}{\ell} + \alpha \right) n + \sum_i \lambda_i c_i + q, \quad (4-38)$$

where  $\alpha$  is a parameter. Instead of  $e^{I(t)}$ , where  $I(t)$  is an integral as in eq. (4-2), we have a simple integrating factor  $e^{\alpha t}$ . From eq. (4-38),

$$n(t) = n(t_0) e^{-\alpha(t-t_0)} + \int_{t_0}^t \left[ \frac{\rho(t') - \beta + \alpha\ell}{\ell} n(t') + \sum_i \lambda_i c_i(t') + q(t') \right] e^{-\alpha(t-t')} dt'. \quad (4-39)$$

For digital computation, eq. (4-39) is coupled with the precursor equations, written as in eq. (4-25), and with standard auxiliary computations of reactivity feedback.

The integrals to be evaluated have the forms

$$\int_0^h f(t_0 + \tau) e^{\alpha\tau} d\tau$$

and

$$\int_0^h f_i(t_0 + \tau) e^{\lambda_i \tau} d\tau,$$

where  $h$  is the time step  $t - t_0$ . The time-step limitation is removed by expanding the slowly varying part in each integral, e.g.,

$$f(t_0 + \tau) = f(t_0) + \tau f'(t_0) + \frac{\tau^2}{2!} f''(t_0) + \dots,$$

and integrating term by term. This generates elementary functions of the form

$$\int_0^1 u^n e^{xu} du,$$

which are easily evaluated (see the problem set at the end of the chapter). In Cohen's method,

$$\alpha = \frac{\beta - \rho(t_0)}{\ell}, \quad (4-40)$$

where  $\rho(t_0)$  is the reactivity at the beginning of the time step. Details of evaluating the coefficients in the truncated expansions are discussed by Cohen (1958).

An alternative procedure that seems to have some advantages is suggested by the work of Adler (1961). Substitute  $c_i(t)$  from eq. (4-25) into eq. (4-39) and remove the resulting double integrals by partial integration. The result is

$$\begin{aligned} n(t) = & n(t_0) e^{-\alpha(t-t_0)} + \int_{t_0}^t \frac{\rho(t') - \beta + \alpha\ell}{\ell} n(t') e^{-\alpha(t-t')} dt' \\ & + \sum_i \frac{\lambda_i c_i(t_0)}{\alpha - \lambda_i} [e^{-\lambda_i(t-t_0)} - e^{-\alpha(t-t_0)}] \\ & + \sum_i \frac{\beta_i \lambda_i}{\ell(\alpha - \lambda_i)} \int_{t_0}^t n(t') [e^{-\lambda_i(t-t')} - e^{-\alpha(t-t')}] dt' \\ & + \int_{t_0}^t q(t') e^{-\alpha(t-t')} dt'. \end{aligned} \quad (4-41)$$

Adler chooses  $\alpha = 1/\ell$ . Also, instead of using power series, Adler uses average values of  $\rho$  and  $n$  in the integrals; the exponentials are integrated analytically and the averages improved at each time step until some predetermined degree of convergence is achieved. The essence of the two methods is the same, and we proceed to use eq. (4-39) to demonstrate practicality and to infer something about the parameter  $\alpha$ .

Let  $h = t - t_0$  and  $q = 0$  in eq. (4-39). Let  $\bar{\rho}$ ,  $\bar{n}$ , and  $\bar{c}_i$  represent suitable averages appropriate to the interval in question. Then eq. (4-39) becomes

$$n(t) = n(t_0)e^{-\alpha h} + \left( \frac{\bar{\rho} - \beta + \alpha\ell}{\ell} \bar{n} + \sum_i \lambda_i \bar{c}_i \right) \int_0^h e^{-\alpha u} du. \quad (4-42)$$

Consider first the case of small  $h$ , such that  $\alpha h \ll 1$ . We find

$$\int_0^h e^{-\alpha u} du = \frac{1 - e^{-\alpha h}}{\alpha} \approx h$$

and

$$n(t) \approx n(t_0)(1 - \alpha h) + \left( \frac{\bar{\rho} - \beta + \alpha\ell}{\ell} \bar{n} + \sum_i \lambda_i \bar{c}_i \right) h. \quad (4-43)$$

Suppose we have a reactivity step from 0 to  $\bar{\rho}$ , with  $n(t_0) = n_0$  representing equilibrium power, and suppose  $\bar{n}$  and  $\bar{c}_i$  are not far from their equilibrium values. Then  $\beta\bar{n}/\ell \approx \sum_i \lambda_i \bar{c}_i$ , and also the terms in  $\alpha$  approximately cancel. Eq. (4-43) becomes

$$n(t) \approx n_0 \left( 1 + \frac{\bar{\rho}}{\ell} h \right), \quad (4-44)$$

which is independent of  $\alpha$  and is approximately the expected response to a reactivity step after a very short time  $h$ .

On the other hand, if  $h$  is large ( $\alpha h \gg 1$ ),

$$e^{-\alpha h} \rightarrow 0$$

and

$$\int_0^h e^{-\alpha u} du \rightarrow \frac{1}{\alpha},$$

so that eq. (4-42) becomes

$$n(t) \approx \left( \frac{\bar{\rho} - \beta + \alpha\ell}{\ell} \bar{n} + \sum_i \lambda_i \bar{c}_i \right) \frac{1}{\alpha}. \quad (4-45)$$

Again consider a reactivity step from 0 to  $\bar{\rho}$  with  $\bar{n}$  and  $\bar{c}_i$  close to their equilibrium values. Eq. (4-45) becomes

$$n(t) \approx \frac{\bar{\rho} + \alpha\ell}{\alpha\ell} n_0. \quad (4-46)$$

All we can really infer from this is that the correct order of magnitude

is preserved if  $\alpha\ell \gg \bar{\rho}$ . This is clearly satisfied by Adler's choice,  $\alpha = 1/\ell$ . Cohen's choice, eq. (4-40), in eq. (4-46) yields

$$n(t) \cong \frac{\bar{\rho} + \beta - \rho(t_0)}{\beta - \rho(t_0)} n_0 \cong \frac{\beta}{\beta - \rho(t_0)} n_0, \quad (4-47)$$

which is highly suggestive of the jump condition in the prompt-jump approximation, eq. (3-10). Another convenient choice is  $\alpha = \beta/\ell$ . We infer that eq. (4-39) or eq. (4-41) yields a numerical method free from the time-step limitation; i.e., fast transients are correctly represented by using very small steps, while slow transients can be represented by using relatively large steps provided  $\alpha \gg \bar{\rho}/\ell$ . Examples are given in sec. 4-8.

Eq. (4-41) with  $\alpha = \beta/\ell$  may be used to derive the prompt-jump approximation directly from the integral equation, using the properties of the kernal as  $\ell \rightarrow 0$ . This is left as an exercise.

#### 4-6. A Weighted-residual Method

The method of weighted residuals (Crandall 1956) is highly successful with these integral forms and is independent of the value of  $\alpha$ . The particular method that has been widely studied in reactor dynamics uses linear, quadratic, or exponential trial functions, with, in Crandall's terminology, "subdomain weighting." The simplest example is the RE-29 code and similar codes developed at Argonne National Laboratory (Brittan 1956), which appear to be the first computer codes for reactor dynamics that were successful for both slow and fast transients over the full range of values of  $\ell$ .

This method with quadratic trial functions is discussed by Kaganove (1960). The method is reviewed in two papers by Flatt (1962, 1968) under the name "collocation method"; we do not use this terminology, because it is reserved by Crandall (1956) for a different type of weighting.

Using either eq. (4-39) or eq. (4-41) with arbitrary  $\alpha$ , one expresses  $n(t')$  and  $c_i(t')$  as trial functions (e.g., linear, quadratic, or exponential functions of  $t'$ ) and integrates analytically. The undetermined coefficients are then evaluated at each time step by demanding that the integral equations be satisfied with zero error at a finite number of points in each interval. For details of the procedure in the quadratic case using eq. (4-39) with  $\alpha = 0$ , see the report by Kaganove (1960). (Kaganove uses the lifetime formulation, but the results are readily simplified to conform to the generation-time formulation.)

We illustrate with a simple integral form, using a linear trial function.

Eq. (4-41) with  $q = 0$  and  $\alpha = 0$  is

$$\begin{aligned} n(t) = & n(t_0) + \frac{1}{\ell} \int_{t_0}^t \rho(t') n(t') dt' \\ & - \frac{1}{\ell} \sum_i \beta_i \int_{t_0}^t n(t') e^{-\lambda_i(t-t')} dt' \\ & + \Sigma_i c_i(t_0) [1 - e^{-\lambda_i(t-t_0)}]. \end{aligned} \quad (4-48)$$

Eq. (4-48) is essentially that used by Brittan as the basis for the RE-29 code. To demonstrate the power and versatility of the method, consider the first time step (one delay group):

$$\begin{aligned} n(h) = & n_0 + \frac{1}{\ell} \int_0^h \rho(t') n(t') dt' \\ & - \frac{\beta}{\ell} \int_0^h n(t') e^{-\lambda(h-t')} dt' + c_0(1 - e^{-\lambda h}). \end{aligned} \quad (4-49)$$

Assume the representations

$$n(t') = n_0 + At', \quad \rho(t') = \rho_0 + Bt'.$$

Evaluate the right-hand side of eq. (4-49) and equate the result to  $n_0 + Ah$ . Assuming the equilibrium initial condition  $c_0 = \beta n_0 / \lambda \ell$  and a time step  $h$  such that  $\lambda h \ll 1$ , we find

$$A = n_0 \frac{\rho_0 h + \frac{1}{2}Bh^2 + O(h^3)}{\ell h + \frac{1}{2}(\beta - \rho_0)h^2 + O(h^3)}. \quad (4-50)$$

For  $h$  very small, eq. (4-50) becomes

$$A \cong \frac{\rho_0}{\ell} n_0,$$

which represents the correct initial derivative in the step-input response. For  $\rho_0 = 0$  and a ramp  $\rho = Bt$ , we have for small  $h$

$$A \cong \frac{Bn_0h}{2\ell},$$

which may be shown to correspond to the correct derivative immediately following a step change in  $d\rho/dt$  from 0 to  $B$ .

If on the other hand one considers a time step  $h$  such that  $\ell/\beta \ll h \ll 1/\lambda$ , eq. (4-50) becomes

$$A \cong 2n_0 \frac{\rho_0 h + \frac{1}{2}Bh^2}{(\beta - \rho_0)h^2}, \quad (4-51)$$

which is independent of  $\ell$ . For a small reactivity step  $\rho_0$ ,

$$n(h) = n_0 + Ah \cong n_0 \frac{\beta + \rho_0}{\beta - \rho_0},$$

which gives the correct order of magnitude for the prompt jump. For the ramp  $\rho = Bt$ , eq. (4-51) becomes

$$A \cong \frac{Bn_0}{\beta},$$

which gives the correct initial derivative in the prompt-jump approximation. We infer that this method is free from time-step limitations.

Note that the linear representation involves the determination of a single coefficient  $A$  for each time step by requiring that eq. (4-49) be satisfied at one point (the endpoint) of each step. With quadratic or exponential trial functions, one may require exact agreement at the midpoint and endpoint of each step and determine two coefficients. It is assumed that  $\rho$  is a known function, or else is obtained by coupling to auxiliary computations, and is represented by a suitable linear or quadratic fitting. Successful use of the method for slow transients in a fast reactor is illustrated in sec. 4-8.

#### 4-7. Hansen's Method

Another elegant numerical method was developed at the Massachusetts Institute of Technology and reported by Hansen, Koen, and Little (1965). It is known as Hansen's largest-eigenvalue method, or Hansen's method. The reactor power and precursor densities appearing in the integrals are assumed exponential in time, with a rise time obtained from the largest eigenvalue (the algebraically largest root of the inhour equation corresponding to some average reactivity appropriate to each time step). The method may be regarded as a variation of the preceding two methods, in that the slowly varying factor is an exponential selected according to an estimate of the "current size" of the largest eigenvalue. (Compare with the Hurwitz WKB method described in sec. 3-6.)

We illustrate by a simple example. The dynamic equations for constant reactivity (source-free, one delay group) may be put in the form

$$\begin{aligned} n(t_0 + h) &= n(t_0)e^{(\rho - \beta)h/\ell} \\ &\quad + \lambda \int_0^h c(t_0 + \tau)e^{(\rho - \beta)(h-\tau)/\ell} d\tau \end{aligned} \quad (4-52)$$

and

$$c(t_0 + h) = c(t_0)e^{-\lambda h} + \frac{\beta}{\ell} \int_0^h n(t_0 + \tau)e^{-\lambda(h-\tau)} d\tau,$$

where  $h$  is the interval  $t - t_0$ . Assume

$$n(t_0 + h) = n(t_0)e^{\omega\tau}$$

and

$$c(t_0 + \tau) = c(t_0)e^{\omega\tau};$$

where  $\omega$  is the algebraically largest root ( $\omega_1$ ) of the inhour equation. Substitution and integration yields

$$\begin{aligned} n(t_0 + h) &= n(t_0)e^{(\rho-\beta)h/\ell} \\ &\quad + \frac{\lambda c(t_0)}{\omega - (\rho - \beta)/\ell} [e^{\omega h} - e^{(\rho-\beta)h/\ell}]; \quad (4-53) \\ c(t_0 + h) &= c(t_0)e^{-\lambda h} + \frac{(\beta/\ell)n(t_0)}{\omega + \lambda} [e^{\omega h} - e^{-\lambda h}]. \end{aligned}$$

If  $\rho = \rho(t)$ , eq. (4-53) is used with  $\omega$  determined from the inhour equation for an average reactivity appropriate to each time step, as determined by auxiliary equations. For the general formulation and proof of stability, see the paper by Hansen, Koen and Little (1965). The extension to  $m$  delay groups is

$$\Psi(t_0 + h) = \mathbf{G}\Psi(t_0), \quad (4-54)$$

where  $\Psi$  is a column vector with components  $n, c_1, c_2, \dots$  and  $\mathbf{G}$  is the matrix

$$\mathbf{G} = \begin{bmatrix} e^{(\rho-\beta)h/\ell} & \lambda_1 \frac{e^{\omega h} - e^{(\rho-\beta)h/\ell}}{\omega - (\rho - \beta)/\ell} & \cdots & \lambda_m \frac{e^{\omega h} - e^{(\rho-\beta)h/\ell}}{\omega - (\rho - \beta)/\ell} \\ \frac{\beta_1}{\ell} \frac{e^{\omega h} - e^{-\lambda_1 h}}{\omega + \lambda_1} & e^{-\lambda_1 h} & \cdots & 0 \\ \cdot & \cdot & \ddots & \cdot \\ \cdot & \cdot & \ddots & \cdot \\ \frac{\beta_m}{\ell} \frac{e^{\omega h} - e^{-\lambda_m h}}{\omega + \lambda_m} & 0 & & e^{-\lambda_m h} \end{bmatrix}. \quad (4-55)$$

The success of this method is quickly understood from our simple example by noting that for small  $h$  and equilibrium initial conditions

eq. (4-53) yields

$$n(t_0 + h) \cong n(t_0) \left( 1 + \frac{\rho}{\ell} h \right), \quad (4-56)$$

which corresponds to the expected initial derivative. For  $\rho < \beta$  and relatively large  $h$  (say  $\omega h$  of the order of unity), however,

$$n(t_0 + h) \cong n(t_0) \frac{\beta}{\beta - \rho} e^{\omega h}, \quad (4-57)$$

which predicts the correct order of magnitude for the prompt jump.

Sample computations are described and compared with other methods in sec. 4-8.

#### 4-8. A Numerical Experiment

The numerical methods described in this chapter have been compared in sample computations of slow transients run on the University of Arizona digital computer (Szeligowski and Hetrick 1967). The test example is one cycle of a sinusoidal reactivity ( $\rho < \beta$ ), with amplitude and frequency arbitrarily related through the inhour equation in an attempt to simulate without auxiliary feedback computations the qualitative features of a nonlinear autonomous negative-feedback system: a substantial range of power variation, a power peak occurring as the reactivity decreases toward zero, and a range of negative reactivity (see chapter 5).

One group of delayed neutrons is used to permit comparison with a complete analytical solution in the prompt-jump approximation (sec. 3-2). For the digital computations, the neutron generation time ranges from  $10^{-3}$  to  $10^{-8}$  sec. Accuracy may be judged by comparing computed values of peak power (which occurs during the second quarter-cycle) and by comparison of the solutions with the prompt-jump approximation in the case of small  $\ell$ .

If a sinusoidal reactivity

$$\rho = \rho_0 \sin \frac{\pi t}{T} \quad (4-58)$$

is used, the analytical solution in the prompt-jump approximation is given by eq. (3-66) or (3-70) with  $A = 0$ ,  $B = \rho_0/\beta$ , and  $\omega = \pi/T$ . Realistic time scales are simulated by arbitrarily equating one quarter-period of the sine wave to a rough estimate of the power-burst width resulting from a self-limiting excursion having maximum reactivity  $\rho_0$ . The Nordheim-Fuchs model (chapter 5) predicts an approximate burst width  $4/\omega_1$ , where  $\omega_1$  is the reciprocal period corresponding to

maximum reactivity; this is an underestimate for slow excursions, but we get the correct order of magnitude for use in these sample calculations by setting the sine-wave quarter-period  $T/2$  equal to  $4/\omega_1$ . If eq. (2-23), the inhour equation for slow transients, is used,

$$\rho_0 = \frac{\beta\omega_1}{\omega_1 + \lambda},$$

and the sine-wave amplitude and half-period are related by

$$\rho_0 = \frac{8\beta}{8 + \lambda T}. \quad (4-59)$$

Parameters for the four cases studied are listed in table 4-1, and a typical solution curve in the prompt-jump approximation (case 4 in table 4-1) is shown in fig. 4-3.

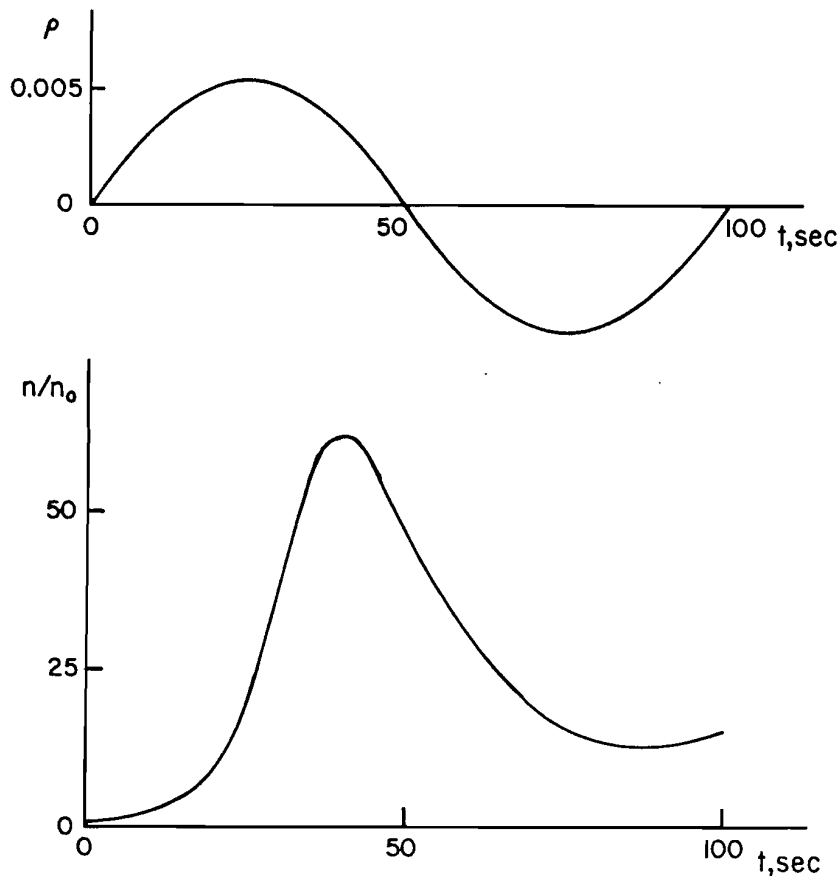


Fig. 4-3. Reactivity and neutron density vs. time for typical test example (prompt-jump approximation);  $n_0 = 1$ ,  $\lambda = 0.077 \text{ sec}^{-1}$ ,  $\beta = 0.0079$ , amplitude  $\rho_0 = 0.005333$  (68 cents), and half-period  $T = 50 \text{ sec}$ .

Peak powers for various digital computations run with different time-step size  $\Delta t$  are shown in figs. 4-4 through 4-7. In all cases,  $n_0 = n(0) = 1$ ,  $\lambda = 0.077 \text{ sec}^{-1}$  and  $\beta = 0.0079$ . The three methods

Table 4-1. Parameters for Numerical Examples

Case No.	Reactivity Amplitude ( $\rho_0$ )	Half-period (T, sec)
1	0.001808 (23 cents)	350
2	0.002319 (29 cents)	250
3	0.003233 (41 cents)	150
4	0.005333 (68 cents)	50

tested extensively are: (1) Adler's iterative method using eq. (4-41) but with  $\alpha$  given by eq. (4-40), (2) the weighted-residual method using eqs. (4-40) and (4-41) with a quadratic trial function, and (3) Hansen's largest-eigenvalue method using eq. (4-53).

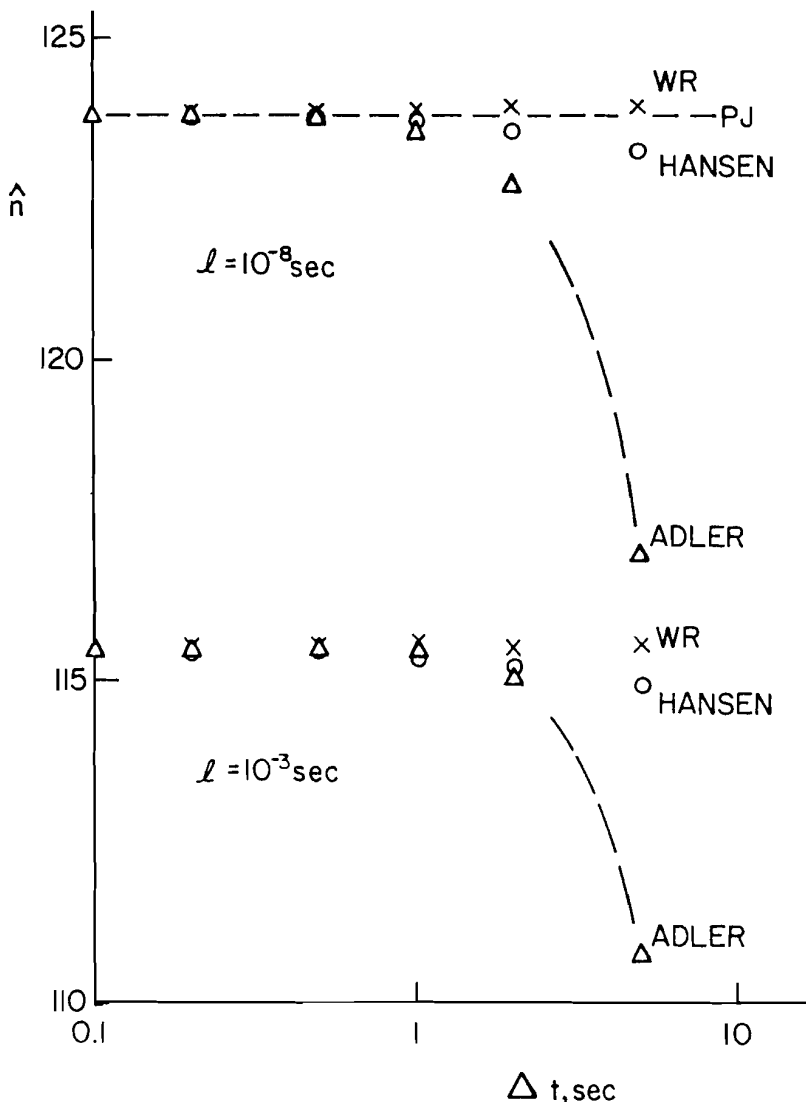


Fig. 4-4. Peak neutron density vs. interval size for various computing methods;  $\rho_0 = 0.001808$  (23 cents) and  $T = 350$  sec (Szeligowski and Hetrick 1967). Dashed line is the prompt-jump approximation.

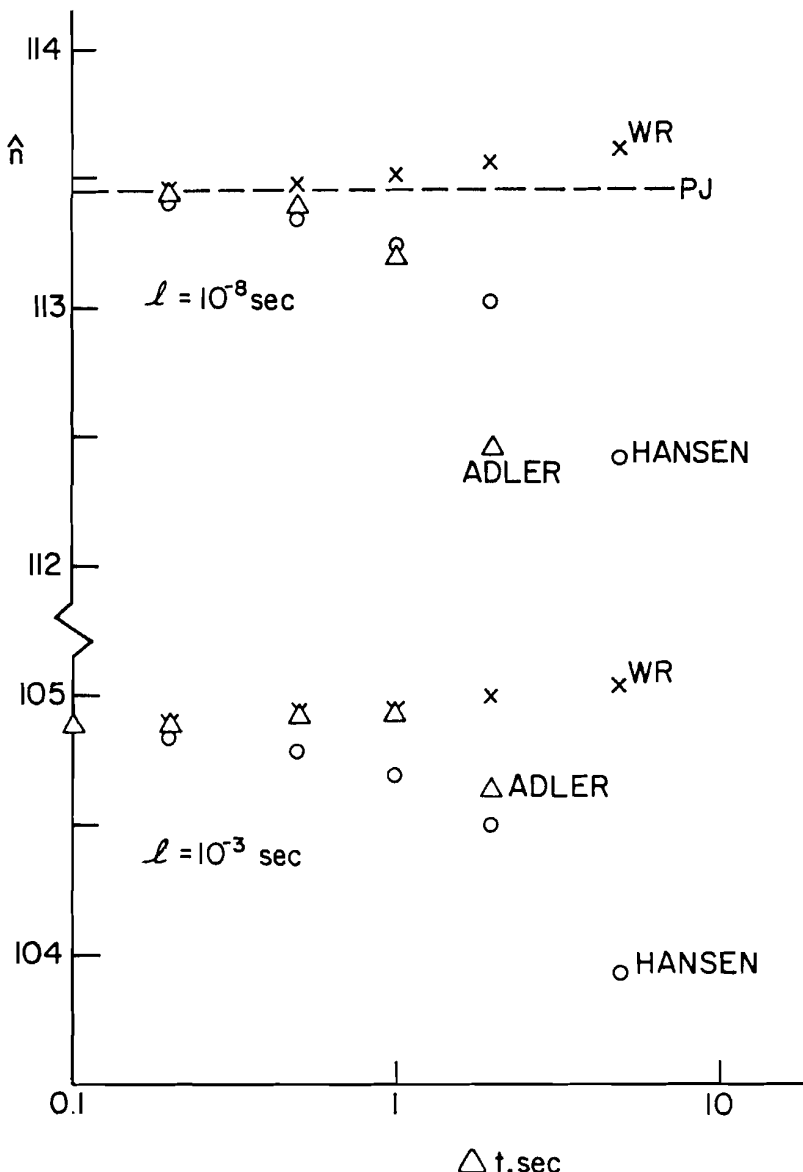


Fig. 4-5. Peak neutron density vs. interval size for various computing methods;  $\rho_0 = 0.002319$  (29 cents) and  $T = 250$  sec (Szeligowski and Hetrick 1967).

The two extreme values for  $\ell$  are illustrated in each of figs. 4-4 through 4-7. As expected, the values of peak power in the cases for small  $\ell$  appear to converge to the value given by the prompt-jump approximation as  $\Delta t$  is reduced. Note that all three methods, even for the fast-reactor examples  $\ell = 10^{-8}$  sec, are successful with interval sizes  $\Delta t$  that are reasonable for the characteristic time scale of the overall dynamic process. In contrast, it has been estimated from sample calculations with  $\ell = 10^{-3}$  sec that comparable accuracy for the example of fig. 4-4 with  $\ell = 10^{-8}$  sec would require  $2 \times 10^8$  time steps using a simple forward-difference method and  $5 \times 10^7$  time steps using the fourth-order Runge-Kutta method (Szeligowski and Hetrick 1967).

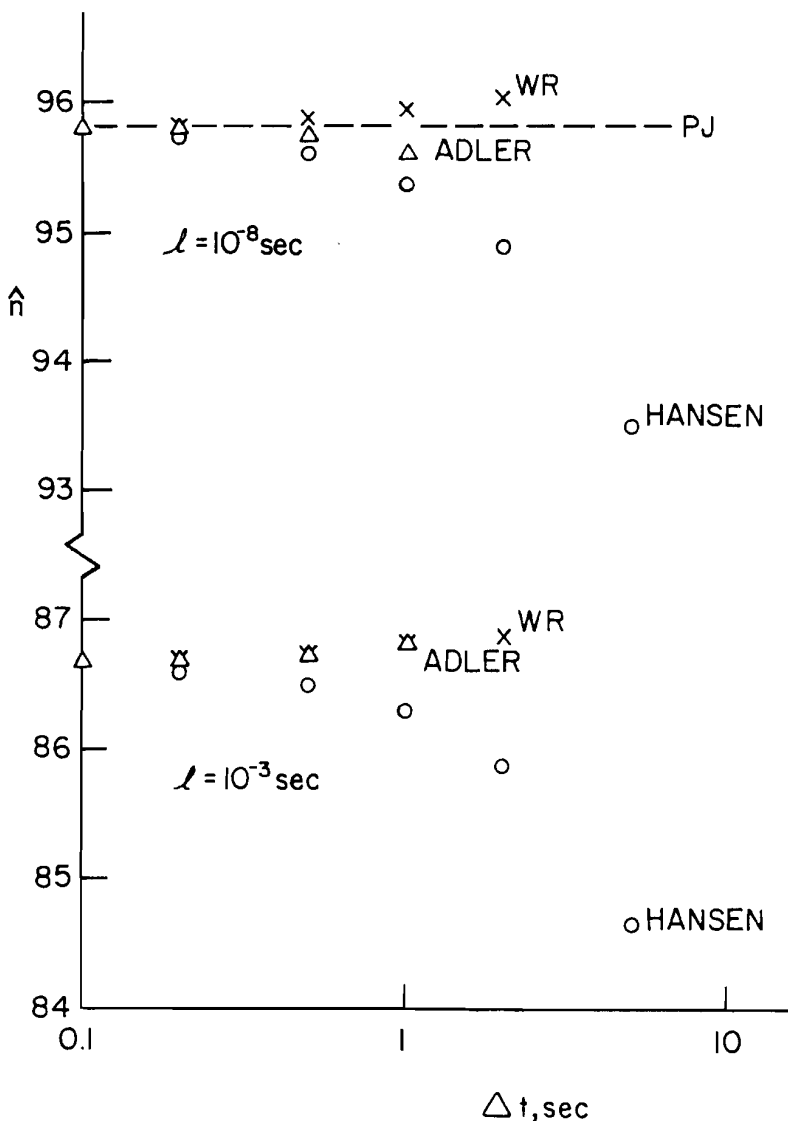


Fig. 4-6. Peak neutron density vs. interval size for various computing methods;  $\rho_0 = 0.003233$  (41 cents) and  $T = 150$  sec (Szeligowski and Hetrick 1967).

Fig. 4-7 includes a few points attributed to Cohen's method. These were computed by using eqs. (4-39) and (4-40) with the precursor density given by eq. (4-25); as in Adler's method, integrals were evaluated by assuming average values and iterating instead of using the original algorithm of Cohen (1958). This permits a comparison of the two formulations, and from the few cases tested it appears that eq. (4-41) may yield a more efficient numerical method than eq. (4-39).

Fig. 4-7 also includes a few points labeled LT (Laplace-transform method). This refers to eq. (4-16), the basis of Keepin's RTS code (Keepin 1965). For the fast reactor ( $\ell = 10^{-8} \text{ sec}$ ), direct numerical integration of the convolution integral in eq. (4-16) is not feasible. A feasible modification may be constructed for small  $\ell$  by approximate analytical integration and subsequent neglect of rapidly decaying transients; this yielded the points LT in fig. 4-7. The result does not

compare favorably with the three chief methods illustrated. For  $\ell = 10^{-3}$  sec, the convolution method is feasible but only with  $\Delta t < 10^{-2}$  sec; points obtained for larger  $\Delta t$  fall off-scale at the bottom of fig. 4-7.

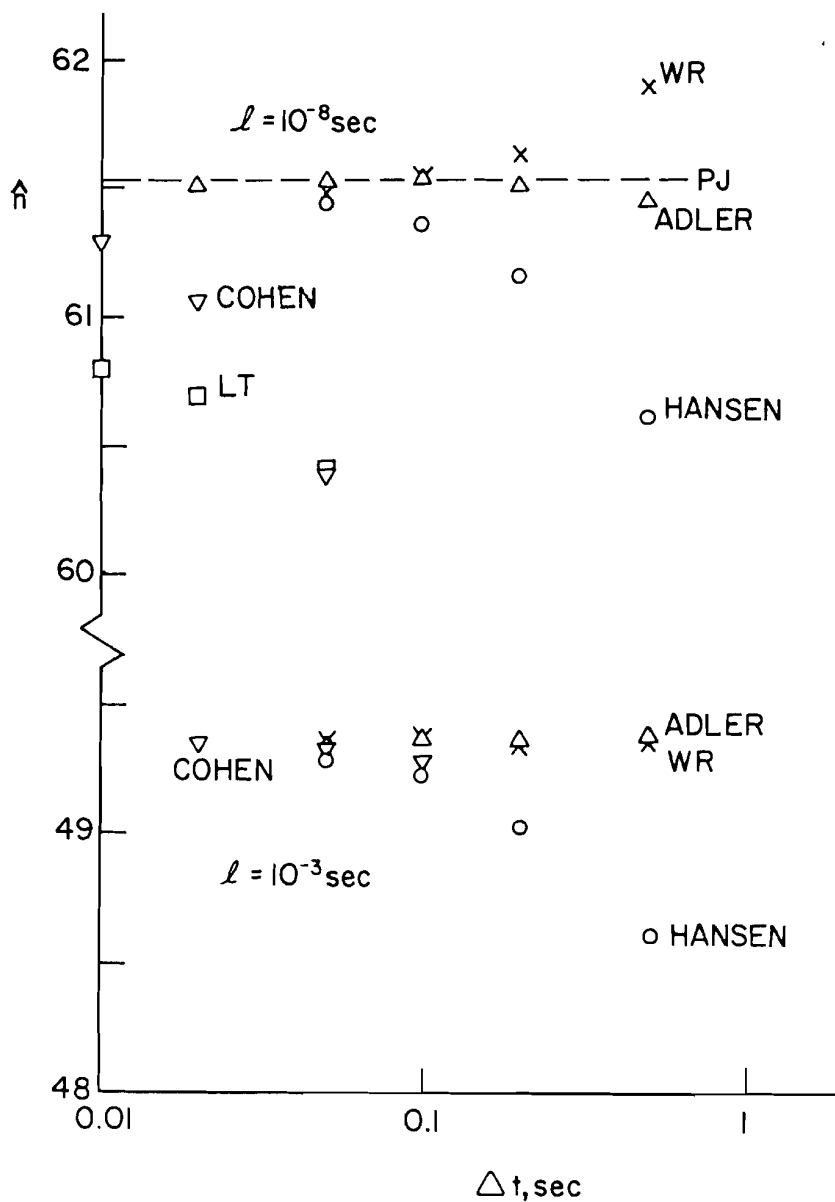


Fig. 4-7. Peak neutron density vs. interval size for various computing methods;  $\rho_0 = 0.005333$  (68 cents) and  $T = 50$  sec (Szeligowski and Hetrick 1967).

Computing times for the three chief methods seem to be comparable. The quadratic weighted-residual method requires slightly more machine time for the same  $\Delta t$  in the examples of figs. 4-4 through 4-7, yielding generally superior accuracy for larger  $\Delta t$ . A few checkpoints using linear trial functions show a slight decrease in computing time

with no significant loss of accuracy at  $\Delta t = 0.1$  sec in fig. 4-7, though it remains to make comparisons at larger  $\Delta t$ .

These comparisons are based on relatively simple numerical methods. The chief purpose here has been to demonstrate that the time-step limitation arising from small  $\ell/\beta$  is easily circumvented. Once this major hurdle is overcome, more sophisticated numerical methods can presumably yield still further gains in computing efficiency over those we have indicated, but it is not our purpose here to investigate this nor to speculate on how far such sophistication can profitably be carried.

Other numerical methods reported recently do seem specially promising. Porsching (1966) has generalized Hansen's method, effecting the approximate integrations by representing exponential functions of a matrix as rational matrix functions. Birkhoff (1966) has proposed a new method based on the recasting of the point-reactor problem in the form of differential-delay equations. A new matrix approach has been reported by Hansen, Kleban, and Chang (1969). The method of Adler and Cohen has been generalized by Secker (1969a, 1969b), who devised a procedure for continually recomputing  $\alpha$  in eq. (4-39) such that the estimated error at each time step is minimized. This method of "optimum integrating factors" includes the possibility of complex values for  $\alpha$ , which may be automatically introduced in oscillatory solutions. The variety of methods is quite large, and the choice of method appropriate for a particular class of problems may depend as much on individual taste as on the nature of the problem. Finally, we reiterate the observation made in sec. 4-4 that the types of problems requiring special treatment are generally those problems (small  $\ell$  and small  $\rho$ ) for which the prompt-jump approximation is adequate. For example, the ANCON code (Vigil 1966) has been used to verify the examples of figs. 4-4 through 4-7, with a switch to an option employing the prompt-jump approximation when  $\ell = 10^{-8}$  sec (computations performed by John C. Vigil, Los Alamos Scientific Laboratory). Other examples using the ANCON code (based on the method of continuous analytic continuation) are given in the paper by Vigil (1967).

For a discussion of matching the actual prompt transient to the asymptotic (prompt-jump) approximation, see MacMillan (1967). A new derivation of a first-order correction to the prompt-jump approximation is given by Goldstein and Shotkin (1969).

Methods developed for reactor dynamics may of course be applied in other fields whenever one encounters an extremely wide spectrum of response times in a dynamic system. Examples are chemical kinetics, missile guidance systems, and certain aerodynamics problems.

#### 4-9. The Inverse Problem

Many writers have derived formulas for calculating the reactivity  $\rho(t)$  from a prescribed power history  $n(t)$ . Some of these formulas and their applications are reviewed by Murray, Bingham, and Martin (1964) and Kovanic (1965). One application is the design of a continuous reactivity monitor, its input the continuous signal from a judiciously located flux monitor. Another application is the computation of instantaneous reactivity during a power excursion in a pulsed reactor. A third use is the planning of a programmed reactivity  $\rho(t)$  that will produce some desired dynamic power  $n(t)$ . In this section we present integral formulas for computing  $\rho(t)$  from a given power history and note the modifications required for slow transients.

From eq. (3-1) we have

$$\rho = \beta + \frac{\ell}{n} \frac{dn}{dt} - \frac{\ell}{n} \sum_i \lambda_i c_i - \frac{\ell q}{n}. \quad (4-60)$$

Substituting eq. (4-25) for the precursor densities, we obtain

$$\begin{aligned} \rho = \beta &+ \frac{\ell}{n} \frac{dn}{dt} - \frac{\ell}{n} \sum_i \lambda_i c_i(t_0) e^{-\lambda_i(t-t_0)} \\ &- \frac{1}{n} \int_{t_0}^t n(t') \sum_i \beta_i \lambda_i e^{-\lambda_i(t-t')} dt' - \frac{\ell q}{n}. \end{aligned} \quad (4-61)$$

This is of course eq. (4-26) solved explicitly for  $\rho$ , and the integral may be represented in terms of the probability density  $D(t)$  of eq. (4-27) and fig. 4-2. Eq. (4-61) is essentially that used for computing reactivity in the SPERT-I reactor excursion experiments (Miller 1957; Corben 1959b) and in the KEWB (Kinetic Experiment Water Boiler) excursions (Dunenfeld 1962).

Using the identity

$$e^{-\lambda_i(t-t_0)} = 1 - \lambda_i \int_{t_0}^t e^{-\lambda_i(t-t')} dt',$$

we may write eq. (4-61) as

$$\begin{aligned} \rho = \beta &+ \frac{\ell}{n} \frac{dn}{dt} - \frac{\ell}{n} \sum_i \lambda_i c_i(t_0) \\ &- \frac{1}{n} \int_{t_0}^t \sum_i [\beta_i \lambda_i n(t') - \ell \lambda_i^2 c_i(t_0)] \\ &\times e^{-\lambda_i(t-t')} dt' - \frac{\ell q}{n}. \end{aligned} \quad (4-62)$$

In the source-free case with equilibrium at  $t = t_0$ , we have

$$\begin{aligned}\rho &= \beta + \frac{\ell}{n} \frac{dn}{dt} - \beta \frac{n(t_0)}{n} \\ &\quad - \frac{1}{n} \int_{t_0}^t [n(t') - n(t_0)] \Sigma_i \beta_i \lambda_i e^{-\lambda_i(t-t')} dt'.\end{aligned}\quad (4-63)$$

An alternate form is generated by partial integration in eq. (4-61):

$$\begin{aligned}\rho &= \frac{\ell}{n} \frac{dn}{dt} + \frac{1}{n} \Sigma_i [\beta_i n(t_0) - \ell \lambda_i c_i(t_0)] e^{-\lambda_i(t-t_0)} \\ &\quad + \frac{1}{n} \int_{t_0}^t \frac{dn(t')}{dt'} \Sigma_i \beta_i e^{-\lambda_i(t-t')} dt' - \frac{\ell q}{n}.\end{aligned}\quad (4-64)$$

The integral in eq. (4-64) may of course be expressed in terms of the delayed-neutron decay function  $f(t)$  of eq. (4-10) and fig. 4-1; when  $t_0 = 0$ , eq. (4-64) reduces to eq. (4-9). In the source-free case with equilibrium at  $t = t_0$ , eq. (4-64) simplifies to

$$\rho = \frac{\ell}{n} \frac{dn}{dt} + \frac{1}{n} \int_{t_0}^t \frac{dn(t')}{dt'} \Sigma_i \beta_i e^{-\lambda_i(t-t')} dt'.\quad (4-65)$$

If instead the reactivity has been a constant  $\rho_0$  for a sufficiently long time before  $t_0$ , one may use the asymptotic relation

$$c_i(t_0) = \frac{\beta_i n(t_0)}{\ell(\omega_1 + \lambda_i)}$$

to find

$$\begin{aligned}\rho &= \frac{\ell}{n} \frac{dn}{dt} + \frac{n(t_0)}{n} (\rho_0 - \ell \omega_1) \Sigma_i e^{-\lambda_i(t-t_0)} \\ &\quad + \frac{1}{n} \int_{t_0}^t \frac{dn(t')}{dt'} \Sigma_i \beta_i e^{-\lambda_i(t-t')} dt'.\end{aligned}\quad (4-66)$$

This is a convenient form for analyzing step-induced excursions, starting from low power, in a pulsed reactor.

In a very fast excursion starting from low power, the initial conditions are unimportant. Further, the time scale is short enough that precursors do not decay appreciably until after the power burst is over. Eq. (4-63) then reduces to

$$\rho = \beta + \frac{\ell}{n} \frac{dn}{dt} - \Sigma_i \beta_i \lambda_i \frac{E}{n},\quad (4-67)$$

where  $E$  is the energy

$$E(t) = \int_{t_0}^t [n(t') - n(t_0)] dt' \cong \int_{t_0}^t n(t') dt'. \quad (4-68)$$

Eq. (4-67) provides an excellent approximation during a fast burst and a convenient limiting case for checking digital computations.

In very slow transients, special attention is needed for the integrals, which have the form

$$\int_0^h f_i(t_0 + \tau) e^{\lambda_i \tau} d\tau$$

as in sec. 4-5. To avoid an excessive number of time steps when  $n(t)$  is changing slowly over intervals that are large compared to  $1/\lambda_i$ , one may use the same scheme as in sec. 4-5: expand only the slowly varying factors in power series and integrate term by term to generate the simple functions

$$\int_0^1 u^n e^{xu} du.$$

Frequently it is adequate to use merely an average value appropriate to each time step, generating only the integrals for  $n = 0$  (simple exponentials).

We mention briefly a few other schemes for computing  $\rho(t)$  from  $n(t)$ . As quoted by Brittan (1956), H. Greenspan proposed a method suitable whenever  $n(t)$  can be represented as a Laplace-transformable function. Solve eq. (4-15) for  $\mathcal{L}(\rho n)$ :

$$\mathcal{L}(\rho n) = \frac{N(s) - n_0/s}{K(s)} - \sum_i \frac{\lambda_i \ell c_{i0} - \beta_i n_0}{s + \lambda_i}. \quad (4-69)$$

We know that  $K(s)$  is essentially the zero-power transfer function, eq. (4-14), and that it may be expressed as a ratio of polynomials. The inversion may then be performed and the result solved for  $\rho$ .

The RTS code (Keepin 1965) has an inverse option. Eq. (4-16), when set up for numerical evaluation of the convolution integral, may be inverted to express the reactivity at each time step. Another method based on eq. (4-16) has been developed by Evans (1964). An attractive feature of the inverse problem is the possibility of studying some aspects of reactor dynamics without having to solve nonlinear differential equations.

## Problems

- 4-1. Verify the steps in deriving Keepin's integral equation, eq. (4-16).

- 4-2. Use the integro-differential form, eq. (4-9), to justify the effective-lifetime model. Neglect the source and initial-condition terms. Hint: Regard the derivative under the integral as slowly varying.
- 4-3. Derive the prompt-jump approximation from eq. (4-16). Neglect the source and initial-condition terms. Hint: Use the impulse response discussed in prob. 2-18.
- 4-4. Verify the subcritical transfer functions, eqs. (4-22) and (4-23).
- 4-5. Derive the alternate form of Keppin's equation, eq. (4-24).
- 4-6. Derive a matrix equation, using backward differences, that corresponds to eq. (4-35). Compare the result with eq. (4-37).
- 4-7. Define the functions  $H_n(x)$  by

$$H_n(x) = \int_0^1 u^n e^{xu} du.$$

Show that

$$H_0(x) = \frac{1}{x} (e^x - 1);$$

$$H_n(x) = \frac{1}{x} [e^x - nH_{n-1}(x)];$$

$$H_n(x) = \sum_{m=0}^{\infty} \frac{x^m}{m!(m+n+1)}.$$

- 4-8. Derive Adler's integral equation, eq. (4-41).
- 4-9. Derive the prompt-jump approximation from a special case of eq. (4-41). Use one delay group with  $\alpha = \beta/\ell$  and  $t_0 = 0$ . Take the limit as  $\ell \rightarrow 0$  and use the fact that

$$\frac{\beta}{\ell} \exp [-(\beta/\ell)t]$$

is similar to the delta function  $\delta(t)$  when  $\ell$  is very small.

- 4-10. Derive eq. (4-50) for the undetermined parameter  $A$  in the linear trial function.
- 4-11. Derive eqs. (4-52) and (4-53) for Hansen's method.
- 4-12. Compute the reactivity function that will produce a ramp change of power from one steady level to another (Murray, Bingham, and Martin 1964).

## **5 Reactivity Feedback and Reactor Excursions**

In the next few chapters, the point-reactor model is extended to include the effect of fission-energy production on the reactivity. That portion of reactivity change arising from the effects of energy production is called reactivity feedback. We shall be concerned primarily with intrinsic feedback, such as the effects of temperature and density changes on the reproduction factor  $k$ , in contrast to reactivity changes generated by feedback signals in automatic control systems.

We first consider some prototype calculations of the temperature coefficient of reactivity for simple models of thermal reactors, and the distinction between prompt and delayed effects is noted. It is pointed out that other physical and chemical effects of fission energy release (e.g., change of state, gas evolution) may accompany a temperature rise, and that it is sometimes useful to speak of an energy coefficient of reactivity. Some special problems of fast reactors are summarized in a separate section.

Next we treat the classic calculations of reactor excursions induced by reactivity steps in systems with prompt linear feedback: the Nordheim-Fuchs model for fast excursions and the prompt-jump model for slow excursions. These are then unified in a single model which permits a new treatment of the transitional case near prompt critical. A nonautonomous case with externally induced reactivity increasing linearly with time (the Fuchs ramp-input model) is treated next, and the final sections deal with excursions in systems having complex energy feedback mechanisms.

### **5-1. Homogeneous Thermal Reactors**

In this section we derive the temperature coefficient of reactivity for a simple model of a homogeneous thermal reactor. The model is that

## 14.2 Reactivity Feedback and Reactor Excursions

used by Lamarsh (1966). It has a few features not included in the reactor model we used in chapter 1.

First, we note that the symbol  $\alpha$  is frequently used to represent a temperature coefficient of reactivity. Lamarsh (1966) more properly uses  $\alpha_T$ . We may start with the relation

$$\alpha_T = \frac{d\rho}{dT}, \quad (5-1)$$

where  $\rho$  is the reactivity of the system and  $T$  is the temperature of some component. Using eq. (1-12), which may be written as  $\rho = 1 - k^{-1}$ , we find

$$\alpha_T = \frac{1}{k^2} \frac{dk}{dT}. \quad (5-2)$$

For all cases of interest,  $k$  is near unity, and eq. (5-2) may be written

$$\alpha_T \cong \frac{1}{k} \frac{dk}{dT}. \quad (5-3)$$

For convenience, eq. (5-3) is frequently adopted as the definition of temperature coefficient.

We shall use  $\alpha_T$  as defined by eq. (5-3) only in the early sections of this chapter. Later, in discussion of self-limiting power excursions, it will be more convenient to use

$$\alpha = -\alpha_T = -\frac{1}{k} \frac{dk}{dT}. \quad (5-4)$$

This is true because stable systems are generally associated with a negative value for  $\alpha_T$  (power increases, temperature rises,  $k$  decreases). A formula for peak power or temperature rise in a self-limiting excursion, if written in terms of  $\alpha_T$ , would contain an awkward minus sign. Further, we will wish to use the control engineer's convention that the sign of the feedback signal is changed before it is combined with the input signal (see chapter 6). We therefore use  $\alpha_T$  as given by eq. (5-3) in deriving temperature coefficients, afterward switching to  $\alpha = -\alpha_T$  when discussing excursions and stability.

We proceed to calculate  $\alpha_T$  for an unreflected homogeneous thermal reactor. We will first treat the temperature change as uniform throughout the reactor, and the particular  $\alpha_T$  obtained is therefore called the *isothermal* temperature coefficient.

The reactor model of chapter 1 is replaced by (Lamarsh 1966)

$$k = k_\infty P_t P_f, \quad (5-5)$$

where the infinite-medium reproduction factor is

$$k_{\infty} = \eta \epsilon p f \quad (5-6)$$

and where  $P_t$  and  $P_f$  are respectively the nonleakage probabilities for thermal and fast neutrons. From diffusion theory,

$$P_t = \frac{1}{1 + B^2 L^2}, \quad (5-7)$$

and from Fermi age theory,

$$P_f = e^{-B^2 t}. \quad (5-8)$$

In eq. (5-6),

$\eta$  = average number of fission neutrons emitted per thermal neutron absorbed in fuel;

$\epsilon$  = average number of neutrons produced in all fissions, fast and thermal, per neutron produced in thermal fission alone (fast-fission factor);

$p$  = probability that a source neutron is not absorbed while slowing down (resonance-escape probability);

$f$  = average number of thermal neutrons absorbed in fuel per thermal neutron absorbed in the reactor (thermal utilization).

In eqs. (5-7) and (5-8),  $B^2$  is the fundamental-mode buckling (as in chapter 1),  $L^2$  is the diffusion area for thermal neutrons, and  $\tau$  is the neutron age or epithermal migration area.

From eqs. (5-3) and (5-5),

$$\alpha_T = \frac{1}{k} \frac{dk}{dT} = \frac{1}{k_{\infty}} \frac{dk_{\infty}}{dT} + \frac{1}{P_t} \frac{dP_t}{dT} + \frac{1}{P_f} \frac{dP_f}{dT}. \quad (5-9)$$

Using the notation

$$\alpha_T(x) = \frac{1}{x} \frac{dx}{dT},$$

we may write eq. (5-9) as

$$\alpha_T = \alpha_T(k) = \alpha_T(k_{\infty}) + \alpha_T(P_t) + \alpha_T(P_f). \quad (5-10)$$

Similarly, from eq. (5-6),

$$\alpha_T(k_{\infty}) = \alpha_T(\eta) + \alpha_T(\epsilon) + \alpha_T(p) + \alpha_T(f), \quad (5-11)$$

and from eqs. (5-7) and (5-8),

$$\alpha_T(P_t) = -\frac{B^2 L^2}{1 + B^2 L^2} [\alpha_T(L^2) + \alpha_T(B^2)] \quad (5-12)$$

and

$$\alpha_T(P_f) = -B^2\tau[\alpha_T(\tau) + \alpha_T(B^2)]. \quad (5-13)$$

The temperature coefficient  $\alpha_T$  of the reactor is now expressed in terms of temperature coefficients of individual parameters by means of eqs. (5-10) through (5-13).

The temperature coefficient of  $\eta$  arises primarily from the fact that the fuel-material cross-sections for thermal fission and radiative capture do not have the same dependence on neutron speed. For a single fissile isotope

$$\eta = v\sigma_f/\sigma_a, \quad (5-14)$$

where  $v$  is the mean number of neutrons per fission (chapter 1) and where  $\sigma_f$  and  $\sigma_a$  are respectively the average thermal fission and total thermal absorption cross-sections in the fuel. The change in  $v$  at thermal energies is very small. Temperature coefficients  $\alpha_T(\eta)$  at 100°C (Lamarsch 1966) derived from the neutron-temperature dependence of  $\eta$  (Westcott 1962) are:  $-3 \times 10^{-5}$  per °C for U<sup>235</sup>,  $-5 \times 10^{-4}$  per °C for Pu<sup>239</sup>, and  $+4 \times 10^{-5}$  per °C for U<sup>233</sup>.

For fuels consisting of a mixture of isotopes,  $\eta$  is computed from a weighted average of macroscopic cross-sections. For natural uranium,  $\alpha_T(\eta)$  is practically zero below about 300°C, changing to about  $-10^{-4}$  per °C above this temperature (Lamarsch 1966). Except for Pu<sup>239</sup>,  $\alpha_T(\eta)$  is usually unimportant in a homogeneous reactor.

The preceding is based on the assumption that the thermal neutron spectrum is Maxwellian and that there is a single temperature throughout the reactor. Limitations imposed by this assumption are discussed in the next section of this chapter.

The fast-fission factor  $\epsilon$  is independent of temperature in a homogeneous thermal reactor. Heterogeneous reactors are discussed in the next section; for the moment we take  $\alpha_T(\epsilon) = 0$ .

The resonance escape probability  $p$  depends on temperature through the Doppler effect (Lamarsch 1966; Weinberg and Wigner 1958). Briefly, increased thermal agitation of fuel atoms, corresponding to a temperature rise, can result in increased neutron absorption. In a homogeneous thermal reactor with its normally low fuel concentration, the Doppler effect is usually negligibly small, and  $\alpha_T(p) \approx 0$ . We discuss the Doppler effect in some detail in the sections on heterogeneous reactors and fast reactors.

The thermal utilization of a homogeneous reactor is given by

$$f = \frac{\Sigma_{aF}}{\Sigma_{aF} + \Sigma_{aM}}, \quad (5-15)$$

where  $\Sigma_{aF}$  and  $\Sigma_{aM}$  are respectively the average macroscopic thermal absorption cross-sections of the fuel and moderator. Differentiating yields

$$\alpha_T(f) = (1 - f)[\alpha_T(\Sigma_{aF}) - \alpha_T(\Sigma_{aM})]. \quad (5-16)$$

Since  $\Sigma = N\sigma$ , where  $N$  is the atom density and  $\sigma$  is a microscopic cross-section, we have for either fuel or moderator

$$\alpha_T(\Sigma_a) = \alpha_T(N) + \alpha_T(\sigma_a). \quad (5-17)$$

The atom density  $N$  is proportional to density (inversely proportional to specific volume) so that

$$\alpha_T(N) = -\beta, \quad (5-18)$$

where  $\beta$  is the volume coefficient of thermal expansion. The average microscopic thermal absorption cross-section may be written (Lamarsch 1966) as

$$\sigma_a = g_a(T)/\sqrt{T}, \quad (5-19)$$

where  $g_a$  may be called the non- $1/v$  factor and where  $T$  is the neutron temperature in °K. If the neutron temperature may be identified with the temperature of the reactor,

$$\alpha_T(\sigma_a) = \alpha_T(g_a) - \frac{1}{2T}. \quad (5-20)$$

More generally, a correction factor should be included to account for the difference between the neutron temperature and the temperature of the moderator-fuel mixture; this is omitted here, though it is clearly important in many cases to distinguish between contributions arising from the temperature of the medium (such as the effect on  $N$ ) and those arising from the neutron temperature (such as the effect on  $\sigma_a$ ).

For a moderator,  $\sigma_a$  frequently has pure  $1/v$  dependence and  $\alpha_T(\sigma_{aM}) = -1/2T$ . From eqs. (5-17) through (5-20) we find, assuming an intimate mixture of fuel and moderator,

$$\alpha_T(\Sigma_{aF}) = -\beta + \alpha_T(g_{aF}) - \frac{1}{2T} \quad (5-21)$$

and

$$\alpha_T(\Sigma_{aM}) = -\beta - \frac{1}{2T}. \quad (5-22)$$

The net result of using eq. (5-16) is

$$\alpha_T(f) = (1 - f)\alpha_T(g_{aF}). \quad (5-23)$$

Some representative values of  $\alpha_T(g_{aF})$  at 500°C are (Lamarsh 1966):  $-3.5 \times 10^{-5}$  per °C for U<sup>235</sup>,  $1.4 \times 10^{-3}$  per °C for Pu<sup>239</sup>, and  $3.1 \times 10^{-5}$  per °C for U<sup>233</sup>. Note the variety in both magnitude and sign. The factor  $1 - f$  is typically 0.1 or 0.2, however, so that  $\alpha_T(f)$  in a homogeneous reactor is usually negligible (except for Pu<sup>239</sup> fuel).

An improved treatment of the temperature coefficient of  $k_\infty$  may be achieved by including epithermal effects. One defines an effective value of the product  $\eta f$  as a weighted average over neutron energy up to the threshold for fast fission. The contribution from  $(\eta f)_{\text{eff}}$  in the temperature coefficient may then be computed with the aid of Westcott's formulation (Argonne National Laboratory 1963a).

We next consider the parameters  $L^2$ ,  $\tau$ , and  $B^2$  appearing in eqs. (5-12) and (5-13). As in chapter 1,

$$L^2 = D/\Sigma_a, \quad (5-24)$$

where  $D$  is the diffusion coefficient. Therefore

$$\alpha_T(L^2) = \alpha_T(D) - \alpha_T(\Sigma_a). \quad (5-25)$$

The dependence of  $D$  on neutron temperature is such that  $D$  is proportional to  $D_0(T/T_0)^m$  where  $m$  is a small constant of the order of 0.1 or less and where  $D_0$  is the monoenergetic diffusion coefficient at temperature  $T_0$ . Since  $D_0$  is proportional to a transport mean-free-path, it varies inversely with the atom density  $N$ . Therefore

$$\alpha_T(D) = \beta + \frac{m}{T}, \quad (5-26)$$

where, as in eq. (5-18),  $\beta$  is the volume coefficient of thermal expansion.

For a homogeneous reactor, we use

$$\Sigma_a = \Sigma_{aF} + \Sigma_{aM}. \quad (5-27)$$

Using eqs. (5-15), (5-21), and (5-22), we find

$$\alpha_T(\Sigma_a) = -\beta - \frac{1}{2T} + f\alpha_T(g_{aF}), \quad (5-28)$$

and as a result,

$$\alpha_T(L^2) = 2\beta + \frac{m + \frac{1}{2}}{T} - f\alpha_T(g_{aF}). \quad (5-29)$$

The last term in eq. (5-29) is usually small.

The age  $\tau$  is affected by increasing temperature in two ways: first by reducing the atom density of the medium, and second by reducing the energy spread from source to thermal. The density effect is usually

dominant. In a homogeneous reactor,  $\tau$  is inversely proportional to  $N^2$ , so that

$$\alpha_T(\tau) = 2\beta. \quad (5-30)$$

The buckling  $B^2$  is inversely proportional to the square of some characteristic linear dimension of the reactor. If the size of the reactor is completely constrained, then  $\alpha_T(B^2) = 0$ . If the reactor is free to expand thermally, then

$$\alpha_T(B^2) = -\frac{2}{3}\beta, \quad (5-31)$$

where again  $\beta$  is the volume coefficient of thermal expansion. The factor  $-\frac{2}{3}$  arises because  $B^2$  varies inversely with radius squared, while volume varies directly as radius cubed. Of course, these simple considerations are not applicable to a reactor that is partially constrained, such as a liquid-core reactor in a partially filled container.

Eqs. (5-12), (5-29), and (5-31) yield

$$\alpha_T(P_i) = -\frac{B^2 L^2}{1 + B^2 L^2} \left[ \frac{4}{3}\beta + \frac{m + \frac{1}{2}}{T} - f\alpha_T(g_{af}) \right], \quad (5-32)$$

while, from eqs. (5-13), (5-30) and (5-31),

$$\alpha_T(P_f) = -\frac{2}{3}B^2\tau\beta. \quad (5-33)$$

If  $\alpha_T(g_{af})$  may be neglected and if, in addition,  $B^2 L^2 \ll 1$ , we may write

$$\alpha_T(P_i) + \alpha_T(P_f) \cong -B^2 L^2 \frac{m + \frac{1}{2}}{T} - \frac{4}{3} B^2 M^2 \beta, \quad (5-34)$$

where  $M^2$  is the migration area

$$M^2 = L^2 + \tau. \quad (5-35)$$

Further, if all terms in eq. (5-11) are small, then  $\alpha_T(k_\infty) \cong 0$  and, by eq. (5-10), the temperature coefficient of reactivity is approximately

$$\alpha_T \cong -B^2 L^2 \frac{m + \frac{1}{2}}{T} - \frac{4}{3} B^2 M^2 \beta. \quad (5-36)$$

Note that the dominant terms in this approximate temperature coefficient of reactivity for a  $U^{235}$ -fueled homogeneous thermal reactor are negative. Further, other things being equal, the presence of  $B^2$  in both terms of eq. (5-34) suggests that a smaller homogeneous reactor will have a temperature coefficient that is larger in magnitude. Finally, the temperature dependence of  $\alpha_T$  in eq. (5-36) is typical of many reactors in that the magnitude of  $\alpha_T$  generally tends to decrease with increasing temperature.

The temperature coefficient of reactivity  $\alpha_T$  for a homogeneous thermal reactor may range from  $-10^{-5}$  per  $^{\circ}\text{C}$  for a large graphite-moderated reactor to  $-3 \times 10^{-4}$  per  $^{\circ}\text{C}$  for a small water-moderated reactor. However, even in homogeneous reactors, the situation may be much more complex than indicated here. For example, in a water-boiler reactor (highly enriched uranium salt solution in light water) the release of fission energy is accompanied by the production of radiolytic gas. In fast excursions, the resulting density change can be more significant than thermal expansion (Atomsics International 1959). In this and other cases it is sometimes possible to use the concept of energy coefficient of reactivity in order to include all the physical effects that accompany a temperature rise during a nuclear excursion.

### 5-2. Heterogeneous Thermal Reactors

The computation of isothermal temperature coefficient of reactivity for a heterogeneous reactor is rather more complicated than that for a homogeneous reactor. Further, the isothermal coefficient may have little relevance in a dynamic situation where a nuclear-induced temperature rise may be far from uniform.

Most of the thermal energy produced in fission comes from fission fragments as they slow down. The fragments are relatively massive and highly charged, and their ranges in solids or liquids are short (millimeters or less). Consequently, the prompt heat source is largely confined to fuel rods or plates, while the effects from moderator, coolant, and supporting structures are delayed in a complex way involving dynamic heat-transfer processes. Reactivity feedback in a nuclear excursion may therefore be exceedingly difficult to calculate, being dependent on a changing temperature distribution. This can become even further complicated when one considers other effects such as melting, vaporization, or expulsion of material from the reactor. (Note also that there will be some prompt heat sources in nonfuel regions arising from neutron and gamma-ray interactions, although this is generally less than 10 percent.)

For approximate treatments of reactor excursions, it is convenient to regard the temperature coefficient for a heterogeneous reactor as made up of prompt and delayed components. Effects that depend on the instantaneous state of the fuel (e.g., thermal distortion of fuel elements, Doppler effect) may be regarded as prompt, while effects that depend primarily on the moderator or coolant (e.g., neutron temperature, thermal expansion of moderator material) are largely delayed. In a fast excursion the delayed effects may be negligible, though they might well dominate in a quasi-static situation. Naturally, in any

case of nonuniform temperature change, the various contributions to the reactivity coefficient would have to be carefully weighted. We proceed to discuss the isothermal temperature coefficient for a simple model of a heterogeneous thermal reactor, noting which components are likely to be prompt and which are generally delayed in a dynamic situation.

First, we note that the temperature coefficient of  $\eta$  may be extremely complicated. Eq. (5-14) should be interpreted in terms of effective average microscopic cross-sections for thermal absorption in the fuel. The spectrum of thermal neutrons in the fuel may be far from Maxwellian, and may also be position dependent, so that standard data tables for average cross-sections may not be useful. Since  $\eta$  is a ratio of microscopic cross-sections, it is dependent primarily on the neutron spectrum as affected by the state of the moderator, and its temperature coefficient may be regarded as a delayed effect. As with homogeneous reactors,  $\alpha_T(\eta)$  is usually small unless the fuel is  $\text{Pu}^{239}$ .

The fast-fission factor  $\epsilon$  in a heterogeneous reactor may vary with temperature for two reasons. First, thermal expansion of fuel elements may alter the escape probabilities of fast neutrons from the fuel; this would be a prompt effect. Second, the thermal flux distribution within a unit cell changes slightly with temperature, and the resulting change in fast neutron source distribution affects the escape probabilities. This flux flattening within a cell is mainly a result of the increase of  $L^2$  with increasing moderator temperature; its effect on  $\epsilon$  may therefore be regarded as delayed. Both effects are usually very small and will not be treated further here.

The effect of temperature on the resonance escape probability  $p$  may be very important in a low-enrichment heterogeneous reactor. The following is a brief description of the Doppler effect and the temperature dependence of the resonance escape probability.

Neutron absorption in heavy elements at epithermal energies is dominated by many resonance peaks in the cross-section vs. neutron-energy curve. An isolated resonance may be described analytically by the Breit-Wigner formula. If this formula is applied to an assembly of capturing atoms in thermal agitation, with the appropriate averaging over the resulting range of relative velocities, it is found that the curve of cross-section vs. neutron energy is broadened and flattened more and more as the fuel temperature increases.

Because the area under the resonance curve does not change, however, the total number of absorptions would not change if the neutron spectrum were flat (independent of neutron energy). The crucial point is that absorption depresses the neutron spectrum in the neighborhood of a resonance. The broadening and flattening that

accompany a temperate rise act to reduce this depression in neutron flux. When the absorption rate  $n(E)v\Sigma_a$  is integrated over energy, the net effect is an increase in absorption with increasing fuel temperature. In thermal reactors, the effect is most likely to be important in heterogeneous systems where the fuel is highly concentrated in plates or rods. Flux depression near the surface of a fuel lump results in a reduced reaction rate in the interior, thus effectively shielding the atoms of resonance absorber inside the lump and increasing the probability of escape from resonance capture. This results in a considerable enhancement of the Doppler effect. The Doppler contribution to the temperature coefficient of  $p$  is prompt because it is due to thermal agitation of fuel atoms.

An approximate formula for resonance escape probability in a heterogeneous reactor is (Lamarsh 1966):

$$p = \exp\left(-\frac{N_F V_F I}{\xi_M \Sigma_{sM} V_M}\right), \quad (5-37)$$

where  $N_F$  is the fuel-atom density,  $V_F$  and  $V_M$  are respectively the fuel and moderator volumes,  $\xi_M \Sigma_{sM}$  is the moderator slowing-down power, and  $I$  is the resonance integral. Here  $\xi_M$  is the average increase in lethargy (logarithm of relative neutron energy) per collision, and  $\Sigma_{sM} = N_M \sigma_{sM}$  is the moderator cross-section. A term in the exponent in eq. (5-37) involving scattering in fuel material has been omitted for simplicity.

It is known both theoretically and empirically (Lamarsh 1966) that the resonance integral for  $U^{238}$  and  $Th^{232}$  and their oxides may be represented approximately as

$$I(T) = I(T_0)[1 + \gamma(\sqrt{T} - \sqrt{T_0})], \quad (5-38)$$

where  $T$  is the fuel temperature (limited to the range from 300°K to 1500°K),  $T_0 = 300°K$ , and  $\gamma$  is roughly a linear function of fuel surface-to-mass ratio. A typical value of  $\gamma$  is  $6 \times 10^{-3}$  per °C<sup>1</sup> as determined for a series of fast excursion tests in SPERT-I with uranium oxide fuel (Spano 1964).

In the prompt case, we note that  $N_F V_F$  is the total number of fuel atoms and that the moderator properties are unaffected. Hence

$$\alpha_T(p) = -\alpha_T(I) \log(1/p). \quad (5-39)$$

In eq. (5-38) we ignore changes in surface-to-mass ratio and find

$$\alpha_T(I) = \frac{I(T_0)}{I(T)} \frac{\gamma}{2\sqrt{T}}; \quad (5-40)$$

therefore

$$\alpha_T(p) = -\frac{I(T_0)}{I(T)} \frac{\gamma}{2\sqrt{T}} \log \frac{1}{p} = -\frac{\gamma}{2\sqrt{T}} \log \frac{1}{p(T_0)}. \quad (5-41)$$

Since  $p(T_0)$  is necessarily less than unity, the prompt temperature coefficient of  $p$  is negative. The inverse square-root dependence on absolute temperature is typical of low-enrichment thermal reactors.

Delayed terms arise from the factor  $\Sigma_{sM} V_M$  in eq. (5-37). This factor may be written as  $N_M \sigma_{sM} V_M$ , where  $N_M V_M$  represents the total number of moderator atoms. Eq. (5-39) is replaced by

$$\alpha_T(p) = [-\alpha_T(I) + \alpha_T(\sigma_{sM}) + \alpha_T(N_M V_M)] \log(1/p). \quad (5-42)$$

The scattering cross-section has sufficiently weak dependence on neutron energy that  $\alpha_T(\sigma_{sM}) \approx 0$  in eq. (5-42). In a solid-moderated reactor,  $N_M V_M$  remains constant and eq. (5-42) reduces to eq. (5-39). In a liquid-moderated reactor that is constrained in a filled tank of fixed volume, some moderator may be expelled from the reactor. If  $\alpha_T(V_M) = 0$ ,

$$\alpha_T(N_M V_M) = \alpha_T(N_M) = -\beta_M; \quad (5-43)$$

where  $\beta_M$  is the moderator volume coefficient of thermal expansion. In this case

$$\alpha_T(p) \approx -[\alpha_T(I) + \beta_M] \log(1/p). \quad (5-44)$$

The expulsion of moderator contributes further to the negative temperature coefficient of  $p$ , as might be expected for an increase of fuel-to-moderator ratio.

The thermal utilization for a heterogeneous reactor may be written

$$f = \frac{\Sigma_{aF} V_F}{\Sigma_{aF} V_F + \Sigma_{aM} V_M \zeta}, \quad (5-45)$$

where again  $V_F$  and  $V_M$  are fuel and moderator volumes and where  $\zeta$  is the disadvantage factor defined by

$$\zeta = \bar{\phi}_M / \bar{\phi}_F. \quad (5-46)$$

In eq. (5-46) the barred quantities denote volume-average thermal neutron flux in moderator and fuel respectively. From eq. (5-45),

$$\alpha_T(f) = (1-f)[\alpha_T(\Sigma_{aF} V_F) - \alpha_T(\Sigma_{aM} V_M) - \alpha_T(\zeta)], \quad (5-47)$$

which may be written

$$\begin{aligned} \alpha_T(f) = (1-f)[ &\alpha_T(N_F V_F) + \alpha_T(\sigma_{aF}) \\ &- \alpha_T(N_M V_M) - \alpha_T(\sigma_{aM}) - \alpha_T(\zeta)]. \end{aligned} \quad (5-48)$$

The disadvantage factor  $\zeta$  decreases with increasing temperature

because of the flux flattening that was mentioned earlier in connection with the fast-fission factor. This flattening is mainly the result of increased  $L^2$  from moderator heating and is therefore a delayed effect. In the prompt case, we take  $\alpha_T(N_F V_F) = 0$ , as before, and note that all other terms in eq. (5-48) would also vanish because they refer to changes in moderator properties. Therefore  $\alpha_T(f) = 0$  in the prompt case.

Ultimately, the moderator heats up and  $f$  changes. As before, we take  $\alpha_T(N_M V_M) = 0$  for a solid moderator. Applying eq. (5-20) and recalling that the moderator is a pure  $1/v$  absorber, we have

$$\alpha_T(\sigma_{aF}) - \alpha_T(\sigma_{aM}) = \alpha_T(g_{aF}). \quad (5-49)$$

Eq. (5-48) yields

$$\alpha_T(f) = (1 - f)[\alpha_T(g_{aF}) - \alpha_T(\zeta)]. \quad (5-50)$$

For a liquid moderator with  $V_M$  fixed, an additional term appears; using eq. (5-43) we find

$$\alpha_f(f) = (1 - f)[\alpha_T(g_{aF}) + \beta_M - \alpha_T(\zeta)]. \quad (5-51)$$

The contribution of  $\alpha_T(g_{aF})$  is generally small for uranium.

The computation of  $\alpha_T(\zeta)$  is usually very involved, but it appears always to be negative (increasing temperature flattens the flux in a cell and reduces  $\zeta$ ). Hence the temperature coefficient of  $f$ , which is a delayed effect, is positive. Its magnitude may vary considerably from one type of reactor to another. Other phenomena not included in this simple treatment may also be important; we have neglected the effects of coolant and structural materials, as well as possible space-dependent spectral effects within the unit cell.

For  $L^2$  we consider only the simple approximate formula, valid if the fuel occupies only a small fraction of the volume,

$$L^2 = (1 - f)L_M^2, \quad (5-52)$$

where  $L_M^2$  refers to moderator material alone. From eq. (5-52),

$$\alpha_T(L^2) = -\frac{f}{1-f} \alpha_T(f) + \alpha_T(L_M^2). \quad (5-53)$$

For  $L_M^2$  we use  $D_M/\Sigma_{aM}$ , so that

$$\alpha_T(L_M^2) = \alpha_T(D_M) - \alpha_T(\Sigma_{aM}) = 2\beta_M + \frac{m + \frac{1}{2}}{T}, \quad (5-54)$$

where we have used eqs. (5-22) and (5-26) with  $\beta = \beta_M$ . Hence

$$\alpha_T(L^2) = 2\beta_M + \frac{m + \frac{1}{2}}{T} - \frac{f}{1-f} \alpha_T(f). \quad (5-55)$$

Since  $\alpha_T(f) = 0$  in the prompt case, we see that the prompt  $\alpha_T(L^2)$  is zero.

As for delayed effects, one could in principle use eq. (5-55) with  $\alpha_T(f)$  given by eq. (5-50) or (5-51). Unfortunately,  $\alpha_T(\zeta)$  depends on the change in  $L^2$ , so that the temperature coefficients of  $L^2$  and  $f$  are interrelated in a complex way. One can hope that at least one of the terms causing this interaction may turn out to be small, and in fact the term in  $f$  in eq. (5-55) is frequently unimportant.

The age  $\tau$  for a heterogeneous reactor is usually very difficult to calculate, and its temperature dependence is highly complicated. It is seldom reliable to assume that  $\tau$  is proportional to  $1/N_M^2$ . Rather, one is forced to use the results of elaborate computations or experimental data for age as a function of the fuel-to-moderator ratio, and correlate the change in age with temperature-induced changes in the reactor composition. Usually, the effect of fuel temperature alone is small, and the prompt  $\alpha_T(\tau)$  is zero. The moderator contribution is usually positive.

The buckling  $B^2$  depends on overall reactor dimensions and is not usually involved in the prompt reactivity coefficient for a heterogeneous reactor. One could imagine special situations where nuclear heating might distort the fuel-element structure in such a way as to produce a prompt change in the lattice pitch, thereby causing complicated effects in all the reactor parameters. Normally, however, the change in  $B^2$  would be delayed and would depend in a complicated way on the detailed structure of the reactor. For a liquid moderator in a filled vessel, one could probably neglect the effect of a change in buckling on the temperature coefficient.

We use eqs. (5-12) and (5-55) to calculate  $\alpha_T(P_i)$ . In the prompt case,  $\alpha_T(P_i) = 0$  because  $L^2$  and  $B^2$  do not change. The delayed coefficient is

$$\alpha_T(P_i) = -\frac{B^2 L^2}{1 + B^2 L^2} \left[ 2\beta_M + \frac{m + \frac{1}{2}}{T} - \frac{f}{1-f} \alpha_T(f) \right], \quad (5-56)$$

provided  $\alpha_T(B^2)$  is negligible. Similarly, by eq. (5-13), the prompt  $\alpha_T(P_f)$  is zero because  $\tau$  and  $B^2$  do not change. The delayed coefficient is

$$\alpha_T(P_f) = -B^2 \tau \alpha_T(\tau). \quad (5-57)$$

Although  $\alpha_T(f)$  is positive, its contribution is small. The other delayed effects are negative, so that  $\alpha_T(P_i)$  and  $\alpha_T(P_f)$  are usually large negative contributions to the overall delayed temperature coefficient.

The temperature coefficient of reactivity is given by eqs. (5-10) and (5-11). A summary is presented in table 5-1 for a nominal low-enrichment uranium-fueled heterogeneous reactor with a liquid moderator. The

### 5-1 Reactivity Feedback and Reactor Excursions

Table 5-1. Temperature Coefficients for a Nominal Uranium-fueled, Liquid-moderated Heterogeneous Reactor

Parameter	Prompt Coefficient	Delayed Coefficient
$\eta$	0	0
$\epsilon$	0	0
$p$	$\gamma_f(1) \log \frac{1}{p} = -\frac{\gamma}{2\sqrt{T}} \log \frac{1}{p(T_0)}$	$-\left[\alpha_T(I) + \beta_M\right] \log \frac{1}{p}$
$f$	0	$(1-f) [\alpha_T(g_{sf}) + \beta_M - \alpha_T(\zeta)]$
$P_e$	0	$-\frac{B^2 L^2}{1+B^2 L^2} \left[ 2\beta_M + \frac{m+1/2}{T} - \frac{f}{1-f} \alpha_T(f) \right]$
$P_f$	0	$-B^2 \tau \alpha_T(\tau)$

zeros indicate negligibly small contributions. The only positive term shown as not negligible is the delayed coefficient of  $f$ , and it is usually small. If moderator material is not expelled by delayed heating, the term  $\beta_M$  in the delayed coefficients of  $p$  and  $f$  should be omitted.

It cannot be overemphasized that the simplified calculation presented here can be applied only to a few special idealized systems. Even in the absence of additional physical phenomena, results computed from the expressions in table 5-1 may be substantially in error. The treatment presented here was motivated rather by a desire to convey the flavor of the general problem and to indicate some of the difficulties.

In practical problems with epithermal or multiregion reactors, one must frequently resort to a set of multigroup calculations in which the reproduction factor  $k$  is computed at a number of temperatures. Further complications arise when the temperature changes are localized or distributed unsymmetrically in the reactor. In such cases it is sometimes feasible to use reactor perturbation theory (Lamarsch 1966).

An important example of complex dynamic effects is encountered with reactors having metal fuel rods or plates distributed in a water moderator. In a sufficiently fast transient, the fuel temperature may rise considerably before significant heat is transferred to the water. If the fuel is highly enriched (primarily  $U^{235}$ ), there will be little reactivity feedback from fuel heating alone, because resonance capture is small while other feedback effects are due primarily to heating of the moderator. This situation is typified by the SPERT-I reactor (Schroeder et al. 1957), in which fast transients are self-limited primarily by steam formation and consequent decrease of moderator density, accompanied in the faster excursions by violent expulsion of moderator caused by

rapid thermal expansion of fuel.

On the other hand, similar reactors with lower enrichment fuel may contain enough  $U^{238}$  to permit self-shutdown by Doppler effect alone, and the delayed effect of moderator heating in a fast transient plays no role until after the excursion is quenched. An example is a later version of SPERT-I, in which the fuel consists of low-enrichment uranium oxide (4 percent  $U^{235}$ ) packed in half-inch rods in a water lattice (Späno 1964). Another example is the PULSTAR pulsed reactor, whose fuel consists of Zircaloy-clad sintered  $UO_2$  pellets (6 percent enrichment) in a water moderator (MacPhee and Lumb 1965).

Boiling-water reactors are particularly difficult to analyze because the void fraction in the water moderator increases with increasing power level. In fast power changes, the void-fraction increase lags behind the power. Here also, the prompt temperature coefficient is highly dependent on the type of fuel.

The TRIGA reactor (Coffer et al. 1966; Stone et al. 1959; West et al. 1967) contains combined fuel-moderator elements, consisting of an intimate mixture of uranium (enriched to 20 percent  $U^{235}$ ) and a zirconium hydride, with aluminium or stainless steel cladding. These elements are spaced in a regular lattice in a pool of water, with an approximate water-volume fraction of  $\frac{1}{3}$ . Moderation is largely produced by hydrogen, both in the zirconium hydride and in the water. The prompt temperature coefficient arises from prompt fission heating of the hydride and is a complicated moderator effect involving quantized energy exchange between neutrons and vibrational quanta (phonons) in the hydride. The result is a large prompt-negative feedback that makes the TRIGA reactor suitable as a pulsed reactor. Again, the delayed effect of water heating plays no role in quenching a fast excursion.

We shall see later that the peak power and energy release in an excursion may depend on the initial power, even when all other parameters are fixed. Also, in an actual system, the feedback coefficients depend on temperature, and the initial temperature may be a significant parameter. Finally, in many heterogeneous systems, the amount of lag exhibited by delayed feedback effects depends on the initial state (e.g., boiling heat transfer might or might not be present, depending on the initial power level).

### 5-3. Fast Reactors

In fast-spectrum reactors, the neutron cycle cannot be separated into the different regimes of slowing down and thermal migration, and the simple formulation of eqs. (5-5) and (5-6) is not applicable. Further, the

neutron spectrum is only slightly affected by temperature. Most neutrons are absorbed or leak out of the system at energies far higher than thermal, and there is no population of neutrons in thermal equilibrium with the reactor materials.

The temperature coefficient of a fast reactor is therefore governed by changes in absorption and leakage at high energies, typically 0.01–1.0 Mev. In a heterogeneous system, consisting of fuel rods, coolant, and structural materials, prompt reactivity effects may arise from longitudinal fuel expansion (change in axial buckling), radial fuel expansion (compression or expulsion of coolant), fuel-rod bowing caused by differential thermal expansion (Dietrich 1964), and the Doppler effect. Delayed effects in such a system may arise from structural heating, thermal expansion of coolant, and additional coolant expulsion. In an extremely fast power excursion, the prompt effects cited above, even if negative, might conceivably be insufficient to quench the excursion before violent disassembly involving some vaporization occurs.

In a small homogeneous fast assembly such as GODIVA (Keepin 1965), which consists of solid highly enriched uranium metal, the dominant prompt effect is the change in leakage caused by thermal expansion. We will discuss such fast-burst reactors in a later section, pointing out how a very fast excursion may be enhanced by mechanical inertia: in effect, a thermal-expansion time lag accompanied by large transient stresses.

The Doppler effect in fast reactors arises from temperature broadening of many closely spaced high-energy resonances in both the fission and parasitic-absorption cross-sections. These resonances interact in a complicated way. Productive and nonproductive processes compete, and the net effect may be either an increase or decrease in reactivity.

The Doppler effect is very sensitive to the neutron spectrum, which in turn is extremely sensitive to many details of the design of a heterogeneous system. For pure U<sup>235</sup> in a hard spectrum (small reactor, mean neutron energy near 0.1 Mev), the Doppler effect is apparently very small and positive, being probably less than 10<sup>-6</sup> per °K (Nordheim 1964). The Experimental Breeder Reactors EBR-I and EBR-II are in this category.

In a slightly softer spectrum (the Enrico Fermi reactor), the Doppler coefficient has been calculated to be  $-2.0 \times 10^{-6}$  per °K (Nicholson 1960). Volume fractions for the reactor model used were: 0.0612 U<sup>235</sup>, 0.1657 U<sup>238</sup>, 0.0472 molybdenum, 0.0382 zirconium, 0.2591 stainless steel, and 0.4286 sodium.

In large dilute systems with uranium oxide or carbide fuels, containing high concentrations of U<sup>238</sup> fertile material, the Doppler effect tends to be much more significant and may be of the order of  $-10^{-5}$ .

per °K (Nordheim 1964). This same magnitude of negative Doppler effect can be found in large fast-breeder reactors with Pu<sup>239</sup> fuel and U<sup>238</sup> fertile material. Here the Pu<sup>239</sup> contributes a positive effect, but the negative effect of U<sup>238</sup> dominates (with some help from Pu<sup>240</sup>).

Doppler coefficients tend to decrease in magnitude with increasing temperature. Earlier, we noted a  $T^{-\frac{1}{4}}$  dependence for a thermal reactor; see eq. (5-41). This has been confirmed experimentally in SPERT-I with low-enrichment oxide fuel (Spano 1964). In fast reactors, the dropoff with increasing temperature is more rapid (McCarthy and Okrent 1964; Nordheim 1964). For large oxide-fuel fast reactors the Doppler coefficient varies somewhat as  $T^{-\frac{1}{2}}$ , while for smaller, highly enriched reactors it tends to approach  $T^{-\frac{3}{4}}$ .

We conclude this section with a brief summary of coolant effects in a sodium-cooled fast reactor (McCarthy and Okrent 1964). The reactivity effect of a reduction in sodium density is difficult to predict because it is the net effect of several competing processes, some of which are extremely complex. First, a reduction of sodium density or a loss of sodium results in increased  $k$  because of the reduced neutron capture. It is therefore a positive contribution, though it is rather small, especially in a hard-spectrum reactor. Second, reduced sodium content increases neutron leakage and decreases  $k$ . The effect is negative, and its contribution is greater for small reactors. Third, a loss of sodium results in an upward spectral shift (hardening) because of the loss of elastic scattering. In a small U<sup>235</sup>-fueled reactor the spectral reactivity effect may be negative. In a large Pu<sup>239</sup> reactor the effect is generally positive because there are more neutrons at low energy where elastic scattering is significant and because Pu<sup>239</sup> exhibits a rapid decrease in capture-to-fission ratio at higher neutron energies. In large fast-breeder reactors, the magnitude of the Doppler coefficient may be significantly reduced by loss of sodium; this is a highly nonlinear and spatially dependent effect.

Since the negative leakage component is less important in a large reactor, whereas the spectral shift effect seems to increase in the positive direction as size increases, it may be expected that the sodium reactivity coefficient may change from negative to positive as reactor volume is increased. This has been confirmed by some detailed computations, of which we quote one example (Yiftah and Okrent 1960). For a plutonium-metal reactor with stainless-steel structure, the removal of 40 percent of the sodium produced the following reactivity changes (expressed as relative change in critical mass needed to duplicate): -0.004 for the 800-liter core, +0.004 for 1,500 liters, and +0.012 for 2,500 liters. This sign change occurs at larger core volume with plutonium carbide or oxide fuels, but the general trend is the same.

Table 5-2. Isothermal Temperature Coefficients of Reactivity for U<sup>235</sup>-fueled Fast Reactors

Mechanism	$10^6 \alpha_T (\text{ }^\circ\text{C}^{-1})$	
	EBR-II	Fermi
Core		
Axial fuel expansion	-3.9	-2.5
Radial fuel expansion (Na expulsion)	-0.9	-0.6
Density change of coolant and subassembly material	-9.1	-7.1
Structure expansion	-9.7	-6.0
Blanket		
Density change of coolant and subassembly material	-9.5	-3.3
Growth of uranium	-1.0	-0.5
Structure expansion	-2.0	-0.6
Total	-36.1	-20.6

SOURCE: McCarthy and Okrent 1964.

One way to alleviate the trend toward positive sodium coefficient in larger reactors is to attempt to retain the negative effect of neutron leakage. This requires keeping the surface-to-volume ratio as large as possible, hence the notion of a flat "pancake-shaped" reactor (volume increased by increasing radius, but not height).

It is important for reactor safety to note that the sodium effect may be highly position dependent. Expulsion of sodium from an outer region will primarily affect the leakage, while expulsion from the central region will have little effect on leakage but may harden the spectrum considerably. A reactor could conceivably have a negative sodium coefficient for a uniform density change but a positive coefficient for expulsion of sodium from the central regions.

Finally, we list in table 5-2 some typical computed isothermal reactivity coefficients for small U<sup>235</sup>-fueled fast reactors (McCarthy and Okrent 1964). These numbers refer to a postulated uniform temperature increase throughout the entire reactor. They are of interest for comparison purposes, but they could be very misleading in any realistic situation (static or dynamic) where temperature gradients exist.<sup>1</sup> Note, however, the indication that the temperature-density effects tend to predominate in the overall coefficient; compare the Doppler coefficient of  $-2.0 \times 10^{-6}$  cited earlier for the Fermi reactor.

For comprehensive studies of reactivity effects in fast reactors, the reader is referred to Thompson and Beckerley (1964), articles from which

1. An important example is the Experimental Breeder Reactor (EBR-I), whose stability is discussed in chapter 6. Two major contributions to reactivity feedback are bowing of the fuel rods and dishing of the shield plate, both arising from differential thermal expansion.

have already been cited in this section, and to the handbook *Reactor Physics Constants* (Argonne National Laboratory 1963a). Also of special interest are the proceedings of conferences at the International Atomic Energy Agency (1961) and at Argonne National Laboratory (1963b, 1965, 1966).

#### 5-4. The Linear Feedback Kernel

In this section we discuss some simple mathematical models for dynamic reactivity feedback in homogeneous reactors. We construct a few models for subsequent use in illustrative dynamic problems, not only for the reactor excursion calculations of this chapter but also for the stability studies of chapters 6 and 7. We then describe the generalized linear feedback kernel  $h(t)$  and discuss its significance and limitations.

Write the reactivity as

$$\rho = \rho_0 - \rho_f, \quad (5-58)$$

where  $\rho_0$  represents some input reactivity and  $\rho_f$  is the intrinsic reactivity feedback. Note the control engineer's convention that the sign of the feedback is changed before it is added to the input.

Consider a simple temperature feedback

$$\rho_f = \alpha(T - T_0) \quad (5-59)$$

with  $\alpha = -\alpha_T$ , where  $\alpha_T$  is the temperature coefficient of reactivity defined by eq. (5-3). For use with the point-reactor model,  $T$  must be regarded as a suitable average reactor temperature. The symbol  $T_0$  represents a reference temperature for which the feedback reactivity is zero. Frequently  $T_0$  will be interpreted as the temperature for stable equilibrium operation, and in later sections it is often set equal to zero for convenience. Note that eq. (5-59) may be regarded as the first term of a Taylor series expansion representing a more general nonlinear relation between reactivity and temperature.

Since the temperature depends on the reactor power, and frequently on the past history of the power, the point-reactor model as represented by eqs. (2-1) and (2-2) is generally nonlinear. Linearized models that are valid for small fluctuations can be constructed as in chapter 6, but feedback effects cannot be ignored unless the reactor power is so small that its fluctuations have negligible effect on the system temperature, density, etc.

To proceed, we need relationships between temperature and power. With the point-reactor model, it is sometimes adequate to represent temperature variations by assuming a single effective coolant temperature  $T_c$  and using Newton's law of cooling:

$$\frac{dT}{dt} = Kn - \gamma(T - T_c). \quad (5-60)$$

If  $n$  is the thermal power, then  $K$  is the reciprocal of the reactor heat capacity. The quantity  $1/\gamma$  is interpreted as the mean time for heat transfer to the coolant. If the reactor structure is complex, or if the coolant temperature varies, the model must be modified. For now we assume that adequate effective values for the parameters in this lumped-parameter model may be obtained.

Suppose that  $T_0$  represents an equilibrium temperature ( $dT/dt = 0$ ) at a steady power  $n_0$ . Then

$$0 = Kn_0 - \gamma(T_0 - T_c). \quad (5-61)$$

By eqs. (5-60) and (5-61),

$$\frac{dT}{dt} = K(n - n_0) - \gamma(T - T_0). \quad (5-62)$$

Note that the coolant temperature does not appear explicitly in eq. (5-62). This equation is very commonly employed in linear stability studies.

Now postulate the existence of another equilibrium state at temperature  $T'_0$  and power  $n'_0$ . We have

$$0 = Kn'_0 - \gamma(T'_0 - T_c). \quad (5-63)$$

Comparing (5-61) and (5-63) yields

$$K(n'_0 - n_0) = \gamma(T'_0 - T_0),$$

which may be written

$$\frac{\delta T'_0}{\delta n_0} = \frac{K}{\gamma}.$$

By eq. (5-59), the difference in feedback reactivity between the two equilibrium states would be

$$\delta\rho_f = \alpha\delta T_0.$$

The ratio

$$\frac{\delta\rho_f}{\delta n_0} = \frac{\alpha K}{\gamma} \quad (5-64)$$

may be called the power coefficient of feedback reactivity. It means that a change between two equilibrium states of different power level must be accompanied by an external reactivity change  $\delta\rho_0 = \delta\rho_f$  to keep the net reactivity in eq. (5-58) equal to zero.

Since a positive increment of  $\rho_f$  means decreased reactivity, we need  $\alpha > 0$  in eq. (5-64) to have a stable system. Otherwise, a small increase in power would produce an increase in reactivity and a possible runaway. (Recall that  $\alpha$  is opposite in sign from the temperature coefficient of reactivity  $\alpha_T$ .)

For very slow transients, it is sometimes adequate to assume that eq. (5-64) still holds. In such a quasi-static model the reactivity feedback would be

$$\rho_f = \text{constant} \times [n(t) - n_0]. \quad (5-65)$$

An opposite extreme might be a large, fast excursion during which all heat loss is negligible. This is the adiabatic model

$$\frac{dT}{dt} = Kn, \quad (5-66)$$

which is the limit of eq. (5-60) when the time constant for heat transfer  $1/\gamma$  is very large compared to the time scale of the excursion. If eq. (5-59) is assumed to hold, then this model gives

$$\frac{d\rho_f}{dt} = \alpha \frac{dT}{dt} = \alpha Kn. \quad (5-67)$$

Another model, frequently used in reactor stability studies, is called the "constant-power-removal" model. It may be regarded as the limit of eq. (5-62) for very large  $1/\gamma$ :

$$\frac{dT}{dt} = K(n - n_0). \quad (5-68)$$

With eq. (5-59), this becomes

$$\frac{d\rho_f}{dt} = \alpha \frac{dT}{dt} = \alpha K(n - n_0). \quad (5-69)$$

Other variations are possible, including cases where the feedback reactivity or its time derivative at time  $t$  may be determined by the reactor power at time  $t - \tau$ . This model can be used to represent the effect of a mass transport process, and in nonlinear systems the transport delay time  $\tau$  might itself be a function of the state of the system. Transport delays have special consequences for stability that will be discussed later.

These and other linear models may be considered as special cases of a general linear feedback

$$\rho_f(t) = \int_{-\infty}^t h(t - t')[n(t') - n_0] dt', \quad (5-70)$$

where  $h(t)$  is the feedback kernel. Eq. (5-70) describes how the reactivity at time  $t$  is affected by the past history of the power, the kernel  $h(t)$  being a weighting function in a linear superposition. The upper limit  $t' = t$  in the integral reflects the fact that the reactivity can be determined only by the power in the past and not in the future. This is equivalent to requiring that  $h(t)$  be a causal function; i.e.,  $h(t) = 0$  for  $t < 0$ . If in addition  $n(t) = n_0$  for all  $t < 0$ , the lower limit may be changed to  $t' = 0$ , and eq. (5-70) would have exactly the form of the convolution integral of Laplace transform theory.

For Newton's law of cooling and a linear temperature feedback, it is readily verified from eqs. (5-59) and (5-62) that

$$h(t) = \alpha K e^{-\gamma t}. \quad (5-71)$$

For reactivity proportional to power,

$$h(t) = \text{constant} \times \delta(t). \quad (5-72)$$

For constant power removal,

$$h(t) = \alpha K. \quad (5-73)$$

The adiabatic model would be obtained by using eq. (5-73) in eq. (5-70) but with  $n_0$  omitted. Finally, a simple example with transport delay would be

$$h(t) = \text{constant} \times \delta(t - \tau). \quad (5-74)$$

It is important to note the distinction between linear feedback kernels  $h(t)$  that represent systems of ordinary differential equations in time and those that do not. Eqs. (5-71) through (5-73) are examples of the first type, and complete solutions may be obtained whenever  $n(t)$  is a known function, provided a sufficient number of initial conditions are known. For such systems, the lower limit of the integral in eq. (5-70) can be replaced by an arbitrary time  $t_0$  whose choice is equivalent to selecting particular sets of initial conditions. When coupled with nonlinear neutron dynamics, stability may depend on initial conditions, but for a particular  $t_0$  it is not necessary to know the shape of  $n(t)$  before  $t_0$ .

On the other hand, the presence of transport delay times in  $h(t)$  corresponds in general to a system of differential-delay equations (Hale and LaSalle 1967). In nonlinear reactor dynamics, stability may depend not only on the initial state but also on the shape of  $n(t)$  before the initial time; i.e., one must consider classes of initial curves as well as initial conditions. As we shall see in chapter 7, this requires modification of the methods of nonlinear stability analysis.

For linearized reactor models, stability is independent of initial

conditions. The lower limit in eq. (5-70) may be taken to be zero, yielding an ordinary convolution integral. Writing  $\delta n = n - n_0$ , and using the convolution relation for Laplace transforms, eq. (5-70) with lower limit zero yields

$$R_f(s) = H(s)\delta N(s), \quad (5-75)$$

where  $R_f(s)$ ,  $H(s)$ , and  $\delta N(s)$  are Laplace transforms of  $\rho_f(t)$ ,  $h(t)$ , and  $\delta n(t)$ . It is seen that  $H(s)$  is the feedback transfer function. This also follows from the fact that  $h(t)$  is the impulse response, or Green's function, for the linear differential operator that represents the feedback.

Finally, we calculate the response to a change in power level between two different equilibrium states resulting from a change in  $\rho_0$ . Suppose  $n$  is to be increased from an initial equilibrium value  $n_0$  to a new equilibrium at  $n_0 + \delta n_0$ . Then

$$\delta N(s) = \frac{\delta n_0}{s},$$

and eq. (5-75) becomes

$$sR_f(s) = \delta n_0 H(s).$$

If the limit as  $t \rightarrow \infty$  exists, the final-value theorem may be invoked to calculate

$$\lim_{t \rightarrow \infty} \rho_f = \lim_{s \rightarrow 0} sR_f(s) = \delta n_0 H(0).$$

We may therefore interpret  $H(0)$  as the static power coefficient of feedback reactivity.

For example, for Newton cooling, eq. (5-71) yields

$$H(s) = \frac{\alpha K}{s + \gamma}, \quad (5-76)$$

and the power coefficient is  $H(0) = \alpha K/\gamma$  in agreement with eq. (5-64). For reactivity proportional to power, eq. (5-72) yields  $H(s) = \text{constant}$ , as expected. For constant power removal, we have from eq. (5-73) that  $H(s) = \alpha K/s$ . The power coefficient  $H(0)$  for this case is not finite; this is due to the fact that eq. (5-68) permits only the one equilibrium state at  $n = n_0$ .

Note that the concept of the feedback kernel is not restricted to temperature effects alone. Any system of linear equations relating power and feedback reactivity through temperature, pressure, void volume, etc., may be cast in the form of eq. (5-70). Nonlinear feedbacks, of course, may not be put in this form.

We will return to the feedback kernel and the power coefficient in

the chapters on stability analysis. The next few sections of this chapter are concerned with power excursions in the absence of heat loss, using the adiabatic model of eqs. (5-66) and (5-67).

### 5-5. The Nordheim-Fuchs Model

Self-limiting power excursions that take place in a very short time may be described analytically by the Nordheim-Fuchs model (Fuchs 1946; Nordheim 1946). The essential approximation, which is meaningful only for sufficiently large reactivity, is that all neutron sources except the production of prompt neutrons are neglected in eq. (2-1) or (3-1). As discussed briefly in chapter 3, this is equivalent to assuming that the reactor power satisfies eq. (3-28), or

$$\frac{dn}{dt} = \frac{\rho - \beta}{\ell} n. \quad (5-77)$$

Physically, this means that the power and its rate of change are so large that the production of delayed neutrons and extraneous source neutrons may be neglected entirely.

We consider first the response to a large step-input of reactivity (Nordheim 1946). Assume that the reactor is initially critical or subcritical at a very low power. Next, assume that the reactor is by some means quickly made superprompt critical (reactivity  $\rho_0 > \beta$ ). We call  $\rho_0$  a step input whenever the reactivity input is sufficiently rapid that the reactivity remains at the value  $\rho_0$  for a brief time before the appearance of appreciable feedback reactivity. We shall see that the subsequent power excursion is then essentially independent of the initial state of the system, which might be critical or subcritical, and which need not be in equilibrium. Of course, the exact time at which the reactor power reaches some predetermined value does depend on the initial power, but the shape of the power-time curve and the values of peak power and energy release in a self-limiting excursion do not.

Write the reactivity as

$$\rho = \rho_0 - \alpha T, \quad (5-78)$$

where  $\rho_0$  is the step input,  $\alpha$  is the negative of the temperature coefficient of reactivity, and  $T$  is the increase of temperature above its initial value. Anticipating a very short time scale for the excursion, we ignore heat loss and use the adiabatic model of eq. (5-66):

$$\frac{dT}{dt} = Kn. \quad (5-79)$$

As before,  $K$  is the reciprocal heat capacity when  $n$  is the reactor power.

Combining eqs. (5-78) and (5-79), we find

$$\frac{d\rho}{dt} = -\alpha Kn. \quad (5-80)$$

When  $n$  is the reactor power,  $\alpha K$  is the energy coefficient of feedback reactivity.

The system is now described by eqs. (5-77) and (5-80), a pair of first-order differential equations. Assume that the time variable may be eliminated by dividing the two equations. This yields a first-order differential equation in  $n$  and  $\rho$ :

$$\frac{dn}{d\rho} = -\frac{\rho - \beta}{\alpha K \ell}. \quad (5-81)$$

A first integral is

$$n = A - \frac{(\rho - \beta)^2}{2\alpha K \ell}. \quad (5-82)$$

This represents a family of parabolic curves in the  $n, \rho$  plane (trajectories in a phase plane). If  $n$  is taken as negligibly small when  $\rho = \rho_0$ , the trajectories may be written

$$n = \frac{1}{2\alpha K \ell} [(\rho_0 - \beta)^2 - (\rho - \beta)^2]. \quad (5-83)$$

The condition for maximum power may be found by setting  $dn/dt = 0$  in eq. (5-77), whence peak power occurs at  $\rho = \beta$ . The power rise is halted when the increment of reactivity above prompt critical is offset by the feedback. Setting  $n = \dot{n}$  when  $\rho = \beta$  in eq. (5-83) yields an equation for peak power

$$\dot{n} = \frac{(\rho_0 - \beta)^2}{2\alpha K \ell}. \quad (5-84)$$

Obviously, eq. (5-84) is meaningful only if  $\alpha$  is positive; with negative  $\alpha$  the model predicts ever increasing reactivity and power. A typical trajectory for  $\alpha > 0$  is shown in fig. 5-1; note the symmetry about the vertical line  $\rho = \beta$ .

Before the feedback becomes significant, the power is small but rising exponentially with a short period. By eq. (2-18) the reciprocal period during this interval is

$$\omega = \frac{\rho_0 - \beta}{\ell}. \quad (5-85)$$

Eq. (5-84) then becomes

$$\dot{n} = \frac{\ell \omega^2}{2\alpha K}. \quad (5-86)$$

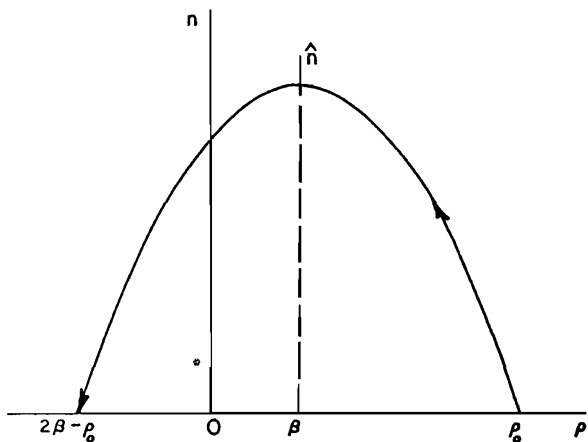


Fig. 5-1. Typical trajectory in the  $n, \rho$  phase plane for a 3.5-dollar reactor excursion (Nordheim-Fuchs model).

This important result that the peak power is proportional to the square of the initial reciprocal period has been verified experimentally for several reactor types.

After the peak, the power falls rapidly and, according to eq. (5-83), becomes again negligibly small when  $\rho - \beta = -(\rho_0 - \beta)$ , i.e., when

$$\rho = 2\beta - \rho_0. \quad (5-87)$$

This may be interpreted as meaning that the fast burst is terminated when the reactivity has been reduced by the amount

$$\rho_0 - \rho = 2(\rho_0 - \beta). \quad (5-88)$$

Actually the power at this time has fallen to a low level determined by the production of delayed-neutron precursors in the burst, and subsequent events cannot be predicted by the Nordheim-Fuchs model. Clearly, eq. (5-87) cannot represent a final equilibrium; it predicts a positive reactivity for an excursion with initial reactivity  $\rho_0 < 2\beta$ . We shall see later that the reactivity ultimately approaches  $-\rho_0$  for the adiabatic model when delayed neutrons are included.

The amount of feedback reactivity at the end of the fast burst is given by eq. (5-88). By eq. (5-78), the temperature rise is

$$T = \frac{2(\rho_0 - \beta)}{\alpha}. \quad (5-89)$$

If  $1/K$  is the heat capacity, the energy production in the fast burst is

$$E = \frac{2(\rho_0 - \beta)}{\alpha K}. \quad (5-90)$$

Note that the problem could have been formulated in terms of energy feedback, using an energy coefficient of reactivity in place of  $\alpha K$ , without reference to the underlying mechanism (Doppler effect, thermal expansion, void production, etc.). In other words, the model requires only that feedback reactivity be proportional to energy, as in eq. (5-80).

An important consequence for reactor safety may be inferred from eqs. (5-84) and (5-90). For a given input reactivity  $\rho_0$ , the burst energy as given by eq. (5-90) is independent of the neutron generation time. Therefore, the same reactivity step in a thermal reactor or a fast reactor yields the same energy, other things being equal. On the other hand, the peak power for a given input  $\rho_0$  is by eq. (5-84) inversely proportional to the neutron generation time. Thus for the same reactivity input and energy release, the fast-reactor accident implies a very much more rapid evolution of energy. This extremely short time scale for fast reactors could have severe consequences, although the comparison is inconclusive for very large reactivities. In a fast reactor, it is impossible to achieve reactivities very much above prompt critical before the effects of feedback or disassembly become significant.

To continue with the mathematical model, the duration of the fast burst may be estimated by taking the ratio of energy release to peak power:

$$E/\bar{n} = 4/\omega. \quad (5-91)$$

The duration of the burst is thus approximately four times the initial exponential period that corresponds to  $\rho_0$ .

Explicit time dependence may be derived by combining eqs. (5-80) and (5-83). We find

$$\frac{d\rho}{dt} = -\frac{1}{ZU} [(\rho_0 - \beta)^2 - (\rho - \beta)^2]. \quad (5-92)$$

It is convenient to set  $t = 0$  at the instant of peak power. Integration of eq. (5-92) then gives

$$\rho = \beta - (\rho_0 - \beta) \tanh \frac{\omega t}{2}, \quad (5-93)$$

where  $\omega$  is given by eq. (5-85).

To find  $n(t)$ , solve eq. (5-80) and obtain

$$n = -\frac{1}{\alpha K} \frac{d\rho}{dt}.$$

Form  $d\rho/dt$  from eq. (5-93) and use eq. (5-85) to find

$$n = \frac{\omega^2}{2\alpha K} \operatorname{sech}^2 \frac{\omega t}{2}.$$

Using eq. (5-86), we have

$$n = \hat{n} \operatorname{sech}^2 \frac{\omega t}{2}. \quad (5-94)$$

The energy as a function of time is

$$E = \frac{\rho_0 - \beta}{\alpha K} \left( 1 + \tanh \frac{\omega t}{2} \right). \quad (5-95)$$

Typical curves are shown in fig. 5-2 for a 3.5-dollar step. Note that the energy at the time of peak power is one-half the total energy. For future

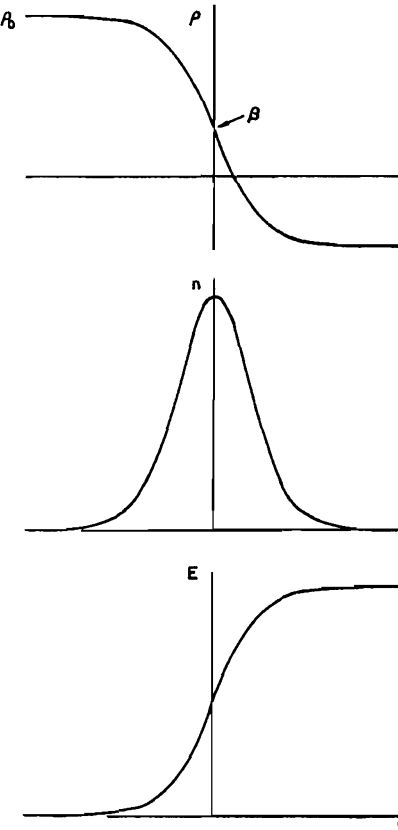


Fig. 5-2. Typical curves of reactivity, power, and energy vs. time for a 3.5-dollar excursion (Nordheim-Fuchs model).

reference, we may write

$$E(\hat{n}) = \hat{E} = \frac{\rho_0 - \beta}{\alpha K}. \quad (5-96)$$

The exact width  $\tau$  of the power burst at half-height is obtained by setting  $n = \frac{1}{2}\hat{n}$  and  $t = \frac{1}{2}\tau$  in eq. (5-94). The result is

$$\tau = \frac{4}{\omega} \cosh^{-1} \sqrt{2} = \frac{3.524}{\omega}. \quad (5-97)$$

This may be compared with the rough estimate of  $4/\omega$  from eq. (5-91).

Experimentally observed departures from the  $\omega^2$  dependence of peak power, eq. (5-86), or from the constant value of  $\omega\tau$ , eq. (5-97), may be used as indications that a system is not adequately described by the simple mathematical model. This may arise from delayed neutrons ( $\rho_0$  too near  $\beta$  or less than  $\beta$ ), from nonlinear or delayed feedback effects, or from a combination of these.

Fig. 5-3 shows experimental results for peak power vs. initial reciprocal period in a number of reactor safety tests and pulsed-reactor systems. These represent many different reactor types and a wide range of values for the neutron generation time (from approximately  $10^{-3}$  sec for TREAT, a graphite-moderated homogeneous thermal reactor, to approximately  $6 \times 10^{-9}$  sec for GODIVA, a solid-metal U<sup>235</sup> fast assembly).

TREAT, the Transient Reactor Test Facility at Argonne National Laboratory in Idaho (Dickerman, Johnson and Gasidlo 1962; Dickerman 1964) is a high-flux pulsed reactor used for engineering tests on fuel-element subassemblies in the fast-reactor safety program of the U.S. Atomic Energy Commission. The  $\omega^2$  dependence of peak power for step-induced transients with sufficiently large  $\omega$  is seen in fig. 5-3 (slope of two on the logarithmic graph). The departure from this at smaller  $\omega$  (slope less than two) is caused by delayed neutrons in excursions near prompt critical and below. As we shall derive in sec. 5-7, the Nordheim-Fuchs formula for peak power in terms of  $\omega$ , eq. (5-86), underestimates peak power about a factor of two when the true value of  $\omega$  at prompt critical is used. For TREAT, prompt critical is near  $\omega = 1.5 \text{ sec}^{-1}$ .

The pulsed reactor IGR (Kurchatov et al. 1964) in the Soviet Union is somewhat similar to TREAT, being also a homogeneous graphite system. In addition, either of these reactors may be operated in an alternate mode in which the power is allowed to rise on a short period and then is maintained at a relatively high level for several seconds by a programmed withdrawal of control rods. The PBF (Power Burst Facility) being constructed at the National Reactor Testing Station

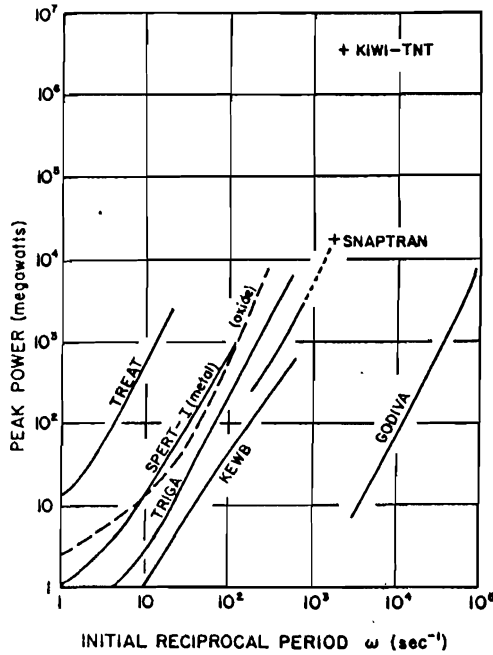


Fig. 5-3. Peak power vs. initial reciprocal period for some reactor safety tests and pulsed reactor systems (see text for references).

(Barton, Bennett, and Carpenter 1965), although a different type of reactor, is also designed for this mode of operation. For a discussion of control and instrumentation requirements for these and other pulsed systems, see the review article by Oakes (1968).

Another type of pulsed system is the TRIGA reactor (Coffer et al. 1966; Stone et al. 1959; West et al. 1967), mentioned earlier in sec. 5-2. For large  $\omega$  the curve in fig. 5-3 has slope two, and for smaller  $\omega$  the slope is reduced by delayed neutrons. Prompt critical is near  $\omega = 6$  sec $^{-1}$ . Improved agreement between theory and experiment is obtained when the Nordheim-Fuchs model is modified to include varying heat capacity (Scalettar 1963).

The fast-burst reactor GODIVA also shows the  $\omega^2$  dependence (Wimett 1956; Wimett et al. 1960). Experimental values of  $\omega$  shown are too large to show a departure from the straight line at small  $\omega$  (at prompt critical  $\omega$  is about 660 sec $^{-1}$ ). On the other hand, the curve breaks sharply upward at large  $\omega$ , indicating the onset of inertial effects (time lag in metal expansion accompanied by transient mechanical stress).

Other fast-burst reactors now in operation include the Sandia

Pulsed Reactor SPR (Coats and O'Brien 1968), the Health Physics Research Reactor HPRR (Mihalczo 1963), the White Sands Missile Range fast-burst reactor (Long 1966), the Aberdeen Pulsed Reactor Facility (Mihalczo et al. 1967), and the British heterogeneous fast reactor VIPER (Long, McTaggart, and Weale 1967).

Data for two versions of the SPERT-I reactor, mentioned earlier in sec. 5-2, are also shown in fig. 5-3. The curve labeled metal is for a core with highly enriched  $U^{235}$  in aluminum-clad fuel plates (Schroeder et al. 1957). The dominant shutdown mechanism is steam-void formation in the water channels, a delayed nonlinear process. Peak power data for large  $\omega$  show an empirical slope of 1.7 on the logarithmic graph in contrast to the Nordheim-Fuchs slope of two.

The curve labeled oxide is for low-enrichment (4 percent)  $UO_2$  fuel rods in water. Here the dominant shutdown mechanism is the Doppler effect, and its nonlinear temperature dependence yields a slope of 2.35 for  $\omega > 160 \text{ sec}^{-1}$  (Spano 1963). (See sec. 5-9 for a later interpretation.)

The PULSTAR reactor (MacPhee and Lumb 1965), also mentioned in sec. 5-2, consists of low-enrichment (6 percent)  $UO_2$  fuel in a water moderator. Its pulsing behavior is similar to that of the SPERT-I oxide core.

The KEWB (Kinetic Experiment Water Boiler) reactor was a small highly enriched homogeneous reactor (uranium sulphate in water solution). Shutdown is produced by the combined effect of thermal expansion and radiolytic gas void (dissociated water). The void effect is nonlinear and seems to be increasingly important as  $\omega$  increases (Dunenfeld 1962). For large  $\omega$ , the slope of the logarithmic curve showing peak power data is about one and a half instead of two.

Safety tests of the SNAP 10A/2 reactor (Satellite Nuclear Auxiliary Power) are also shown in fig. 5-3 (Johnson 1966). The solid line has a slope less than two, indicating that the temperature feedback in this uranium-zirconium hydride reactor is nonlinear. The broken line connects a series of excursions with a destructive test in which fuel disintegration and hydrogen release may have played a part (Moss and Buttrey 1964).

The large destructive test KIWI-TNT was conducted as part of the nuclear rocket safety program (King 1965). The nuclear rocket reactor is a thermal reactor containing uranium fuel in graphite with hydrogen propellant. The excursion resulted in violent disassembly involving some vaporization.

Analytical models for fast excursions in some complex systems are discussed in secs. 5-9 and 5-10. For the moment we return to the simple Nordheim-Fuchs model to discuss one of the effects of delayed neutrons.

In deriving eq. (5-83) we neglected delayed-neutron production

## 17.2 Reactivity Feedback and Reactor Excursions

entirely. The trajectory in fig. 5-1 approaches  $n = 0$  at  $\rho = 2\beta - \rho_0$ , and we referred to this as the end of the fast burst. Actually the power falls to a small but nonzero value immediately following the burst, and for fast assemblies this value may be estimated from the production of delayed-neutron precursors during the burst.

The precursors are described by eq. (3-2):

$$\frac{dc_i}{dt} = \frac{\beta_i}{\ell} n - \lambda_i c_i. \quad (5-98)$$

Regard the fast burst as an impulse in  $n(t)$  representing an energy release given by eq. (5-90):

$$n(t) = \frac{2(\rho_0 - \beta)}{\alpha K} \delta(t). \quad (5-99)$$

When used in eq. (5-98), this represents a jump in  $c_i$  from some negligible initial value to

$$c_i = \frac{2\beta_i(\rho_0 - \beta)}{\alpha K \ell}. \quad (5-100)$$

At this time,  $dn/dt$  is small, and we may use the prompt-jump approximation. From eq. (3-6) with  $q = 0$ ,

$$n = \frac{\sum_i \lambda_i \ell c_i}{\beta - \rho}. \quad (5-101)$$

The reactivity at this instant is  $2\beta - \rho_0$  by eq. (5-87). Eq. (5-101) yields

$$n = \frac{2}{\alpha K} \sum_i \beta_i \lambda_i = \frac{2\beta \lambda'}{\alpha K}, \quad (5-102)$$

where  $\lambda'$  is the mean weighted decay constant of table 1-3. Eq. (5-102) means that the power immediately after the burst is independent of the initial reactivity. In a fast assembly the power spike is followed by a plateau given by eq. (5-102), and the power remains at that value until significant decay of precursors (Wimett 1956).

Fig. 5-4 shows digital computer results for a typical fast assembly with delayed neutrons included ( $\ell/\beta = 10^{-6}$ ,  $\alpha K/\beta = 1$ ,  $n_0 = 10^{-6}$ ; computations performed by John Szeligowski, University of Arizona, 1967). These cases are just slightly above prompt critical and are slow enough that the delayed-neutron tail has undergone some decay. Eq. (5-102) predicts  $n = 0.8$ , while the three curves in fig. 5-4 join near  $t = 0.01$  sec, where  $n$  is about 0.6. Extrapolation of the tails back to  $t = 0$  is consistent with the value 0.8. The three values of peak power are 3.05, 4.65, and 6.65; the Nordheim-Fuchs model using eq. (5-86) predicts 2.88, 4.50, and 6.50. The correspondence would improve rapidly at larger values of  $\omega$ .

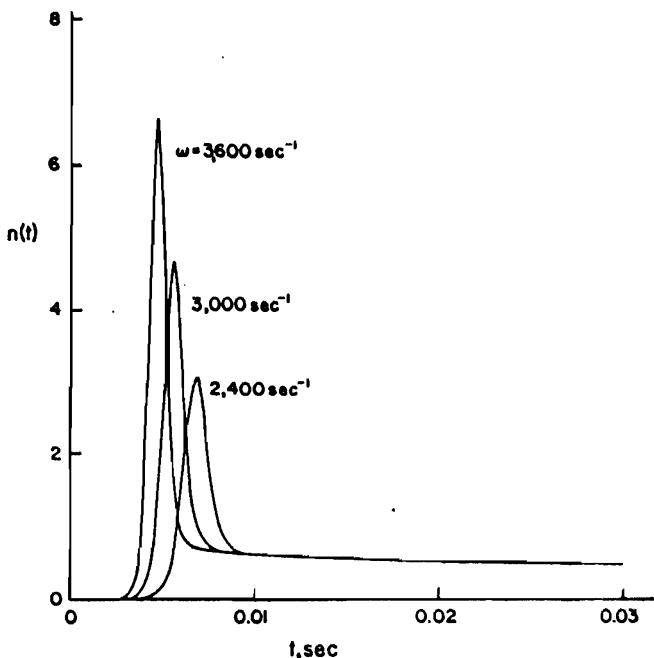


Fig. 5-4. Power vs. time for the adiabatic model with six groups of delayed neutrons:  $\ell/\beta = 10^{-6}$  (fast reactor);  $\omega = 2,400, 3,000, 3,600 \text{ sec}^{-1}$ ; reactivity steps 1.00223, 1.00286, 1.00349 dollars;  $\alpha K/\beta = 1$ ;  $n_0 = 10^{-6}$ .

In a thermal reactor, the delayed-neutron tail is less noticeable because the precursors have more time to decay during the burst. In fig. 5-5,  $\ell/\beta = 10^{-1}$  with  $\alpha K/\beta = 1$  and  $n_0 = 10^{-6}$  as before (computations by John Szeligowski, University of Arizona, 1967). Eq. (5-102) is no longer applicable. The reactivities are much greater for these cases than for the fast assembly, but the time scale is greatly lengthened by the larger neutron generation time. The peak powers in fig. 5-5 are 3.32, 5.13, and 7.33; the Nordheim-Fuchs model predicts 3.20, 5.00, and 7.20.

The digital computer results reported in this chapter were obtained using delayed-neutron data for thermal fission in  $U^{235}$ . Although this is not strictly consistent when  $\ell/\beta$  varies from  $10^{-1}$  sec (thermal) to  $10^{-6}$  sec (fast), the variation is small. In any case, as observed in sec. 3-2, it would be pointless to attempt a description of delayed-neutron data that varied continuously with  $\ell$ .

We will return to fast-excursion calculations in later sections. The next section deals with slow excursions initiated by small reactivity steps ( $\rho_0 < \beta$ ).

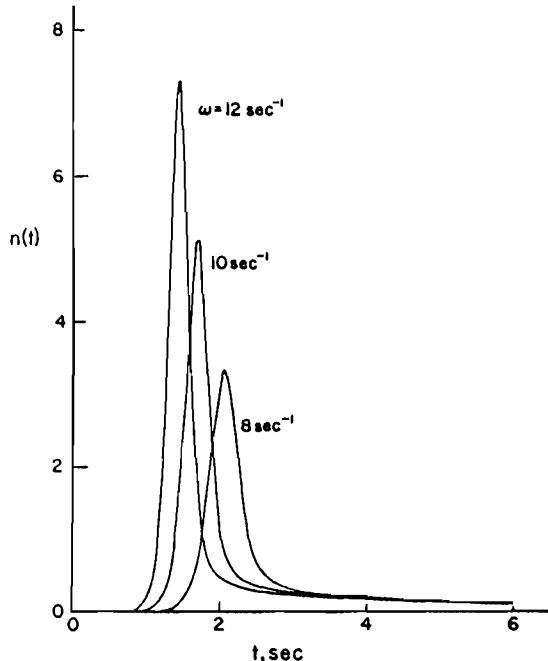


Fig. 5-5. Power vs. time for the adiabatic model with six groups of delayed neutrons:  $\gamma/\beta = 10^{-4}$  (thermal reactor);  $\omega = 8, 10, 12 \text{ sec}^{-1}$ ; reactivity steps 1.756, 1.964, 2.170 dollars;  $\alpha K/\beta = 1$ ;  $n_0 = 10^{-6}$ .

### 5-6. Small Reactivity Excursions

If the maximum reactivity in a power excursion is sufficiently less than  $\beta$ , then the transient is slow and the prompt-jump approximation may yield useful results.<sup>2</sup> If, in addition, the transient is not too slow, we may still use the adiabatic feedback model as in the previous section.

Assume that the reactor power satisfies eq. (3-13) with  $q = 0$  (one delay group, no source):

$$(\beta - \rho) \frac{dn}{dt} = \left( \lambda \rho + \frac{d\rho}{dt} \right) n. \quad (5-103)$$

As in the previous section, let the reactivity be given by

$$\rho = \rho_0 - \alpha T$$

2. Results in this section were derived by the author in 1957. Some are reported in the review paper by Cohen (1958). Other results, obtained independently, appear in a paper by Simets and Gyftopoulos (1959).

with

$$\frac{dT}{dt} = Kn$$

so that

$$\frac{d\rho}{dt} = -\alpha Kn. \quad (5-104)$$

Eliminating the time variable in eqs. (5-103) and (5-104),

$$\frac{dn}{d\rho} = \frac{\alpha Kn - \lambda\rho}{\alpha K(\beta - \rho)}. \quad (5-105)$$

This may be rearranged as

$$\alpha K(\beta - \rho) dn + (\lambda\rho - \alpha Kn) d\rho = 0.$$

The left-hand side is an exact differential, and the integral may be written as

$$\frac{1}{2}\lambda\rho^2 + \alpha K(\beta - \rho)n = A. \quad (5-106)$$

As in the Nordheim-Fuchs treatment, assume that  $n$  is very small when  $\rho = \rho_0$ . The trajectories in the  $n, \rho$  plane may then be written

$$n = \frac{\lambda(\rho_0^2 - \rho^2)}{2\alpha K(\beta - \rho)}. \quad (5-107)$$

A typical trajectory for  $\alpha > 0$  is shown in fig. 5-6. Here  $\rho_0 = \beta/2$  (reactivity step, 50 cents). The reactivity at peak power is  $0.134\beta$ , and, if  $\lambda\beta/\alpha K = 1$ , the peak value of  $n$  is 0.134. Note the lack of symmetry about the peak, and note that the final reactivity is  $-\rho_0$ .

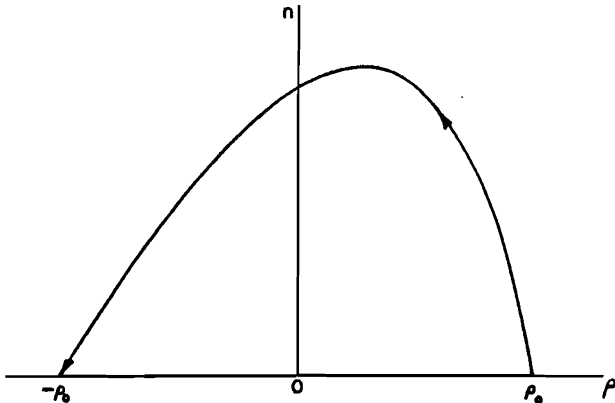


Fig. 5-6. Typical trajectory in the  $n, \rho$  phase plane for a 0.5-dollar reactor excursion (prompt-jump approximation, one delay group, adiabatic).

By eq. (5-103), the peak power  $\hat{n}$  occurs when

$$\frac{d\rho}{dt} = -\lambda\rho.$$

Incorporating this in eq. (5-104), we see that the relation between peak power and the reactivity at the time of peak power is

$$\hat{n} = \lambda\hat{\rho}/\alpha K. \quad (5-108)$$

Eq. (5-107) must also hold at peak power, with the result that the reactivity at peak power satisfies

$$\hat{\rho}^2 - 2\beta\hat{\rho} + \rho_0^2 = 0. \quad (5-109)$$

One root of eq. (5-109) violates the condition  $\rho < \beta$ . The other root is

$$\hat{\rho} = \beta - \sqrt{(\beta^2 - \rho_0^2)}. \quad (5-110)$$

From eq. (5-108), the peak power is

$$\hat{n} = \frac{\lambda}{\alpha K} [\beta - \sqrt{(\beta^2 - \rho_0^2)}]. \quad (5-111)$$

It is useful that  $\hat{n}$  converges to  $\lambda\beta/\alpha K$  as  $\rho_0 \rightarrow \beta$ , even though eq. (5-103) becomes meaningless. The significance of this will be discussed later.

We can express these results in terms of the initial inverse period  $\omega$  by means of an approximate inhour equation. For small  $\ell$ , eq. (2-28) is

$$\rho_0 = \frac{\beta\omega}{\omega + \lambda}. \quad (5-112)$$

Eqs. (5-110) and (5-111) become

$$\hat{\rho} = \beta \left[ 1 - \frac{\lambda}{\omega + \lambda} \sqrt{(1 + 2\omega/\lambda)} \right] \quad (5-113)$$

and

$$\hat{n} = \frac{\lambda\beta}{\alpha K} \left[ 1 - \frac{\lambda}{\omega + \lambda} \sqrt{(1 + 2\omega/\lambda)} \right]. \quad (5-114)$$

Note that  $\hat{n}$  converges to  $\lambda\beta/\alpha K$  as  $\omega \rightarrow \infty$ . This observation, which is related to the divergence of the approximation as  $\rho \rightarrow \beta$ , will be useful later.

At the other extreme of very small  $\omega$ , the adiabatic feedback model would fail. It is nevertheless interesting to expand the radical in eq. (5-114) in powers of  $\omega/\lambda$  and drop terms higher than quadratic. The result is

$$\hat{n} = \frac{\beta\omega^2}{2\lambda\alpha K} + O(\omega^3). \quad (5-115)$$

This would be useful in a very slow transient that is yet fast enough to justify using the adiabatic model and also neglecting the initial power.

Comparison with eq. (5-86) for the Nordheim-Fuchs model shows that peak power varies as  $\omega^2$  for both very slow and very fast excursions. This is of course a consequence of the fact that the effective-lifetime model ( $\omega \ll \lambda$ ) has the same mathematical form as reactor dynamics without delayed neutrons. Compare eq. (5-86) with the leading term of eq. (5-115), recalling that the effective lifetime is  $\beta/\lambda$ .

More useful is the comparison of eqs. (5-86) and (5-114). This is shown in fig. 5-7, together with digital computer results for two values of  $\ell$  using one group of delayed neutrons with  $\lambda = 0.0767 \text{ sec}^{-1}$  and  $\alpha K/\beta = 1$  (computations by John Szeligowski, University of Arizona, 1967). The striking feature is the overlap of the two types of approximation, with almost the entire range of  $\omega$  well represented by one or the other. The overlap, of course, is a result of using the appropriate form of the inhour equation for each range, eq. (5-85) for fast excursions

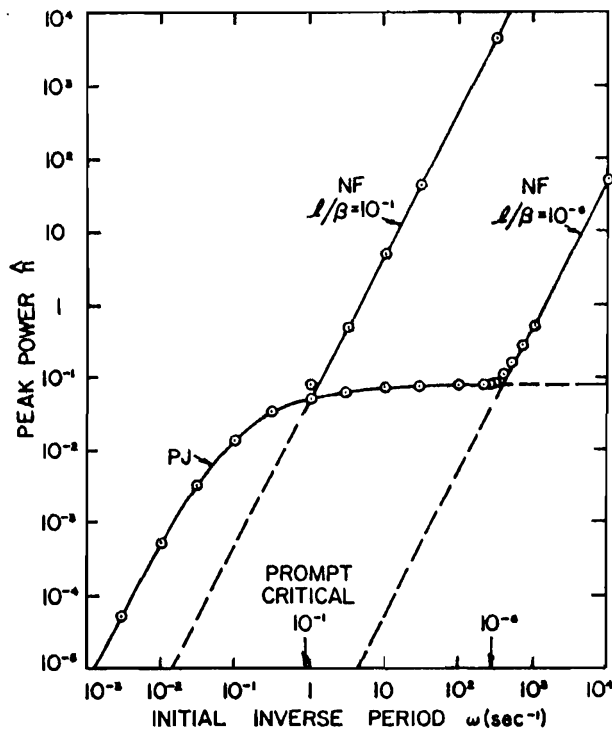


Fig. 5-7. Peak power vs. initial inverse period (one group of delayed neutrons, linear adiabatic model, initial power negligible,  $\alpha K/\beta = 1$ ).

and eq. (5-112) for slow transients, and extending the resulting graphs outside their ranges of validity. This must not be used to infer that the two types of approximation merge smoothly into each other across prompt critical. As was indicated in sec. 3-1 and will be discussed in the next section, the transition is singular.

Nevertheless, fig. 5-7 indicates that peak power for the full range of  $\omega$  may be closely predicted from the two simple approximations, at least for one group of delayed neutrons. The exact solution is very close to the prompt-jump approximation until the two approximate curves have nearly intersected. It is shown in the next section that the peak power near prompt critical for one delay group is very close to  $\lambda\beta/\alpha K$ . The inhour equation for one delay group, eq. (2-28), may be written

$$\rho_0 = \ell\omega + \beta - \frac{\beta\lambda}{\omega + \lambda}$$

so that at prompt critical

$$\omega^2 \cong \beta\lambda/\ell, \quad (5-116)$$

where  $\lambda \ll \omega \ll \beta/\ell$ . If eq. (5-116) is substituted into eq. (5-86), the result is

$$\hat{n} \cong \lambda\beta/2\alpha K, \quad (5-117)$$

which indicates that the Nordheim-Fuchs model expressed in terms of  $\omega$  underestimates the peak power by a factor of two when a realistic  $\omega$  for prompt critical is used. This serves to locate prompt critical on a graph such as fig. 5-7, and it indicates how narrow the transition region is between the prompt-jump and Nordheim-Fuchs models.

Further insight into the transition may be gained by considering  $\hat{\rho}$ , the reactivity at peak power, as a function of  $\rho_0$ . This is shown in fig. 5-8, where we take eq. (5-110) for  $\hat{\rho}$  when  $\rho_0 < \beta$  and then switch to the Nordheim-Fuchs result  $\hat{\rho} = \beta$ . The transition is now seen to be abrupt.

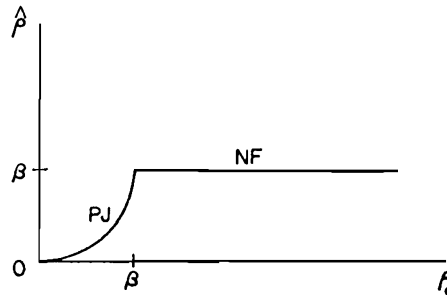


Fig. 5-8. Reactivity at peak power vs. initial reactivity, comparing prompt-jump (one delay group) and Nordheim-Fuchs models.

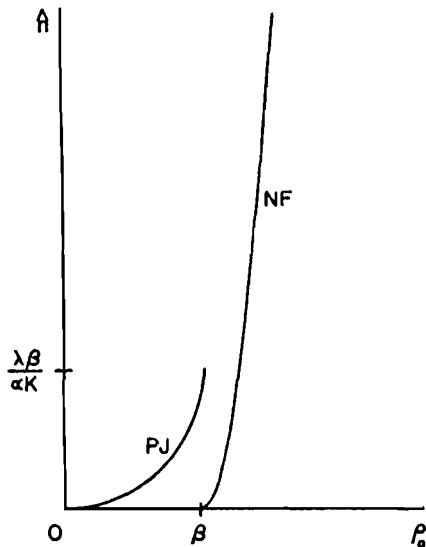


Fig. 5-9. Peak power vs. initial reactivity, comparing prompt-jump (one delay group) and Nordheim-Fuchs models.

This is emphasized by plotting peak power vs.  $\rho_0$  as in fig. 5-9, using eq. (5-111) below prompt critical and eq. (5-84) above. (The parabolic curve for  $\rho_0 > \beta$  would rise very rapidly with a realistic value of  $\ell$ .)

Next, consider the reactivity compensated at the instant peak power is reached ( $\rho_0 - \hat{\rho}$ ). This is shown in fig. 5-10 as  $E(\hat{\rho})$ , the energy produced at peak power (integrated power to peak), where the energy and compensated reactivity are numerically equal if  $\alpha K / \beta = 1$ . The lines represent eq. (5-110) below prompt critical and the Nordheim-Fuchs value  $\rho_0 - \beta$  above prompt critical. The points are from some of the digital computations used in fig. 5-7. The approximations predict a sharp drop to zero at prompt critical. With exact solutions and experimental tests the transition is smooth, but the minimum near prompt critical is very pronounced when  $\ell$  is very small.

Figs. 5-7 and 5-10 indicate the utility of the prompt-jump approximation for representing exact solutions with one group of delayed neutrons. With several delayed-neutron groups the situation is more complex. A many-group version of the prompt-jump approximation is a good asymptotic solution for the exact many-group equations in most of the range  $\rho < \beta$ , but it is still a high-order system of equations. The one-group prompt-jump approximation is a good asymptotic solution for the exact many-group equations, but in a more restricted range.

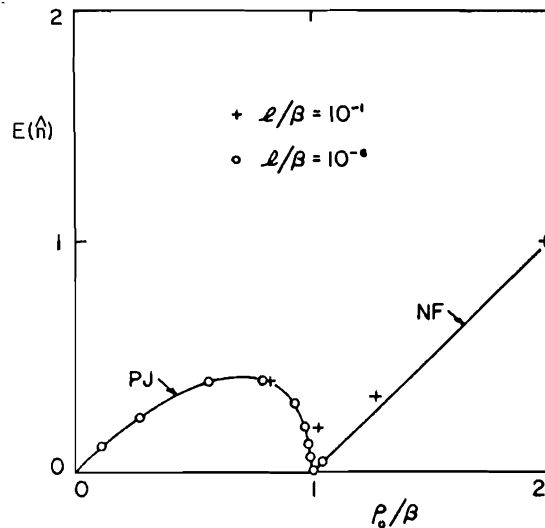


Fig. 5-10. Energy or compensated reactivity at peak power vs. initial reactivity (one group of delayed neutrons).

Fortunately, the results of one-delay-group analysis may be adapted to permit construction of curves similar to those in fig. 5-7. The key is the use of two different one-group representations, one using the weighted mean decay time  $1/\lambda$  appropriate for small  $\omega$ , and the other using the mean decay constant  $\lambda'$  appropriate near prompt critical, where  $\lambda$  and  $\lambda'$  are given by eqs. (2-27) and (2-31).

In fig. 5-11 there are two curves for  $\hat{h}$  vs.  $\omega$  in the prompt-jump approximation, both computed from eq. (5-114). The curve labeled  $\lambda$  is the curve shown in fig. 5-7 ( $\lambda = 0.0767 \text{ sec}^{-1}$ ). The curve labeled  $\lambda'$  is the same but with  $\lambda$  replaced by  $\lambda' = 0.405 \text{ sec}^{-1}$ . The Nordheim-Fuchs curves are identical to those in fig. 5-7. The points are digital computer results for two values of  $\ell$  using six groups of delayed neutrons. As before,  $\alpha K/\beta = 1$ .

It is seen that the exact solutions are near the prompt-jump curve for  $\lambda$  when  $\omega$  is small. As  $\omega$  increases the exact results begin to drop below, and then tend toward the prompt-jump curve for  $\lambda'$ . The plateau near prompt critical is still very pronounced for small  $\ell$ , and the peak power at prompt critical is very close to  $\lambda' \beta / \alpha K$ . For the larger value of  $\ell$ ,  $\lambda'$  and  $\beta/\ell$  are too close together to permit a clear separation, but a consistent prescription can still be made. Sketch the curves for eq. (5-114) using both  $\lambda$  and  $\lambda'$ , together with the straight line given by eq. (5-86). The exact solution for six delay groups may then be predicted

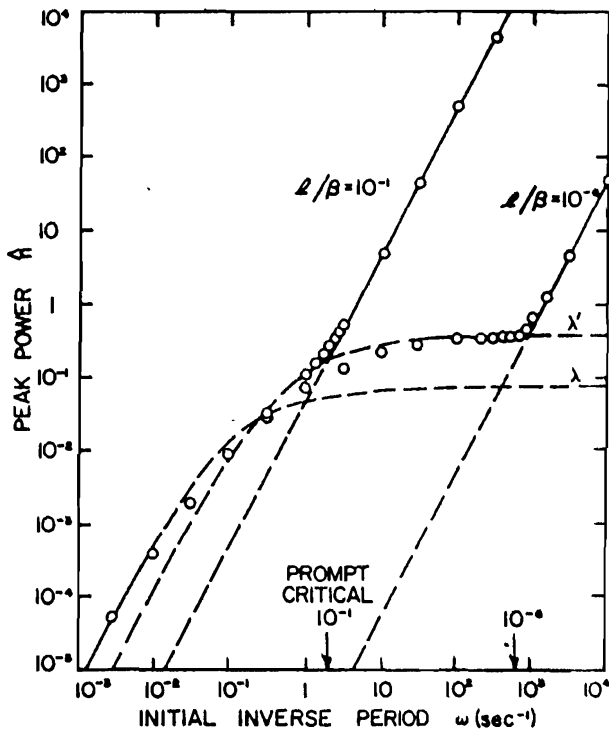


Fig. 5-11. Peak power vs. initial inverse period (six groups of delayed neutrons, linear adiabatic model, initial power negligible,  $\alpha K/\beta = 1$ ).

by sketching a smooth transition from one to another of the three approximate curves, noting that the peak power at prompt critical does not exceed  $\lambda'\beta/\alpha K$ .

The energy, or compensated reactivity, at peak power is shown in fig. 5-12. The curves for various values of  $\ell/\beta$  are interpolated among digital computer points for six groups of delayed neutrons. A curve for a six-delay-group prompt-jump approximation is indistinguishable on this scale from the curve for  $\ell/\beta = 10^{-6}$  in the entire range below prompt critical. For comparison, the one-delay-group prompt-jump curve from fig. 5-10 is reproduced as a dashed line.

The same data, plotted logarithmically as  $E(\dot{n})$  vs.  $\omega$  in fig. 5-13, shows how small the energy release at the time of peak power can be for small  $\ell$  in an excursion near prompt critical. Inspection of fig. 5-13 suggests that the minimum value of  $E(\dot{n})$  is roughly proportional to the square root of  $\ell$ . The theoretical basis for this appears in the next section, together with citations of experimental data.

18.2 Reactivity Feedback and Reactor Excursions

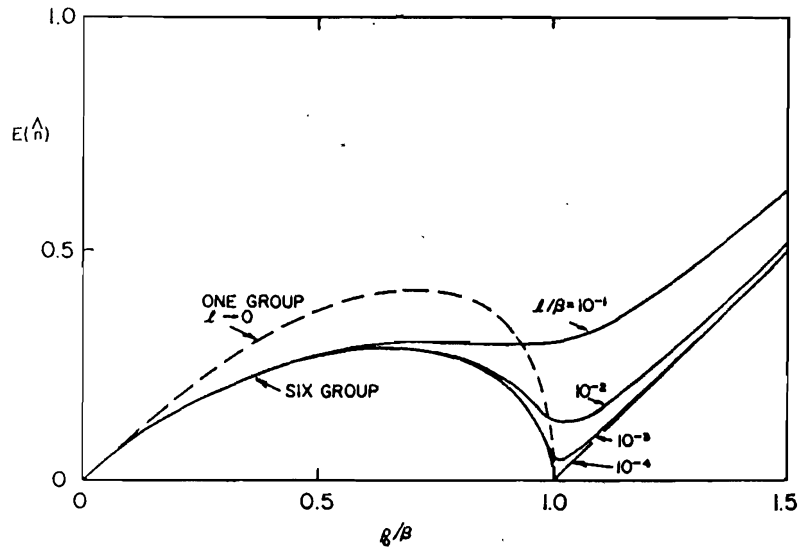


Fig. 5-12. Energy or compensated reactivity at peak power vs. initial reactivity.

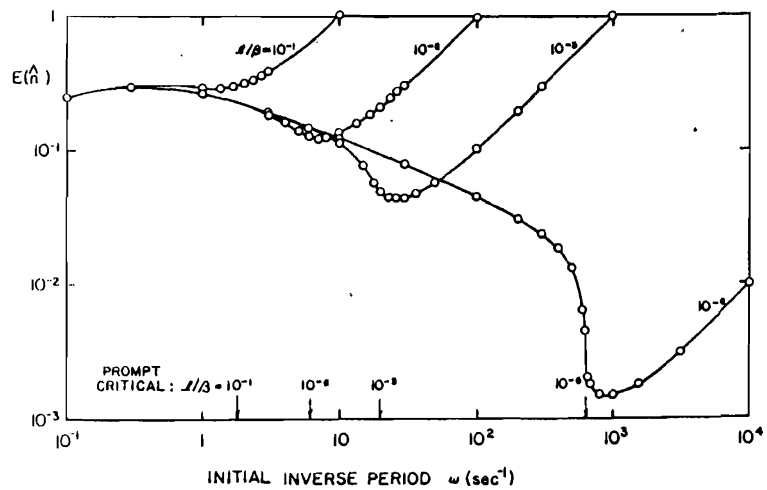


Fig. 5-13. Energy or compensated reactivity at peak power vs. initial inverse period (six groups of delayed neutrons).

Digital computer runs for two slow excursions having the same initial period ( $\omega = 0.1 \text{ sec}^{-1}$ ) are shown in fig. 5-14. Values of  $\rho_0/\beta$  are 0.4092 and 0.3992 for  $\tau/\beta = 10^{-1} \text{ sec}$  and  $10^{-6} \text{ sec}$  respectively. For

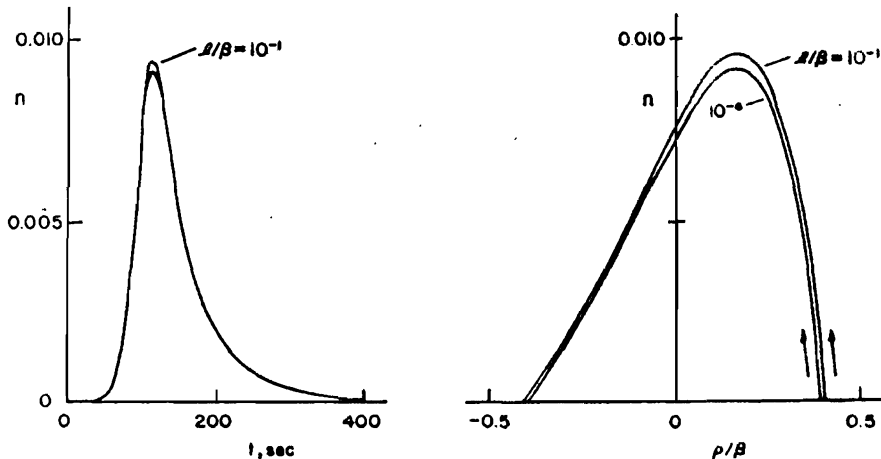


Fig. 5-14. Power vs. time and power-reactivity trajectories for the adiabatic model with six groups of delayed neutrons; initial inverse period  $\omega = 0.1 \text{ sec}^{-1}$ .

these cases  $n_0 = 10^{-6}$ , and, as before,  $\alpha K/\beta = 1$ . The two trajectories would be even closer together if initial reactivities rather than initial periods had been the same.

To complete this section, we note that the one-group prompt-jump model does not admit explicit solutions for the time dependence of  $\rho$  and  $n$  that would be analogous to eqs. (5-93) and (5-94) for the Nordheim-Fuchs model. One has instead an implicit relationship for reactivity (or energy) that is derived by eliminating  $n$  in eqs. (5-104) and (5-107). The result is

$$\lambda(t - t_1) = \frac{\beta - \rho_0}{\rho_0} \log \frac{\rho_0 - \rho(t)}{\rho_0 - \rho(t_1)} - \frac{\beta + \rho_0}{\rho_0} \log \frac{\rho_0 + \rho(t)}{\rho_0 + \rho(t_1)}, \quad (5-118)$$

where the time integration is from  $t_1$  to  $t$ . In both the prompt-jump and Nordheim-Fuchs models with initial power neglected, the solutions are functions that extend backward in time to  $\rho \rightarrow \rho_0$  and  $n \rightarrow 0$  as  $t \rightarrow -\infty$ . Any initial point for which  $\rho$  and  $\rho_0$  are indistinguishable (any very small initial power) will ultimately produce essentially the same excursion, though of course the actual time at which peak power occurs depends on the value of the initial power. For the digital computations reported in this chapter, various small but nonzero values of initial power were selected to start the computations, with the choices made to minimize computing time without affecting the result for peak power.

### 5-7. Excursions near Prompt Critical

In this section we study the point-reactor equations with one group of delayed neutrons and the adiabatic feedback model. This yields a single model for reactor excursions that is valid both above and below prompt critical and contains information about excursions near prompt critical. The development is essentially that of Canosa (1964), who recognized that the system of equations in three variables could be reduced to one first-order differential equation in two variables.

One result is the development of asymptotic expansions in powers of a small parameter, the first term of each expansion representing either the prompt-jump or Nordheim-Fuchs model, depending on the initial reactivity. Another result is insight into the highly asymmetrical power bursts near prompt critical in which very small energy yields are produced before peak power. We show that the minimum in the curve for compensated reactivity at peak power (see fig. 5-13) varies roughly as the square root of the neutron generation time  $\ell$ .

Assume that the reactor is described by eqs. (3-24) and (3-25) with  $q = 0$ :

$$\frac{dn}{dt} = \frac{\rho - \beta}{\ell} n + \lambda c \quad (5-119)$$

and

$$\frac{dc}{dt} = \frac{\beta}{\ell} n - \lambda c. \quad (5-120)$$

As in the preceding two sections, assume that the feedback is

$$\rho = \rho_0 - \alpha T, \quad (5-121)$$

$$\frac{dT}{dt} = K n, \quad (5-122)$$

$$\frac{d\rho}{dt} = -\alpha K n. \quad (5-123)$$

As shown by Canosa (1964), it is possible to carry through the analysis with a more general feedback  $\rho = \rho_0 + f(T)$  in place of eq. (5-121). We choose to illustrate the method using the simpler model.

Eqs. (5-119), (5-120), and (5-123) are a system of equations in the three state variables  $n$ ,  $c$ , and  $\rho$ . The solution trajectories are curves in a three-dimensional space. Equilibrium occurs for  $n = c = 0$  with  $\rho$  arbitrary. The nature of the equilibrium states may be studied by writing the system in the form

$$\frac{d}{dt} \begin{bmatrix} n \\ c \\ \delta\rho \end{bmatrix} = \begin{bmatrix} (\rho - \beta)/\ell & \lambda & 0 \\ \beta/\ell & -\lambda & 0 \\ -\alpha K & 0 & 0 \end{bmatrix} \begin{bmatrix} n \\ c \\ \delta\rho \end{bmatrix}, \quad (5-124)$$

where  $n$ ,  $c$ , and  $\delta\rho$  may be regarded as small departures from an equilibrium at  $n = c = 0$  and  $\rho$  arbitrary. In a small neighbourhood of an equilibrium point the matrix element containing  $\rho$  is nearly a constant. It is readily verified that two eigenvalues of the system matrix are the roots of eq. (2-29), the inhour equation corresponding to reactivity  $\rho$ , while the third eigenvalue is zero.

As discussed in connection with fig. 2-4, there are two roots of opposite sign when  $\rho > 0$ , and two negative roots when  $\rho < 0$ . As will be discussed in chapter 7, this means that the equilibrium is unstable (a saddle point) when  $\rho > 0$  and stable when  $\rho < 0$ . This unstable zero-power equilibrium for arbitrary positive reactivity corresponds to a supercritical reactor "waiting for a neutron to come along." The presence of the zero eigenvalue is a reflection of the arbitrary reactivity at equilibrium.

Following Canosa (1964), except that we are using  $n$ ,  $c$ , and  $\rho$  instead of  $n$ ,  $c$ , and  $T$ , we proceed to eliminate  $c$  from the system given by eqs. (5-119), (5-120), and (5-123). Adding the first two equations, we have

$$\frac{d}{dt}(n + c) = \frac{\rho}{\ell} n. \quad (5-125)$$

Eliminating the time variable between eqs. (5-123) and (5-125) yields

$$\frac{d(n + c)}{d\rho} = -\frac{\rho}{\alpha K \ell}. \quad (5-126)$$

Integrating, we find

$$c = A - n - \frac{\rho^2}{2\alpha K \ell}. \quad (5-127)$$

Substituting this into eq. (5-119) yields

$$\frac{dn}{dt} = \frac{\rho - \beta}{\ell} n + \lambda A - \lambda n - \frac{\lambda \rho^2}{2\alpha K \ell}. \quad (5-128)$$

The next step is elimination of the time variable between eqs. (5-123) and (5-128) to find

$$\frac{dn}{d\rho} = \frac{\beta + \lambda \ell - \rho}{\alpha K \ell} - \frac{\lambda A}{\alpha K n} + \frac{\lambda \rho^2}{2\alpha^2 K^2 \ell n}. \quad (5-129)$$

We now have a differential equation for curves in the  $n$ ,  $\rho$  plane,

representing planar projections of the three-dimensional  $n, c, \rho$  solution trajectories.

We select a subset of all possible integral curves, including the integral curve through the two points  $n = 0, c = 0, \rho = \pm\rho_0$ , by setting

$$A = \frac{\rho_0^2}{2\alpha K \ell} \quad (5-130)$$

in eq. (5-127). The point  $\rho = \rho_0$  is unstable, and the point  $\rho = -\rho_0$  is stable. Therefore, an excursion beginning at reactivity  $\rho_0$  and very low power will ultimately terminate at  $\rho = -\rho_0$ . When eq. (5-130), is used in eq. (5-129), the differential equation for these trajectories is

$$\frac{dn}{d\rho} = \frac{\beta + \lambda\ell - \rho}{\alpha K \ell} + \frac{\lambda(\rho^2 - \rho_0^2)}{2\alpha^2 K^2 \ell n}. \quad (5-131)$$

No explicit integrating factor for eq. (5-131) has been found. However, it is not difficult to construct graphical solutions in the  $n, \rho$  plane. By eq. (5-123),  $n$  and  $d\rho/dt$  are proportional, so that this is essentially a conventional phase plane. (Later we occasionally use the term phase plane to denote a two-dimensional state space even when one variable is not the time derivative of the other.)

One very straightforward graphical method is the construction of the direction field. Eq. (5-131) gives the slope of a trajectory at each point  $(n, \rho)$  on an integral curve. One draws short straight lines in the plane whose slopes are given by eq. (5-131). The direction of motion is given by a time derivative; for example, eq. (5-123) shows that  $\rho$  is always decreasing for  $\alpha > 0$  and  $n > 0$ . Equilibrium points yield indeterminate slopes.

Once the direction field is plotted, it is not difficult to draw approximate trajectories among the lines representing the slopes. Here we are interested in a particular trajectory connecting the points  $n = 0, \rho = \rho_0$  and  $n = 0, \rho = -\rho_0$ .

It is often helpful to construct isolines. An isocline is the locus of all points in the direction field for which the slope is the same. In this particular example, we can deduce much by considering the zero-slope isocline (ZSI), obtained by setting the right-hand side of eq. (5-131) equal to zero. Clearly, the trajectory crosses the ZSI at maximum power.

From eq. (5-131), the ZSI is

$$n = \frac{\lambda(\rho_0^2 - \rho^2)}{2\alpha K(\beta + \lambda\ell - \rho)}. \quad (5-132)$$

This is a hyperbola in the  $n, \rho$  plane. Its asymptotes are the straight lines

$$\rho = \beta + \lambda t \quad (S-133)$$

and

$$n = \frac{\lambda}{2\alpha K} (\rho + \beta + \lambda t). \quad (S-134)$$

Note that these asymptotes are independent of  $\rho_0$ .

A case for  $\rho_0 = 0.8\beta$  is shown in fig. 5-15. The numerical values  $\lambda = 0.405 \text{ sec}^{-1}$ ,  $\ell/\beta = 0.1 \text{ sec}$ , and  $\alpha K/\beta = 1$  were chosen for illustration. The integral curve is almost indistinguishable from the ZSI (the crossing is at peak power near  $\rho = 0.4\beta$ ). This behaviour is not surprising when one compares eqs. (5-107) and (5-132). If  $t$  may be

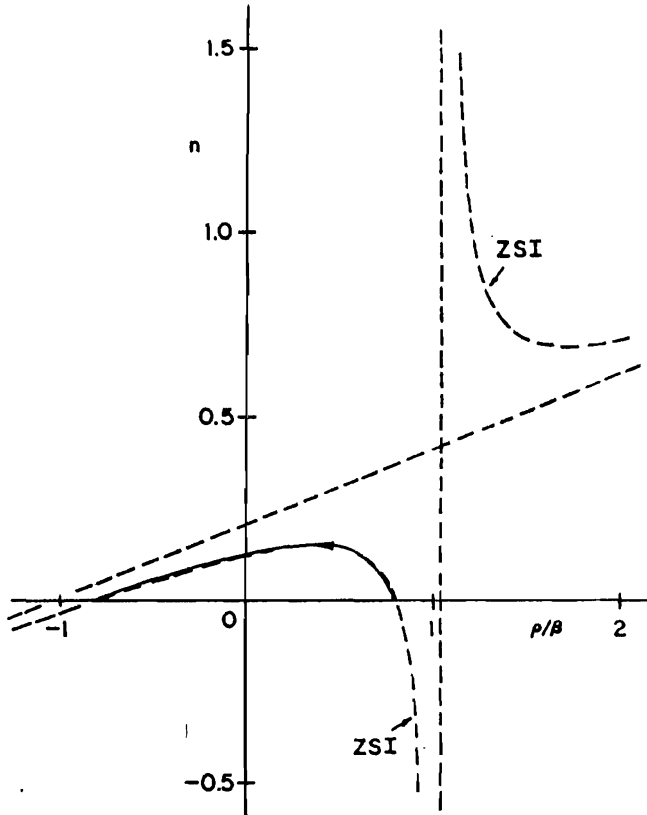


Fig. 5-15. The  $n, \rho$  plane for  $\rho_0 = 0.8\beta$ , showing the zero-slope isocline, its asymptotes, and the trajectory ( $\alpha K/\beta = 1$ ,  $\lambda = 0.405$ , and  $\ell/\beta = 0.1$ ).

neglected, the ZSI becomes the integral curve of the prompt-jump approximation.

A case for  $\rho_0 = 1.8\beta$ , with the other parameters unchanged, is shown in fig. 5-16. The integral curve of the Nordheim-Fuchs model, eq. (5-84), is included for comparison. For smaller values of  $\ell$ , the two curves would peak much closer together. The similarity of the two curves during the fast part of the burst is expected from eq. (5-131), which reduces to the Nordheim-Fuchs model when  $\lambda$  may be neglected.

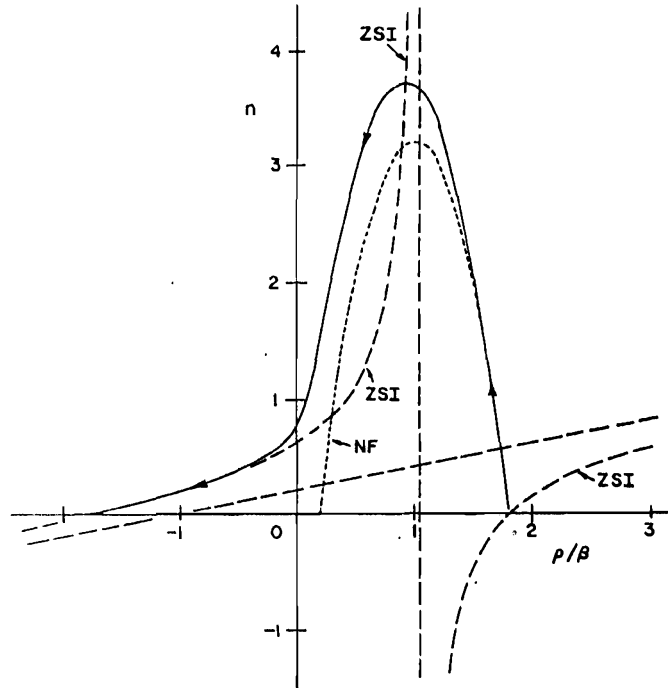


Fig. 5-16. The  $n, \rho$  plane for  $\rho_0 = 1.8\beta$ , showing the zero-slope isocline, its asymptotes, the trajectory, and the Nordheim-Fuchs approximate trajectory ( $\alpha K/\beta = 1$ ,  $\lambda = 0.405$ , and  $\gamma/\beta = 0.1$ ).

After the fast burst, the exact solution quickly approaches the ZSI from above. The remaining trajectory is the delayed-neutron tail, for which  $n \rightarrow 0$  and  $\rho \rightarrow -\rho_0$ . The beginning of the tail may be estimated by substituting the “final” reactivity  $2\beta - \rho_0$  from the Nordheim-Fuchs model into eq. (5-132) for the ZSI. The result is

$$n \geq 2\beta\lambda/\alpha K. \quad (5-135)$$

This may be compared with eq. (5-102), if we recall that  $\lambda'$  should be used for  $\lambda$  immediately after a fast burst. For small  $\ell$ , this point becomes

the intersection of the Nordheim-Fuchs curve and the ZSI, and the ZSI essentially plays the role of the prompt-jump approximation once the fast burst is over.

Additional insight may be obtained by considering other trajectories in the plane. On the ZSI, where  $dn/dt = 0$ , let  $n = n_z$ . Eq. (5-128) becomes

$$0 = \frac{\rho - \beta}{\ell} n_z + \lambda A - \lambda n_z - \frac{\lambda \rho^2}{2\alpha K \ell}. \quad (5-136)$$

Subtract eq. (5-136) from eq. (5-128) at the same value of  $\rho$  to find

$$\frac{dn}{dt} = -\frac{\beta + \lambda \ell - \rho}{\ell} (n - n_z). \quad (5-137)$$

This suggests that all integral curves, no matter what their initial conditions, rapidly converge toward the ZSI when  $\rho < \beta + \lambda \ell$ . This corresponds to the rapidly decaying starting transient that is represented by the prompt jump or drop. It explains why the integral curve is so close to the ZSI throughout in fig. 5-15, and why it approaches the ZSI so rapidly after the fast burst in fig. 5-16.

The preceding represents a single model that provides information about both slow and fast excursions, as illustrated in figs. 5-15 and 5-16. The two phase planes are very different, as exemplified by the shapes of the ZSI. The transition, which is a turning point for the system of differential equations, occurs at  $\rho_0 = \beta + \lambda \ell$ , where the hyperbola degenerates into its asymptotes. Note that the turning point is not precisely at  $\rho_0 = \beta$  (the value one might expect from the derivations of the prompt-jump and Nordheim-Fuchs models).

An integral curve starting at  $\rho_0 = \beta + \lambda \ell$  is highly asymmetrical, as shown in fig. 5-17 (computations by John Szeligowski, University of Arizona, 1967). For smaller  $\ell$  the curve closely approaches a triangular shape. The limiting value of peak power for small  $\ell$  is the intersection of the two asymptotes:

$$\hat{n} = \frac{\lambda(\beta + \lambda \ell)}{\alpha K} \rightarrow \frac{\lambda \beta}{\alpha K}. \quad (5-138)$$

This corresponds to eq. (5-111) of the prompt-jump approximation in the limit  $\rho_0 \rightarrow \beta$ . The difference between initial reactivity and reactivity at peak power becomes smaller and smaller as  $\ell$  is reduced, explaining the deep minimum in the curve of energy or compensated reactivity at peak power that is seen in figs. 5-12 and 5-13.

The small energy production at peak power requires that the curve of  $n(t)$  also be highly asymmetrical. This is seen in fig. 5-18 (compu-

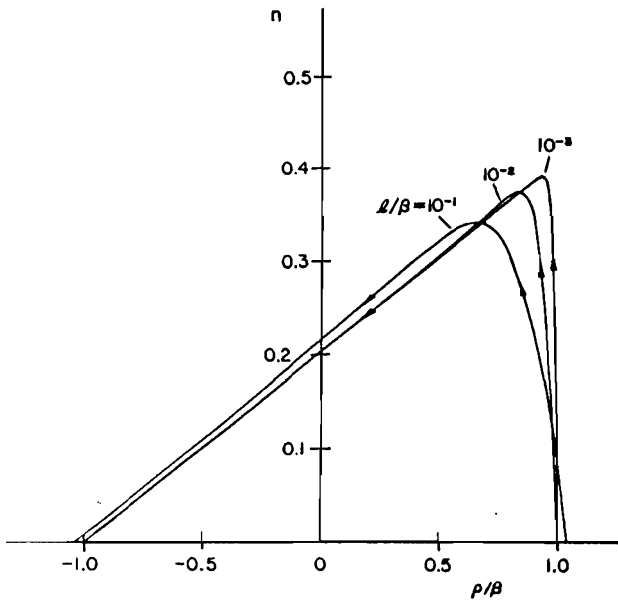


Fig. 5-17. The  $n, \rho$  plane for  $\rho_0 = \beta + \lambda\ell$  ( $\alpha K/\beta = 1$ ,  $\lambda = 0.405$ ). The zero-slope isolines, which are identical to their asymptotes, are given by eqs. (5-133) and (5-134).

tions by John Szeligowski, University of Arizona, 1967). The detailed shape after peak power would be different with six groups of delayed neutrons, but the essential features are the same.

Next, we consider one method of generating asymptotic series in powers of a small parameter to represent approximate trajectories in the  $n, \rho$  plane. For this purpose, it will be convenient to define new variables

$$x = \frac{\rho}{\beta} \quad (5-139)$$

and

$$y = \frac{\alpha K}{\lambda \beta} n. \quad (5-140)$$

The parameters are

$$x_0 = \frac{\rho_0}{\beta} \quad (5-141)$$

and

$$\epsilon = \frac{\lambda\ell}{\beta}. \quad (5-142)$$

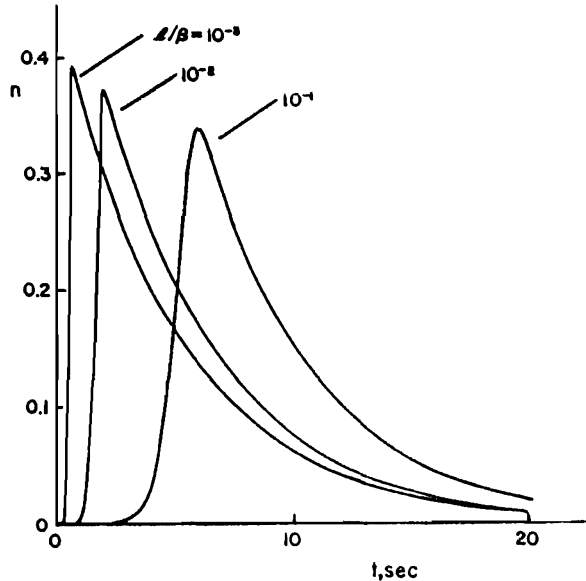


Fig. 5-18. Power vs. time for the adiabatic model with one group of delayed neutrons:  
 $\rho_0 = \beta + \lambda^2; \lambda = 0.405; \alpha K / \beta = 1; n_0 = 10^{-6}$ .

With this transformation, eq. (5-131) becomes

$$\epsilon y \frac{dy}{dx} = (1 + \epsilon - x)y + \frac{1}{2}(x^2 - x_0^2). \quad (5-143)$$

For small reactivity excursions, we expect that the dominant term in the solution will be independent of  $\epsilon$  or  $\ell$ . Hence let

$$y = y_1 + \epsilon y_2 + O(\epsilon^2), \quad (5-144)$$

as in sec. 3-1. Substituting into eq. (5-143) and equating coefficients of like powers of  $\epsilon$ , we find, for  $O(\epsilon^0)$ ,

$$y_1 = \frac{x_0^2 - x^2}{2(1 - x)}, \quad (5-145)$$

which is identified with eq. (5-107) in the prompt-jump approximation. For  $O(\epsilon^1)$ ,

$$y_2 = \frac{y_1}{1 - x} \left( \frac{dy_1}{dx} - 1 \right). \quad (5-146)$$

Taking  $y_1$  as given by eq. (5-145), we find

$$y_2 = \frac{1}{2}(x_0^2 - x^2)[x - 1 + \frac{1}{2}(x_0^2 - x^2)](1 - x)^{-4}. \quad (5-147)$$

## 19.2 Reactivity Feedback and Reactor Excursions

If eq. (5-144) is used, the solution of eq. (5-143) takes the form

$$y = \frac{x_0^2 - x^2}{2(1-x)} \left[ 1 + \frac{x-1 + \frac{1}{2}(x_0^2 - x^2)}{(1-x)^3} \epsilon + O(\epsilon^2) \right]. \quad (5-148)$$

This series differs from that obtained by Canosa (1964) in two respects. Canosa used temperature rather than reactivity as the independent variable. Further, the leading term of his series contains a parameter  $B$  which is essentially  $x_0 - 1 - \epsilon$ ; we have chosen instead to regard  $\epsilon$  as a small parameter wherever it appears, so that all terms of order  $\epsilon$  are incorporated in the second term of the series. The leading term of the series, eq. (5-148), is therefore identical to the prompt-jump approximation, and the series is valid for  $x < 1$ .

To find a first-order correction to the peak power, we calculate  $\hat{x}$  for the function  $y_1$  (the value of  $x$  for maximum  $y_1$ ) and use it in eq. (5-148) to approximate  $\hat{y}$ . It is readily verified that  $y_1$  is a maximum at

$$\hat{x} = 1 - \sqrt{1 - x_0^2}. \quad (5-149)$$

This result corresponds to eq. (5-110) in the prompt-jump approximation. Substituting into eq. (5-148), we find

$$\hat{y} = 1 - \sqrt{1 - x_0^2} + \left[ 1 - \frac{1}{\sqrt{1 - x_0^2}} \right] \epsilon + O(\epsilon^2). \quad (5-150)$$

The leading term corresponds to the right-hand side of eq. (5-111) in the prompt-jump approximation. Note that the first-order correction is negative ( $x_0 < 1$ ) and that it diverges as  $x_0 \rightarrow 1$ . Like the prompt-jump approximation, eq. (5-150) has a limited range of usefulness in which prompt critical must be avoided more widely when larger values of  $\epsilon$  are used. The divergence as  $x_0 \rightarrow 1$  is characteristic of singular perturbation expansions, and a smooth joining of eq. (5-148) or (5-150) with a series derived for fast excursions is not generally to be expected.

One way to find a first-order correction to  $\hat{x}$  is to locate the value of  $x$  for which the sum of the first two terms in eq. (5-148) is a maximum. This turns out to be rather laborious, and an alternative estimate may be made by assuming, as suggested earlier, that the exact trajectory is very close to the ZSI. The ZSI for eq. (5-143) is

$$y = \frac{x_0^2 - x^2}{2(1 + \epsilon - x)}, \quad (5-151)$$

and its maximum occurs at

$$\hat{x} = 1 - \sqrt{1 - x_0^2} + \left[ 1 - \frac{1}{\sqrt{1 - x_0^2}} \right] \epsilon + O(\epsilon^2). \quad (5-152)$$

As it happens, eq. (5-152) is very close to the result obtained by maximizing eq. (5-148), except in the limit  $x_0 \rightarrow 1$ . As in the case of  $\hat{y}$ , the first-order correction to  $\hat{x}$  is negative and divergent as  $x_0 \rightarrow 1$ .

For large reactivity excursions, it may be inferred from the Nordheim-Fuchs model, eq. (5-83), that the dominant term in  $y(x)$  will be of order  $1/\epsilon$ . Let

$$y = \frac{y_1}{\epsilon} + y_2 + O(\epsilon). \quad (5-153)$$

This is similar to the treatment in sec. 3-1, although here we explicitly write  $1/\epsilon$  in the leading term. Substituting in eq. (5-143) and equating coefficients of like powers of  $\epsilon$ , we find, for  $O(\epsilon^{-1})$ ,

$$\frac{dy_1}{dx} = 1 - x. \quad (5-154)$$

Integrating with  $y_1 = 0$  at  $x = x_0$ , we have

$$y_1 = \frac{1}{2}[(1 - x_0)^2 - (1 - x)^2], \quad (5-155)$$

which is equivalent to eq. (5-83). For  $O(\epsilon^0)$ ,

$$y_2 \frac{dy_1}{dx} + y_1 \frac{dy_2}{dx} = y_1 + (1 - x)y_2 + \frac{1}{2}(x^2 - x_0^2). \quad (5-156)$$

Using eqs. (5-154) and (5-155), one finds

$$\frac{dy_2}{dx} = \frac{1}{1 - \frac{1}{2}(x + x_0)}.$$

Integrating with  $y_2 = 0$  at  $x = x_0$  yields

$$y_2 = 2 \log \frac{1 - x_0}{1 - \frac{1}{2}(x + x_0)}. \quad (5-157)$$

The solution trajectory may be written as

$$y = \frac{1}{2}[(1 - x_0)^2 - (1 - x)^2] \frac{1}{\epsilon} + 2 \log \frac{1 - x_0}{1 - \frac{1}{2}(x + x_0)} + O(\epsilon). \quad (5-158)$$

Again, the result differs from one obtained by Ganosa (1964), as cited earlier in connection with eq. (5-148). In particular, the coefficient of  $1/\epsilon$  in eq. (5-158) is independent of  $\epsilon$ .

This series is useful during the fast part of the excursion. After the fast burst, the trajectory rapidly approaches the ZSI, eq. (5-151).

The first term of eq. (5-158) peaks at  $\hat{x} = 1$ , as in the Nordheim-Fuchs model. The exact trajectory peaks when it crosses the ZSI, eq.

(5-151). To obtain the first-order correction to  $\dot{x}$ , we set the right-hand side of eq. (5-151) equal to the first term of eq. (5-158) and solve for  $x$ . The result is

$$\dot{x} = 1 - \frac{x_0 + 1}{x_0 - 1} \epsilon + O(\epsilon^2). \quad (5-159)$$

To find the first-order correction to  $\dot{y}$ , we set  $x = 1$  in eq. (5-158). This yields

$$\dot{y} = \frac{(1 - x_0)^2}{2\epsilon} + 2 \log 2 + O(\epsilon). \quad (5-160)$$

The first term is eq. (5-84) of the Nordheim-Fuchs approximation. The lack of smooth matching with eqs. (5-150) and (5-152) at  $x_0 = 1$  is evident.

As pointed out by Canosa (1964), these expansions are asymptotic series that could be used for numerical calculation in limited regimes. The generation of higher-order terms would be laborious, and their practical value would be small. The underlying idea, however, is of great importance in understanding how approximate solutions, valid in different regimes of a dependent variable, may be generated and placed in proper relation to each other.

The use of approximate inhour equations to generate asymptotic series for  $\dot{y}$  and  $\dot{x}$ , with  $\omega$  as a parameter instead of  $x_0 = \rho_0/\beta$ , is reserved for the problem set at the end of the chapter. This is of interest because the initial inverse period  $\omega$  is more directly related to experimental observation than is the initial reactivity  $\rho_0$ .

To conclude this section, we discuss an approximate treatment of the transition case  $\rho_0 = \beta + \lambda\epsilon$  or  $x_0 = 1 + \epsilon$ . It will be convenient to work with the variable

$$u = x_0 - x, \quad (5-161)$$

which is proportional to compensated reactivity or temperature rise. Eq. (5-143) is transformed into

$$\epsilon y \frac{dy}{du} = (x_0 - 1 - \epsilon)y + x_0 u - uy - \frac{1}{2}u^2. \quad (5-162)$$

At the transition  $x_0 = 1 + \epsilon$ , this reduces to

$$\epsilon y \frac{dy}{du} = (1 + \epsilon)u - uy - \frac{1}{2}u^2. \quad (5-163)$$

We seek the trajectory through the origin in the  $y, u$  plane. Note that the slope at the origin is indeterminate in eq. (5-163).

Consider the family of isoclines given by

$$\epsilon yM = (1 + \epsilon)u - uy - \frac{1}{2}u^2. \quad (5-164)$$

We note that the ZSI ( $M = 0$ ) consists of the two intersecting straight lines

$$u = 0 \quad (5-165)$$

and

$$y = 1 + \epsilon - \frac{1}{2}u. \quad (5-166)$$

The origin is a saddle point. To find the initial slope, we select the special trajectory that can emerge from the saddle point. As we shall see in chapter 7, such a trajectory must itself coincide with a particular isocline as it passes through the saddle point. Differentiating eq. (5-164), we obtain

$$\epsilon M \frac{dy}{du} = 1 + \epsilon - u \frac{dy}{du} - y - u,$$

where  $dy/du$  is now the slope of an isocline. At the origin, we have

$$\epsilon M \frac{dy}{du} = 1 + \epsilon. \quad (5-167)$$

For a trajectory to coincide with an isocline,  $M$  must equal  $dy/du$ . The initial slope is therefore

$$M = \sqrt{\frac{1 + \epsilon}{\epsilon}} \cong \frac{1}{\sqrt{\epsilon}}. \quad (5-168)$$

This initial slope is very large because  $\epsilon$  is a small parameter. The trajectory peaks where it crosses the ZSI as given by eq. (5-166), and this must be at small  $u$  because of the initial steepness. The peak must therefore be  $\hat{y} \cong 1$ . The value of  $u$  at  $\hat{y}$  may be estimated roughly from eq. (5-168) by means of the initial slope,

$$\hat{y}/\hat{u} \cong 1/\hat{u} \cong 1/\sqrt{\epsilon},$$

so that a zero-order approximation to  $\hat{u}$  is

$$\hat{u} \cong \sqrt{\epsilon}. \quad (5-169)$$

By eqs. (5-139), (5-141), and (5-161),  $\hat{u}$  is the reactivity in dollars compensated at the instant of peak power. Since  $\epsilon = \lambda\varepsilon/\beta$ , eq. (5-169) states that for initial reactivity  $1 + \epsilon$  the compensated reactivity at peak is proportional to the square root of  $\varepsilon$ .

A better approximation may be derived using eq. (5-163). Assume

that  $u$  remains sufficiently small that  $u^2$  may be neglected in the differential equation. The resulting approximate trajectory satisfies

$$\epsilon \frac{dy}{du} = (1 + \epsilon)u - uy \cong u - uy. \quad (5-170)$$

The approximate integral curve is

$$\epsilon \log \frac{1}{1 - y} - \epsilon y = \frac{1}{2}u^2. \quad (5-171)$$

Eq. (5-171) is a good approximate trajectory provided  $u$  is  $O(\sqrt{\epsilon})$  or smaller.

We seek relationships at peak by investigating the intersection of eq. (5-171) with the ZSI. By eq. (5-166), the ZSI for small  $\epsilon$  is

$$y = 1 - \frac{1}{2}u. \quad (5-172)$$

The intersection yields a transcendental equation for  $\hat{u}$ . To find an approximate solution, rewrite eq. (5-171) as

$$y = 1 - \exp\left(-\frac{u^2}{2\epsilon} - y\right). \quad (5-173)$$

We may set  $y \cong 1$  in the exponent. Comparison with eq. (5-172) shows that the approximate  $\hat{u}$  is the solution of

$$\exp\left(-1 - \frac{u^2}{2\epsilon}\right) = \frac{1}{2}u. \quad (5-174)$$

The Gaussian function that appears in the left-hand side of eq. (5-174) has a half-width  $u = \sqrt{(2\epsilon)}$ . The solution  $u = \hat{u}$  of eq. (5-174) is small, so that the approximation

$$\hat{u} \cong \sqrt{(2\epsilon)} \quad (5-175)$$

is better than eq. (5-169) and is also seen to be a lower limit for  $\hat{u}$ . We arbitrarily select eq. (5-175) as our first approximation.

Next, we rewrite eq. (5-174) as

$$u = \sqrt{\left[2\epsilon \left(\log \frac{2}{u} - 1\right)\right]}. \quad (5-176)$$

A second approximation that is very close to the exact solution of eq. (5-174) is obtained by substituting eq. (5-175) into the right-hand side of eq. (5-176):

$$\hat{u} \cong \sqrt{\left[\epsilon \left(\log \frac{2}{\epsilon} - 2\right)\right]}. \quad (5-177)$$

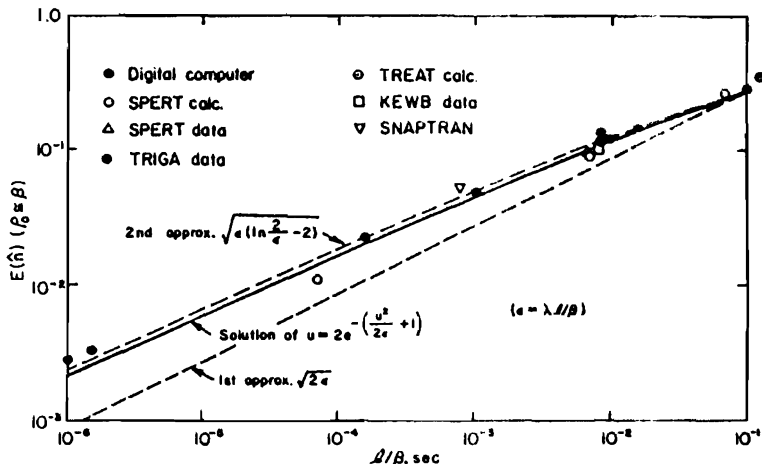


Fig. 5-19. Compensated reactivity at peak power vs.  $t/\beta$  for one-dollar reactivity step. For prompt linear shutdown, ordinate also represents energy (normalized to a reactivity coefficient of one dollar per unit energy).

Precise values for the exact solution of eq. (5-174) may be quickly obtained by an iterative procedure using eq. (5-176), the next approximation being the result of using eq. (5-177) in the right-hand side of eq. (5-176).

Comparisons with experiment and with precise digital computations are good, even for systems with complex shutdown mechanisms. Compensated reactivity (dollars) at peak power for  $\rho_0 = \beta + \lambda$  is shown in fig. 5-19 as a function of  $t/\beta$ . Digital computer results are by Szeligowski and Hetrick (1967) and by Vigil<sup>3</sup>. The SPERT reactor calculations are semiempirical estimates (Forbes 1959). The experimental point for the SPERT-I reactor represents reactivity computed from power excursion data (Miller 1957). Data for TRIGA were supplied by Kurstedt<sup>4</sup> and Leonard<sup>5</sup>. The computational result for TREAT was supplied by Dickerman<sup>6</sup>. The experimental point for KEWB was reported by Hetrick and Gamble (1958), and the point for SNAPTRAN was reported by Johnson (1966). Fast-burst reactors are represented only by computed points; it is extremely difficult to perform the precise experiment in this range because the period is highly sensitive to small uncertainties in reactivity input.

It is well established that the compensated reactivity at peak power

3. J. C. Vigil, Los Alamos Scientific Laboratory, private communication (1967).

4. H. A. Kurstedt, Ohio State University, private communication (1967).

5. B. E. Leonard, Defense Atomic Support Agency, private communication (1967).

6. C. E. Dickerman, Argonne National Laboratory, private communication (1967).

has a minimum near one-dollar initial reactivity, consistent with the computations shown in fig. 5-13. The occurrence of this phenomenon even with complex nonlinear shutdown mechanisms suggests that it is essentially a manifestation of delayed neutrons.

### 5-8. The Fuchs Ramp-Input Model

Self-limiting power excursions induced by ramp inputs of reactivity (initial reactivity increasing linearly with time) are considered next. Important contributions to the subject were made by Fuchs (1946), Hansen (1952), Brittan (1956), Nyer (1958), Smets (1959a), and Canosa (1967a, 1968a). We first summarize the main features of the classic Fuchs model for fast excursions and then give Canosa's derivation of a necessary condition for the net reactivity to exceed prompt critical in the presence of delayed neutrons.

As in sec. 5-5, neglect the production rates of delayed neutrons and source neutrons, and use eq. (5-77) for the neutron density:

$$\frac{dn}{dt} = \frac{\rho - \beta}{\ell} n. \quad (5-178)$$

For the reactivity, assume

$$\rho = \rho_0 + \gamma t - \alpha T, \quad (5-179)$$

where  $\rho_0$  is an unspecified constant,  $\gamma$  is the reactivity ramp rate, and  $T$  is the temperature rise. Other symbols have the same meanings as in sec. 5-5; the significance of  $t = 0$  will be discussed later.

We use the adiabatic model of eq. (5-66) or (5-79):

$$\frac{dT}{dt} = Kn. \quad (5-180)$$

As pointed out by Smets (1959a), the form of the equations is not altered by using the constant-power-removal model of eq. (5-68). We choose the simpler case for this exposition. From eqs. (5-179) and (5-180),

$$\frac{d\rho}{dt} = \gamma - \alpha Kn. \quad (5-181)$$

Upon eliminating the time variable between eqs. (5-178) and (5-181), we have

$$\frac{dn}{d\rho} = \frac{(\rho - \beta)n}{\ell(\gamma - \alpha Kn)}. \quad (5-182)$$

Eq. (5-182) is a differential equation for trajectories in the  $n, \rho$  plane,

and the problem has been effectively transformed into the solution of an autonomous system.

It is convenient to work with the instantaneous reciprocal period

$$\omega = \frac{1}{n} \frac{dn}{dt} = \frac{\rho - \beta}{\ell} \quad (5-183)$$

so that eq. (5-182) is replaced by

$$\frac{dn}{d\omega} = \frac{\ell \omega n}{\gamma - \alpha K n}. \quad (5-184)$$

With variables separated,

$$\frac{dn}{n} - \frac{\alpha K}{\gamma} dn = \frac{\ell}{\gamma} \omega d\omega. \quad (5-185)$$

By eqs. (5-181) and (5-183), the maximum reactivity  $\rho_m$  and maximum reciprocal period  $\omega_m$  occur at  $n = n_m$  given by

$$n_m = \frac{\gamma}{\alpha K}. \quad (5-186)$$

This is an important parameter of the system, and it is usually referred to as the power at minimum period. It is seen that  $n_m$  is also the power at minimum reactivity (maximum period) following a neutron burst.

Eq. (5-185) may be written as

$$\frac{dn}{n} - \frac{dn}{n_m} = \frac{\ell}{\gamma} \omega d\omega. \quad (5-187)$$

By eq. (5-183),  $n$  will be a maximum ( $\hat{n}$ ) or a minimum ( $n_{min}$ ) when  $\omega = 0$ . Integrating eq. (5-187) from  $n = n_{min}$  and  $\omega = 0$ , we have

$$\log \frac{n}{n_{min}} - \frac{n - n_{min}}{n_m} = \frac{\ell}{2\gamma} \omega^2, \quad (5-188)$$

a family of closed curves in the  $n, \omega$  plane that represents periodic solutions for power and reactivity. If we introduce

$$x = \left(\frac{\ell}{\gamma}\right)^{\frac{1}{2}} \omega, \quad y = \frac{n}{n_m}, \quad y_0 = \frac{n_{min}}{n_m}, \quad (5-189)$$

the trajectories are

$$\log \frac{y}{y_0} - (y - y_0) = \frac{1}{2}x^2. \quad (5-190)$$

Trajectories are shown in fig. 5-20, with  $1/y_0 = n_m/n_{min}$  used as the parameter. Note that the value of  $y$  becomes exceedingly small along

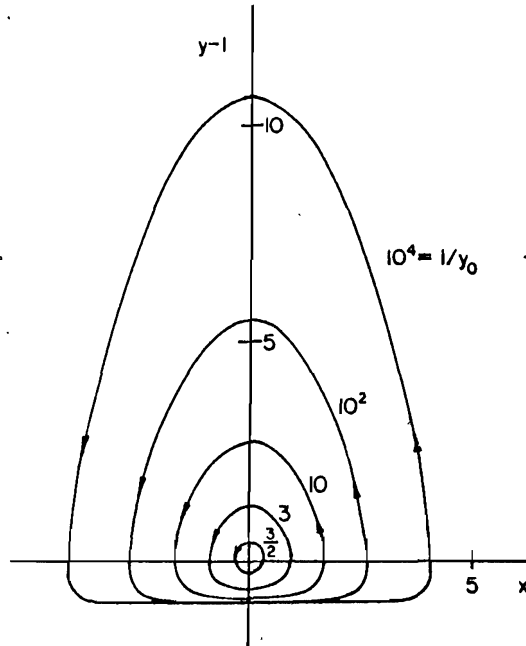


Fig. 5-20. Solution trajectories for the Fuchs ramp-input model:  $x = (\ell/\gamma)^{1/2}\omega$ ,  $y = n/n_m$ ,  $n_m$  = power at minimum period; parameter is  $1/y_0 = n_m/n_{\min}$ .

the bottom of a large trajectory. In fact, the line  $y = 0$ , corresponding to  $n(t) = 0$  and  $d\rho/dt = \gamma$ , is a separatrix that bounds the region of closed curves.

It may be noted that fig. 5-20 is closely related to the phase plane for a second-order differential equation obtained by eliminating  $n$  between eqs. (5-178) and (5-181),

$$\frac{d^2\rho}{dt^2} - (\rho - \beta) \frac{d\rho}{dt} + \gamma(\rho - \beta) = 0. \quad (5-191)$$

By eqs. (5-181) and (5-189),  $y - 1$  corresponds to  $-d\rho/dt$ , and, by eqs. (5-183) and (5-189),  $x$  corresponds to  $\rho - \beta$ . Fig. 5-20 is the phase plane  $d\rho/dt$  vs.  $\rho - \beta$  with the vertical axis reversed and the scales changed. Canosa (1967a) used eq. (5-191) as the basis for a singular perturbation treatment of this problem.

Next, return to eq. (5-187) and integrate from  $n = n_m$  and  $\omega = \omega_m$ :

$$\log \frac{n}{n_m} - \frac{n - n_m}{n_m} = \frac{\ell}{2\gamma} (\omega^2 - \omega_m^2). \quad (5-192)$$

If one sets  $n = \hat{n}$  and  $\omega = 0$  (peak power), this equation becomes

$$\frac{\hat{n}}{n_m} - 1 - \log \frac{\hat{n}}{n_m} = \frac{\ell}{2\gamma} \omega_m^2. \quad (5-193)$$

It may be mentioned that solving eq. (5-193) for  $\ell$  in terms of experimentally measured quantities yields an indirect measurement of the neutron generation time. Eq. (5-193) also yields an important theoretical result for large excursions (large  $\hat{n}/n_m$ ). In the limit of large  $\hat{n}$ , eq. (5-193) is approximately

$$\hat{n} \cong \frac{\ell n_m \omega_m^2}{2\gamma} = \frac{\ell \omega_m^2}{2\alpha K}. \quad (5-194)$$

We may compare eq. (5-194) with eq. (5-86) for large step-induced excursions, recalling that  $\omega$  in that case also corresponds to minimum period (maximum reactivity). This suggests a concept of approximate equivalence between step and ramp excursions, although the approximation may not be very good. (Even for the largest trajectory in fig. 5-20 the error is about 30 percent.) Other examples of the step-to-ramp equivalence are discussed by Canosa (1967a).

Returning now to eq. (5-192), we set  $n = n_{\min}$  and  $\omega = 0$  to find

$$\log \frac{n_m}{n_{\min}} - 1 + \frac{n_{\min}}{n_m} = \frac{\ell}{2\gamma} \omega_m^2. \quad (5-195)$$

Even for moderate-size trajectories, the term  $n_{\min}/n_m$  is small and may be neglected in eq. (5-195). Solving for  $\omega_m$ , we have

$$\omega_m = \pm \sqrt{\left[ \frac{2\gamma}{\ell} \left( \log \frac{n_m}{n_{\min}} - 1 \right) \right]}. \quad (5-196)$$

Eq. (5-196) may be combined with eq. (5-194) to yield

$$\frac{\hat{n}}{n_m} \cong \log \frac{n_m}{n_{\min}} - 1. \quad (5-197)$$

As mentioned in connection with eq. (5-194), this cannot be expected to yield a good approximation. In a rather laborious analysis, Fuchs (1946) obtained

$$\frac{\hat{n}}{n_m} \cong \log \frac{4n_m}{n_{\min}},$$

which gives a rough idea of the amount by which eq. (5-194) or (5-197) is an underestimate of the peak power.

Eq. (5-196) itself is a good approximation, and it may be used to deduce other properties of the periodic solution. Using eq. (5-183), we

find the extremes in reactivity to be

$$\rho_m = \beta \pm \sqrt{\left[ 2\gamma\ell \left( \log \frac{n_m}{n_{\min}} - 1 \right) \right]}. \quad (5-198)$$

A single burst corresponds to a reactivity excursion of

$$\Delta\rho = 2\sqrt{\left[ 2\gamma\ell \left( \log \frac{n_m}{n_{\min}} - 1 \right) \right]}. \quad (5-199)$$

The energy in one burst is  $E = \Delta\rho/\alpha K$ . Using eq. (5-186), we have

$$E = 2n_m \sqrt{\left[ \frac{2\ell}{\gamma} \left( \log \frac{n_m}{n_{\min}} - 1 \right) \right]}. \quad (5-200)$$

Between bursts, the reactivity loss  $\Delta\rho$  is restored at the input rate  $\gamma$  per sec. The cycle time  $\Delta t$ , or interval between bursts, is therefore  $\Delta\rho/\gamma$ , or

$$\Delta t = 2\sqrt{\left[ \frac{2\ell}{\gamma} \left( \log \frac{n_m}{n_{\min}} - 1 \right) \right]}. \quad (5-201)$$

Finally, we may roughly estimate the duration of each burst as  $\tau \cong E/\dot{n}$ . Using eqs. (5-197) and (5-200), we find

$$\tau \cong 2\sqrt{\left[ 2\ell/\gamma \left( \log \frac{n_m}{n_{\min}} - 1 \right) \right]}. \quad (5-202)$$

The situation is pictured qualitatively in fig. 5-21, where the point  $t = 0$  is placed at prompt critical. Actually, as far as the periodic solution itself is concerned, the time axis is arbitrary. Since  $n$  is never zero on a closed trajectory, there is no initial equilibrium point for which  $dT/dt$  vanishes. (For a discussion of this, and for approximate time-domain solutions, see Canosa 1967a).

In fact, the major difficulty in using this model for a practical problem is the selection of an appropriate closed trajectory that may be matched in some fashion to a ramp solution without feedback, the latter originating at critical ( $\rho = 0$ ) with some initial power  $n_0$ . The Fuchs model is derived under the assumption that the reactor has already exceeded prompt critical before feedback becomes appreciable. For a slow ramp, it is to be expected that the neutron burst may be over without the net reactivity ever reaching prompt critical.

Limiting cases of very fast ramps may be treated using the asymptotic solution given in sec. 3-4. Assume  $\gamma$  is large enough that the asymptotic solution without feedback, eq. (3-129), is valid for an interval after prompt critical is reached but before the onset of feedback. The parabolic curve of fig. 3-16 may then be identified as the lower portion of a

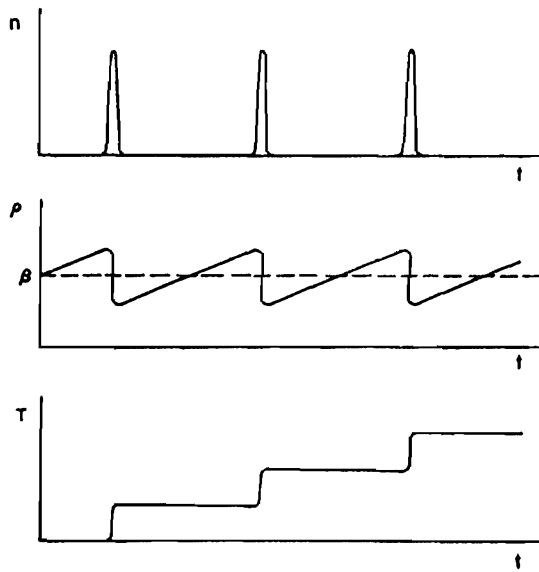


Fig. 5-21. Qualitative response to a large ramp input of reactivity.

Fuchs-model trajectory taken from fig. 5-20 (recall that fig. 3-16 has a logarithmic scale).

Extrapolation of eq. (3-129) back to prompt critical gave eq. (3-131):

$$n(t^*) \cong n_0 \beta \sqrt{(2\pi/\gamma\ell)}. \quad (5-203)$$

We may now identify this  $n(t^*)$  as  $n_{min}$ , thereby selecting a particular closed trajectory. This permits the calculation of unique values for peak power, maximum reactivity, energy release, etc., by using the equations derived in this section. Such results would be applicable only to very fast ramps initiated at very low power, and they would be meaningless if the net reactivity actually remained less than  $\beta$ .

A criterion for validity of the procedure just outlined may be derived intuitively as follows: In eq. (5-203),  $n(t^*)$  varies inversely as  $\gamma^{\frac{1}{2}}$ . If  $\gamma$  is too small, then  $n(t^*)$  will exceed  $n_m$  as calculated from eq. (5-186). Therefore, a necessary condition for identifying eq. (5-203) with  $n_{min}$  is

$$n(t^*) < n_m. \quad (5-204)$$

In fact, if this inequality is not satisfied, prompt critical cannot be reached before appreciable feedback appears. Using eqs. (5-186) and (5-203), we conclude that

$$\left(\frac{\ell}{2\pi}\right)^{\frac{1}{2}} \frac{\gamma^{\frac{1}{2}}}{\beta\alpha Kn_0} > 1 \quad (5-205)$$

is a necessary condition for the identification of  $n(t^*)$  with  $n_{\min}$  (and for the attainment of prompt critical before appreciable feedback). Of course, eq. (3-129) is an asymptotic form valid for large  $\gamma$ , and one should first check to see that the condition  $\gamma \gg \lambda\beta$  is satisfied (see secs. 3-3 and 3-4).

We now turn to the derivation of a related criterion obtained by Canosa (1968a). We shall find that eq. (5-205) is essentially a special case that is valid for sufficiently small initial power  $n_0$ . We shall also discuss Canosa's more general results for maximum net reactivity.

Let the initial state be  $\rho = 0$ ,  $n = n_0$ . Assume that the excursion is fast enough that the  $c_i$  remain at their equilibrium values. Eqs. (3-1) and (3-2), with  $q = 0$  and  $dc_i/dt = 0$ , yield (constant-source approximation):

$$\frac{dn}{dt} = \frac{\rho - \beta}{\ell} n + \frac{\beta}{\ell} n_0. \quad (5-206)$$

As discussed in sec. 3-1, this will be valid for  $t \ll 1/\lambda$ . Since with ramp rate  $\gamma$  prompt critical would be reached at  $t = \beta/\gamma$ , we may infer that this model is useful provided  $\gamma \gg \lambda\beta$ .

Represent the reactivity as

$$\rho = \gamma t - \alpha T \quad (5-207)$$

for  $t > 0$ , with  $\rho = 0$  for  $t < 0$ , and use the constant-power-removal model of eq. (5-68):

$$\frac{dT}{dt} = K(n - n_0). \quad (5-208)$$

Eliminating  $T$ , we have

$$\frac{d\rho}{dt} = \gamma - \alpha K(n - n_0). \quad (5-209)$$

To proceed, eliminate  $n$  using eqs. (5-206) and (5-209). This yields

$$\frac{d^2\rho}{dt^2} + (\beta - \rho) \frac{d\rho}{dt} + (\gamma + \alpha Kn_0)\rho - \gamma\beta = 0. \quad (5-210)$$

If  $n_0 \rightarrow 0$ , eq. (5-210) reduces to eq. (5-191), which is homogeneous in the variable  $\rho - \beta$ . Eq. (5-210) may be made homogeneous by the substitution

$$u = \rho - \frac{\gamma\beta}{\gamma + \alpha Kn_0} \quad (5-211)$$

or

$$u = \rho - \frac{\beta}{1 + \delta}, \quad (5-212)$$

where

$$\delta = \alpha K n_0 / \gamma. \quad (5-213)$$

The transformed equation is

$$\epsilon \frac{d^2 u}{dt^2} + \left( \frac{\beta \delta}{1 + \delta} - u \right) \frac{du}{dt} + \gamma(1 + \delta)u = 0.$$

Next, introduce the dimensionless time  $\tau$  and the parameter  $\epsilon$ ,

$$\tau = \gamma t, \quad \epsilon = \gamma \ell, \quad (5-214)$$

and obtain

$$\epsilon \frac{d^2 u}{d\tau^2} + \left( \frac{\beta \delta}{1 + \delta} - u \right) \frac{du}{d\tau} + (1 + \delta)u = 0. \quad (5-215)$$

The latter may be converted to the pair of first-order equations

$$\frac{du}{d\tau} = v \quad (5-216)$$

and

$$\frac{dv}{d\tau} = \frac{1}{\epsilon} \left[ uv - \frac{\beta \delta}{1 + \delta} v - (1 + \delta)u \right], \quad (5-217)$$

where the phase variable  $v$  is identified as  $d\rho/dt$ . Trajectories in the phase plane are given by

$$\frac{dv}{du} = \frac{1}{\epsilon v} \left[ uv - \frac{\beta \delta}{1 + \delta} v - (1 + \delta)u \right]. \quad (5-218)$$

The zero-slope isocline (ZSI) in the phase plane is the hyperbola

$$uv - \frac{\beta \delta}{1 + \delta} v - (1 + \delta)u = 0 \quad (5-219)$$

with asymptotes

$$u = \frac{\beta \delta}{1 + \delta} \quad \text{and} \quad v = 1 + \delta. \quad (5-220)$$

By eq. (5-212), the vertical asymptote corresponds to prompt critical.

The initial state is  $\rho = 0$ ,  $d\rho/dt = \gamma$ . By eqs. (5-212), (5-214), and (5-216), the initial point in the phase plane is

$$u = -\frac{\beta}{1 + \delta}, \quad v = 1. \quad (5-221)$$

From eq. (5-219), it is seen that the initial point is on the ZSI. Fig. 5-22 is a qualitative illustration. Each time the trajectory crosses to the right of the vertical asymptote, the net reactivity exceeds prompt critical.

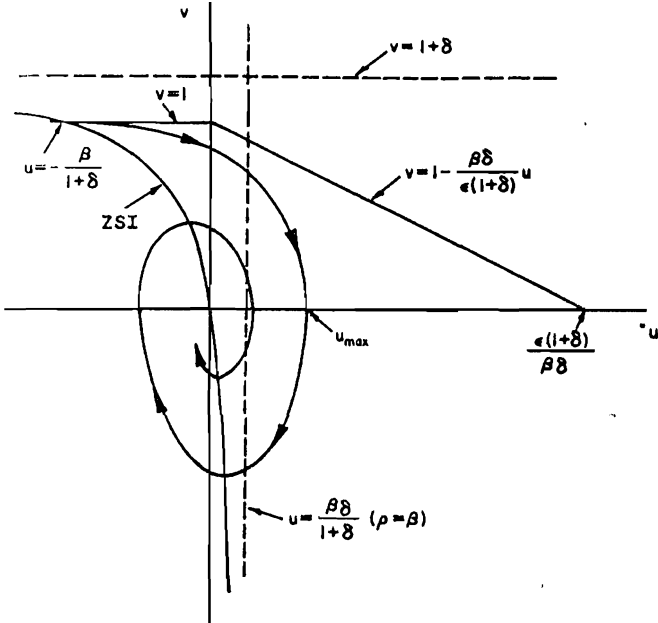


Fig. 5-22. Qualitative illustration of Canosa's criterion for a ramp excursion with delayed neutrons.

An upper bound to the trajectory is found as follows: From the initial point to the  $v$ -axis, the trajectory lies below the line  $v = 1$ . The trajectory crosses the  $v$ -axis ( $u = 0$ ) with a slope

$$M = -\frac{\beta\delta}{\epsilon(1 + \delta)}, \quad (5-222)$$

as given by eq. (5-218). The straight line

$$v = 1 - \frac{\beta\delta}{\epsilon(1 + \delta)} u \quad (5-223)$$

is therefore an upper bound in the first quadrant. This straight line intersects the  $u$ -axis at

$$u = \frac{\epsilon(1 + \delta)}{\beta\delta}, \quad (5-224)$$

as shown in fig. 5-22.

The reactivity exceeds prompt critical only if the trajectory crosses the vertical asymptote. A necessary condition for this crossing is

$$\frac{\epsilon(1 + \delta)}{\beta\delta} > \frac{\beta\delta}{1 + \delta},$$

which is

$$\frac{\epsilon^2(1 + \delta)}{\beta\delta} > 1. \quad (5-225)$$

Using eqs. (5-213) and (5-214), we may express this criterion of Canosa's in terms of physical variables as

$$\frac{(\gamma\ell)^{\frac{1}{2}}(\gamma + \alpha Kn_0)}{\beta\alpha Kn_0} > 1. \quad (5-226)$$

In the special case  $n_0 \ll \gamma/\alpha K$ , this reduces to eq. (5-205) except for the factor  $\sqrt{(2\pi)}$ . Eq. (5-205), which was derived for small  $n_0$  on a simple intuitive basis, is somewhat more restrictive than eq. (5-226) in the limit of small  $n_0$  because of the factor  $\sqrt{(2\pi)}$ .

Eq. (5-224), used in the derivation of Canosa's criterion, is not a useful upper limit for estimating  $u_{\max}$  (see fig. 5-22). Instead, we note that  $\epsilon$  and  $\delta$  are both small parameters in a realistic model of a fast excursion. This means that the ZSI is very close to its straight-line asymptotes, turning a very sharp corner near the  $v$ -axis and consequently crowding the trajectory very close to the line  $v = 1$  as it approaches the  $v$ -axis.

The trajectory crosses the  $v$ -axis near  $v = 1$  with a slope given by eq. (5-222). In a fast excursion, the magnitude of this slope could be either greater or less than unity. However, the vertical asymptote ( $\rho = \beta$ ) is very close to the  $v$ -axis (small  $\delta$ ), so that the trajectory crosses this asymptote near  $v = 1$ .

We may construct an approximate trajectory in three segments. First, let the trajectory follow the ZSI until the slope  $M$  of eq. (5-222) is attained. Then let the trajectory switch to a tangent line of slope  $M$ , crossing the  $v$ -axis and extending to the vertical asymptote. From this point on, one neglects the term  $v\beta\delta/(1 + \delta)$  in eq. (5-218) and integrates to obtain the equation of an approximate trajectory. This curve then crosses the  $u$ -axis near  $u_{\max}$ .

This approximate trajectory is sketched in fig. 5-23. From the initial point to point 1, the curve is the ZSI, eq. (5-219). To locate point 1, form  $dv/du$  from eq. (5-219), set it equal to  $M$  as given by eq. (5-222), and solve for

$$u_1 = \frac{\beta\delta}{1 + \delta} - \sqrt{[\epsilon(1 + \delta)]} \quad (5-227)$$

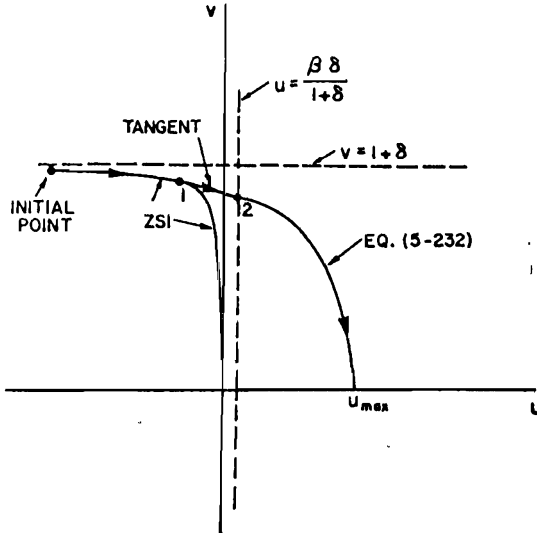


Fig. 5-23. Sketch of approximate trajectory for a fast ramp excursion with delayed neutrons.

and

$$v_1 = 1 + \delta - \frac{\beta\delta}{\sqrt{[\epsilon(1 + \delta)]}}. \quad (5-228)$$

The tangent at point 1 with slope  $M$  is extended to point 2, given by

$$u_2 = \frac{\beta\delta}{1 + \delta} \quad (5-229)$$

and

$$v_2 = 1 + \delta - \frac{2\beta\delta}{\sqrt{[\epsilon(1 + \delta)]}}. \quad (5-230)$$

After point 2, use eq. (5-218) in the approximate form

$$\frac{dv}{du} = \frac{1}{\epsilon v} \left[ uv - (1 + \delta)u \right]. \quad (5-231)$$

The approximate trajectory is the integral curve for eq. (5-231) that passes through point 2:

$$u^2 - u_2^2 = 2\epsilon \left[ v - v_2 + (1 + \delta) \log \frac{1 + \delta - v}{1 + \delta - v_2} \right]. \quad (5-232)$$

To obtain  $u_{\max}$ , set  $v = 0$  in eq. (5-232). The result may be used in eq. (5-212) to obtain

$$\rho_{\max} = \frac{\beta}{1 + \delta} + \sqrt{\left\{ u_2^2 + 2\epsilon \left[ (1 + \delta) \log \frac{1 + \delta}{1 + \delta - v_2} - v_2 \right] \right\}}. \quad (5-233)$$

In the limit of small  $\delta$ , eq. (5-233) becomes

$$\rho_{\max} \cong \beta + \sqrt{\left[ 2\epsilon \left( \log \frac{\sqrt{\epsilon}}{2\beta\delta} - 1 \right) \right]}, \quad (5-234)$$

in terms of the physical variables, it is

$$\rho_{\max} \cong \beta + \sqrt{\left[ 2\gamma \left( \log \frac{\gamma\sqrt{(\gamma\ell)}}{2\beta\alpha K n_0} - 1 \right) \right]}. \quad (5-235)$$

It is interesting to compare this result with eq. (5-198), recalling that  $n_m = \gamma/\alpha K$ . We find

$$n_{\min} \cong \frac{2\beta}{\sqrt{(\gamma\ell)}} n_0. \quad (5-236)$$

But  $n_{\min}$  is the minimum power on a closed trajectory (power at prompt critical) and  $n_0$  is the initial power (power at delayed critical). Note that eqs. (5-203) and (5-236) agree except for the factor  $\sqrt{(\pi/2)}$ , lending confirmation to the validity of the approximations used.

The approximate trajectory, eq. (5-232), may be extended to its minimum (second crossing of the ZSI). For small  $\delta$ , the minimum occurs near  $u = 0$ , yielding a transcendental equation for  $v_{\min}$ . Transforming back to physical variables and using eq. (5-209) yield a transcendental equation for peak power; for fast excursions this new equation reduces to eq. (5-193).

We conclude this section with a brief discussion of excursions for which  $\delta$  is not small (e.g., large  $n_0$  or small  $\gamma$ ). If  $\epsilon$  is a small parameter but  $\delta$  is not, then by eq. (5-222) the trajectory crosses the  $v$ -axis of fig. 5-22 with an extremely large negative slope. In such a case  $u_{\max}$  will be small compared to  $\beta\delta/(1 + \delta)$ . In fact, for  $u_{\max}$  near zero, eq. (5-212) yields

$$\rho_{\max} \cong \frac{\beta}{1 + \delta}. \quad (5-237)$$

Canosa has shown (1968a) that this is an excellent approximation for a very wide range of subprompt-critical excursions.

Approximate time-domain solutions for both slow and fast ramp excursions, obtained by matching singular-perturbation expansions, are given in the paper by Canosa (1968a).

### 5-9. Complex Shutdown Mechanisms: Thermal Reactors

The linear, prompt-feedback model for reactor shutdown given by eqs. (5-78) and (5-79) must be modified considerably for certain reactor types. Several examples have been selected as detailed illustrations: the SPERT-I reactor, either with highly enriched metal fuel or with low-enrichment oxide fuel; a modification developed for the TRIGA reactor using a temperature-dependent heat capacity; and the homogeneous solution reactor KEWB. Fast reactors are considered in the section that follows.

As discussed in sec. 5-2, the major shutdown mechanism in SPERT-I with highly enriched fuel is steam formation in the water moderator. Steam production is delayed because the fission heat must be transferred from the fuel to the moderator and the moderator temperature must be raised to the boiling point. Typical experimental power traces are quite asymmetrical, showing a rapid drop after peak power (Forbes 1958; Haire 1961; Nyer 1964; Nyer and Forbes 1958; Schroeder et al. 1957).

A semiempirical model was devised by Forbes (1958) in an attempt to correlate the large amount of data on fast power excursions. This model is a modification of the Nordheim-Fuchs approximation in which the reactivity feedback is both delayed and nonlinear.

Assume that eq. (5-77) describes the neutron dynamics, as in sec. 5-5:

$$\frac{dn}{dt} = \frac{\rho - \beta}{\ell} n. \quad (5-238)$$

In the simple Nordheim-Fuchs model of sec. 5-5, the reactivity feedback is proportional to energy, so that eq. (5-238) might be written

$$\frac{1}{n} \frac{dn}{dt} = \omega - bE, \quad (5-239)$$

where  $\omega$  is the initial inverse period corresponding to the initial reactivity  $\rho_0$ , as given by eq. (5-85), and  $b$  is the energy coefficient of reactivity divided by the neutron generation time. If  $n(t)$  represents power,  $n = dE/dt$ .

One way to modify eq. (5-239) to simulate the observed asymmetry of the power bursts is to introduce a nonlinear feedback, proportional to  $E^r$ , where  $r > 1$ . This yields

$$\frac{1}{n} \frac{dn}{dt} = \omega - bE^r, \quad (5-240)$$

where the interpretation of  $b$  is to be modified accordingly. An addi-

tional modification is the introduction of a feedback delay time  $\tau$  such that  $E = 0$  for  $t < \tau$ , with  $E(t)$  replaced by  $E(t - \tau)$  for  $t > \tau$ ; i.e.,

$$\frac{1}{n} \frac{dn}{dt} = \begin{cases} \omega, & (t < \tau); \\ \omega - bE^r(t - \tau), & (t > \tau). \end{cases} \quad (5-241)$$

Two special cases may be integrated analytically. We consider first the special case represented by eq. (5-240), known as the "zero-delay" model. Using  $n = dE/dt$ , we integrate eq. (5-240) as

$$n = \omega E - \frac{b}{r + 1} E^{r+1}, \quad (5-242)$$

where the initial power  $n_0$  is neglected as in sec. 5-5. At peak power ( $n = A$ ) the energy  $\hat{E}$  is found from eq. (5-240) with  $dn/dt = 0$ :

$$\hat{E} = (\omega/b)^{1/r}. \quad (5-243)$$

Using this in eq. (5-242) yields

$$\hat{n} = \frac{r\omega^{1+1/r}}{(r + 1)b^{1/r}}. \quad (5-244)$$

Energy as a function of time is obtained by using  $n = dE/dt$  in eq. (5-242). We integrate from the time of peak power ( $t = t_m$ ) with  $E(t_m) = \hat{E}$  as given by eq. (5-243). The result is

$$E(t) = [(r + 1)\omega/b]^{1/r} [1 + re^{-r\omega(t - t_m)}]^{-1/r}. \quad (5-245)$$

Differentiating and using eq. (5-244), we have

$$n(t)/\hat{n} = \left[ \frac{1 + r}{1 + re^{-r\omega(t - t_m)}} \right]^{1+1/r} e^{-r\omega(t - t_m)}. \quad (5-246)$$

It is easy to show that this function exhibits the desired type of asymmetry. During the rising portion, where  $t \ll t_m$ , eq. (5-246) reduces to

$$n/\hat{n} \cong (1 + 1/r)^{1+1/r} e^{\omega(t - t_m)}$$

with a rise time  $1/\omega$ . After the peak, where  $t \gg t_m$ , we have

$$n/\hat{n} \cong (1 + r)^{1+1/r} e^{-r\omega(t - t_m)}$$

with a decay time  $1/r\omega$ . The decay time is smaller than the rise time if  $r > 1$ .

Burst shapes calculated from eq. (5-246) using various values of  $r$  are compared with a typical SPERT-I experiment in fig. 5-24, where  $\phi$  is power relative to peak and "time" is  $\omega(t - t_m)$ ; i.e., relative to peak, measured in units of the initial period  $T = 1/\omega = 9.5$  millisec. The correspondence is not quantitatively good.

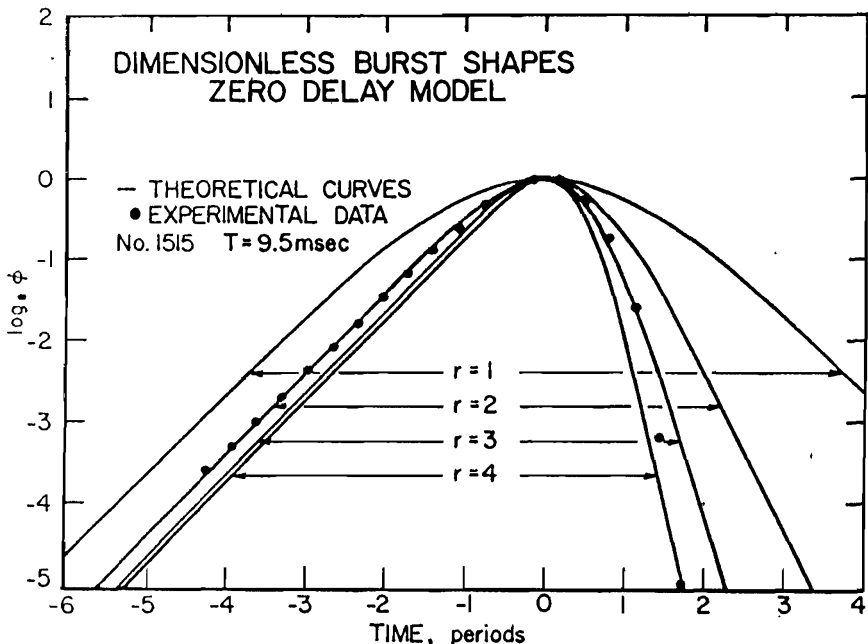


Fig. 5-24. Burst shapes for the zero-delay model compared with SPERT-I data for highly enriched metal fuel (Forbes 1958).

An additional difficulty in using the zero-delay model for this reactor type is found by comparing eq. (5-244) with data for  $\hat{n}$  vs.  $\omega$ . In sec. 5-5, in connection with fig. 5-3, it was noted that  $\hat{n}$  varies as  $\omega^{1.7}$  for this reactor core, so that eq. (5-244) would predict  $r = 1.4$ . From fig. 5-24, the predicted burst would be much too wide.

Better results are obtained when a delay time is used in conjunction with nonlinear feedback. In particular, consider the second special case of eq. (5-241) that may be integrated analytically. This is the "long-delay" model in which the delay time is assumed to be larger than the burst width. The energy feedback during the burst is then derived explicitly from the exponentially rising power.

While the power is rising exponentially, with  $n = n_0$  at  $t = 0$ , the energy is

$$E = \frac{n_0}{\omega} (e^{\omega t} - 1) \cong \frac{n_0}{\omega} e^{\omega t}.$$

Eq. (5-241) for  $t > \tau$  becomes

$$\frac{1}{n} \frac{dn}{dt} = \omega - b(n_0/\omega)^r e^{r\omega(t-\tau)}. \quad (5-247)$$

This may be integrated approximately as

$$\log \frac{n}{n_0} = \omega t - (bn_0^r/r\omega^{r+1}) e^{r\omega(t-\tau)} \quad (5-248)$$

At peak power ( $t = t_m$ ) eq. (5-247) yields

$$bn_0^r/\omega^{r+1} = e^{r\omega(t-t_m)}, \quad (5-249)$$

and eq. (5-248) becomes

$$\log \frac{n}{n_0} = \omega t - \frac{1}{r} e^{r\omega(t-t_m)}. \quad (5-250)$$

At peak power

$$\log \frac{n}{n_0} = \omega t_m - \frac{1}{r}. \quad (5-251)$$

Eliminating  $n_0$ , we may write the burst shape as

$$\log \frac{n}{n_0} = \omega(t - t_m) + \frac{1}{r} [1 - e^{r\omega(t-t_m)}]. \quad (5-252)$$

Further, we may eliminate  $n_0$  between eqs. (5-249) and (5-251) to obtain

$$\hat{n} = \frac{\omega^{1+1/r}}{b^{1/r}} e^{\omega t - 1/r}. \quad (5-253)$$

This may be compared with eq. (5-244) for the zero-delay model.

Burst shapes calculated from eq. (5-252) using various values of  $r$  are shown in fig. 5-25 together with the experimental points for the 9.5-millisec burst shown in fig. 5-24. The correspondence is fairly good at  $r = 1.5$ . Another example is shown in fig. 5-26, where raw data from a linear recording of a 7.4-millisec burst corresponds well with a calculated curve for  $r = 2$ .

Examination of a large volume of data for the SPERT-IA core, using both the burst shapes and the compensated reactivity curves, leads to the conclusion that the best correlation occurs for  $r = 2$  (Forbes 1958). This may then be used in eq. (5-253) to permit a comparison with data for  $\hat{n}$  vs.  $\omega$  and an empirical determination of  $\tau$ . The result is that  $\omega t$  is nearly constant over a range of periods (2.2 at 20 millisec to 2.6 at 5 millisec). The power-time curves confirm that these are indeed sufficient times for the long-delay model to be realistic. Additional confirmation comes from compensated reactivity curves (Forbes 1958).

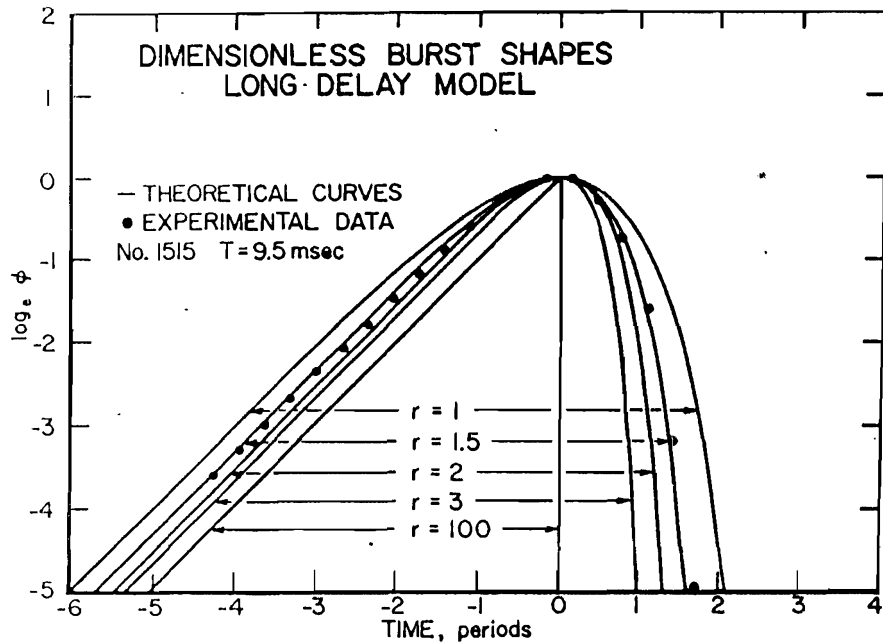


Fig. 5-25. Burst shapes for the long-delay model compared with SPERT-I data for highly enriched metal fuel (Forbes 1958).

The exponent  $r$  and the delay time  $\tau$  are most certainly not to be regarded as basic physical parameters. Rather, they are convenient devices for correlating data and for predicting over a limited range. The analysis has been presented here as an ingenious example of successful "model-building" for a highly complex system.

Other empirical models have been proposed for correlating power excursions in this type of reactor (e.g., Forbes 1959; Garner 1962). A review is given by Nyer (1964). More recently, a moderately successful model was derived from more basic considerations including details of boiling and nonboiling heat transfer (Turner 1968). A deeper treatment is beyond the scope of this book.

The behaviour of SPERT-I with low-enrichment uranium-oxide fuel is quite different, the dominant shutdown mechanism being the Doppler effect (see sec. 5-2). Data for peak power vs.  $\omega$  in fig. 5-3 have been fitted by using a slope of 2.35 on a logarithmic graph for  $\omega > 160 \text{ sec}^{-1}$  (Spano 1963). More recently, an analytical model using a square-root temperature dependence for the Doppler effect has been developed and found in good agreement with experiments (Spano 1964).

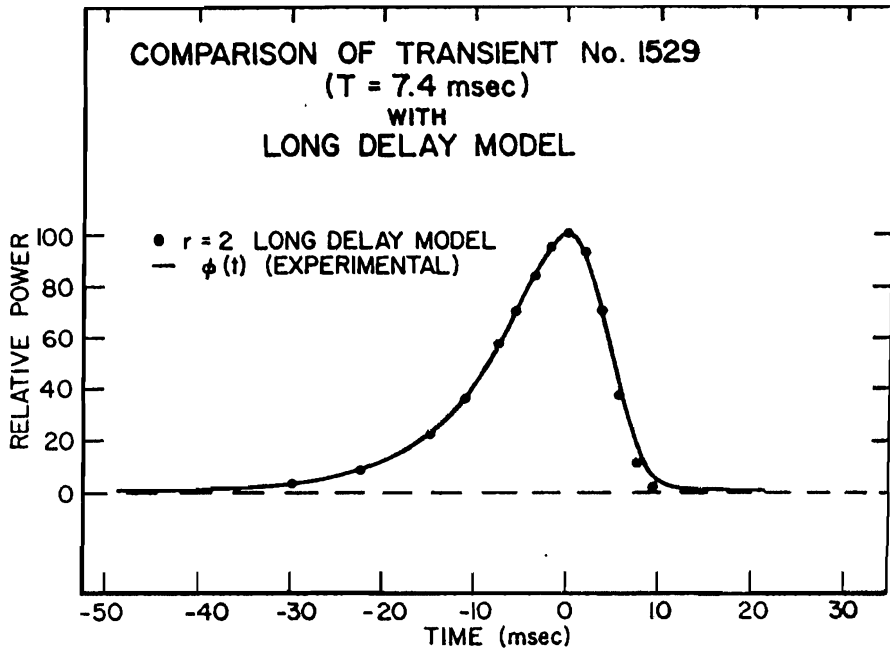


Fig. 5-26. Burst shape for the long-delay model with  $r = 2$  compared with SPERT-I data for highly enriched metal fuel (Forbes 1958).

We use eqs. (5-77) and (5-85), together with

$$\rho = \rho_0 - \rho_f = \rho_0 - \beta b \{ \sqrt{[1 + AE(t)]} - 1 \}, \quad (5-254)$$

where  $E(t)$  is the energy and  $b$  and  $A$  are given in terms of resonance parameters by Spano (1964). We have

$$\frac{1}{n} \frac{dn}{dt} = \omega + \frac{\beta b}{\ell} [1 - \sqrt{(1 + AE)}]. \quad (5-255)$$

Using  $n = dE/dt$  and  $B = \beta b/\ell$ , we have a second-order differential equation for  $E$ :

$$\frac{d^2 E}{dt^2} = [\omega + B - B\sqrt{(1 + AE)}] \frac{dE}{dt}. \quad (5-256)$$

Since we neglect the initial power, as in sec. 5-5, the initial conditions are  $E = 0$  and  $dE/dt = 0$ .

With the transformation

$$y = 1 + AE, \quad x = \omega/B, \quad (5-257)$$

we have

$$\frac{d^2y}{dt^2} = [(1+x)B - B\sqrt{y}] \frac{dy}{dt}. \quad (5-258)$$

This may be integrated with initial conditions  $y = 1$  and  $dy/dt = 0$ :

$$\frac{dy}{dt} = (1+x)By - \frac{2}{3}By^{\frac{1}{2}} - \frac{1}{3}B(1+3x). \quad (5-259)$$

The second integration is facilitated by the transformation

$$w = 1 + 2/\sqrt{y} = 1 + 2/\sqrt{1 + AE}. \quad (5-260)$$

Substituting and rearranging, we find

$$\frac{1}{B} \frac{dw}{dt} = \frac{1+3x}{24} (w-3)(w+M)(w-M), \quad (5-261)$$

where

$$M^2 = \frac{9+3x}{1+3x}. \quad (5-262)$$

Using partial fractions, we may rewrite eq. (5-261) as

$$\begin{aligned} \frac{dw}{2M(M+3)(w+M)} &= \frac{dw}{2M(3-M)(w-M)} \\ &- \frac{dw}{(3+M)(3-M)(3-w)} = \frac{1+3x}{24} B dt. \end{aligned} \quad (5-263)$$

Some factors have been rearranged for convenience; note that  $w$  decreases from three, and  $M$  is between one and three.

Integrating eq. (5-263) from  $t_m$  to  $t$ , we obtain

$$(w+M)^{3-M}(3-w)^{2M}(w-M)^{-3-M} = Ke^{2Mw(t-t_m)}, \quad (5-264)$$

where  $K$  may be evaluated in terms of  $w(t_m)$ . If  $t_m$  is chosen as the time of peak power where  $d^2E/dt^2 = 0$ , then, by eq. (5-258),  $\sqrt{y} = 1 + x$ , and by eq. (5-260),

$$w(t_m) = \frac{3+x}{1+x}. \quad (5-265)$$

The initial value in eq. (5-264) is

$$\lim_{t \rightarrow -\infty} w = 3,$$

while the final value is

$$\lim_{t \rightarrow \infty} w = M. \quad (5-266)$$

The initial state must be perturbed to start the solution along a physically meaningful trajectory. This is realized as a small positive  $E$  in eq. (5-260), which corresponds to a value of  $w$  slightly less than three. The derivative in eq. (5-261) is therefore negative, and  $w$  subsequently decreases.

By eq. (5-260), the energy at any time may be found from

$$AE = \frac{4}{(w - 1)^2} - 1. \quad (5-267)$$

From eq. (5-265), the energy at the time of peak power is

$$AE = 2x + x^2, \quad (5-268)$$

while from eq. (5-266) the total energy is

$$AE = \frac{4}{(M - 1)^2} - 1. \quad (5-269)$$

To find  $n(t)$ , form  $dw/dt$  in terms of  $n = dE/dt$  from eq. (5-260). This yields

$$\frac{1}{A} \frac{dw}{dt} = -\frac{1}{8}(w - 1)^3 n(t).$$

Combining this with eq. (5-261) yields

$$\frac{A}{B} n(t) = \frac{(1 + 3x)(3 - w)(w + M)(w - M)}{3(w - 1)^3}. \quad (5-270)$$

Using eqs. (5-262) and (5-265), we may ultimately obtain the peak power

$$\frac{A}{B} n = x^2 + \frac{1}{3}x^3. \quad (5-271)$$

Noting that  $x = \omega/B$ , we have the prediction that  $n$  varies as  $\omega^2$  for the smaller fast excursions, with a gradual shift toward  $\omega^3$ -dependence as  $\omega$  increases. This is consistent with fig. 5-3, where the slope of the logarithmic curve increases from two as  $\omega$  increases from about fifty sec<sup>-1</sup>. Later data shows confirmation of eq. (5-271) up to  $\omega \cong 450$  sec<sup>-1</sup> (Spano 1964).

Another successful modification of the simple fast-excursion model was derived and applied to the TRIGA reactor by Scalettar (1963).<sup>7</sup> Eqs. (5-77) and (5-78) of the Nordheim-Fuchs model are used, but eq.

7. See also: Wolfe (1964); Kazi, Tomonto, and Cherry (1966).

(5-79) is replaced by

$$C \frac{dT}{dt} = n, \quad (5-272)$$

where the heat capacity  $C$  is a linear function of temperature:

$$C = C_0 + \gamma T. \quad (5-273)$$

The resulting system of equations has a first integral,

$$n = \frac{(\rho_0 - \beta)C_0}{\ell} T - \frac{\alpha C_0}{2\ell} T^2 + \frac{\gamma(\rho_0 - \beta)}{2\ell} T^2 - \frac{\gamma\alpha}{3\ell} T^3, \quad (5-274)$$

which reduces to the Nordheim-Fuchs result if  $\gamma \rightarrow 0$ ; this is easily verified by using eqs. (5-78) and (5-83) with  $C_0 = 1/K$ .

As before, we have neglected the initial power. The temperature in the fast burst ranges from zero to

$$T = \frac{\rho_0 - \beta}{\alpha} \left\{ -\frac{3}{4}(\sigma - 1) + \frac{3}{4}\sqrt{[(\sigma - 1)^2 + \frac{16}{3}\sigma]} \right\}, \quad (5-275)$$

where

$$\sigma = \frac{\alpha C_0}{\gamma(\rho_0 - \beta)}.$$

By expanding the radical for small  $\gamma$  (large  $\sigma$ ), one finds

$$T = \frac{2(\rho_0 - \beta)}{\alpha} \left( 1 - \frac{1}{3\sigma} + \dots \right), \quad (5-276)$$

so that eq. (5-276) reduces to eq. (5-89) as  $\gamma \rightarrow 0$ . The other extreme (large  $\gamma$ , small  $\sigma$ ) would be

$$T \rightarrow \frac{3(\rho_0 - \beta)}{2\alpha}. \quad (5-277)$$

The use of a constant heat capacity with the simple Nordheim-Fuchs model thus leads to an overestimate of the final temperature, the extreme case exhibiting a ratio of four to three.

By eqs. (5-77) and (5-78), the power peaks when  $\rho = \beta$  or  $T = (\rho_0 - \beta)\alpha$ . Eq. (5-274) yields

$$n = \frac{(\rho_0 - \beta)^2 C_0}{2\alpha\ell} \frac{1 + 3\sigma}{3\sigma}. \quad (5-278)$$

For large  $\sigma$ , this reduces to eq. (5-84). For a meaningful comparison of the other extreme (small  $\sigma$ ), we may compare eq. (5-278) with the simple Nordheim-Fuchs model using a temperature-averaged heat

capacity. The initial heat capacity is  $C_0$ . The final heat capacity is found by substituting eq. (5-89) into eq. (5-273). The average heat capacity is therefore

$$\bar{C} = C_0 + \gamma(\rho_0 - \beta)/\alpha = C_0(1 + 1/\sigma).$$

Using this for  $1/K$  in eq. (5-84) yields

$$n(NF) = \frac{(\rho_0 - \beta)^2 C_0}{2\alpha\ell} \frac{1 + \sigma}{\sigma}. \quad (5-279)$$

Eqs. (5-278) and (5-279) are identical for  $\sigma \gg 1$ , but for the other extreme ( $\sigma \rightarrow 0$ ) eq. (5-279) would overestimate the peak power by a factor of three. The peak power is therefore somewhat sensitive to variations in heat capacity.

A second integral giving  $T(t)$  implicitly may be obtained from eqs. (5-272) through (5-274). Alternatively, one could compute  $E$  from

$$E = \int C dT$$

and use the result in eq. (5-274) together with  $n = dE/dt$ . This example will not be carried further here.

To complete this section on thermal-reactor excursions, we consider briefly the homogeneous-solution reactor KEWB (Kinetic Experiment Water Boiler), which consisted of highly enriched uranium salt solution (ordinary water) partially filling a one-foot diameter stainless-steel vessel placed inside a graphite reflector (Dunensfeld 1962; Dunensfeld and Stitt 1963; Marable 1961 and 1963; Remley et al. 1958; Silberberg 1965).

Correlation of fast-excursion data was moderately successful when a prompt, nonlinear shutdown model was used (Dunensfeld and Gamble 1959; Hetrick and Gamble 1958). Eq. (5-77) is used together with

$$\rho = \rho_0 - \alpha T - \phi V, \quad (5-280)$$

$$\frac{dT}{dt} = Kn, \quad (5-281)$$

$$\frac{dV}{dt} = vnE, \quad (5-282)$$

where  $\phi V$  is the radiolytic-gas feedback reactivity ( $\phi$  = void-volume coefficient;  $V$  = void volume),  $v$  is a constant, and  $n = dE/dt$ . Eq. (5-281) represents the prompt temperature feedback produced in fission fragments in the solution. Eq. (5-282) is a crude model for radiolytic decomposition of water followed by nucleation of gas

bubbles (dissolved gas concentration proportional to energy; nucleation rate proportional to power). Integration yields

$$T = KE$$

and

$$V = \frac{1}{2}\phi v E^2.$$

Substituting these into eq. (5-280) gives the reactivity

$$\rho = \rho_0 - \alpha KE - \frac{1}{2}\phi v E^2. \quad (5-283)$$

Using eq. (5-77), we find the first integral to be

$$n = \frac{1}{\ell} [(\rho_0 - \beta)E - \frac{1}{2}\alpha KE^2 - \frac{1}{6}\phi v E^3]. \quad (5-284)$$

As before, the power peaks at  $\rho = \beta$ . Eq. (5-283) yields a quadratic in  $E$  whose positive root is

$$\hat{E} = \frac{\alpha K}{\phi v} \left\{ -1 + \left[ 1 + 2\phi v(\rho_0 - \beta)/\alpha^2 K^2 \right]^{\frac{1}{2}} \right\}. \quad (5-285)$$

For large reactivity steps, this becomes

$$\hat{E} \approx \left[ \frac{2(\rho_0 - \beta)}{\phi v} \right]^{\frac{1}{2}} = \left[ \frac{2\ell\omega}{\phi v} \right]^{\frac{1}{2}}, \quad (5-286)$$

where  $\omega$  is the initial reciprocal period of eq. (5-85). The peak power is obtained by substituting eqs. (5-283) and (5-285) into eq. (5-284):

$$\dot{n} = \frac{2}{3}\omega\hat{E} - \frac{\alpha K}{6\ell} \hat{E}^2. \quad (5-287)$$

For large  $\omega$ , eqs. (5-286) and (5-287) give

$$\dot{n} \approx \frac{2}{3}(2\ell/\phi v)^{\frac{1}{2}}\omega^{\frac{1}{2}}. \quad (5-288)$$

Experimental data for this reactor are consistent with the exponent  $\frac{1}{2}$  for large  $\omega$  (Dunensfeld 1962); see also fig. 5-3. By using exact solutions of the complete equations, the peak-power data were fitted by a single empirical constant  $v$  over the range from  $\omega = 100 \text{ sec}^{-1}$  to  $500 \text{ sec}^{-1}$  (Herrick and Gamble 1958). Detailed power-time curves were reproduced with only moderate success.

As in other model-building exercises, the parameter  $v$  in eq. (5-282) should not be endowed with any basic physical meaning. Further, this model is unable to predict transient pressures. More recently, the transient pressure data were successfully correlated with the power data using an energy-threshold concept (Dunensfeld 1961; Dunensfeld and Stitt 1963; Marable 1963). Instead of using  $\phi V$ , with  $V$  given by

eq. (5-282), the void reactivity is represented as

$$\rho_v = \begin{cases} 0, & E < E_0 \\ k_1 \int_0^t (t - t') p(t') dt', & E \geq E_0 \end{cases}$$

where  $E_0$  is the threshold energy for the appearance of inertial pressure,  $k_1$  is a constant, and  $p(t)$  is the pressure as measured at the bottom of the core. This model assumes that the acceleration in the fluid is proportional to the transient pressure and that the reactivity feedback is proportional to the surface displacement. The observed threshold energy  $E_0$  is about 0.9 megajoule for a wide range of excursions. Reactor power data were successfully reproduced by computations, using measured transient pressures and a fixed value of  $k_1$  in this feedback model, for  $\omega$  ranging from 10 to 1,000 sec<sup>-1</sup> (Dunensfeld 1961).

Excursions in this type of system would be much more severe if the container were initially completely filled with solution. The shutdown reactivity would be greatly reduced by the container, and it is conceivable that the elastic limit (or even the ultimate strength) of the container might be exceeded. Excursions in constrained solutions are discussed in a report by Hansen (1952).

This completes the discussion of special excursion calculations for thermal reactors. For more details, and for discussions of other reactor types, see the compilation edited by Thompson and Beckerley (1964).

### 5-10. Complex Shutdown Mechanisms: Fast Reactors

The calculation of large excursions in fast reactors is complicated by the possibility of extremely high power densities and very short characteristic times. This possibility is seen from eqs. (5-84) and (5-90). Other things being equal (if that were possible), a given superprompt-critical reactivity would result in a certain energy release, independent of the neutron generation time, but the peak power in a fast reactor would be orders of magnitude larger.

In reality, the situation is much more complex. Once the reactivity in a fast system exceeds prompt critical by a very small amount, the characteristic time becomes extremely small. The sharp power increase may produce extreme internal shocks resulting in violent disassembly. The problem is further complicated by the possibility of internal zones of rapid melting and vaporization of metal, and the behaviour of reactor materials under such extreme conditions is very difficult to predict.

One of these phenomena is beautifully illustrated in the prototype fast-burst reactor GODIVA (Wimett 1956; Wimett et al. 1960). As seen in fig. 5-3, the peak power is proportional to  $\omega^2$  over a wide range. Near  $\omega = 5 \times 10^4 \text{ sec}^{-1}$  (reactivity about five cents above prompt critical;  $\beta/\gamma = 1.1 \times 10^6 \text{ sec}^{-1}$ ) the slope of the peak-power curve begins to increase sharply.

This reactor is composed of highly enriched solid uranium metal. The shutdown mechanism is predominantly thermal expansion, which is prompt and approximately linear, so that the simple Nordheim-Fuchs model is a good description over a wide range. However, for the faster bursts, an inertial time lag appears between the fission heating and the metal expansion. This results in enhanced power excursions accompanied by transient inertial stresses.

The use of a simple hydrodynamic model led to the estimate that this mechanical inertia increases the peak power and total energy by a factor of  $1 + \tau^2 \omega^2$ , where  $\tau$  is a characteristic time for mechanical vibration (Wimett et al. 1960). For GODIVA I, a value of  $\tau \approx 10^{-5} \text{ sec}$  was derived from the excursion data. A more recent study of delayed feedbacks in fast reactors was made by Köhler (1969).

More complex calculations have been performed using coupled sets of equations representing neutronic, hydrodynamic, and thermodynamic phenomena (Hansen 1952; Okrent et al. 1959; Lazarus, Stratton, and Hughes 1968). Detailed studies of thermal shocks have been published (Austin 1964; Burgreen 1967; Reuscher 1968). Studies of the combined effects of elastic waves and Doppler coefficient have been made by Randles (1966) and Vaughan (1969). Reduction of thermal shocks and attainment of larger bursts without damage have been realized in more recent designs. A comprehensive review of fast-burst reactors is contained in the proceedings edited by Long and O'Brien (1969).

The situation in a fast-spectrum power reactor is extremely complex. The shutdown mechanism in a large excursion is the net effect of many interdependent phenomena: Doppler effect, fuel and structure expansion, coolant vaporization, fuel melting and vaporization, and the propagation of mechanical shock waves (Bethe and Tait 1956; IAEA 1961; Jankus 1962; McCarthy et al. 1958; McCarthy and Okrent 1964; Nicholson 1964; Stratton, Colvin, and Lazarus 1958). Here we present only a brief outline of one type of accident calculation, selecting from the above references a few features of the analysis of a hypothetical fast-reactor meltdown accident.

It is postulated that a fast reactor accidentally loses its coolant as a result of a pumping failure or a power excursion. Some fuel may be melted by fission heating or delayed fission-product heating. An

accident involving partial melting of the core in the experimental fast reactor EBR-I occurred (without injury to personnel) in 1955 (Brittan 1958; Thompson 1964). Such accidents in existing and future systems are extremely unlikely because of improved design ensuring both intrinsic safety and the reliable operation of safety devices.

Nevertheless, because of the potential hazard, one unlikely consequence of fuel melting has been studied in detail. It is postulated that a loss of coolant is followed by a structural collapse in which a mass of molten fuel assumes a supercritical configuration. One estimate of the possible reactivity-addition rate, assuming gravitational collapse of a melting core, is forty to fifty dollars per sec (Bethe and Tait 1956). It is assumed that this reactivity increase continues unchecked until the reactivity is somewhere above prompt critical. Fission heating in this new excursion will cause expansion, but it is assumed that no reactivity feedback appears until the metal has expanded to fill the internal voids. When this threshold is reached, there will be a sudden pressure surge followed by rapid disassembly. It is further assumed that the disassembly is so rapid that the net reactivity exceeds the threshold value by only a negligible amount.

The calculation proceeds by estimation of the reactivity-addition rate and the threshold energy. One estimate of threshold energy is about one megajoule per kilogram (Bethe and Tait 1956). The reactivity at this energy is then calculated from the ramp-response equations without feedback, and this is taken to be the maximum reactivity. Finally, the excess energy above the threshold is calculated as the energy required to disassemble the mass to the point where the reactivity is reduced from its maximum (threshold) value to  $\beta$  (prompt critical). The total energy in the excursion is then the sum of the threshold energy and the disassembly energy.

To estimate the maximum reactivity, use eq. (5-77) with

$$\rho = \beta + \gamma t, \quad (5-289)$$

where the system is taken to be prompt critical at  $t = 0$ . Eq. (5-77) becomes

$$\frac{dn}{dt} = \frac{\gamma tn}{\ell}.$$

This may be integrated as

$$n = n(0) \exp(\gamma t^2/2\ell). \quad (5-290)$$

The energy is

$$E = \int_0^t n(\tau) d\tau = n(0) \int_0^t \exp(\gamma \tau^2/2\ell) d\tau. \quad (5-291)$$

### 2.2.4 Reactivity Feedback and Reactor Excursions

The use of the asymptotic form for the error function of imaginary argument (Abramowitz and Stegun 1964) enables us to write eq. (5-291), assuming  $\gamma t^2/2\ell \gg 1$ , as

$$E \approx \frac{\ell n(0)}{\gamma t} \exp(\gamma t^2/2\ell). \quad (5-292)$$

This equation may also be derived by changing the variable of integration from  $\tau$  to  $z = t - \tau$ , dropping  $z^2$  in the exponent, and integrating. Given  $E = E_0$ , eq. (5-292) is a transcendental equation to be solved for the corresponding time  $t_0$ .

An iterative solution is generated by writing

$$\frac{\gamma t_0^2}{2\ell} \approx \log \frac{\gamma E_0 t_0}{\ell n(0)}.$$

This is conveniently rewritten as

$$\frac{\gamma t_0^2}{\ell} \approx \log \left[ \frac{\gamma E_0 t_0}{\ell n(0)} \right]^2 = \log \xi + \log \frac{\gamma t_0^2}{\ell}, \quad (5-293)$$

where

$$\xi = \frac{\gamma}{\ell} \left[ \frac{E_0}{n(0)} \right]^2. \quad (5-294)$$

A first approximation is

$$t_0 \approx [(\ell/\gamma) \log \xi]^{\frac{1}{2}}, \quad (5-295)$$

while a second approximation may be obtained by using eq. (5-295) in the right-hand side of eq. (5-293). Using this result together with eq. (5-289) gives the prompt reactivity at the threshold energy  $E_0$ :

$$\delta\rho = \rho_{\max} - \beta = \gamma t_0 \approx [\gamma \ell (\log \xi + \log \log \xi)]^{\frac{1}{2}}. \quad (5-296)$$

This is the amount of reactivity to be compensated by disassembly.

The excursion will be more severe for small  $n(0)$ , because the reactivity will have more time to increase prior to threshold. As a sample, choose  $\gamma/\beta = 50$  dollars/sec,  $\ell/\beta = 10^{-6}$  sec,  $E_0 = 10^6$  joule/kgm, and  $n(0) = 1$  watt/kgm. Then  $\log \xi = 45.3$ ,  $t_0 = 1$  millisecond, and  $\delta\rho/\beta = 5$  cents. If  $n(0)$  were  $10^{-3}$ ,  $\log \xi$  would be 59.1, yielding  $t_0 = 1.13$  millisecond; if  $n(0)$  were  $10^3$ ,  $\log \xi$  would be 31.5, giving  $t_0 = 0.84$  millisecond. From the extremes of this range, it is seen that a variation of  $10^6$  in  $n(0)$  corresponds to a 35-percent variation in  $t_0$  and  $\delta\rho$ . Since  $\log \xi$  is so insensitive in this range, rough estimates may be used for both  $E_0$  and  $n(0)$ . Further, by eq. (5-296),  $\delta\rho$  may be taken as nearly proportional to the square root of  $\gamma\ell$ .

Disassembly begins at time  $t_0$  when the reactivity is given by eq. (5-296). The excess energy  $E - E_0$  produces pressure, resulting in outward displacement of material which reduces the reactivity. Following Nicholson (1964), assume that the reactivity feedback is

$$\delta\rho = \int \mathbf{u} \cdot \nabla W dV \quad (5-297)$$

where  $\mathbf{u}(r, t)$  is the displacement of a volume element  $dV$  initially at the point  $\mathbf{r}$ ,  $W(\mathbf{r})$  is the reactivity weighting function (reactivity decrease caused by removal of a unit volume of homogenized core material at  $\mathbf{r}$ ), and the integral extends over the core volume; in eq. (5-297),  $\mathbf{u} \cdot \nabla W$  is the reactivity change when a unit volume is displaced from  $\mathbf{r}$  to  $\mathbf{r} + \mathbf{u}$ . For spherical symmetry,  $dV = 4\pi r^2 dr$  and

$$\delta\rho = 4\pi \int u \frac{dW}{dr} r^2 dr, \quad (5-298)$$

where the integral extends over the radius of the core.

For the equation of motion, assume

$$m \frac{\partial^2 u}{\partial t^2} = \frac{\partial p}{\partial r}, \quad (5-299)$$

where  $m$  is the mass of a unit volume and  $p$  is the pressure. From eq. (5-298),

$$\frac{d^2 p}{dt^2} = -\frac{4\pi}{m} \int \frac{\partial p}{\partial r} \frac{dW}{dr} r^2 dr. \quad (5-300)$$

To obtain the form used by McCarthy and Okrent (1964), assume that  $W$  is parabolic

$$W(r) = 1 - r^2/a^2. \quad (5-301)$$

Substituting and integrating by parts yields

$$\frac{d^2 p}{dt^2} = -C_1 \int pr^2 dr, \quad (5-302)$$

where  $C_1$  is a constant.

It is difficult to justify eq. (5-302) by a more general first-order perturbation theory in which absorption effects are weighted by the flux squared and changes in the diffusion coefficient are weighted by the flux gradient squared (see any standard text on reactor theory). Some authors have used a formula in which the flux gradient squared is a weighting factor for the function  $u/r$  in a volume integral (Bethe and Tait 1956; McCarthy et al. 1958; McCarthy and Okrent 1964).

The derivations are no more convincing than the one we have used here, though the same result is obtained when a parabolic flux distribution is assumed.

To relate reactivity feedback and energy, the pressure in eq. (5-302) must be expressed in terms of the energy  $E - E_0$  produced after the threshold is reached. We assume a very simple equation of state (Bethe and Tait 1956; McCarthy et al. 1958; McCarthy and Okrent 1964),

$$p = (\gamma - 1)m(E - E_0), \quad (5-303)$$

where  $\gamma$  is the ratio of specific heats and  $m$  is the density. More complex equations of state are discussed by Hansen (1952), Nicholson (1964), and Stratton, Colvin and Lazarus (1958). Next, assume that  $E$  may be written as

$$E(r, t) = N(r)Q(t),$$

where

$$N(r) = 1 - qr^2/b^2, \quad 0 < q < 1, \quad (5-304)$$

inside the core ( $r < b$ ), and  $N = 0$  outside ( $r > b$ ).

Pressure first appears at the center when  $Q = E_0 = Q^*$ . We have

$$p = (\gamma - 1)m(Q - Q^* - Qqr^2/b^2)$$

for  $Q > Q^*$  and  $p = 0$  for  $Q < Q^*$ . Pressure appears at the surface  $r = b$  when  $Q = Q^*/(1 - q)$ .

We have two cases. For  $Q^* < Q < Q^*/(1 - q)$ , the integral in eq. (5-302) extends from 0 to  $b_1$  where

$$b_1 = bq^{-\frac{1}{2}}(1 - Q^*/Q)^{\frac{1}{2}}.$$

The integral yields

$$\frac{d^2\rho}{dt^2} = -C_2Q(1 - Q^*/Q)^{\frac{1}{2}}, \quad Q^* < Q < Q^*/(1 - q), \quad (5-305)$$

where  $C_2$  is another constant. The second case applies after the threshold is reached at  $r = b$ . For  $Q > Q^*/(1 - q)$ , the integral extends from 0 to  $b$ . We find

$$\frac{d^2\rho}{dt^2} = -C_3(1 - 0.6q)Q - Q^*, \quad Q > Q^*/(1 - q) \quad (5-306)$$

where  $C_3$  is a constant.

Assuming  $n$  is proportional to  $dQ/dt$ , eqs. (5-305) and (5-306) represent the reactivity feedback to be used in conjunction with eq. (5-77). Solution by numerical methods is straightforward. However, approximate values for the energy may be obtained analytically by assuming,

as suggested earlier, that the reactivity exceeds the threshold value by only a negligible amount. The net reactivity during disassembly is then calculated from eqs. (5-305) and (5-306) using an exponential energy rise; the reciprocal period is  $\delta\rho/\ell$  with  $\delta\rho$  given by eq. (5-296). The excess energy above threshold is then taken to be the energy required to reduce the reactivity from  $\rho_{\max}$  to  $\beta$ . This overestimates the energy during the power rise, but the error is more or less offset by neglecting the energy produced after peak power.

Consider first a limiting case in which the power rise is terminated before the threshold is reached at  $r = b$ , so that eq. (5-305) applies throughout. Let

$$Q = Q^* \exp(\delta\rho\delta t/\ell), \quad (5-307)$$

where  $\delta t$  is the time after threshold is reached at the center. To integrate eq. (5-305), let  $\delta\rho\delta t \ll \ell$  and represent the exponential as a power series. Assuming  $d\rho/dt \cong 0$  and  $\rho = \rho_{\max}$  when  $\delta t = 0$ ,

$$\rho \cong \rho_{\max} - C_4(\ell/\delta\rho)^2(Q - Q^*)^{\frac{1}{2}}$$

where  $C_4$  is a constant. The final energy is found by setting  $\rho = \beta$ . Recall that  $\rho_{\max} - \beta = \delta\rho$ ; therefore

$$Q - Q^* \cong C_5x^{\frac{1}{2}} \quad (5-308)$$

where  $C_5$  is a constant and

$$x = K(\delta\rho)^3/\ell^2. \quad (5-309)$$

In eq. (5-309),  $K$  is a constant depending on  $b, q, Q^*$ , and other physical parameters.

The other extreme is a very fast excursion in which the final energy is large compared to  $Q^*$  and the intermediate stage described by eq. (5-305) is of little importance. Using eqs. (5-306) and (5-307) with  $Q \gg Q^*$  yields

$$\rho \cong \rho_{\max} - C_3(1 - 0.6q)(\ell/\delta\rho)^2Q.$$

When  $\rho = \beta$ ,

$$Q \cong \frac{x}{C_3(1 - 0.6q)}, \quad (5-310)$$

where  $x$  is again given by eq. (5-309).

One may infer that the range from small to large excursions is characterized by the parameter  $x$ , raised to an exponent whose value ranges from  $\frac{1}{2}$  to 1. Indeed, in the example by Bethe and Tait (1956), the exponent for an intermediate case was approximately 0.5. Fig. 5-27 shows the result of a set of numerical computations (Nicholson

1964); see also the report by Jankus (1962). The slope of the curve is about  $\frac{2}{3}$  for small  $x$ . The range of  $x$  is too small to exhibit the full range of the exponent ( $\frac{2}{3}$  to 1). The upper curve is for a different case with the core surface constrained.

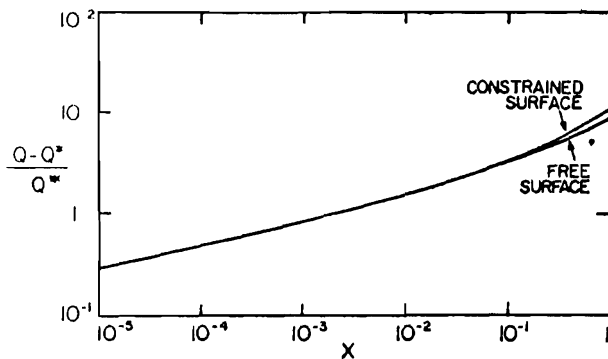


Fig. 5-27. Ratio of excess energy to threshold energy as a function of  $x = K(\delta\rho)^3/\epsilon^2$ , using the modified Bethe-Tait method (Nicholson 1964).

Maximum reactivity and total energy for a particular reactor model are shown in fig. 5-28; the points are taken from a table by Nicholson (1964). These results are for the so-called modified Bethe-Tait method, which is essentially the use of eqs. (5-305) and (5-306) as reactivity feedback in a numerical calculation. In the same paper, Nicholson describes improved numerical calculations using a more realistic equation of state (the saturated-vapor-pressure equation). Further, there is no division into separate time regimes; reactivity input and feedback are present throughout. Comparison shows that fig. 5-28 overestimates the maximum reactivity slightly (20 percent at small  $\gamma$  and 2 percent at large  $\gamma$ ). Fig. 5-28 also overestimates the energy release (a factor of two at small  $\gamma$  and 3 percent at large  $\gamma$ ). This comparison, of course, is between two numerical calculations for a particular idealized reactor model. No experimental results are available. Further, it is very difficult to estimate the fraction of the total energy that appears as mechanical work (kinetic energy of fragments, structural damage, etc.).

Other conclusions of this improved calculation are that the initial power and the neutron generation time are not highly significant parameters. This might be expected from eqs. (5-296) and (5-309). We saw in connection with eq. (5-296) that  $\delta\rho$  is very insensitive to  $n(0)$ , and that  $\delta\rho$  is approximately proportional to the square root of  $\gamma\ell$ . Using this in eq. (5-309) shows that  $x$  would be proportional to  $\gamma^{\frac{1}{2}}\ell^{-\frac{1}{2}}$ , and the energy would be proportional to  $x^n$  with  $n$  between  $\frac{2}{3}$  and 1. The dependence of energy on  $\ell$  is therefore slight, especially for the

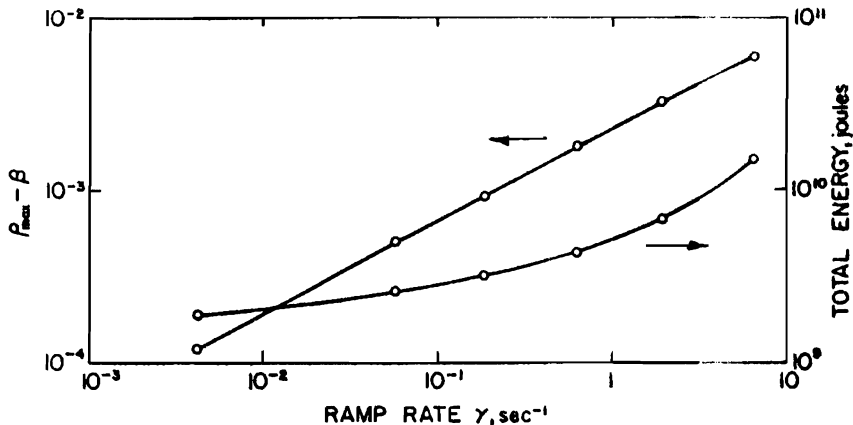


Fig. 5-28. Maximum reactivity and total energy vs. ramp rate for a hypothetical fast-reactor accident, using the modified Bethe-Tait method (Nicholson 1964)

smaller excursions. Another conclusion, also expected, is that delayed neutrons have negligible effect unless the maximum reactivity is very close to prompt critical (or below). Finally, computed curves of  $n(t)$ , both with and without negative Doppler effect, are highly asymmetric, most of the energy being produced before peak power.

The role of the parameter  $x$  may be seen by using a very simple dimensional argument. Assuming that  $Q$  and  $\nabla p$  are both rising exponentially, and that the radius has an acceleration proportional to  $\nabla p$ ,

$$\frac{d^2r}{dt^2} \sim \exp(\delta\rho\delta t/\ell).$$

Integrating twice, we have

$$\delta r \sim (\ell/\delta\rho)^2 \exp(\delta\rho\delta t/\ell) \sim (\ell/\delta\rho)^2 Q.$$

If the feedback reactivity is proportional to  $\delta r$ , then

$$Q \sim (\delta\rho)^3/\ell^2.$$

Hence  $Q$  is proportional to  $x$  as in eq. (5-310). This type of argument is apparently useful only in the limiting case of very fast excursions.

Another analytical procedure may be helpful in certain cases. For fast excursions, eq. (5-306) gives the second derivative of the reactivity as proportional to the energy. In contrast, the Nordheim-Fuchs model assumes that the feedback reactivity and energy are proportional. A generalized empirical feedback model may be studied in which the  $r$ th derivative of reactivity is proportional to the energy raised to the

exponent  $s$ . For fast excursions using eq. (5-77), a first integral may be obtained which gives the path of the excursion in the  $n, \rho$  plane and the ratio of total energy to peak power. These results for various values of  $r$  and  $s$  are given by Soodak (1962).

We conclude this chapter with a few remarks on reactor safety. Many of the examples of reactor excursions that we discussed represent hypothetical situations taken out of the context of realistic reactor operation. In particular, the use of reactivity input as an independent variable has little relevance to a realistic problem in reactor safety because the reactivity is only one variable in a complex chain of interacting quantities. Further, many if not most of the potential operating problems in a power-reactor system may be completely independent of the reactivity. Finally, we emphasize that spectacular calculations of energy release as a function of ramp rate (note the energy ordinate in fig. 5-28) have little use in overall safety evaluation unless they can be put in proper perspective. The central problem in reactor safety analysis is the quantitative evaluation of reliability of the entire system, and this is beyond the scope of this book. The interested reader is referred to the literature, e.g., Denielou (1967); Farmer (1963); IAEA (1962); Okrent (1965); Russell (1962); Thompson and Beckerley (1964); Wolfe (1969). Details of recent improved calculations are given by Azzoni et al. (1969); Braess, Küsters, and Thürnay (1967); Moss and Rhoades (1968); Oyama, An, and Kondo (1967); Renard and Stiévenart (1967); and Russell and Morris (1965).

### Problems

- 5-1. Verify the temperature coefficients of  $P_t$  and  $P_f$ , eqs. (5-12) and (5-13).
- 5-2. Verify the temperature coefficients of  $f$  and  $L^2$ , eqs. (5-16) and (5-29).
- 5-3. Verify the prompt temperature coefficient of  $p$ , eq. (5-41).
- 5-4. Using data from a standard reactor-theory textbook (e.g., Lamarsh 1966), estimate the isothermal temperature coefficient of reactivity for an unreflected homogeneous  $U^{235}$ -graphite reactor with 1,200 carbon atoms per  $U^{235}$  atom.
- 5-5. Estimate the isothermal temperature coefficient of reactivity for an unreflected reactor consisting of thin  $U^{235}$ -aluminium fuel plates in water. The metal-to-water volume ratio is 1.0 and the aluminium-to- $U^{235}$  atom ratio is 150 (Lamarsh 1966).
- 5-6. When a liquid homogeneous core in a partially filled spherical vessel is heated, the expansion produces a change in shape

(decreased surface-to-volume ratio). Estimate the effect on the temperature coefficient of reactivity. Assume 2 kgm of  $\text{U}^{235}$  in a sulphate solution in water and a one-foot diameter sphere that is critical when 80 percent filled.

- 5-7. The reactivity coefficients for a water-boiler reactor (Remley et al. 1958) are: temperature,  $-0.02$  dollar per  $^{\circ}\text{C}$ ; void volume,  $-0.005$  dollar per  $\text{cm}^3$ . The heat capacity is  $5 \times 10^4$  joules per  $^{\circ}\text{C}$ . The gas evolution rate is 4 liters per megajoule at standard conditions. Calculate the energy coefficient of reactivity assuming atmospheric pressure. What would be the effect of a pressure rise during a transient?
- 5-8. Verify the feedback kernels for the special cases given by eqs. (5-71) through (5-74).
- 5-9. Derive eqs. (5-94) and (5-95) for the power and energy in a fast excursion.
- 5-10. Show that  $n(t)$  for the Nordheim-Fuchs model is a solution of

$$\frac{d^2n}{dt^2} = \frac{1}{n} \left( \frac{dn}{dt} \right)^2 - \frac{\alpha K}{\ell} n^2.$$

- 5-11. Derive eq. (5-115) from eq. (5-114) using a series expansion in powers of  $\omega$ .
- 5-12. Given the set of peak-power data for step transients, find the shutdown coefficient  $\alpha K/\beta$  in dollars per megawatt-sec and the value of  $\ell/\beta$ . Use  $\lambda = 0.077 \text{ sec}^{-1}$  and assume that heat-transfer effects may be neglected.

Initial period (Seconds)	Peak power (Watts)
400	100
250	260
173	520
100	1600
40	6000
12	$2.5 \times 10^4$
2.2	$1.0 \times 10^5$
0.50	$3.2 \times 10^5$
0.20	$7.0 \times 10^5$
0.080	$1.8 \times 10^6$
0.031	$1.1 \times 10^7$
0.020	$2.5 \times 10^7$
0.010	$1.0 \times 10^8$
0.0050	$4.0 \times 10^8$

5.3. *Reactivity Feedback and Reactor Excursions*

- 5-13. Derive the implicit reactivity-time relationship for slow transients, eq. (5-118).
- 5-14. Show that the two nonzero eigenvalues of the matrix in eq. (5-124) are the roots of the inhour equation.
- 5-15. Verify that eqs. (5-133) and (5-134) are the asymptotes of the hyperbola representing the ZSI.
- 5-16. By expanding the one-group inhour equation in powers of  $\epsilon$ , obtain asymptotic series corresponding to eqs. (5-150), (5-152), (5-159), and (5-160) with  $\omega$  as a parameter instead of the initial reactivity  $x_0$ .
- 5-17. Verify the approximate trajectory, eq. (5-171), and show by means of a series expansion that the initial derivative agrees with eq. (5-168).
- 5-18. Using the one-group adiabatic model, eqs. (5-119) through (5-123), together with the approximate relation

$$\frac{\int_0^t n(t') dt'}{\int_0^t c(t') dt'} \approx \frac{n - n_0}{c - c_0},$$

derive an approximate integral curve  $n(\rho)$ . Show that the reactivity at peak power is the solution of a cubic equation whose physically meaningful root is a good approximation over the full range of initial reactivity  $\rho_0$  (suggested by E. J. Britt, University of Arizona, 1969).

- 5-19. Show that the lower portions of the larger trajectories in fig. 5-20 are such that  $\log n$  is approximately quadratic in time with the same time dependence as in eq. (3-129).
- 5-20. A reactor is subjected to a reactivity rate of 10 dollars/sec such that the power at the instant of prompt critical is 1 watt. Compute the peak power and the burst duration if the reactivity coefficient is 0.5 dollar/kilowatt-sec and  $\epsilon/\beta = 10^{-3}$  sec.
- 5-21. Verify the expressions for maximum reactivity, eqs. (5-233) and (5-234).
- 5-22. Derive an equation for peak power by extending the approximate trajectory, eq. (5-232). Show that the result reduces to eq. (5-193).
- 5-23. Derive eq. (5-236) for the power at prompt critical by comparing eq. (5-230) with the exact value of  $v$  at prompt critical (suggested by H. B. Smets, Université de Liège, 1969).

- 5-24. Verify the equations for the zero-delay nonlinear feedback model, eqs. (5-242) through (5-246).
- 5-25. Derive the equation for  $n(t)$  in the long-delay model, eq. (5-248).
- 5-26. Derive the equations for the thermal uranium-oxide reactor with Doppler shutdown, eqs. (5-255) through (5-271).
- 5-27. Derive the asymptotic energy formula, eq. (5-292).
- 5-28. Verify the limiting cases, eq. (5-308) and (5-310), for the energy production in a fast-reactor accident.



---

## 6 Linear System Stability

We now turn to the question of stability of dynamical systems. The central problem is, Will a given system initially at equilibrium, when perturbed in some manner throughout a finite time interval, eventually return to its equilibrium state? The goal is to answer this question without explicitly solving the equations of motion.

This chapter is concerned with linear systems representing nuclear reactors with reactivity feedback. Starting with the concept of linear systems with feedback, we describe some of the widely used methods for linear-stability analysis. Then, with the reactor equations put in suitable form, we proceed to analyze a number of special reactor models for linear stability. Particular attention is paid to the system with two reactivity feedbacks because of the great variety of cases arising in this simple model and because of its utility in illustrating the effects of delayed neutrons on stability.

As mentioned earlier, we will be concerned primarily with intrinsic feedback (reactivity effects caused by reactor temperature, density, etc.). The control-system engineer may then use the results of this type of analysis (for example, a description of a reactor system with temperature and density effects included) as the starting point in designing an external automatic-control system.

The equations of reactor dynamics are nonlinear when the reactivity depends on the power. A linear system is therefore only a first approximation. However, as we shall see in chapter 7, some important conclusions about a nonlinear system may be made by studying its associated linear approximation. In particular, the stability of a nonlinear system for small perturbations may often be deduced by examining the stability of an associated linear system.

### 6-1. Linear Systems with Feedback

It will be convenient to formulate the linear stability problem in terms of transfer functions and block diagrams. The reader is referred to sec. 2-6 for an introduction. The transfer function characterizes the inhomogeneous part of a solution to the system equations, i.e., the response (output) to a driving signal (input) in the absence of initial conditions. The transfer function is defined as the ratio of Laplace transforms of output and input and is equal to the Laplace transform of the impulse response. The transient response of a linear system is characterized by the poles of the transfer function (the roots of the characteristic equation). For further reference the reader may consult books on automatic-control theory (Chestnut and Mayer 1951; Evans 1954; James, Nichols, and Phillips 1947; Thaler 1955; Truxal 1955) and on reactor-system analysis (Harrer 1963; Schultz 1961; Weaver 1963).

For the moment, we restrict our attention to linear time-invariant systems and assume the validity of superposition of solutions. The most common systems of this type are those represented by ordinary linear differential equations with constant coefficients. Linear systems with simple transport-time delays may also be treated.

Block diagrams for a linear system with feedback are shown in fig. 6-1. The block  $G(s)$  represents the forward-loop transfer function and the block  $H(s)$  represents the feedback transfer function. In fig. 6-1,  $r(t)$  is the input,  $c(t)$  is the output, and  $e(t)$  is the difference between the

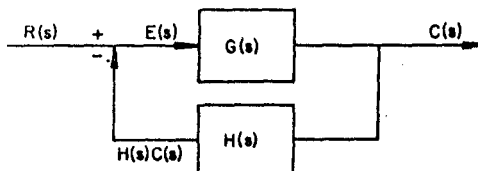
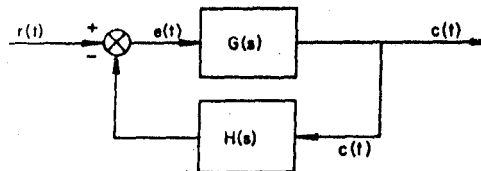


Fig. 6-1. Block diagrams for a linear system with feedback.

input to the system and the output of the feedback element. In control-system terminology,  $e(t)$  may be thought of as an error signal that is to be minimized by proper choice of  $H(s)$ , hence the convention of subtracting the feedback signal.

It is important to recognize that a block diagram represents the flow of information. If  $H(s)$  represented a controlling device, the diagram would signify a sensing of  $c(t)$  by some detector without drawing off appreciable energy. In general,  $c(t)$  represents information that may be received by  $H(s)$  and also by elements of other systems not shown.

The two diagrams in fig. 6-1 are two of many different ways of representing the same system. We will generally use the second diagram, in which the signals are represented by their Laplace transforms and in which the control engineer's conventional symbol for subtraction is indicated merely by the symbols + and -. Arrows will often be omitted where no possibility of confusion exists.

Applying eq. (2-71) to the diagram in fig. 6-1, we have

$$C(s) = G(s)E(s) \quad (6-1)$$

and

$$E(s) = R(s) - H(s)C(s). \quad (6-2)$$

Eliminating  $E(s)$ , we may write the overall-system transfer function (closed-loop transfer function) as

$$Y(s) = \frac{C(s)}{R(s)} = \frac{G(s)}{1 + G(s)H(s)}. \quad (6-3)$$

The product  $G(s)H(s)$  is called the open-loop transfer function, and it plays a central role in stability analysis for systems with feedback.

As we saw in sec. 2-6, the transfer function of a system described by a linear differential equation with constant coefficients may be written as a ratio of two polynomials in  $s$ . If we have

$$G(s) = P_G(s)/D_G(s), \quad H(s) = P_H(s)/D_H(s),$$

then

$$Y(s) = \frac{P_G(s)D_H(s)}{P_G(s)P_H(s) + D_G(s)D_H(s)}.$$

Note that the zeros of  $Y(s)$  coincide with the zeros of  $G(s)$  and the poles of  $H(s)$ . The transient response of the system is characterized by the poles of  $Y(s)$ , which are the roots of the characteristic equation

$$1 + G(s)H(s) = 0. \quad (6-4)$$

The characteristic equation may also be written as

$$D(s) = P_G(s)P_H(s) + D_G(s)D_H(s) = 0, \quad (6-5)$$

where  $D(s)$  is the characteristic polynomial.

The transient response is a linear combination of terms  $\exp(s_j t)$  where the  $s_j$  are the roots of eq. (6-4) or (6-5). If one or more of the  $s_j$  has a positive real part, the response to a perturbation will grow indefinitely and the linear system is unstable. If all the  $s_j$  have negative real parts, the response to a perturbation will ultimately decay to zero as  $t \rightarrow \infty$ ; the system returns arbitrarily close to its equilibrium and is said to be asymptotically stable. If no root has a positive real part but at least one root has a zero real part, we have a borderline case whose time response contains decaying transients together with constant terms or sustained oscillations. This type of system will be called "critical."

Linear asymptotic stability is assured if all the roots  $s_j$  have negative real parts; i.e., if all the poles of  $Y(s)$  are in the left half of the complex  $s$ -plane. For simplicity, throughout this chapter we shall refer to linear systems as stable (meaning asymptotically stable), critical, or unstable.<sup>1</sup> A criterion for linear stability is therefore a statement of conditions under which all roots of the characteristic equation have negative real parts, i.e., all poles of  $Y(s)$  are in the left-half-plane.

For a linear system, the size of the perturbation is not relevant to stability because the principle of superposition applies. Once the perturbation is removed, all solutions are expressible as linear combinations of the same time functions. This observation may be used to deduce the fact that a stable linear system has one and only one equilibrium state (equilibrium point in state space).

It should be emphasized that these concepts of stability may be applied directly to a given  $Y(s)$  without decomposing the system into a forward loop and a feedback loop. However, stability analysis is often greatly facilitated by arranging the system in this form and using concepts originally developed for analysis and design of feedback control systems.

The decomposition of a given  $Y(s)$  into  $G(s)$  and  $H(s)$  is not unique unless either  $G(s)$  or  $H(s)$  is specified in advance. This is clear if eq. (6-3) is written as

$$H(s) = Y^{-1}(s) - G^{-1}(s). \quad (6-6)$$

A unique choice may be accomplished by selecting the variable that is to be identified with the feedback  $C(s)H(s)$  in fig. 6-1.

In general, we will consider only physically realizable systems. One consequence is that all the polynomials in the transfer functions and

<sup>1</sup> More precise terminology will be defined and used for nonlinear systems in chapter 7. For example, the critical case may be characterized as stable but not asymptotically stable.

characteristic equations have real coefficients. The roots  $s_j$  are therefore real numbers or pairs of complex conjugates. A second consequence of physical realizability is that a transfer function should tend to zero as  $|s| \rightarrow \infty$ . This is suggested by the interpretation of a transfer function as a frequency response when  $s = j\omega_0$  (see sec. 2-6) and by the observation that the frequency response of a real system tends to become negligible at sufficiently high frequencies. Therefore, a transfer function expressed in terms of polynomials should have more poles than zeros. We shall see, however, that linear-stability criteria for systems with feedback are still meaningful in approximations where either  $G(s)$  or  $H(s)$  fails to have this property, provided the product  $G(s)H(s)$  tends to zero as  $|s| \rightarrow \infty$ . By eq. (6-3), this is equivalent to the provision that  $Y(s) \rightarrow G(s)$  at large  $s$ .

We proceed by discussing the Routh criterion, the Nyquist criterion, and the root-locus method, illustrating each method by simple examples. We then examine a variety of reactor systems for linear stability.

### 6-2. The Routh Criterion

Linear stability is assured if all poles of the system transfer function are in the left half-plane, i.e., if all roots of the characteristic equation are negative or have negative real parts. The Routh criterion gives necessary and sufficient conditions that all complex roots of a polynomial with real coefficients be negative or have negative real parts.

The general problem for a polynomial with complex coefficients was solved by Hermite (1850). A simple algorithm for polynomials with real coefficients was derived by Routh (1877). Later formulations of the problem were made by Hurwitz (1895) and Bilharz (1944). The four criteria associated with these four authors are equivalent to, or are special cases of, Hermite's criterion (Lehnigk 1966). Routh's algorithm is a simple practical formulation of the Hurwitz criterion, and it is generally known as the Routh-Hurwitz criterion or the Routh criterion.

Let the characteristic polynomial be

$$D(s) = a_n s^n + a_{n-1} s^{n-1} + a_{n-2} s^{n-2} + \cdots + a_1 s + a_0, \quad (6-7)$$

where the  $a_i$  are real numbers. Form the Routh array

$$\begin{array}{ccccccc} a_n & a_{n-2} & a_{n-4} & a_{n-6} & \cdots \\ a_{n-1} & a_{n-3} & a_{n-5} & \cdots & & & \\ b_1 & b_2 & b_3 & \cdots & & & \\ c_1 & c_2 & \cdots & & & & \\ d_1 & \cdots & & & & & \\ \vdots & & & & & & \\ \vdots & & & & & & \end{array} \quad (6-8)$$

240      *Linear System Stability*

where typical entries in the third and subsequent rows are given by

$$b_1 = a_{n-2} - \frac{a_n a_{n-3}}{a_{n-1}}, \quad (6-9)$$

$$b_2 = a_{n-4} - \frac{a_n a_{n-5}}{a_{n-1}}, \quad (6-10)$$

$$b_3 = a_{n-6} - \frac{a_n a_{n-7}}{a_{n-1}}, \quad (6-11)$$

$$c_1 = a_{n-3} - \frac{a_{n-1} b_2}{b_1}, \quad (6-12)$$

$$d_1 = b_2 - \frac{b_1 c_2}{c_1}. \quad (6-13)$$

Missing entries at the right-hand end of each row may be regarded as zeros. The calculation proceeds in the manner indicated by eqs. (6-9) through (6-13),  $n + 1$  rows being generated. The last entry in the first column is  $a_0$ .

The necessary and sufficient condition that all zeros of  $D(s)$  be in the left half-plane is that all entries in the first column (the Routh numbers) have the same sign. If  $D(s)$  is written so that  $a_n > 0$  (usually  $a_n = 1$  for convenience), the stability criterion is that all the Routh numbers be positive. If a zero denominator is encountered in calculating the array, one may investigate an auxiliary polynomial constructed by adding a parameter in a coefficient. If the second last Routh number is zero, there is a pair of characteristic roots equal in magnitude and opposite in sign.

To illustrate the application of the Routh criterion, consider the fourth-degree characteristic polynomial

$$D(s) = s^4 + 3s^3 + 2s^2 - 2s - 4. \quad (6-14)$$

The Routh array is

1	2	-4
3	-2	0
$\frac{8}{3}$	-4	0
$\frac{5}{2}$	0	
-4		

The first column consists of four positive and one negative number (the Routh numbers). The roots of  $D(s)$  are not all in the left half-plane. As may be shown by factoring, the roots are  $+1, -2, -1 \pm j$ .

As another example, consider

$$D(s) = s^4 + 2s^3 + 2s^2 + 2s + 1. \quad (6-15)$$

The Routh array is

$$\begin{array}{ccc} 1 & 2 & 1 \\ 2 & 2 & 0 \\ 1 & 1 & 0 \\ 0 & 0 & \end{array}$$

The fourth Routh number is zero, and the algorithm fails. There is a pair of roots of equal magnitude and opposite sign, but stability is not ascertained.

Instead, consider an auxiliary polynomial

$$D(s) = s^4 + 2s^3 + 2s^2 + 2s + 1 + \epsilon. \quad (6-16)$$

The array is

$$\begin{array}{ccc} 1 & 2 & 1 + \epsilon \\ 2 & 2 & 0 \\ 1 & 1 + \epsilon & 0 \\ -2\epsilon & 0 & \\ 1 + \epsilon & & \end{array}$$

There is no longer an indeterminate form in computing the last Routh number. The auxiliary system is stable if  $\epsilon < 0$ . The original system has Routh numbers 1, 2, 1, 0, and 1 and is therefore critical (see sec. 6-1). The roots are  $-1, -1$ , and  $\pm j$ .

This example suggests that when the second-last Routh number is zero, it may simply be replaced by a small parameter that is permitted to vanish when the array is complete. As can be inferred from the examples, the last Routh number would still be  $a_0$ . The net result is a simple rule: whether the second-last Routh number is zero or not, terminate the computation and write  $a_0$  for the last Routh number.

The situation is more complex if a zero is encountered earlier in the first column. An auxiliary polynomial can be constructed, and the stability studied parametrically. Another alternative is to construct the Hurwitz determinants (Lehnigk 1966). These are related to the Routh numbers, but the Hurwitz criterion (stability assured if the determinants are all positive) is free from infinities and indeterminate forms. We will not pursue this further, because most of our applications will involve problems containing one or more adjustable parameters. There is no danger of misinterpretation if one is careful about indeterminate forms.

We mention in passing that the Routh numbers for a quadratic are just the coefficients  $a_2$ ,  $a_1$ , and  $a_0$ . As may be quickly verified by inspection of the standard quadratic formula, the roots are in the left half-plane if and only if all three coefficients have the same sign.

We now consider five examples of simple systems with feedback. Each in turn will be studied by other methods in later sections, and the designations as example 1, etc., will be retained.

*Example 1*

$$G(s)H(s) = \frac{K}{s(s+a)(s+b)}. \quad (6-17)$$

Eq. (6-17) could represent any of several feedback systems. Two possibilities are shown in fig. 6-2. As seen from eq. (6-3), each system corresponds to a different closed-loop transfer function  $Y(s)$ . However, they all have the same characteristic equation, eq. (6-4), so their stability properties are the same.

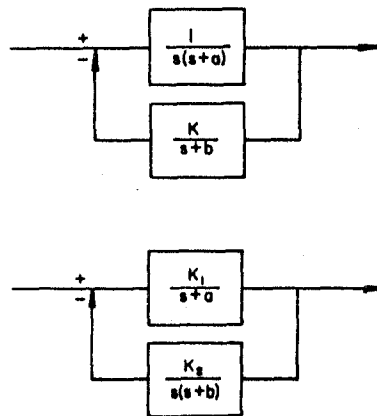


Fig. 6-2. Two possible closed-loop systems corresponding to example 1.

The characteristic polynomial is

$$D(s) = s^3 + (a+b)s^2 + abs + K. \quad (6-18)$$

The Routh array is

1	$ab$
$a+b$	$K$
$ab - \frac{K}{a+b}$	0
	$K$

Assume for the moment that  $a$  and  $b$  are positive. Then the closed-loop system is stable if

$$0 < K < ab(a + b). \quad (6-19)$$

This example might represent a system in which  $a$  and  $b$  are fixed (reciprocal time constants) and  $K$  is an adjustable gain factor. By eq. (6-19), there is a range of  $K$  for stability. This is an example of *conditional stability* (stability conditional upon the values of one or more parameters).

Let us examine the endpoints of the range of  $K$  in eq. (6-19) by studying the characteristic equation. If  $K = 0$ , the characteristic equation is

$$s^3 + (a + b)s^2 + abs = 0. \quad (6-20)$$

Its roots are  $0$ ,  $-a$ , and  $-b$ . This is a critical system, and  $K = 0$  is called the "static stability boundary" because of the zero characteristic root. Note that the last Routh number (the constant term in the characteristic equation) is zero.

If  $K = ab(a + b)$ , the characteristic equation is

$$s^3 + (a + b)s^2 + abs + ab(a + b) = 0. \quad (6-21)$$

This may be factored as

$$(s + a + b)(s^2 + ab) = 0.$$

The roots are  $-(a + b)$  and  $\pm j\omega$ , where  $\omega^2 = ab$ . This is another critical system, this time with two conjugate imaginary roots representing a sustained oscillation (periodic after the decaying transient arising from the negative real root has died away). We call  $K = ab(a + b)$  the "dynamic stability boundary." Note that this corresponds to the vanishing of the second-last Routh number (roots equal in magnitude and opposite in sign).

It is generally easier to seek a dynamic stability boundary by postulating  $s = j\omega$  and substituting in the original characteristic equation. We find

$$-j\omega^3 - (a + b)\omega^2 + jab\omega + K = 0.$$

Separating real and imaginary parts and assuming  $\omega \neq 0$ , we obtain

$$\omega^2 = ab, \quad K = \omega^2(a + b) = ab(a + b).$$

A simple algorithm is based on the numbers in the Routh array. The second-last Routh number vanishes if  $K = ab(a + b)$ . From the first and second entries in the row immediately above, we form the equation

#### 6.4. Linear System Stability

$$(a + b)s^2 + K = 0.$$

Combining with the previous condition yields  $s^2 = -ab$  or  $\omega^2 = ab$ .

The case of negative  $a$  or  $b$  is left as an exercise.

#### Example 2

$$G(s)H(s) = \frac{K}{(s-1)(s+2)}. \quad (6-22)$$

A possible block diagram is shown in fig. 6-3. The open-loop system is unstable because of the pole at  $s = 1$ . For the closed-loop system,

$$D(s) = s^2 + s + K - 2. \quad (6.23)$$

The Routh numbers are 1, 1, and  $K - 2$ . The closed-loop system is stable for  $K > 2$  (stabilized by sufficiently large negative feedback). The point  $K = 2$  is a static stability boundary.

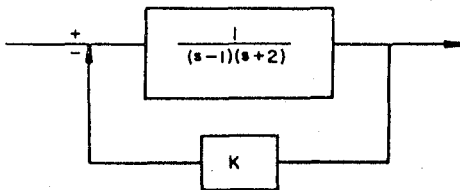


Fig. 6-3. Stabilization of an open-loop unstable system (example 2).

#### Example 3

$$G(s)H(s) = \frac{K(s+a)}{s(s-b)}. \quad (6-24)$$

With positive  $a$  and  $b$ , eq. (6-24) represents another open-loop unstable system. For the closed-loop system,

$$D(s) = s^2 + (K-b)s + Ka. \quad (6-25)$$

The Routh numbers are 1,  $K - b$ , and  $Ka$ . The system is stable for  $K > b$ . The point  $K = b$  is a dynamic stability boundary, with  $\omega^2 = ab$ .

#### Example 4

$$G(s)H(s) = \frac{K(s-a)}{s(s+b)}. \quad (6-26)$$

Taking  $a$  and  $b$  as positive, we may call eq. (6-26) an open-loop critical

system (poles at 0 and  $-b$ ). For the closed-loop system,

$$D(s) = s^2 + (K + b)s - Ka. \quad (6-27)$$

The Routh numbers are 1,  $K + b$ , and  $-Ka$ . The stability range is  $-b < K < 0$ . The point  $K = 0$  is a static stability boundary, and the point  $K = -b$  is a dynamic stability boundary with  $\omega^2 = ab$ .

The way this example is formulated, its stability range includes only negative values of  $K$ . This frequently arises in systems with a zero in the right half-plane (sometimes called nonminimum-phase systems; see sec. 6-3). Some authors prefer to write the numerator in eq. (6-26) as  $K(a - s)$ , in effect reversing the sign of  $K$ . We will not do this because of the confusion it would introduce into parametric studies where a zero may be in either half-plane.

#### *Example 5*

$$G(s)H(s) = \frac{K}{(s - 1)(s + 2)(s + \alpha)}. \quad (6-28)$$

Eq. (6-28) could represent the system of fig. 6-3 but with the feedback replaced by the two-parameter system  $K/(s + \alpha)$ . For the closed-loop system,

$$D(s) = s^3 + (\alpha + 1)s^2 + (\alpha - 2)s + K - 2\alpha. \quad (6-29)$$

The Routh array is

$$\begin{array}{cc} 1 & \alpha - 2 \\ \alpha + 1 & K - 2\alpha \\ \hline \alpha^2 + \alpha - 2 - K & 0 \\ \alpha + 1 & \\ \hline K - 2\alpha & \end{array}$$

The stability conditions are  $\alpha > -1$  and

$$2\alpha < K < \alpha^2 + \alpha - 2. \quad (6-30)$$

The condition expressed by eq. (6-30) cannot be satisfied for arbitrary  $\alpha$ . No  $K$  exists for  $-1 < \alpha < 2$ . Further, since  $\alpha > -1$  is necessary, the stability condition may be restated as eq. (6-30) together with the requirement  $\alpha > 2$ .

These considerations may be summarized in terms of stability boundaries in a parameter space. Fig. 6-4 shows the  $K$  vs.  $\alpha$  plane for this example. The stable region and the stability boundaries are as labeled. Along the dynamic stability boundary we find  $\omega^2 = \alpha - 2$ , so

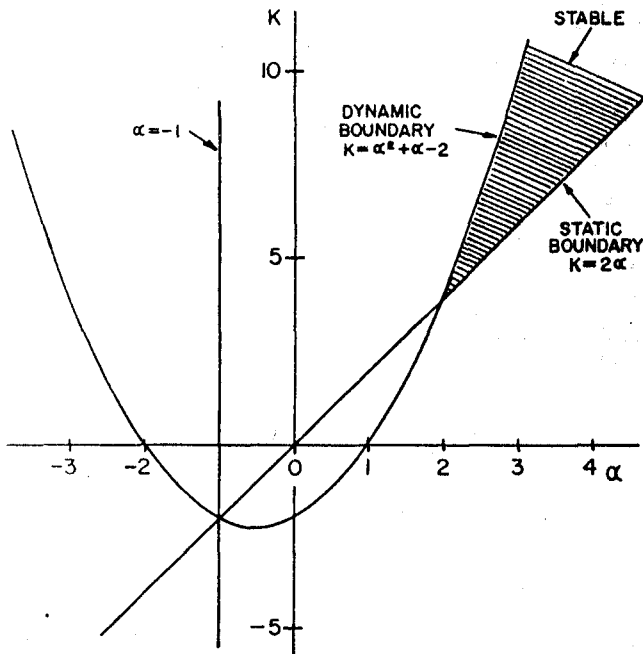


Fig. 6-4. Stability boundaries in parameter space for example 5.

that pure imaginary roots are possible only for  $\alpha > 2$ . Note that only portions of each boundary actually border on the stable region. Also, the line  $\alpha = -1$  is not a border of the stable region. This is not surprising, because this line represents the locus of points for which the sum of the characteristic roots is zero. For example, at the intersection  $\alpha = -1$  and  $K = -2$ , the characteristic roots are 0 and  $\pm\sqrt{3}$ .

In addition to static and dynamic stability boundaries, a parametric system could also exhibit an "infinity stability boundary." If a coefficient in the characteristic equation changes sign by passing through infinity ( $1/a_i \rightarrow 0$ ), a Routh number also changes sign. We have not included an example of this type of stability boundary.

We shall find the concept of stability regions in a parameter space very useful for studying reactor systems. First, we shall summarize some other methods for linear-stability analysis.

### 6-3. Representations for Frequency Response

The next method for linear stability analysis that we shall discuss (sec. 6-4) depends upon the behavior of  $G(j\omega)H(j\omega)$ , i.e., the open-loop

transfer function evaluated at  $s = j\omega$  (the imaginary axis of the  $s$ -plane). By the discussion in sec. 2-6, this function is the open-loop frequency response. This section is concerned with ways of representing the frequency response.

Consider the complex function

$$F(s) = \frac{1}{s + a}, \quad (6-31)$$

where  $a$  is a real number. For  $s = j\omega$ ,

$$F(j\omega) = \frac{1}{j\omega + a} = \frac{a - j\omega}{\omega^2 + a^2}. \quad (6-32)$$

We have

$$\operatorname{Re} F(j\omega) = \frac{a}{\omega^2 + a^2}, \quad (6-33)$$

$$\operatorname{Im} F(j\omega) = -\frac{\omega}{\omega^2 + a^2}, \quad (6-34)$$

$$F(j\omega) = |F(j\omega)| e^{j\theta}, \quad (6-35)$$

$$|F(j\omega)| = (\omega^2 + a^2)^{-\frac{1}{2}}, \quad (6-36)$$

$$\tan \theta = -\omega/a. \quad (6-37)$$

For small  $\omega$ ,

$$F(j\omega) \rightarrow 1/a, \quad \theta \rightarrow 0. \quad (6-38)$$

For  $\omega = a$ ,

$$F(j\omega) = 1/(ja + a), \quad |F(j\omega)| = 1/(a\sqrt{2}), \quad \theta = -45^\circ. \quad (6-39)$$

For large  $\omega$ ,

$$F(j\omega) \rightarrow -j/\omega, \quad |F(j\omega)| \rightarrow 1/\omega, \quad \theta \rightarrow -90^\circ. \quad (6-40)$$

A convenient representation is the Bode plot in which  $\log |F(j\omega)|$  is plotted against  $\log \omega$ . For small  $\omega$ , eq. (6-38) represents a horizontal line. For large  $\omega$ , eq. (6-40) yields a straight line of slope  $-1$ . These two asymptotes intersect at  $\omega = a$ , which is called the break frequency. The true magnitude at  $\omega = a$  is  $1/\sqrt{2}$  times the horizontal asymptote. In communications and control engineering, the decibel unit (db) is often used (ten times the common logarithm of the intensity ratio, or twenty times the common logarithm of the amplitude ratio). An amplitude ratio of  $\sqrt{2}$  corresponds to about 3 db, hence for the example

248      *Linear System Stability*

the magnitude at the break frequency is 3 db below the horizontal asymptote. As the frequency is increased from zero, the response is "flat" up to the neighborhood of the break frequency, is attenuated  $1/\sqrt{2}$  (3 db) at the break frequency, and falls off as  $1/\omega$  above the break frequency (slope -1 on a log-log plot, or an attenuation of 20 db per decade of frequency). Note that frequency here is in radians per sec. The phase varies smoothly from 0 to  $-90^\circ$  over the frequency range, being  $-45^\circ$  at the break frequency. This is illustrated in fig. 6-5 for eq. (6-31) with  $a = 1$ .

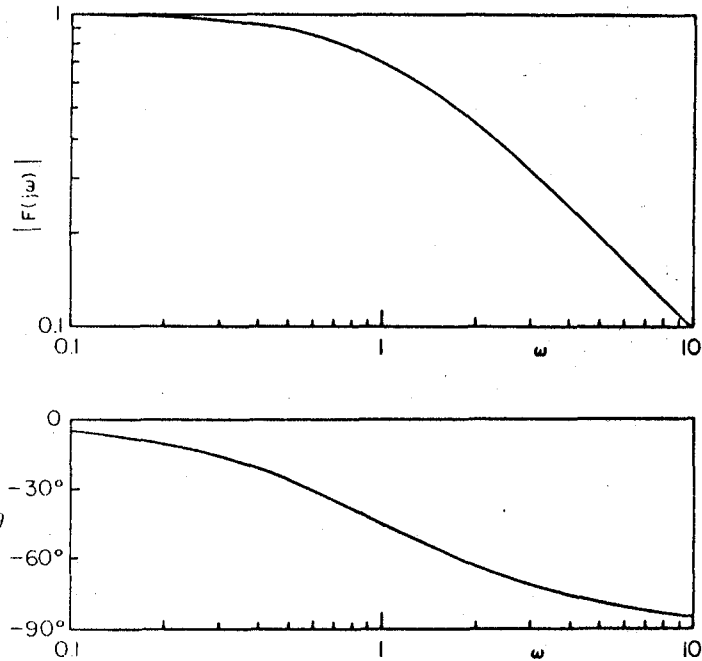
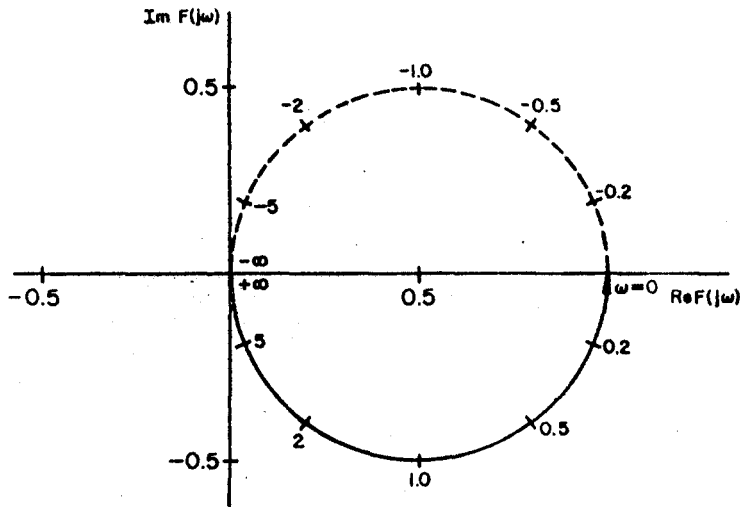


Fig. 6-5 Magnitude and phase plots for  $F(s) = 1/(s + 1)$ .

A polar plot of  $F(j\omega)$  is made by taking the real and imaginary parts, eqs. (6-33) and (6-34), as a pair of  $x, y$  coordinates. For our example it is quickly verified that the polar plot is a half-circle through the origin with radius  $1/2a$ . See fig. 6-6. Negative values of  $\omega$  yield the upper half-circle, shown dotted. Note the symmetry about the real axis; eqs. (6-33) and (6-34) show that the real part is an even function of  $\omega$  and the imaginary part is an odd function.

The full circle in fig. 6-6 may be regarded as a mapping of the entire imaginary axis in the  $s$ -plane into the complex  $F(j\omega)$  plane. The direc-

Fig. 6-6. Polar plot for  $F(s) = 1/(s + 1)$ .

tion of the arrow is rather arbitrarily taken as indicating a traverse from  $\omega = +\infty$  to  $\omega = 0$ , because we later choose to integrate along a contour coming down the imaginary axis of the  $s$ -plane when we discuss the Nyquist criterion. For further discussion of this, see sec. 6-4; for additional hints in sketching polar plots, see the examples in sec. 6-4 (especially example 1).

Note that multiplication of  $F(j\omega)$  by  $-1$  has no effect on the magnitude. The phase is increased (or decreased) by  $180^\circ$ , corresponding to a rotation of the polar plot through  $180^\circ$ .

Next, consider a more complicated function

$$H(s) = \frac{s + a}{(s + b)(s + c)} \quad (6-41)$$

having two poles and a zero. For illustration, suppose  $b \ll a \ll c$ . We have

$$\begin{aligned} H(s) &\cong a/bc, & |s| \ll b; \\ H(s) &\cong a/cs, & b \ll |s| \ll a; \\ H(s) &\cong 1/c, & a \ll |s| \ll c; \\ H(s) &\cong 1/s, & |s| \gg c. \end{aligned} \quad (6-42)$$

The frequency response is flat at the value  $a/bc$  for small  $\omega$ , breaks at  $\omega = b$  to fall off as  $a/c\omega$ , breaks again at  $\omega = a$  and becomes flat (at a lower level  $1/c$ ), and finally rolls off at  $\omega = c$  to fall as  $1/\omega$ . If the

250      *Linear System Stability*

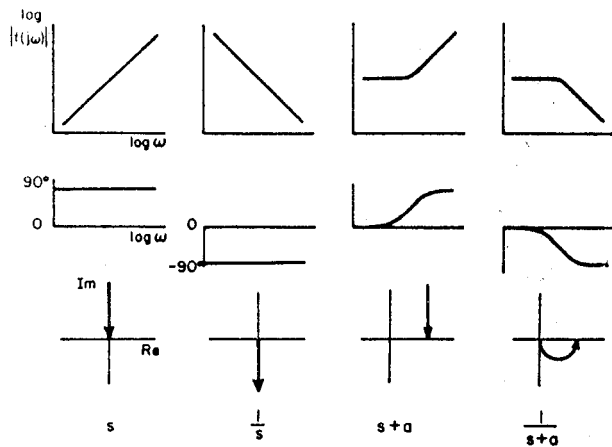


Fig. 6-7. Magnitude, phase, and polar plots for various functions  $f(s)$ .

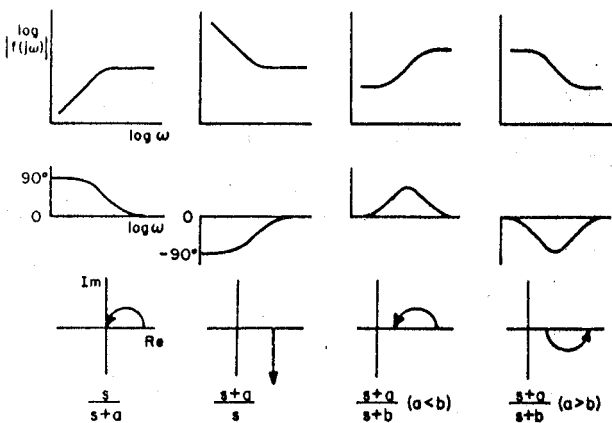


Fig. 6-8. Magnitude, phase, and polar plots for various functions  $f(s)$ .

poles and zeros were very widely separated, then the phase would fluctuate from zero to  $-90^\circ$ , back to zero, and again back to  $-90^\circ$ , passing through  $-45^\circ$  at each of the three break frequencies. When the poles and zeros are not well separated, the fluctuations of slope and phase are smoothed out considerably. With a little practice, rough sketches of magnitude and phase for complicated polynomial functions may be quickly constructed once the poles and zeros are located.

Magnitude, phase, and polar plots are sketched in figs. 6-7 through 6-14 for a number of functions ( $a$ ,  $b$ , and  $c$  are positive real numbers except as otherwise indicated). Figs. 6-9 and 6-10 contain cases in which

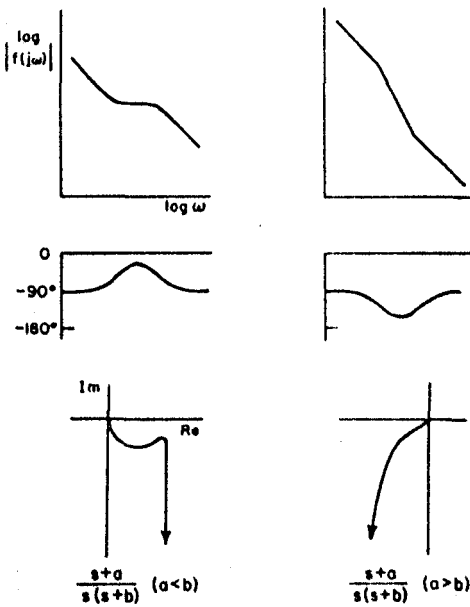


Fig. 6-9. Magnitude, phase, and polar plots for  $f(s) = (s + a)/(s + b)$ .

the transfer function varies as  $1/s^2$  or  $1/s^3$  over limited ranges, corresponding to slopes of  $-2$  or  $-3$  in the logarithmic magnitude plots.

Figs. 6-11 through 6-14 represent various sample cases for the function given by eq. (6-41) with magnitudes normalized to  $|H(0)| = 1$ . Note that the poles and zeros are fairly closely spaced in these four examples. The straight-line asymptotes are included in the magnitude plots for comparison.

The function given by eq. (6-41) is interesting because of the variety of cases. This variety appears later in the two-path feedback reactor model. It is left to the reader, as an exercise, to show that the real part of  $H(j\omega)$  can vanish for finite  $\omega$  (as in fig. 6-11) only when  $a > b + c$ , while the imaginary part can vanish for finite  $\omega$  (as in fig. 6-13) only when  $a < bc/(b + c)$ . Note the presence of phase lead ( $\theta > 0$ ) in figs. 6-13 and 6-14.

Fig. 6-14 illustrates a nonminimum-phase system. The effect of putting the zero in the right half-plane is a phase variation through  $270^\circ$  instead of only  $90^\circ$  (as in figs. 6-11 through 6-13) when  $\omega$  varies from  $0$  to  $\infty$ . The magnitude curve for this case is the same as that in fig. 6-12 because  $b < |a| < c$  in both figures, and of course  $|j + 1| = |j - 1|$ . This illustrates an important point: a unique phase curve may be deduced from a magnitude curve only if it is known that no zeros or poles are in the right half-plane.

## Linear System Stability

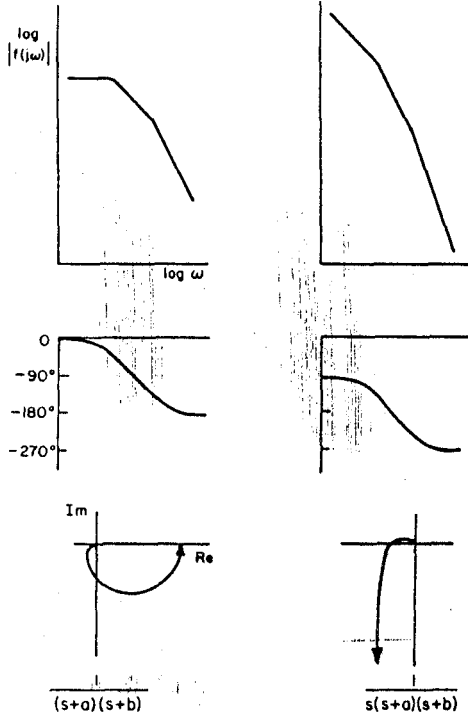


Fig. 6-10. Magnitude, phase, and polar plots for  $1/(s + a)(s + b)$  and  $1/s(s + a)(s + b)$ .

The reader should verify the qualitative features of the curves in figs. 6-7 through 6-14 and should also investigate the effects on phase curves and polar plots in figs. 6-7 through 6-10 when a pole or zero is shifted from the left to the right-half-plane.

Thus far we have considered combinations of linear factors representing poles or zeros on the real axis. A quadratic factor with real coefficients could represent a pair of complex conjugate poles or zeros. For example, consider

$$G(s) = \frac{\omega_0^2}{s^2 + 2\zeta\omega_0 s + \omega_0^2}. \quad (6-43)$$

This function has poles at

$$s = -\omega_0[\zeta \pm \sqrt{(\zeta^2 - 1)}].$$

For  $0 < \zeta < 1$ , there is a pair of complex conjugate poles in the left half-plane. We call  $\zeta$  the damping factor and  $\omega_0$  the natural frequency (frequency for undamped oscillations).

Magnitude and phase plots for various values of  $\zeta$  are shown in

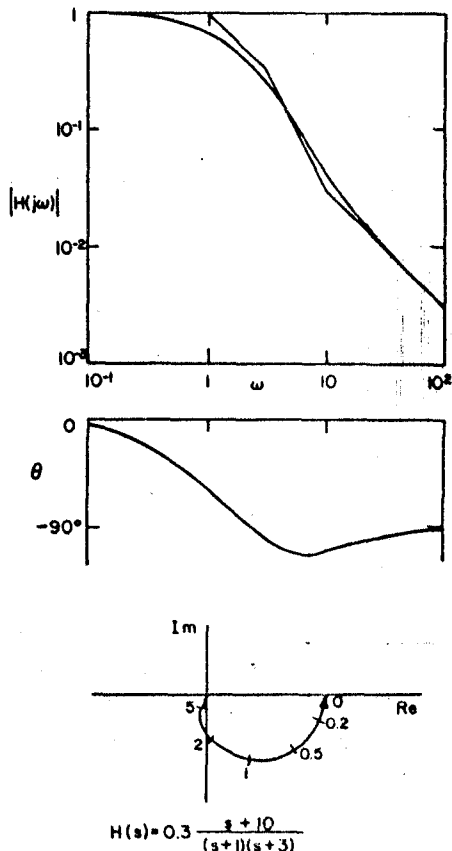


Fig. 6-11. Magnitude, phase, and polar plots (two poles and one zero in left half-plane).

figs. 6-15 and 6-16. The curve for  $\zeta = 1$  is for the case of a double pole at  $s = -\omega_0$ . Note the resonance, which becomes more pronounced as  $\zeta$  decreases. Of course, one could simulate the magnitude curves with their peaks by using a combination of several linear factors with real poles and zeros, but this would yield a false description of the system. This is another illustration of the fact that a magnitude curve alone is not sufficient to characterize a linear system.

Consider now the low-power reactor transfer function discussed in sec. 3-2. The input is a reactivity oscillation and the output is an oscillation of power or neutron density. By eq. (3-48), the zeros are at  $s = -\lambda_i$  and the poles are the roots of the inhour equation (fig. 2-1). There are  $m$  zeros and  $m + 1$  poles alternating along the negative real axis. If  $p_0 = 0$  (no source) then one pole is at the origin.

214      *Linear System Stability*

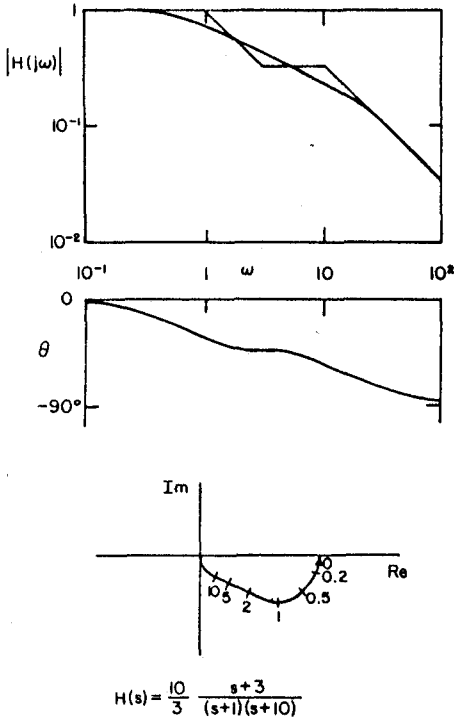


Fig. 6-12. Magnitude, phase, and polar plots (two poles and one zero in left half-plane).

For one group of delayed neutrons, there are two poles and one zero; see eq. (3-55) or (3-57). Since  $\lambda \ll \beta/\ell$ , the critical-reactor transfer function is qualitatively given in fig. 6-9 by the case for  $a < b$ . For the subcritical reactor, one would have a curve like fig. 6-12, though the poles and zeros would be much further apart (see figs. 3-9 and 3-10).

For six delay groups, there are six closely spaced alternating poles and zeros and one pole far out on the negative real axis. The effect is seen in figs. 3-4 and 3-5. The neutron generation time affects only the high-frequency pole as shown in figs. 3-6 and 3-7. Fig. 3-8 shows the one-group transfer function in various approximations as given by eqs. (3-59) through (3-63). The reader should compare these with appropriate cases in figs. 6-7 and 6-8.

To see the effect of linear feedback reactivity, we replace  $\delta\rho$  in eq. (3-40) by  $\delta\rho - \rho_f$ , where  $\rho_f$  is the feedback reactivity of eq. (5-70). We neglect both  $\rho_f\delta n$  and  $\delta\rho\delta n$  and take Laplace transforms; the Laplace transform of the feedback kernel  $h(t)$  is the feedback transfer function  $H(s)$  of eq. (5-75). Proceeding as in sec. 3-2, we solve for the

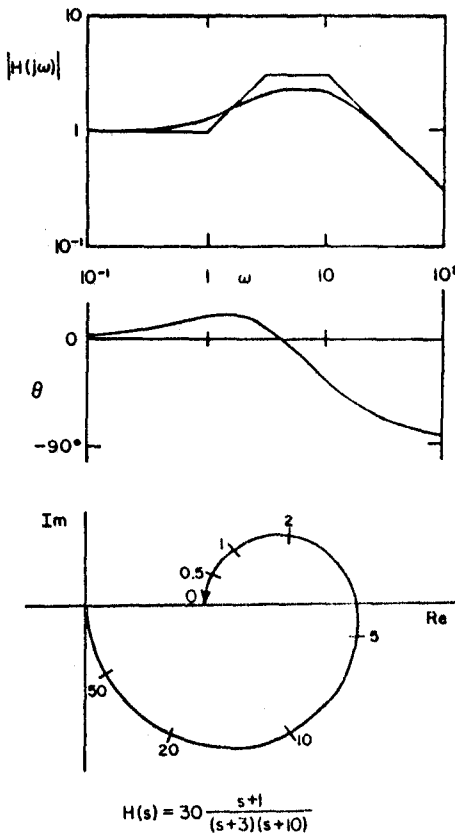


Fig. 6-13. Magnitude, phase, and polar plots (two poles and one zero in left half-plane).

Laplace transform of the steady-state portion of the response:

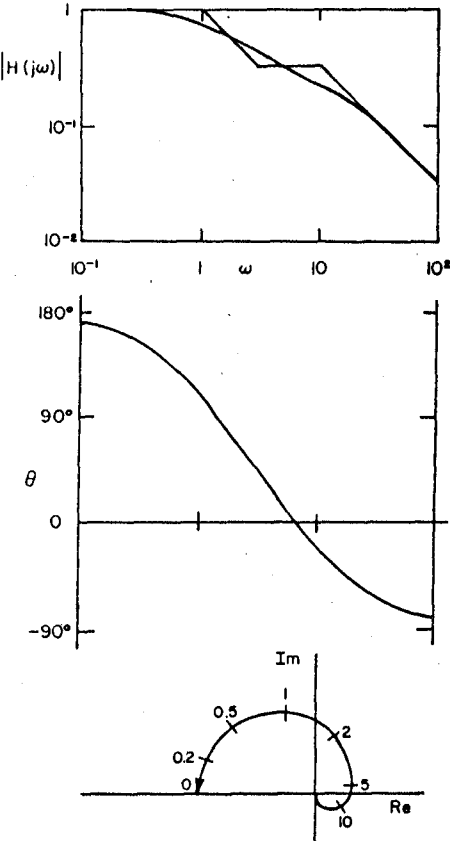
$$\delta N(s) = \frac{n_0 \delta R(s)}{\zeta s + \beta - \rho_0 - \sum_i \frac{\beta_i \lambda_i}{s + \lambda_i} + n_0 H(s)}. \quad (6-44)$$

This may be compared with eq. (3-42). From eqs. (3-43) and (6-44), the closed-loop transfer function is

$$Y(s) = \frac{\delta N(s)}{\delta R(s)} = \frac{G(s)}{1 + G(s)H(s)}. \quad (6-45)$$

This establishes the closed-loop formulation of eq. (6-3), represented by the block diagram of fig. 6-1, from another viewpoint. Note that  $G(s)$  from eq. (3-43) is proportional to the equilibrium power  $n_0$ , while

286      Linear System Stability



$$H(s) = \frac{10}{3} \frac{s-3}{(s+1)(s+10)}$$

Fig. 6-14. Magnitude, phase, and polar plots (two poles in left half-plane, one zero in right-half plane).

$H(s)$  in sec. 5-4 contains feedback parameters only; this means that the open-loop gain is proportional to  $n_0$ .

Next, we describe a simple graphical method for sketching the closed-loop transfer function when the forward and feedback transfer functions  $G(s)$  and  $H(s)$  are known. If there is a frequency range for which  $|G(j\omega)H(j\omega)| \gg 1$ , then by eq. (6-45),

$$|Y(j\omega)| \cong 1/|H(j\omega)|. \quad (6-46)$$

On the other hand, when  $|G(j\omega)H(j\omega)| \ll 1$ ,

$$|Y(j\omega)| \cong |G(j\omega)|. \quad (6-47)$$

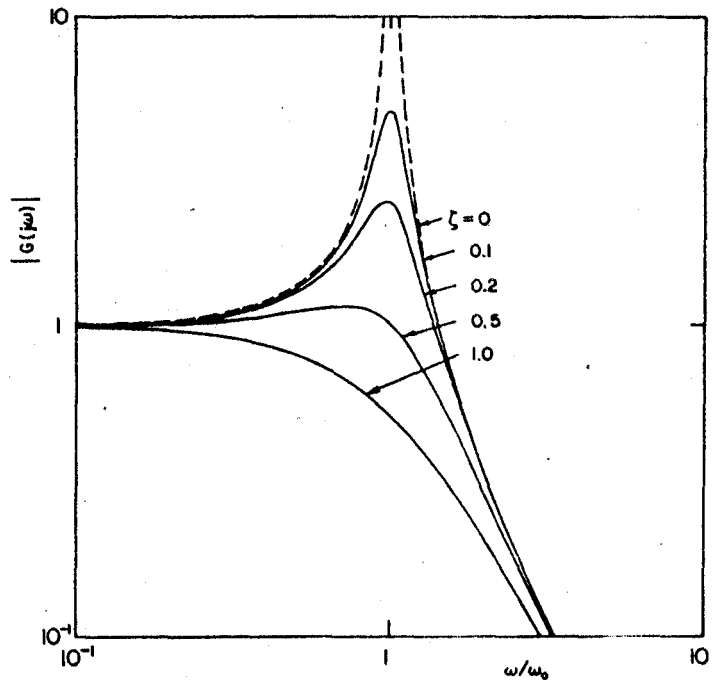


Fig. 6-15. Magnitude plots for quadratic factor with complex poles.

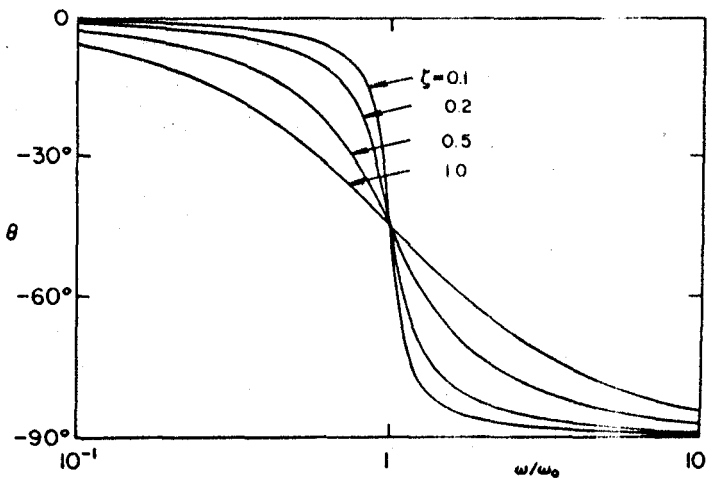


Fig. 6-16. Phase plots for quadratic factor with complex poles.

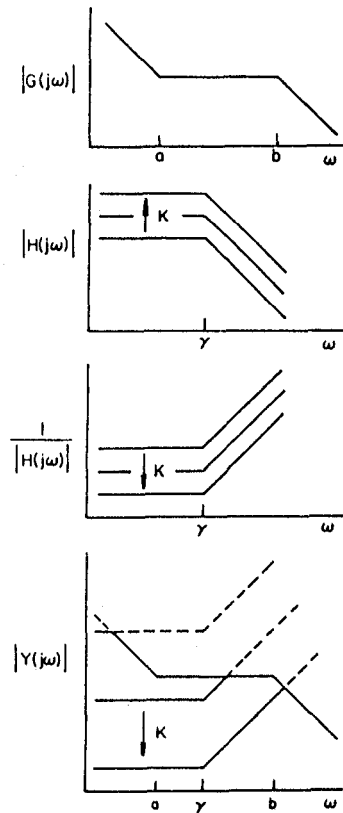


Fig. 6-17. Construction of qualitative magnitude plot for a closed-loop transfer function (log-log plots).

If one sketches magnitude plots for  $G$  and  $1/H$ , then the magnitude plot for  $Y$  follows the lower of the two curves. This is true because  $Y$  follows  $1/H$  when  $G$  is larger, and  $Y$  follows  $G$  when  $1/H$  is larger. The scheme fails near the crossing of  $G$  and  $1/H$  because the denominator of eq. (6-45) might approach zero in certain cases; this will be discussed in connection with the Nyquist stability criterion.

We illustrate by a simple example, shown in fig. 6-17. Suppose

$$G(s) = \frac{s + a}{s(s + b)}$$

and

$$H(s) = \frac{K}{s + \gamma},$$

where  $a < \gamma < b$ . Increasing  $K$  depresses the magnitude curve for  $1/H$ . Three possibilities for  $Y$  are shown (three different values for the magnitude of the gain). If one has the additional information that  $G(j\omega)H(j\omega)$  is not close to  $-1$  when its magnitude is near one (i.e., if the phase is not near  $180^\circ$ ), these composite curves are qualitatively correct for the entire frequency range.

Such is the case for the simple reactor model with a temperature feedback that follows Newton's law of cooling.

Using eq. (3-57) for  $G(s)$  and eq. (5-76) for  $H(s)$ , where we identify  $a$  with  $\lambda$  and  $\gamma$  with the reciprocal time constant for heat transfer, we use fig. 6-17 to deduce the magnitude curve in fig. 6-18 for the case  $\gamma > \lambda$ . The parameter is  $\alpha$ , the magnitude of the negative temperature coefficient of reactivity, and we do not include the unrealistic case of  $\alpha$  so great that the pole at  $s \cong -\beta/\alpha$  is suppressed. In this particular case, it can be shown that  $Y$  represents a minimum-phase system and that the phase can be correctly inferred from the magnitude of  $Y(j\omega)$  as sketched in fig. 6-18.

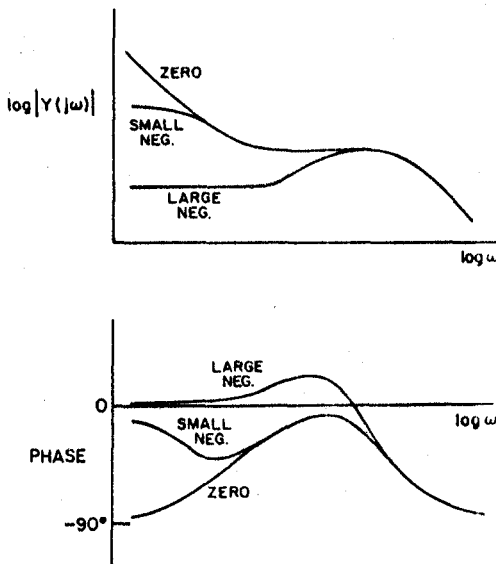


Fig. 6-18. Reactor transfer function (qualitative) for negative temperature coefficient of reactivity in the case  $\gamma > \lambda$ .

The open-loop gain for this system may be taken as  $\alpha K n_0 / \lambda$ . One might associate the factor  $n_0$  with the feedback by plotting  $G/n_0$  and  $n_0 H$ . The curves in fig. 6-18 could therefore be interpreted as showing the effect on  $Y/n_0$  when any of the three parameters  $\alpha$ ,  $K$ , or  $n_0$  is increased.

The student should construct curves corresponding to those in fig. 6-18 for the case  $\gamma < \lambda$ .

Finally, we note the utility of eq. (6-6), which expresses the feedback transfer function in terms of the forward and closed-loop transfer functions. By measuring the reactor transfer functions at low and high power and identifying them with  $G$  and  $Y$  respectively, the feedback transfer function can be calculated from the data. This has proved useful in a number of reactor stability studies (e.g., Smith et al. 1960).

#### 6-4. The Nyquist Criterion

The denominator of the system transfer function  $Y(s)$  of eq. (6-3) may be written as

$$f(s) = 1 + G(s)H(s). \quad (6-48)$$

The zeros of  $f(s)$  are the roots of the characteristic equation. A method of determining whether  $f(s)$  has zeros in the right half of the complex  $s$ -plane was developed by Nyquist (1932). The method is based on a theorem in the theory of complex variables relating a certain closed-contour integral to the number of zeros and poles within the contour (Titchmarsh 1939; Whittaker and Watson 1940; Wylie 1960).

We paraphrase the theorem as follows: Let  $f(s)$  be analytic and different from zero on a simple closed contour  $C$ , and let  $f(s)$  be analytic within  $C$  except at a finite number of poles. Then

$$\frac{1}{2\pi j} \oint_C \frac{f'(s)}{f(s)} ds = Z - P, \quad (6-49)$$

where  $Z$  and  $P$  are respectively the number of zeros and poles of  $f(s)$  within  $C$ , each counted according to its multiplicity. The contour is traversed counterclockwise, and  $f'(s)$  means  $df/ds$ .

Now  $f(s)$  may be regarded as a mapping, and a traverse of  $C$  in the  $s$ -plane corresponds to a traverse of the mapped contour  $C'$  in the  $f$ -plane. Since

$$\frac{f''}{f'} ds = \frac{df}{f} = d(\log f),$$

each counterclockwise encirclement of the origin in the  $f$ -plane contributes  $2\pi j$  to the integral along  $C$ . Eq. (6-49) becomes

$$E = Z - P, \quad (6-50)$$

where  $E$  is the number of counterclockwise encirclements of the origin by  $C'$  in the  $f$ -plane as the closed contour  $C$  is traversed once in the  $s$ -plane.

To apply this result in linear stability analysis, we select a contour which encloses the entire right half of the  $s$ -plane. Examples of this so-called  $\Gamma$ -contour are shown in fig. 6-19. If  $G(s)H(s)$  represents a physically realizable system, then  $f(s) \rightarrow 1$  on the large semicircle at infinity, and the conditions of the theorem are not violated. However, there may be poles on the imaginary axis that must be bypassed on small semicircles as indicated in fig. 6-19; as a radius is made infinitesimal, the corresponding part of the map in the  $f$ -plane remains highly significant.

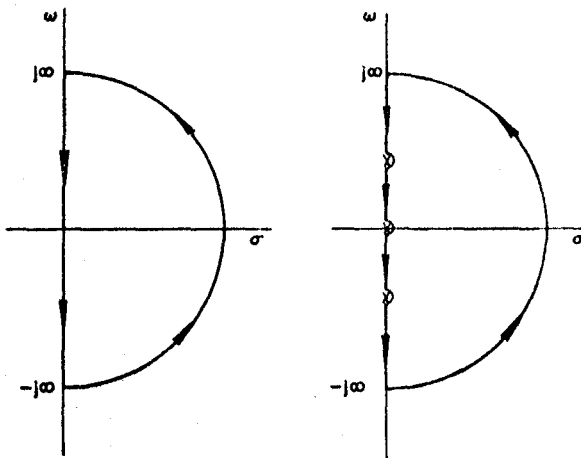


Fig. 6-19. Integration contours ( $\Gamma$ -contours) enclosing the right half of the  $s$ -plane.

To apply the method to feedback systems, we note that the origin in the  $f$ -plane is the point  $-1$  in the  $GH$ -plane. It is generally simpler to work with the mapping  $GH$ , and we regard  $E$  as the number of counter-clockwise encirclements of the  $-1$  point in the  $GH$ -plane as  $\Gamma$  is traversed once. If the closed-loop system is stable, then  $f$  has no zero inside  $\Gamma$  and  $Z = 0$ . The Nyquist criterion (necessary and sufficient) may now be stated as follows: The linear feedback system represented by eq. (6-3) is stable if

$$E = -P, \quad (6-51)$$

where  $E$  is the number of counterclockwise encirclements of the  $-1$  point in the  $GH$ -plane for each traverse of  $\Gamma$  and  $P$  is the number of poles of  $GH$ , or  $f$ , within  $\Gamma$ . This may be summarized by saying that the system is stable if there is one clockwise (negative) encirclement of the  $-1$  point for each pole of  $GH$  in the right half-plane. The locus, or mapping, in the  $GH$ -plane is called the Nyquist plot.

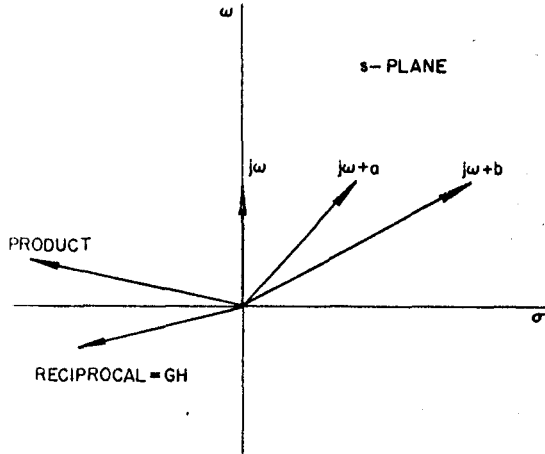


Fig. 6-20. Vector diagram (Argand diagram) for example 1.

*Example 1.* The open-loop transfer function is given by eq. (6-17),

$$G(s)H(s) = \frac{K}{s(s + a)(s + b)}, \quad (6-52)$$

where  $a$  and  $b$  will be taken as positive. Select a  $\Gamma$ -contour as in fig. 6-19 with one indentation to circumvent the pole at the origin. On the imaginary axis,

$$G(j\omega)H(j\omega) = \frac{K}{j\omega(j\omega + a)(j\omega + b)}. \quad (6-53)$$

For large  $\omega$ ,

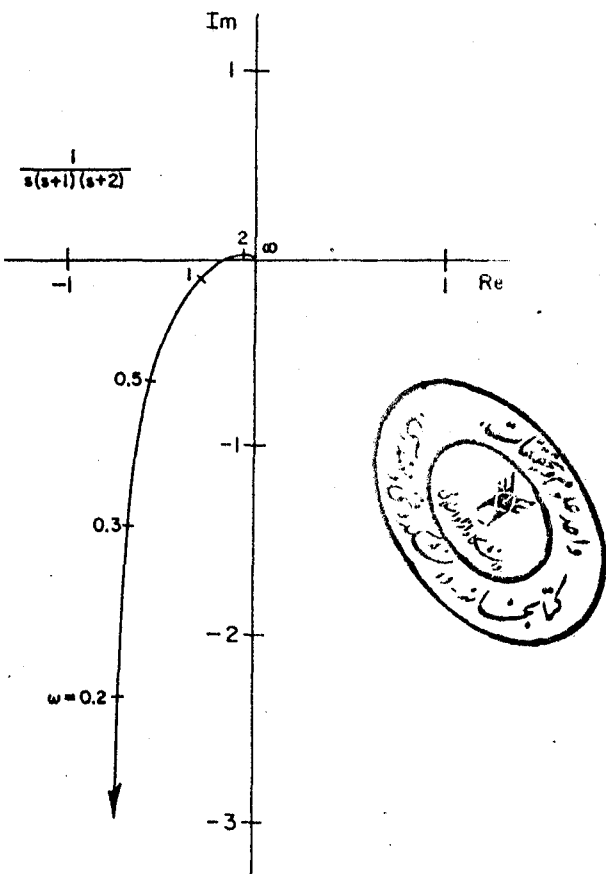
$$G(j\omega)H(j\omega) \cong jK/\omega^3, \quad (6-54)$$

while for small  $\omega$ ,

$$G(j\omega)H(j\omega) \cong -jK/ab\omega. \quad (6-55)$$

As we come down the positive imaginary axis in the  $s$ -plane, the locus traced out in the  $GH$ -plane emerges from the origin at the phase angle  $90^\circ$  and eventually approaches infinity at a phase angle  $-90^\circ$  (or  $270^\circ$ ).

To determine the behavior at intermediate frequencies, select a frequency near  $a$  or  $b$  and sketch a vector diagram (Argand diagram) representing the factors in eq. (6-53), as shown in fig. 6-20. The denominator is found by adding the phases of the three vectors, and  $GH$  is the reciprocal whose phase is found by changing the sign of the phase of the denominator (assuming  $K > 0$ ). It is seen that because  $GH$  has a

Fig. 6-21. The polar plot (Nyquist plot) for  $K = 1, a = 1, b = 2$  in example 1.

negative real part the locus is to the left of the origin in the  $GH$ -plane. This portion of the locus is the polar plot sketched for this function in fig. 6-10, and a numerical example ( $K = 1, a = 1, b = 2$ ) is plotted to scale in fig. 6-21. This corresponds to the segment  $AB$  in the  $GH$ -plane in fig. 6-22.

Near the origin in the  $s$ -plane, we detour on the small semicircle  $BCD$  in fig. 6-22. From eq. (6-52),

$$G(s)H(s) \cong K/abs.$$

Let  $s = \rho \exp(j\phi)$ , where  $\rho$  is small. Then

$$GH \cong (K/ab\rho) \exp(-j\phi).$$

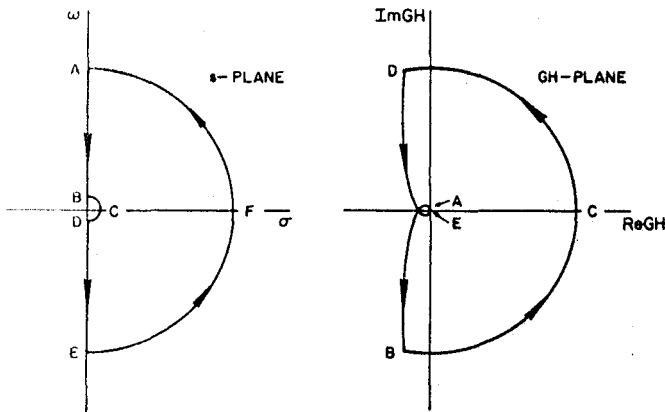


Fig. 6-22. The  $\Gamma$ -contour in the  $s$ -plane and its map (the Nyquist plot) in the  $GH$ -plane for example 1.

As the small circle in the  $s$ -plane is traversed clockwise from  $+90^\circ$  to  $-90^\circ$ , a large circle in the  $GH$ -plane is traversed in the opposite direction ( $-90^\circ$  to  $+90^\circ$ ).

The segment  $DE$  maps into a mirror image of the polar plot, obtained by taking the complex conjugate (replace  $j\omega$  by  $-j\omega$ ). This brings us back to the origin in the  $GH$ -plane (approaching, however, from below). The  $\Gamma$ -contour is not yet closed. From eq. (6-52),

$$G(s)H(s) \cong K/s^3.$$

Let  $s = R \exp(j\theta)$ , where  $R$  is large. Then

$$GH \cong (K/R^3) \exp(-j3\theta).$$

The large semicircle in the  $s$ -plane, traversed counterclockwise, maps into one and one-half tiny circles in the  $GH$ -plane, traversed clockwise. This closes the  $\Gamma$ -contour and puts the phase right at the origin of the  $GHI$ -plane.

We now apply the Nyquist criterion. There is no pole in the right half-plane, and by eq. (6-51) the system is stable if  $E = 0$  (no encirclement of the  $-1$  point in the  $GH$ -plane). Multiplication by a positive number  $K$  simply changes the scale of the Nyquist plot. From fig. 6-22, there will be no encirclement of the  $-1$  point if  $K$  is small, but there will be a counterclockwise encirclement if  $K$  is sufficiently large. This system is stable for small positive  $K$  and unstable for large positive  $K$ , in agreement with the Routh criterion as applied in sec. 6-2. For negative  $K$ , the Nyquist plot is rotated  $180^\circ$  so that it always encircles the  $-1$  point, and the system is unstable for all  $K < 0$ .

The threshold of instability occurs when  $G(j\omega)H(j\omega) = -1$ . From eq. (6-53) we may derive

$$\operatorname{Re}[G(j\omega)H(j\omega)] = -\frac{K(a+b)}{(\omega^2 + a^2)(\omega^2 + b^2)} \quad (6-56)$$

and

$$\operatorname{Im}[G(j\omega)H(j\omega)] = \frac{K(\omega^2 - ab)}{\omega(\omega^2 + a^2)(\omega^2 + b^2)}. \quad (6-57)$$

Note that the real part is an even function of  $\omega$  and the imaginary part an odd function, whence the symmetry of the Nyquist plot about the real axis. By eq. (6-57), the imaginary part vanishes at  $\omega^2 = ab$ , giving the resonance frequency found in sec. 6-2. Substituting this in the right-hand side of eq. (6-56), setting the left-hand side equal to  $-1$ , and solving for  $K$  yields

$$K = ab(a+b),$$

which confirms the upper limit of the stability range as given in eq. (6-19).

*Example 2.* From eq. (6-22),

$$G(s)H(s) = \frac{K}{(s-1)(s+2)} \quad (6-58)$$

and

$$G(j\omega)H(j\omega) = \frac{K}{(j\omega-1)(j\omega+2)}. \quad (6-59)$$

For large  $\omega$ ,

$$G(j\omega)H(j\omega) \cong -K/\omega^2,$$

and for  $\omega = 0$ ,

$$GH = -K/2.$$

A quick sketch like that in fig. 6-20 shows that  $GH$  is in the third quadrant for  $\omega > 0$ . A scale drawing for  $K = 1$  is shown in fig. 6-23. Since there are no poles of  $GH$  on the imaginary axis, there is no need to indent the  $\Gamma$ -contour.

There is a pole in the right half-plane ( $P = 1$ ). Because stability requires  $E = -1$  by eq. (6-51), the loop must enclose the  $-1$  point for stability (one clockwise encirclement). The threshold is  $GH = -1$ , which occurs at  $\omega = 0$  and  $K = 2$ . No encirclement is possible for negative  $K$ ; therefore the stability range is  $K > 2$ .

(a) *Linear System Stability*

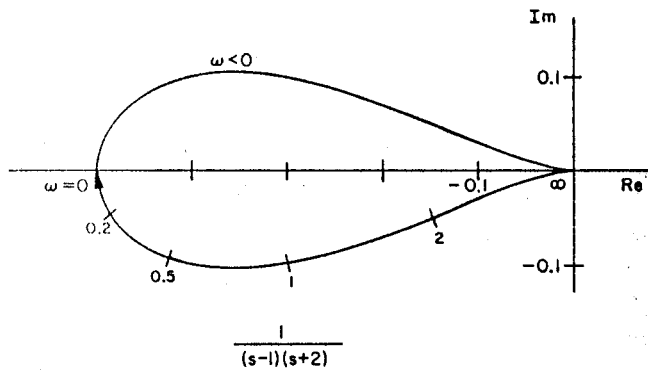


Fig. 6-23. Nyquist plot for  $K = 1$  in example 2.

*Example 3.* From eq. (6-24),

$$G(s)H(s) = \frac{K(s+a)}{s(s-b)}, \quad (6-60)$$

where  $a$  and  $b$  are positive. We find that the Nyquist plot starts from the origin at  $-90^\circ$  and tends to infinity at  $+90^\circ$ . The real part remains negative throughout. Since there is a pole at the origin, a large semicircle is traced counterclockwise. Since there is a pole in the right half-plane, one clockwise encirclement of the  $-1$  point is required for stability. As seen in fig. 6-24, this can occur only for sufficiently large  $K$ .

We find

$$\operatorname{Re}[G(j\omega)H(j\omega)] = -\frac{K(a+b)}{\omega^2 + b^2}$$

and

$$\operatorname{Im}[G(j\omega)H(j\omega)] = \frac{K(ab - \omega^2)}{\omega(\omega^2 + b^2)}.$$

The threshold is  $GH = -1$ , which yields  $\omega^2 = ab$  and  $K = b$ . The stability range is  $k > b$ , in agreement with the Routh criterion.

*Example 4.* From eq. (6-26),

$$G(s)H(s) = \frac{K(s-a)}{s(s+b)}, \quad (6-61)$$

where  $a$  and  $b$  are positive. Again, the Nyquist plot starts from the origin at  $-90^\circ$  and tends to infinity at  $+90^\circ$ . This time, however, the real part is positive. See fig. 6-25.

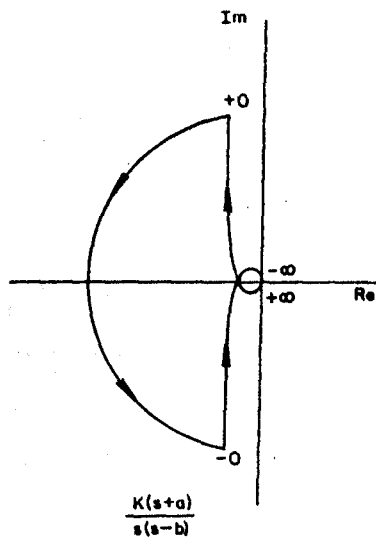


Fig. 6-24. Nyquist plot for example 3.

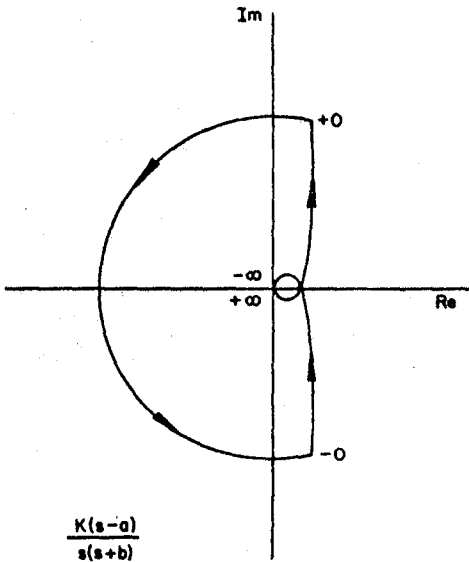


Fig. 6-25. Nyquist plot for example 4.

Since there is no pole in the right half-plane, stability requires that there be no encirclement of the  $-1$  point. This can happen only for a negative  $K$  of sufficiently small magnitude (rotate the Nyquist plot  $180^\circ$ ). By setting  $GH = -1$ , the threshold is found to be  $\omega^2 = ab$ ,

$K = -b$ . The stability range is therefore  $-b < K < 0$ .

For negative  $K$ , one could just as well look at the Nyquist plot as is and consider encirclement of the  $+1$  point. We prefer not to do this because of the risk of confusion about the sign of the feedback.

*Example 5.* From eq. (6-28),

$$G(s)H(s) = \frac{K}{(s-1)(s+2)(s+\alpha)}. \quad (6-62)$$

The Nyquist plot emerges from the origin at  $+90^\circ$  and ends at  $-K/2\alpha$  on the negative real axis (for positive  $K$  and  $\alpha$ ). For intermediate values of  $\omega$  the situation is more complicated than in the previous examples.

By making a few vector sketches as in fig. 6-20, it can be ascertained that the locus for  $\omega > 0$  is entirely in the second quadrant only for sufficiently small  $\alpha$ . This means that the Nyquist plot is a counter-clockwise loop. Since there is a pole in the left half-plane, stability requires a clockwise encirclement of the  $-1$  point, which is impossible for any  $K$  when  $\alpha$  is small.

For large  $\alpha$ , the locus enters the third quadrant as  $\omega$  decreases. The Nyquist plot is a figure 8, with a clockwise loop on the left. For intermediate  $K$ , the  $-1$  point can be captured in the clockwise loop, making the system stable.

We find

$$\operatorname{Re}[G(j\omega)H(j\omega)] = -K \frac{(\alpha+1)\omega^2 + 2\alpha}{(\omega^2 + 1)(\omega^2 + 4)(\omega^2 + \alpha^2)}$$

and

$$\operatorname{Im}[G(j\omega)H(j\omega)] = K \frac{\omega(\omega^2 - \alpha + 2)}{(\omega^2 + 1)(\omega^2 + 4)(\omega^2 + \alpha^2)}.$$

The imaginary part vanishes three times if  $\alpha > 2$ . Examples are shown in fig. 6-26. Setting  $\omega^2 = \alpha - 2$  in the equation for the real part and requiring  $GH = -1$  yields the upper threshold  $K = \alpha^2 + \alpha - 1$ . This is the dynamic stability boundary found by the Routh criterion. Since the other threshold is  $\omega = 0$ ,  $K = 2\alpha$ , the stability range is  $2\alpha < K < \alpha^2 + \alpha - 1$ .

Fig. 6-4 shows the parameter space for the system of example 5. The student may sketch a Nyquist plot for negative  $\alpha$  and verify the instability.

Note that the qualitative features of fig. 6-26 could have been deduced from fig. 6-23 together with the polar plot for  $1/(s + \alpha)$  in fig. 6-7. If frequencies are labeled on two polar plots, the polar plot for the product is easily sketched.

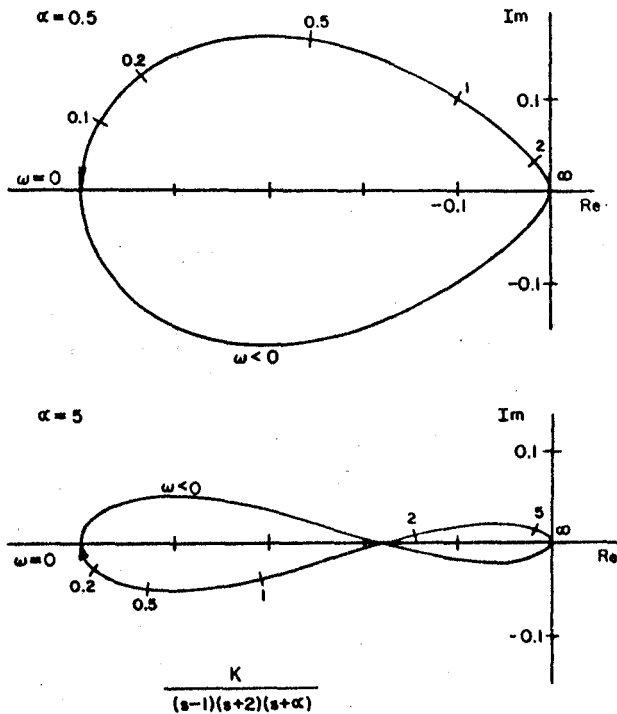


Fig. 6-26. Nyquist plots for example 5.

This completes the five special examples. We shall return to them in the next section after outlining the root-locus method. We complete the present section with a few additional observations about stability and the frequency response.

An advantage of the Nyquist method is that it can be applied to a system with a transport time delay. A signal  $f(t)$  transmitted with a time delay  $T$  may be represented by  $f(t - T)$ . If the Laplace transform of  $f(t)$  is  $F(s)$ , and if  $f(t) = 0$  for  $t < 0$ , then the transform of the delayed signal is  $\exp(-Ts) \cdot F(s)$ . The Nyquist method may be applied in the presence of the exponential factor; the essential singularity at infinity does not affect the contour in the right half-plane.

A simple example is shown in fig. 6-27. The system without time delay would be stable for all positive  $K$  because the Nyquist plot for  $1/s$  is closed by a large half-circle to the right. With time delay, the Nyquist plot is altered by the exponential factor, whose polar plot is also given in fig. 6-27. The Nyquist plot for the system is the spiral shown in fig. 6-28.

270      Linear System Stability

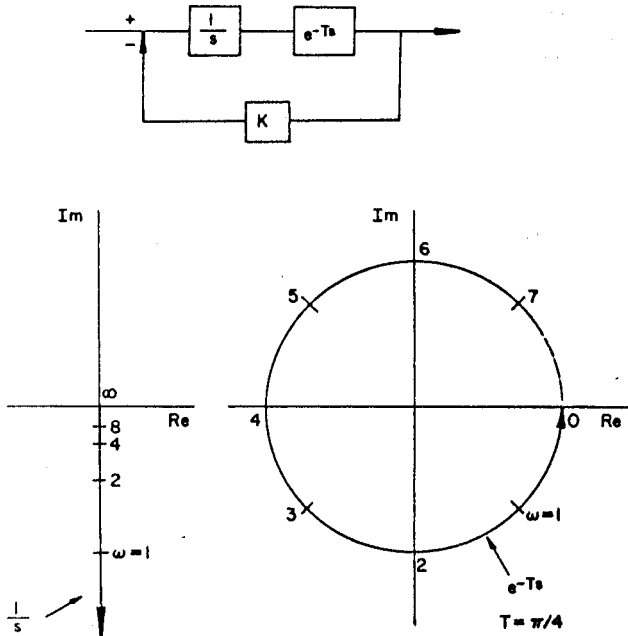


Fig. 6-27. Example with transport time delay.

The system is stable for small  $K$ . As  $K$  increases, the  $-1$  point is encircled twice, then four times, etc. The first crossing of the real axis occurs at  $\omega T = \pi/2$ , and the system is unstable for  $K > \pi/2T$ . The time delay has converted a system that is stable for all positive  $K$  into a conditionally stable system whose stability range decreases as the delay increases.

The time-delay operator may be approximated by a rational function of  $s$  (a ratio of polynomials) by using truncated power series. Higher accuracy naturally requires a larger number of poles and zeros.

Next, we note that the stability of simple systems may often be inferred directly from the magnitude plot of the open-loop frequency response. Consider the system of example 1 (figs. 6-21 and 6-22). The magnitude and phase plots are shown in fig. 6-10. The threshold of instability occurs when the Nyquist plot crosses the real axis at  $-1$ . This means a magnitude of one and a phase of  $-180^\circ$ . If  $K$  is such that the magnitude drops to one (0 db) before the phase reaches  $-180^\circ$ , the system is stable. A minimum-phase system such as this example can be evaluated roughly just by looking at the magnitude plot.

The closeness of approach to the instability threshold in conditionally stable systems of this type may be expressed quantitatively by the phase

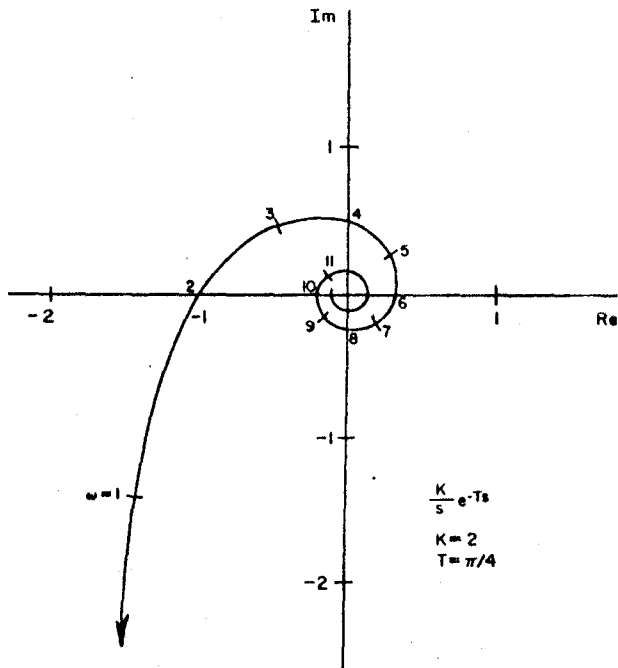


Fig. 6-28. Open-loop transfer function for example with transport time delay.

margin and the gain margin. These are defined as shown in fig. 6-29, where a Nyquist plot for a typical stable system is shown in relation to the unit circle in the  $GH$ -plane.

Another graphical method for determining linear stability may be expressed in terms of the forward and feedback transfer functions separately. Suppose we have a forward transfer function  $G(s)$  and a feedback  $KH(s)$ . We construct polar plots for  $1/G(j\omega)$  and  $-KH(j\omega)$  as shown in fig. 6-30. If these two loci can be made to intersect at the same  $\omega$  for some critical gain  $K_c$ , then the system is conditionally stable and  $K_c$  represents the threshold of instability.

This method is difficult to apply in practice. A related method which gives a sufficient condition for linear stability and is much simpler to use will now be described. Consider the example of fig. 6-30. Since the phase angles are negative (phase lags) for all frequencies, the critical condition may be expressed as

$$1/|G(j\omega)| = K|H(j\omega)| \quad (6-63)$$

and

$$|\theta_G(j\omega)| + |\theta_H(j\omega)| = \pi. \quad (6-64)$$

272 • Linear System Stability

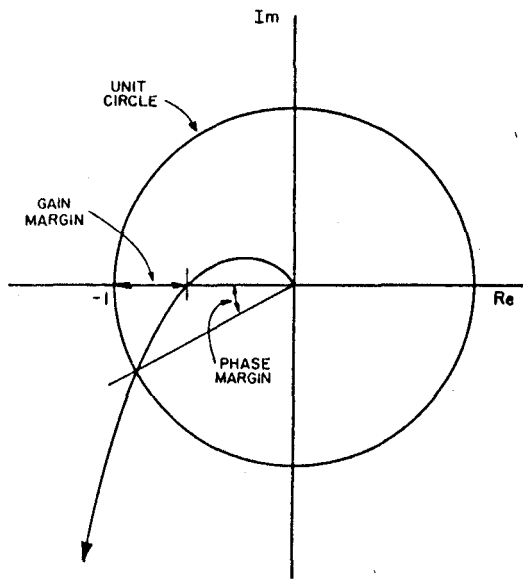


Fig. 6-29. Phase margin and gain margin for a conditionally stable system.

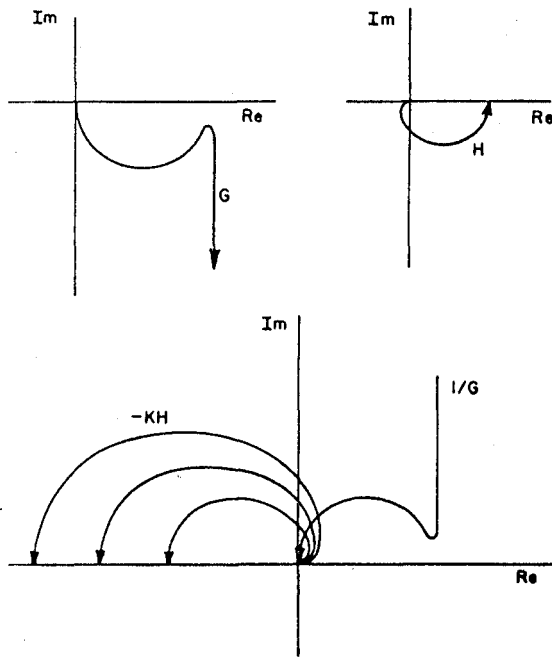


Fig. 6-30. Polar plots showing intersections of  $1/G$  and  $-KH$ .

We plot

$$\tau_G(j\omega) = \frac{\pi - |\theta_G|}{\omega} \quad (6-65)$$

and

$$\tau_H(j\omega) = \frac{|\theta_H|}{\omega} \quad (6-66)$$

as functions of  $1/|G(j\omega)|$  and  $K|H(j\omega)|$  respectively. These are sketched in fig. 6-31 as semilog plots. The arrows show the direction of decreasing frequency.

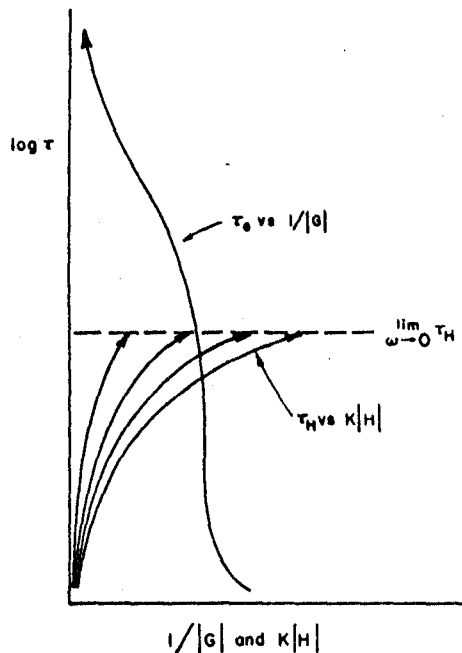


Fig. 6-31. Illustration of sufficient condition for linear stability (Störmer 1960).

As in fig. 6-30, the system is critical if the forward and feedback loci can be made to intersect at the same frequency. However, unlike the sketch in fig. 6-30, this figure has a range of  $K$  for which no intersection occurs. Note that all feedback curves approach the same limiting value of  $\tau_H$  as  $\omega \rightarrow 0$ . If  $K$  is sufficiently small that the limit point lies to the left of the  $\tau_H$  locus, no intersection is possible at any frequency and the system is stable. This is a sufficient but not necessary condition for linear stability.

274      *Linear System Stability*

Consider the limiting value of  $\tau_H$ . For example, if

$$KH(s) = \frac{K}{(s+a)(s+b)}, \quad (6-67)$$

as in the present example (see fig. 6-10), then

$$\tan \theta_H(j\omega) = \frac{(a+b)\omega}{\omega^2 - ab}.$$

We find

$$\lim_{\omega \rightarrow 0} \tau_H(j\omega) = \frac{a+b}{ab} = \frac{1}{a} + \frac{1}{b}.$$

If in addition  $a \ll b$ , then

$$\lim_{\omega \rightarrow 0} \tau_H(j\omega) \cong 1/a. \quad (6-68)$$

The limit point of the  $\tau_H$  locus is therefore characterized by the largest time constant in the feedback system and by the magnitude  $KH(0)$ .

One can take advantage of this in experimental investigations of stability. Suppose  $G$  is well known over the entire frequency range, as with the zero-power reactor transfer function. In fact, if the reactor transfer function is normalized by multiplying by  $\beta/n_0$ , the  $\tau_G$  curve is essentially a universal curve for reactors (except for the break at the lower right beyond  $\omega = \beta/\ell$ ). Suppose in addition that the feedback is well known only for low frequencies; i.e., the values of  $KH(0)$  and the largest time constant are known. This gives the limit point of the  $\tau_H$  locus. If, in addition, it can be assumed that

$$|H(j\omega)| \leq |H(0)| \quad (6-69)$$

and

$$\tau_H(j\omega) \leq \lim_{\omega \rightarrow 0} \tau_H(j\omega), \quad (6-70)$$

as in fig. 6-31, stability may be inferred from the location of the limit point of  $\tau_H$  without detailed knowledge of the  $\tau_H$  locus at higher frequencies. We therefore have a sufficient condition for linear stability that requires only partial knowledge of the feedback.

The conditions represented by eqs. (6-69) and (6-70) are frequently, but not always, satisfied. For example, see fig. 6-13. However, for many practical situations, the method is successful. It was devised and applied to fast-breeder reactors by Störrer (1960), and a summary is reproduced in the book by Keppin (1965).

Finally, consider the method of sketching magnitude plots for  $Y(s)$  when the magnitudes for  $G(s)$  and  $H(s)$  are known (see fig. 6-17). At the

crossing of the magnitude curves for  $G$  and  $1/H$ , the Nyquist plot for  $GH$  crosses the unit circle in the  $GH$ -plane. If  $Y(s)$  is a minimum-phase system, its phase can be inferred from its magnitude plot.

For example, suppose the magnitude curve for  $Y$  changes its slope from 0 to  $-1$  at the crossover point. If  $Y$  represents a minimum-phase system, its phase goes from  $0^\circ$  to  $-90^\circ$ . If the slope changes from 1 to  $-2$ , or 0 to  $-3$ , the net phase variation is  $-270^\circ$ .

Instability arises when the complex number  $1 + G(j\omega)H(j\omega)$  goes through zero. This is accompanied by a sudden phase change, which is reflected in the phase of  $Y(j\omega)$ . Therefore, a large change of slope in the magnitude curve for  $Y$  that occurs at the crossing of  $G$  and  $1/H$  is associated with instability. A useful rule of thumb for minimum-phase systems may be stated as follows: If the net change of slope in the magnitude curve for  $Y(s)$  at the crossover point (magnitude of  $G$  equals magnitude of  $1/H$ ) is zero or  $-1$ , the system is stable. If the net change of slope is  $-3$ ,  $-4$ , etc., the system is unstable. If the net change is  $-2$ , further investigation is necessary.

There are many other varieties of stability tests based on representations of the frequency response. The reader may consult the texts cited at the beginning of sec. 6-1.

### 6-5. The Root-Locus Method

In the root-locus method, the roots of the characteristic equation are investigated by determining how these roots change position in the  $s$ -plane as a parameter (usually the gain  $K$ ) is varied. A stable linear system becomes unstable when a root (or pair of roots) crosses the imaginary axis and enters the right half-plane. This may be contrasted with the Nyquist method, in which the open-loop transfer function is studied as a function of position along the imaginary axis in the  $s$ -plane.

The root-locus method as used in control-system stability analysis was developed by Evans (1950, 1954), who also contrived a mechanical device to aid in the graphical construction of root-locus plots. A basic ingredient of the method is the classical idea of equiphase plots in the theory of complex variables: given a function of a complex variable  $F(s)$ , lines may be constructed in the  $s$ -plane along which the phase of  $F(s)$  is a constant. The method is not restricted to rational functions (ratios of polynomials).

We write eq. (6-48), the denominator of the system transfer function  $Y(s)$ , as

$$f(s) = 1 + G(s)H(s) = 1 + KF(s), \quad (6-71)$$

where  $K$  is real. The roots of the characteristic equation are the roots of

$$F(s) = -1/K.$$

Consequently, the root locus is the  $180^\circ$  equiphase line of  $F(s)$  for positive  $K$  and the zero equiphase line for negative  $K$ . We proceed to enumerate several rules for construction of the root locus for  $F(s)$  a ratio of polynomials such that  $F(s) \rightarrow 0$  as  $|s| \rightarrow \infty$  (corresponding to a physically realizable open-loop transfer function).

Suppose the open-loop transfer function is

$$G(s)H(s) = KF(s) = K \frac{(s - r_1)(s - r_2)\dots(s - r_n)}{(s - p_1)(s - p_2)\dots(s - p_{m+n})}, \quad (6-72)$$

where  $m$  and  $n$  are positive integers. The roots  $r_i$  and  $p_i$  are assumed to be real or to occur in conjugate pairs. Note first that

$$\lim_{K \rightarrow 0} G(s)H(s) = 0 \quad (6-73)$$

except for  $s \rightarrow p_i$ . The characteristic equation

$$G(s)H(s) = -1 \quad (6-74)$$

cannot be satisfied for  $K \rightarrow 0$  unless  $s \rightarrow p_i$ , which leads to:

*Rule 1.* As  $K \rightarrow 0$ , the locus coincides with the poles of the open-loop transfer function.

Next, note that

$$\lim_{K \rightarrow \infty} G(s)H(s) = \infty \quad (6-75)$$

unless  $s \rightarrow r_i$  or  $s \rightarrow \infty$ . The characteristic equation cannot be satisfied for  $K \rightarrow \pm \infty$  unless  $F(s) \rightarrow 0$ , which leads to:

*Rule 2.* As  $K \rightarrow \pm \infty$ , the locus approaches the zeros of the open-loop transfer function, including the  $m$  zeros at infinity.

Now consider the phase (the argument) of  $G(s)H(s)$ . From eqs. (6-72) and (6-74),

$$\begin{aligned} \arg [G(s)H(s)] &= \arg(K) + \sum_{i=1}^n \arg(s - r_i) - \sum_{i=1}^{m+n} \arg(s - p_i) \\ &= (2k + 1)\pi, \end{aligned} \quad (6-76)$$

where  $k$  is an integer. For  $K > 0$ , the phase of  $K$  is zero. We have

$$\sum_{i=1}^n \arg(s - r_i) - \sum_{i=1}^{m+n} \arg(s - p_i) = (2k + 1)\pi. \quad (6-77)$$

On the real axis to the right of all roots and poles, the phases of all

factors arising from roots and poles on the real axis are zero. On the real axis the phases from conjugate pairs always add to zero. The left-hand side of eq. (6-77) is zero and the equation cannot be satisfied for any  $k$ .

On the real axis to the left of one root or pole (the algebraically largest of the  $r_i$  and  $p_i$ ), the left-hand side of eq. (6-77) is  $\pm\pi$  and the equation can be satisfied. Since  $\arg(K) = \pi$  for  $K < 0$ , these considerations lead to:

*Rule 3.* For positive (negative)  $K$ , the locus contains the real axis to the left (right) of an odd number of points  $s = r_i$  and  $s = p_i$ .

Next, consider the behavior as  $|s| \rightarrow \infty$ . From eq. (6-72),

$$G(s)H(s) \cong K/s^m.$$

On the locus,  $s^m \cong -K$ . Let

$$s = |s|e^{j\theta},$$

and for  $K > 0$ ,

$$-K = Ke^{j(2k+1)\pi}.$$

We find

$$\theta = \frac{2k+1}{m}\pi, \quad K > 0. \quad (6-78)$$

For  $K < 0$ , let

$$K = |K|e^{j(2k+1)\pi},$$

whence

$$\theta = 2k\pi/m, \quad K < 0. \quad (6-79)$$

As  $K \rightarrow \pm\infty$ , the locus is asymptotic to  $m$  straight lines radiating at the angles given by eq. (6-78) or (6-79).

If the system had no zeros and one pole of order  $m$  at  $s = B$ , the equation for the root locus would be

$$\frac{K}{(s - B)^m} = -1. \quad (6-80)$$

This represents  $m$  straight lines radiating from the point  $s = B$ . Comparing eqs. (6-72) and (6-80) and retaining only first-order terms, we find

$$B = \frac{\sum p_i - \sum r_i}{m}, \quad (6-81)$$

correct to first order. Calling eq. (6-80) the asymptotic locus, we have:

*Rule 4.* The asymptotic locus for large  $s$  consists of  $m$  straight lines radiating from a point  $s = B = (\sum p_i - \sum r_i)/m$  on the real axis, at angles  $\theta = (2k + 1)\pi/m$  for  $K > 0$  and  $\theta = 2k\pi/m$  for  $K < 0$ .

Symmetry about the real axis is assured because the replacement  $\omega \rightarrow -\omega$  in  $s = \sigma + j\omega$  is equivalent to  $s \rightarrow s^*$  and because  $P(s^*) = P^*(s)$  for a polynomial with real coefficients.

Following these rules, the root locus for many cases can be quickly sketched and the stability determined from the location of the roots. The magnitude of the gain at any point on the locus may be determined graphically from

$$|K| = \frac{|s - p_1| |s - p_2| \dots |s - p_{m+n}|}{|s - r_1| |s - r_2| \dots |s - r_n|}, \quad (6-82)$$

where, for example,  $|s - p_i|$  is the distance from the pole at  $p_i$  to the point in question.

The method has a unique advantage in that the root locus displays the presence or absence of oscillations for various values of  $K$ . The onset of oscillation is the point where the locus departs from the real axis (double root of the characteristic equation). To study this further, let  $s = \sigma + j\omega$  and write

$$K \frac{(\sigma - r_1 + j\omega)(\sigma - r_2 + j\omega) \dots}{(\sigma - p_1 + j\omega)(\sigma - p_2 + j\omega) \dots} = -1.$$

Each factor may be written as, for example,

$$\sigma - r_i + j\omega = (\sigma - r_i) \left( 1 + \frac{j\omega}{\sigma - r_i} \right).$$

Near the real axis ( $\omega \ll \sigma - r_i$ , etc.) we have, correct to the first order in  $\omega$ ,

$$K \frac{(\sigma - r_1)(\sigma - r_2) \dots}{(\sigma - p_1)(\sigma - p_2) \dots} \left[ 1 + j\omega \left( \frac{1}{\sigma - r_1} + \frac{1}{\sigma - r_2} + \dots - \frac{1}{\sigma - p_1} - \frac{1}{\sigma - p_2} - \dots \right) \right] = -1. \quad (6-83)$$

Since both sides of this equation must be real, we have either  $\omega = 0$  (on the real axis) or else

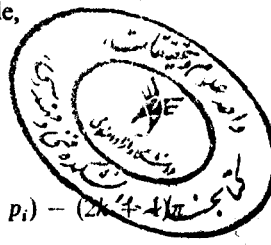
$$\begin{aligned} \frac{1}{\sigma - r_1} + \frac{1}{\sigma - r_2} + \dots + \frac{1}{\sigma - r_n} \\ = \frac{1}{\sigma - p_1} + \frac{1}{\sigma - p_2} + \dots + \frac{1}{\sigma - p_{m+n}}. \end{aligned} \quad (6-84)$$

Eq. (6-84) may be solved for  $\sigma$ , the real roots  $\sigma_d$  giving the locations of the departure points.

A useful rule is that the locus always departs from the real axis at right angles. This may be proved by retaining second-order terms in eq. (6-83) and then noting that the derivative  $d\omega/d\sigma$  becomes infinite as  $s \rightarrow \sigma_d$  from a point off the real axis.

When the open-loop transfer function has complex poles, it is helpful to compute the angle at which the locus emerges from such a pole. This may be accomplished by using eq. (6-76). For example,

$$\arg(s - p_1) = \arg(K) + \sum_{i=1}^n \arg(s - r_i) - \sum_{i=1}^{m+n} \arg(s - p_i) - (2k + 1)\pi$$



and

$$\lim_{s \rightarrow p_1} \arg(s - p_1) = \arg(K) + \sum_{i=1}^n \arg(p_1 - r_i) - \sum_{i=1}^{m+n} \arg(p_1 - p_i) - (2k + 1)\pi. \quad (6-85)$$

The angle of emergence from  $p_1$  is therefore expressed in terms of the angles to  $p_1$  from every other pole and zero.

A few apparent ambiguities not resolved by these rules will occasionally arise. We will encounter some later in the applications to reactor systems. As we shall see, these questions are usually answered by consideration of limiting cases.

*Example 1.* Given the open-loop transfer function of eq. (6-17),

$$G(s)H(s) = \frac{K}{s(s + a)(s + b)},$$

where  $a$  and  $b$  are real and positive (take  $a < b$ ). The locus begins at the real poles at 0,  $-a$ , and  $-b$ , and terminates at infinity. For  $K > 0$  the locus contains the real axis from 0 to  $-a$  and from  $-b$  to  $-\infty$ . Since  $m = 3$ , there are three asymptotes. By eq. (6-78),  $\theta = \pi/3$ ,  $\pi$ , and  $5\pi/3$ . By eq. (6-81), the three asymptotes radiate from the point  $s = B = -(a + b)/3$ .

The root locus for  $a = 1$ ,  $b = 2$  is shown in fig. 6-32. For  $K < 0$ , the

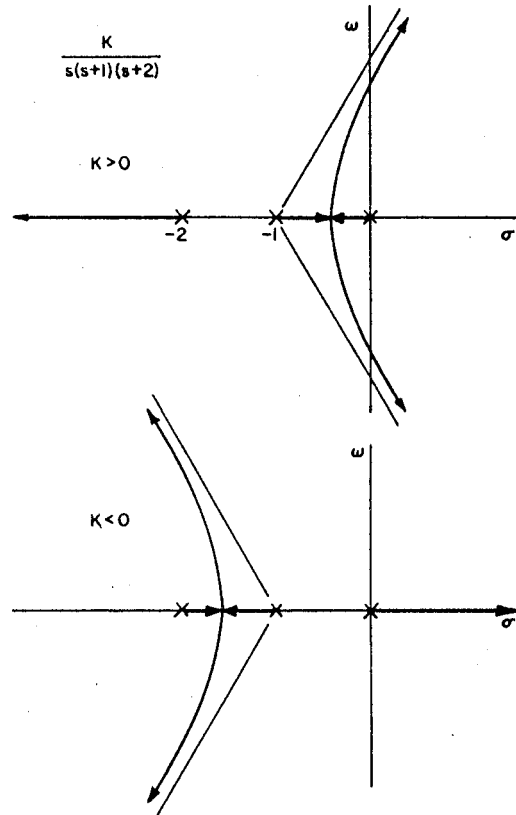


Fig. 6-32. Root locus for example 1.

asymptotes are at  $2\pi/3$ ,  $4\pi/3$ , and  $2\pi$  (zero). Arrows conventionally indicate the direction of increasing magnitude of  $K$ .

As shown by the Routh criterion (sec. 6-2), this system becomes unstable at  $K = ab(a + b) = 6$  with a critical frequency  $\omega = \sqrt{(ab)} = \sqrt{2}$ . This value of  $K$  is easily verified from the root locus by means of eq. (6-82). The departure point for positive  $K$  is  $\sigma_d = -0.423$ ,  $K = 0.384$ . This value of  $K$  may also be verified graphically using eq. (6-82). The system is unstable for all negative  $K$ , as shown by the positive real root.

*Example 2.* From eq. (6-22),

$$G(s)H(s) = \frac{K}{(s - 1)(s + 2)}.$$

The locus begins at the poles at  $+1$  and  $-2$  and terminates at infinity.

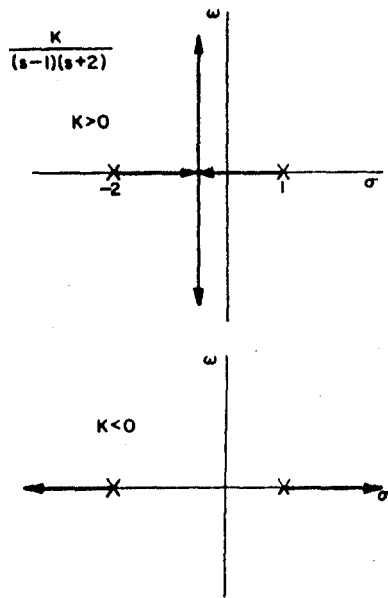


Fig. 6-33. Root locus for example 2.

The locus for positive  $K$  contains the real axis between the two poles. From eq. (6-78) for  $m = 2$ ,  $\theta = \pi/2$  and  $3\pi/2$ . From eq. (6-81),  $B = (1 - 2)/2 = -\frac{1}{2}$ . The locus is shown in fig. 6-33. The system is stable for  $K > 2$ .

The equation of the locus in the  $\sigma, \omega$  plane is easily derived for the general case of two poles and no zeros. The locus always consists of two perpendicular straight lines, and the departure point is midway between the poles.

*Example 3.* From eq. (6-24),

$$G(s)H(s) = \frac{K(s + a)}{s(s - b)},$$

where  $a$  and  $b$  are positive. The locus begins at  $s = 0$  and  $s = b$  and terminates at  $s = -a$  and infinity. For  $K > 0$ , the locus contains the real axis from 0 to  $b$  and from  $-a$  to  $-\infty$ . By eq. (6-78) with  $m = 1$ ,  $\theta = \pi$ . The system is stable for  $K > b$ . See fig. 6-34.

As with the previous example, it is not difficult to derive the equation for the locus in the  $\sigma, \omega$  plane. When the zero is not between two real poles, the locus consists of the real axis together with a circle whose center is at the zero location.

No. 2      *Linear System Stability*

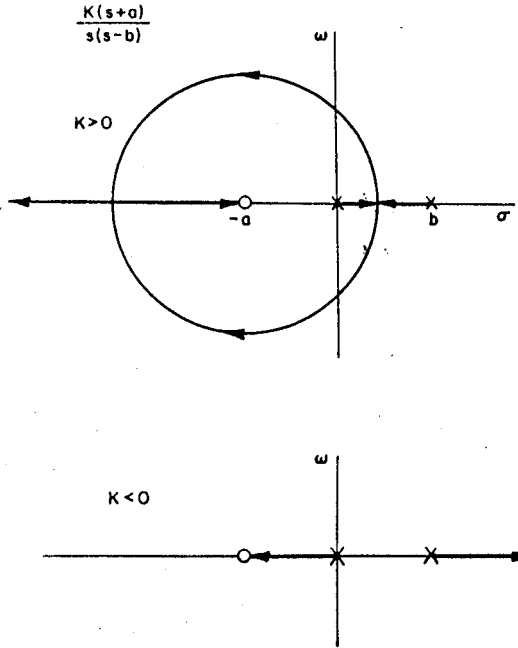


Fig. 6-34. Root locus for example 3.

*Example 4.* From eq. (6-26),

$$G(s)H(s) = \frac{K(s-a)}{s(s+b)}$$

The locus is shown in fig. 6-35. The system is stable for  $-b < K < 0$ .

*Example 5.* From eq. (6-28),

$$G(s)H(s) = \frac{K}{(s-1)(s+2)(s+\alpha)}$$

As shown by the Routh criterion, stability is possible only for  $\alpha > 2$ . Root-locus plots for  $\alpha = 0.5$  and  $\alpha = 5$  are shown in fig. 6-36 for positive  $K$ . The locus never leaves the right half-plane for small  $\alpha$ . It is easily shown that the departure point is at the origin for  $\alpha = 2$ .

*Example 6.* We conclude this section with an additional example to illustrate complex poles. Suppose

$$G(s)H(s) = \frac{K(s+2)}{s(s+3)(s^2+2s+2)}$$

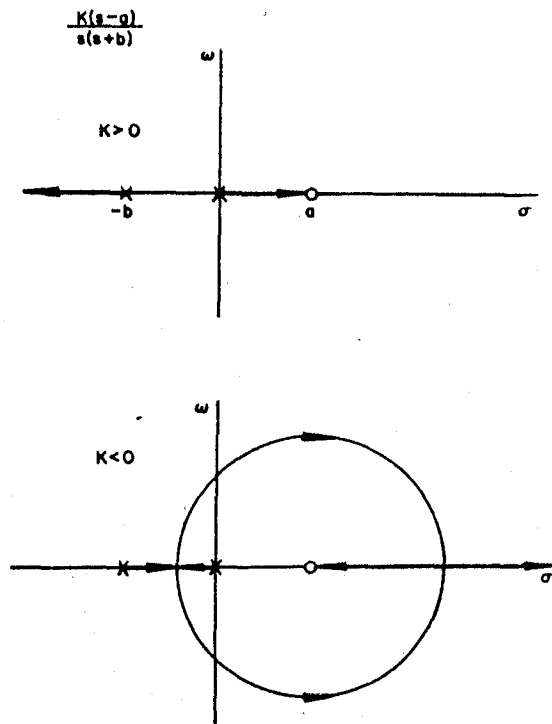


Fig. 6-35. Root locus for example 4.

The locus begins at the poles  $(0, -3, \text{ and } -1 \pm j)$  and terminates at  $-2$  and infinity. The locus for  $K > 0$  contains the real-axis segments from  $0$  to  $-2$  and  $-3$  to  $-\infty$ . Since  $m = 3$ , there is a segment from the upper pole to an asymptote at  $60^\circ$  ( $B = -1$ ). Call this pole  $p_1$  and apply eq. (6-85). The angles are then (poles labeled in clockwise order):

$$\begin{aligned}\arg(p_1 - r_1) &= 45^\circ; \\ \arg(p_1 - p_2) &= 135^\circ; \\ \arg(p_1 - p_3) &= 90^\circ; \\ \arg(p_1 - p_4) &= 26.5^\circ.\end{aligned}$$

With the convenient choice  $k = -1$ , we find

$$\lim_{s \rightarrow p_1} \arg(s - p_1) = -206.5^\circ + 180^\circ = -26.5^\circ.$$

The root locus for  $K > 0$  is shown in fig. 6-37.

The student should verify that the critical gain is 7.03 at a frequency  $\omega = 1.614$ . Since the asymptote crosses the imaginary axis at

### 28.4 Linear System Stability

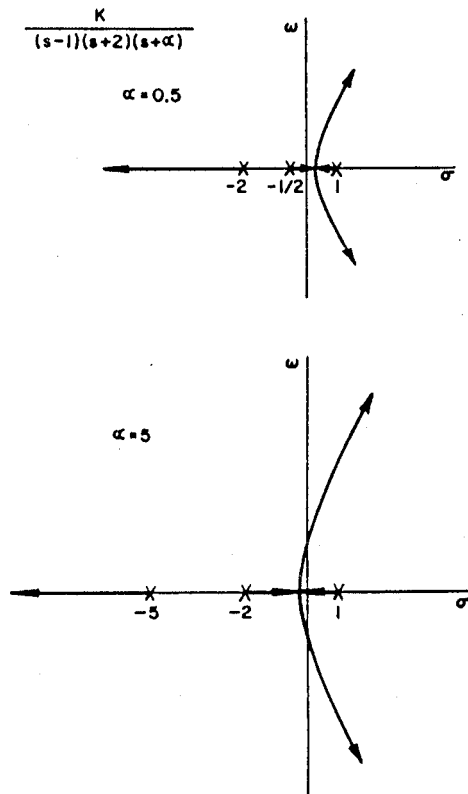


Fig. 6-36. Root-locus plots ( $K > 0$ ) for example 5.

$\tan^{-1} 60^\circ = 1.732$ , the locus must cross the asymptote before entering the right half-plane.

This completes the introduction to methods of linear stability analysis. We are now in a position to study the stability of a large number of nuclear reactor models.

### 6-6. Stability of Simple Reactor Systems

In this section we apply the methods of linear stability analysis to a variety of simple reactor models. The purpose is to study the effect of using different approximations for the zero-power reactor transfer function with (1) a single reactivity feedback following Newton's law of cooling and (2) a two-path feedback where one path is independent of frequency (constant power coefficient of reactivity).

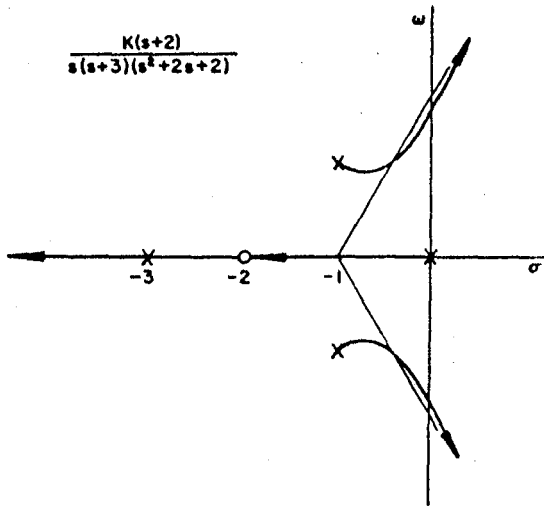


Fig. 6-37. Root locus for a system with complex open-loop poles.

For the first case, use the effective-lifetime model, eq. (3-61),

$$G(s) = n_0/\ell' s, \quad (6-86)$$

with eq. (5-76) for the feedback

$$H(s) = \frac{\alpha K_0}{s + \gamma}, \quad (6-87)$$

where  $\alpha$  is the negative of the temperature coefficient of reactivity,  $K_0$  is the reciprocal heat capacity,<sup>2</sup> and  $\gamma$  is the reciprocal time constant for heat loss. Of course, this feedback could arise from some physical effect other than temperature, provided the constants are properly interpreted.

We have

$$1 + G(s)H(s) = 1 + \frac{\alpha K_0 n_0}{\ell' s(s + \gamma)}. \quad (6-88)$$

Recall that the same form for  $G(s)$  is also used for a reactor with no delayed neutrons; compare eqs. (3-61) and (3-63). We choose to use the effective lifetime  $\ell' = \beta/\lambda$  in what follows. Eq. (6-88) becomes

$$1 + G(s)H(s) = 1 + \frac{K\lambda}{s(s + \gamma)}, \quad (6-89)$$

2. We use a subscript here so that the symbol  $K$  may be reserved for a different meaning.

where  $K = \alpha K_0 n_0 / \beta$ .

The characteristic equation is

$$D(s) = s^2 + \gamma s + K\lambda = 0. \quad (6-90)$$

This system is stable if  $\gamma > 0$  and  $K\lambda > 0$ . Because the only physical parameter that could have either sign is  $\alpha$ , the system is stable provided  $\alpha > 0$  (negative temperature coefficient). Nyquist and root-locus plots are sketched in fig. 6-38. Oscillations occur for  $K\lambda > \gamma^2/4$ , which suggests that too large a negative reactivity feedback may not always be desirable.

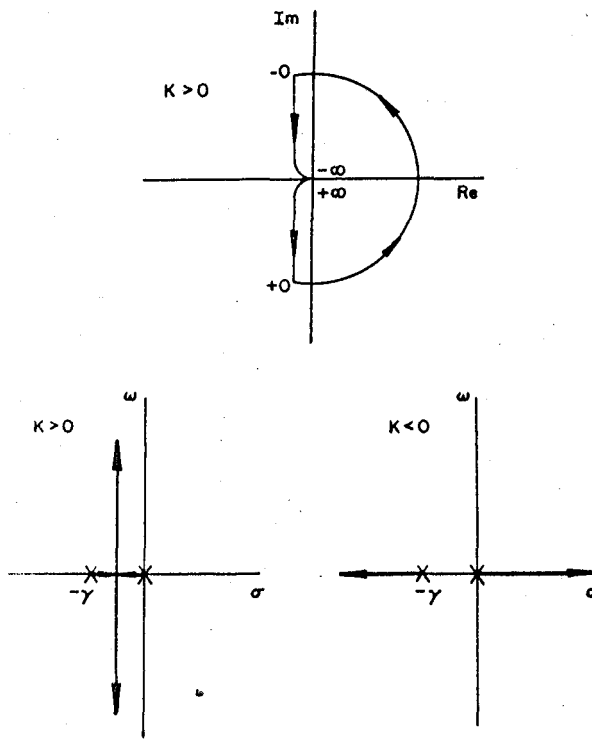


Fig. 6-38. Nyquist and root-locus plots for the effective-lifetime model with one reactivity feedback.

Note the special case  $\gamma \rightarrow 0$ . This is the "constant power removal" model (see sec. 5-4). The open-loop system has a double pole at the origin, and the closed-loop system is critical at all power levels. The characteristic equation is

$$s^2 = -K\lambda = -\alpha K_0 n_0 / \ell'.$$

This is the origin of the term "reactor natural frequency" used by many authors and given by the formula

$$\Omega = \sqrt{(\alpha K_0 n_0 / \ell')}. \quad (6-91)$$

For the second case, we introduce delayed neutrons by using the prompt-jump approximation. From eq. (3-59),

$$G(s) = \frac{n_0(s + \lambda)}{\beta s}. \quad (6-92)$$

With eq. (6-87), we have

$$1 + G(s)H(s) = 1 + \frac{\alpha K_0 n_0 (s + \lambda)}{\beta s (s + \gamma)}.$$

Again using  $K = \alpha K_0 n_0 / \beta$ , we have

$$1 + G(s)H(s) = 1 + \frac{K(s + \lambda)}{s(s + \gamma)}. \quad (6-93)$$

The characteristic equation is

$$D(s) = s^2 + (K + \gamma)s + K\lambda = 0. \quad (6-94)$$

This system is stable if  $K + \gamma > 0$  and  $K\lambda > 0$ . Again, the only physical parameter that can change sign is  $\alpha$ . The system is stable for  $\alpha > 0$  ( $K\lambda > 0$ ) because the condition  $K + \gamma > 0$  is automatically satisfied in that case. Nyquist and root-locus plots are shown in figs. 6-39 and 6-40.

The addition of delayed neutrons has not changed the range of stability, but there are other important differences. For example, it is more difficult to make this system oscillate, and, as seen most readily from the root-locus plots, it will not oscillate for any  $K$  if  $\gamma > \lambda$ .

We note for future reference the effect of delayed neutrons on the characteristic equations. Eq. (6-94) reduces to eq. (6-90) in the limit  $K \rightarrow 0$  but with  $K\lambda$  nonzero. This implies  $\lambda \rightarrow \infty$ . The physical meaning is that eq. (6-90) is valid only for  $|s| \ll \lambda$ , which is of course the range in which the effective-lifetime model and the prompt-jump approximation are equivalent (see fig. 3-8). This is reflected in the fact that the open-loop transfer functions in eqs. (6-89) and (6-93) are equivalent for  $|s| \ll \lambda$ .

This means that the simplest realistic procedure for studying the effect of delayed neutrons on stability is to use the one-group prompt-jump approximation and to compare it with its limit for  $|s| \ll \lambda$ . One is then comparing two systems whose low-frequency behaviors are the same. Compare, for example, the root-locus plots in figs. 6-38 and 6-39.

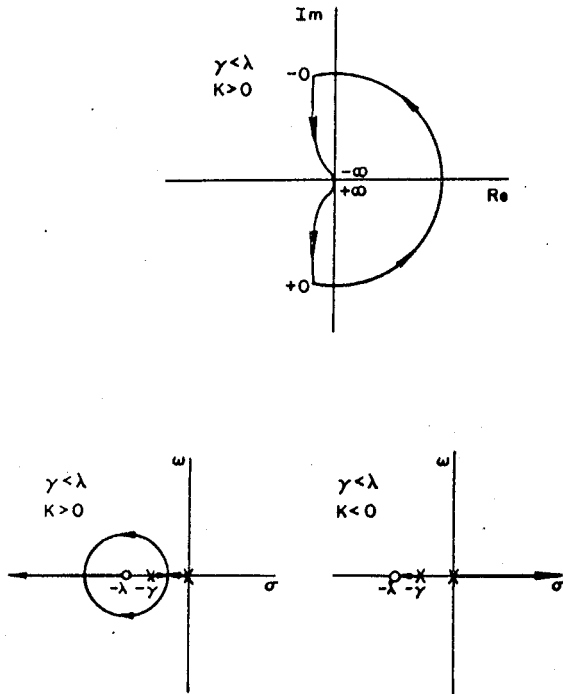


Fig. 6-39. Nyquist and root-locus plots for the prompt-jump model with one reactivity feedback ( $\gamma < \lambda$ ).

This is certainly more realistic than using eq. (3-57), which contains the neutron generation time, and then studying the effect of  $\beta \rightarrow 0$ ; this compares two models that coincide only for very high frequencies  $|s| \gg \beta/\ell$ , completely obscuring important phenomena in the low-frequency range.

Indeed, one can assert that eq. (6-93) and figs. 6-39 and 6-40 represent the simplest realistic model of a nuclear reactor with both delayed neutrons and reactivity feedback. This will be made particularly clear by the next example.

The second-order zero-power transfer function (one group of delayed neutrons), as given by eq. (3-58), is

$$G(s) = \frac{n_0(s + \lambda)}{\ell s(s + \beta/\ell)}. \quad (6-95)$$

Recall that the pole is really at  $s = -(\lambda + \beta/\ell)$ , but that  $\lambda \ll \beta/\ell$ .

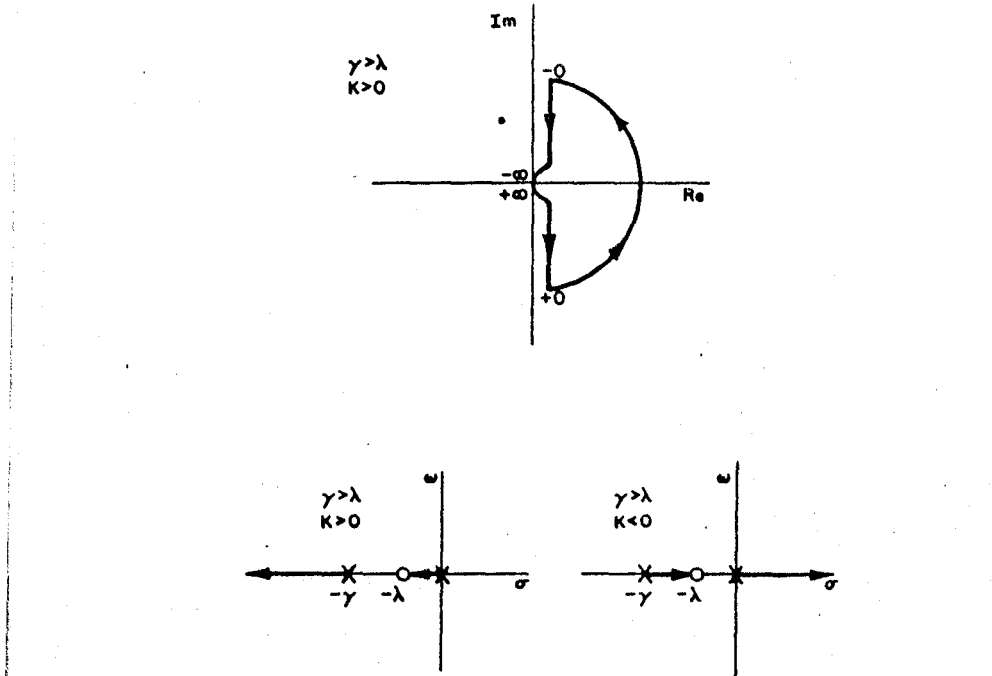


Fig. 6-40. Nyquist and root-locus plots for the prompt-jump model with one reactivity feedback ( $\gamma > \lambda$ ).

With eq. (6-87), we have

$$G(s)H(s) = \frac{\alpha K_0 n_0 (s + \lambda)}{\ell s(s + \gamma)(s + \beta/\ell)}. \quad (6-96)$$

For the moment, use  $K' = \alpha K_0 n_0 / \ell$  and write

$$G(s)H(s) = \frac{K'(s + \lambda)}{s(s + \gamma)(s + \beta/\ell)}. \quad (6-97)$$

The characteristic equation is

$$D(s) = s^3 + (\gamma + \beta/\ell)s^2 + (K' + \gamma\beta/\ell)s + K'\lambda = 0. \quad (6-98)$$

In terms of  $K = \alpha K_0 n_0 / \beta = K' \ell / \beta$ , this may be written as

$$D(s) = (\ell/\beta)s^3 + (1 + \gamma\ell/\beta)s^2 + (K + \gamma)s + K\lambda = 0. \quad (6-99)$$

The relation to eq. (6-94) in the limit  $\ell \rightarrow 0$  is now clear. More properly, this limit is  $|s| \ll \beta/\ell$  and  $\gamma \ll \beta/\ell$ .

The Routh array for eq. (6-99) is

$$\begin{array}{cc}
 \ell/\beta & K + \gamma \\
 1 + \gamma\ell/\beta & K\lambda \\
 K + \gamma - \frac{K\lambda\ell}{\beta + \gamma\ell} & 0 \\
 & K\lambda
 \end{array}$$

The condition  $K\lambda > 0$  is familiar, corresponding to  $\alpha > 0$  as in the previous examples. The second-last Routh number yields

$$K(\gamma - \lambda + \beta/\ell) + \gamma(\gamma + \beta/\ell) > 0. \quad (6-100)$$

The system will be stable for all positive  $K$  unless  $\lambda > \gamma + \beta/\ell$ , which is physically unrealistic. Actually, if we had retained the proper factor  $s + \lambda + \beta/\ell$  in  $G(s)$ , even this unrealistic possibility would not appear. The root locus cannot enter the right half-plane because the zero at  $-\lambda$  is always to the right of a pole at  $-(\lambda + \beta/\ell)$ . The system therefore has the same stability properties as the prompt-jump model.

Multiplying eq. (6-100) by  $\ell$  and letting  $\ell \rightarrow 0$  yields  $K + \gamma > 0$ , exactly as in the prompt-jump model. The relation between the second-order model and the prompt-jump model is illustrated by the Nyquist plots of fig. 6-41 and the root-locus plots of figs. 6-42 and 6-43. Comparison of these root-locus plots with those in figs. 6-39 and 6-40 is instructive. Because  $\ell$  is small, the pole at  $-\beta/\ell$  has very little effect on the

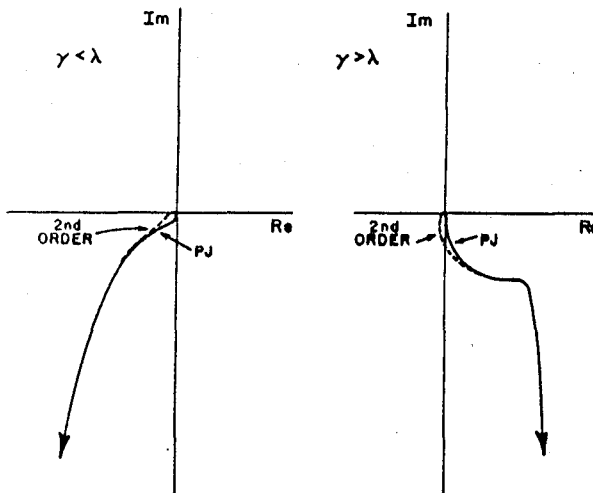
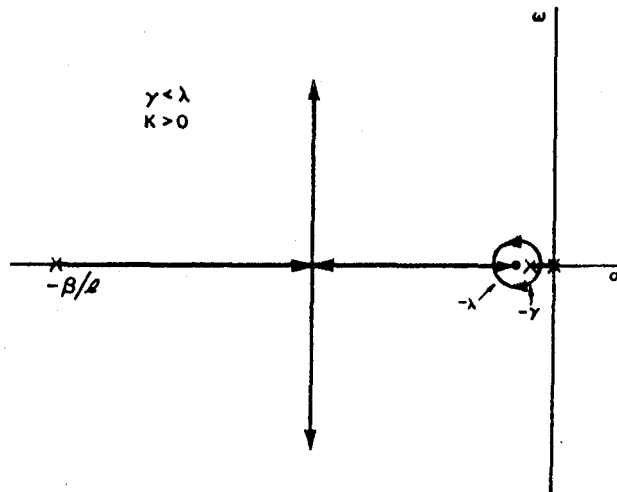
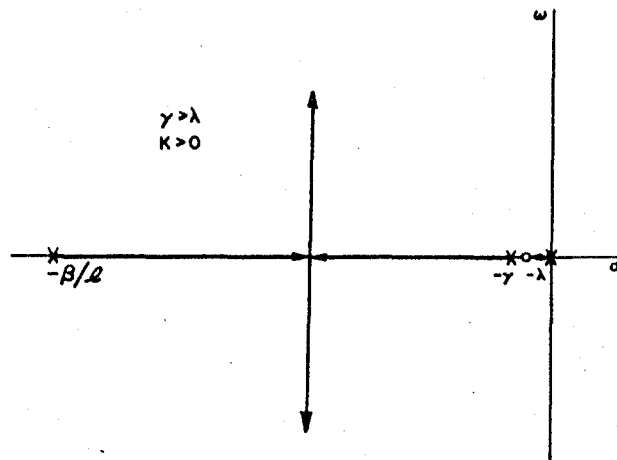


Fig. 6-41. Comparison of Nyquist plots for prompt-jump model and second-order model with one reactivity feedback.

Fig. 6-42. Root-locus plot for the second-order model with one reactivity feedback ( $\gamma < \lambda$ ).Fig. 6-43. Root-locus plot for the second-order model with one reactivity feedback ( $\gamma > \lambda$ ).

low-frequency behavior. The plots for the prompt-jump model are essentially magnified views of that portion of the *s*-plane where the physically significant phenomena are represented.

It must not be forgotten that these examples have only one group of delayed neutrons. The student should investigate, at least qualitatively, the effect of several groups (for example, sketch a root locus).

Return now to the effective-lifetime model, eq. (3-61) or (6-86), but add a second feedback loop in parallel:

$$H(s) = \kappa + \frac{\alpha K_0}{s + \gamma}, \quad (6-101)$$

where  $\kappa$  represents a constant power coefficient of reactivity arising from some unspecified phenomenon. The block diagram is shown in fig. 6-44. The feedback represented by  $\kappa$  is understood to be some process whose characteristic time is short compared to all other time constants in the system. We shall refer to this model as "one feedback region plus a power coefficient."

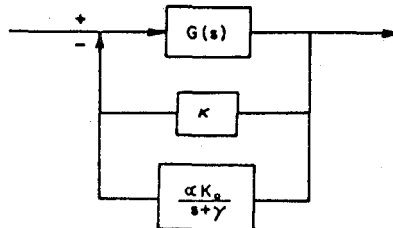


Fig. 6-44. Block diagram for the reactor model with one feedback region plus a power coefficient.

We have

$$G(s)H(s) = \frac{n_0}{\ell's} \left( \kappa + \frac{\alpha K_0}{s + \gamma} \right).$$

Using  $\ell' = \beta/\lambda$ , we may write

$$G(s)H(s) = \frac{\lambda}{s} \left( A + \frac{B}{s + \gamma} \right),$$

where

$$A = \kappa n_0 / \beta, \quad B = \alpha K_0 n_0 / \beta. \quad (6-102)$$

We find

$$G(s)H(s) = \lambda A \frac{s + \gamma + B/A}{s(s + \gamma)}. \quad (6-103)$$

The characteristic equation is

$$D(s) = s^2 + (\gamma + \lambda A)s + \lambda(\gamma A + B) = 0. \quad (6-104)$$

The system is stable if

$$A > -\gamma/\lambda \quad (6-105)$$

and

$$B > -\gamma A. \quad (6-106)$$

The parameter space is shown in fig. 6-45. The line  $A = -\gamma/\lambda$  is the dynamic stability boundary, and the line  $B = -\gamma A$  is the static stability boundary. This latter boundary has an important physical meaning in that the static power coefficient of reactivity

$$H(0) = \kappa + \alpha K_0 / \gamma \quad (6-107)$$

vaniishes on the static stability boundary. As we shall see,  $H(0) > 0$  is a necessary condition for stability with any of the various  $G(s)$  representing reactors.

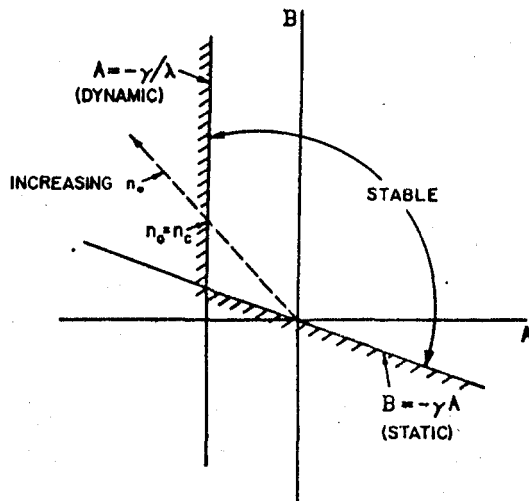


Fig. 6-45. Parameter space for a reactor with one feedback region plus a power coefficient (effective-lifetime model).

Note several features of this parameter space. By the definitions in eq. (6-102) together with our sign convention, both feedbacks are negative in the first quadrant. Further, a vertical line represents fixed  $\kappa$ , and a horizontal line fixed  $\alpha K_0$  for constant  $n_0$ . Since  $A/B$  is independent of  $n_0$ , increasing the power level with other parameters fixed is equivalent to moving outward on a radial line. One such line is shown in fig. 6-45, and the critical power  $n_c$  is designated. We say that the portion of the second quadrant defined by  $A < 0, B > -\gamma A$  is a region of conditional stability, while the region  $A > 0, B > -\gamma A$  is unconditionally stable.

Since the parameter  $\lambda A$  plays the role of the gain in eq. (6-103), the second quadrant represents systems with negative gain. The open-loop transfer function has a zero at  $s = -\gamma - B/A$ . Since in the region of conditional stability we have  $B/A < -\gamma$ , the zero is in the right half-plane. The root locus for this negative-gain nonminimum-phase system

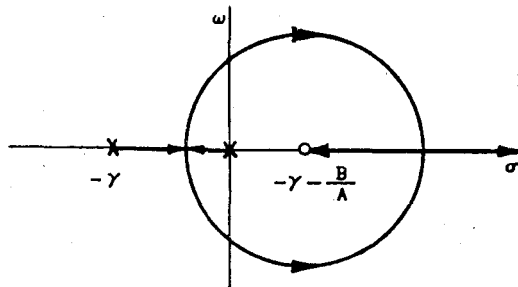


Fig. 6-46. Root locus showing conditional stability (one feedback region plus a power coefficient; effective-lifetime model).

is shown in fig. 6-46. We shall see that many of the interesting reactor systems are of this type.

The student should construct the other five root-locus plots that represent the rest of the possible cases for this example. It is also instructive to find the oscillation boundary in the  $A, B$  plane (locus of points for which the characteristic equation has two equal real roots). This is easily done for a quadratic characteristic equation, so that all the possible cases in the  $A, B$  plane (stable, unstable; oscillatory, non-oscillatory) may be correlated with points on root-locus plots. For example, a point on the oscillation boundary corresponds to a departure point of a root locus. The student will also find it helpful to sketch the Nyquist plots for the various cases.

We now introduce delayed neutrons by using eq. (6-92) for  $G(s)$ . We find

$$G(s)H(s) = \frac{n_0(s + \lambda)}{\beta s} \left( \kappa + \frac{\alpha K_0}{s + \gamma} \right).$$

Using eq. (6-102) to define  $A$  and  $B$ , we have

$$G(s)H(s) = \frac{A(s + \lambda)(s + \gamma + B/A)}{s(s + \gamma)}. \quad (6-108)$$

The characteristic equation is

$$D(s) = (1 + A)s^2 + (\gamma + \lambda A + \gamma A + B)s + \lambda(\gamma A + B) = 0. \quad (6-109)$$

The system is stable if all coefficients in eq. (6-109) are positive:

$$A > -1, \quad (6-110)$$

$$B > -(\lambda + \gamma)A - \gamma, \quad (6-111)$$

$$B > -\gamma A. \quad (6-112)$$

However, according to the Routh criterion, the system represented by eq. (6-109) is stable if all coefficients have the same sign (positive or negative). This would imply stability, not only as stated by eqs. (6-110) through (6-112), but also with these three inequalities reversed. This is physically unreasonable, particularly because the static power coefficient would have the wrong sign.

This pitfall of the prompt-jump approximation arises because the open-loop transfer function in eq. (6-108) does not vanish as  $s \rightarrow \infty$ . At least one of the two functions  $G$  or  $H$  should vanish for large  $s$ . Later, in sec. 6-8, we put things right by giving each of the two regions its own time constant. For the moment, however, we shall press into service the pole of  $G(s)$  at  $s \cong -\beta/\ell$ .

By using the second-order model of eq. (6-95) together with the feedback of eq. (6-101), and retaining  $A$  and  $B$  as defined by eq. (6-102), one obtains the characteristic equation

$$\begin{aligned} D(s) = & (\ell/\beta)s^3 + (1 + A + \gamma\ell/\beta)s^2 \\ & + (\gamma + \lambda A + \gamma A + B)s + \lambda(\gamma A + B) = 0. \end{aligned} \quad (6-113)$$

The Routh criterion may now be used to find stability boundaries in the  $A, B$  plane. The dynamic stability boundary is a hyperbola that degenerates to its straight-line asymptotes in the limit  $\ell \rightarrow 0$ , yielding stability requirements that are identical with eqs. (6-110) through (6-112).

One might be tempted to take the limit  $\ell \rightarrow 0$  in eq. (6-113), thus reproducing eq. (6-109). More properly, the leading term should be retained, if only as a reminder that positive (not negative) coefficients in eq. (6-109) correspond to a stable system.

The consequences of eqs. (6-110) through (6-112) may now be explored in terms of stable regions in the  $A, B$  plane. There are three stability boundaries:

$$\begin{aligned} A &= -1, \\ B &= -(\lambda + \gamma)A - \gamma, \\ B &= -\gamma A. \end{aligned}$$

The last two are the dynamic and static stability boundaries respectively, and they coincide at the point  $A = -\gamma/\lambda$ ,  $B = \gamma^2/\lambda$ . This is also the point where dynamic and static boundaries for the effective-lifetime model coincide in fig. 6-45. This is not surprising, since the characteristic equations for both the effective-lifetime and prompt-jump models, eqs. (6-104) and (6-109), have double roots  $s = 0$  at this point.

Consider first the case  $\gamma < \lambda$ , shown in fig. 6-47. The stability boundary  $A = -1$  lies to the left of the boundary  $A = -\gamma/\lambda$  (the dashed line) that we found for the effective-lifetime model. Comparing

figs. 6-45 and 6-47, we see that the stable region has been enlarged by delayed neutrons. The relation between the two reactor models may be clarified by comparing eqs. (6-104) and (6-109). The latter reduces to the former when  $A$  and  $B$  are small, provided the products  $\lambda A$  and  $\lambda B$  are not regarded as small.

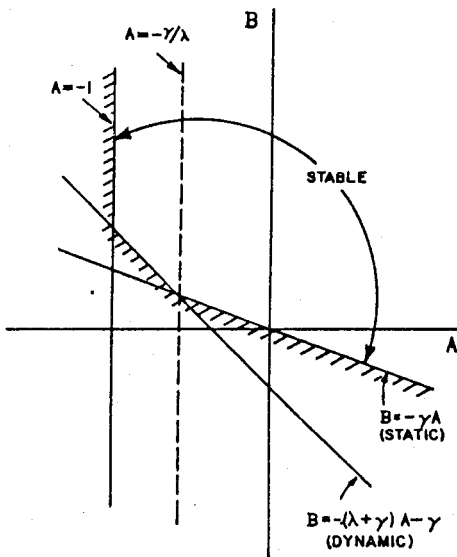


Fig. 6-47. Parameter space for a reactor with one feedback region plus a power coefficient (prompt-jump model,  $\gamma < \lambda$ ).

The case  $\gamma > \lambda$  is rather different, as shown in fig. 6-48. The boundary  $A = -1$  lies to the right of the line  $A = -\gamma/\lambda$ . Comparison of figs. 6-45 and 6-48 reveals that the stable region is smaller with delayed neutrons than with the effective-lifetime model. The area enclosed by *abcd* in fig. 6-48 is destabilized by the addition of delayed neutrons.

This example illustrates an extremely important point. Stability studies made by neglecting delayed neutrons in order to have a simpler system to analyze may be highly misleading. One might be tempted to leave out delayed neutrons on the intuitive basis that they should always help stability, and then attempt to approximate reality by using the effective lifetime. In our example this procedure is safe only for  $\gamma < \lambda$ .

We shall see in sec. 6-8 that this example is only a special case of a more general two-region reactor model, so that this behavior is not caused by the presence of a constant power coefficient. Nor is this a

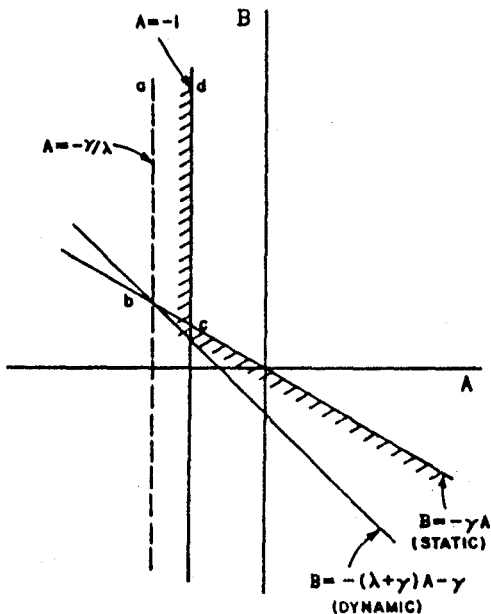


Fig. 6-48. Parameter space for a reactor with one feedback region plus a power coefficient (prompt-jump model,  $\gamma > \lambda$ ; area  $abcd$  is destabilized by delayed neutrons).

peculiarity of the prompt-jump approximation, as may be seen by comparing the Nyquist plots shown in fig. 6-49, where the stable system is the effective-lifetime model of eq. (6-103) and the unstable system is the second-order model of eq. (6-95) with the same feedback and with  $\gamma > \lambda$ . These two curves are for the same power level  $n_0$ , chosen to lie within the area  $abcd$  of fig. 6-48. When  $\gamma > \lambda$ , the zero at  $s = -\lambda$  has a chance to be effective at low frequency, hence the destabilizing effect of the delayed neutrons. (The parameters in fig. 6-49 are  $\lambda = 0.08 \text{ sec}^{-1}$ ,  $\gamma = 0.10 \text{ sec}^{-1}$ , and  $B/A = -0.11$ , with  $\beta/\ell$  sufficiently large that its effect is completely isolated. The gain is adjusted so that the two transfer functions are identical in the limit of zero frequency.)

Finally, another viewpoint is provided by the root locus shown in fig. 6-50. The large loop is not quite a circle unless one of the zeros is made to coincide with a neighboring pole. As  $\ell \rightarrow 0$ , the pole recedes to  $-\infty$  and the circle becomes infinite. As the magnitude of the negative gain increases, the locus approaches  $-\infty$  and reappears from  $+\infty$ . The transition occurs at the critical gain  $A = -1$ , as seen by eq. (6-108) and as expected from fig. 6-48.

A careful analysis of another destabilizing effect of delayed neutrons (improved stability as  $\beta \rightarrow 0$ ) appears in a paper by Smets (1966).

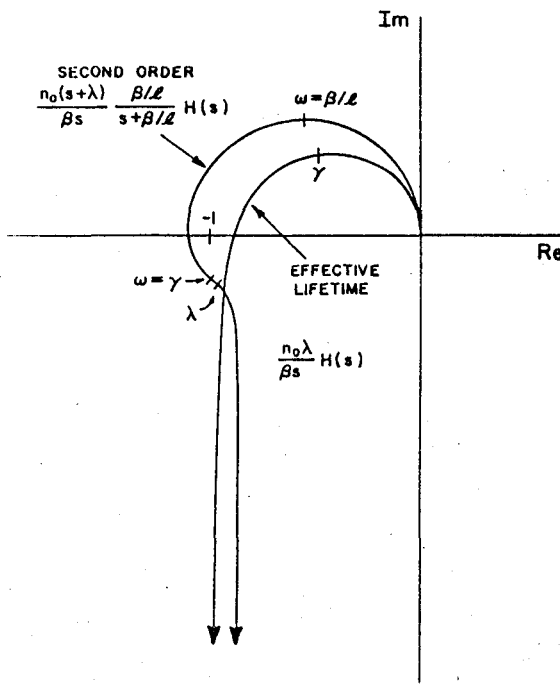


Fig. 6-49. Comparison of Nyquist plots showing destabilizing effect of delayed neutrons.

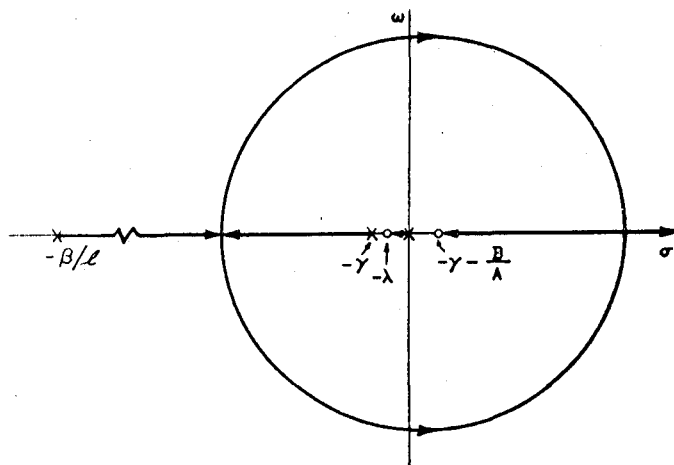


Fig. 6-50. Root locus for a reactor with one feedback region plus a power coefficient.

The question is further discussed by Tan (1969a, 1969b) and by Smets (1969). The conclusion is drawn that delayed neutrons will not necessarily increase the critical power and the damping of natural oscillations unless the feedback is a low-pass phase-lagging system. As we shall see, many of the interesting cases in the two-region reactor model do not have that type of feedback.

### 6-7. Two-Path Feedback: Effective-Lifetime Model

The point-reactor model with two reactivity feedbacks, each feedback having its own time constant (see fig. 6-51), has been the subject of much attention. Nonlinear examples without delayed neutrons have been studied by Ergen, Lipkin, and Nohel (1957), Gyftopoulos (1961), Lellouche (1966), and Shotkin (1963, 1964a). A detailed analysis of the linear system without delayed neutrons was made by Agresta (1961). Studies of linear stability with delayed neutrons are reported by Miida and Suda (1961), Schultz (1961), Skinner and Hetrick (1958), and Weaver (1963). Several other special examples are cited in later sections of this chapter and in chapter 7.

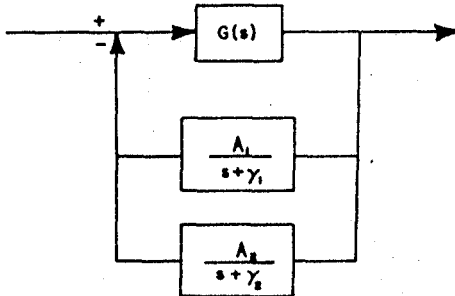


Fig. 6-51. Block diagram for a reactor with two-path feedback.

At first glance, the system of fig. 6-51 appears to be a very special case in that the two feedbacks are completely independent of each other. Actually, this decoupled system serves to represent infinitely many coupled systems, as will now be described.

Suppose we have two regions, each characterized by a space-average temperature. Let

$$\frac{dT_1}{dt} = b_1(n - n_0) - h_1(T_1 - T_2) - h_2 T_1 \quad (6-114)$$

and

$$\frac{dT_2}{dt} = b_2(n - n_0) + h_3(T_1 - T_2) - h_4 T_2,$$

where the  $h_i$  are reciprocal time constants for heat transfer. The terms  $h_1 n$  represent a split of the total power  $n$  between the two regions, and  $n_0$  is the total power at equilibrium. Each temperature is incremental, representing the temperature difference between operating and equilibrium states in each region. The terms  $-h_1(T_1 - T_2)$  and  $h_3(T_1 - T_2)$  represent a balance for heat transfer between regions; the coefficients are unequal because eq. (6-114) represents rates of temperature change and not rates of heat flow. The terms  $-h_2 T_1$  and  $-h_4 T_2$  represent heat loss from each region to constant-temperature reservoirs. The student should derive these equations, starting with total heat generation rates and actual temperatures (including the reservoirs), calculating the equilibrium relations, and introducing the incremental variables.

Analogous equations could represent physical phenomena other than heat flow and temperature feedback. For simplicity we shall refer to two temperatures in what follows. Eq. (6-114) is coupled to the neutron dynamics by

$$\rho = \rho_0 - \alpha_1 T_1 - \alpha_2 T_2 \quad (6-115)$$

where  $\alpha_1$  and  $\alpha_2$  represent the negatives of temperature coefficients of reactivity and where  $\rho_0 = 0$  at the equilibrium state  $n = n_0, T_1 = T_2 = 0$ .

Eqs. (6-114) and (6-115) may be transformed into a decoupled, or canonical, system for which

$$\frac{dT'_1}{dt} = K_1(n - n_0) - \gamma_1 T'_1, \quad (6-116)$$

$$\frac{dT'_2}{dt} = K_2(n - n_0) - \gamma_2 T'_2,$$

and

$$\rho = \rho_0 - \alpha_1' T'_1 - \alpha_2' T'_2. \quad (6-117)$$

This is most easily accomplished by seeking a similarity transformation that diagonalizes the matrix of heat transfer coefficients (Ergen, Lipkin, and Nohel 1957; Lellouche, 1966). In our two-region example, the matrix of coefficients is

$$\begin{bmatrix} h_1 + h_2 & -h_1 \\ -h_3 & h_3 + h_4 \end{bmatrix}$$

and its eigenvalues are  $\gamma_1$  and  $\gamma_2$ . The student can demonstrate that the eigenvalues are positive and real if the  $h_i$  are positive and real.

A convenient transformation matrix is<sup>3</sup>

$$M = \frac{1}{r_2 - r_1} \begin{bmatrix} r_2 & -r_1 \\ -1 & 1 \end{bmatrix}$$

where

$$r_i = (h_1 + h_2 - \gamma_i)/h_3, \quad (i = 1, 2).$$

The canonical variables are

$$T'_i = T_i + r_i T_2.$$

From eqs. (6-114) through (6-117) we find

$$K_i = b_1 + r_i b_2,$$

$$\alpha_1' = \frac{r_2 \alpha_1 - \alpha_2}{r_2 - r_1},$$

$$\alpha_2' = \frac{r_1 \alpha_1 - \alpha_2}{r_1 - r_2}.$$

The inverse relations are

$$T_1 = \frac{r_2 T'_1 - r_1 T'_2}{r_2 - r_1},$$

$$T_2 = \frac{T'_1 - T'_2}{r_1 - r_2},$$

$$b_1 = \frac{r_2 K_1 - r_1 K_2}{r_2 - r_1},$$

$$b_2 = \frac{K_1 - K_2}{r_1 - r_2},$$

$$\alpha_1 = \alpha_1' + \alpha_2',$$

$$\alpha_2 = r_1 \alpha_1' + r_2 \alpha_2'.$$

We may now work with the decoupled system of eqs. (6-116) and (6-117). We set  $\rho_0 = 0$  and use

$$A_1 = \alpha_1' K_1, \quad A_2 = \alpha_2' K_2. \quad (6-118)$$

As indicated by fig. 6-51, the feedback is

$$H(s) = \frac{A_1}{s + \gamma_1} + \frac{A_2}{s + \gamma_2}. \quad (6-119)$$

<sup>3</sup> We assume that the matrix of coefficients is nonsingular and that its eigenvalues are distinct.

302      *Linear System Stability*

This may be written as

$$H(s) = \frac{(A_1 + A_2)s + A_1\gamma_2 + A_2\gamma_1}{(s + \gamma_1)(s + \gamma_2)}$$

or

$$H(s) = \frac{(A_1 + A_2)(s + \xi)}{(s + \gamma_1)(s + \gamma_2)}, \quad (6-120)$$

where

$$\xi = \frac{A_1\gamma_2 + A_2\gamma_1}{A_1 + A_2}. \quad (6-121)$$

The feedback has one zero and two poles. The feedback gain may have either sign, and the zero may be in either half-plane, because the temperature coefficient of either region may be positive or negative. Typical magnitude, phase, and polar plots are shown in figs. 6-11 through 6-14.

Using now the effective-lifetime model of eq. (3-61) or (6-86),

$$G(s) = n_0/\ell' s = n_0\lambda/\beta s, \quad (6-122)$$

we have

$$G(s)H(s) = \frac{K\lambda(s + \xi)}{s(s + \gamma_1)(s + \gamma_2)}, \quad (6-123)$$

where

$$K = (A_1 + A_2)n_0/\beta. \quad (6-124)$$

The characteristic equation is

$$D(s) = s^3 + (\gamma_1 + \gamma_2)s^2 + (\gamma_1\gamma_2 + K\lambda)s + K\lambda\xi = 0. \quad (6-125)$$

From the Routh criterion, with  $\gamma_1$  and  $\gamma_2$  assumed positive, the system is stable if

$$\gamma_1\gamma_2 + K\lambda - \frac{K\lambda\xi}{\gamma_1 + \gamma_2} > 0 \quad (6-126)$$

and

$$K\lambda\xi > 0. \quad (6-127)$$

The first of these conditions yields the dynamic stability boundary, and the second the static stability boundary. It is seen from eqs. (6-120) and (6-124) that the second stability condition corresponds to  $H(0) > 0$ . It may be written as

$$A_1\gamma_2 + A_2\gamma_1 > 0. \quad (6-128)$$

Using eqs. (6-121) and (6-124), we may write the first stability condition as

$$(n_0\lambda/\beta)(A_1\gamma_1 + A_2\gamma_2) + \gamma_1\gamma_2(\gamma_1 + \gamma_2) > 0. \quad (6-129)$$

The system will be unconditionally stable (stable at all power levels  $n_0$ ) if

$$A_1\gamma_1 + A_2\gamma_2 > 0. \quad (6-130)$$

If eq. (6-128) is satisfied, but not eq. (6-130), we have conditional stability. The system is stable for  $n_0 < n_c$ , where

$$n_c = -\frac{\beta\gamma_1\gamma_2(\gamma_1 + \gamma_2)}{\lambda(A_1\gamma_1 + A_2\gamma_2)}. \quad (6-131)$$

It is convenient to introduce the parameters

$$x = A_1n_0/\beta, \quad y = A_2n_0/\beta. \quad (6-132)$$

The dynamic stability boundary becomes

$$\gamma_1x + \gamma_2y = -\gamma_1\gamma_2(\gamma_1 + \gamma_2)/\lambda. \quad (6-133)$$

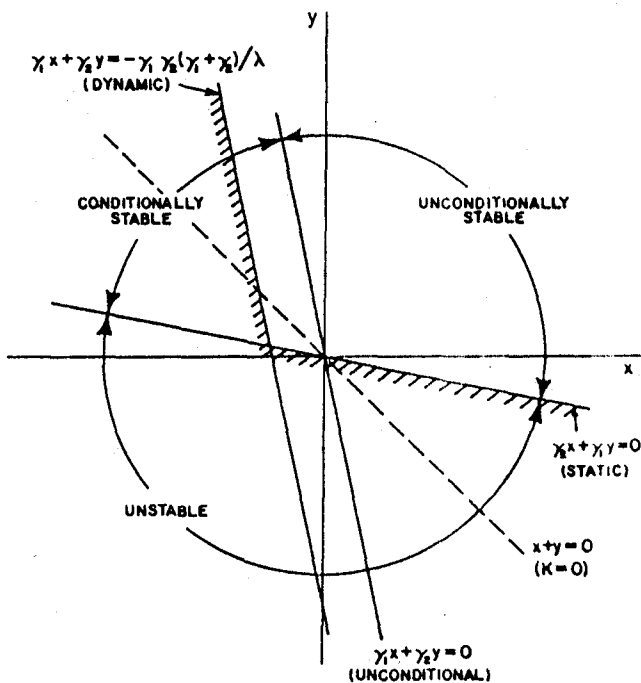


Fig. 6-52. Parameter space for a reactor with two-path feedback (effective-lifetime model),  $\gamma_1 > \gamma_2$ .

The static stability boundary is

$$\gamma_2 x + \gamma_1 y = 0. \quad (6-134)$$

The locus of points for which  $K = 0$  is

$$x + y = 0. \quad (6-135)$$

The unconditional stability boundary is

$$\gamma_1 x + \gamma_2 y = 0. \quad (6-136)$$

These boundaries and the various types of regions are shown in fig. 6-52 for  $\gamma_1 > \gamma_2$ . Recalling our sign convention, we see that conditional stability occurs only for positive reactivity feedback in the faster loop and negative in the slower (the second quadrant). Of course, there is complete symmetry upon interchange of  $x$  with  $y$  and subscript 1 with 2.

By eqs. (6-121) and (6-132), we have

$$\xi = \frac{\gamma_2 x + \gamma_1 y}{x + y}. \quad (6-137)$$

Lines of constant  $\xi$  are straight lines through the origin, and an increase of power level  $n_0$  (with other parameters fixed) corresponds to moving

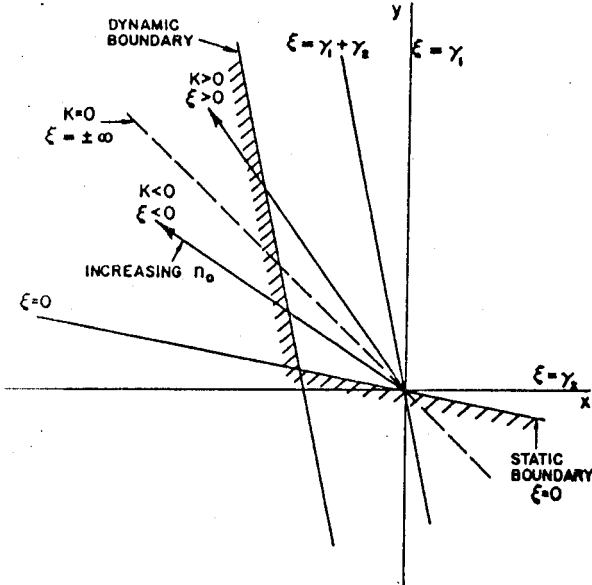


Fig. 6-53. Parameter space for a reactor with two-path feedback illustrating two types of conditional stability.

radially outward in the  $x, y$  plane. Two such lines in the conditionally stable region are shown in fig. 6-53, together with ranges of values for  $K$  and  $\xi$ . Note that the unconditional stability boundary corresponds to

$$\xi = \gamma_1 + \gamma_2. \quad (6-138)$$

The two types of conditional stability illustrated in fig. 6-53 are shown in fig. 6-54 as root-locus plots. The student should sketch the root locus for every other possible case, with particular attention to the significance of eq. (6-138).

We note for future reference that the intersection of the two stability boundaries in fig. 6-53 is at the point

$$x = -\frac{\gamma_1^2 \gamma_2}{\lambda(\gamma_1 - \gamma_2)}, \quad y = \frac{\gamma_1 \gamma_2^2}{\lambda(\gamma_1 - \gamma_2)}. \quad (6-139)$$

The reader may verify that the characteristic equation yields two zero roots and one negative real root  $s = -(\gamma_1 + \gamma_2)$  at this point. This corresponds to the vanishing of the two pure imaginary roots as one approaches this point along the dynamic stability boundary from above.

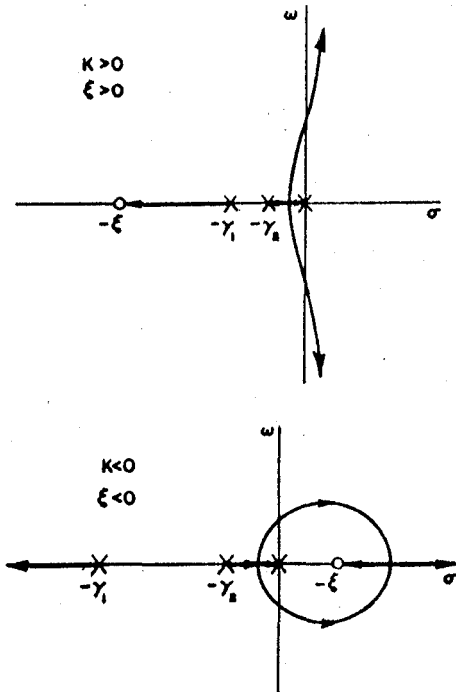


Fig. 6-54. Root-locus plots illustrating two types of conditional stability.

308      *Linear System Stability*

Recall that the units of  $A_1$  and  $A_2$  are reactivity per unit energy. The  $x, y$  plane may therefore be regarded as a parameter space of energy coefficients of reactivity (normalized by the factor  $n_0/\beta$ ). Recall that  $A_1/\gamma_1$  and  $A_2/\gamma_2$  are static power coefficients of reactivity, hence this information may be displayed as a parameter space of power coefficients using the  $x/\gamma_1, y/\gamma_2$  plane. This merely changes the slopes of the lines, and the static stability boundary would have a slope of  $-1$ .

Another viewpoint is afforded by a different parameter space used by Shotkin (1963, 1964a), who plots  $\gamma_1/\gamma_2$  vs.  $A_1/A_2 = x/y$ . Such a graph, as shown in fig. 6-55, includes the effect of varying  $\gamma_1$  and  $\gamma_2$ . However, the dynamic stability boundary cannot be plotted in this space (a radial line in fig. 6-53 corresponds to one point in fig. 6-55). Note that  $y$  is assumed positive to exclude any unstable systems in the first quadrant. To understand the region  $\gamma_1/\gamma_2 < 1$ , we must interchange  $\gamma_1$  and  $\gamma_2$  in fig. 6-53, thus putting the conditionally stable region into the fourth quadrant of the  $x, y$  plane and out of the range of fig. 6-55.

In the next section, we add delayed neutrons to this system and show that the region of unconditional stability is greatly enlarged. At the same time, certain nonminimum phase conditionally stable systems are destabilized by the delayed neutrons.

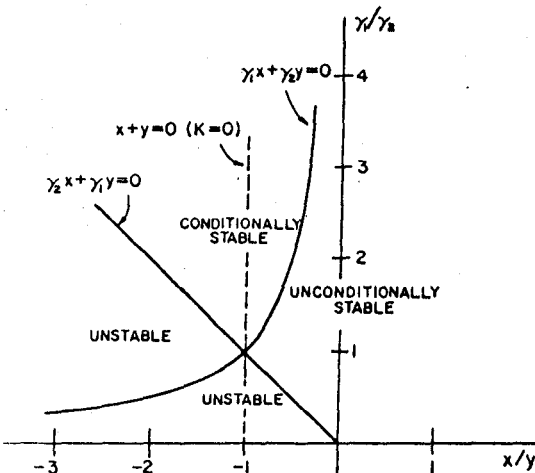


Fig. 6-55. Alternative parameter space for a reactor with two-path feedback (Shotkin 1964a).

#### 6-8. Two-Path Feedback: Delayed Neutrons

To study the effect of delayed neutrons, we use the one-group prompt-jump approximation, eq. (3-59) or (6-92),

$$G(s) = \frac{n_0(s + \lambda)}{\beta s}. \quad (6-140)$$

The two-path feedback is given by eq. (6-120). We have

$$G(s)H(s) = \frac{K(s + \lambda)(s + \xi)}{s(s + \gamma_1)(s + \gamma_2)}, \quad (6-141)$$

where  $K$  is given by eq. (6-124) and  $\xi$  by eq. (6-121). The characteristic equation is

$$D(s) = s^3 + (\gamma_1 + \gamma_2 + K)s^2 + (\gamma_1\gamma_2 + K\lambda + K\xi)s + K\lambda\xi = 0. \quad (6-142)$$

Note that this reduces to eq. (6-125) for  $|s| \ll \lambda$  and  $K$  small, keeping the product  $K\lambda$  as is.

Applying the Routh criterion, we find three conditions for stability:

$$\gamma_1 + \gamma_2 + K > 0, \quad (6-143)$$

$$\gamma_1\gamma_2 + K\lambda + K\xi - \frac{K\lambda\xi}{\gamma_1 + \gamma_2 + K} > 0, \quad (6-144)$$

$$K\lambda\xi > 0. \quad (6-145)$$

The second of these conditions yields the dynamic stability boundary, while the third condition, identical to eq. (6-127), yields the familiar static boundary. Eqs. (6-143) and (6-144) together replace eq. (6-126) of the effective-lifetime model.

If we introduce the parameters  $x$  and  $y$ , given by eq. (6-132), the stability boundaries corresponding to eqs. (6-143) through (6-145) are

$$x + y + \gamma_1 + \gamma_2 = 0, \quad (6-146)$$

$$(1 + \gamma_2)x^2 + (2\lambda + \gamma_1 + \gamma_2)xy + (1 + \gamma_1)y^2 + (\lambda\gamma_1 + 2\gamma_1\gamma_2 + \gamma_2^2)x + (\lambda\gamma_2 + 2\gamma_1\gamma_2 + \gamma_1^2)y + \gamma_1\gamma_2(\gamma_1 + \gamma_2) = 0, \quad (6-147)$$

and

$$\gamma_2x + \gamma_1y = 0. \quad (6-148)$$

The dynamic stability boundary, eq. (6-147), is a hyperbola in the  $x, y$  plane. There is a wide variety of cases.

The case shown in fig. 6-56 is for  $\gamma_1 = 0.05 \text{ sec}^{-1}$ ,  $\gamma_2 = 0.01 \text{ sec}^{-1}$ , and  $\lambda = 0.10 \text{ sec}^{-1}$  (Meenan and Hetrick 1966). The dynamic stability boundary of the effective-lifetime model, eq. (6-133), is included for comparison, as is the unconditional stability boundary of that model (see fig. 6-52). The dynamic stability boundaries of the two models

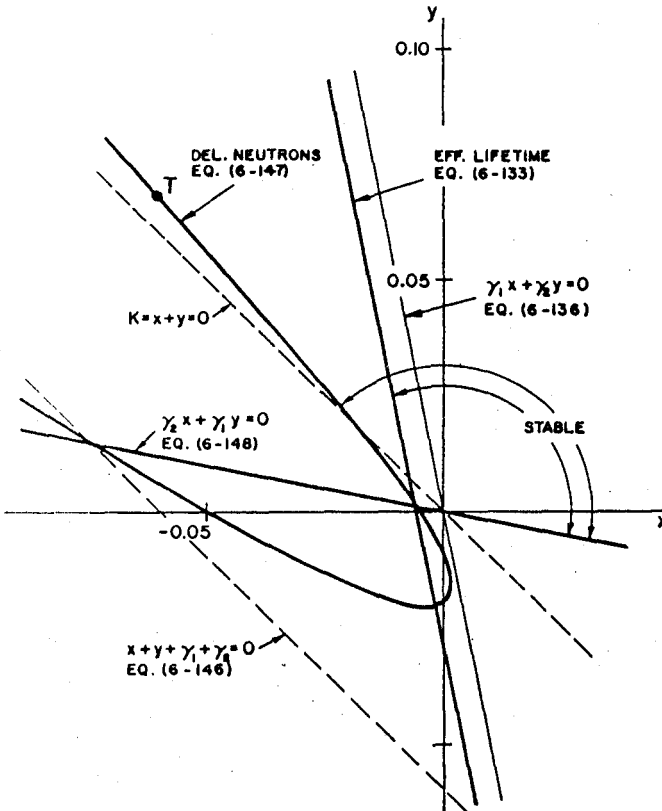


Fig. 6-56. Parameter space for a reactor with two-path feedback and delayed neutrons ( $\gamma_1 = 0.05$ ,  $\gamma_2 = 0.01$ ,  $\lambda = 0.1$ ).

intersect twice. One of these intersections is on the static stability boundary, at the point given by eq. (6-139). The stable region is enlarged by delayed neutrons, as indicated by the arrows. In particular, the region of unconditional stability is greatly increased. A system is stable at all power levels if one can move outward on a radial line from the origin without encountering a stability boundary. When delayed neutrons are added, the unconditional stability boundary is moved from the line given by eq. (6-136) to a line from the origin tangent to the hyperbola at  $T$ .

A radial line in the space between  $T$  and the dashed line  $K = 0$  will intersect the hyperbola twice. This represents a unique type of system that is stable at low power, unstable at intermediate power, and again stable at high power. A Nyquist plot illustrating this possibility for

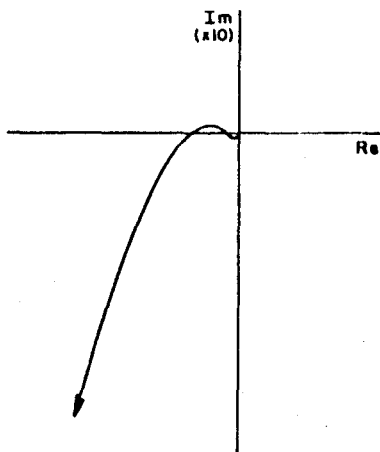


Fig. 6-57. Nyquist plot illustrating conditional stability.

$\xi = 0.4$  is shown in fig. 6-57. A root locus for a similar system is shown in fig. 6-58.

A condition for this type of behavior may be derived by considering the asymptotes of the hyperbola. These are

$$y = -x + \lambda - \gamma_1 - \gamma_2 \quad (6-149)$$

and

$$y = -\frac{\lambda + \gamma_2}{\lambda + \gamma_1} x - \frac{\lambda^2 + \gamma_1 \gamma_2}{\lambda + \gamma_1}. \quad (6-150)$$

When  $\gamma_1 > \gamma_2$ , eq. (6-149) represents the steeper asymptote. If it passes above the origin ( $\lambda > \gamma_1 + \gamma_2$ ), a tangent line from the origin to  $T$  is possible. Otherwise, a radial line from the origin that is above the line  $K = 0$  will not meet the hyperbola. To summarize, we may say that the region of unconditional stability extends to a tangent line if  $\lambda > \gamma_1 + \gamma_2$  and to the line  $K = x + y = 0$  if  $\lambda < \gamma_1 + \gamma_2$ . This condition may also be derived by seeking two crossings of the real axis in the Nyquist plot, as in fig. 6-57, or by seeking two crossings of the positive imaginary axis in a root locus, as in fig. 6-58.

The other type of conditional stability, which occurs more frequently with this system, is found for  $K < 0$  and  $\xi < 0$ . The feedback has its zero in the right half-plane. A typical root locus for  $\lambda > \gamma_1 > \gamma_2$  is shown in fig. 6-59.

Now consider the trend as  $\gamma_1$  increases. (In plotting the parameter spaces, we keep  $\gamma_1 = 5\gamma_2$  for convenience.) The upper asymptote of the

Fig. 6-59. Root locus illustrating conditional stability.

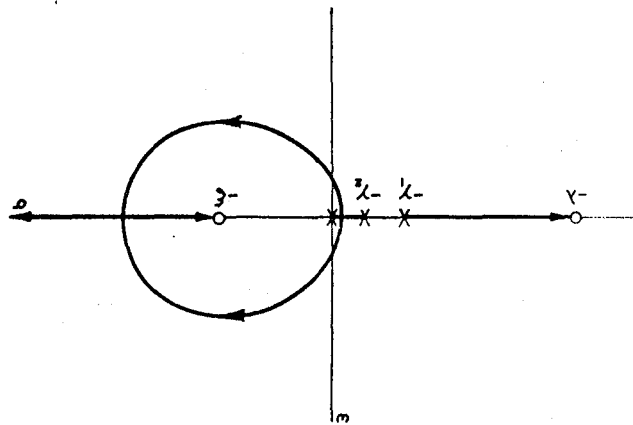
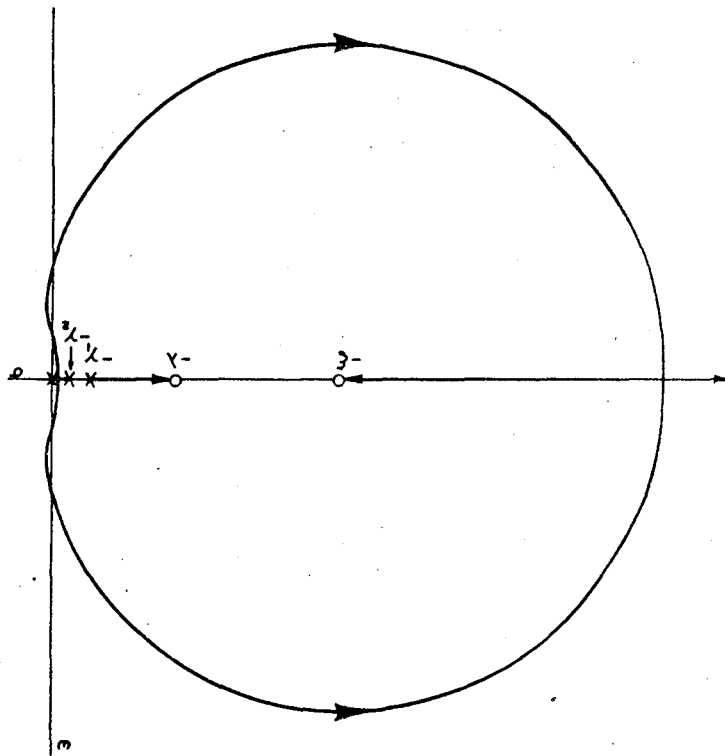


Fig. 6-58. Root locus illustrating conditional stability.



hyperbola drops below the origin. The first degenerate case appears at  $\lambda = \gamma_1$  (the hyperbola degenerates to its asymptotes when  $\lambda$  coincides with either  $\gamma$ ). For  $\gamma_1 > \lambda > \gamma_2$ , the curvature of the hyperbola is reversed, and we have the case shown in fig. 6-60 ( $\gamma_1 = 0.15$ ,  $\gamma_2 = 0.03$ ,  $\lambda = 0.10$ ). Delayed neutrons again enlarge the region of stability. The region of unconditional stability extends to the line  $K = 0$ , and all the conditionally stable cases are nonminimum-phase systems.

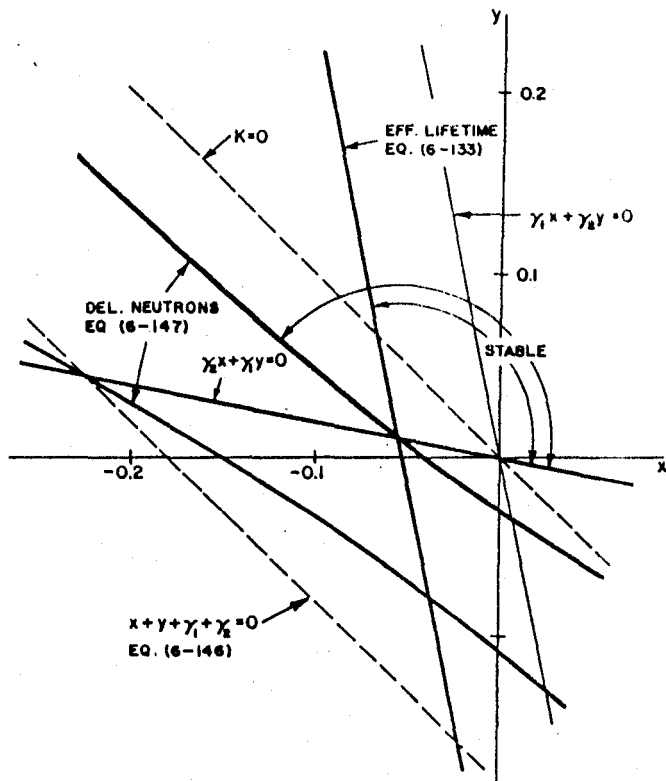


Fig. 6-60. Parameter space for a reactor with two-path feedback and delayed neutrons ( $\gamma_1 = 0.15$ ,  $\gamma_2 = 0.03$ ,  $\lambda = 0.1$ ).

A root locus for the latter type of system is shown in fig. 6-61. This locus has two departure points and is similar to that in fig. 6-59. However, there is an ambiguity not covered by the rules of sec. 6-5 unless one actually computes the departure points. This same ordering of poles and zeros may produce a locus with four departure points, as shown in fig. 6-62. As mentioned in sec. 6-5, the ambiguity is resolved by studying limiting cases. As  $\gamma_1 \rightarrow \lambda$ , the locus is a circle with radius determined by

### 312 Linear System Stability

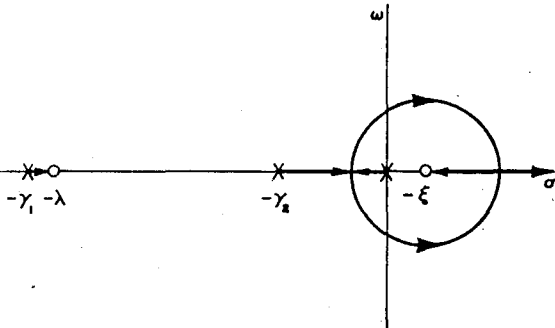


Fig. 6-61. Root locus illustrating conditional stability.

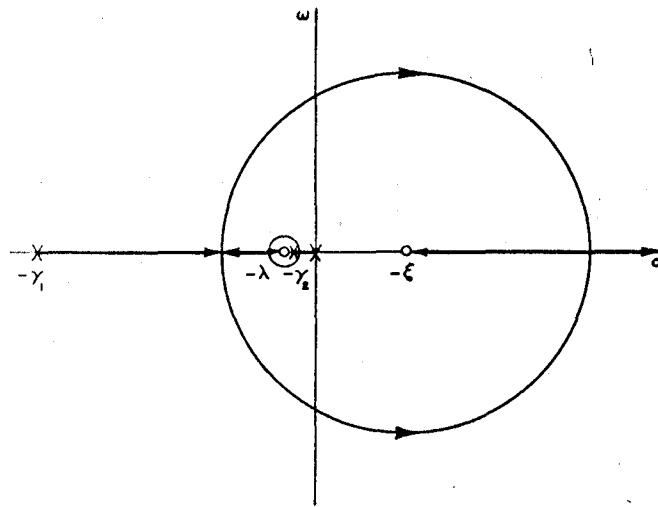


Fig. 6-62. Root locus illustrating conditional stability and four departure points.

$y_2$  and  $\xi$ . When  $y_2 \rightarrow \lambda$ , the radius is determined by  $y_1$  and  $\xi$ . For  $\lambda$  close to  $y_2$ , and  $y_2$  sufficiently small, there may be two loops, as seen in fig. 6-62.

For  $y_1 > y_2 > \lambda$ , the curvature of the hyperbola again reverses. Eventually, we reach the case where all three stability boundaries intersect. This occurs when the values of  $x$  and  $y$  given by eq. (6-139) are also solutions of eq. (6-146), which is possible if

$$\frac{1}{\lambda} = \frac{1}{y_1} + \frac{1}{y_2}. \quad (6-151)$$

However, before this point is reached, a much more significant special case is found.

Recall that the hyperbola, eq. (6-147), intersects the dynamic stability line of the effective-lifetime model, eq. (6-133), in two places. One intersection is at the point where each of these lines encounters the static stability boundary; its coordinates are given by eq. (6-139). The other intersection lies in the unstable region in figs. 6-56 and 6-60. Its coordinates are

$$x = -\frac{\gamma_2(\gamma_1 + \gamma_2)}{\lambda(\gamma_1 - \gamma_2)} \frac{\gamma_1^2 + (\gamma_1 - \lambda)\gamma_2}{\gamma_1 + \gamma_2 + \lambda} \quad (6-152)$$

and

$$y = \frac{\gamma_1(\gamma_1 + \gamma_2)}{\lambda(\gamma_1 - \gamma_2)} \frac{\gamma_2^2 + (\gamma_2 - \lambda)\gamma_1}{\gamma_1 + \gamma_2 + \lambda}.$$

At a value of  $\gamma_2$  between  $\gamma_2 = \lambda$  and the value given by eq. (6-151), this second intersection moves into the region above the static stability boundary. The hyperbola now penetrates into the stable region for the effective-lifetime model, and we have systems that are destabilized by delayed neutrons. An example is shown in fig. 6-63 (Hetrick 1967), where  $\gamma_1 = 1.0$ ,  $\gamma_2 = 0.2$ , and  $\lambda = 0.1$ .

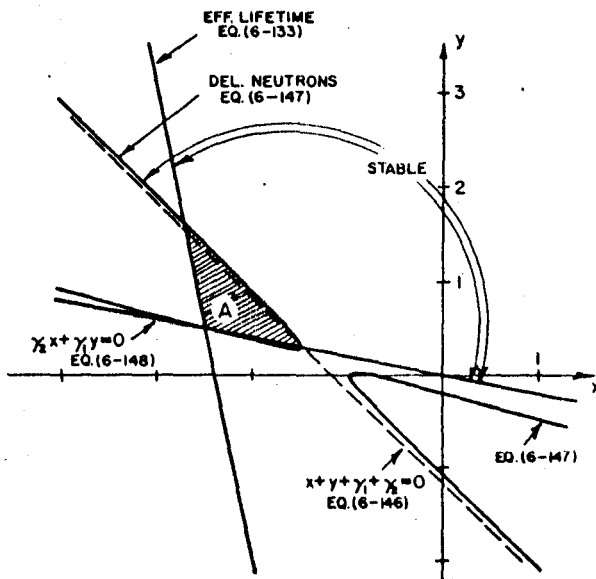


Fig. 6-63. Parameter space for a reactor with two-path feedback and delayed neutrons ( $\gamma_1 = 1.0$ ,  $\gamma_2 = 0.2$ ,  $\lambda = 0.1$ ); shaded area destabilized by delayed neutrons.

### 314 Linear System Stability

To find the crossover point, we seek the condition on the parameters for which eqs. (6-139) and (6-152) represent the same point. This is the case for which the two dynamic stability boundaries, eqs. (6-133) and (6-147), are tangent. The resulting condition is

$$\frac{1}{\lambda} = \frac{1}{\gamma_1} + \frac{1}{\gamma_2} - \frac{1}{\gamma_1 + \gamma_2}. \quad (6-153)$$

The condition for the existence of systems that are destabilized by delayed neutrons is therefore

$$\frac{1}{\lambda} > \frac{1}{\gamma_1} + \frac{1}{\gamma_2} - \frac{1}{\gamma_1 + \gamma_2}. \quad (6-154)$$

It may be noted that eq. (6-154) reduces to  $\gamma > \lambda$  if  $\gamma_1 \rightarrow \infty$  and  $\gamma_2 = \gamma$ . This is just the case of one region plus a power coefficient that we studied in sec. 6-6 (see fig. 6-48).

Nyquist plots for point A in fig. 6-63, chosen so that the  $-1$  point falls between the two curves, are shown in fig. 6-64. Destabilization by

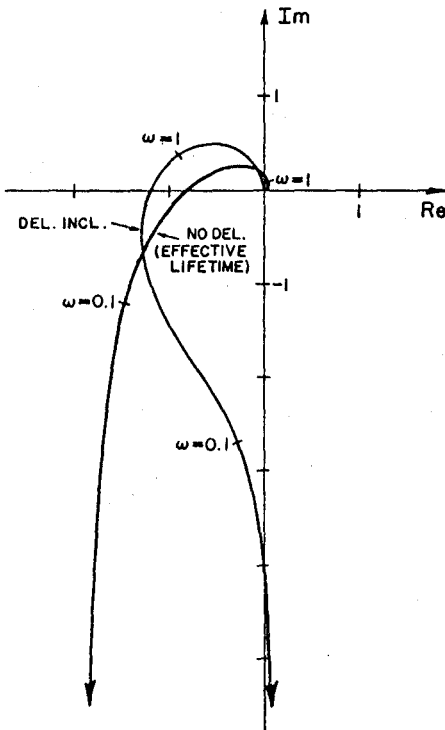


Fig. 6-64. Nyquist plots showing destabilizing effect of delayed neutrons (point A in fig. 6-63).

delayed neutrons is possible because the zero at  $s = -\lambda$  becomes effective at low frequency when the condition of eq. (6-154) is satisfied. When the pole at  $-\beta/\ell$  is included, the upper curve crosses into the right half-plane before approaching the origin as  $\omega \rightarrow \infty$ ; the effect, even for  $\beta/\ell = 10$ , is too small to show in the figure. Fig. 6-64 may be compared with the related curves in fig. 6-49 for the case of one region plus a power coefficient.

A root locus for a possible system with delayed neutrons is shown in fig. 6-65. Another root locus for the same ordering of poles and zeros is shown in fig. 6-66. This latter case does not satisfy the condition of eq. (6-154), and it is included mainly to illustrate the variety of possible cases.

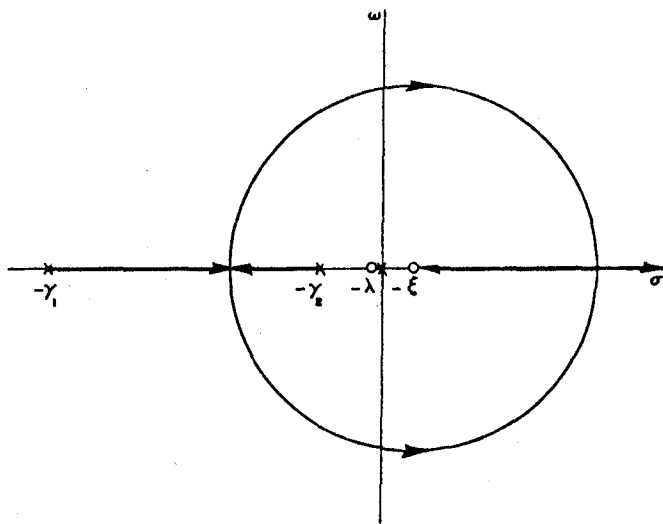


Fig. 6-65. Root locus illustrating conditional stability.

The variety is great. Suppose the parameters  $\gamma_1$ ,  $\gamma_2$ , and  $\lambda$  are fixed. The additional zero at  $s = -\xi$  may be added in any of four ways (to the left of all poles, between a pair of poles, or in the right half-plane). This yields eight root-locus plots, counting four for each sign of  $K$ . In addition, a single configuration may show either two or four departure points.

This refers only to one possible ordering of the parameters  $\gamma_1$ ,  $\gamma_2$ , and  $\lambda$ . From another viewpoint, starting with three poles we can add two zeros in ten different ways; two indistinguishable objects in three boxes may be arranged in  $(5!)/(2!)(3!) = 10$  configurations. One of the ten configurations is excluded because there can be at most one zero in the

right half-plane ( $\lambda > 0$ ). There are therefore nine configurations, producing eighteen root-locus cases (with additional variety depending on the number of departure points).

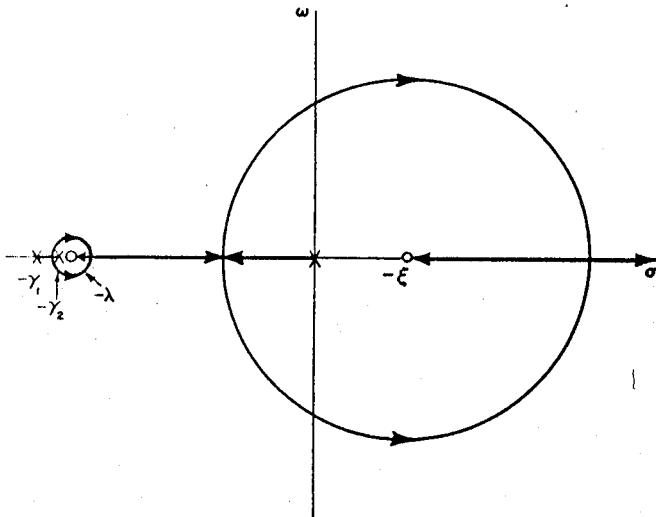


Fig. 6-66. Root locus illustrating conditional stability and four departure points.

The reader should not be inspired to make a profusion of fruitless sketches. Instead, return to a particular case such as that shown in fig. 6-63. The parameter space is completely covered by eight root-locus cases (four for each sign of  $K$ ). By sketching root-locus plots and noting the possible departure points, one can locate approximately the boundary line that separates oscillatory from nonoscillatory regions in the  $x, y$  plane. A parameter space showing the stability boundaries and the oscillation boundaries contains nearly all the essential information about a linear system.

The treatment in this section was inspired by the work of Miida and Suda (1961), who found the regions of unconditional stability in the parameter space of power coefficients, and by the work of Hans Bethe (1956), who pointed out the great utility of the prompt-jump approximation in reactor stability studies.

Miida and Suda included the pole at  $-\beta/\ell$ , making the system somewhat more complicated, and they did not attempt to find the dynamic stability boundaries. The use of the prompt-jump approximation makes the derivation of dynamic stability boundaries less formidable. Fortunately, the pole at  $-\beta/\ell$  has extremely little effect for realistic values of  $\gamma$ . The reader is encouraged to set up the two-region problem using the

second-order model of eq. (6-95) and to apply the Routh criterion. When plotted in the  $x, y$  plane with  $\beta/\ell > 10$ , the stability boundaries are practically indistinguishable from those shown in figs. 6-56, 6-60, and 6-63.

#### 6-9. Stability of Fast Reactors

As mentioned in chapter 5, the Doppler effect may lead to a prompt positive feedback in a fast reactor. Another prompt-positive effect may be caused by fuel-rod bowing, as was observed in EBR-I (McCarthy and Okrent 1964; Smith et al. 1961). The qualitative behavior of such a system may be understood with the aid of a two-path feedback model with  $\alpha_1 < 0$  and  $\alpha_2 > 0$ .

Consider the reactivity feedback

$$\rho = -\alpha_1 T_1 - \alpha_2 T_2, \quad (6-155)$$

where the incremental temperatures are given by

$$\frac{dT_1}{dt} = b(n - n_0) - \eta_1 T_1 \quad (6-156)$$

and

$$\frac{dT_2}{dt} = \eta_2 T_1 - \eta_3 T_2.$$

This system is a special case of the coupled system of eq. (6-114). Heat loss from region 1 depends on  $T_1$  only, and back transfer from region 2 to region 1 is neglected. There is no heat generation in region 2. This model was applied to a prototype fast-breeder reactor by Kinchin (1956). The same model has been used to analyze stability in a fast reactor with in-core thermionic diodes (Brehm, Hetrick, and Schmidt 1969).

Region 1 represents the fuel and any immediate surroundings whose temperature changes follow the fuel temperature without appreciable time lag. Region 2 represents the remaining structure. We refer to  $\alpha_1$  and  $\alpha_2$  as prompt and delayed coefficients respectively.

A block diagram is shown in fig. 6-67. The prompt feedback transfer function is

$$H_1(s) = \frac{\alpha_1 b}{s + \eta_1}.$$

The delayed feedback is

$$H_2(s) = \frac{\alpha_2 b \eta_2}{(s + \eta_1)(s + \eta_3)}.$$

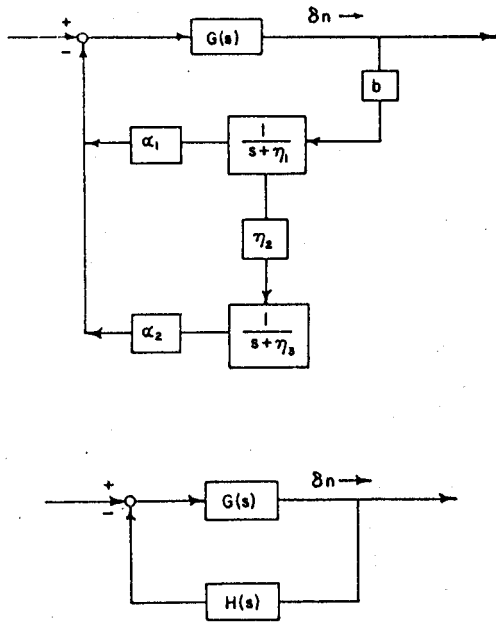


Fig. 6-67. Block diagrams for a simple coupled system.

The total feedback may be written

$$H(s) = \alpha_1 b \frac{s + \eta_3 + \eta_2 \alpha_2 / \alpha_1}{(s + \eta_1)(s + \eta_3)}. \quad (6-157)$$

Using the prompt-jump approximation, eq. (3-59) or (6-140), we may write

$$G(s)H(s) = \frac{K(s + \lambda)(s + \xi)}{s(s + \eta_1)(s + \eta_3)}, \quad (6-158)$$

where

$$K = \alpha_1 b n_0 / \beta, \quad \xi = \eta_3 + \eta_2 \alpha_2 / \alpha_1. \quad (6-159)$$

To refer to the effective-lifetime model, replace  $s + \lambda$  by  $\lambda$ .

The relation to the canonical system, eq. (6-141), is straightforward. The characteristic equations have the same form as eq. (6-125) or (6-142). One immediately identifies  $\eta_1 = \gamma_1$  and  $\eta_3 = \gamma_2$ . This is also seen upon comparing eqs. (6-114) and (6-156); we have  $b_1 = b$ ,  $b_2 = 0$ ,  $h_1 = 0$ ,  $h_2 = \eta_1$ ,  $h_3 = \eta_2$ , and  $h_3 + h_4 = \eta_3$ . The matrix of heat-transfer coefficients (see sec. 6-7) is

$$\begin{bmatrix} \eta_1 & 0 \\ -\eta_2 & \eta_3 \end{bmatrix},$$

and its eigenvalues are  $\eta_1$  and  $\eta_3$ . Carrying out the transformation to canonical coordinates, we find

$$T_1' = T_1,$$

$$T_2' = T_1 + \frac{\eta_1 - \eta_3}{\eta_2} T_2,$$

$$\alpha_1' = \alpha_1 - \frac{\eta_2}{\eta_1 - \eta_3} \alpha_2,$$

$$\alpha_2' = \frac{\eta_2}{\eta_1 - \eta_3} \alpha_2,$$

$$K_1 = K_2 = b.$$

The inverse transformation is

$$T_1 = T_1',$$

$$T_2 = \frac{\eta_2}{\eta_1 - \eta_3} (T_2' - T_1'),$$

$$\alpha_1 = \alpha_1' + \alpha_2',$$

$$\alpha_2 = \frac{\eta_1 - \eta_3}{\eta_2} \alpha_2',$$

$$b = K_1.$$

The stability properties of the coupled system may be studied in the  $x, y$  plane of the canonical system, as shown in secs. 6-7 and 6-8.

However, more insight into the coupled system may be gained by working with a parameter space that is closer to the original physical parameters. Define

$$u = \alpha_1 b n_0 / \beta, \quad v = \eta_2 \alpha_2 b n_0 / \eta_3 \beta. \quad (6-160)$$

From eq. (6-159),

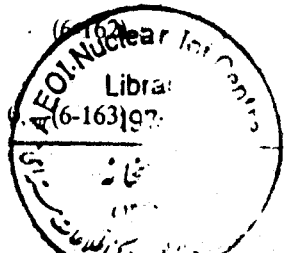
$$K = u, \quad \xi = \eta_3(1 + v/u). \quad (6-161)$$

The stability boundaries in the  $u, v$  plane are

$$u + \eta_1 + \eta_3 = 0,$$

$$(\lambda + \eta_3)u^2 + \eta_3 uv + (\eta_3^2 + \lambda\eta_1 + 2\eta_1\eta_3)u$$

$$+ \eta_3(\eta_1 + \eta_3 - \lambda)v + \eta_1\eta_3(\eta_1 + \eta_3) = 0. \quad (6-163)$$



6.10      *Linear System Stability*

and

$$u + v = 0. \quad (6-164)$$

These correspond respectively to eqs. (6-146) through (6-148). The dynamic stability boundary of the effective-lifetime model is

$$\eta_1 u - \eta_3 v = -\eta_1 \eta_3 (\eta_1 + \eta_3)/\lambda, \quad (6-165)$$

corresponding to eq. (6-133), and the unconditional stability boundary of that model is

$$\eta_1 u - \eta_3 v = 0, \quad (6-166)$$

corresponding to eq. (6-136). In all cases,  $K = 0$  corresponds to  $u = 0$  (the  $v$ -axis). The first quadrant in the  $u, v$  plane represents cases for which both feedbacks are negative ( $\alpha_1$  and  $\alpha_2$  positive), and the second quadrant is the prompt-positive feedback region of special interest ( $\alpha_1 < 0, \alpha_2 > 0$ ).

The case for  $\eta_1 = 0.05, \eta_3 = 0.01$ , and  $\lambda = 0.1$  is shown in fig. 6-68. This corresponds to the  $x, y$  plane of fig. 6-56. The relation between the two parameter spaces is

$$\begin{aligned} x &= u - \frac{\eta_3}{\eta_1 - \eta_3} v, & y &= \frac{\eta_3}{\eta_1 - \eta_3} v, \\ u &= x + y, & v &= \frac{\eta_1 - \eta_3}{\eta_3} y. \end{aligned} \quad (6-167)$$

The coupling coefficient  $\eta_2$  does not appear because it was absorbed in the definition of  $v$ . We retain  $\eta_1 = 5\eta_3$  in the cases illustrated so that  $v = 4y$ .

Perhaps the most remarkable feature of fig. 6-68 is that both the dynamic stability boundaries enter the first quadrant. The physical interpretation is that a coupled system may be unstable even though both feedbacks are negative. This can occur if the magnitude of the prompt coefficient is small and the magnitude of the delayed coefficient is sufficiently large. This possibility, which is obscured in the transformation to canonical coordinates (and which cannot occur in a physically decoupled system), was pointed out by Lellouche (1966) in discussing higher-order coupled systems.

In the present system, it is seen from eq. (6-165) that the effective-lifetime model will always exhibit this type of instability. For the prompt-jump model, we may inspect the asymptotes of the hyperbola, which are

$$u = \lambda - \eta_1 - \eta_3$$

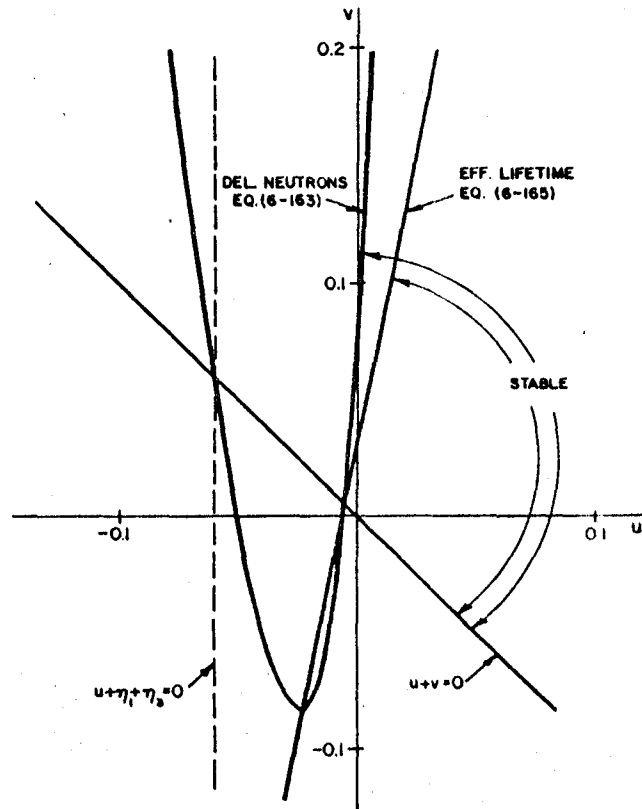


Fig. 6-68. Parameter space for a reactor with coupled two-path feedback ( $\eta_1 = 0.05$ ,  $\eta_3 = 0.01$ ,  $\lambda = 0.1$ ).

and

(6-168)

$$v = -\frac{\lambda + \eta_3}{\eta_3} u - \frac{\lambda^2 + \eta_1 \eta_3}{\eta_3}.$$

The vertical asymptote is in the right half-plane, permitting the hyperbola to enter the first quadrant, only if  $\lambda > \eta_1 + \eta_3$ . The latter is therefore a necessary condition for instability in the first quadrant with the coupled two-region prompt-jump model, and it is the necessary condition for the type of instability shown in fig. 6-58. Note that this instability occurs for very slow systems (large characteristic times for heat transfer). The system of fig. 6-68 is unconditionally stable above the line  $u + v = 0$  and, when delayed neutrons are included, to the right of a line through the origin that is tangent to the hyperbola.

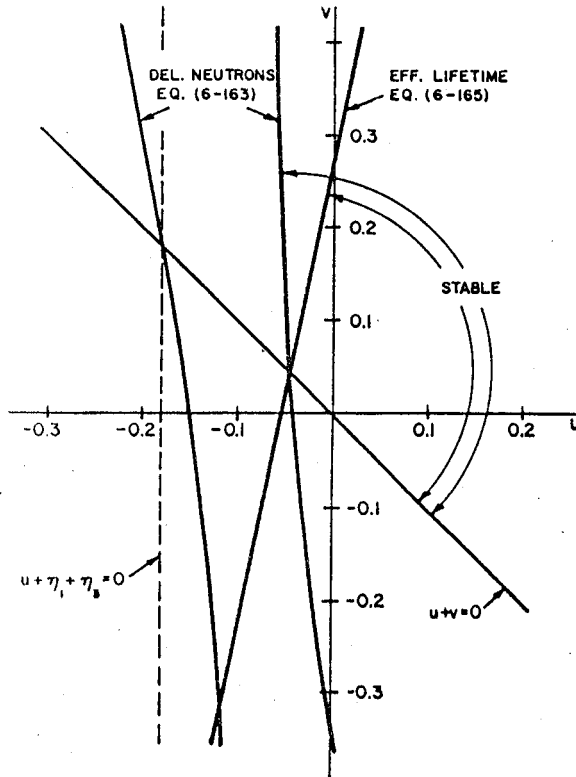


Fig. 6-69. Parameter space for a reactor with coupled two-path feedback ( $\eta_1 = 0.15$ ,  $\eta_3 = 0.03$ ,  $\lambda = 0.1$ ).

For  $\lambda < \eta_1 + \eta_3$ , the region of unconditional stability is broadened to include the entire first quadrant. This is illustrated by fig. 6-69 for  $\eta_1 = 0.15$ ,  $\eta_3 = 0.03$ , and  $\lambda = 0.1$  (corresponding to fig. 6-60); and by fig. 6-70 for  $\eta_1 = 1.0$ ,  $\eta_3 = 0.2$ ,  $\lambda = 0.1$  (corresponding to fig. 6-63). Note the shaded area that is destabilized by delayed neutrons. The Nyquist plots of fig. 6-64 apply to point A as shown in boths figs. 6-63 and 6-70. The necessary condition for destabilization by delayed neutrons, eq. (6-154), may be written

$$\frac{1}{\lambda} > \frac{1}{\eta_1} + \frac{1}{\eta_3} - \frac{1}{\eta_1 + \eta_3}. \quad (6-169)$$

Let us now turn to the practical consequences of operating a system with a prompt-positive and a delayed-negative feedback. Consider first the time domain. If the power is sufficiently low, the characteristic

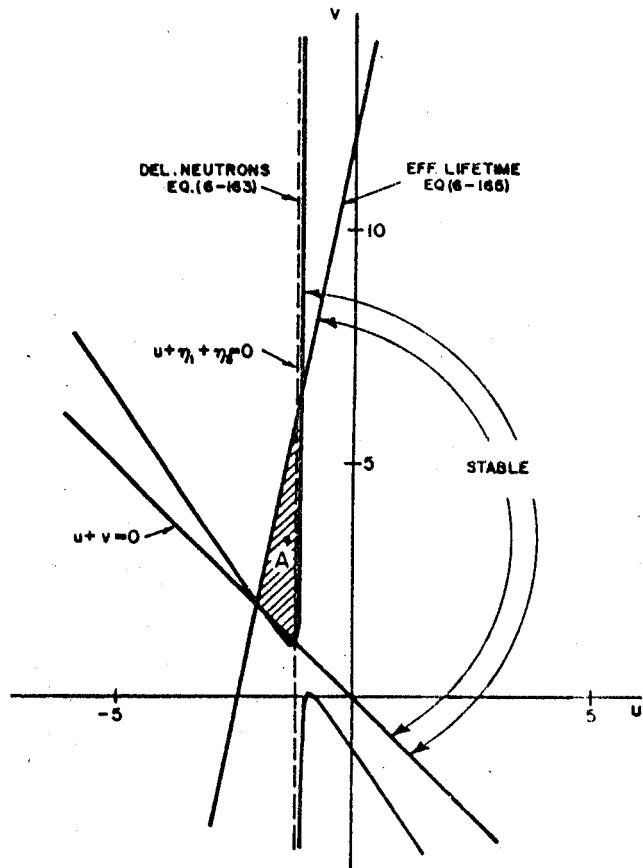


Fig. 6-70. Parameter space for a reactor with coupled two-path feedback ( $\eta_1 = 1.0$ ,  $\eta_2 = 0.2$ ,  $\lambda = 0.1$ ); shaded area destabilized by delayed neutrons.

roots are all negative real numbers and there is no oscillation. Nevertheless, there may be some potential operating problems. The response to a sudden increase of coolant temperature for two hypothetical systems is shown in fig. 6-71. The ordinates represent incremental power relative to the final equilibrium power (in arbitrary units). The time scale is typical for operation in the nonoscillatory range.

In the case of one region with negative feedback, the temperature rise is immediately felt as a power reduction, and the system monotonically approaches a new equilibrium at lower power. However, in the system chosen to illustrate a prompt positive effect, the immediate response to a temperature rise is a power increase. The negative feedback soon comes into play, causing some overcompensation and an eventual approach to

124 *Linear System Stability*

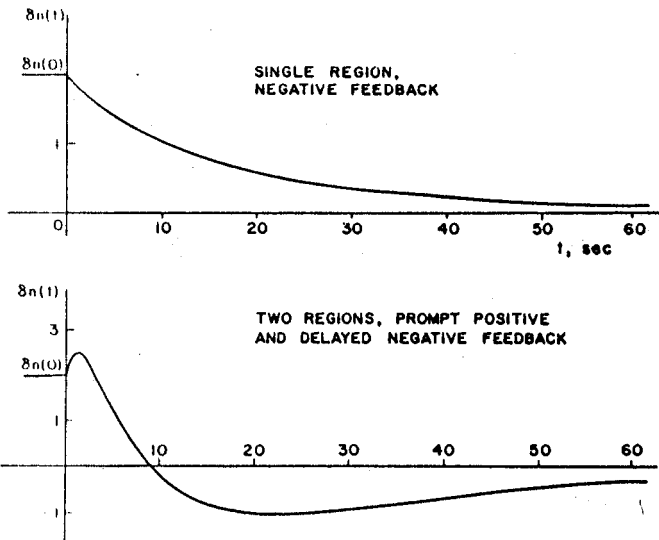


Fig. 6-71. Response to a sudden increase of coolant temperature (plotted as power fluctuation about final equilibrium).

a new equilibrium at reduced power. The initial power rise may or may not be a problem, depending on the system parameters and the amount of reactivity involved. We shall see in chapter 7 that a large excursion in such a reactor may take the system into a range dominated by nonlinear effects, and that a linearly stable system of this type may be highly unstable for large perturbations.

The meltdown accident in EBR-I Mark II illustrates what may be called the autocatalytic effect of prompt-positive feedback (Brittan 1958; Thompson 1964). The accident occurred during a low-power experimental operation, and a small positive reactivity resulted in a rapidly decreasing period. The core of the reactor was severely damaged before it was shut down.

Returning to the linear stability problem, consider the effect of increasing the equilibrium power  $n_0$ . The systems in question all lie in the second quadrant of the  $u, v$  plane above the line  $u + v = 0$  (see figs. 6-68 through 6-70). Increasing  $n_0$  means moving outward on a radial line through the origin. At first, all characteristic roots are negative real numbers. At higher power, two roots become complex with negative real parts. As the power is increased, the dynamic stability boundary is crossed (real parts of complex roots change from negative to positive). This process may be followed on a root locus such as that shown in fig. 6-59. Eventually, the roots return to the real axis,

and the second crossing of the hyperbola corresponds to real roots of equal magnitude and opposite sign (far inside the unstable region).

The value of  $n_0$  at the first encounter with the dynamic stability boundary may be called the critical, or resonance, power. In terms of the frequency response  $Y(j\omega)$ , this corresponds to unbounded amplitude at the resonant frequency. The approach to resonance may also be observed in a graph like that in fig. 6-30, using an appropriate feedback such as that shown in fig. 6-14 but with  $K < 0$ . Measurement of the frequency response in a neighborhood just below critical power will yield a peak in the amplitude because the complex number  $G(j\omega)H(j\omega)$  is near  $-1$  for frequencies near resonance.

The neighborhood of critical power was explored extensively by oscillator tests in EBR-I (Ackroyd et al. 1958; Thalgott et al. 1958). Some typical data taken in 1955 are reproduced in fig. 6-72 (Brittan 1956). In principle, a large set of such data could be extrapolated to predict the critical condition. In practice, it is often difficult to vary only one parameter at a time. There is also some risk that a small change near resonance could cause the system to exceed some operating limit and result in damage.

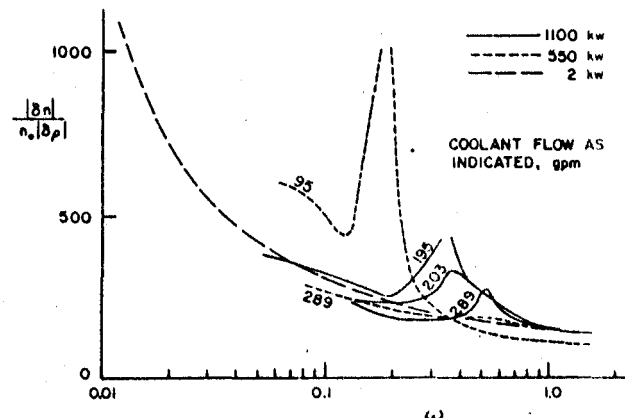


Fig. 6-72. Amplitude response in EBR-I Mark II oscillator tests (Brittan 1956).

It was mentioned earlier that the model of eq. (6-156) was applied to EBR-I Mark II by Kinchin (1956). The agreement with oscillator data such as that in fig. 6-72 was qualitatively correct but quantitatively poor. Kinchin proposed instead a model containing a transport time delay for the passage of coolant between the core and the external structure above the core, postulating that thermally induced motions of the structure produced a delayed-negative reactivity feedback.

### 3.6 Linear System Stability

Such a model was applied by Bethe (1956), using for the delayed feedback

$$H_2(s) = \frac{\eta_1 \eta_3 H_2(0) \exp(-\tau s)}{(s + \eta_1)(s + \eta_3)}.$$

By fitting parameters to the amplitude data, he found a prompt positive power coefficient of  $8 \times 10^{-4}$  per Mw, a delayed negative power coefficient of  $3.8 \times 10^{-3}$  per Mw, and time constants  $1/\eta_1 = 0.6$  sec,  $1/\eta_3 = 1.51$  sec, and  $\tau = 10$  sec. However, this procedure produces only empirical constants for a restricted mathematical model and cannot explain the underlying physical mechanisms. Another limitation is a discrepancy between steady-state power coefficients determined in this way as compared to those measured in other types of experiments. The oscillator experiment can miss low-frequency processes whose time constants are too long to affect the available data; the measured coefficients are in effect quasi-static. Still another difficulty is that the transport time delay  $\tau$  is very difficult to correlate with the mass flow rate of coolant. Indeed, it depends on the thermal properties of the system in a complicated way, and the effective transport time may be much larger than the actual mass transport time (Störrer 1960).

Subsequent to the studies by Kinchin and Bethe, a large program of feedback transfer-function measurements was undertaken in EBR-I Mark III (Smith et al. 1960). Magnitude and phase data were used in eq. (6-6) to determine the feedback

$$H(j\omega) = Y^{-1}(j\omega) - G^{-1}(j\omega),$$

where  $Y$  and  $G$  are the closed-loop (high-power) and the forward (zero-power) transfer functions respectively.

During this work, a comparison was made using two types of fuel element, one type equipped with ribs designed to minimize fuel-rod bowing. In this way it was determined that the prompt-positive coefficient of EBR-I Mark II was indeed largely caused by fuel-rod bowing.

A number of mathematical models for the feedback were contrived and compared with oscillator measurements. One model for EBR-I Mark II is given by Smith et al. (1960):

$$-H(s) = \frac{A}{s + \eta_1} - \frac{B}{(s + a)(s + b)} - \frac{C \exp(-\tau s)}{s + c}.$$

The first term is the prompt rod-bowing effect. The second term was attributed to axial fuel-rod expansion, and the third to "ligamental expansions in the lower shield plate." Coolant, flowing upward through the core, was presumably responsible for periodic thermal distortion of

the lower shield plate (the first main structural member that is passed), producing flexing of the fuel rods and a delayed negative feedback. This type of structure was eliminated in the highly stable Mark III design.

A later model for Mark II is given by Smith et al. (1961):

$$-H(s) = \frac{A}{s + \eta_1} - \frac{B \exp(-\tau s)}{(s + \eta_1)(s + a)} - \frac{C \exp(-\tau s)}{(s + \eta_1)(s + b)}$$

where all core feedback processes, including rod bowing and axial expansion, are lumped in the first term. The second term represents shield plate flexing, and the third represents shield plate radial expansion ( $b \ll a$ ). This model was consistent with laboratory tests on a dummy shield plate, and it was made to fit detailed measurements of the EBR-I Mark II transfer function. Good data fitting, however, was accomplished only by permitting  $B$ ,  $C$ , and  $\tau$  to be frequency dependent. Incidentally, higher resonances that might be expected from the transport-delay terms (as with the spiral in fig. 6-28) were never observed. This is attributed to large attenuation of  $B$  and  $C$  at high frequencies.

The history of the instability in EBR-I Mark II and the subsequent experimental program with EBR-I Mark III may be traced in a number of sources. Additional references may be sought in the documents already cited. The title of ANL-6354 (Smith et al. 1961) is misleading in that it refers to the "instability of EBR-I Mark III"; the title is indeed cited more properly in some sources as referring to Mark II. Quoting from ANL-6354: "... it has been demonstrated conclusively that the Mark III loading of EBR-I is characterized by extreme stability under all operating conditions."

The significant conclusion of these studies is that there is nothing intrinsic in the neutronic or mechanical features of a fast reactor that prevents highly stable operation over a wide range. The observed instabilities were caused by mechanical features that are not present in later designs; see, for example, a study of the dynamics of EBR-II (DeShong 1969).

We close this section by observing that the main limitation of the model given by eq. (6-158) is in the lumped-parameter representation. One way to generalize the model is to include transport time delays. Alternatively, the model may be generalized to that given by eqs. (6-114) and (6-141), and the approximate stability properties deduced using the canonical  $x$ ,  $y$  space of sec. 6-8. For good quantitative results, it may be necessary to employ a complicated analysis using more than one group of delayed neutrons, particularly if the thermal time constants are close to the delayed-neutron lifetimes. The stability criterion developed by Störner (1960), described earlier in connection with fig. 6-31, will frequently prove helpful. Finally, we note that both fast and thermal

reactors that are free from highly space-dependent neutronic properties are adequately described for the purposes of linear stability analysis by the point-reactor model using the prompt-jump approximation.

#### 6-10. Boiling-Water Reactors

In this section we outline briefly the development of one type of lumped-parameter model for a natural circulation boiling-water reactor. An example is the Experimental Boiling Water Reactor (EBWR), and the simplified model is that described by DeShong and Lipinski (1958). Other descriptions of the model are given by Ash (1965), Harrer (1963), and Lipinski (1960). Additional information on boiling-water reactor stability analysis is given by Akcasu (1960), Beckjord (1958), Fleck (1961), George and Sesonske (1959), Nahavandi and von Hollen (1964a), Thie (1958, 1959, 1964), and Weaver (1963).

In a simplified description, the core consists of a lattice of metal-clad fuel plates in water inside a closed vessel. In normal operation, water flows upward through the core and reaches the boiling point at a height inside the core called the boiling boundary. Above this boundary is a region of two-phase flow, and above the water level is a steam dome from which steam passes to the external power system. Water emerging from the core recirculates to the bottom of the vessel, where it is joined by entering water from feedwater inlets.

The dominant reactivity feedback is the negative effect of steam voids in the undermoderated core. The void fraction is affected by direct heat flow into the water (power-void effect) and by the system pressure. The pressure acts in two ways, by changing the void fraction in the boiling region (flashing-void effect) and by changing the location of the boiling boundary (boundary-void effect). The pressure is a complicated function of the instantaneous power and the load on the external power system. Neglecting all temperature coefficients of reactivity, an elementary description of the system is based on three steam-void feedbacks in parallel: power-void, flashing-void, and boundary-void.

Consider the block diagram in fig. 6-73, in which the reactor has been decoupled from the steam turbine system. The zero-power reactor transfer function is  $G(s)$ . Heat transfer into the water is represented with two time constants,  $T_1$  and  $T_2$ , in a manner analogous to the delayed portion of the feedback in fig. 6-67. Here  $\delta q$  represents the heat power delivered to the water.

Assume that a heat impulse in the water produces steam in the boiling region, and that its effect lasts for a mean time  $\tau$  (the steam transit time). The power coefficient of void volume  $V$  may be expressed in  $\text{ft}^3/\text{Mw}$ .

The loop is closed by multiplying by  $\phi$ , the void-volume coefficient of reactivity.

Let  $\sigma$  represent the mass of steam per unit energy. The output of this block is therefore  $dm/dt$  (rate of change of steam mass). The model used for converting this information into a rate of change of pressure is a simplified representation of the pressure-vessel thermodynamics, derived by DeShong and Lipinski (1958). The steam constants  $\eta$  and  $\gamma$  are expressed in lb/psi, and  $T_s$  is the time constant for water recirculation. In this study,  $\eta > \gamma$  so that the pole of this thermodynamic transfer function is at a higher frequency than the zero. (Another pole at very high frequency is neglected.)

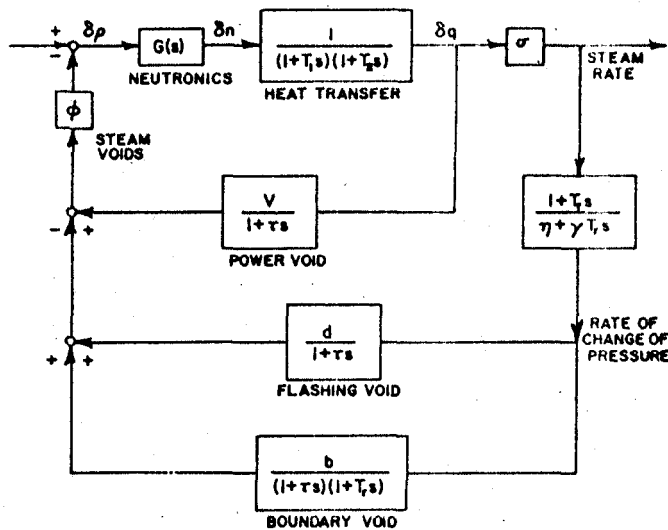


Fig. 6-73. Block diagram for a natural circulation boiling-water reactor (DeShong and Lipinski 1958).

A pressure pulse causes a compression of steam in the boiling region. Assume that the steam transit time  $\tau$  is small enough for the duration of this effect to be determined by  $\tau$ . The same pressure pulse reduces the size of the boiling region, but the relaxation of this effect is additionally delayed by the recirculation time  $T_r$ . The coefficients  $b$  and  $d$  ( $\text{ft}^3/\text{sec}/\text{psi}$ ) are discussed by DeShong and Lipinski (1958). The plus and minus signs in fig. 6-73 are used to emphasize the fact that a power pulse tends to increase the steam void by direct heat transfer and, at the same time, to suppress the steam void by increased pressure.

We have three contributions to the transfer function from  $\delta q$  to steam voids:

$$\frac{V}{1 + \tau s},$$

$$-\frac{\sigma d(1 + T_r s)}{(1 + \tau s)(\eta + \gamma T_r s)},$$

and

$$\frac{\sigma b}{(1 + \tau s)(\eta + \gamma T_r s)}.$$

The power-to-reactivity feedback transfer function is

$$H(s) = \phi \frac{\eta V - \sigma d - \sigma b + (\gamma V - \sigma d) T_r s}{(1 + T_1 s)(1 + T_2 s)(1 + \tau s)(\eta + \gamma T_r s)}, \quad (6-170)$$

where the numerical values are such that  $H(0) > 0$  and the zero is in the left half-plane. Fig. 6-74 shows the calculated magnitude of  $H(s)$  for one set of operating conditions (DeShong and Lipinski 1958):

$$\begin{aligned} n_0 &= 20 \text{ Mw (300 psi)}, \\ \phi &= 1.5 \text{ dollar/ft}^3, \\ V &= 2.2 \text{ ft}^3/\text{Mw}, \\ \sigma &= 23 \text{ lb/Mw sec}, \\ d &= 0.010 \text{ ft}^3 \text{ sec/psi}, \\ b &= 0.57 \text{ ft}^3 \text{ sec/psi}, \\ T_1 &= 0.23 \text{ sec}, \\ T_2 &= 0.14 \text{ sec}, \\ \tau &= 0.062 \text{ sec}, \\ T_r &= 28 \text{ sec}, \\ \eta &= 9.32 \text{ lb/psi}, \\ \gamma &= 1.08 \text{ lb/psi}. \end{aligned}$$

For these operating parameters, eq. (6-170) is

$$H(s) = \frac{1.12(1 + s/0.12)}{(1 + s/0.31)(1 + s/4.4)(1 + s/7)(1 + s/16)}. \quad (6-171)$$

Eq. (6-6) was used to derive the feedback transfer function from oscillator data taken with the turbine off. Agreement between analytical and measured transfer functions, both in amplitude and phase, was satisfactory.

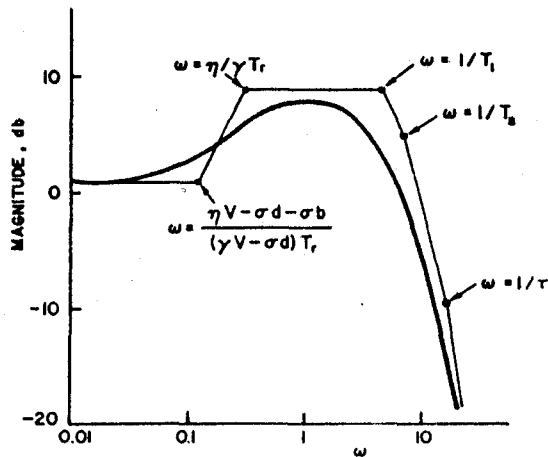


Fig. 6-74. Feedback transfer function for a natural circulation boiling water reactor (DeShong and Lipinski 1958).

The feedback given by eq. (6-171) has one zero at low frequency and four poles at higher frequencies. The open-loop function  $G/H$  represents a positive-gain minimum-phase system. We saw in sec. 6-8 that a minimum-phase feedback with one zero and two poles will not lead to instability except for a special pole-zero configuration such as that in fig. 6-58 (high-frequency zero and low-frequency poles). If there is to be conditional stability with the feedback of eq. (6-171), it must be related to the additional poles.

This possibility is seen in the root-locus sketches of fig. 6-75, for which the prompt-jump model for the neutron dynamics is used. The first sketch is a highly stable example of a feedback with one zero and two poles. The addition of one pole permits oscillation at high gain, but the system is still unconditionally stable. It is the addition of the fourth pole in the feedback, which produces root-locus asymptotes at  $60^\circ$ , that introduces conditional stability.

It was established for the 20-Mw test in EBWR that the gain margin was 0.8 and the phase margin  $50^\circ$  (see fig. 6-29). Gain- and phase-margin curves were used, and the series of tests at various stable power levels was extrapolated to predict an instability threshold at about 65 Mw (DeShong and Lipinski 1958).

Boiling-water reactors and pressurized-water reactors have proved to be highly stable and practical systems for use in electrical power generation. As with fast reactors, there is no intrinsic feature that prevents a wide range of stable operation.

## 6-7 Linear System Stability

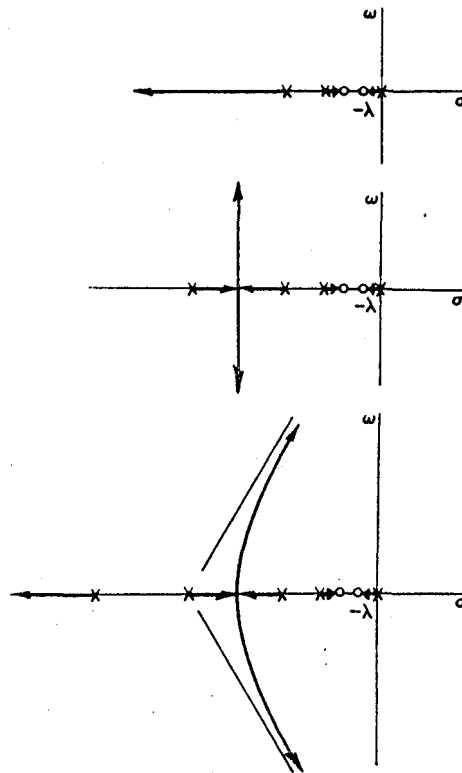


Fig. 6-75. Root-locus sketches for a reactor with one zero in the feedback, illustrating trend toward instability as poles are added (prompt-jump model).

### 6-11. Nuclear Rocket Reactors

Nuclear rocket engines have attracted wide attention because of the promise of higher performance than with chemical rockets and because of many successful ground tests. The reader may consult the books by Ash (1965) and Bussard and DeLauer (1958) for general information. Some dynamic measurements are reported by Bodenschatz et al. (1966) and by Ortenberg (1967). We present a brief analysis of a two-path feedback model used by Smith and Stenning (1961), by Smith (1962, 1964), and by Wiberg and Woyski (1968).

The reactor core is a homogeneous mixture of  $U^{235}$  and graphite, penetrated by propellant passages. The propellant is hydrogen, pumped by a turbine and preheated while the rocket nozzle and the reactor reflector are cooled. The reactivity is determined by the reactor core temperature and the density of hydrogen passing through the core.

Assume that the reactor core and the hydrogen in the core are characterized by a single temperature  $T$ . The reactivity is<sup>4</sup>

$$\rho = \rho_0 - \alpha_T T - \alpha_H P/T, \quad (6-172)$$

where  $T$  and  $P$  are absolute temperature and pressure,  $\rho_0$  is a constant, and  $\alpha_T$  and  $\alpha_H$  are feedback reactivity coefficients. Since  $P/T$  is proportional to density for an ideal gas,  $\alpha_H$  is essentially a density coefficient of reactivity. Increased temperature reduces reactivity ( $\alpha_T > 0$ ) and increased hydrogen density increases reactivity ( $\alpha_H < 0$ ).

The temperature and pressure equations are

$$\frac{dT}{dt} = K_0 n - APT^{\frac{1}{2}} \quad (6-173)$$

and

$$\frac{dP}{dt} = BPT^{\frac{1}{2}} - CP^2T^{-\frac{1}{2}}, \quad (6-174)$$

where  $K_0$  is the reciprocal heat capacity,  $n$  is the total power, and  $A$ ,  $B$ , and  $C$  are positive constants. Eq. (6-174) is the model for turbopump operation given by Smith and Stenning (1961). This two-point nonlinear feedback model has been used in a number of simulation studies (e.g., Wiberg and Woyski 1968).

To investigate linear stability, we must reduce eqs. (6-172) through (6-174) to a set of linear equations correct to first order in the deviations from equilibrium. Using the subscript zero to denote equilibrium, we have

$$BT_0 = CP_0 \quad (6-175)$$

and

$$K_0 n_0 = AP_0 T_0^{\frac{1}{2}} = (AB/C) T_0^{\frac{1}{2}} = A(C/B)^{\frac{1}{2}} P_0^{\frac{1}{2}}. \quad (6-176)$$

Expanding the nonlinear terms in powers of  $\delta T = T - T_0$  and  $\delta P = P - P_0$  and retaining only the linear terms yields

$$\rho = -(\alpha_T - \alpha_H P_0/T_0^2)\delta T - (\alpha_H/T_0)\delta P, \quad (6-177)$$

$$\frac{d}{dt}\delta T = K_0(n - n_0) - \frac{AB}{2C}\sqrt{T_0}\delta T - B\sqrt{T_0}\delta P, \quad (6-178)$$

and

$$\frac{d}{dt}\delta P = \frac{B^2}{C}\sqrt{T_0}\delta T - A\sqrt{T_0}\delta P. \quad (6-179)$$

This is now in the form of the linear coupled system discussed in sec. 6-7.

4. The model proposed by Smith and Stenning (1961) has  $\alpha_c\sqrt{T}$  in place of  $\alpha_T T$  in eq. (6-172). The linearized system and the stability conclusions are essentially the same.

### 3.3.4 Linear System Stability

The matrix of coefficients is

$$\begin{bmatrix} AB \\ 2C\sqrt{T_0} & A\sqrt{T_0} \\ -\frac{B^2}{C}\sqrt{T_0} & B\sqrt{T_0} \end{bmatrix}$$

Note that the time constants and coupling coefficients are all proportional to  $\sqrt{T_0}$ . This means that because the equilibrium power enters into the characteristic equation in a complicated way the simple parameter spaces of secs. 6-7 and 6-8 may not be used (except perhaps in the small neighbourhood of a unique equilibrium). This situation is often encountered with linearized versions of nonlinear systems.

The eigenvalues  $\gamma_1$  and  $\gamma_2$  are the solutions of

$$\gamma^2 - B(T_0)^{\frac{1}{2}}(1 + A/2C)\gamma + 3AB^2T_0/2C = 0. \quad (6-180)$$

It may be shown that the eigenvalues are complex when

$$0.202 < A/C < 19.8$$

and real for other positive values of  $A$  and  $C$ . This possibility of complex poles in the feedback transfer function is another departure from the systems studied in secs. 6-7 and 6-8; the parameter spaces are designed for real eigenvalues only.

However, one can still construct the open-loop transfer function and the characteristic equation as before. With the prompt-jump model, eq. (6-142) is still the characteristic equation; the reader should carry out the algebra and identify  $K$  and  $\xi$ . Since the eigenvalues  $\gamma_1$  and  $\gamma_2$  appear in the characteristic equation only as a sum or product, the characteristic equation has real coefficients (and the Routh numbers are real) whether the eigenvalues are real or complex. This means that the stability conditions of eqs. (6-143) through (6-145) are still useful.

Fortunately, the operating range for a typical nuclear rocket is such that the only significant stability requirement is on the sign of the static power coefficient. This is of course the requirement that the last Routh number be positive. The other stability boundaries are far away from the operating range, and, if  $\rho$  is the net reactivity, the stability requirement may be expressed as

$$T_0 \left( \frac{\partial \rho}{\partial T} \right)_P + P_0 \left( \frac{\partial \rho}{\partial P} \right)_T < 0$$

at equilibrium (Smith and Stenning 1961). It is left as an exercise to show that the pressure effect cancels out using eq. (6-177), and that the stability condition is simply  $\alpha_T > 0$ .

We will not carry this example any further, and we use it to close this chapter on linear stability. Many other important and instructive applications of linear stability analysis to reactor systems may be found in the literature. The classic problems of fission-product poisoning and of the circulating-fuel reactor are included in the problem set. Other topics of interest are coupled-core reactors (Avery 1958; Chezem and Köhler 1967; Keepin 1965; Weaver 1968) and space-dependent feedback (Ergen and Nohel 1959; Gyftopoulos and Smets 1959; Hitchcock 1960; Lellouche 1967a; Sanathanan et al. 1967). The reader is encouraged to study the important subject of reactor noise (Albrecht 1962; Cohn 1960; Keepin 1965; Moore 1958, 1959; Pacilo 1969; Thie 1963; Uhrig 1967) as well as the related topics of Rossi-alpha measurements (Feynman, deHoffman, and Serber 1956; Keepin 1965; Orndoff 1957) and reactor startup in the presence of extremely weak sources (Hansen 1960; Hurwitz et al. 1963; MacMillan and Storm 1963). General discussions of reactor dynamics as a stochastic process are given in the book by Osborn and Yip (1967) and in papers by Natelson, Osborn, and Shure (1966), by Barrett and Thompson (1969), by Harris and Prescop (1969), and by Stacey (1969b).

We have not considered the problem of control-system design; for a conventional background in that field the reader is referred to the books cited at the beginning of sec. 6-1, while more modern techniques (including the "method of state-variable feedback") are described in the books by Schultz and Melsa (1967) and Weaver (1968). A recent contribution to reactor control design is described by Slivinsky and Weaver (1969).

### Problems

- 6-1. Analyze the stability of the system used for example 1, eq. (6-17), with negative  $a$  and positive  $b$ .
- 6-2. In the system of eq. (6-24), regard  $b$  as a fixed positive number and sketch the stable region in the  $K, \alpha$  plane.

In probs. 6-3 through 6-8,  $G(s)H(s)$  is the open-loop transfer function. Plot the stable region for the closed-loop system in the  $K, \alpha$  plane.

$$6-3. \quad G(s)H(s) = \frac{K}{(s+2)(s+\alpha)}.$$

$$6-4. \quad G(s)H(s) = \frac{K + \alpha}{(s+2)(s+\alpha)}.$$

336      *Linear System Stability*

6-5.       $G(s)H(s) = \frac{K\alpha}{(s + 2)(s + \alpha)}.$

6-6.       $G(s)H(s) = \frac{K}{(s + 1)^2(s + \alpha)}.$

6-7.       $G(s)H(s) = \frac{K + \alpha}{(s - 1)(s + 2)(s + \alpha)}.$

6-8.       $G(s)H(s) = \frac{K(s + 1)}{(s - 1)(s + 2)(s + \alpha)}.$

6-9.      Given the open-loop transfer function

$$G(s)H(s) = \frac{K(s + \lambda)}{s(s^2 + \theta_1 s + \theta_1 \theta_2)},$$

where  $\lambda$ ,  $\theta_1$ , and  $\theta_2$  are positive, plot an appropriate two-dimensional parameter space and label stable and unstable regions.

6-10. For the function  $H(s)$  given by eq. (6-41), show that for finite  $\omega$  the real part of  $H(j\omega)$  can vanish only when  $a > b + c$ , and the imaginary part can vanish only when  $a < bc/(b + c)$ .

6-11. Construct graphs like those in figs. 6-17 and 6-18 for the case  $\gamma < \lambda$ .

6-12. Derive a formula for numerical evaluation of a transfer function from step-input response data (Chapin 1969; Weaver 1963).

6-13. Sketch a Nyquist plot for example 5, eq. (6-28), for  $\alpha < 0$ .

6-14. Sketch a Nyquist plot for

$$G(s)H(s) = \frac{K}{s^2 + 1}$$

and for

$$G(s)H(s) = \frac{K}{s(s^2 + 1)}.$$

6-15. Sketch Nyquist and root-locus plots for the various cases in prob. 6-3.

6-16. Sketch Nyquist and root-locus plots for the various cases in prob. 6-6.

6-17. Sketch Nyquist and root-locus plots for the various cases in prob. 6-8.

6-18. If the open-loop transfer function has two poles on the real axis and no zeros, show that the root locus is two perpendicular straight lines in the  $s$ -plane ( $s = \sigma + j\omega$ ) as in fig. 6-33. Show that the departure point is midway between the poles.

- 6-19. Given the open-loop transfer function

$$G(s)H(s) = \frac{K(s + a)}{s(s + b)},$$

find the equation for the root locus in the  $s$ -plane ( $s = \sigma + j\omega$ ). Show that part of the locus may be a circle; locate the center and find the radius.

- 6-20. Given the open-loop transfer function

$$G(s)H(s) = \frac{K(s + 4)}{s^2 + 4s + 20},$$

show that the root locus consists of the real axis and a circle in the  $s$ -plane. Find the radius of the circle and locate its center.

- 6-21. Construct the root locus for the system whose open-loop transfer function is

$$G(s)H(s) = \frac{K(s + 2)}{s(s^2 + 2s + 2)}.$$

- 6-22. Given the open-loop transfer function

$$G(s)H(s) = \frac{K}{(s + a)(s^2 + b^2)},$$

study the stability of the closed-loop system using the Routh, Nyquist, and root-locus methods.

- 6-23. Given the open-loop transfer function

$$G(s)H(s) = \frac{K(s + a)}{s^2(s + b)},$$

sketch possible root-locus plots. Verify the departure points analytically.

- 6-24. For example 5, eq. (6-28), plot the boundary in fig. 6-4 that separates oscillatory and nonoscillatory regions.

- 6-25. Find the range of  $K$  for which the prompt-jump model with Newton cooling, eq. (6-93), exhibits damped oscillations.

- 6-26. Sketch the six root-locus cases for the effective-lifetime model with one feedback plus a power coefficient, eq. (6-103). One of the cases is shown in fig. 6-46.

- 6-27. Calculate and plot the oscillation boundary in the parameter space of fig. 6-45.

- 6-28. Sketch the oscillation boundaries in the parameter spaces of figs. 6-47 and 6-48.

### 6.3. Nuclear System Stability

- 6-29. Find the stability boundaries in the  $A, B$  plane for eq. (6-113). Show that the limit  $\ell \rightarrow 0$  yields figs. 6-47 and 6-48.
- 6-30. Derive eq. (6-114) for the two-region heat balance, starting with total heat-generation rates and nonincremental temperatures (including reservoir temperatures).
- 6-31. Show that the eigenvalues of the heat-transfer matrix
- $$\begin{bmatrix} h_1 + h_2 & -h_1 \\ -h_3 & h_3 + h_4 \end{bmatrix}$$
- are real and positive if the  $h_i$  are real and positive.
- 6-32. Derive the linear transformation relating eqs. (6-114) and (6-116).
- 6-33. Sketch the possible root-locus cases for the effective-lifetime model with two feedbacks and correlate each case with a region in parameter space (fig. 6-52).
- 6-34. Verify the intersection of the two stability boundaries as given by eq. (6-139) and show that the characteristic equation has two zero roots and one negative real root at this point.
- 6-35. Verify the equation for the dynamic stability boundary, eq. (6-147), and show that it is a hyperbola with asymptotes given by eqs. (6-149) and (6-150).
- 6-36. By estimating angles in the  $s$ -plane, show that the root locus in fig. 6-58 cannot cross the imaginary axis unless  $\lambda > \gamma_1 + \gamma_2$ .
- 6-37. Derive the condition for destabilization by delayed neutrons, eq. (6-154).
- 6-38. A dynamic stability boundary such as eq. (6-147) corresponds to two pure imaginary roots whenever the line borders on the stable region. Show that when
- $$\frac{1}{\lambda} > \frac{1}{\gamma_1} + \frac{1}{\gamma_2},$$
- as is the case in fig. 6-63, pure imaginary roots also appear in part of the unstable region.
- 6-39. Discuss the two-region model in the special case  $\gamma_2 \rightarrow 0$  (constant power removal in region 2).
- 6-40. Using polar sketches such as in fig. 6-30, discuss the effect of including a transport delay factor in the delayed feedback for the two-region coupled system (Bethe 1956).

- 6-41. The large neutron absorption of  $Xe^{135}$  is an important reactivity effect in a high-flux reactor. Linearize the system

$$\frac{dI}{dt} = \gamma_I \Sigma_f \phi - \lambda_I I$$

and

$$\frac{dX}{dt} = \gamma_x \Sigma_f \phi + \lambda_I I - \lambda_x X - \sigma_x \phi X,$$

where  $I$  and  $X$  are the concentrations of  $I^{135}$  and  $Xe^{135}$  respectively,  $\phi$  is the neutron flux, and  $\Sigma_f$  is the fission cross-section. Derive the transfer function  $\delta X(s)/\delta \phi(s)$ , which is proportional to the xenon reactivity feedback. Show that this transfer function has a zero that moves into the right half-plane when the equilibrium flux exceeds  $\phi_0 = 3 \times 10^{11}$ . Use

$$\gamma_I = \text{iodine yield fraction} = 0.056;$$

$$\gamma_x = \text{xenon yield fraction} = 0.003;$$

$$\lambda_I = \text{iodine decay constant} = 2.9 \times 10^{-5} \text{ sec}^{-1};$$

$$\lambda_x = \text{xenon decay constant} = 2.1 \times 10^{-5} \text{ sec}^{-1};$$

$$\sigma_x = \text{xenon absorption cross-section} = 3.5 \times 10^{-18} \text{ cm}^2$$

(Schultz 1961; Weaver 1963).

- 6-42. A reactor with a negative temperature coefficient ( $\alpha > 0$ ) is stable at all power levels, and the closed-loop transfer function is a constant at very low frequencies. Add the xenon feedback and explain the possibility of unstable operation for flux levels above  $\phi_0 = 3 \times 10^{11}$  when the magnitude of the temperature coefficient is not sufficiently large.
- 6-43. A one-delay-group model for a circulating-fuel reactor uses a modified precursor equation,

$$\frac{dc}{dt} = \frac{\beta}{\ell} n(t) - \lambda c(t) - \frac{c(t)}{T_1} + \frac{c(t - T_2)}{T_1} e^{-\lambda T_2},$$

where  $T_1$  is the core residence time and  $T_2$  is the residence time in the external loop. Derive the reactivity-to-power transfer function. Show that for low frequencies and small values of  $\lambda T_2$  the transfer function reduces to the usual form with  $\beta$  diminished by a factor

$$a = \frac{T_1}{T_1 + T_2}$$

(MacPhee 1958).



---

## 7 Nonlinear System Stability

In this chapter we present a brief introduction to nonlinear mechanics and some applications to nuclear reactor systems. The emphasis is on analytical methods for investigating stability in the absence of exact solutions, though some graphical and computer solutions are discussed as illustrations.

The presence of the product  $\rho n$  in the point-reactor equations means that the system is nonlinear if there is reactivity feedback. In addition, the feedback itself may be nonlinear. No general method is available for solving nonlinear differential equations, and much theoretical effort has been devoted to stability studies.

An understanding of linear stability theory is an essential prerequisite because many of the concepts used in nonlinear studies are related to those used for linear systems and because nonlinear stability may sometimes be inferred from an associated linearized system. There are, of course, essential differences. For example, a linear system that is stable (in the sense of the preceding chapter) will be stable for any size perturbation. This is not generally true for nonlinear systems; we shall see examples of systems that are stable for small perturbations (linearly stable) but unstable for large perturbations.

Further, a homogeneous linear system with constant coefficients cannot have a solution that grows more rapidly than an exponential function of time. Nonlinear models, including some very simple illustrations, may exhibit solutions that approach infinity in a finite time interval (finite escape time). The study of such systems is inhibited by the fact that Laplace and Fourier transforms do not exist for some or all of their solutions. Another important nonlinear phenomenon is the limit cycle, an isolated periodic motion that is independent of initial conditions.

Two basic problems of nonlinear stability are the determination of regions in a parameter space for which a system is stable for all perturbations (stability in the large) and the determination of regions in state space (or phase space) in which a system is stable (if not stable in the large). However, one should not lose sight of practical considerations; we study the stability of a mathematical model and not the stability of a real reactor system. For example, a system that is asymptotically stable in the large approaches equilibrium as  $t \rightarrow \infty$ ; yet subsequent to certain initial perturbations one or more of the variables may temporarily exceed the system's operating limits. On the other hand, a system that is unstable by definition (see sec. 7-4) may be bounded or easily controllable so that it is stable for all practical purposes. Further, one should not exclude a model from consideration solely because it exhibits nonphysical behaviour in some range; real reactors may not experience finite escape times, but there is useful information in mathematical models that exhibit such behaviour. Of course, the ability to judge whether the mathematical model or the reactor fails first is an essential ingredient of the engineer's art.

The field of nonlinear mechanics was born in the work of Poincaré (1892). The modern approach to nonlinear stability was founded by Liapunov (1892). A collection of translated papers was recently published (1966). A brief history and summary of the state of the art is given in the essay by Lefschetz (1967). The books by Hahn (1963) and by LaSalle and Lefschetz (1961) are devoted to Liapunov's direct method. Nonlinear oscillations are treated by Minorsky (1962) and nonlinear control systems by Lefschetz (1965) and by Minorsky (1969). For deeper study in nonlinear differential equations, one may consult treatises by Cesari (1959), Coddington and Levinson (1955), Krasovskii (1963), Lefschetz (1963), and Malkin (1952).

The subject of nonlinear reactor stability is reviewed briefly by Welton (1961) and later by Chernick (1962) and Kasten (1962). Some stability concepts and considerations of delayed-neutron effects are presented in two papers by Robinson (1954, 1955). Some basic theorems are discussed in the book by Smets (1962). Several advances are reported in the symposium volumes edited by Weaver (1964) and by Hetrick and Weaver (1966). A brief summary appears in the book by Keepin (1965). Later advances are included in the book by Weaver (1968) and in the proceedings of a conference at Brookhaven National Laboratory (1968). The most thorough treatment is that by Akcasu, Lellouche, and Shotkin (forthcoming). Other source materials are cited at the end of sec. 1-1.

We begin by studying the equilibrium points and the state space (phase plane) for second-order systems, with applications to simple

reactor models. We then introduce the direct method of Liapunov and discuss several reactor applications. This is followed by the topic of boundedness and Lagrange stability. The chapter concludes with discussions of frequency-domain stability criteria and nonlinear oscillations.

### 7-1. Equilibrium Points

We may classify the elementary types of equilibrium points exhibited by a nonlinear system of second order by studying the associated linear equations. Suppose we have the nonlinear system

$$\frac{dx}{dt} = P(x, y)$$

and

$$\frac{dy}{dt} = Q(x, y),$$

(7-1)

where  $P$  and  $Q$  are real analytic functions of  $x$  and  $y$ . We assume that  $P$  and  $Q$  both vanish at the origin, so that the origin is an equilibrium point (sometimes called a singular point or critical point). If  $P$  and  $Q$  do not vanish at the origin, we can always make a linear change of variables that "brings the equilibrium point to the origin." In general, a system such as eq. (7-1) may have any number of equilibrium points, in contrast with a linear system, which can have only one.

In chapter 5, we used the state-space technique of eliminating the time variable. Eq. (7-1) becomes

$$\frac{dy}{dx} = \frac{Q(x, y)}{P(x, y)}. \quad (7-2)$$

Occasionally eq. (7-2) may be integrated to yield equations for the integral curves or trajectories in the  $x, y$  plane. The equilibrium points are the points where the right-hand side of eq. (7-2) has the indeterminate form 0/0.

Return to eq. (7-1) and expand  $P$  and  $Q$  in power series,

$$\frac{dx}{dt} = Ax + By + p(x, y)$$

and

$$\frac{dy}{dt} = Cx + Dy + q(x, y),$$

(7-3)

where  $p$  and  $q$  are power series beginning with terms of degree at least two. To investigate the neighborhood of the equilibrium point, we

### 3.4 Nonlinear System Stability

study the associated linear system

$$\frac{dx}{dt} = Ax + By \quad (7-4)$$

and

$$\frac{dy}{dt} = Cx + Dy.$$

Eq. (7-4) is the set of linearized equations valid in a small neighborhood of the equilibrium point. There is a different linearized set for the neighborhood of each equilibrium point of eq. (7-1), with  $\dot{x}$  and  $\dot{y}$  in each neighborhood representing small deviations around one particular equilibrium point.

We may write eq. (7-4) as

$$\frac{d}{dt} \begin{bmatrix} x \\ y \end{bmatrix} = \begin{bmatrix} A & B \\ C & D \end{bmatrix} \begin{bmatrix} x \\ y \end{bmatrix}. \quad (7-5)$$

The eigenvalues of the coefficient matrix are the solutions of

$$s^2 - (A + D)s + AD - BC = 0, \quad (7-6)$$

which is the characteristic equation for the linear system eq. (7-4). The solutions of eq. (7-4) are linear combinations of two exponentials  $e^{st}$ . If the coefficients are real, linear stability corresponds to two negative real roots or a conjugate complex pair with negative real parts. Since conclusions about stability of the nonlinear system eq. (7-3) are valid only in a small neighborhood of the equilibrium point, we use the term "stability in the small."

We proceed to study the types of linear trajectories that can arise with different possible pairs of eigenvalues. To do this, we seek a convenient canonical representation (canonical, decoupled, or normal coordinates) for the general second-order linear system. We then classify the various types of equilibrium points for a nonlinear system in terms of the types of trajectories in the small neighborhood of each equilibrium point.

An eigenvector belonging to the eigenvalue  $s$  may be derived from

$$\begin{bmatrix} A & B \\ C & D \end{bmatrix} \begin{bmatrix} e \\ f \end{bmatrix} = s \begin{bmatrix} e \\ f \end{bmatrix}.$$

The components of the eigenvector must satisfy

$$\frac{f}{e} = \frac{s - A}{B} = \frac{C}{s - D}.$$

We select a pair of eigenvectors

$$K_1 \begin{bmatrix} s_1 - D \\ C \end{bmatrix} \text{ and } K_2 \begin{bmatrix} s_2 - D \\ C \end{bmatrix}$$

corresponding to eigenvalues  $s_1$  and  $s_2$  respectively. The sum of the eigenvalues is, by eq. (7-6),

$$s_1 + s_2 = A + D,$$

so that the two eigenvectors may be written

$$K_1 \begin{bmatrix} A - s_2 \\ C \end{bmatrix} \text{ and } K_2 \begin{bmatrix} A - s_1 \\ C \end{bmatrix}.$$

It is this device that permits a simple canonical representation.

The transformation is

$$\begin{bmatrix} \xi \\ \eta \end{bmatrix} = T^{-1} \begin{bmatrix} x \\ y \end{bmatrix},$$

where

$$T = \begin{bmatrix} K_1(A - s_2) & K_2(A - s_1) \\ K_1C & K_2C \end{bmatrix}.$$

Forming  $T^{-1}$  and selecting

$$K_1 = -K_2 = \frac{1}{C(s_1 - s_2)}$$

yields

$$T^{-1} = \begin{bmatrix} C & s_1 - A \\ C & s_2 - A \end{bmatrix}.$$

The canonical variables are

$$\xi = Cx + (s_1 - A)y$$

and

(7-7)

$$\eta = Cx + (s_2 - A)y.$$

It is easily verified that

$$\frac{d\xi}{dt} = s_1 \xi$$

### 11. Nonlinear System Stability

and

(7-8)

$$\frac{d\eta}{dt} = s_2 \eta.$$

Eliminating the time variable yields

$$\frac{d\eta}{d\xi} = \frac{s_2 \eta}{s_1 \xi},$$

which may be integrated as

$$\eta = C_1 \xi^{s_2/s_1}. \quad (7-9)$$

Before studying eq. (7-9) further, we note that it is not convenient for complex eigenvalues. However, we have selected a transformation that is well adapted to this possibility. Suppose

$$s_1 = a + jb, \quad s_2 = a - jb.$$

Then eq. (7-7) becomes

$$\dot{\xi} = Cx + (a - A + jb)y$$

and

(7-10)

$$\eta = Cx + (a - A - jb)y,$$

and we note that  $\eta = \xi^*$ . Separating into real and imaginary parts, let

$$\xi = u + jv, \quad \eta = u - jv.$$

Substituting into eq. (7-8) yields

$$\frac{du}{dt} = au - bv$$

and

(7-11)

$$\frac{dv}{dt} = bu + av.$$

Again eliminating the time variable, we have

$$\frac{dv}{du} = \frac{bu + av}{au - bv}. \quad (7-12)$$

The final step is to introduce polar coordinates in the  $u, v$  plane:

$$u = r \cos \phi, \quad v = r \sin \phi.$$

Upon substitution, eq. (7-12) reduces to

$$ar d\phi = b dr,$$

which may be integrated as

$$r = C_2 \exp(a\phi/b). \quad (7-13)$$

Eqs. (7-9) and (7-13) may now be used to classify linear trajectories in the  $\xi, \eta$  or the  $u, v$  plane.

*Case 1. Eigenvalues real and positive.* From eq. (7-9),

$$\eta = C_1 \xi^n, \quad (7-14)$$

where  $n = s_2/s_1 > 0$ . Possible trajectories are shown in fig. 7-1. It can be deduced from eq. (7-8) that the motion is always away from the origin. The equilibrium point is called an *unstable node*. The time variable is a parameter, which increases in the direction of the arrow. By choosing a pair of initial values (any point in the plane except the origin), one selects a unique trajectory. Of course, any point on a trajectory may be regarded as  $t = 0$ . The special case  $s_1 = s_2$  (straight-line trajectories) is sometimes called a star. (The transformation  $T$  is singular in this degenerate case. Later we discuss a case in the  $x, y$  plane that has equal eigenvalues.)

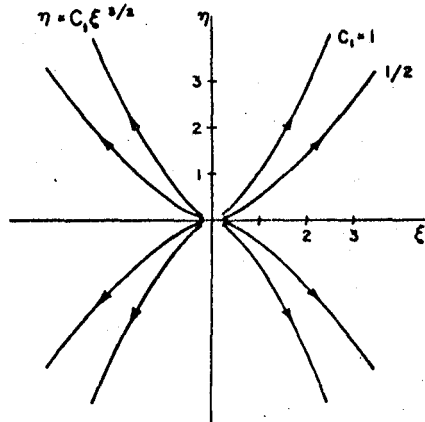


Fig. 7-1. Unstable node (eigenvalues real and positive).

*Case 2. Eigenvalues real and negative.* Eq. (7-14) with  $n > 0$  still applies. By eq. (7-8) the motion is always toward the origin, and the equilibrium point is a *stable node* as shown in fig. 7-2. Note that a trajectory does not continue through the origin; a single smooth curve represents two distinct trajectories that approach the origin as  $t \rightarrow \infty$ .

*Case 3. Eigenvalues real with opposite sign.* Eq. (7-14) may be written

$$\eta = C_1 \xi^{-|n|}, \quad (7-15)$$

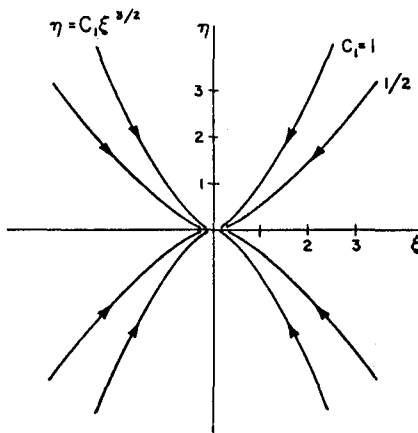
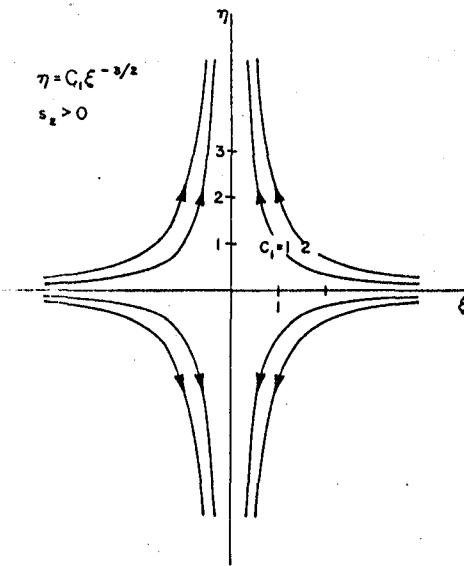


Fig. 7-2. Stable node (eigenvalues real and negative).

where  $n = s_2/s_1 < 0$ . An example is shown in fig. 7-3 for  $s_2 > 0$ . This case, called a *saddle point*, is unstable, though there are two special trajectories along the  $\xi$ -axis that approach the origin as  $t \rightarrow \infty$ . These trajectories may be regarded as metastable in that the slightest perturbation away from the  $\xi$ -axis will grow indefinitely. Trajectories along either coordinate axis correspond to the excitation of only one of the two normal modes (this applies to figs. 7-1 and 7-2 as well).

Fig. 7-3. Saddle point (eigenvalues real with opposite sign,  $s_2 > 0$ ).

**Case 4. Eigenvalues complex with positive real part.** Eq. (7-13) represents a logarithmic spiral. It may be deduced from eq. (7-11) that the motion is away from the origin if  $a > 0$ . The equilibrium point is called an *unstable focus* or *spiral point*. The system executes an unbounded growing oscillation. A typical trajectory is shown in fig. 7-4.

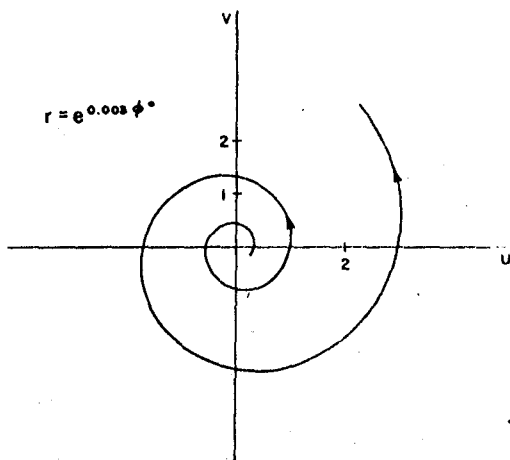


Fig. 7-4. Unstable focus or spiral point (eigenvalues complex with positive real part).

**Case 5. Eigenvalues complex with negative real part.** Motion along the spiral is toward the origin if  $a < 0$ . The equilibrium point is called a *stable focus* or *spiral point*, as shown in fig. 7-5. The system undergoes a damped oscillation.

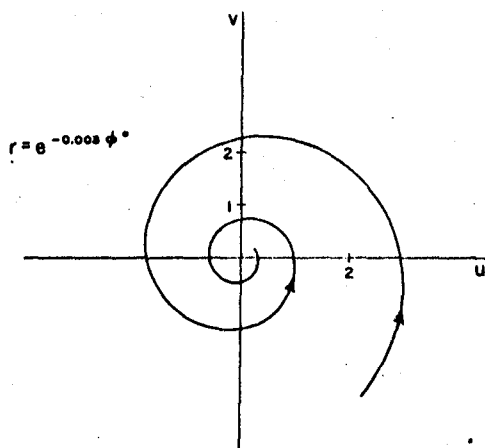


Fig. 7-5. Stable focus or spiral point (eigenvalues complex with negative real part).

*Case 6. Eigenvalues purely imaginary.* The spiral degenerates to a circle when  $a = 0$ . The equilibrium point is a *center* or *vortex point*, shown in fig. 7-6. The motion is periodic, and the particular closed orbit is selected by the initial state. This type of sustained oscillation can also occur in some nonlinear systems, but it must not be confused with a limit cycle, which is an isolated periodic motion that neighboring trajectories tend to approach (or diverge from). Limit cycles do not exist in linear systems.

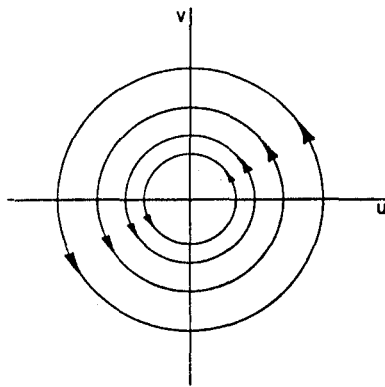


Fig. 7-6. Center or vortex point (eigenvalues imaginary).

*Case 7. Eigenvalues equal.* One type of motion with  $s_1 = s_2$  was mentioned earlier as a special case of a node. The trajectories in the  $\xi, \eta$  plane are radial lines, and such a case is called a star point.

However, when the system of eq. (7-4) has equal eigenvalues, the transformation  $T$  is singular. Consider an example for which  $A = D$  and  $B = 0$ :

$$\begin{aligned} \frac{dx}{dt} &= Ax, \\ \frac{dy}{dt} &= Cx + Ay. \end{aligned} \tag{7-16}$$

There are two eigenvalues  $s = A$ . One standard procedure for solution is to eliminate  $x$  and then solve the second-order equation

$$\frac{d^2y}{dt^2} - 2A \frac{dy}{dt} + A^2y = 0 \tag{7-17}$$

in terms of  $e^{At}$  and  $te^{At}$ .

Trajectories in the  $x, y$  plane are found from

$$\frac{dy}{dx} = \frac{Cx + Ay}{Ax}, \quad (7-18)$$

which has the integral

$$y = kx + (C/A)x \log x. \quad (7-19)$$

An example for  $C = A < 0$  is shown in fig. 7-7. Clearly, stability depends on the sign of  $A$ .

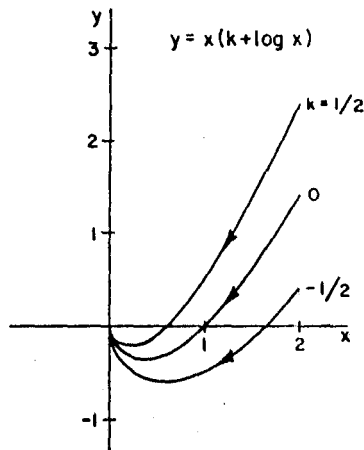


Fig. 7-7. A system with equal negative eigenvalues.

*Case 8. One eigenvalue zero.* Canonical coordinates for eq. (7-4) may be found (it is the matrix of coefficients that is singular), and the coordinate corresponding to the zero eigenvalue is independent of time. This means that there is no unique equilibrium point.

Consider a simple example in the  $x, y$  space ( $A = B = 0, C = 1, D = -2$ ):

$$\begin{aligned} \frac{dx}{dt} &= 0, \\ \frac{dy}{dt} &= x - 2y. \end{aligned} \quad (7-20)$$

The eigenvalues are  $s = 0$  and  $-2$ . We find

$$x = 2k_1$$

and

$$y = k_1 + k_2 e^{-2t}.$$

### 3.3 Nonlinear System Stability

The trajectories are the lines  $x = \text{constant}$ , as shown in fig. 7-8. Note that the line  $y = x/2$  is an "equilibrium line." Stability is determined by the sign of the nonzero eigenvalue.

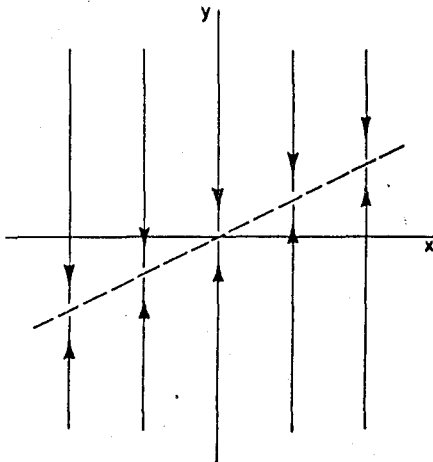


Fig. 7-8. A system with one negative and one zero eigenvalue.

The use of these concepts in analyzing nonlinear systems may be illustrated by an example. Consider the system (Cunningham 1958, 1963):

$$\begin{aligned}\frac{dx}{dt} &= -2x + xy, \\ \frac{dy}{dt} &= -y + xy.\end{aligned}\tag{7-21}$$

This nonlinear system has two equilibrium points:  $x = 0, y = 0$  and  $x = 1, y = 2$ . In the neighborhood of the origin, the associated linear system is

$$\begin{aligned}\frac{dx}{dt} &= -2x, \\ \frac{dy}{dt} &= -y.\end{aligned}\tag{7-22}$$

The eigenvalues are  $-2$  and  $-1$ , and the origin is a stable node.

However, there is no guarantee that the system is stable outside this small neighborhood (stable in the large). To investigate the other equilibrium point, let

$$\begin{aligned}x &= 1 + x', \\y &= 2 + y',\end{aligned}$$

where  $x'$  and  $y'$  are small. Substituting into eq. (7-21) and neglecting nonlinear terms, we find

$$\begin{aligned}\frac{dx'}{dt} &= y', \\ \frac{dy'}{dt} &= 2x'.\end{aligned}\tag{7-23}$$

The coefficient matrix is

$$\begin{bmatrix} 0 & 1 \\ 2 & 0 \end{bmatrix}.$$

Since the eigenvalues are  $\pm\sqrt{2}$ , the point  $x = 1, y = 2$  is a saddle point.

The  $x, y$  plane is shown in fig. 7-9. The trajectories were computed numerically (Cunningham 1963). Note the metastable trajectories to the saddle point; together these two trajectories form the separatrix between the stable and unstable regions of the plane. The special trajectory from the saddle point to the origin may also be regarded as a separatrix.

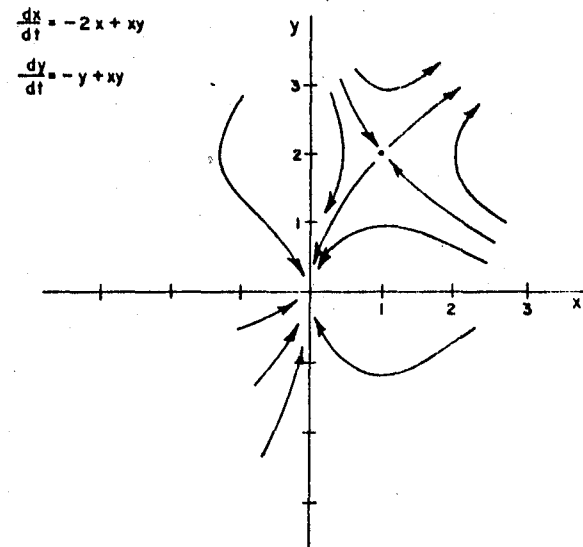


Fig. 7-9. A nonlinear system with a stable node and a saddle point (Cunningham 1963; reprinted by special permission from *American Scientist*, December 1963. © 1963 by the Society of the Sigma Xi).

### 35-1 Nonlinear System Stability

The coordinate axes have special properties in this example. Along the  $x$ -axis,  $dx/dt = -2x$ , while along the  $y$ -axis,  $dy/dt = -y$ . These special trajectories may also be regarded as separatrices in the sense that no trajectory may cross a coordinate axis.

In the next section, we discuss some graphical aids for making rough sketches of the trajectories and thereby deducing the stability properties of a second-order nonlinear system without recourse to numerical solutions. Unfortunately, third-order systems are not generally amenable to such analysis, and systems of order higher than third require much more sophisticated analytical techniques.

The system of fig. 7-9 has a unique feature that is not generally found even in simple second-order systems. We can rewrite eq. (7-21) as

$$\begin{aligned} \frac{dx}{dt} &= -2 + y, \\ \frac{dy}{dt} &= -1 + x. \end{aligned} \tag{7-24}$$

In the quarter-plane  $x < 1, y < 2$ , the variables and their time derivatives have opposite signs. Therefore, all trajectories are heading toward the origin, and the entire quarter-plane is stable. Such a direct determination of a large region of stability is a special feature of this particular system.

### 7-2. Geometry of the Phase Plane

Trajectories discussed in the preceding section are, strictly speaking, representations of solutions in a two-dimensional state space (a state plane). Figs. 7-1 through 7-6 are canonical state planes. However, the terminology "phase space" or "phase plane" is quite commonly employed for such examples, though a distinction remains between state variables and phase variables.

We say that an  $n$ th order system is characterized by the time dependence of  $n$  state variables. Canonical variables constitute a decoupled set of state variables. In contrast, a set of phase variables consists of one function and its first  $n - 1$  time derivatives.

To illustrate the use of phase variables, consider a second-order nonlinear differential equation:

$$\frac{d^2x}{dt^2} + x + x^2 = 0. \tag{7-25}$$

Select phase variables  $x$  and  $y = dx/dt$ . We have

$$\begin{aligned}\frac{dx}{dt} &= y, \\ \frac{dy}{dt} &= -x - x^2.\end{aligned}\tag{7-26}$$

The differential equation for trajectories in the phase plane is

$$\frac{dy}{dx} = -\frac{x + x^2}{y}.\tag{7-27}$$

Solutions of  $dy/dx = f(x, y)$  exist in closed form only for special cases; in this example the integral curves are

$$y^2 + x^2 + \frac{2}{3}x^3 = C.\tag{7-28}$$

The phase plane is shown in fig. 7-10. Note the curve for  $C = \frac{1}{3}$  that separates the stable and unstable regions.

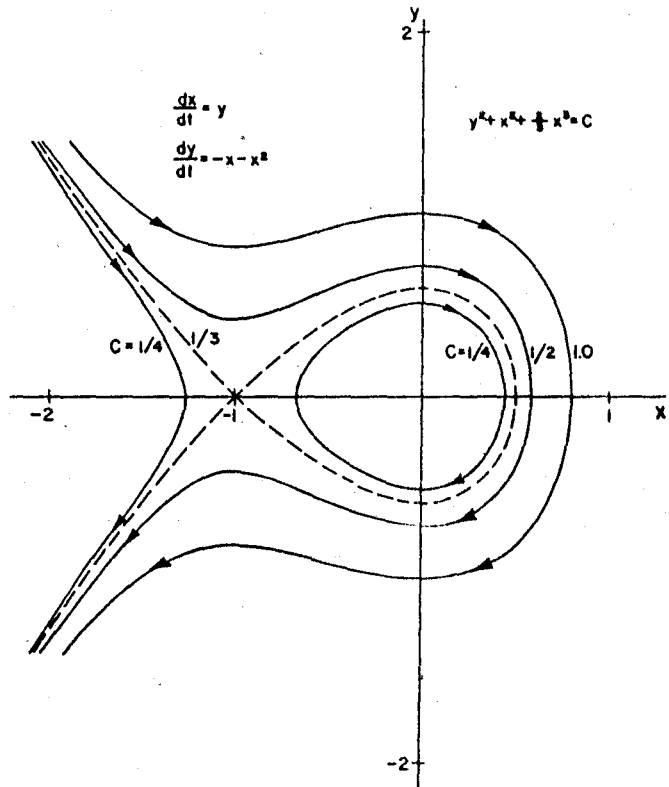


Fig. 7-10. Trajectories for a nonlinear system with a center and a saddle point.

### 7.6 Nonlinear System Stability

The example illustrates a number of features of the phase plane. This is, of course, a state space, as is the plane shown in fig. 7-9. Note, however, one unique feature of using phase variables: trajectories always cross the  $x$ -axis perpendicular to it ( $dy/dx \rightarrow \infty$  as  $y \rightarrow 0$ ).

The equilibrium points are the origin and the point  $(-1, 0)$ . The former is a center with eigenvalues  $\pm j$ , and the latter is a saddle point with eigenvalues  $\pm 1$ . The slope  $dy/dx$  is unique at every point except an equilibrium point, and all trajectories are smooth curves except the separatrix  $C = \frac{1}{3}$  and the stable equilibrium  $C = 0$ .

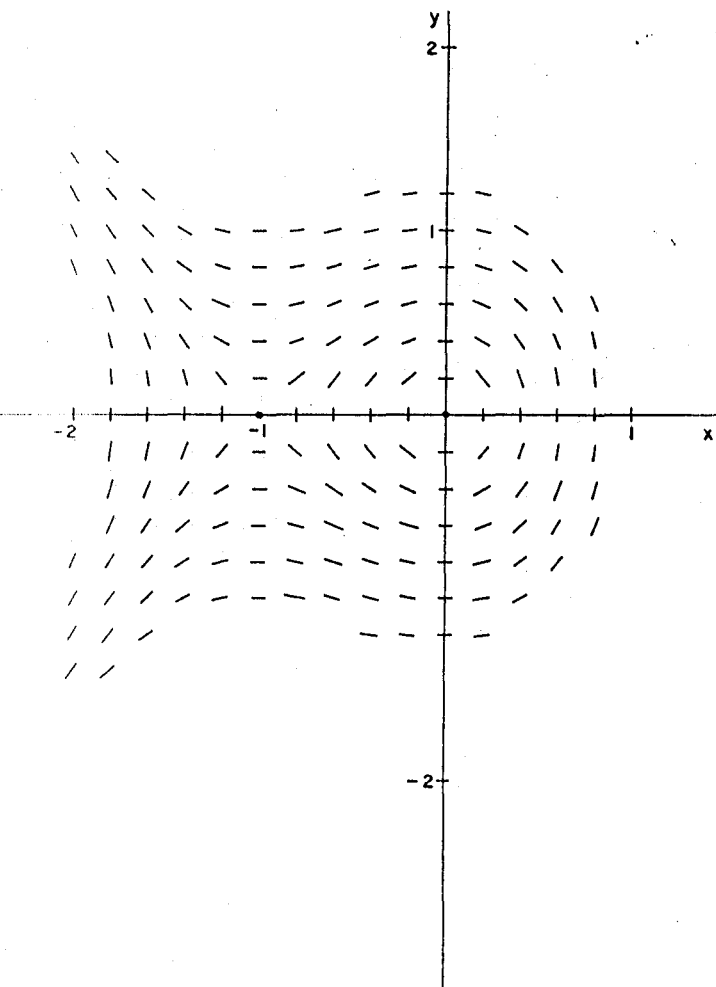


Fig. 7-11. The direction field for the system of fig. 7-10.

Now suppose eq. (7-27) had no simple integral. We could still sketch a set of trajectories, using the direction field mentioned earlier in sec. 5-7 and shown for this example in fig. 7-11. One computes  $dy/dx$  at each point from eq. (7-27) and draws a short line having the specified slope. The direction of motion is found from eq. (7-26). Trajectories may then be sketched, and the accuracy depends on one's care and patience.

Another aid is the method of isoclines, also mentioned in sec. 5-7. An isocline is the locus of points in the direction field having fixed  $dy/dx = M$ . From eq. (7-27),

$$M = -(x + x^2)/y,$$

and the isoclines are the parabolas

$$y = -(x^2 + x)/M. \quad (7-29)$$

A set is shown in fig. 7-12. Note that isoclines radiate from equilibrium points (indeterminate  $M$ ). The zero-slope isocline is the pair of lines  $x = 0$  and  $x = -1$ . The infinite-slope isocline is the  $x$ -axis because we are using phase variables.

It is often helpful to find the slope of a separatrix at a node or saddle point. Such a special trajectory must enter or leave along an isocline. From eq. (7-29), the derivative along an isocline is

$$\frac{dy}{dx} = -(2x + 1)/M. \quad (7-30)$$

We set  $dy/dx = M$  at the saddle point  $(-1, 0)$  and solve for  $M$  to find  $M = \pm 1$ . The separatrix in fig. 7-10 is seen to approach the saddle point with slope  $\pm 1$ . This technique was used in sec. 5-7 to find the initial slope of the trajectory for eq. (5-163) that emerges from the saddle point at the origin. From another viewpoint, this is a representation of eigenvectors in the  $x, y$  plane.

All these considerations also apply to phase planes representing state variables that are not phase variables (except the observation that the  $x$ -axis is always an infinite-slope isocline). There is another special advantage of using phase variables. We have, for small increments,

$$y = \frac{dx}{dt} \cong \frac{\Delta x}{\Delta t}, \quad \Delta t \cong \Delta x/\bar{y}, \quad (7-31)$$

where  $\bar{y}$  is an average value of  $y$  corresponding to an increment  $\Delta x$  on a trajectory. One can therefore graphically construct curves of time functions from a phase-variable trajectory.

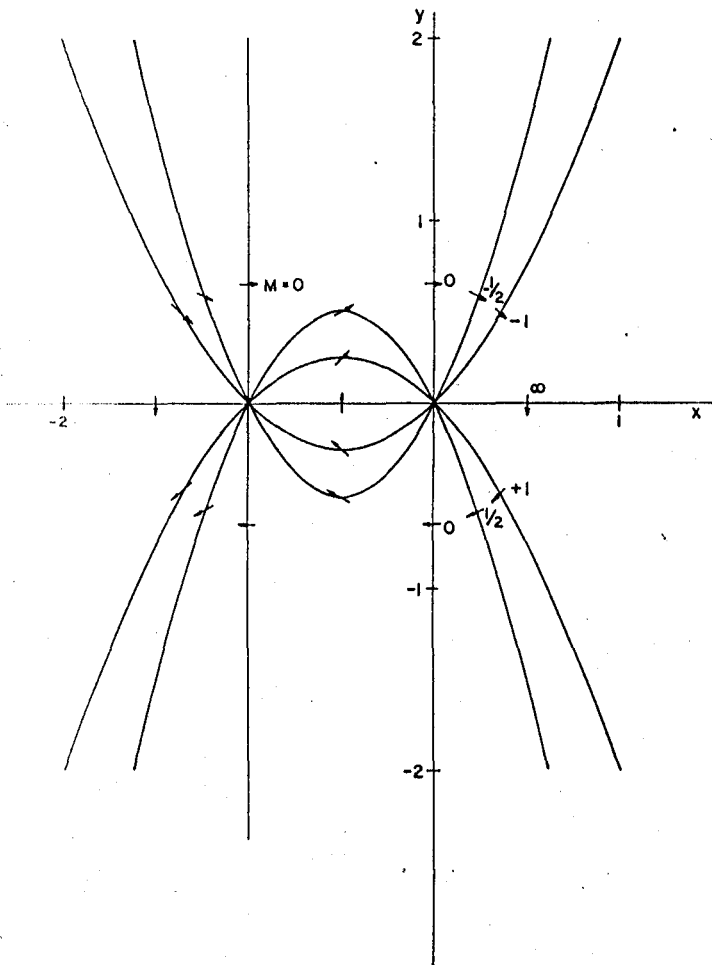


Fig. 7-12. Isoclines for the system of fig. 7-10.

One other advantage of phase variables is the simple correspondence between an  $n$ th order differential equation and the associated matrix of coefficients. Given the linear equation with constant coefficients,

$$a_n \frac{d^n x}{dt^n} + a_{n-1} \frac{d^{n-1} x}{dt^{n-1}} + \cdots + a_1 \frac{dx}{dt} + a_0 x = 0, \quad (7-32)$$

and the set of phase variables  $x_1 = x$ ,  $x_2 = dx/dt$ ,  $x_3 = d^2x/dt^2$ , etc., one finds

$$\frac{d}{dt} \begin{bmatrix} x_1 \\ x_2 \\ x_3 \\ \vdots \\ x_{n-1} \\ x_n \end{bmatrix} = \begin{bmatrix} 0 & 1 & 0 & \cdots & 0 \\ 0 & 0 & 1 & \cdots & 0 \\ 0 & 0 & 0 & \cdots & 0 \\ \vdots & \vdots & \vdots & \ddots & \vdots \\ 0 & 0 & 0 & \cdots & 1 \\ -\frac{a_0}{a_n} & -\frac{a_1}{a_n} & -\frac{a_2}{a_n} & \cdots & -\frac{a_{n-1}}{a_n} \end{bmatrix} \begin{bmatrix} x_1 \\ x_2 \\ x_3 \\ \vdots \\ x_{n-1} \\ x_n \end{bmatrix}. \quad (7-33)$$

Returning now to state variables that are not phase variables, consider the example

$$\begin{aligned} \frac{dx}{dt} &= -x + y + x^2, \\ \frac{dy}{dt} &= -2y - 2xy. \end{aligned} \quad (7-34)$$

This system has three equilibrium points: a stable node at the origin (eigenvalues  $-1$  and  $-2$ ) and two saddle points:  $(1, 0)$  and  $(-1, -2)$ . Each saddle point has eigenvalues  $+1$  and  $-4$ . The trajectories shown

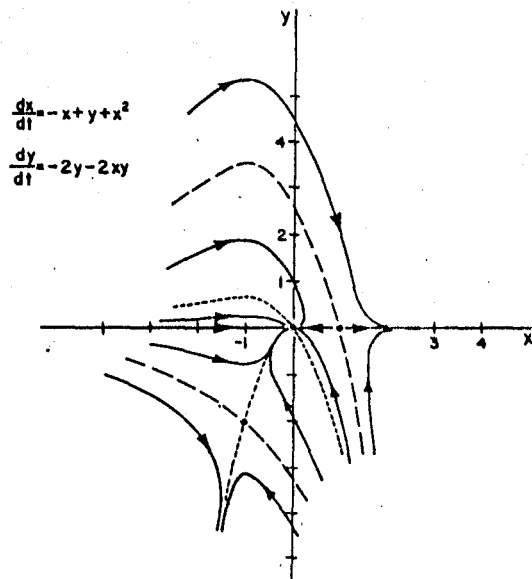


Fig. 7-13. A nonlinear system with a stable node and two saddle points, stable region between heavy dashed lines.

160      *Nonlinear System Stability*

in fig. 7-13 were constructed graphically by use of the direction field and verified on an analogue computer (computations by Peter Meenan, University of Arizona, 1966).

Note that the line  $y = 0$  is a separatrix. Other separatrices in fig. 7-13, shown as dashed lines, were determined graphically. The separatrices that bound the stable region of the phase plane are shown as heavy dashed lines.

This example indicates how the stability of a second-order nonlinear system may be determined by simple geometrical methods in the absence of an exact solution. In the next section, we apply these geometrical ideas to a few simple nonlinear reactor examples.

### 7-3. Some Simple Reactor Systems

The concepts of the preceding two sections may now be applied to a variety of second-order nonlinear models for nuclear reactors. The reader is referred to two classic papers: Chernick (1951) and Ergen and Weinberg (1954). In this section we treat the effective-lifetime model and the prompt-jump approximation, using with each a linear feedback (either constant power removal or Newton's law of cooling).

The first example is the effective-lifetime model, eq. (3-27):

$$\frac{dn}{dt} = \frac{\rho}{\ell'} n, \quad (7-35)$$

where

$$\rho = -\alpha T \quad (7-36)$$

with  $T$  the incremental temperature ( $T = 0$  at equilibrium). Assume  $\alpha > 0$ . We have

$$\frac{dn}{dt} = -\frac{\alpha}{\ell'} nT. \quad (7-37)$$

For constant power removal, use eq. (5-68):

$$\frac{dT}{dt} = K_0(n - n_0), \quad (7-38)$$

where we retain the subscript on  $K$  that was introduced in sec. 6-6. There is one equilibrium point:  $n = n_0$ ,  $T = 0$ .

The linearized system, which may be obtained by setting  $n = n_0 + \delta n$  and neglecting  $T\delta n$  in eq. (7-37), was treated in sec. 6-6 ( $\gamma \rightarrow 0$ ). The characteristic equation is

$$s^2 = -\alpha K_0 n_0 / \ell' = -\Omega^2,$$

and the eigenvalues are  $\pm j\Omega$ ; see eq. (6-91). The equilibrium point is a center.

For the nonlinear system, we may eliminate the time in eqs. (7-37) and (7-38) to find

$$\frac{dn}{dT} = -\frac{\alpha n T}{\ell' K_0 (n - n_0)}. \quad (7-39)$$

Rearranging, we have

$$\ell' K_0 n_0 \frac{dn}{n} - \ell' K_0 dn = \alpha T dT.$$

Maximum and minimum power occur at  $T = 0$ . Integrating from  $n = n_{\min}$  and  $T = 0$ , we have

$$\log \frac{n}{n_{\min}} - \frac{n - n_{\min}}{n_0} = \frac{\alpha}{2\ell' K_0 n_0} T^2. \quad (7-40)$$

The trajectories are closed curves in the  $n, T$  plane for  $\alpha > 0$ , and we have an undamped nonlinear oscillator (a nonlinear center).

We take advantage of the similarity to eq. (5-188) and define

$$x = \left( \frac{\alpha}{\ell' K_0 n_0} \right)^{\frac{1}{2}} T, \quad y = \frac{n}{n_0}, \quad y_0 = \frac{n_{\min}}{n_0}. \quad (7-41)$$

Eq. (7-40) becomes

$$\log \frac{y}{y_0} - (y - y_0) = \frac{1}{2} x^2, \quad (7-42)$$

which is identical to eq. (5-190) except that the variables have different physical meanings. The  $x, y$  plane is shown in fig. 7-14, with the parameter  $1/y_0 = n_0/n_{\min}$ . This time the closed curves are traversed clockwise, as seen from eq. (7-37). The line  $y = 0$ , corresponding to  $n(t) = 0$  and  $dT/dt = -K_0 n_0$ , is a separatrix that bounds the region of closed curves; the system cannot cross into the unstable region of negative  $n$ , as discussed in sec. 2-1. The similarity of figs. 5-20 and 7-14 suggests that the ramp-input problem and the present problem can be combined in a single treatment if  $x$  and  $y$  are properly defined and  $\ell'$  instead of  $\ell$  is used throughout. This was described in a paper by Smets (1959a).

We can express the present problem as a second-order differential equation

$$\ell' \frac{d^2 \rho}{dt^2} - \rho \frac{d\rho}{dt} + \alpha K_0 n_0 \rho = 0. \quad (7-43)$$

162 Nonlinear System Stability

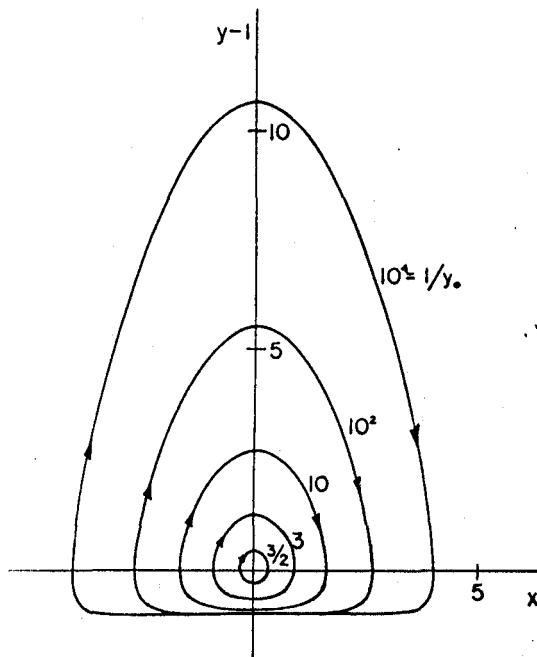


Fig. 7-14. Trajectories for the effective-lifetime model with constant power removal;  $x = (\gamma \ell' / K_0 n_0)^{1/2} T$ ,  $y = n/n_0$ , and  $1/y_0 = n_0/n_{\min}$ .

Compare this with eq. (5-191). Fig. 7-14 may therefore be converted into the phase plane  $d\rho/dt$  vs.  $\rho$  (reverse signs and change scales, noting that  $y - 1$  corresponds to  $-d\rho/dt$  and  $x$  to  $-\rho$ ).

The closed curves of fig. 7-14 have important consequences for stability. If we replace eq. (7-38) by eq. (5-62), using  $K_0$  for  $K$  and  $T_0 = 0$  for the equilibrium,

$$\frac{dT}{dt} = K_0(n - n_0) - \gamma T, \quad (7-44)$$

the equilibrium point  $n = n_0$ ,  $T = 0$  is either a stable node or focus. The linear system is

$$\frac{d}{dt} \begin{bmatrix} \delta n \\ T \end{bmatrix} = \begin{bmatrix} 0 & -\alpha n_0 / \ell' \\ K_0 & -\gamma \end{bmatrix} \begin{bmatrix} \delta n \\ T \end{bmatrix}, \quad (7-45)$$

where  $\delta n = n - n_0$ . The eigenvalues are

$$\lambda = -\frac{\gamma}{2} \pm \sqrt{\left(\frac{\gamma^2}{4} - \frac{\alpha K_0 n_0}{\ell'}\right)}, \quad (7-46)$$

and the linear system oscillates if  $\alpha K_0 n_0 / \ell' > \gamma^2 / 4$ . (See sec. 6-6 and the root locus of fig. 6-38.)

If eqs. (7-37) and (7-44) are used, the nonlinear trajectories satisfy

$$\frac{dn}{dT} = -\frac{\alpha n T}{\ell'[K_0(n - n_0) - \gamma T]}. \quad (7-47)$$

If  $\alpha > 0$  is assumed, eq. (7-39) gives the slope  $dn/dT$  on a closed curve ( $\gamma = 0$ ). By comparing eq. (7-39) with eq. (7-47) for  $\gamma > 0$ , we may deduce that the trajectories for  $\gamma > 0$  must cross closed curves from the outside toward the inside everywhere in the half plane  $n > 0$  (see fig. 7-15). This can be formalized as a geometric proof of asymptotic stability for the nonlinear system eqs. (7-37) and (7-44) in the entire half plane  $n > 0$  provided  $\alpha > 0$  (the other parameters must physically be always positive).

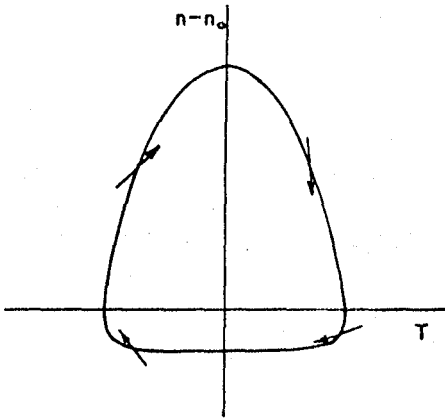


Fig. 7-15. Sketch of the  $n, T$  plane for the effective-lifetime model, illustrating the effect of the heat-loss term on the trajectories.

This type of geometric or topological argument is frequently useful in establishing stability. In third-order systems it may be applied by finding closed surfaces in state space across which all trajectories are directed inward (e.g., Smets and Gyftopoulos 1959).

Next, consider eqs. (7-37) and (7-44) and note the second equilibrium point  $n = 0, T = -K_0 n_0 / \gamma$ . This is the shutdown equilibrium, and by eq. (7-36) the shutdown reactivity is

$$\rho_s = \alpha K_0 n_0 / \gamma. \quad (7-48)$$

Note that  $\rho_s > 0$  if the equilibrium at  $n = n_0$  is to be stable ( $\alpha > 0$ ). Of course, a real reactor at shutdown has a small power  $n > 0$  because of neutron sources, but, as discussed in sec. 2-1, the nonphysical

concept of zero-power equilibrium is very useful in nonlinear stability analysis.

Therefore let  $n = \delta n$  and  $T = -K_0 n_0 / \gamma + \delta T$ . Substituting into eqs. (7-37) and (7-44) and neglecting  $\delta n \delta T$  yields

$$\frac{d}{dt} \begin{bmatrix} \delta n \\ \delta T \end{bmatrix} = \begin{bmatrix} \alpha K_0 n_0 / \gamma \ell' & 0 \\ K_0 & -\gamma \end{bmatrix} \begin{bmatrix} \delta n \\ \delta T \end{bmatrix}. \quad (7-49)$$

Since the eigenvalues are  $s = -\gamma$  and  $s = \alpha K_0 n_0 / \gamma \ell'$ , the shutdown equilibrium is a saddle point for  $\alpha > 0$ .

An example in which the equilibrium  $n = n_0$  is a stable focus is sketched in fig. 7-16. The ordinate is  $n/n_0$  and the abscissa is  $\alpha T / \ell'$ . Here,  $\gamma = 2$  and  $\alpha K_0 n_0 / \ell' = \Omega^2 = 2$ ; hence the equilibrium points are  $(0, 1)$  and  $(-1, 0)$ . The stable focus has eigenvalues  $-1 \pm j$ , and the shutdown saddle point has eigenvalues  $+1$  and  $-2$ . Each coordinate axis is a zero-slope isocline (ZSI). Note the separatrix from the shutdown to the operating point; if the technique outlined in sec. 7-2 is used, the two separatrices at the saddle point have slopes  $M = 0$  and  $M = \frac{3}{2}$ . Trajectories for  $n < 0$ , of course, have no physical significance.

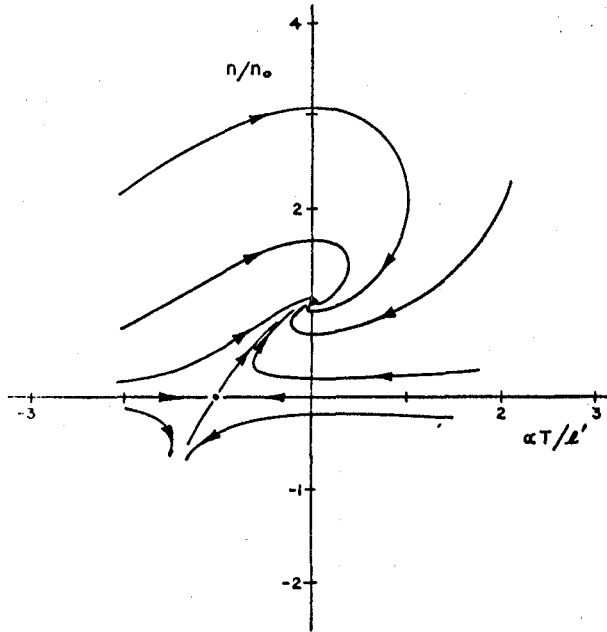


Fig. 7-16. Trajectories for the effective-lifetime model with Newton cooling;  $\gamma = 2$  and  $\Omega^2 = 2$ .

A second example, in which the equilibrium  $n = n_0$  is a stable node, is sketched in fig. 7-17. Here  $\gamma = 6$  and  $\Omega^2 = 6$ . The equilibrium points are again  $(0, 1)$  and  $(-1, 0)$ . The stable node has eigenvalues  $-3 \pm \sqrt{3}$ , and the saddle-point eigenvalues are  $+1$  and  $-6$ . The separatrices at the saddle point have slopes  $M = 0$  and  $M = \frac{1}{6}$ ; the separatrices at the node have slopes  $M = 0.211$  and  $M = 0.789$ .

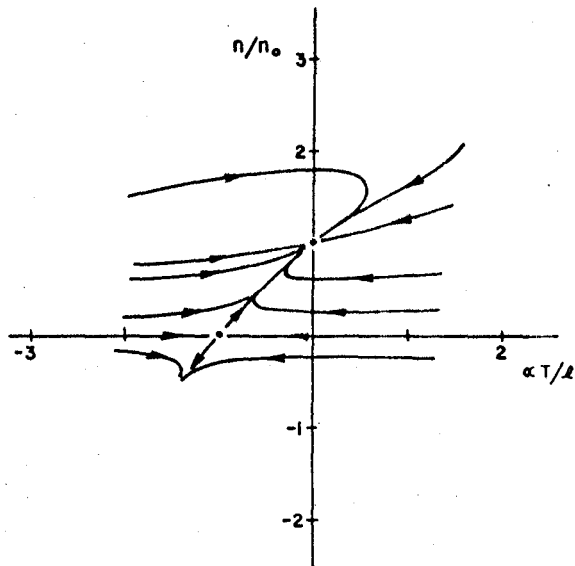


Fig. 7-17. Trajectories for the effective-lifetime model with Newton cooling;  $\gamma = 6$  and  $\Omega^2 = 6$ .

Unfortunately, the examples in figs. 7-16 and 7-17 do not have much physical significance. The swing in reactivity from shutdown to the operating equilibrium is much too large to be encompassed by the effective-lifetime model.

To be more realistic, consider the prompt-jump model, eq. (3-19):

$$(\beta - \rho) \frac{dn}{dt} = \left( \lambda\rho + \frac{d\rho}{dt} \right) n. \quad (7-50)$$

Using eqs. (7-36) and (7-44), we have

$$\frac{dn}{dt} = -\frac{[\alpha K_0(n - n_0) + (\lambda - \gamma)\alpha T]n}{\beta + \alpha T}, \quad (7-51)$$

$$\frac{dT}{dt} = K_0(n - n_0) - \gamma T, \quad (7-52)$$

and

$$\frac{dn}{dT} = -\frac{[\alpha K_0(n - n_0) + (\lambda - \gamma)\alpha T]n}{(\beta + \alpha T)[K_0(n - n_0) - \gamma T]}. \quad (7-53)$$

The case of constant power removal is the limit as  $\gamma \rightarrow 0$ . In this case,

$$\frac{dn}{dt} = -\frac{[\alpha K_0(n - n_0) + \lambda\alpha T]n}{\beta + \alpha T}, \quad (7-54)$$

$$\frac{dT}{dt} = K_0(n - n_0), \quad (7-55)$$

and

$$\frac{dn}{dT} = -\frac{[\alpha K_0(n - n_0) + \lambda\alpha T]n}{(\beta + \alpha T)K_0(n - n_0)}. \quad (7-56)$$

This system has the equilibrium point  $n = n_0$ ,  $T = 0$ . There are two other singular points (indeterminate  $dn/dT$ ); these are  $n = 0$ ,  $T = -\beta/\alpha$  and  $n = n_0 + \lambda\beta/\alpha K_0$ ,  $T = -\beta/\alpha$ . The vertical line  $T = -\beta/\alpha$  is a separatrix; trajectories in the prompt-jump model cannot cross  $\rho = \beta$ . The physical meaning is that  $dn/dt$  has a very large magnitude near prompt critical, and the prompt-jump model must be replaced by higher-order dynamic equations in that neighborhood.

Trajectories are sketched in fig. 7-18 for a case in which the equilibrium point is a stable focus. The ordinate is  $n/n_0$  and the abscissa is  $\alpha T/\beta$ . The parameter is  $\alpha K_0 n_0 / \lambda \beta = \frac{1}{8}$ . The system is stable in the physically meaningful range  $n > 0$  and  $T > -\beta/\alpha$ ; trajectories outside this region are not shown. The student should investigate the associated linear system and calculate the eigenvalues; it is easily shown that the equilibrium point for eqs. (7-54) and (7-55) is a stable focus for  $0 < \alpha K_0 n_0 / \lambda \beta < 4$  and a stable node for larger  $n_0$ .

Add the heat-loss term  $-\gamma T$  and return to eqs. (7-51) and (7-52). This system has two equilibrium points:  $n = n_0$ ,  $T = 0$  and the shutdown point  $n = 0$ ,  $T = -K_0 n_0 / \gamma$ . The other two singular points are  $n = 0$ ,  $T = -\beta/\alpha$  and  $n = n_0 + (\lambda - \gamma)\beta/\alpha K_0$ ,  $T = -\beta/\alpha$ . Again, the vertical line  $T = -\beta/\alpha$  may not be crossed.

The operating equilibrium point of this system was studied in sec. 6-6. The characteristic equation is eq. (6-94). With  $\alpha > 0$  assumed, this equilibrium point is always a stable node for  $\gamma > \lambda$ , and it may be either a stable node or focus for  $\gamma < \lambda$ . See the root-locus plots in figs. 6-39 and 6-40. The condition for linear oscillation may be expressed as

$$\frac{\lambda}{\gamma} > \frac{(\beta + \rho_s)^2}{4\beta\rho_s}, \quad (7-57)$$

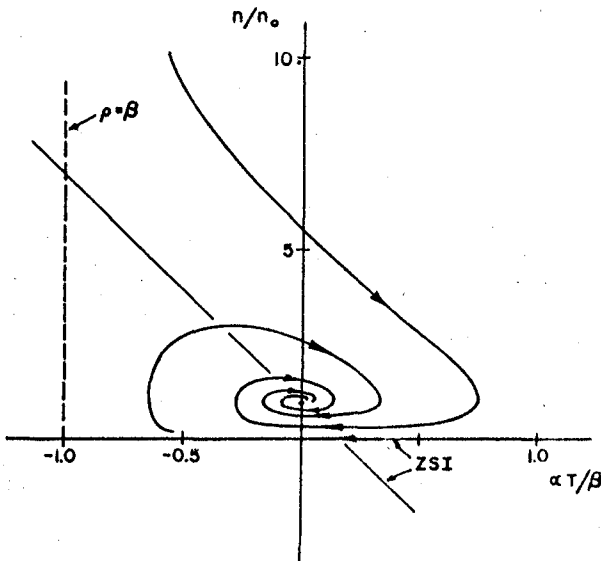


Fig. 7-18. Trajectories for the prompt-jump model with constant-power removal:  $\alpha K_0 n_0 / \lambda \beta = 1/6$ .

where  $\rho_s$  is the shutdown reactivity given by eq. (7-48).

The shutdown equilibrium point is a saddle point, with eigenvalues

$$s = -\gamma, \quad s = \frac{\lambda \rho_s}{\beta - \rho_s}.$$

The positive eigenvalue is simply the approximate root of the inhour equation corresponding to the shutdown reactivity  $\rho_s$ ; see eq. (2-45).

Trajectories are sketched in fig. 7-19 for a case in which the equilibrium at  $n_0$  is a stable focus (Hetrick 1965a). The parameters are  $\alpha K_0 n_0 / \lambda \beta = \frac{1}{3}$  and  $\lambda/\gamma = 3$ . The shutdown reactivity is  $\rho_s = \beta/3$ . The system is stable in the physically meaningful range  $n > 0$  and  $T > -\beta/\alpha$ .

Note that the shutdown point would be in the nonphysical region  $T < -\beta/\alpha$  for  $\rho_s > \beta$ . This is another consequence of the fact that a system above prompt critical must be described by higher-order equations. Nevertheless, the prompt-jump model is more useful than the effective-lifetime model. Even for  $\rho_s$  small compared to  $\beta$ , curves such as those in figs. 7-16 and 7-17 would be misleading because of the absence of delayed-neutron effects.

The prompt-jump approximation is particularly valuable because it permits analysis of a reactor model that is only second order and yet exhibits both delayed-neutron and reactivity-feedback effects. As discussed in chapters 3 and 5, the prompt-jump model is a valid

608      *Nonlinear System Stability*

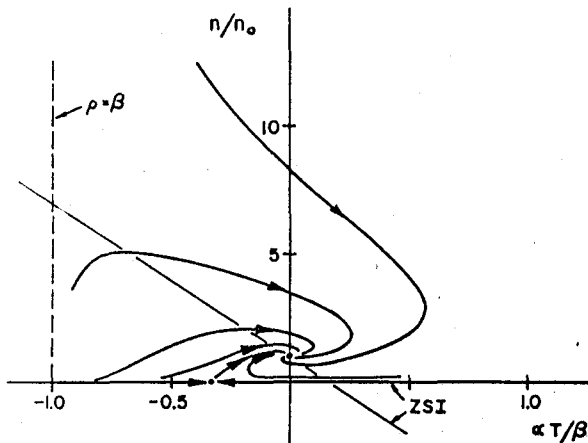


Fig. 7-19. Trajectories for the prompt-jump model with Newton cooling;  $\alpha K_0 n_0 / \lambda \beta = 1/9$  and  $\lambda/\gamma = 3$  (Hetrick 1965a).

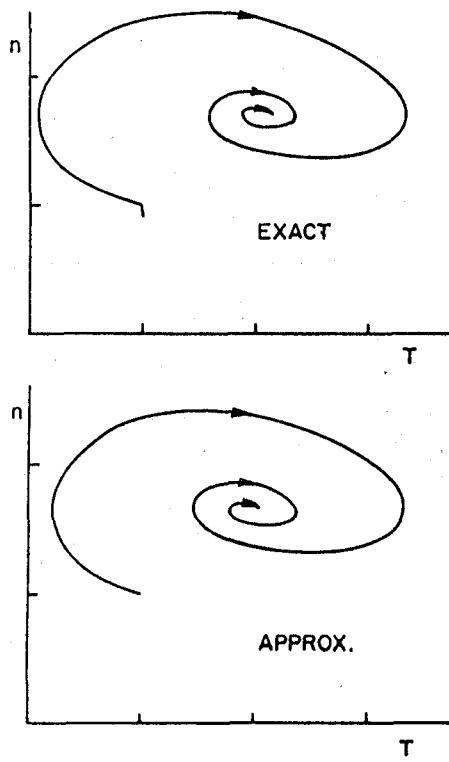


Fig. 7-20. Comparison of second-order neutron dynamics ( $\beta/\ell = 10$ ) with the prompt-jump approximation (constant power removal).

asymptotic solution for  $\rho < \beta$ . The  $n, T$  curves in figs. 7-18 and 7-19 are approximate projections of three-dimensional  $n, c, T$  space curves.

This asymptotic behavior is illustrated by the analogue computer solutions in fig. 7-20 (computations by Peter Meenan, University of Arizona, 1966). The curve labeled "exact" is for a third-order system, one group of delayed neutrons ( $\beta/\ell = 10$ ) with eqs. (7-36) and (7-38). The "approximate" curve is for the prompt-jump model using eqs. (7-54) and (7-55). The approximate initial condition for the "exact" curve was computed from eq. (3-10) with  $\rho(-0) = 0$  to account for the fast-decaying transient, which is missing in the asymptotic solution and appears as a short vertical jump at the start of the exact curve. The case illustrated is similar to those in fig. 7-18 except that the  $T$ -scale is shifted to the left.

#### 7-4. Definitions of Stability

To proceed further, we need to refine the stability concepts that were introduced for linear systems in sec. 6-1. This requires careful definitions of several types of stability, because distinctions may arise in nonlinear systems that are not found in linear systems.

Consider the dynamical system<sup>1</sup>

$$\frac{dx_i}{dt} = X_i(x_1, \dots, x_n, t), \quad (7-58)$$

where  $i = 1, \dots, n$ . Let the origin be an equilibrium point:

$$X_i(0, \dots, 0, t) = 0. \quad (7-59)$$

We restrict our attention to momentary perturbations; i.e., given initial values at time  $t_0$ ,

$$x_i(t_0) = x_{i0}, \quad (7-60)$$

we inquire into the behavior of the system for  $t > t_0$ . Constantly acting perturbations, described by adding a forcing function to the right-hand side of eq. (7-58), will not be considered. Further, we will be primarily concerned with time-invariant (autonomous) systems (functions  $X_i$  independent of time).

It is convenient to adopt a definition of distance in the state space. Regarding the  $x_i$  as components of a vector, let the displacement from the origin be measured by the Euclidean norm

$$\bar{x}(t) = \{\sum_i [x_i(t)]^2\}^{1/2}. \quad (7-61)$$

1. We use the term "dynamical system" rather loosely. A proper definition contains several restrictions, including the requirement that all solutions be defined and continuous for  $-\infty < t < \infty$ . For further details, see Zubov (1957).

### 7.0 Nonlinear System Stability

We define stability as follows: The equilibrium of the system given by eq. (7-58) is said to be *stable* if, for any given positive number  $\epsilon$ , a positive number  $\delta$  can be found such that

$$\bar{x}(t_0) < \delta \quad (7-62)$$

implies

$$\bar{x}(t) < \epsilon \quad (7-63)$$

for all  $t > t_0$ . In general,  $\delta$  is a function of  $\epsilon$  and  $t_0$ . If  $\delta$  is independent of  $t_0$ , as in an autonomous system, the stability is said to be *uniform*. We may paraphrase the definition of stability by saying that a solution  $x_i(t)$ , sometimes called a "motion," is stable if a region  $R(\delta)$  can be found such that all trajectories originating inside  $R(\delta)$  remain inside a specified region  $R(\epsilon)$  for all subsequent time.

The solution is *unstable*, if, as  $\delta$  is made arbitrarily small, there is at least one solution trajectory for which the condition given by eq. (7-63) is not satisfied.

A motion is *asymptotically stable* if it is stable and if, in addition,

$$\lim_{t \rightarrow \infty} \bar{x}(t) = 0. \quad (7-64)$$

The motion is *asymptotically stable in the large* if it is asymptotically stable and  $\delta$  may be made arbitrarily large. We avoid the term "globally asymptotically stable" because it is used for different concepts by various authors.

There are motions for which the limit in eq. (7-64) holds; yet the condition given by eq. (7-63) is not satisfied. Such a motion is called *quasi-asymptotically stable*. Examples are given by Lehnigk (1966).

Periodic motions may sometimes be said to possess *orbital stability*, a special case in which there is stability but not asymptotic stability. Figs. 7-6, 7-10, and 7-14 are examples. Planetary motion is another example.

A motion that is not asymptotically stable, but for which all solutions are bounded, is called stable in the sense of Lagrange, or *Lagrange stable*. There are many examples in the form of systems that are unstable for small perturbations; yet all solutions are bounded. These may be called *unstable in the small*, but *stable in the large* and hence Lagrange stable. Fig. 7-21 shows one type of Lagrange stability: a stable limit cycle enclosing an unstable focus, forming a system that may be called *orbitally asymptotically stable*. Limit cycles, unlike centers, are independent of initial conditions.

The set of all initial points  $x_{i0}$  for which subsequent motions are stable is called the *domain of attraction* of the equilibrium point. If the

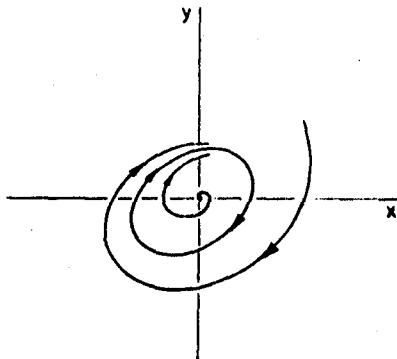


Fig. 7-21. A stable limit cycle.

motion is asymptotically stable but the domain of attraction does not include the entire state space, we have *asymptotic stability in the small*. Figs. 7-9 and 7-13 are examples of this. Another example, sketched in fig. 7-22, is an unstable limit cycle enclosing a stable focus. Fig. 7-10 is an example that has orbital stability in the small. Such examples are frequently characterized as "instability in a linearly stable system."

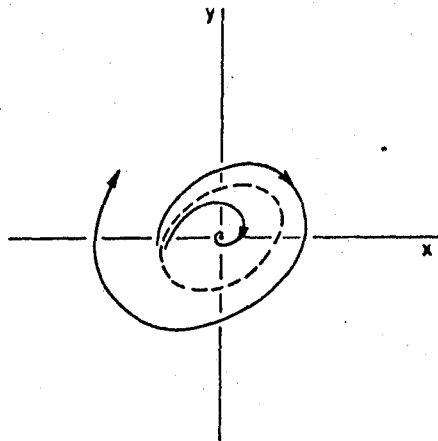


Fig. 7-22. An unstable limit cycle.

A motion that is asymptotically stable in the large for some class of functions  $X_t$  is called *absolutely stable*. This term is also applied to motions that are asymptotically stable in the large for all values of one or more parameters. If the stability is restricted to a limited region of a parameter space, one may speak of *structural ability*.

If the solution  $x_i(t)$  may be extended from the initial point  $x_{i0}$  for all  $t > t_0$ , then  $x_i(t)$  is said to be *defined in the future*. If, on the other hand,

### 372 Nonlinear System Stability

there is a time  $t_e > t_0$  such that  $\bar{x}(t) \rightarrow \infty$  as  $t \rightarrow t_e$ , the solution is said to have a *finite escape time*. An elementary example of this is the particular solution

$$x(t) = 1/(1 - t)$$

of the differential equation

$$\frac{dx}{dt} = x^2.$$

Such solutions are not Laplace-transformable. It is important to the theory of reactor stability that finite escape times can occur in systems that are stable in the small (Akcasu and Noble 1966a).

Limit cycles and finite escape times do not occur in linear systems. The autonomous second-order linear systems classified in sec. 7-1 as cases 1 through 8 (figs. 7-1 through 7-8) may be characterized as follows: Cases 1, 3, and 4 are unstable. Cases 2, 5, and 7 are asymptotically stable. Cases 6 and 8 are stable but not asymptotically stable; case 6 is orbitally stable. Of course, stability in a linear system is stability in the large because the principle of superposition applies.

The extension to linear systems of higher order than two is easily visualized. For example, a third-order linear system is asymptotically stable if its three eigenvalues are negative, or if one is negative real and two are complex with negative real parts. One positive eigenvalue, or a complex pair with positive real parts, will assure instability in a system of any order.

We now state three theorems of Liapunov that relate a nonlinear system to its associated linear system. Given the autonomous nonlinear system

$$\frac{dx_i}{dt} = \sum_j a_{ij}x_j + F_i(x_1, \dots, x_n), \quad (7-65)$$

where the  $a_{ij}$  are constants and where the  $F_i$  are power series beginning with terms of degree at least two, the associated linear system (sometimes called the linearized system or the abridged system) is

$$\frac{dx_i}{dt} = \sum_j a_{ij}x_j. \quad (7-66)$$

Let  $s_j$  be the roots of the characteristic equation for the linear system (the eigenvalues of the matrix whose elements are  $a_{ij}$ ). The theorems are (Minorsky 1962):

1. If  $Re(s_j) < 0$  for all roots  $s_j$ , the equilibrium point  $x_i = 0$  of eq. (7-65) is asymptotically stable for all functions  $F_i$ .

2. If  $\operatorname{Re}(s_j) > 0$  for at least one of the roots  $s_j$ , the equilibrium point is unstable for all  $F_i$ .
3. If no root  $s_j$  has a positive real part but at least one root has a zero real part (critical case), the equilibrium point may be either stable or unstable depending on the functions  $F_i$ .

The theorems say nothing about stability in the large; they refer only to stability in some neighborhood of the equilibrium point (stability in the small). The theorems justify the procedure that was followed in sec. 7-1 in analyzing second-order systems. The reference to "all functions  $F_i$ " is qualified, in that we assumed power series beginning with terms of at least second degree. This restriction can be relaxed somewhat; some variations are discussed by Minorsky (1962).

The first two theorems are easily proved by the direct method of Liapunov, which we discuss in the next section. The third theorem, covering the critical cases, requires special treatment. For proofs, see Minorsky (1962). We have already seen examples of critical cases: Fig. 7-10 shows a center at the origin that is made unstable by the nonlinearity except in a small region of the plane. Fig. 7-14 is a center that remains orbitally stable in an entire half-plane when the nonlinearity is added. Finally, we note that the system

$$\begin{aligned}\frac{dx}{dt} &= y - x^3, \\ \frac{dy}{dt} &= -x - y^3\end{aligned}\tag{7-67}$$

has a center at the origin; compare this with eq. (7-26) and fig. 7-10. However, all trajectories of eq. (7-67) spiral in toward the origin, as we may verify by sketching a few isolines. Asymptotic stability for this system will be proved in the next section.

Application of the three theorems is sometimes called the *first method of Liapunov*. It is the formal justification for the studies of equilibrium points in the preceding three sections.

### 7-5. The Direct Method of Liapunov

The modern approach to the study of nonlinear stability was founded by A. M. Liapunov (1892). The *direct method*, also known as the *second method of Liapunov*, is a generalization of the concept of energy in theoretical mechanics. If a particle moves in a force field such that its total energy is nonincreasing, the motion is confined to a restricted region of state space and is stable. If the total energy is continually

#### 7.4 Nonlinear System Stability

decreasing, it ultimately approaches zero and the motion is asymptotically stable.

An example is the harmonic oscillator. Without damping, the total energy remains constant and the motion is a closed orbit in state space. With a frictional force proportional to velocity, the rate of change of energy is negative and proportional to the square of the velocity. Except at two instants in each cycle where the velocity is zero, the total energy is decreasing and must ultimately decay to zero. The motion, a damped oscillation, is asymptotically stable.

Potential energy is proportional to the square of the displacement, and kinetic energy is proportional to the square of the velocity. The total energy is a function of the state-space coordinates that is positive everywhere except at the origin, where it is zero. Such a function is called a *positive definite function* of the coordinates. The spirit of the direct method is to identify some positive definite function of the coordinates. If its total time derivative, expressed in terms of the coordinates by means of the equations of motion, can be shown to be zero or negative (a negative semidefinite function), the positive definite function is a Liapunov function and the motion is stable. If the time derivative is negative definite (vanishing only when all its arguments are zero), the motion is asymptotically stable.

Before stating the theorem and outlining a proof, we need the definitions:

1. A scalar function  $V(x_1, \dots, x_n)$  is *positive definite* in a region  $R$  about the origin if  $V > 0$  in  $R$  when  $x_i \neq 0$  and  $V(0, \dots, 0) = 0$ .
2. The time derivative of  $V$  along a solution trajectory of eq. (7-58) is

$$\frac{dV}{dt} = \mathbf{X} \cdot \nabla V = \sum_i X_i \frac{\partial V}{\partial x_i} \quad (7-68)$$

where  $\mathbf{X}$  is a vector whose components are  $X_i$ .

3. A positive-definite function  $V$  in  $R$  is a *Liapunov function* if  $V$  and its first partial derivatives are continuous and  $dV/dt \leq 0$  in  $R$ .

The theorem, which gives a sufficient (but not necessary) condition for stability, may be stated as follows:

If there exists a Liapunov function in an open region  $R$  containing the origin, then the equilibrium of eq. (7-58) is stable.

A proof may be outlined briefly as follows: Since Liapunov functions are increasing functions of their arguments, the equation  $V(x_1, \dots, x_n) = C$  represents a concentric family of closed surfaces enclosing the origin. Two such surfaces are shown in fig. 7-23, where

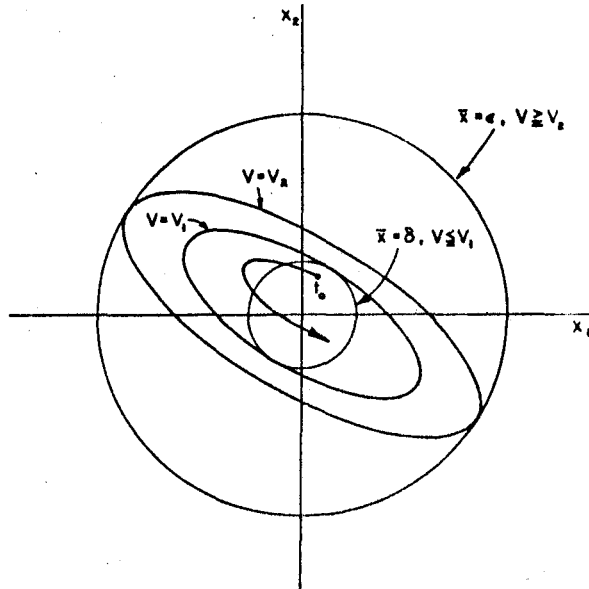


Fig. 7-23. Regions of state space used in proving the theorem of Liapunov.

$0 < V_1 < V_2$ . By the assumed continuity,  $V \geq V_2$  on the surface  $\bar{x} = \epsilon$ , which is assumed to be entirely within the region  $R$ .

In part of the region  $\bar{x} < \epsilon$ ,  $V$  is less than  $V_2$ . Therefore, there exists a  $\delta$ , depending on  $\epsilon$ , such that  $0 < \delta < \epsilon$  and  $V \leq V_1 < V_2$  for all  $\bar{x} \leq \delta$ . Clearly, there are points in the shell  $\delta < \bar{x} < \epsilon$  where  $V < V_1$ .

Consider an initial point ( $t = t_0$ ) inside  $\bar{x} = \delta$ . Because the Liapunov function  $V$  is nonincreasing on the trajectory,  $V$  at time  $t > t_0$  is less than or equal to the initial value of  $V$ , which in turn is less than  $V_2$ . Since  $V \geq V_2$  on  $\bar{x} = \epsilon$ , the trajectory cannot cross the surface  $\bar{x} = \epsilon$ . Therefore,  $\bar{x}(t) < \epsilon$  for all  $t > t_0$  when  $\bar{x}(t_0) < \delta$ , and the motion is stable as defined in sec. 7-4.

As seen in fig. 7-23, the trajectory may temporarily leave the region  $\bar{x} \leq \delta$ . Clearly, it cannot leave the region  $V \leq V_1$ . The formal definition of stability is satisfied because  $V_1 < V_2$ . Of course, the figure is merely a symbolic representation of an  $n$ -dimensional state space.

As a corollary, the motion is asymptotically stable if  $dV/dt < 0$ . This is true because the trajectory must not only remain inside  $\bar{x} = \epsilon$  but also must be characterized by decreasing  $V$ . The trajectory eventually reaches the origin. A converse theorem may also be established as a corollary: the equilibrium is unstable if  $V$  is positive definite and  $dV/dt > 0$  in a neighborhood surrounding the origin.

As an example, consider the second-order system

$$\begin{aligned}\frac{dx}{dt} &= -2x, \\ \frac{dy}{dt} &= -y - y^3.\end{aligned}\tag{7-69}$$

The equilibrium point is a stable node, as is the origin in fig. 7-9. Select the positive definite function

$$V(x, y) = x^2 + y^2.\tag{7-70}$$

We have

$$\frac{dV}{dt} = 2x \frac{dx}{dt} + 2y \frac{dy}{dt}.\tag{7-71}$$

Substituting from eq. (7-69), we have

$$\frac{dV}{dt} = -4x^2 - 2y^2 - 2y^4.\tag{7-72}$$

The motion is asymptotically stable in the large, because  $dV/dt$  is negative definite in the entire  $x, y$  space. The reader may verify that the trajectories are

$$\frac{y^2}{1 + y^2} = Cx\tag{7-73}$$

and that the motion is always toward the origin.

As a second example, consider the system of eq. (7-67), which has a center at the origin. If eqs. (7-70) and (7-71) together with the equations of motion are used,

$$\frac{dV}{dt} = -2x^4 - 2y^4.\tag{7-74}$$

The system is asymptotically stable in the large.

Next, consider the example of eq. (7-21) and fig. 7-9. The origin is a stable node, but the saddle point precludes asymptotic stability in the large. We can identify a subdomain of the asymptotically stable region as follows: Again using eqs. (7-70) and (7-71), we find (Cunningham 1963)

$$\frac{dV}{dt} = -4x^2 + 2x^2y - 2y^2 + 2xy^2.\tag{7-75}$$

Clearly,  $dV/dt$  is not sign-definite in the entire plane. However,  $dV/dt$  is negative in a neighborhood surrounding the origin.

The locus of points for which  $dV/dt = 0$  is the origin together with a curve having three branches:

$$x^2(2 - y) + y^2(1 - x) = 0. \quad (7-76)$$

The curves  $V = C$  are concentric circles about the origin. The region for which asymptotic stability is proved is the interior of the largest circle that may be inscribed in the region for which  $dV/dt < 0$ , i.e., the circle tangent to the curve of eq. (7-76), as shown in fig. 7-24. The significant branch of the locus of eq. (7-76) contains the saddle point  $(1, 2)$ .

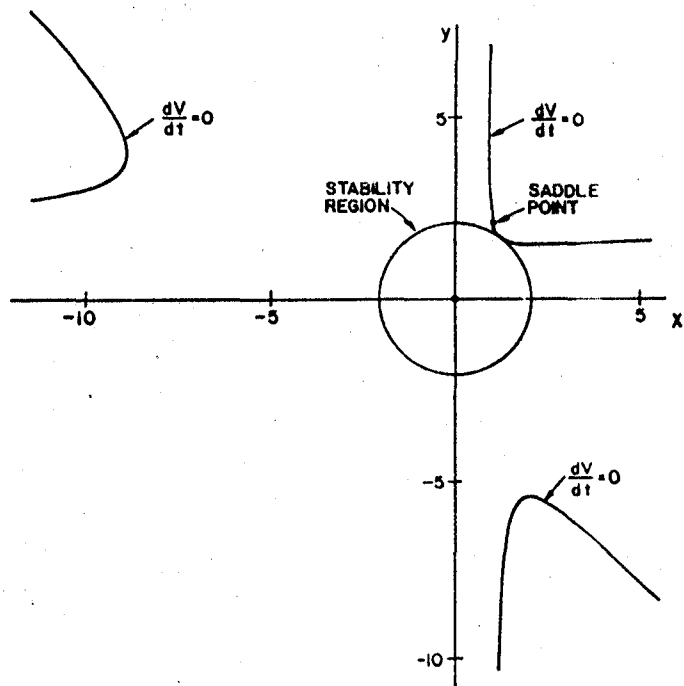


Fig. 7-24. Subdomain of the asymptotically stable region and locus of  $dV/dt = 0$  for the example of fig. 7-9.

Note that the size and shape of the region for which stability is proved depends on the choice of the function  $V$ . Elliptical curves of constant  $V$  would have yielded a different region for this example. To illustrate, consider the system of fig. 7-13 and eq. (7-34). We could find a circular region about the origin by using eq. (7-70); instead we select

$$V(x, y) = (x + y)^2 + y^2. \quad (7-77)$$

378      *Nonlinear System Stability*

In this case, the curves  $V = C$  are a family of concentric ellipses. We find

$$\frac{dV}{dt} = 2x \frac{dx}{dt} + 2x \frac{dy}{dt} + 2y \frac{dx}{dt} + 4y \frac{dy}{dt}. \quad (7-78)$$

Using the equations of motion, we have

$$\frac{dV}{dt} = -2x^2 - 4xy - 6y^2 + 2x^3 - 2x^2y - 8xy^2. \quad (7-79)$$

Again,  $dV/dt$  is negative in a neighborhood of the origin, and the locus of  $dV/dt = 0$  is the origin plus a curve of three branches:

$$x^2 + 2xy + 3y^2 - x^3 + x^2y + 4xy^2 = 0. \quad (7-80)$$

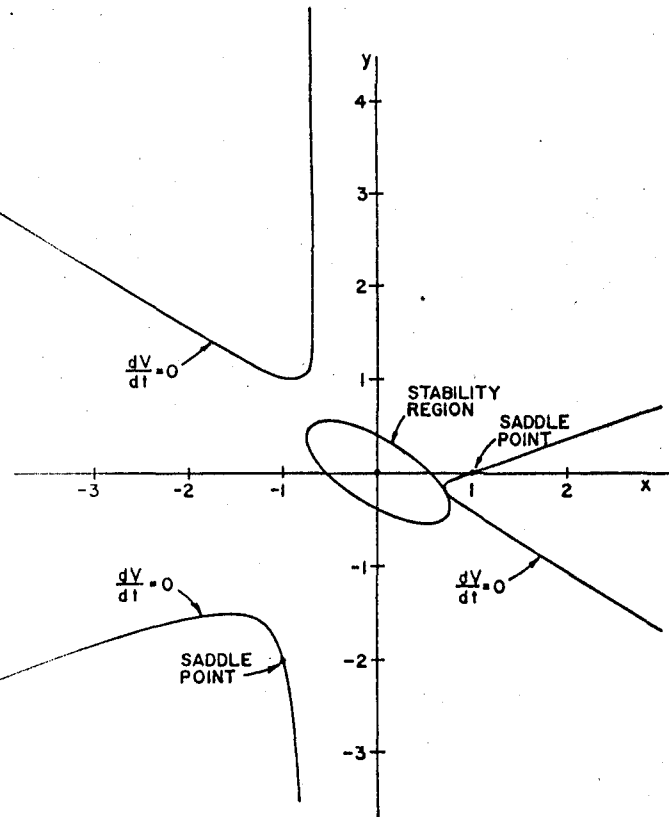


Fig. 7-25. Subdomain of the asymptotically stable region and locus of  $dV/dt = 0$  for the example of fig. 7-13.

The region for which asymptotic stability is proved is the interior of an ellipse tangent to the nearest branch of eq. (7-80). There is a branch through each of the saddle points of eq. (7-34), as shown in fig. 7-25.

Asymptotic stability may be proved for each of a set of different  $V$ -functions. The results may be combined, and the region of asymptotic stability is the union of all the regions so obtained. There is still no guarantee that the entire region of asymptotic stability is discovered in this manner, because the theorem only provides a sufficient condition.

Application of the method requires both insight and artistry. As we shall see, there is no need to restrict  $V$  to a quadratic form. Quadratic forms are sufficient for describing the stability properties of linear systems; indeed, the Routh criterion may be derived in this way (Parks 1962). Much effort has been devoted to the invention of systematic methods for constructing  $V$ -functions for nonlinear systems, and some of these are discussed in the remainder of this section.

First, we note that it is frequently helpful to seek a first integral of some related, but simpler, system. For example, consider the system

$$\begin{aligned}\frac{dx}{dt} &= -\alpha x + y, \quad \alpha \geq 0, \\ \frac{dy}{dt} &= -x - x^3.\end{aligned}\tag{7-81}$$

The origin is the only equilibrium point (a center for  $\alpha = 0$ , a stable focus for  $0 < \alpha < 2$ , and a stable node for  $\alpha > 2$ ). The function  $V = x^2 + y^2$  is not very useful, because it yields

$$\frac{dV}{dt} = -2\alpha x^2 - 2x^3 y.$$

Instead, consider the special case  $\alpha = 0$ , for which a first integral is

$$y^2 + x^2 + \frac{1}{2}x^4 = C.\tag{7-82}$$

The left-hand side is a positive definite function, and eq. (7-82) represents a concentric family of closed curves. Let

$$V(x, y) = y^2 + x^2 + \frac{1}{2}x^4.\tag{7-83}$$

We have

$$\frac{dV}{dt} = 2y \frac{dy}{dt} + 2x \frac{dx}{dt} + 2x^3 \frac{dx}{dt}.\tag{7-84}$$

We now apply this to the original system, eq. (7-81). We find

$$\frac{dV}{dt} = -2\alpha x^2 - 2\alpha x^4.\tag{7-85}$$

The equilibrium is stable in the large for  $\alpha = 0$  and asymptotically stable in the large for  $\alpha > 0$ .

The method of Aizerman (1958) is useful in the study of automatic control systems; see also Hahn (1963) and Minorsky (1962). Its greatest utility lies with systems of the form

$$\frac{dx_1}{dt} = a_{11}x_1 + a_{12}x_2 + \cdots + f(x_k) \quad (7-86)$$

and

$$\frac{dx_i}{dt} = a_{i1}x_1 + a_{i2}x_2 + \cdots + a_{in}x_n, \quad (i \neq 1),$$

in which the nonlinearity appears as a function of one state variable in one equation. The essence of the method is to replace  $f(x_k)$  by the linear term  $px_k$  such that the resulting linear system is asymptotically stable for a range  $p_1 < p < p_2$ . Using the quadratic form  $V$  that demonstrates this linear stability, one then constructs from it and from eq. (7-86) a form  $dV/dt$  for the nonlinear system. The nonlinear system is then asymptotically stable in a suitable region for which this  $dV/dt < 0$ .

One may ask the following question: If the linear system is asymptotically stable for  $p_1 < p < p_2$  and if  $f(x_k)$  satisfies

$$p_1x_k^2 < x_kf(x_k) < p_2x_k^2,$$

will the nonlinear system be asymptotically stable in the large? Unfortunately, the answer is affirmative only for  $n = 2$  (Hahn 1963). Additional restrictions on the form of the nonlinearity are required for higher-order systems.

The method of Aizerman has limited utility in reactor dynamics because the nonlinearity usually arises from the product  $\rho\delta n$ . With a simple linear feedback, and in the absence of delayed neutrons, the transformation

$$\sigma = \log(n/n_0) \quad (7-87)$$

removes the product nonlinearity and introduces the nonlinearity

$$f(\sigma) = e^\sigma - 1 \quad (7-88)$$

into the feedback. However, this device fails in the presence of delayed neutrons. Moreover,  $V$  is always constrained to be a quadratic form, and we will not pursue this method further.

The method of Szego (1963), as described by Schultz (1965), begins by postulating a quadratic form whose coefficients may be functions of the state variables. Formally,

$$V = \sum_{ij} a_{ij}(x_i, x_j) x_i x_j, \quad (7-89)$$

subject to the restrictions that  $a_{ij} = a_{ji}$  and that the  $a_{ij}$  are independent of at least one state variable (say  $x_n$ ). One forms  $dV/dt$ , using eq. (7-89) and the equations of motion, and then seeks relations for determining the variable coefficients subject to constraints on  $V$  and  $dV/dt$ .

As an example, consider the second-order system of eq. (7-81). Let

$$V = a_{11}(x)x^2 + 2a_{12}(x)xy + y^2 \quad (7-90)$$

where  $y$  is identified as  $x_n$  and where  $a_{22} = 1$  without loss of generality. Of course, we know in advance from eq. (7-83) that the alternative (identifying  $x$  as  $x_n$ ) would not be fruitful, though in the absence of this information, each alternative would be tried. We find

$$\begin{aligned} \frac{dV}{dt} = & 2a_{11}x \frac{dx}{dt} + x^2 \frac{da_{11}}{dx} \frac{dx}{dt} + 2a_{12}x \frac{dy}{dt} \\ & + 2a_{12}y \frac{dx}{dt} + 2xy \frac{da_{12}}{dx} \frac{dx}{dt} + 2y \frac{dy}{dt}. \end{aligned} \quad (7-91)$$

Substituting from eq. (7-81) leads to

$$\begin{aligned} \frac{dV}{dt} = & -2\alpha a_{11}x^2 - \alpha \frac{da_{11}}{dx} x^3 - 2a_{12}x^2 - 2a_{12}x^4 \\ & + \left( 2a_{11}x + \frac{da_{11}}{dx} x^2 - 2\alpha a_{12}x \right. \\ & \left. - 2\alpha \frac{da_{12}}{dx} x^2 - 2x - 2x^3 \right) y \\ & + \left( 2a_{12} + 2 \frac{da_{12}}{dx} x \right) y^2. \end{aligned} \quad (7-92)$$

Regarding eq. (7-92) as a quadratic in  $y$ , we infer that the locus of  $dV/dt = 0$  has two branches in the  $x, y$  plane. The two branches coincide if the discriminant vanishes, and a simple way to ensure this is to set  $a_{12} = 0$  and

$$2a_{11}x + \frac{da_{11}}{dx} x^2 - 2x - 2x^3 = 0. \quad (7-93)$$

Regard eq. (7-93) as a linear differential equation for the variable coefficient  $a_{11}$ . A particular solution is

$$a_{11} = 1 + \frac{1}{2}x^2.$$

Eq. (7-90) now reduces to the desired form, eq. (7-83), and upon noting

### 38.2 Nonlinear System Stability

that eq. (7-92) reduces to eq. (7-85) we see that the example is complete.

Even in this simple illustration, the method requires either foresight or artifice. In a more complex example, the forms for  $V$  and  $dV/dt$  must be juggled to find conditions consistent with the Liapunov theorem, and the differential equations for the variable coefficients may become rather complicated. The results are often somewhat arbitrary, and different sets of coefficients may lead to different subregions of the region of stability.

The variable-gradient method, which is very useful and somewhat more systematic, was developed by Schultz (1965). The essential ideas are that, given a desired form  $dV/dt$ , eq. (7-68) is a partial differential equation for  $V$ , and that under certain conditions  $V$  may be obtained as a line integral of the gradient  $\nabla V$ . Indeed, the necessary and sufficient conditions for a scalar function  $V$  to be obtained uniquely from a vector function  $\nabla V$  are (Lass 1950)

$$\frac{\partial}{\partial x_i} (\nabla V)_j = \frac{\partial}{\partial x_j} (\nabla V)_i, \quad (i, j = 1, \dots, n). \quad (7-94)$$

The vector  $\nabla V$  is written as

$$\begin{bmatrix} (\nabla V)_1 \\ (\nabla V)_2 \\ \vdots \\ (\nabla V)_n \end{bmatrix} = \begin{bmatrix} a_{11}x_1 + a_{12}x_2 + \dots + a_{1n}x_n \\ a_{21}x_1 + a_{22}x_2 + \dots + a_{2n}x_n \\ \vdots \\ \vdots \\ a_{n1}x_1 + a_{n2}x_2 + \dots + a_{nn}x_n \end{bmatrix} \quad (7-95)$$

where the coefficients  $a_{ij}$  are undetermined functions of the state variables. In three dimensions, the conditions of eq. (7-94) guarantee that the curl of the gradient vanishes identically. In general, these conditions, which assure that  $V$  has continuous first partial derivatives, provide relations among the off-diagonal elements of the matrix of coefficients  $a_{ij}$ . If these off-diagonal elements are constants,  $a_{ij} = a_{ji}$  (Schultz 1965).

The derivative  $dV/dt$  is

$$\frac{dV}{dt} = \frac{\partial V}{\partial x_1} \frac{dx_1}{dt} + \frac{\partial V}{\partial x_2} \frac{dx_2}{dt} + \dots \quad (7-96)$$

The procedure is to compute  $dV/dt$  in terms of the variable coefficients, select coefficients such that  $dV/dt$  is negative definite or semidefinite in some region  $R$ , and then obtain  $V$  as a line integral in state space such that  $V = 0$  at the origin. If the resulting  $V$  is positive definite in  $R$ , then  $R$  is the region of stability.

The integration is justified provided the conditions of eq. (7-94) are fulfilled. The line integral is then independent of the path and may be conveniently represented as

$$\begin{aligned} V = & \int_0^{x_1} \nabla V^{(1)}(\xi_1, 0, \dots, 0) d\xi_1 \\ & + \int_0^{x_2} \nabla V^{(2)}(x_1, \xi_2, \dots, 0) d\xi_2 + \dots \\ & + \int_0^{x_n} \nabla V^{(n)}(x_1, x_2, \dots, \xi_n) d\xi_n. \end{aligned} \quad (7-97)$$

where the superscript indicates the appropriate component of  $\nabla V$ .

To illustrate, consider once again the example of eq. (7-81). Let

$$\nabla V = \begin{bmatrix} a_{11}x + a_{12}y \\ a_{21}x + a_{22}y \end{bmatrix}. \quad (7-98)$$

We have

$$\frac{dV}{dt} = (a_{11}x + a_{12}y) \frac{dx}{dt} + (a_{21}x + a_{22}y) \frac{dy}{dt}.$$

Substituting from eq. (7-81) and letting  $a_{12} = a_{21} = \text{constant}$  leads to

$$\begin{aligned} \frac{dV}{dt} = & -a_{12}(1+x^2)x^2 + [a_{11} - a_{22}(1+x^2)]xy + a_{12}y^2 \\ & - \alpha a_{11}x^2 - \alpha a_{12}xy. \end{aligned}$$

The last two terms vanish if  $\alpha \rightarrow 0$  (no damping). Pretending not to know the answer, we explore the possibility that  $dV/dt \rightarrow 0$  for all  $x$  and  $y$  when  $\alpha \rightarrow 0$ . A possible set of coefficients is then

$$\begin{aligned} a_{11} &= 2(1+x^2), \\ a_{12} &= 0, \\ a_{22} &= 2. \end{aligned}$$

This yields precisely eq. (7-85):

$$\frac{dV}{dt} = -2\alpha x^2 - 2\alpha x^4.$$

The components of the gradient are  $2x + 2x^3$  and  $2y$ . Integrating as suggested in eq. (7-97) yields eq. (7-83):

$$V = x^2 + \frac{1}{2}x^4 + y^2.$$

### 7.8-4 Nonlinear System Stability

For the system of eq. (7-81), the Szego method and the variable-gradient method both yield the simple result we obtained earlier by considering a first integral for  $\alpha = 0$ . Clearly, more difficulties will be encountered in studying systems that are not so simple. Some systems are more easily handled by one method, some by another. No method yields guaranteed success in all cases, and the ingenuity of the investigator is probably the most important prerequisite.

In any method, one is concerned with functions  $V$  and  $dV/dt$  that are to be made sign definite. For simple forms like eqs. (7-83) and (7-85) the judgment is very easy. Frequently one encounters the form

$$V = a_{11}x^2 + 2a_{12}xy + a_{22}y^2$$

or the general quadratic form

$$V = [x_1 \ x_2 \ \dots \ x_n] \begin{bmatrix} a_{11} & a_{12} & \dots & a_{1n} \\ a_{12} & a_{22} & & \\ \vdots & & \ddots & \\ \vdots & & & a_{nn} \end{bmatrix} \begin{bmatrix} x_1 \\ x_2 \\ \vdots \\ x_n \end{bmatrix}, \quad (7-99)$$

where the  $a_{ij}$  are constants. The necessary and sufficient condition for this quadratic form to be positive definite is that the principal minors of the determinant of the matrix in eq. (7-99) be positive (Sylvester's theorem; Schultz 1965; Wylie 1960). That is,  $a_{11} > 0$ , and

$$\begin{vmatrix} a_{11} & a_{12} \\ a_{12} & a_{22} \end{vmatrix} > 0, \quad \begin{vmatrix} a_{11} & a_{12} & a_{13} \\ a_{12} & a_{22} & a_{23} \\ a_{13} & a_{23} & a_{33} \end{vmatrix} > 0,$$

etc., up to the  $n \times n$  determinant of the full matrix. Thus,  $x^2 + xy + y^2$  is positive definite, while  $x^2 + 2xy + y^2$  and  $x^2 + 3xy + y^2$  are not. Note that a symmetric matrix is used ( $a_{ij} = a_{ji}$ ). In two dimensions, curves of constant  $V > 0$  are elliptical for positive-definite  $V$ . As a corollary to the theorem, the necessary and sufficient condition for the quadratic form to be negative definite is that  $a_{11} < 0$  and that the remaining principal minors, taken in increasing order, be of alternating sign.

Another type of Liapunov function was developed for nonlinear control systems (Lur'e 1951; Letov 1955; Lefschetz 1965). Given the system

$$\frac{dx_i}{dt} = \sum_j a_{ij}x_j - b_i u, \quad i = 1, \dots, n,$$

$$\frac{du}{dt} = f(\sigma), \quad (7-100)$$

$$\sigma = \sum_j c_j x_j - ru,$$

where the  $a_{ij}$  are the constant elements of the  $n \times n$  coefficient matrix,  $b_i$  and  $c_i$  are components of constant vectors,  $u$  is a scalar function of time (the control variable), and  $r$  is a parameter. The nonlinearity is described by the characteristic function  $f(\sigma)$ , which is assumed to satisfy the conditions  $\sigma f(\sigma) > 0$  for  $\sigma \neq 0$  and  $f(0) = 0$ .

Using the transformation  $\xi_i = dx_i/dt$ , we may write the system equations as

$$\frac{d\xi_i}{dt} = \sum_j a_{ij} \xi_j - b_i f(\sigma)$$

and

$$\frac{d\sigma}{dt} = \sum_j c_j \xi_j - rf(\sigma).$$

A Liapunov function of the Lur'e type is

$$V = \sum_{ij} B_{ij} \xi_i \xi_j + \int_0^\sigma f(\sigma') d\sigma', \quad (7-102)$$

and the stability analysis reduces to the algebraic problem of making  $V$  and  $dV/dt$  conform to the requirements of the Liapunov theorem. Unfortunately, as with the Aizerman method, the equations of reactor dynamics cannot be put in this form unless delayed neutrons are neglected. Essentially the same system was studied by Popov (1961), who derived a frequency-domain stability criterion that we discuss in a later section.

An important special case of eq. (7-101) arises when the coefficient matrix is diagonal ( $a_{ij} = \gamma_i$  for  $i = j$ ; and  $a_{ij} = 0$  for  $i \neq j$ ). A transformation yielding such a canonical form was derived by Lur'e (1951). It is then convenient to include in  $V$  a special quadratic form for which

$$B_{ij} = \frac{g_i g_j}{\gamma_i + \gamma_j} \quad (7-103)$$

where the  $g_i$  are real numbers and the  $\gamma_i$  are the eigenvalues. The quadratic form becomes

$$\begin{aligned} \sum_{ij} \frac{g_i g_j}{\gamma_i + \gamma_j} \xi_i \xi_j &= \int_0^\infty \sum_{ij} g_i g_j \xi_i \xi_j e^{-(\gamma_i + \gamma_j)u} du \\ &= \int_0^\infty (\sum_i g_i \xi_i e^{-\gamma_i u})^2 du \geq 0. \end{aligned} \quad (7-104)$$

This type of quadratic form has been used in a special Liapunov function by Akcasu, Lellouche, and Shotkin (forthcoming) to analyze stability in the presence of delayed neutrons; in their case the  $\xi_i$  are the canonical feedback variables and the  $\gamma_i$  are the real eigenvalues of the heat-transfer matrix. Note that since eq. (7-104) demonstrates only that this form is positive semidefinite, additional terms are required to construct a Liapunov function.

Another method of constructing Liapunov functions for systems such as eq. (7-101) was proposed by Rosen (1961) and applied to a simple reactor model without delayed neutrons by Devooght and Smets (1967). This method also requires the computation of a canonical form, but it has an advantage over Lur'e canonical systems in that  $g(\sigma)$  is not constrained to be positive. The reactor example is discussed in the next section, with a different method used.

It was suggested earlier in connection with the variable-gradient method that eq. (7-68) may be regarded as a partial differential equation for  $V$ . This viewpoint has been developed by Zubov (1957), who has devised special examples for which the entire region of asymptotic stability is obtained by deriving such a Liapunov function. Details are given by Hahn (1963). Unfortunately, the difficulties of practical application seem to be very great.

In addition to quadratic forms and functions like those in eqs. (7-83) and (7-102), many other special functions may be used. As we shall see in the next section, the form

$$V(x) = x - \log(1 + x)$$

is particularly useful in reactor dynamics. This form is positive definite for  $x > -1$  and reduces to  $\frac{1}{2}x^2$  in the neighborhood of the origin.

The requirement that  $dV/dt$  be negative definite is often overrestrictive. The condition may be relaxed as follows (see any of the standard references cited earlier):

*If there exists a Liapunov function in an open region  $R$  containing the origin, and if  $dV/dt$  is not identically zero along any solution trajectory other than the origin (the trivial solution), the equilibrium of eq. (7-58) is asymptotically stable.*

Clearly,  $V \rightarrow 0$  through positive values as  $t \rightarrow \infty$  in an asymptotically stable system. At the same time,  $dV/dt \rightarrow 0$  through negative values. Conceivably, one could have  $V \rightarrow V_0 > 0$  as  $t \rightarrow \infty$  and still have  $dV/dt \rightarrow 0$ . Linear examples are the critical systems (stable systems with a zero eigenvalue or a pair of pure imaginary eigenvalues). A nonlinear system may, in addition, exhibit a limit cycle, on which  $dV/dt = 0$ . To establish asymptotic stability with  $dV/dt$  only negative

semidefinite, one must establish the nonexistence of arbitrary constant solutions and of stable periodic solutions (centers and limit cycles). The concepts may be formalized in terms of Birkhoff's limiting sets (LaSalle 1960, 1968; LaSalle and Lefschetz 1961); we will not go into the subject here.

Another variation of the Liapunov direct method may be formulated as follows: If a function  $V$  can be found that is positive in some region  $R$ , while  $dV/dt$  is negative or zero in the same region, and if, in addition, there exists auxiliary information that no trajectory may leave  $R$ , all solutions originating in  $R$  are stable. Further, if  $dV/dt = 0$  only at the equilibrium point (which may be on the boundary of  $R$ ), all solutions originating in  $R$  are asymptotically stable. This follows because all trajectories must cross curves of constant  $V$  in the direction of decreasing  $V$ .

Such functions are not Liapunov functions, because they are not positive definite. The region of stability is no longer bounded by a closed curve of constant  $V$ , but rather by a portion of a curve of constant  $V$  together with separatrix trajectories that cannot be crossed. We illustrate briefly for the system of eq. (7-21) and fig. 7-9. Since both coordinate axes are separatrix trajectories, a trajectory originating in the first quadrant must remain there. Let

$$V = x + y. \quad (7-105)$$

By eq. (7-21),

$$\frac{dV}{dt} = -2x - y + 2xy.$$

The locus of  $dV/dt = 0$  is

$$y = \frac{2x}{2x - 1}. \quad (7-106)$$

We have  $V > 0$  and  $dV/dt < 0$  in a triangular region bounded by the coordinate axes and the line  $x + y = C$ , where  $C > 0$  characterizes a straight-line tangent to the curve given by eq. (7-106). Any trajectory originating in this triangle must tend to the origin as  $t \rightarrow \infty$ .

In fact, the function  $V = |x| + |y|$  may be used for each quadrant in turn (for example,  $V = x - y$  in the fourth quadrant), and one has functions  $V > 0$  for which  $dV/dt < 0$  throughout the second, third, and fourth quadrants. Because the separatrix along each coordinate axis tends to the origin, the region of asymptotic stability is the triangle in the first quadrant plus all of the other three quadrants, as shown in fig. 7-26. This technique has application in reactor dynamics because  $n(t)$  and  $c_i(t)$  are never negative, as discussed in sec. 2-1; therefore a

function  $V$  containing terms like  $n + \sum_i c_i$  may be used in stability analysis, even though these terms are not positive definite and there are no closed curves of constant  $V$  (Smets and Gyftopoulos 1959; Smets 1962). These functions are state functions in the same sense as positive-definite Liapunov functions because they depend explicitly on the state variables and not on the path to the representative point in state space.

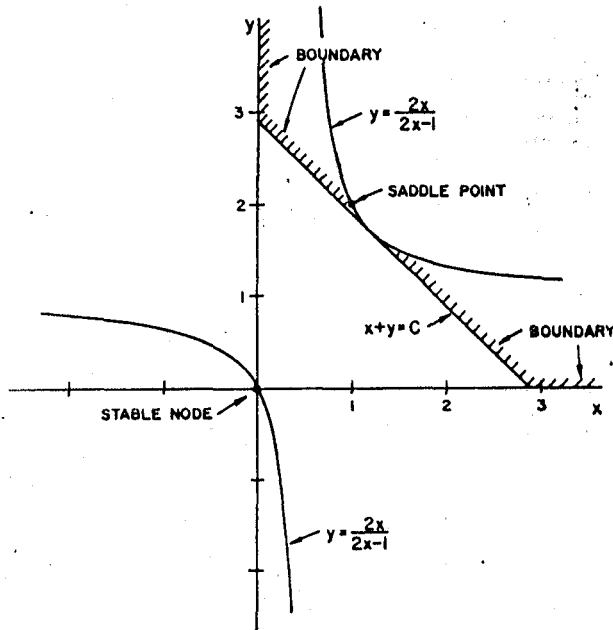


Fig. 7-26. Stability boundary for the system of fig. 7-9 using  $V = |x| + |y|$ .

Finally, we note that this introduction to the direct method of Liapunov has been confined to autonomous systems. The extensions to systems with time-dependent coefficients and continually acting perturbations are discussed by many authors (e.g., Hahn 1963; LaSalle and Lefschetz 1961; Minorsky 1962).

#### 7-6. Application to Reactor Systems

The use of positive-definite functions in the study of nonlinear reactor stability was introduced by Ergen and Weinberg (1954). Using analogies with kinetic and potential energy, they constructed the total energy (the Hamiltonian function) as a function of generalized coordinates

and velocities. This function was identified as a Liapunov function by Ergen, Lipkin, and Nohel (1957).

The classic example is the effective-lifetime model with one feedback variable, eqs. (7-35) and (7-36) with various heat-transfer models such as eq. (7-38) or (7-44). We showed in sec. 7-3 that the case for constant power removal, eq. (7-38), admits a first integral, eq. (7-40). Noting that  $dT/dt = 0$  at  $n = n_0$ , one may integrate eq. (7-39) from  $n = n_0$  and  $T = T_{\max}$  and obtain an alternate expression for the first integral

$$n - n_0 - n_0 \log \frac{n}{n_0} + \frac{\alpha}{2\ell' K_0} T^2 = \frac{\alpha}{2\ell' K_0} T_{\max}^2. \quad (7-107)$$

This may also be derived directly from eq. (7-40). The closed curves of fig. 7-14 represent curves of constant  $T_{\max}$ . Therefore let

$$V = n - n_0 - n_0 \log \frac{n}{n_0} + \frac{\alpha}{2\ell' K_0} T^2, \quad (7-108)$$

from which

$$\frac{dV}{dt} = \frac{dn}{dt} - \frac{n_0}{n} \frac{dn}{dt} + \frac{\alpha T}{\ell' K_0} \frac{dT}{dt}. \quad (7-109)$$

Eq. (7-108) is a positive-definite function in the half-space  $n > 0$ . Fig. 7-27 shows how  $V$  behaves as a function of  $n$  for  $T = 0$ . Substituting the equations of motion, eqs. (7-37) and (7-38), into eq. (7-109) yields  $dV/dt = 0$ , whence eq. (7-108) is a Liapunov function and the system is stable. The trajectories are closed orbits following the curves of constant

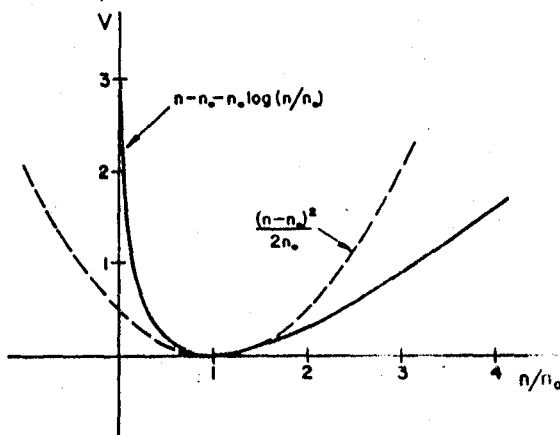


Fig. 7-27. The function  $n - n_0 - n_0 \log(n/n_0)$  and its first-order approximation  $(n - n_0)^2/2n_0$  (normalized to  $n_0 = 1$ ).

$V$ ; see fig. 7-14. Since  $V \rightarrow \infty$  as  $n \rightarrow 0$  or  $\infty$  and as  $T \rightarrow \pm\infty$ , the closed curves fill the half-plane and the system is stable in the entire half-plane.

Using Newton's law of cooling, eq. (7-44) instead of eq. (7-38), and substituting into eq. (7-109) yields

$$\frac{dV}{dt} = -\frac{\alpha\gamma}{\ell'K_0} T^2. \quad (7-110)$$

The effective-lifetime model with Newton cooling is therefore asymptotically stable in the half-plane  $n > 0$ .

A more general result is obtained by using eq. (7-37) together with

$$\frac{dT}{dt} = K_0(n - n_0) - f(T), \quad (7-111)$$

from which

$$\frac{dV}{dt} = -\frac{\alpha}{\ell'K_0} Tf(T). \quad (7-112)$$

The system is therefore asymptotically stable for any cooling law such that  $Tf(T) > 0$  for all  $T \neq 0$ .

The mechanical analogy is obtained by defining the coordinate

$$x = -\log(n/n_0). \quad (7-113)$$

From eq. (7-37) the velocity is

$$v = \frac{dx}{dt} = (\alpha/\ell')T. \quad (7-114)$$

Eq. (7-111) may be written as

$$\frac{\ell'}{\alpha K_0} \frac{dv}{dt} = n_0(e^{-x} - 1) - f(T)/K_0.$$

In analogy with Newton's law of motion,  $m(dv/dt) = F$ , one has a force

$$F = n_0(e^{-x} - 1) - f(T)/K_0$$

and a mass

$$m = \ell'/\alpha K_0.$$

The kinetic energy becomes

$$K = \frac{1}{2}mv^2 = \frac{\alpha}{2\ell'K_0} T^2.$$

The potential energy is defined as

$$U(x) = n_0(x + e^{-x} - 1) = n - n_0 - n_0 \log \frac{n}{n_0}$$

so that  $U(0) = 0$  and the conservative force is

$$-\frac{dU}{dx} = n_0(e^{-x} - 1).$$

The total energy  $U + K$  is the Hamiltonian, or the Liapunov function, of eq. (7-108). The term  $-f(T)/K_0$  plays the role of a dissipative force, and the product of force and velocity is the rate of energy dissipation given by eq. (7-112). The analogy is therefore complete, and it serves to lend some physical feeling to the ideas of the Liapunov method.

The same Liapunov function may be generated by other methods. Before illustrating this, and generalizing to delayed neutrons and more than one feedback region, we observe that a Liapunov function may be constructed for the case of one feedback region using the prompt-jump approximation (Herrick 1965b; Weaver 1968).

The system is defined by eqs. (7-36), (7-44), and (7-50). We seek an auxiliary system that has a first integral. This we achieve by setting  $\gamma = 0$  in eq. (7-44) and by dropping the term  $d\rho/dt$  in eq. (7-50). We find

$$\frac{dn}{dT} = -\frac{\lambda\alpha T n}{K_0(n - n_0)(\beta + \alpha T)}.$$

This may be integrated as

$$V = n - n_0 - n_0 \log \frac{n}{n_0} + \frac{\lambda}{K_0} T - \frac{\lambda\beta}{\alpha K_0} \log \left(1 + \frac{\alpha}{\beta} T\right). \quad (7-115)$$

The auxiliary system has  $dV/dt = 0$ .

Now restore the term  $d\rho/dt$  in eq. (7-50), keeping  $\gamma = 0$ . One finds

$$\frac{dV}{dt} = -\frac{\alpha K_0(n - n_0)^2}{\beta + \alpha T}. \quad (7-116)$$

Eq. (7-115) is a Liapunov function for the region  $n > 0$ ,  $T > -\beta/\alpha$  (i.e.,  $\rho < \beta$ ), and by eq. (7-116) the stability is asymptotic in that region. Note that  $n = n_0$  with  $T$  arbitrary cannot be a trajectory; see eq. (7-44). Recall that this model reduces to the effective-lifetime model ( $\ell' = \beta/\lambda$ ) when  $\rho$  and  $d\rho/dt$  are small, and that eq. (7-109) yielded  $dV/dt = 0$  for that model. Therefore, we have shown that the one-region reactor model with constant power removal ( $\gamma = 0$ ) is made more stable by

(9.1) Nonlinear System Stability

delayed neutrons, at least in the region where the prompt-jump approximation has meaning.

When  $\gamma > 0$ , eq. (7-115) leads to

$$\frac{dV}{dt} = -[\alpha K_0(n - n_0)^2 - \alpha\gamma(n - n_0)T + \lambda\alpha\gamma T^2/K_0]/(\beta + \alpha T). \quad (7-117)$$

We have a quadratic form in  $n - n_0$  and  $T$ . By Sylvester's theorem (sec. 7-5),  $dV/dt$  is negative definite and the stability is asymptotic provided  $\gamma < 4\lambda$ . If this condition is not satisfied, no conclusion about stability is possible using the Liapunov function of eq. (7-115). Presumably, some other Liapunov function would serve to extend the region of stability in parameter space, but the problem has not been studied further.

Curves of constant  $V$  and some trajectories are shown in fig. 7-28. The trajectories are taken from fig. 7-19. The curves of constant  $V$  are given by

$$\log \frac{y}{y_0} - (y - y_0) = \frac{x}{\epsilon} - \frac{1}{\epsilon^2} \log(1 + \epsilon x), \quad (7-118)$$

where  $x$ ,  $y$ , and  $y_0$  are defined by eq. (7-41) and where the parameter  $\epsilon$ , given by

$$\epsilon = (\alpha K_0 n_0 / \beta \lambda)^{\frac{1}{2}},$$

is a measure of the left-right asymmetry. Compare with eq. (7-42) and fig. 7-14.

Next, we apply the variable-gradient method (see sec. 7-5), using as the first example the effective-lifetime model with Newton cooling, eqs. (7-37) and (7-44) (Weaver 1968). It will be convenient to work with the state variables  $x_1 = n - n_0$  and  $x_2 = T$  and to use parameters  $\xi = \alpha/\beta$  and  $K = K_0$ . The system equations are

$$\frac{dx_1}{dt} = -\xi x_2(n_0 + x_1) \quad (7-119)$$

and

$$\frac{dx_2}{dt} = Kx_1 - \gamma x_2.$$

As suggested by eq. (7-95), let

$$\nabla V = \begin{bmatrix} a_{11}x_1 + a_{12}x_2 \\ a_{21}x_1 + a_{22}x_2 \end{bmatrix}. \quad (7-120)$$

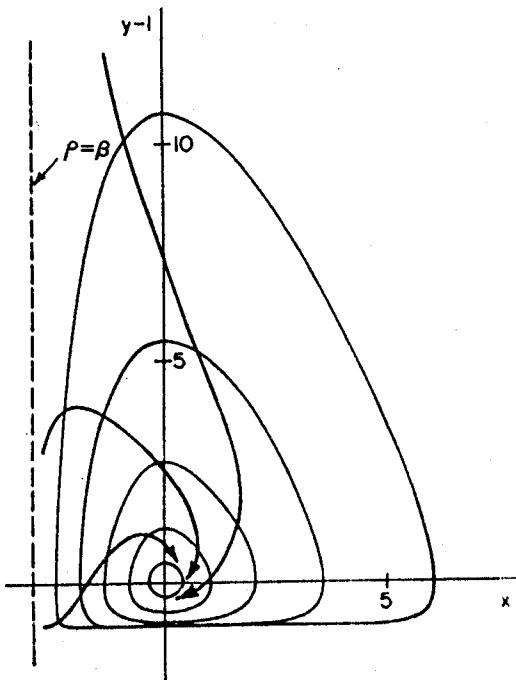


Fig. 7-28. Trajectories and curves of constant  $V$  for the prompt-jump approximation with Newton cooling (Hetrick 1965b).

We set  $a_{11} = a_{12} = 0$  as the simplest way of satisfying the generalized curl condition, eq. (7-94). Then by eqs. (7-96) and (7-119),

$$\frac{dV}{dt} = -a_{11}\xi n_0 x_1 x_2 - a_{11}\xi x_1^2 x_2 + a_{22}K x_1 x_2 - a_{22}\gamma x_2. \quad (7-121)$$

To make this form negative definite, choose  $a_{22} > 0$  and

$$a_{11} = \frac{Ka_{22}}{\xi(n_0 + x_1)}.$$

Assuming  $\alpha > 0$ , let  $a_{22} = \xi/K$  and

$$a_{11} = 1/(n_0 + x_1).$$

Eq. (7-120) becomes

$$\nabla V = \begin{bmatrix} x_1 \\ \frac{n_0 + x_1}{\xi} \\ \frac{\xi x_2}{K} \end{bmatrix}.$$

394 *Numerical System Stability*

By eq. (7-97),

$$\begin{aligned} V' &= \int_0^{x_1} \frac{x_1'}{n_0 + x_1'} dx_1' + \frac{\xi}{K} \int_0^{x_2} x_2' dx_2' \\ &= x_1 - n_0 \log\left(1 + \frac{x_1}{n_0}\right) + \frac{\xi}{2K} x_2^2. \end{aligned} \quad (7-122)$$

Eq. (7-122) is the Liapunov function of eq. (7-108). Substitution of the coefficients into eq. (7-121) verifies that

$$\frac{dV}{dt} = -\frac{\xi\gamma}{K} x_2^2$$

in conformity with eq. (7-110).

It has been shown that the method of Szego will yield this same Liapunov function.<sup>2</sup> The method of Aizerman fails because it uses a quadratic form with constant coefficients. The variable-gradient method was selected for the study of higher-order systems, as will now be described.

Consider first the point-reactor model with one group of delayed neutrons and one feedback region with Newton cooling:

$$\frac{dn}{dt} = -\frac{\alpha T + \beta}{\ell} n + \lambda c,$$

$$\frac{dc}{dt} = \frac{\beta}{\ell} n - \lambda c,$$

$$\frac{dT}{dt} = K(n - n_0) - \gamma T,$$

where  $\ell$  is the true neutron generation time. The equilibrium is  $n = n_0$ ,  $c = c_0 = \beta n_0 / \lambda \ell$ , and  $T = 0$ . Introduce the state variables  $x_1 = n - n_0$ ,  $x_2 = c - c_0$ , and  $x_3 = T$  and the parameters  $\omega = \beta/\ell$  and  $\xi = \alpha/\ell$ . The system equations are

$$\begin{aligned} \frac{dx_1}{dt} &= -\omega x_1 + \lambda x_2 - \xi(n_0 + x_1)x_3, \\ \frac{dx_2}{dt} &= \omega x_1 - \lambda x_2, \end{aligned} \quad (7-123)$$

and

$$\frac{dx_3}{dt} = Kx_1 - \gamma x_3.$$

<sup>2</sup> Unpublished studies by R. L. Brehm, University of Arizona, 1968.

We attempt a representation in which  $a_{ij} = 0$  for  $i \neq j$ :

$$\nabla V = \begin{bmatrix} a_{11}x_1 \\ a_{22}x_2 \\ a_{33}x_3 \end{bmatrix}. \quad (7-124)$$

Using eqs. (7-96) and (7-123), we find

$$\frac{dV}{dt} = a_{11}[-\omega x_1 + \lambda x_2 - \xi(n_0 + x_1)x_3]x_1 + a_{22}(\omega x_1 - \lambda x_2)x_2 + a_{33}(Kx_1 - \gamma x_3)x_3. \quad (7-125)$$

Terms in  $x_1x_3$  vanish if we select

$$a_{11} = \frac{Ka_{33}}{\xi(n_0 + x_1)}.$$

This is similar to the previous example, and it is convenient to select

$$a_{11} = \frac{1}{n_0 + x_1}, \quad a_{33} = \frac{\xi}{K}.$$

Eq. (7-125) becomes

$$\frac{dV}{dt} = -\left(\frac{x_1}{n_0 + x_1} - a_{22}x_2\right)(\omega x_1 - \lambda x_2) - \frac{\xi\gamma}{K}x_3^2. \quad (7-126)$$

We now seek a function  $a_{22}$  that will make  $dV/dt$  negative semi-definite. This we accomplish by setting

$$a_{22}(x_2) = f(x_2)/g(x_2).$$

We have

$$\frac{x_1}{n_0 + x_1} - a_{22}x_2 = \frac{x_1g - n_0x_2f - x_1x_2f}{(n_0 + x_1)g}.$$

We set the numerator of this expression equal to  $\omega x_1 - \lambda x_2$  to generate a perfect square. Since  $f$  and  $g$  are independent of  $x_1$ , let

$$f = \lambda/n_0, \quad x_1g - x_1x_2f = \omega x_1,$$

from which

$$g = \omega + \lambda x_2/n_0$$

and

$$a_{22} = \frac{1}{(\omega n_0/\lambda) + x_2} = \frac{1}{c_0 + x_2}.$$

Eq. (7-126) becomes

$$\frac{dV}{dt} = -\frac{n_0}{\lambda} \frac{(\omega x_1 - \lambda x_2)^2}{(n_0 + x_1)(c_0 + x_2)} - \frac{\xi\gamma}{K} x_3^2. \quad (7-127)$$

The gradient is

$$\nabla V = \begin{bmatrix} \frac{x_1}{n_0 + x_1} \\ \frac{x_2}{c_0 + x_2} \\ \frac{\xi x_3}{K} \end{bmatrix}.$$

Integrating, we have

$$V = x_1 - n_0 \log \left( 1 + \frac{x_1}{n_0} \right) + x_2 - c_0 \log \left( 1 + \frac{x_2}{c_0} \right) + \frac{\xi}{2K} x_3^2. \quad (7-128)$$

This function, which may be written as

$$V = n - n_0 - n_0 \log \frac{n}{n_0} + c - c_0 - c_0 \log \frac{c}{c_0} + \frac{\alpha}{2K\ell} T^2, \quad (7-129)$$

and for which

$$\frac{dV}{dt} = -\frac{n_0}{\lambda} \frac{[(\beta/\ell)(n - n_0) - \lambda(c - c_0)]^2}{nc} - \frac{\alpha\gamma}{K\ell} T^2, \quad (7-130)$$

is essentially that used by many writers (e.g., Hsu 1967; Popov 1958; Smets 1962, 1963). The preceding derivation is due to R. L. Brehm, University of Arizona.

Here we have  $V$  positive definite and  $dV/dt$  negative semidefinite provided  $n$  and  $c$  are positive and  $\xi > 0$  ( $\alpha > 0$ ). Since  $n$  and  $c$  cannot change sign, we need only show that there exist no solution trajectories (other than the equilibrium point) for which  $dV/dt$  is identically zero. By eq. (7-127), such a trajectory must satisfy  $\omega x_1 = \lambda x_2$  and  $x_3 = 0$  for all  $t$ . By eq. (7-123),  $dx_3/dt = Kx_1$ , so that  $x_1 = x_2 = 0$  and the system is asymptotically stable for  $n > 0$ ,  $c > 0$ , and  $\alpha > 0$ . The case  $\gamma = 0$  requires special attention, but it is easily shown that  $dV/dt = 0$  implies either  $x_3 = 0$  or  $n_0 + x_1 = 0$ . Since the latter is the shutdown point  $n = 0$ , which is clearly excluded by the form of  $V$ , the stability remains asymptotic.

These conditions for asymptotic stability have been obtained by many writers. Our purpose in deriving them by the variable-gradient method is to suggest ways in which that method may be used for more complicated systems. We illustrate, using one group of delayed neutrons with a two-region feedback.

The reactor model is

$$\begin{aligned}\frac{dn}{dt} &= -\frac{\alpha_1 T_1 + \alpha_2 T_2 + \beta}{\ell} n + \lambda c, \\ \frac{dc}{dt} &= \frac{\beta}{\ell} n - \lambda c, \\ \frac{dT_1}{dt} &= K_1(n - n_0) - \gamma_1 T_1, \\ \frac{dT_2}{dt} &= K_2(n - n_0) - \gamma_2 T_2.\end{aligned}$$

We select the state variables  $x_1 = n - n_0$ ,  $x_2 = c - c_0$ ,  $x_3 = T_1$ , and  $x_4 = T_2$ . The parameters are  $\omega = \beta/\ell$ ,  $\xi_1 = \alpha_1/\ell$ , and  $\xi_2 = \alpha_2/\ell$ . The system is

$$\begin{aligned}\frac{dx_1}{dt} &= -\omega x_1 + \lambda x_2 - (\xi_1 x_3 + \xi_2 x_4)(n_0 + x_1), \\ \frac{dx_2}{dt} &= \omega x_1 - \lambda x_2, \\ \frac{dx_3}{dt} &= K_1 x_1 - \gamma_1 x_3, \\ \frac{dx_4}{dt} &= K_2 x_1 - \gamma_2 x_4.\end{aligned}\tag{7-131}$$

The complete expression for  $dV/dt$  is

$$\begin{aligned}\frac{dV}{dt} &= (a_{11}x_1 + a_{12}x_2 + a_{13}x_3 + a_{14}x_4)[- \omega x_1 \\ &\quad + \lambda x_2 - (\xi_1 x_3 + \xi_2 x_4)(n_0 + x_1)] \\ &\quad + (a_{21}x_1 + a_{22}x_2 + a_{23}x_3 + a_{24}x_4)(\omega x_1 - \lambda x_2) \\ &\quad + (a_{31}x_1 + a_{32}x_2 + a_{33}x_3 + a_{34}x_4)(K_1 x_1 - \gamma_1 x_3) \\ &\quad + (a_{41}x_1 + a_{42}x_2 + a_{43}x_3 + a_{44}x_4)(K_2 x_1 - \gamma_2 x_4).\end{aligned}\tag{7-132}$$

As a first step in simplifying this expression, it is reasonable to exclude triple products like  $x_1x_2x_3$ . This implies  $a_{12} = a_{13} = a_{14} = 0$ . Then, the simplest way to cause eq. (7-132) to conform with eq. (7-94) is to let  $a_{21} + a_{31} = a_{41} = 0$ . Next, taking advantage of the previous example, let

$$a_{11} = \frac{1}{n_0 + x_1}, \quad a_{22} = \frac{1}{c_0 + x_2}.$$

At this point,  $dV/dt$  still contains a number of products  $x_1x_2$ ,  $x_1x_3$ , etc. Suspecting from previous experience that it may be fruitful to abandon all these except  $x_3x_4$  (the cross-product in a quadratic function of the two temperatures), we obtain the conditions

$$a_{32}K_1 + a_{42}K_2 = 0, \quad (7-133)$$

$$a_{23}\omega + a_{33}K_1 + a_{43}K_2 - \xi_1 = 0, \quad (7-134)$$

$$a_{24}\omega + a_{34}K_1 + a_{44}K_2 - \xi_2 = 0, \quad (7-135)$$

$$a_{23}\lambda + a_{32}\gamma_1 = 0, \quad (7-136)$$

$$a_{24}\lambda + a_{42}\gamma_2 = 0. \quad (7-137)$$

We now have

$$\begin{aligned} \frac{dV}{dt} = & -\frac{n_0}{\lambda} \frac{(\omega x_1 - \lambda x_2)^2}{(n_0 + x_1)(c_0 + x_2)} - a_{33}\gamma_1 x_3^2 \\ & - (a_{34}\gamma_1 + a_{43}\gamma_2)x_3 x_4 - a_{44}\gamma_2 x_4^2. \end{aligned} \quad (7-138)$$

The gradient is

$$\nabla V = \begin{bmatrix} \frac{x_1}{n_0 + x_1} \\ \frac{x_2}{c_0 + x_2} \\ a_{33}x_3 + a_{34}x_4 \\ a_{43}x_3 + a_{44}x_4 \end{bmatrix},$$

and the integral is

$$\begin{aligned} V = & x_1 - n_0 \log \left( 1 + \frac{x_1}{n_0} \right) + x_2 - c_0 \log \left( 1 + \frac{x_2}{c_0} \right) \\ & + \frac{1}{2} a_{33}x_3^2 + a_{43}x_3 x_4 + \frac{1}{2} a_{44}x_4^2. \end{aligned} \quad (7-139)$$

The conditions expressed by eqs. (7-133), (7-136), and (7-137) are

most easily satisfied if we choose

$$a_{23} = a_{32} = a_{24} = a_{42} = 0.$$

Eqs. (7-134) and (7-135) become

$$a_{33}K_1 + a_{43}K_2 - \xi_1 = 0 \quad (7-140)$$

and

$$a_{34}K_1 + a_{44}K_2 - \xi_2 = 0. \quad (7-141)$$

One method of satisfying these two conditions and of following the lead of the one-region example would be to take  $a_{34} = a_{43} = 0$ ,  $a_{33} = \xi_1/K_1$ , and  $a_{44} = \xi_2/K_2$ . This is unnecessarily restrictive; by eqs. (7-138) and (7-139), there would be no hope of establishing stability unless  $\alpha_1 > 0$  and  $\alpha_2 > 0$  (the first quadrant in figs. 6-52, 6-56, etc.).

Instead, we retain eq. (7-138) as is, and use eqs. (7-140) and (7-141) to express two of the undetermined coefficients in terms of the other one. Taking eq. (7-94) into account, we have

$$a_{34} = a_{43} = \frac{a_{33}K_1 - \xi_1}{K_2} \quad (7-142)$$

and

$$a_{44} = \frac{a_{33}K_1^2 - \xi_1 K_1 + \xi_2 K_2}{K_2^2}. \quad (7-143)$$

We next apply Sylvester's theorem to the quadratic forms in eqs. (7-138) and (7-139), and, using eqs. (7-142) and (7-143), we find that  $V$  is positive definite and  $dV/dt$  negative semidefinite provided  $a_{33} > 0$  and that

$$(\xi_1 K_1 + \xi_2 K_2)a_{33} - \xi_1^2 > 0 \quad (7-144)$$

and

$$-(\gamma_1 - \gamma_2)^2 K_1^2 a_{33}^2 + [2(\gamma_1^2 + \gamma_2^2)\xi_1 K_1 + 4\gamma_1\gamma_2\xi_2 K_2]a_{33} - (\gamma_1 + \gamma_2)^2 \xi_1^2 > 0. \quad (7-145)$$

We note that  $a_{33}$  must not be too large, or the condition expressed by eq. (7-145) will not be satisfied.

If we replace the inequality in eq. (7-145) by an equal sign, we find, after some manipulation, two critical values for  $a_{33}$  between which the inequality is satisfied:

$$a_{33} = \frac{1}{(\gamma_1 - \gamma_2)^2 K_1^2} \{ \gamma_1(\gamma_1\xi_1 K_1 + \gamma_2\xi_2 K_2) + \gamma_2(\gamma_2\xi_1 K_1 + \gamma_1\xi_2 K_2) \\ \pm 2[\gamma_1\gamma_2(\gamma_1\xi_1 K_1 + \gamma_2\xi_2 K_2)(\gamma_2\xi_1 K_1 + \gamma_1\xi_2 K_2)]^{1/2} \}. \quad (7-146)$$

This result is meaningful only if the two roots are real and distinct. Therefore we must have

$$\gamma_1\xi_1K_1 + \gamma_2\xi_2K_2)(\gamma_2\xi_1K_1 + \gamma_1\xi_2K_2) > 0.$$

Note that the two factors appear in eq. (7-146) in the form of arithmetic and geometric means, and that we require  $a_{33} > 0$ . Each factor alone must therefore be positive:

$$\gamma_1\xi_1K_1 + \gamma_2\xi_2K_2 > 0, \quad (7-147)$$

$$\gamma_2\xi_1K_1 + \gamma_1\xi_2K_2 > 0. \quad (7-148)$$

Recalling the definitions of the parameters involved, we see that eqs. (7-147) and (7-148) are respectively identical to eqs. (6-130) and (6-128). These are the necessary and sufficient conditions that the two-region reactor, in the absence of delayed neutrons, be linearly stable at all equilibrium power levels  $n_0$ . In other words, we are in the process of proving that the nonlinear two-region model with delayed neutrons is asymptotically stable in the large in the same region of parameter space for which the linearized system without delayed neutrons is unconditionally stable (stable at all power levels). As we shall see in a later section, this is a well-known result that has been derived by other methods.

To complete the present proof, it is necessary to establish that a positive number  $a_{33}$  can be chosen such that the inequalities expressed by eqs. (7-144) and (7-145) are both satisfied. This we may accomplish by rejecting the minus sign in eq. (7-146) and replacing the factor two by  $\epsilon$ , where  $0 < \epsilon < 2$ . The resulting value of  $a_{33}$  satisfies eq. (7-145) and also satisfies the condition

$$a_{33} > \frac{\gamma_1(\gamma_1\xi_1K_1 + \gamma_2\xi_2K_2) + \gamma_2(\gamma_2\xi_1K_1 + \gamma_1\xi_2K_2)}{(\gamma_1 - \gamma_2)^2 K_1^2}. \quad (7-149)$$

If eq. (7-144) is satisfied by the right-hand side of eq. (7-149), it will be satisfied by any  $a_{33}$  in the specified range. Substituting the right-hand side of eq. (7-149) into eq. (7-144) yields, after some manipulation,

$$\gamma_1\gamma_2(\xi_1K_1 + \xi_2K_2)^2 + (\gamma_1\xi_1K_1 + \gamma_2\xi_2K_2)(\gamma_2\xi_1K_1 + \gamma_1\xi_2K_2) > 0,$$

which is a true inequality whenever eq. (7-147) and (7-148) are satisfied. Finally, by arguments similar to those employed in the one-region example, it may be established that  $dV/dt = 0$  only at the equilibrium point. The two-region system with delayed neutrons is therefore asymptotically stable for all  $n > 0$  and  $c > 0$  whenever the conditions of eqs. (7-147) and (7-148) are met.

Systems with more than two regions were also considered in the paper by Ergen, Lipkin, and Nohel (1957). A review of the many-region problem, with some applications, is given by Akcasu, Lefouche, and Shotkin (forthcoming). Their Liapunov function, a generalization of eq. (7-139), may be written as

$$V = n - n_0 - n_0 \log \frac{n}{n_0} + \sum_i \left( c_i - c_{i0} - c_{i0} \log \frac{c_i}{c_{i0}} \right) + \sum_i \frac{g_i g_j}{\gamma_i + \gamma_j} \xi_i \xi_j + \sum_j A_j \xi_j^2,$$

where the  $\xi_i$  are the canonical feedback variables, as mentioned earlier in connection with eq. (7-104). This is a Liapunov function of the Lur'e-Letov type, modified for application to reactor dynamics. Stability criteria are expressed as relations among the feedback parameters and the coefficients  $g_i$  and  $A_j$ .

The stability conditions obtained by these methods are sufficient but not necessary. As we saw in chapter 6, the two-region system without delayed neutrons is linearly stable in a larger region of the parameter space provided the equilibrium power is sufficiently small (conditional stability). Further, the region of unconditional linear stability is enlarged by delayed neutrons. The treatments we have discussed contain no information about these possibilities. These considerations naturally lead one to suggest that the Liapunov function of eq. (7-139) is more restrictive than necessary. A number of restrictive assumptions were made in the course of applying the variable-gradient method to this system, and it is conceivable that larger, more realistic domains of stability might be obtained using other assumptions. The question deserves further investigation.

We now turn to a different example that is interesting because it illustrates stability in a finite region of state space. Consider the effective-lifetime model with a one-region temperature coefficient (Newton cooling) plus a power coefficient, as formulated by Devooght and Smets (1967):

$$\begin{aligned} \frac{dn}{dt} &= \frac{\rho}{\ell} n, \\ \rho &= \rho_0 - \alpha T - \kappa n, \\ \frac{dT}{dt} &= Kn - \gamma T. \end{aligned} \tag{7-150}$$

The linear stability of this system was studied in sec. 6-6. Here we have a slightly different notation; the prime on  $\ell$  and the subscript on  $K$

have been dropped, and the temperature  $T$  is now referred to  $T = 0$  as the shutdown state. The equilibrium conditions are

$$\rho_0 = \alpha T_0 + \kappa n_0,$$

$$n_0 = \frac{\gamma \rho_0}{\alpha K + \gamma \kappa},$$

$$T_0 = \frac{K \rho_0}{\alpha K + \gamma \kappa},$$

where  $\rho_0$  is the reactivity at zero power. If we express eqs. (6-105) and (6-106) in terms of the present physical quantities, the requirements for linear stability are

$$\kappa n_0 > -\gamma \ell \quad (7-151)$$

and

$$\alpha K + \gamma \kappa > 0. \quad (7-152)$$

The latter expresses the requirement  $H(0) > 0$ ; see eq. (6-107). The former expresses the possibility of conditional stability when  $\kappa < 0$  (positive power coefficient of reactivity).

We will look for conditions for nonlinear asymptotic stability with  $\kappa < 0$ , assuming that eqs. (7-151) and (7-152) are satisfied. The system equations are

$$\frac{dn}{dt} = -[\alpha(T - T_0) + \kappa(n - n_0)]n/\ell \quad (7-153)$$

and

$$\frac{dT}{dt} = K(n - n_0) - \gamma(T - T_0).$$

The Liapunov function postulated by Devooght and Smets (1967) may be written as

$$V = n - n_0 - n_0 \log \frac{n}{n_0} + \frac{[\alpha(T - T_0) - \gamma \ell \log(n/n_0)]^2}{2\ell(\alpha K + \gamma \kappa)}. \quad (7-154)$$

This function is positive definite in the half-space  $n > 0$  provided eq. (7-152) is satisfied. We find

$$\frac{dV}{dt} = -\frac{1}{\ell}[\kappa(n - n_0)^2 + \gamma \ell(n - n_0) \log(n/n_0)]. \quad (7-155)$$

The locus of  $dV/dt = 0$  is the origin plus a straight line in the  $n, T$  plane given by the solution of the transcendental equation

$$\gamma \ell \log(n/n_0) = -\kappa(n - n_0). \quad (7-156)$$

A solution  $n > n_0$  exists if eq. (7-151) is satisfied (asymptotic stability in the small). The region of nonlinear asymptotic stability is determined by plotting the curve  $V = \text{constant}$  that is just tangent to the line  $n = n_1$  where  $n_1$  is the root of eq. (7-156).

The procedure is to solve eq. (7-156) for  $n = n_1$ , compute  $T_1$  (the value of  $T$  at the tangent point) from

$$T_1 = T_0 + \frac{\gamma \ell}{\alpha} \log \frac{n}{n_0} \quad (7-157)$$

and then compute  $V_{\max}$  by using  $n_1$  and  $T_1$  in eq. (7-154). Eq. (7-157) results from setting  $dV/dT = 0$  at constant  $n$ . The curve  $V = V_{\max}$  is plotted in the  $n, T$  plane by solving eq. (7-154) for  $T$  in terms of  $n$  and  $V_{\max}$ .

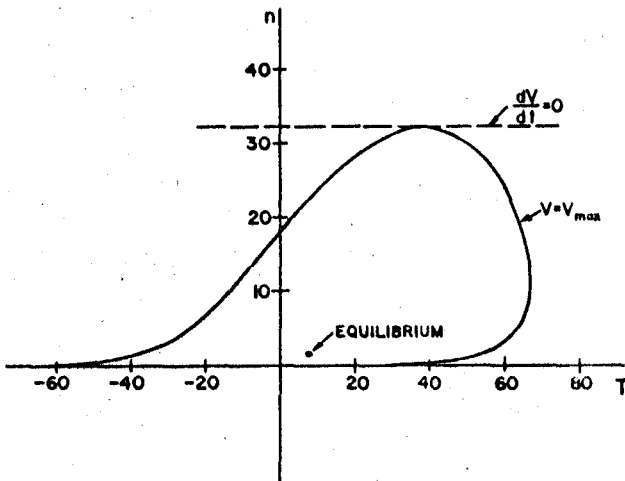


Fig. 7-29. The domain of asymptotic stability for the effective-lifetime model with one feedback region plus a power coefficient (Devooght and Smets 1967).

An example is shown in fig. 7-29. The parameters are  $K = 50$ ,  $\rho_0/\ell = 6$ ,  $\alpha/\ell = 1$ ,  $\kappa/\ell = -1$ , and  $\gamma = 10$ . Derived parameters are  $n_0 = 1.5$ ,  $T_0 = 7.5$ ,  $n_1 = 32.15$ ,  $T_1 = 38.15$ , and  $V_{\max} = 26.05$ . The region of stability does not include the  $T$ -axis. The region becomes infinitesimally thin as  $T$  becomes large negative. Of course, an initial point in the range  $T < 0$  is somewhat unreal because it would represent a reactor cooled below the temperature of its surroundings.

This problem has been treated by a number of writers, and it is rapidly becoming a classic test case. It has been shown that a class of functions

### 4.11 Linear System Stability

containing the function of eq. (7-154) can be generated by the variable-gradient method, and that eq. (7-154) represents the particular member of this class that yields the largest domain of stability (Brehm 1969). Other methods have been applied by Devooght and Smets (1967), Hsu and Sha (1969), Kalinowski and Bailey (1968), and Shotkin (1969a), each method yielding a different stability domain. No analytical method has yet been found that describes the full stability domain as determined for this example by trial-and-error computer studies (Shotkin 1969a). We shall return to the last-mentioned paper by Shotkin in a later section.

We close this section with two simple examples illustrating the use of state functions that are not positive definite. Consider the one-region model plus a power coefficient, but with delayed neutrons included: eqs. (3-1) and (3-2) with  $q = 0$  together with the feedback used in eq. (7-150). Let

$$V_1 = n + \sum_i c_i + \frac{\alpha}{2\ell K} T^2. \quad (7-158)$$

We find

$$\frac{dV_1}{dt} = \frac{dn}{dt} + \sum_i \frac{dc_i}{dt} + \frac{\alpha T}{\ell K} \frac{dT}{dt} = \frac{\rho_0}{\ell} n - \frac{\kappa}{\ell} n^2 - \frac{\alpha\gamma}{\ell K} T^2.$$

Since  $n$  and  $c_i$  may not be negative, we have  $V_1 > 0$  and  $dV_1/dt < 0$  for  $\rho_0 < 0$ ,  $\kappa > 0$ , and  $\alpha > 0$ , so that this shutdown state is asymptotically stable in the large ( $n > 0$ ,  $c_i > 0$ ). It is easily verified that the other mathematically possible equilibrium state has negative  $n_0$ . A similar function was used by Smets (1962) to establish this type of behavior for a more general linear feedback.

As a second example using this reactor model, let

$$V_2 = n + \sum_i c_i \quad (7-159)$$

and

$$\frac{dV_2}{dt} = \frac{\rho_0}{\ell} n - \frac{\alpha}{\ell} n T - \frac{\kappa}{\ell} n^2.$$

The locus of  $dV_2/dt = 0$  is the origin plus the line  $\rho = 0$ . Since the line  $\rho = 0$  extends into the region  $n > 0$ , no assertion may be made concerning all possible values of  $n$ . However, if  $\rho_0 > 0$ , there is a neighborhood of the origin for which  $n > 0$  and  $dV_2/dt > 0$ . Therefore, for positive shutdown reactivity, all physically possible trajectories originating near the origin are directed away from the origin and the shutdown equilibrium point is locally unstable.

Many other reactor applications of the direct method of Liapunov and its variations may be found in the literature. An important theoretical study of the effect of delayed neutrons was made by Popov (1958), using functions like those in eq. (7-129). An example of nonlinear feedback is given by Smets (1961). Several matrix methods are compared in a recent study by Sha and Hsu (1968). Other references have been cited throughout this section.

Finally, we emphasize one basic limitation of the direct method of Liapunov. The system equations must be of the form of eq. (7-58), which for a reactor means that the feedback must not contain a transport time delay. For linear feedbacks, the feedback kernel of eq. (5-70) is therefore constrained to be the Green's function (impulse response) of a linear differential operator; i.e., a linear feedback system must be expressible as a set of linear differential equations in  $t$ . The theoretical problem arising from time delays is treated by Krasovskii (1963). Modifications of the method to include time delays are possible (e.g., Murray and Schultz 1966), but the subject is beyond the scope of this book, as are other methods for treating nonlinear systems with time delays (e.g., Jacobowitz, Akcasu, and Shotkin, 1966).

### 7-7. Boundedness and Lagrange Stability

Asymptotic stability guarantees that a system returns to equilibrium after being perturbed. In some cases, the demand for asymptotic stability is an unnecessarily great restriction on the design or operation of a system. Some systems that are not asymptotically stable can operate satisfactorily as long as the physical variables remain within limits fixed by considerations of safety, material properties, or other constraints. In fact, the system might not even be stable in the small; the stable limit cycle of fig. 7-21 could be an example. It might be pointed out that a mechanical clock operates on a limit cycle. Of course, one could establish either asymptotic stability or boundedness as properties of a mathematical model and yet be unable to predict safe operation of a corresponding physical system. Further information about the system response would be needed, because a relatively small perturbation might cause a physical variable to exceed some crucial limit before settling down to an acceptable value.

Keeping this limitation in mind, we look for mathematical conditions that assure bounded solutions; i.e., solutions for which the norm  $\bar{x}(t)$  of eq. (7-61) has a finite upper bound for all  $t$  following an initial disturbance. When a particular solution or a limited class of solutions is bounded, we use the term *boundedness*. When all solutions are bounded, we say that the system possesses *Lagrange stability*.

First, we describe a general criterion for boundedness that was derived by Akcasu.<sup>3</sup> We repeat the system equations:

$$\frac{dn}{dt} = \frac{\rho - \beta}{\ell} n + \sum_i \lambda_i c_i$$

and

$$\frac{dc_i}{dt} = \frac{\beta_i}{\ell} n - \lambda_i c_i.$$

Define the function (not a Liapunov function)

$$V = n - n_0 - n_0 \log \frac{n}{n_0} + \sum_i \left( c_i - c_{i0} - c_{i0} \log \frac{c_i}{c_{i0}} \right) - \frac{1}{\ell} \int_{-\infty}^t \dot{\rho}(t') [n(t') - n_0] dt'. \quad (7-161)$$

Using the system equations with  $\lambda_i c_{i0} = \beta_i n_0 / \ell$ , we have

$$\frac{dV}{dt} = - \sum_i \frac{n_0}{\lambda_i n c_i} \left( \frac{\beta_i}{\ell} n - \lambda_i c_i \right)^2. \quad (7-162)$$

We saw in the previous section that  $V$  without the integral term would be positive definite for  $n > 0, c_i > 0$ . Also, we have  $dV/dt \leq 0$ , so that  $V$  is constant or monotonically decreasing along every solution trajectory. Extending the ideas of the Liapunov theorem (sec. 7-5), we assert that all solutions are bounded if  $V$  is bounded. Since  $V$  is never increasing, the criterion for boundedness may be stated as

$$\int_{-\infty}^t \dot{\rho}(t') [n(t') - n_0] dt' \leq 0 \quad (7-163)$$

provided the initial value of  $V$  is bounded. Then, as  $t \rightarrow \infty$ ,  $V \rightarrow V_0 \geq 0$  and  $dV/dt \rightarrow 0$  (assuming  $V$  is uniformly continuous).

The criterion is very general. The reactivity is unspecified, and the feedback need not be linear. The initial state prior to the perturbation need not be the equilibrium state. Moreover, the criterion may be interpreted to include feedbacks with transport time delays. In this case, one may establish eq. (7-163) for all physically admissible initial curves (all possible power histories for  $t < 0$ ) and for arbitrary functions  $\eta(t)$  for  $t > 0$ , and derive sufficient conditions for boundedness. Of course, if  $n = n_0$  for  $t < 0$ , the lower limit in the integral may be replaced by zero. A rigorous discussion is given by Akcasu, Lellouche,

3. I am grateful to A. Z. Akcasu of the University of Michigan for the opportunity to study his notes prior to their publication (Akcasu, Lellouche, and Shotkin, forthcoming).

and Shotkin (forthcoming). We shall make use of eq. (7-163) later in deriving a frequency-domain stability criterion.

A criterion for boundedness of certain solutions (but not Lagrange stability) was obtained by Akcasu and Noble (1966a). Starting from the integro-differential equation for reactor dynamics, eq. (4-31), and using the general linear feedback, eq. (5-70), i.e.,

$$\begin{aligned}\rho &= - \int_{-\infty}^t h(t-t')[n(t') - n_0] dt' \\ &= - \int_0^\infty h(u)[n(t-u) - n_0] du,\end{aligned}\quad (7-164)$$

one separates out for special treatment all integral terms that involve the reactor power for  $t < 0$ . Assuming that  $n(t)$  is of exponential order, one may solve the transformed equation for the Laplace transform of  $n$  and investigate its singularities in the  $s$ -plane. It is found that the Laplace-transformable solutions are bounded if  $H(s)$ , the Laplace transform of the linear feedback kernel  $h(t)$ , does not vanish on the positive real axis, and if  $H(0) > 0$ . Recall that  $h > 0$  corresponds to negative reactivity with our sign convention. Note that this is not a sufficient condition for Lagrange stability, because solutions that contain  $\exp(t^2)$  and solutions that exhibit finite escape time (sec. 7-4) are not Laplace transformable. The criterion has been established both with and without delayed neutrons (Akcasu and Noble 1966a).

We illustrate the application of this criterion for the two-region reactor model of secs. 6-7 and 6-8. By eq. (6-119),

$$H(s) = \frac{A_1}{s + \gamma_1} + \frac{A_2}{s + \gamma_2} \quad (7-165)$$

and

$$h(t) = A_1 e^{-\gamma_1 t} + A_2 e^{-\gamma_2 t}, \quad t \geq 0, \quad (7-166)$$

with  $h(t) = 0$  for  $t < 0$ , where  $A_1 = \alpha_1' K_1$  and  $A_2 = \alpha_2' K_2$ . These are the parameters of the decoupled feedback system of eqs. (6-116) and (6-117). Eq. (7-165) may be written as eq. (6-120), with the zero exhibited at  $s = -\xi$ . The criterion for boundedness requires that  $\xi > 0$  and  $(A_1 + A_2)\xi > 0$ . Using eq. (6-121), we find that all Laplace-transformable solutions of this model are bounded if

$$A_1 \gamma_2 + A_2 \gamma_1 > 0 \quad (7-167)$$

and

$$A_1 + A_2 > 0. \quad (7-168)$$

Using eq. (6-132) we can locate the corresponding region in the parameter space of fig. 6-52. The region is defined by

$$\gamma_2 x + \gamma_1 y > 0, \quad x + y > 0.$$

The boundary contains the static stability boundary and the locus for  $K = 0$ ; see eqs. (6-134) and (6-135). The region is therefore the region of unconditional linear stability without delayed neutrons, plus that subregion of conditional stability where  $K$ , the open-loop gain in eq. (6-123), is positive. This is precisely the region of stable minimum-phase positive-gain feedback systems. Since the criterion applies also when delayed neutrons are included, it is interesting to consult figs. 6-56, 6-60, and 6-63; the only cases of conditional linear stability that satisfy the new criterion appear in fig. 6-56.

Later, we discuss stable limit cycles that have been demonstrated for linearly unstable but bounded cases in both figs. 6-52 and 6-56. This is as expected, though we have not yet ruled out the possibility of unbounded solutions that are not Laplace-transformable.

We have already demonstrated nonlinear asymptotic stability, with and without delayed neutrons, for the region of linear unconditional stability in fig. 6-52 using the Liapunov function of eq. (7-139); see the discussion following eq. (7-148). Lagrange stability of the nonlinear system is therefore assured in this region because it follows from a proof of asymptotic stability. This applies to the same region in figs. 6-56, 6-60, and 6-63.

A necessary condition for the existence of solutions with finite escape time was also derived by Akcasu and Noble (1966a):

$$h(0) = \lim_{s \rightarrow \infty} sH(s) < 0 \quad (7-169)$$

provided  $h(0)$  is finite. This criterion also is valid with or without delayed neutrons. Finite escape times cannot exist with linear feedback unless the feedback kernel is initially negative (prompt-positive reactivity effects). For the two-region model of eq. (7-166), the necessary condition is

$$A_1 + A_2 < 0. \quad (7-170)$$

This corresponds to  $x + y < 0$  in fig. 6-52 and the other parameter planes. Ruling out cases below the static stability boundary, we see that finite escape times may exist in those conditionally stable systems for which  $K < 0$ . These are the nonminimum-phase, negative-gain feedbacks. Finite escape times in linearly stable systems of this type have been demonstrated—without delayed neutrons by Shotkin (1964a), and with delayed neutrons by Akcasu and Noble (1966a) and by Schmidt (1969).

This criterion establishes that finite escape times do not occur in those systems whose Laplace-transformable solutions are bounded according to the preceding criterion. This still does not rule out other types of nontransformable solutions, such as  $\exp(t^2)$ , for these systems. It is therefore conceivable that a stable limit cycle could occur in conjunction with an unbounded solution (e.g., a stable limit cycle inside an unstable limit cycle). Such behaviour has not been found with the two-region model of eq. (7-166).<sup>4</sup>

We now turn to several criteria for boundedness that do not depend on an assumption of Laplace transformability and that are therefore criteria for Lagrange stability. Unfortunately, the proofs do not apply to systems with delayed neutrons.

A sufficient criterion for boundedness with a linear feedback kernel  $h(t)$  and no delayed neutrons is that  $h(t) > 0$  for all  $t > 0$  (Smets 1960, 1962). For our two-region example, with  $\gamma_1 > \gamma_2$ , this reduces to

$$A_1 + A_2 > 0, \quad A_2 > 0, \quad (7-171)$$

which corresponds to  $x + y > 0$ ,  $y > 0$  in fig. 6-52 (for  $\gamma_1 < \gamma_2$ , interchange the subscripts). This region does not include all the cases of unconditional linear stability in fig. 6-52, but it does establish that there are no unbounded nontransformable solutions in the region of conditional stability where  $K > 0$  (in the absence of delayed neutrons). For the application of this criterion to the case of two regions plus a power coefficient, see Smets (1963).

If a power coefficient is included, there is a constant term  $\kappa$  in  $H(s)$  and a corresponding term  $\kappa\delta(t)$  in the feedback kernel  $h(t)$ . We may write

$$H(s) = \kappa + H_1(s), \quad h(t) = \kappa\delta(t) + h_1(t),$$

where  $h_1(t)$  is bounded. It was shown by Akcasu and Noble (1966b) that all solutions (without delayed neutrons) are bounded if  $h_1(t)$  is bounded and integrable, if the power variation for  $t < 0$  is bounded and integrable from  $-\infty$  to 0, and if  $\kappa + H_1(s) > 0$  for all  $s$  on the real axis. It is shown in the same paper that the case  $\kappa = 0$  is bounded if the power variation for  $t < 0$  is bounded and integrable and if

$$\int_0^t h(t') dt' \geq 0 \quad (7-172)$$

for all  $t \geq 0$ . This last condition was also derived by Smets.<sup>5</sup> When the

4. Since this section was written, the criterion for boundedness (Akcasu and Noble 1966a) has been established without the restriction to Laplace-transformable solutions (Smets 1970). In addition, it has been shown that  $h(0) < 0$  is a sufficient condition for the existence of solutions with finite escape time (H. B. Smets, private communication, 1970).

5. H. B. Smets, private communication (1965). See also Smets (1967).

criterion of eq. (7-172) is applied to the two-region model of eq. (7-166), one obtains precisely the conditions of eqs. (7-167) and (7-168). In other words, all solutions without delayed neutrons are bounded in the region of unconditional linear stability and in the region of conditional stability in which  $K > 0$ . This extends the region given by eq. (7-171) to include those linearly stable systems with  $A_2 < 0$ , so that all the cases of nonlinear asymptotic stability for the two-region model without delayed neutrons are included. Unfortunately, it is not clear how to include delayed neutrons in these particular criteria for Lagrange stability.

The situation for the two-region model without delayed neutrons (i.e., the effective-lifetime model) is summarized in fig. 7-30, using the parameters of fig. 6-52 as defined by eqs. (6-132) and (6-118). Of course,

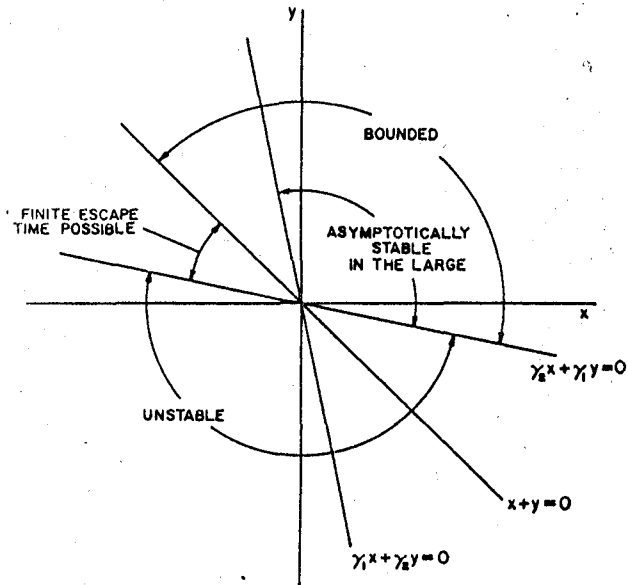


Fig. 7-30. Nonlinear stability characteristics for a reactor with two-path feedback and no delayed neutrons (effective-lifetime model) using the parameter space of fig. 6-52 (regions for bounded and asymptotically stable solutions derived from sufficient but not necessary conditions).

bounded or asymptotically stable solutions may exist outside the regions indicated, because these regions are derived from conditions that are sufficient but not necessary. The unstable region is the same as that in fig. 6-52; here it means that the nonlinear system is unstable for all initial perturbations, including small perturbations at any power

level  $n_0$ . The same figure applies for the two-region system with delayed neutrons except for one modification: the region that is bounded but not asymptotically stable in the large must instead be characterized as "bounded for all solutions that are Laplace-transformable."<sup>6</sup>

We mention one other approach to Lagrange stability, based on an extension of the Liapunov direct method (LaSalle and Lefschetz 1961). The essential features of the relevant theorem are: If  $V$  is positive definite and properly continuous in the entire state space, and if  $dV/dt$  is negative everywhere outside some bounded region surrounding the origin, then the system possesses Lagrange stability. The application to reactors appears in a paper by Gyftopoulos (1964a), in which it is shown that the two-region reactor without delayed neutrons has Lagrange stability when the conditions of eqs. (7-167) and (7-168) are satisfied, as shown in fig. 7-30.

Closely related to Lagrange stability is the question of estimating the size of the domain of asymptotic stability for a linearly stable system that is not asymptotically stable in the large. We have already seen examples of this in figs. 7-24, 7-25, and 7-29, using Liapunov's direct method. Other methods exist, and a classic example is given in the technical note by Akcasu (1966).

A major advance in this direction was achieved by Shotkin (1969a), who developed and applied an idea that originated with Malkin (1952). The essence of this method is that any linearly stable system possesses a dominant canonical coordinate associated with the least negative eigenvalue (or a complex pair of canonical coordinates associated with a dominant pair of complex eigenvalues). These dominant eigenvalues belong to the term or pair of terms in the linearized solution (an exponential decay or a damped oscillation) that is the last to disappear as  $t \rightarrow \infty$ . In this sense, these dominant terms represent the asymptotic solutions of linearized problems.

First, one finds a linear transformation that diagonalizes the linear system. If a complex pair of eigenvalues is dominant, it is convenient to select a transformation such that the associated canonical variables are complex conjugates of each other. The complete nonlinear system is then expressed in terms of the set of canonical variables. One then seeks a nonlinear transformation that expresses the dominant variable (or dominant pair) in terms of all the remaining variables, with the goal of eliminating all the nondominant coordinates. This transformation usually appears as a power series beginning with terms of at least second degree in the nondominant coordinates. The coefficients in the series are determined by substituting the series into the nonlinear

6. This restriction has recently been removed by Smets (1970).

#### 41.2 Nonlinear System Stability

canonical equations and equating terms of the same degree. In the case of a dominant real eigenvalue, the result is a first-order differential equation in the dominant canonical coordinate. The range of stability of this first-order system is then indicative of the magnitude of a perturbation that can be tolerated without instability in the original nonlinear system. As is usual in power series approximations, both the accuracy and the computational labor increase as the number of terms is increased. Of course, if the original system were asymptotically stable in the large, this could not be determined conclusively with a finite number of terms in the nonlinear transformation.

As an illustration, consider the second-order system of eq. (7-21) and figs. 7-9 and 7-24. With respect to the stable node at the origin, this system is already in canonical form:

$$\begin{aligned}\frac{dx}{dt} &= -2x + xy, \\ \frac{dy}{dt} &= -y + xy.\end{aligned}\tag{7-173}$$

Since the dominant coordinate is  $y$ , we attempt a transformation

$$x = Ay^2 + By^3 + \dots\tag{7-174}$$

Taking the time derivative of eq. (7-174), substituting eq. (7-173), and using eq. (7-174) to eliminate  $x$ , we find

$$-2Ay^2 + (A - 2B)y^3 + By^4 = -2Ay^2 - 3By^3 + 2A^2y^4 + \dots\tag{7-175}$$

Ignoring the equilibrium solution  $A = B = 0$ , we have, from the terms in  $y^3$  and  $y^4$ ,  $A = -\frac{1}{2}$  and  $B = \frac{1}{2}$ . Eq. (7-174) becomes

$$x = -\frac{1}{2}y^2 + \frac{1}{2}y^3 + \dots\tag{7-176}$$

From eq. (7-173) we find

$$\frac{dy}{dt} = -y - \frac{1}{2}y^3 + \frac{1}{2}y^4 + \dots\tag{7-177}$$

Eq. (7-177) is a first-order differential equation for the dominant canonical variable  $y$ . When terms through  $y^4$  are retained, the right-hand side vanishes at the equilibrium point and at  $y = 1.696$  (the only real solution of a cubic equation in  $y$ ). We observe that

$$\frac{1}{y} \frac{dy}{dt} < 0$$

for  $-\infty < y < 1.696$ , which is therefore the range of stability of eq. (7-177) in this approximation.

Substitution of the maximum value of  $y$  into eq. (7-176) yields  $x = 1$ . We infer that the point  $x = 1$ ,  $y = 1.696$  is near the threshold of instability for the system, and this is confirmed by figs. 7-9 and 7-24. In fact, this point is just slightly inside the circle in fig. 7-24.

Information of this type, particularly when combined with a knowledge of the locations of nearby unstable critical points, is very useful in analyzing complicated nonlinear systems. Of course, it does not tell the whole story; when the dominant eigenvalue is real, one obtains only one point on the approximate stability boundary.

When a complex conjugate pair is dominant, one obtains instead a two-dimensional curve in the state space. In this case, once the non-dominant coordinates have been eliminated, one has two canonical equations,

$$\frac{dx_1}{dt} = s_1 x_1 + f_1(x_1, x_2) \quad (7-178)$$

and

$$\frac{dx_2}{dt} = s_2 x_2 + f_2(x_1, x_2),$$

with  $x_1 = x_2^*$  and  $s_1 = s_2^*$ . Following Bogoliubov and Mitropolsky (1961), we seek a solution in terms of two time-dependent functions  $A$  and  $\theta$  (representing an amplitude and a phase):

$$x_1 = A e^{j\theta} + A^2 u_2(\theta) + A^3 u_3(\theta) + \dots, \quad (7-179)$$

where the  $u_n$  are periodic functions of  $\theta$ . Letting  $s_1 = b + j\omega$ , we assume that

$$\frac{dA}{dt} = bA + B_2 A^2 + B_3 A^3 + \dots \quad (7-180)$$

and

$$\frac{d\theta}{dt} = \omega + \Omega_2 A + \Omega_3 A^2 + \dots.$$

After substitution and comparison of coefficients of like powers of  $A$ , one derives a first-order differential equation for  $A$  analogous to eq. (7-177). The maximum value of  $A$  for stability is determined by setting  $dA/dt = 0$ .

Using eq. (7-179) with  $x_2 = x_1^*$ , one finds equations for  $x_1$  and  $x_2$  in terms of the parameter  $\theta$ , that give the approximate stability bound. When transformed back to the original state variables, these become

parametric equations for a two-dimensional curve in the state space. The most informative application of this method is found in a second-order system, because the curve of maximum  $A$  represents an approximation to the complete two-dimensional stability boundary.

A beautiful example of this method is the application to the second-order system, eq. (7-150), representing a reactor with one feedback region plus a power coefficient (Shotkin 1969a). Stability boundaries for the first two approximations are shown in fig. 7-31. The case labeled  $O(A^2)$  is for  $u_3(\theta) = 0$ . Comparison is made with the Liapunov stability bound shown in fig. 7-29 and with a computer-determined stability bound (note the logarithmic scale for  $n$ ). The analytic approximations are rather conservative, especially in view of the observation that the computer shows stability well beyond  $T = 1,000$  for  $n < 100$  (Shotkin 1969a). As mentioned in sec. 7-6, other methods of estimating bounds for this example are discussed by Devooght and Smets (1967), Hsu and Sha (1969), and Kalinowski and Bailey (1968).

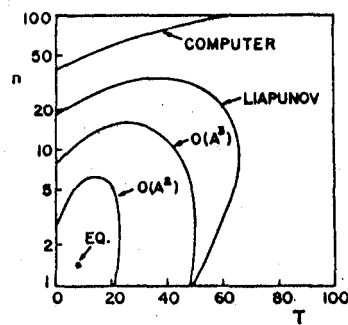


Fig. 7-31. Stability bounds for the effective-lifetime model with one feedback region plus a power coefficient (Shotkin 1969a).

Although the computational labor may become great for a high-order system, the present method has some important advantages. It is closely related to the associated linear system, it may be used with either linear or nonlinear feedback, and it is free from any worries about Laplace-transformability or the possibility of a finite escape time. Further, the nonlinear transformation may be regarded as the equation of a particular solution trajectory in the sense that eq. (7-177) is valid along the curve given by eq. (7-176). This suggests that the method may also be used for estimating the behavior near an unstable critical point (Shotkin 1969a). For example, this method will select the separatrix trajectory that emerges from a saddle point and will permit an estimate of its behavior as it comes under the influence of the nonlinear effects.

### 7-8. Frequency-Domain Stability Criteria

A sufficient criterion for asymptotic stability of a nuclear reactor system with arbitrary linear feedback was derived by Welton (1955a, 1955b). This section is primarily devoted to a new derivation of Welton's criterion that is due to Akcasu.<sup>7</sup> A heuristic derivation of Welton's criterion published by Smets (1959b, 1962) is also described. Several variations and attempts to find useful generalizations are also mentioned.

We use the function  $V$  defined by eq. (7-161). Its time derivative, when the point-reactor equations are used, is given by eq. (7-162). Using  $\rho = -\rho_f$  in eq. (7-163), we may write the criterion for boundedness as

$$I = \int_{-\infty}^t \rho_f(t') [n(t') - n_0] dt' \geq 0. \quad (7-181)$$

Then for  $t \rightarrow \infty$ , as described in the last section,  $V \rightarrow V_0 \geq 0$  and  $dV/dt \rightarrow 0$ .

We do not attempt to use the Liapunov theorem, which would restrict the form of the feedback kernel and would be difficult to apply in view of the integral that appears in eq. (7-161). Instead, we note from eq. (7-162) that  $dV/dt \rightarrow 0$  implies

$$\frac{\beta_i}{\ell} n - \lambda_i c_i \rightarrow 0. \quad (7-182)$$

From eq. (7-160), this implies  $dc_i/dt \rightarrow 0$ . Also, if  $n$  and  $c_i$  are uniformly continuous, eq. (7-182) implies

$$\frac{\beta_i}{\ell} \frac{dn}{dt} - \lambda_i \frac{dc_i}{dt} \rightarrow 0. \quad (7-183)$$

From  $dc_i/dt \rightarrow 0$ , we have  $dn/dt \rightarrow 0$ . Next, from eq. (7-160),

$$\frac{dn}{dt} + \sum_i \frac{dc_i}{dt} = \frac{\rho}{\ell} n.$$

Since the derivatives vanish, we have  $\rho n \rightarrow 0$ , and, because  $n \rightarrow 0$  is not compatible with a finite  $V$ , we have  $\rho \rightarrow 0$  and  $n \rightarrow \text{constant}$ . If this constant is the equilibrium value  $n_0$ , the system is asymptotically stable. Therefore, we conclude that the system is asymptotically stable in the large if eq. (7-181) is satisfied ( $I \geq 0$ ) and if the feedback is such that  $\rho = -\rho_f \rightarrow 0$  implies  $n \rightarrow n_0$ .

7. This derivation (Akcasu, Lellouche, and Shotkin, forthcoming) is a refinement of an earlier treatment by Akcasu and Dales (1960).

This procedure fails if there are no delayed neutrons, because  $dV/dt$  would be identically zero along the trajectories. One could conclude boundedness but not asymptotic stability. As a consequence, a reactor undergoing a periodic oscillation without delayed neutrons will become asymptotically stable when delayed neutrons are added, provided eq. (7-181) is satisfied ( $I \geq 0$ ).

The remaining steps in the proof of Welton's criterion are based on a linear feedback, eq. (5-70) or (7-164):

$$\rho_f(t) = \int_{-\infty}^t h(t-u)[n(u) - n_0] du.$$

From eq. (7-181),

$$I = \int_{-\infty}^t \left[ \int_{-\infty}^{t'} h(t'-u)x(u) du \right] x(t') dt',$$

where  $x = n - n_0$ . It will be convenient to use  $t$  for the upper limit of the inner integral. This may be done because  $h(t'-u) = 0$  for  $t' - u < 0$ , as discussed in sec. 5-4; there is, therefore, no contribution from the inner integral in the range  $t' < u < t$ . Hence

$$I = \int_{-\infty}^t \left[ \int_{-\infty}^t h(t'-u)x(u) du \right] x(t') dt'. \quad (7-184)$$

Next, we need a frequency-domain representation for  $h(t)$ . The Laplace transform is

$$H(s) = \int_0^\infty h(t)e^{-st} dt.$$

Since  $h(t) = 0$  for  $t < 0$ , we may write

$$H(s) = \int_{-\infty}^\infty h(t)e^{-st} dt$$

or

$$H(j\omega) = \int_{-\infty}^\infty h(t)e^{-j\omega t} dt.$$

The inverse Fourier transform is

$$h(t) = \frac{1}{2\pi} \int_{-\infty}^\infty H(j\omega)e^{j\omega t} d\omega. \quad (7-185)$$

This is the desired representation, and eq. (7-184) becomes

$$I = \int_{-\infty}^t \left\{ \int_{-\infty}^t \left[ \frac{1}{2\pi} \int_{-\infty}^\infty H(j\omega)e^{j\omega(t'-u)} d\omega \right] x(u) du \right\} x(t') dt'.$$

Rearranging, we have

$$I = \frac{1}{2\pi} \int_{-\infty}^{\infty} H(j\omega) \left[ \int_{-\infty}^t x(t') e^{j\omega t'} dt' \right] \left[ \int_{-\infty}^t x(u) e^{-j\omega u} du \right] d\omega,$$

which may be written

$$I = \frac{1}{2\pi} \int_{-\infty}^{\infty} H(j\omega) |f(j\omega)|^2 d\omega, \quad (7-186)$$

where

$$f(j\omega) = \int_{-\infty}^t x(t') e^{j\omega t'} dt'.$$

Eq. (7-186) is

$$I = \frac{1}{2\pi} \int_0^{\infty} [H(j\omega) + H(-j\omega)] |f(j\omega)|^2 d\omega.$$

As in sec. 2-6, we assume that the linear feedback is characterized by

$$H(-j\omega) = H^*(j\omega),$$

and therefore

$$I = \frac{1}{\pi} \int_0^{\infty} \operatorname{Re} H(j\omega) |f(j\omega)|^2 d\omega. \quad (7-187)$$

By eq. (7-187), we have  $I \geq 0$  provided  $\operatorname{Re} H(j\omega) \geq 0$  for all  $\omega$ . By eq. (7-181), a sufficient condition for boundedness is

$$\operatorname{Re} H(j\omega) \geq 0 \quad (7-188)$$

for all  $\omega$ .

Finally, to establish asymptotic stability, it is necessary to show that  $n \rightarrow n_0$  as  $\rho \rightarrow 0$ . In other words, we need to be able to deduce that  $x \rightarrow 0$  as  $t \rightarrow \infty$  whenever

$$\lim_{t \rightarrow \infty} \int_{-\infty}^t h(t-u)x(u) du = 0. \quad (7-189)$$

This is accomplished by invoking Pitt's form of Wiener's theorem (Widder 1946): If  $h(t)$  is absolute-integrable in  $-\infty < t < \infty$ , if  $x(t)$  is bounded, if  $dx/dt$  is greater than some negative constant, if  $H(j\omega) \neq 0$ , and if

$$\lim_{t \rightarrow \infty} \int_{-\infty}^t h(t-u)x(u) du = A \int_{-\infty}^{\infty} h(u) du, \quad (7-190)$$

then

$$\lim_{t \rightarrow \infty} x(t) = A. \quad (7-191)$$

The first three conditions are satisfied for bounded, physically realistic systems. We apply the theorem with  $A = 0$  and with  $h(t) = 0$  for  $t < 0$ , so that eq. (7-190) reduces to eq. (7-189). Therefore, the sufficient condition for asymptotic stability in the large becomes

$$\operatorname{Re} H(j\omega) > 0 \quad (7-192)$$

for all  $\omega$ . This is known as Welton's criterion, originally deduced by Welton (1955a, 1955b) using a mechanical analogy.

Conditions under which eq. (7-188) may also imply asymptotic stability (i.e., Welton's criterion with the equality sign included) are discussed by Akcasu, Lellouche, and Shotkin (forthcoming). We will not go into this question here, except for the following observation: We cannot conclude stability if  $\operatorname{Re} H(j\omega)$  changes sign. It is frequently true (and it is easily demonstrated for the two-region reactor system) that  $\operatorname{Re} H(j\omega)$  is an even function of  $\omega$  that could vanish at  $\omega = 0$ , and that  $\operatorname{Im} H(j\omega)$  is an odd function that does vanish at  $\omega = 0$ . But this would correspond to  $H(0) = 0$ , for which there is no unique equilibrium point and therefore no asymptotic stability. Hence we will take eq. (7-192) as the sufficient condition for asymptotic stability (Welton's criterion without the equality sign).

Another viewpoint was used by Smets (1959b, 1962). Consider the function

$$V_1 = n - n_0 - n_0 \log \frac{n}{n_0} + \sum_i \left( c_i - c_{i0} - c_{i0} \log \frac{c_i}{c_{i0}} \right). \quad (7-193)$$

From eq. (7-160),

$$\frac{dV_1}{dt} = \frac{\rho}{\ell} (n - n_0) - \sum_i \frac{n_0}{\lambda_i n c_i} \left( \frac{\beta_i}{\ell} n - \lambda_i c_i \right)^2. \quad (7-194)$$

Using eq. (7-164) and letting  $x = n - n_0$ , we integrate eq. (7-194) to find

$$\begin{aligned} V_1(\infty) - V_1(0) &= -\frac{1}{\ell} \int_0^\infty \int_0^\infty h(u) x(t-u) x(t) du dt \\ &\quad - \int_0^\infty \sum_i \frac{n_0}{\lambda_i n c_i} \left( \frac{\beta_i}{\ell} n - \lambda_i c_i \right)^2 dt. \end{aligned} \quad (7-195)$$

Consider the real part of the transfer function,

$$\operatorname{Re} H(j\omega) = \operatorname{Re} \int_0^\infty h(t)e^{-j\omega t} dt = \int_0^\infty h(t) \cos \omega t dt.$$

If this is nonnegative for all  $\omega$ , the integral in the first term on the right-hand side of eq. (7-195) is analogous to the energy dissipated by a passive network (positive or zero impedance). This energy is necessarily nonnegative. The integrand in the second term is positive for  $n > 0$ ,  $c_i > 0$ , unless  $dc_i/dt = 0$  for all  $t$ , in which case the integral is zero. Therefore,  $V_1(0) \geq V_1(\infty) \geq 0$ , which establishes boundedness.

However, the integrals in eq. (7-195) do not exist unless  $x \rightarrow 0$ ,  $n \rightarrow n_0$ , and  $c_i \rightarrow c_{i0}$ . The stability must therefore be asymptotic. The case  $H(0) = 0$  must be ruled out because there is no unique equilibrium point. Therefore, we may say that asymptotic stability is assured provided the linear feedback system behaves like a passive network for which  $\operatorname{Re} H(j\omega) \geq 0$  for all  $\omega \neq 0$  and provided  $H(0) > 0$ . For most applications, this is equivalent to Welton's criterion as expressed by eq. (7-192).

Welton's criterion contains feedback parameters only, and is therefore unaffected by the presence or absence of delayed neutrons. As an elementary example, consider one region with Newton cooling. From eqs. (7-36) and (7-44) we find

$$H(s) = \frac{\alpha K_0}{s + \gamma} \quad (7-196)$$

and

$$H(j\omega) = \alpha K_0 \frac{\gamma - j\omega}{\omega^2 + \gamma^2}.$$

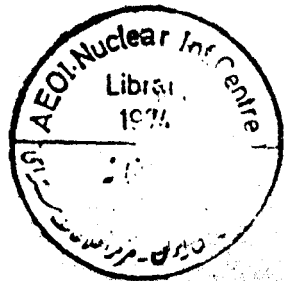
Since the only parameter that can change sign is  $\alpha$ , Welton's criterion is satisfied if  $\alpha > 0$ . This is the same condition for asymptotic stability found for the effective-lifetime model and for one group of delayed neutrons in sec. 7-6.

For the two-region reactor, use eq. (7-165) to find

$$\operatorname{Re} H(j\omega) = \frac{\gamma_1 \gamma_2 (A_1 \gamma_2 + A_2 \gamma_1) + (A_1 \gamma_1 + A_2 \gamma_2) \omega^2}{(\omega^2 + \gamma_1^2)(\omega^2 + \gamma_2^2)}. \quad (7-197)$$

By Welton's criterion,

$$\begin{aligned} A_1 \gamma_2 + A_2 \gamma_1 &> 0, \\ A_1 \gamma_1 + A_2 \gamma_2 &> 0. \end{aligned}$$



The former is the requirement on the static power coefficient,  $H(0) > 0$ , discussed in chapter 6; see for example eq. (6-128) or eq. (6-134). The latter is the necessary requirement for unconditional linear stability in the effective-lifetime model (no delayed neutrons); see eq. (6-130) or eq. (6-136). Welton's criterion for the two-region reactor, with or without delayed neutrons, is thus identical to the necessary and sufficient conditions for linear stability at all equilibrium power levels in the absence of delayed neutrons. These are also the conditions for asymptotic stability in the large with one group of delayed neutrons, as found in sec. 7-6 by constructing a Liapunov function using the variable-gradient method; see eqs. (7-147) and (7-148). The region is shown in fig. 7-30. For this particular feedback model, all we have gained from Welton's criterion is the extension from one group of delayed neutrons to several groups. The region in parameter space for asymptotic stability in the large is not changed. Other simple examples are discussed in the problem set.

Welton's criterion represented a major advance in the understanding of nonlinear reactor stability. A stability criterion of Popov (1961) represented a major advance in nonlinear control theory. Since, unfortunately, the reactor model with delayed neutrons cannot be put into Popov's standard form, the criterion is not proved for systems with delayed neutrons. The criterion is mentioned here because it is often cited in the literature on reactor stability, but not always with a proper statement of its limitations.

The system studied by Popov is

$$\begin{aligned} \frac{dx_i}{dt} &= \sum_j a_{ij}x_j + b_i f(\sigma), \\ \frac{d\xi}{dt} &= f(\sigma), \\ \sigma &= \sum_j c_j x_j - \gamma \xi. \end{aligned} \tag{7-198}$$

As in eq. (7-100),  $f(\sigma)$  is the characteristic function describing the nonlinearity. Eqs. (7-100) and (7-198) are related by a simple linear transformation (Lefschetz 1965), and either system can represent a nuclear reactor by means of the transformation  $\sigma = \log(n/n_0)$  provided the delayed neutrons are ignored.

The criterion may be stated as follows: A sufficient condition for the asymptotic stability in the large of the system represented by eq. (7-198) is that for all real  $\omega$  there exists a number  $q \geq 0$  such that

$$\operatorname{Re}[(1 + j\omega q)K(j\omega)] \geq 0, \tag{7-199}$$

where  $K(s)$  is the transfer function for the linear part (transfer function around the closed loop from the output  $f$  to the input  $\sigma$  of the nonlinearity). It can be shown that  $K(s)$  is essentially  $G(s)H(s)$  for the linearized reactor system. Delayed neutrons not being admissible, we replace  $K(s)$  by  $H(s)/s$  and obtain Popov's first criterion for reactor stability: A reactor with linear feedback and no delayed neutrons is asymptotically stable in the large if for all real  $\omega$  there exists a number  $p > 0$  ( $p = 1/q$ ) such that

$$\operatorname{Re} H(j\omega) + \frac{p}{\omega} \operatorname{Im} H(j\omega) \geq 0. \quad (7-200)$$

It is left as an exercise to show that eq. (7-200) is more restrictive than Welton's criterion for the simple two-region reactor model. Other applications are discussed in the paper by Lellouche (1967b). The relationship to Liapunov functions is discussed by Kalman (1963) and by Lefschetz (1965). A Liapunov function for the two-temperature model without delayed neutrons was constructed using Kalman's procedure by Pai, Sastry, and Mohan (1970). A direct derivation of eq. (7-200) from an integral equation of reactor dynamics is given by Akcasu, Lellouche, and Shotkin (forthcoming).

The first frequency-domain stability criterion for nuclear reactors to contain delayed neutron effects not only in the derivation but also in the statement of the criterion appears to be due to Popov (1963); we shall call this Popov's second criterion for reactor stability. The proof, which is difficult, is reproduced by Akcasu, Lellouche, and Shotkin (forthcoming). The sufficient criterion for asymptotic stability is

$$|G_1(j\omega)|^2 \operatorname{Re} H(j\omega) + r \left[ \operatorname{Re} G_2(j\omega) + \frac{1}{h_2 - h_1} \right] > 0 \quad (7-201)$$

for all  $\omega$ , where  $r \geq 0$  with

$$G_1(s) = \frac{G(s)}{1 + h_1 G(s)H(s)} \quad (7-202)$$

and

$$G_2(s) = G_1(s)H(s) \quad (7-203)$$

and where  $h_1 < 1$  and  $h_2 > 1$  are nonnegative parameters describing a range of equilibrium power levels for which the associated linear system is stable. Specifically,  $h = n'_0/n_0$ , where  $n_0$  is the equilibrium power and  $n'_0$  is another equilibrium power for the same system. Clearly,  $h_2$  must not exceed  $n_c/n_0$ , where  $n_c$  is the critical power at

#### 4.2.2 Nonlinear System Stability

which the linear system ceases to be stable (if such exists). Note that  $r = 0$  corresponds to Welton's criterion.

This criterion shows much promise because of the possibility of investigating conditionally stable systems. Further, the proof of the criterion contains the possibility of estimating bounds for permissible perturbations in systems that are not asymptotically stable in the large. Unfortunately, the criterion is difficult to apply except in simple special cases.

When  $r \rightarrow \infty$ ,  $h_1 \rightarrow 0$ , and  $h_2 \rightarrow \infty$ , eq. (7-201) becomes

$$\operatorname{Re}[G(j\omega)H(j\omega)] > 0 \quad (7-204)$$

for all  $\omega$ , which corresponds to the sufficient criterion derived by Baran and Meyer (1966). This criterion is rather restrictive, at least for simple systems, as can be seen by inspecting a few Nyquist plots (e.g., figs. 6-38 and 6-39).

A frequency-domain stability criterion that is similar to Popov's second criterion, eq. (7-201), was reported by Gyftopoulos (1966). For commentaries, see Kalinowski (1968) and Di Pasquantonio and Kappel (1970).<sup>8</sup>

Some general words of caution regarding frequency-domain stability criteria are in order. The derivations of such criteria generally depend upon the assumption that all solutions are of exponential order. In the case of Welton's criterion, there is no difficulty because all systems that satisfy the criterion are guaranteed to have bounded solutions only. However, eq. (7-201) must be qualified by excluding cases that can exhibit such phenomena as finite escape time. This is unfortunate, because many of the interesting cases that exhibit conditional linear stability are also the cases that satisfy the necessary condition for the existence of finite escape time. This condition, derived by Akcasu and Noble (1966a) and expressed by our eq. (7-169), applies to all the nonminimum-phase conditionally stable systems that we studied in secs. 6-7 and 6-8. When delayed neutrons are included in the two-region model, almost all cases of conditional stability are of this type (see figs. 6-56, 6-60, and 6-63). It appears that further progress must await the discovery of useful sufficient conditions for the non-existence of finite escape time.

Another limitation is that many frequency-domain stability criteria (Welton's criterion excepted) are derived for systems of ordinary differential equations in time. This excludes the possibility of transport delay times, which cannot be accommodated in such models.

8. Since this section was written, a new frequency-domain stability criterion has been published (Smets 1970). This new criterion appears to establish asymptotic stability in the large for certain minimum-phase conditionally stable systems at low equilibrium power.

### 7-9. Nonlinear Oscillations

The limit cycles that have been mentioned throughout this chapter are periodic solutions of the system equations, and it is natural to think of Fourier series representations. This turns out to be a useful idea, not only in the study of limit cycles (autonomous oscillations), but also in the search for nonlinear corrections to the transfer function (the response to forced oscillations).

The relevance of limit cycles to nonlinear stability is illustrated by figs. 7-21 and 7-22. A stable limit cycle may exist in a system that is linearly unstable. A small perturbation produces a disturbance that grows until the nonlinearity becomes appreciable. All solution trajectories approach a closed orbit, and one may speak of "orbital asymptotic stability." This is a common phenomenon in systems that are linearly unstable but are stable in the sense of Lagrange (all solutions bounded).

On the other hand, a linearly stable system may be unstable for large perturbations, and an unstable limit cycle is a dramatic example. One is therefore encouraged to seek analytical criteria for the existence of autonomous periodic solutions in a nonlinear system. When such a solution is found, one suspects the possibility of a stable limit cycle if the associated linear system is unstable, or an unstable limit cycle if the linear system is stable. This does not tell the complete story, because there are such things as concentric nests of limit cycles (e.g., a stable limit cycle inside an unstable limit cycle). There is also the possibility of a semistable limit cycle (e.g., a stable point enclosed by a limit cycle such that all solutions, both inside and outside, decay with time). These possibilities are discussed by Akcasu and Shotkin (1967), but these phenomena have not been observed in reactor systems with linear feedback and no transport delay effects.

A brief introduction to large-amplitude forced oscillations appears at the end of sec. 3-2. Alternatively, one may use the concept of a modified transfer function, commonly called a "describing function," that contains amplitude-dependent nonlinear correction terms. We include it here because it is so closely related to the Fourier representation of a limit cycle. Essentially the same equations are used in the derivations, the limit-cycle equations arising from a special case, and the only real difference is a shift in viewpoint.

An early application of Fourier series in reactor dynamics was made by Rumsey (1947), who obtained a first-order correction to a transfer function by solving for Fourier coefficients of the neutron density in terms of the coefficients of a periodic reactivity input. Essentially the same approach was used by Nelkin (1955). Both authors recognized

#### 4.14      *Nonlinear System Stability*

that a negative reactivity bias is necessary to maintain a steady oscillation, but neither recognized the need to distinguish between the equilibrium power level and the time-average power. The negative reactivity bias in a large oscillation was also investigated by Akcasu (1958), but without reactivity feedback.

A consistent set of equations for forced oscillations was obtained by Sandmeier (1959), with the power shift included. A review of the earlier work is included in the thesis by Wasserman (1962), who discussed the relationship to the usual describing-function technique. Another treatment appears in the thesis by Lauber (1962). A distinction between "direct" and "indirect" methods of deriving a describing function was made by Smets (1964, 1965). The latter paper suggested the application of Fourier series to autonomous oscillations, but only stable limit cycles were considered.

More recently, the nuclear-reactor describing function was examined by means of the WKB method (see sec. 3-6) in the paper by Tan (1967). It was concluded that the earlier formulations are incomplete.

Torlin (1966), using an iterative scheme, derived a formula for the magnitude of the first harmonic of an autonomous reactivity oscillation, with one harmonic assumed in reactivity and two in power. He recognized the possibility of either stable or unstable limit cycles. Unfortunately, the particular model he selected for illustration was incorrectly analyzed in the paper. Torlin's contribution was to specify the procedure: obtain a formula for the magnitude of a Fourier component in terms of the frequency  $\omega$ , and then search for regions in parameter space that simultaneously correspond to real positive numbers for  $\omega^2$  and for the magnitude of the Fourier component.

Recent contributions to the theory of describing functions were made by Akcasu and Shotkin (1967, 1968). They succeeded in proving the nonexistence of unstable limit cycles for the case of linear feedback without delayed neutrons (the effective-lifetime model). A brief review of describing functions is given by Vaurio and Pulkki (1970).

Unstable limit cycles with linear feedback and delayed neutrons are now known to exist. An example is given by Hetrick and Schmidt (1968) in which a low-order approximation is used. Higher approximations, together with conclusive evidence from digital computer studies, are given by Schmidt (1969) and by Schmidt and Hetrick (1969, 1970). An analytical proof that delayed neutrons introduce the possibility of unstable limit cycles with linear feedback (contributed by L. M. Shotkin) is discussed in the papers by Shotkin, Hetrick, and Schmidt (1969, 1970).

We proceed to derive an expression for the describing function that contains in a consistent manner the first two harmonics and the shifts

in reactivity and power levels. Then, building on the same foundation, we derive the magnitudes of the first-harmonic components in reactivity and power for autonomous oscillations, and we illustrate their use in searching for limit cycles. By starting with the integro-differential equation of sec. 4-3, we bypass the iterative scheme used by Schmidt and by Torlin and obtain directly the complete result for the case of two harmonics in reactivity and power.

The starting point is eq. (4-31) with  $q = 0$ :

$$\frac{\ell}{\beta} \frac{dn}{dt} = \frac{\rho}{\beta} n(t) + \int_0^\infty [n(t-u) - n(t)] D(u) du, \quad (7-205)$$

where  $D$  is the delayed-neutron kernel (emission probability) of eq. (4-27) and fig. 4-2:

$$D(t) = \frac{1}{\beta} \sum_i \beta_i \lambda_i e^{-\lambda_i t}, \quad (7-206)$$

$$\int_0^\infty D(u) du = 1. \quad (7-207)$$

Eq. (7-205) may be written

$$\frac{\ell}{\beta} \frac{dn}{dt} = \frac{\rho}{\beta} n(t) - n(t) + \int_0^\infty n(t-u) D(u) du. \quad (7-208)$$

We let

$$\frac{\rho}{\beta} = 2b_1 \cos \omega t + \sum_{-\infty}^{\infty} a_k e^{jk\omega t} \quad (7-209)$$

and

$$\frac{n}{n_0} = 1 + \sum_{-\infty}^{\infty} A_m e^{jm\omega t}, \quad (7-210)$$

where  $a_{-k} = a_k^*$ ,  $A_{-m} = A_m^*$ , and where we include  $k = 0$  and  $m = 0$ . For a forced oscillation,  $b_1$  and  $\omega$  are given parameters, and we note

$$2b_1 \cos \omega t = b_{-1} e^{-j\omega t} + b_1 e^{j\omega t}, \quad (b_{-1} = b_1),$$

where  $b_1$  is real. For autonomous oscillations, we set  $b_1 = 0$  and regard  $\omega$  as undetermined.

We substitute eqs. (7-209) and (7-210) into eq. (7-208), noting that

$$\int_0^\infty n(t-u) D(u) du = n_0 + n_0 \sum_m A_m \bar{D}(jm\omega) e^{jm\omega t},$$

### 3.26 Nonlinear System Stability

where  $\bar{D}(s)$  is the Laplace transform of  $D(t)$  and where we abbreviate the infinite summation by using a simple subscript. Equating coefficients of terms in like harmonics, and noting that the double sum

$$\sum_r \sum_s a_r A_s e^{j(r+s)\omega t}$$

contributes in the  $m$ th harmonic only if  $r + s = m$ , we find

$$[1 - \bar{D}(jm\omega) + jm\omega\ell/\beta]A_m = a_m + \sum_k a_k A_{m-k} \quad (7-211)$$

when  $b_1 = 0$ ; if  $b_1 \neq 0$  we replace  $a_{-1}$  by  $a_{-1} + b_{-1}$  and  $a_1$  by  $a_1 + b_1$ . We define

$$Z_m = Z(jm\omega) = 1 - \bar{D}(jm\omega) + jm\omega\ell/\beta \quad (7-212)$$

and identify the low-power reactor transfer function from eq. (3-56),

$$G(jm\omega) = \frac{n_0}{\beta} Z^{-1}(jm\omega). \quad (7-213)$$

We are now in a position to apply eq. (7-211), dropping third and higher harmonics. For  $m = 0$ , noting that  $Z(0) = 0$ , we find

$$0 = a_0 + 2 \operatorname{Re} a_1 A_1^* + 2b_1 \operatorname{Re} A_1 + a_0 A_0 + 2 \operatorname{Re} a_2 A_2^*. \quad (7-214)$$

For  $m = 1$ ,

$$A_1 Z_1 = a_1 + b_1 + a_1^* A_2 + a_0 A_1 + a_1 A_0 + a_2 A_1^* + b_1 (A_0 + A_2). \quad (7-215)$$

For  $m = 2$ ,

$$A_2 Z_2 = a_2 + a_1 A_1 + b_1 A_1 + a_0 A_2 + a_2 A_0. \quad (7-216)$$

All first and second harmonics are accounted for. The next step is to identify the likely orders of magnitude of the various terms.

We assume that  $a_1$ ,  $b_1$ , and  $A_1$  are of the same order of magnitude. We further assume that  $a_0$ ,  $A_0$ ,  $a_2$  and  $A_2$  are all of order  $a_1^2$ . A further breakdown than this appears to lead to inconsistencies. We therefore have the consistent approximations

$$0 = a_0 + 2 \operatorname{Re} a_1 A_1^* + 2b_1 \operatorname{Re} A_1, \quad (7-217)$$

correct to order  $a_1^2$ ,

$$A_1 Z_1 = a_1 + b_1, \quad (7-218)$$

correct to order  $a_1$ , and

$$A_2 Z_2 = a_2 + a_1 A_1 + b_1 A_1, \quad (7-219)$$

correct to order  $a_1^2$ . To proceed, we use eqs. (7-217) through (7-219) to derive approximate expressions for the higher-order terms in the fundamental formula eq. (7-215).

The first important result appears upon substitution of eqs. (7-218) and (7-219) in eq. (7-217):

$$a_0 = -2|A_1|^2 \operatorname{Re} Z_1, \quad (7-220)$$

correct to order  $a_1^2$ . But the low-power transfer function has a real part only if delayed neutrons are included. Therefore, the negative reactivity shift is absent unless delayed neutrons are included.

Next, we note that the higher-order terms in eq. (7-215) may be approximated in such a way that  $a_0$ ,  $A_1$ , and  $A_2$  do not appear on the right-hand side. The approximate relations are

$$a_0 = -2[|a_1|^2 + b_1(b_1 + 2 \operatorname{Re} a_1)] \operatorname{Re} Z_1^{-1}, \quad (7-221)$$

$$A_1 = (a_1 + b_1)Z_1^{-1}, \quad (7-222)$$

and

$$A_2 = [a_2 + (a_1 + b_1)^2 Z_1^{-1}] Z_2^{-1}. \quad (7-223)$$

Eq. (7-215) may be written as

$$\begin{aligned} A_1 Z_1 = & \\ & (a_1 + b_1)\{1 + A_0 - [2|a_1|^2 + 2b_1(b_1 + 2 \operatorname{Re} a_1)]Z_1^{-1} \operatorname{Re} Z_1^{-1}\} \\ & + (a_1^* + b_1)[(a_1 + b_1)^2 Z_1^{-1} Z_2^{-1} + a_2(Z_{-1}^{-1} + Z_2^{-1})]. \end{aligned} \quad (7-224)$$

This is the complete equation with all first and second harmonics properly included.

The goal is to express the right-hand side of eq. (7-224) in terms of  $b_1$  and the transfer functions. This requires the elimination of  $a_1$ ,  $a_2$ , and  $A_0$ . The feedback is expressed by

$$a_m = -K_m A_m, \quad (7-225)$$

where  $K_m = K(jm\omega) = (n_0/\beta)H(jm\omega)$ . The three relations we need are

$$a_0 = -K_0 A_0, \quad a_1 = -K_1 A_1, \quad a_2 = -K_2 A_2, \quad (7-226)$$

where  $K_0 = (n_0/\beta)H(0)$ . It turns out to be simpler to return to eq. (7-215) and, with the aid of eqs. (7-217) through (7-219) for approximating the higher-order terms, to introduce the feedback at that point.

Some of the intermediate steps yield

$$A_0 = 2|A_1|^2 K_0^{-1} \operatorname{Re} Z_1, \quad (7-227)$$

$$A_1 = \frac{b_1}{Z_1 + K_1}, \quad (7-228)$$

and

$$A_2 = \frac{b_1 - A_1 K_1}{Z_2 + K_2} A_1, \quad (7-229)$$

all of which are used only in approximating higher-order terms. Note that the shift in time-average power disappears in the absence of delayed neutrons, according to eq. (7-227). Note also that eq. (7-228) represents the linear approximation (the closed-loop transfer function) because

$$\frac{A_1}{b_1} = \frac{1}{Z_1 + K_1} = \frac{Z_1^{-1}}{1 + Z_1^{-1} K_1}. \quad (7-230)$$

Eq. (7-215) yields

$$A_1 Z_1 = (b_1 - A_1 K_1) Q, \quad (7-231)$$

where

$$Q = 1 + \frac{b_1^2}{|Z_1 + K_1|^2} \left[ 2(K_0^{-1} - Z_1^{-1}) \operatorname{Re} Z_1 + \frac{Z_1^{-1} - K_2}{Z_2 + K_2} \right]. \quad (7-232)$$

This expresses the reactor describing function.<sup>9</sup>

According to eq. (7-228), the linear approximation is

$$A_1 Z_1 = b_1 - A_1 K_1, \quad (7-233)$$

which corresponds to the describing function for small  $b_1$ . Since from eq. (7-231) we find

$$\frac{A_1}{b_1} = \frac{Z_1^{-1} Q}{1 + Z_1^{-1} Q K_1}, \quad (7-234)$$

the first-order describing function may be represented as in the block diagram of fig. 7-32.

Combining eqs. (7-220) and (7-228) yields

$$d_0 = -\frac{2b_1^2 \operatorname{Re} Z_1}{|Z_1 + K_1|^2}, \quad (7-235)$$

9. A possible source of confusion is that, in conventional describing-function analysis, one assumes that the second harmonic is negligible when it returns through the feedback loop. This assumption appears to be inadequate for reactor systems.

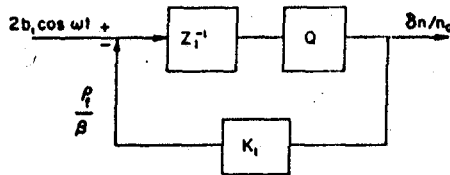


Fig. 7-32. Block diagram for the describing-function representation (the linear system corresponds to  $Q = 1$ ).

which is to be identified as the negative steady-state reactivity component that must be supplied externally. With the effective-lifetime model this component is zero. In the absence of feedback, eq. (7-235) becomes

$$a_0 = -2b_1^2 \operatorname{Re} Z_1 / |Z_1|^2. \quad (7-236)$$

In the prompt-jump approximation, this becomes

$$a_0 = -2b_1^2, \quad (7-237)$$

which corresponds to eq. (3-69) with  $A = a_0$  and  $B = 2b_1$ . Using eq. (7-236) with delayed neutrons and  $\ell \neq 0$ , we may easily show that eq. (7-237) remains valid for  $\omega \ll \beta/\ell$ .

This describing function is clearly limited to small amplitudes and two harmonics. Since it can be shown that a third harmonic makes no contribution of order  $a_1^2$ , the amplitude limitation is dominant.

The describing function may be used to infer nonlinear corrections to linear stability by using a Nyquist plot. Interpreting eq. (7-234) as the modified closed-loop transfer function, we see that the threshold of instability corresponds to

$$Z_1^{-1}K_1 = -1/Q. \quad (7-238)$$

One replaces the  $-1$  point by a locus of  $-1/Q$  (different for each amplitude  $b_1$ ) and infers stability from its location relative to the locus of  $Z_1^{-1}K = GH$ .

To study autonomous oscillations we set  $b_1 = 0$  in eq. (7-224):

$$\begin{aligned} A_1 Z_1 &= a_1 [1 + A_0 - 2|a_1|^2 Z_1^{-1} \operatorname{Re} Z_1^{-1} + |a_1|^2 Z_1^{-1} Z_2^{-1}] \\ &\quad + a_1 * a_2 (Z_{-1}^{-1} + Z_2^{-1}). \end{aligned} \quad (7-239)$$

Set  $b_1 = 0$  in eq. (7-221) and use eq. (7-226):

$$A_0 = 2|a_1|^2 K_0^{-1} \operatorname{Re} Z_1^{-1}. \quad (7-240)$$

Set  $b_1 = 0$  in eq. (7-223) and use eq. (7-226):

4.30      *Nonlinear System Stability*

$$a_2 = -\frac{Z_1^{-1}Z_2^{-1}}{Z_2^{-1} + K_2^{-1}} a_1^2. \quad (7-241)$$

Use eq. (7-226) to eliminate  $A_1$ . One obtains from eq. (7-239) an equation that may be solved for  $|a_1|^2$ , with the result

$$|a_1|^2 = \frac{1 + Z_1^{-1}K_1}{Z_1^{-1}K_1[2(Z_1^{-1} - K_0^{-1})\operatorname{Re} Z_1^{-1} - Z_1^{-1}Z_2^{-1}(1 - Z_{-1}^{-1}K_2)(1 + Z_2^{-1}K_2)^{-1}]} \quad (7-242)$$

An analogous procedure leads to

$$|A_1|^2 = \frac{1 + Z_1^{-1}K_1}{Z_1^{-1}K_1[-2(K_1^{-1} + K_0^{-1})\operatorname{Re} Z_1^{-1} + K_{-1}Z_2^{-1}(1 + K_{-1}^{-1}K_2)(1 + Z_2^{-1}K_2)^{-1}]} \quad (7-243)$$

Note that these amplitudes vanish when  $Z_1^{-1}K_1 = -1$ , which corresponds to  $GH = -1$  (resonance or critical power). We therefore expect these equations to be useful in the neighborhood of critical, where the amplitudes, if they exist, are small.

Next, we require that the right-hand sides of eqs. (7-242) and (7-243) be real and positive. A convenient procedure is first to demand real numbers. This leads to the vanishing of certain polynomials in  $\omega^2$ . One then rejects all roots  $\omega^2$  that are not real and positive. The remaining roots are then tested in the appropriate amplitude expression, eq. (7-242) or (7-243), and those that produce positive numbers for both squared magnitudes are accepted as corresponding to limit cycles.

The procedure generally leads to polynomials of high degree in  $\omega^2$  that must be solved numerically for each set of parameters (Schmidt 1969). One simple example, a two-region reactor with the effective-lifetime model, yields a quadratic in  $\omega^2$  if the terms in  $K_2$  are neglected in eqs. (7-242) and (7-243). This example, which is given by Schmidt, does predict stable limit cycles. However, the predicted range is too large, and the model is too simple to be conclusive. We include the calculation in the problem set because of its value as an illustration.

Another simple example, a two-region reactor with the one-delay-group prompt-jump approximation, appears in the paper by Hetrick and Schmidt (1968). This example is both incomplete and inconclusive because only eq. (7-242) is used and the terms in  $K_2$  are omitted.<sup>10</sup> One

10. This yields eq. (17) of the paper by Torlin (1966).

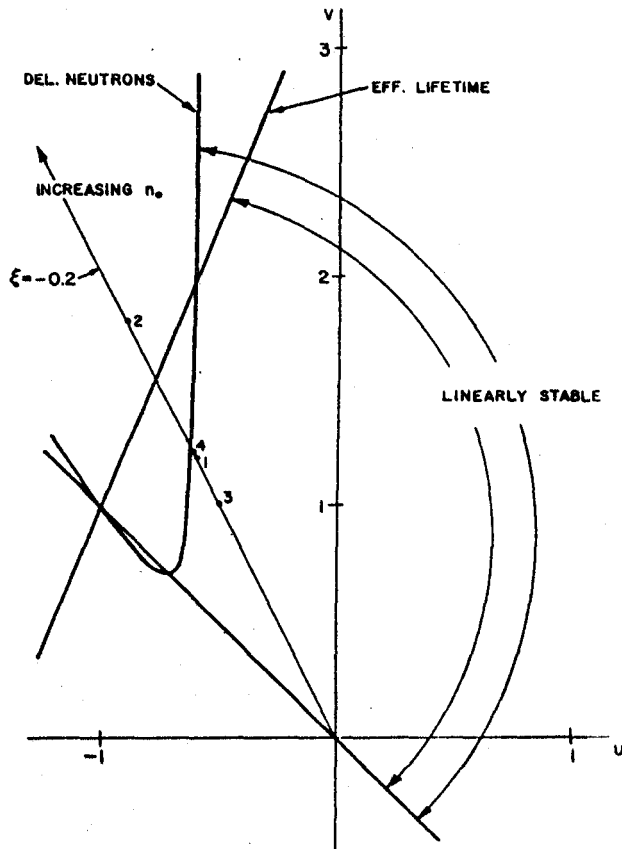


Fig. 7-33. Parameter space for a reactor with coupled two-path feedback, showing cases for nonlinear studies ( $\eta_1 = 0.5$ ,  $\eta_3 = 0.2$ ,  $\lambda = 0.1$ ).

finds a cubic equation in  $\omega^2$  whose coefficients can be examined analytically for sign changes in real roots, leading to one of the first tentative predictions of unstable limit cycles with delayed neutrons. These two examples are also cited in the review paper by Hetrick and Weaver (1968).

We have selected some examples that use eqs. (7-242) and (7-243), with all terms included, from the thesis by Schmidt (1969). Fig. 7-33 is a parameter space for a two-region coupled system, as given by eq. (6-156), and for which fig. 6-70 is a different example. Here the parameters are  $\eta_1 = 0.5$ ,  $\eta_2 = 0.25$ , and  $\eta_3 = 0.2$  ( $\text{sec}^{-1}$ ). Also,  $\lambda = 0.1 \text{ sec}^{-1}$ ,  $\beta = 0.01$ ,  $b = 100 \text{ C}^\circ/\text{mw} - \text{sec}$ ,  $\alpha_1 = -3.33 \times 10^{-7} \text{ per C}^\circ$ , and  $\alpha_2 = 5.33 \times 10^{-7} \text{ per C}^\circ$  (prompt-positive and delayed-negative

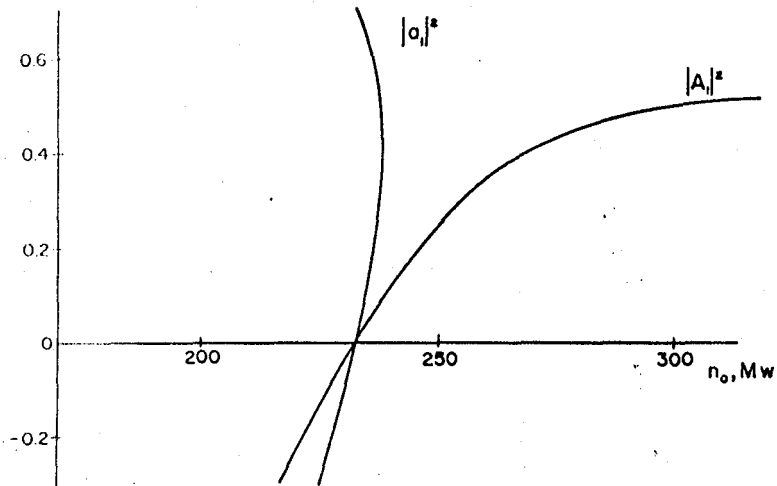


Fig. 7-34. Oscillation amplitudes vs. equilibrium power for the effective-lifetime model.

feedback). By eq. (6-159), this is a negative-gain, nonminimum-phase system with  $\xi = -0.2$ . Increasing the equilibrium power  $n_0$  corresponds to moving outward along the radial line of constant  $\xi$ .

Consider first the effective-lifetime model. Reactivity and power amplitudes, computed from eqs. (7-242) and (7-243), are plotted as functions of equilibrium power  $n_0$  in fig. 7-34. Both amplitudes, which vanish at critical power, are positive above critical and negative below. This suggests a stable limit cycle in the linearly unstable region.

This is confirmed by digital computer solutions shown in figs. 7-35 and 7-36 (labeled respectively cases 1 and 2 in the parameter space of fig. 7-33). The trajectories are projections on the  $n, T_1$  plane (power vs. temperature of the prompt region). Fig. 7-35 represents a linearly stable system. Note the separatrix from the shutdown point (a saddle point) to the operating point (a stable focus). Fig. 7-36 represents a linearly unstable system, and the separatrix from shutdown winds onto the stable limit cycle. Both figures show the possibility of unstable solutions for large perturbations.

Reactivity and power amplitudes for the one-group prompt-jump approximation are shown in fig. 7-37. Both amplitudes are positive below critical power, indicating an unstable limit cycle. Trajectories for case 3 of fig. 7-33 are shown in fig. 7-38. One can infer a separatrix between stable and unstable regions, but it does not appear to be a closed curve. Note also the trajectory from the shutdown point; it is clearly unstable (compare with figs. 7-35 and 7-36).

The unstable limit cycle appears as one approaches critical power

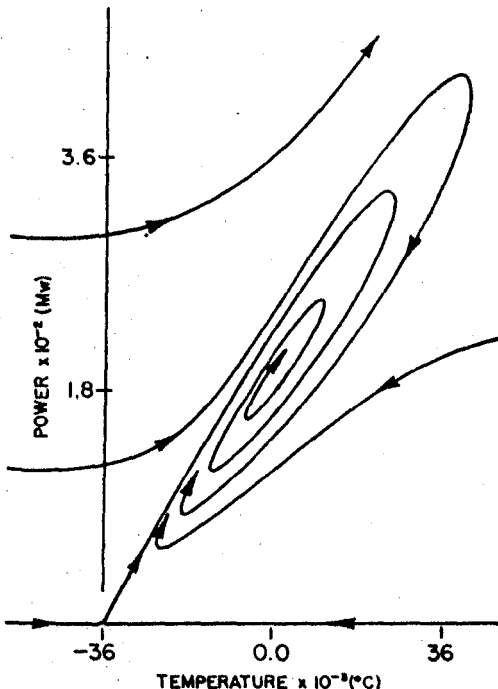


Fig. 7-35. Trajectories in the  $n, T_1$  plane for case 1 (linearly stable,  $n_0 = 180$  mw, effective-lifetime model). Temperature extremes are unrealistic because small reactivity coefficients were assumed.

from below. It is seen in fig. 7-39 (case 4 of fig. 7-33). One infers a separatrix between stable and unstable regions such that an unstable trajectory can wind around the outside of a closed curve an arbitrary number of times before diverging to infinity.

The first reactor example of this behaviour was discovered by Akcasu and Noble (1966a), and it is presented in their paper as an example of finite escape time in a linearly stable system. The example was not fully recognized as an unstable limit cycle until later.

As the power level is increased, the unstable limit cycle becomes smaller. It disappears at critical, in keeping with fig. 7-37, and there are no limit cycles above critical power in this particular system. In fact, when the two-region linear feedback is used, the only stable limit cycles observed with delayed neutrons are for cases such as those shown in figs. 6-56 and 6-68, where there are two critical power levels bracketing an unstable region in parameter space. This is predicted by the amplitude equations (Schmidt 1969).

The search for limit cycles quickly becomes tedious. Surveys of many

4.3.4 Nonlinear System Stability

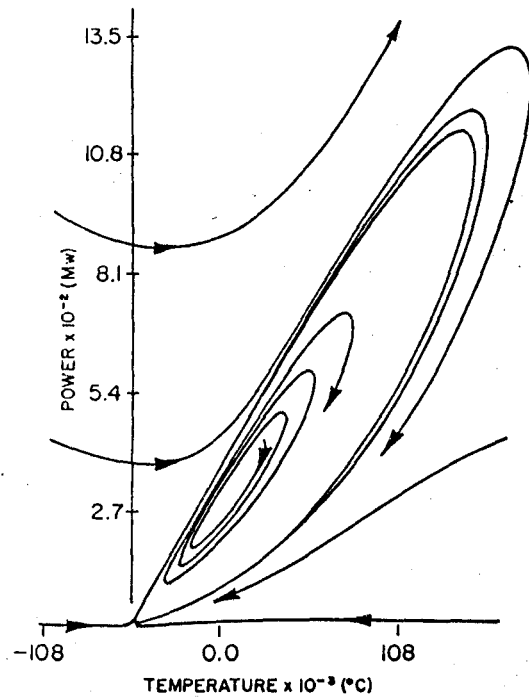


Fig. 7-36. Trajectories in the  $n, T_1$  plane for case 2, showing a stable limit cycle (linearly unstable,  $n_0 \approx 270$  mw, effective-lifetime model).

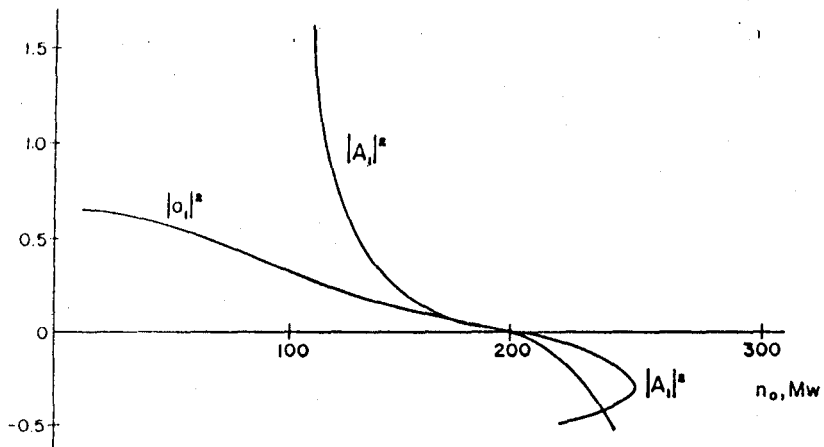


Fig. 7-37. Oscillation amplitudes vs. equilibrium power for the prompt-jump approximation.

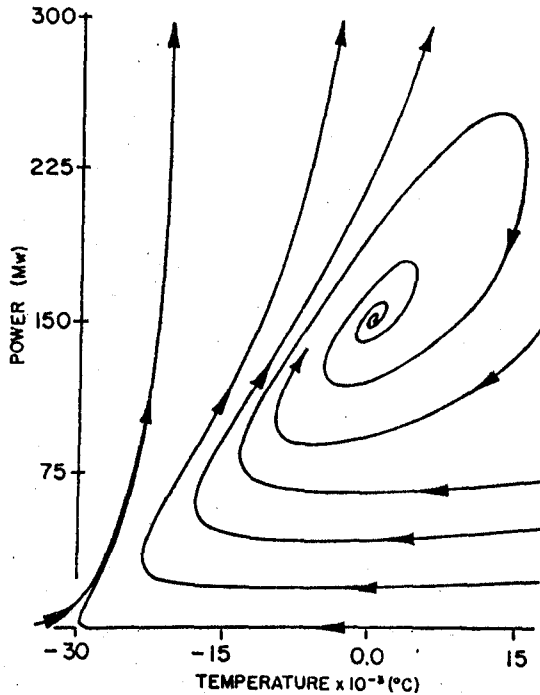


Fig. 7-38. Trajectories in the  $n, T_1$  plane for case 3 (linearly stable,  $n_0 = 150$  mw, prompt-jump approximation).

cases have led to the conclusion that eqs. (7-242) and (7-243) are reliable near critical, but that otherwise they tend to predict limit cycles over too broad a range. Fig. 7-38 is an example, in that the unstable limit cycle apparently opens out to infinity as the equilibrium power is reduced. Furthermore, cases apparently exist where the amplitude equations predict unstable limit cycles but where the range of their existence (just below critical power) seems to be extremely small. This does not preclude instability in linearly stable systems of this type; the behavior shown in fig. 7-38 is apparently quite common in non-minimum-phase systems.

It is interesting that eqs. (7-242) and (7-243) consistently predict a subharmonic oscillation that has not been observed. This is related to the fact that both amplitudes vanish when  $Z_2^{-1}K_2 = -1$ . This appears to be a nonphysical manifestation of the approximate analytical treatment.

Finally, we reiterate that the prompt-jump approximation is a useful representation for systems with delayed neutrons. Proper initial

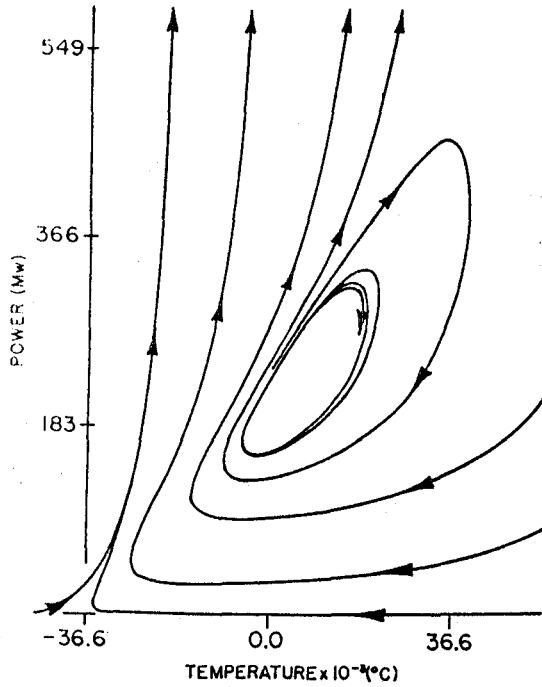


Fig. 7-39. Trajectories in the  $n, T_1$  plane for case 4, showing an unstable limit cycle (linearly stable,  $n_0 = 183$  mw, prompt-jump approximation).

conditions should be used to account for the fast-decaying transient that is neglected; see eq. (3-10). The main concern would be a possible approach to prompt critical, but this was ruled out for figs. 7-38 and 7-39 by monitoring the reactivity. However, one must be careful about deducing the presence of finite escape time when using this approximation; a rapidly growing solution may indicate only an approach to prompt critical, and a more complete model would be needed for studying the ultimate behavior.

This concludes our treatment of reactor stability. We turn now to space-dependent reactor dynamics. Some references to space-dependent effects on stability are given in the next chapter, but a study of these effects is beyond the scope of this book.

#### Problems

- 7-1. Find eigenvalues and eigenvectors for the matrix

$$\Lambda = \begin{bmatrix} -3 & 1 \\ 4 & 0 \end{bmatrix}$$

and show that

$$T = \begin{bmatrix} 1 & -1 \\ 4 & 1 \end{bmatrix}$$

is a diagonalizing transformation.

- 7-2. Find eigenvalues and eigenvectors for the matrix

$$A = \begin{bmatrix} 0 & 2 \\ -1 & -2 \end{bmatrix}$$

and show that

$$T = \begin{bmatrix} 1+j & 1-j \\ -1 & -1 \end{bmatrix}$$

is a diagonalizing transformation.

- 7-3. Derive the equation for the integral curves of eq. (7-21) and fig. 7-9.

- 7-4. Find eigenvalues and eigenvectors for the coefficient matrix obtained by linearizing eq. (7-26). Show that

$$T = \begin{bmatrix} 1 & 1 \\ j & -j \end{bmatrix}$$

is a diagonalizing transformation.

- 7-5. Show that the integral curves for eq. (7-26) are given by eq. (7-28).

- 7-6. Study the system

$$\frac{dx}{dt} = -x + xy,$$

$$\frac{dy}{dt} = -y + xy$$

in the  $x, y$  plane. Obtain an expression for the separatrix between stable and unstable regions.

- 7-7. Calculate the slopes with which the integral curves approach or leave the equilibrium points of eq. (7-34).

- 7-8. Study the system

$$\frac{dx}{dt} = -xy,$$

4.33 Nonlinear System Stability

$$\frac{dy}{dt} = x - xy$$

in the  $x, y$  plane.

- 7-9. Study the system

$$\frac{dx}{dt} = -xy,$$

$$\frac{dy}{dt} = x - 2y$$

by sketching trajectories in the  $x, y$  plane. (The equilibrium point is a half-node, half-saddle.)

- 7-10. Study the system

$$\frac{dx}{dt} = y - x$$

$$\frac{dy}{dt} = (a - x)y, \quad a \geq 0$$

in the  $x, y$  plane. Note the relationship to figs. 7-16 and 7-17 when  $a \neq 0$ . Sketch trajectories for the critical case  $a = 0$ , and identify the physical significance of this case. (For a rigorous treatment of stability in this type of critical system, see Di Pasquantonio 1968.)

- 7-11. Show that the effective-lifetime model with Newton cooling and  $\alpha < 0$  has a saddle point for  $n = n_0$  and a stable node for  $n = 0$ .

- 7-12. Given the reactor model

$$\frac{dn}{dt} = \frac{\rho}{\ell} n,$$

$$\rho = -\alpha T + \epsilon T^2,$$

$$\frac{dT}{dt} = K(n - n_0) - \gamma T,$$

find and classify the equilibrium points and discuss stability.

- 7-13. Study the modified system corresponding to eq. (7-51) when  $\rho$  is neglected in the left-hand side of eq. (7-50).

- 7-14. Find the eigenvalues for the linearized system corresponding to eqs. (7-54) and (7-55) and derive the condition for damped oscillations.

- 7-15. Verify the condition for oscillations as given by eq. (7-57).

- 7-16. Sketch a few of the spiral trajectories for eq. (7-67).
- 7-17. Show that the integral curves for eq. (7-69) are given by eq. (7-73). Sketch a few trajectories in the  $x, y$  plane.
- 7-18. Find an elliptical region of asymptotic stability for eq. (7-21) using the  $V$ -function of eq. (7-77).
- 7-19. Study the system of eq. (7-81) in the  $x, y$  plane for two cases:  $\alpha = 1$  and  $\alpha = 4$ .
- 7-20. Study the system

$$\frac{dx}{dt} = -x + 2x^2y,$$

$$\frac{dy}{dt} = -y$$

in the  $x, y$  plane. Show that Zubov's  $V$ -function

$$V = 1 - \exp \left[ -\frac{y^2}{2} - \frac{x^2}{2(1-xy)} \right]$$

yields the exact stability boundary  $xy = 1$  (Hahn 1963).

- 7-21. Carry out the detailed steps in the application of the variable gradient method of the two-temperature model with one group of delayed neutrons, eqs. (7-131) through (7-149).
- 7-22. Consider the system of eq. (7-153), which has one temperature region plus a power coefficient. Show that there is a solution trajectory that approaches  $n = A + BT$  for large  $n$  and  $T$ . Sketch some isolines for the case in fig. 7-29 and show that  $n = A + BT$  approaches a separatrix between stable and unstable regions. Identify a semi-infinite stable region (suggested by J. M. Kendall, University of Arizona, 1970).
- 7-23. Verify eq. (7-162) for  $dV/dt$ .
- 7-24. Apply the boundedness criterion of eq. (7-172) to the two-temperature model and correlate the result with the parameter space of fig. 7-30.
- 7-25. Using the two-temperature model, express each of the following as boundaries in the parameter space of fig. 7-30:

$$\int_0^\infty h(t') dt' = 0;$$

$$h(0) = 0;$$

4-10 *Nonlinear System Stability*

$$\left. \frac{dh}{dt} \right|_{t=0} = 0.$$

7-26. Apply the method of dominant canonical coordinates to the system given by eq. (7-34).

7-27. Apply the method of dominant canonical coordinates to the system

$$\frac{dx}{dt} = -2x + 2y,$$

$$\frac{dy}{dt} = -x - xy.$$

7-28. Verify eq. (7-197) and the application of Welton's criterion to the two-region model.

7-29. Apply Welton's criterion to the model with one region plus a power coefficient.

7-30. Apply Popov's first criterion, eq. (7-200), to the two-region model. Show that Welton's criterion is less restrictive in this case.

7-31. Verify the limit-cycle amplitude equations, eqs. (7-242) and (7-243).

7-32. Apply eqs. (7-242) and (7-243), with the  $K_2$  terms neglected, to the two-region reactor with the effective-lifetime model.

## 8 Space-dependent Neutron Dynamics

This final chapter is mainly concerned with three subjects: a derivation of the point-reactor model from neutron transport theory, some descriptions of methods used in space-dependent reactor dynamics, and a brief introduction to the theory of neutron pulses and waves. Each of these subjects deserves much more elaboration; in particular, the important and difficult field of space-dependent reactor dynamics has grown very rapidly in recent years. However, our purpose here is to present a few fundamental ideas and to stimulate an interest in further study.

Many important topics are mentioned only briefly. Furthermore, the attempt to make the bibliography exhaustive had to be abandoned because of the sheer magnitude of the task. Special attention is called to some review articles that contain large bibliographies, and it is hoped that this will partially compensate for the deficiencies and omissions.

### 8-1. The Transport Equation

The Boltzmann transport equation for a reactor may be written

$$\begin{aligned} \frac{1}{v} \left[ \frac{\partial}{\partial t} \Phi(\mathbf{r}, v, t) + \mathbf{v} \cdot \nabla \Phi(\mathbf{r}, v, t) \right] = \\ - \Sigma_i(\mathbf{r}, v, t) \Phi(\mathbf{r}, v, t) \\ + \int \Sigma_s(\mathbf{r}, \mathbf{v}' \rightarrow \mathbf{v}, t) \Phi(\mathbf{r}, \mathbf{v}', t) d\mathbf{v}' \\ + \int \chi(v) (1 - \beta) v \Sigma_f(\mathbf{r}, v', t) \Phi(\mathbf{r}, v', t) d\mathbf{v}' \\ + \Sigma_i \lambda_i C_i(\mathbf{r}, t) \chi_i(v) \\ + S(\mathbf{r}, v, t), \end{aligned} \quad (8-1)$$

#### 4.1.2 Space-dependent Neutron Dynamics

where  $\Phi$  is the directional flux, such that  $\Phi(\mathbf{r}, \mathbf{v}, t) d\mathbf{r} d\mathbf{v}$  is  $v$  times the number of neutrons in the six-dimensional volume element of phase space  $d\mathbf{r} d\mathbf{v}$  at point  $\mathbf{r}$  with velocity  $\mathbf{v}$  at time  $t$ . The macroscopic cross-sections  $\Sigma_i$ ,  $\Sigma_s$ , and  $\Sigma_f$  refer respectively to all interactions, to scattering interactions which change the neutron velocity from  $\mathbf{v}'$  to  $\mathbf{v}$ , and to fission events. The neutron emission spectra  $\chi(v)$  and  $\chi_i(v)$  are for prompt neutrons and delayed neutrons of the  $i$ th group respectively. The average number of prompt neutrons per fission is  $(1 - \beta)v$ . For the  $i$ th delayed neutron group,  $\lambda_i$  and  $C_i$  are the decay constant and precursor density. Sources extraneous to the fission chain are represented by  $S$ .

The integrals in eq. (8-1) are triple integrals over neutron velocity space. The cross-sections are written as functions of the scalar speed  $v$ , as is frequently the case. Explicit time dependence is indicated in the cross-sections to account for externally imposed control or for feedback. The total cross-section  $\Sigma$  has units of reciprocal length, while the other cross-sections, as written here, have additional units (per unit volume in velocity space).

The gradient term in eq. (8-1) may be transposed to the right-hand side, and the partial derivative is seen to represent a rate of change of neutron density in phase space consisting of six terms: losses arising from streaming and from neutron interactions, offset by gains consisting of scattering from other velocities, production of prompt fission neutrons, production of delayed neutrons, and contributions from extraneous sources.

If the delayed-neutron precursors are assumed to be stationary, we may write

$$\frac{\partial C_i}{\partial t} = \int \beta_i v \Sigma_f(\mathbf{r}, \mathbf{v}', t) \Phi(\mathbf{r}, \mathbf{v}', t) d\mathbf{v}' - \lambda_i C_i(\mathbf{r}, t). \quad (8-2)$$

Eqs. (8-1) and (8-2) are easily extended to systems with more than one fuel isotope by including a term in  $\chi(1 - \beta)v\Sigma_f$  and a set of delayed neutrons appropriate to each isotope.

Following Henry (1958) and Keepin (1965), we postulate a fictitious steady state with  $S = 0$  and  $\Phi = \phi_s(\mathbf{r}, \mathbf{v})$ . To achieve a steady state with the same parameters that appear in eq. (8-1) at any given instant, we must introduce a fictitious reproduction factor  $k_s$ . We write

$$k_s \left[ (\mathbf{v}/v) \cdot \nabla \phi_s(\mathbf{r}, \mathbf{v}) + \Sigma_i \phi_s(\mathbf{r}, \mathbf{v}) - \int \Sigma_s(\mathbf{r}, \mathbf{v}' \rightarrow \mathbf{v}) \phi_s(\mathbf{r}, \mathbf{v}') d\mathbf{v}' \right] \\ = \int [(1 - \beta)\chi(v) + \Sigma_i \beta_i \chi_i(v)] v \Sigma_f(\mathbf{r}, \mathbf{v}') \phi_s(\mathbf{r}, \mathbf{v}') d\mathbf{v}', \quad (8-3)$$

where we have grouped all the terms representing nonfission events on the left-hand side and where we have used eq. (8-2) with  $\partial C_v / \partial t = 0$  to eliminate  $C_p$ .

Eq. (8-3) may be symbolically rearranged in the form

$$\mathcal{O}[\phi_s] = k_s \phi_s, \quad (8-4)$$

where  $\mathcal{O}$  represents a complicated integro-differential operator and  $k_s$  is an eigenvalue belonging to the eigenfunction  $\phi_s$  (if it exists). Actually, this is a symbolic way of representing the "reactivity eigenfunctions," or "lambda modes" (Cohen 1958; Kaplan et al. 1964). The spectrum of eigenvalues may be discrete or continuous or both. We assume that there is a "fundamental mode" eigenfunction  $\phi_0$  corresponding to a largest eigenvalue  $k$ . This is equivalent to assuming that the solution of eqs. (8-1) and (8-2) may be written as

$$\Phi(\mathbf{r}, v, t) = \sum_{s=0}^{\infty} f_s(t) \phi_s(\mathbf{r}, v) \quad (8-5)$$

and that the term in  $\phi_0$  represents a useful approximate solution for small departures from steady state. Note that  $f_0(t)\phi_0(\mathbf{r}, v)$  can be a complete solution only if space and time (as well as velocity and time) are separable. The identification of  $\phi_0$  as a fundamental mode is seen to be analogous to the procedure used for the diffusion equation in sec. 1-2, where we assumed the separable solution

$$N(\mathbf{r}, t) = f(\mathbf{r})n(t)$$

and identified  $f$  as the fundamental-mode eigenfunction of the Helmholtz equation. The use of modal expansions such as eq. (8-5) for solving nonseparable problems is basic to most methods in space-dependent reactor dynamics. As we shall see, many different types of eigenfunctions may be used.

Of course, there is no reason to assume in advance that an arbitrary set of eigenfunctions is either complete or orthogonal, and there is no guarantee that expansion coefficients may be found. The usual procedure is to assume biorthogonality and to generate adjoint functions  $\phi_s^+$ . Following Morse and Feshbach (1953), we generate an equation adjoint to eq. (8-3) by changing the signs of the first derivatives and by interchanging  $v$  and  $v'$  in the kernels of the integral operators. The equation for the fundamental-mode adjoint function  $\phi_0^+$  is

$$\begin{aligned} k & \left[ -(\mathbf{v}/v) \cdot \nabla \phi_0^+(\mathbf{r}, v) + \Sigma_i \phi_0^+(\mathbf{r}, v) - \int \Sigma_s(\mathbf{r}, v \rightarrow v') \phi_0^+(\mathbf{r}, v') dv' \right] \\ & = \int [(1 - \beta)\chi(v') + \Sigma_i \beta_i \chi_i(v')] v \Sigma_j(\mathbf{r}, v) \phi_0^+(\mathbf{r}, v') dv'. \quad (8-6) \end{aligned}$$

444 *Space-dependent Neutron Dynamics*

We now interpret  $k$  and the cross-sections in eq. (8-6) as time dependent, and identify the cross-sections with those in eq. (8-1). Multiply eq. (8-1) by  $\phi_0^+(\mathbf{r}, \mathbf{v})$  and integrate over  $\mathbf{r}$  and  $\mathbf{v}$ , multiply eq. (8-6) by  $\Phi(\mathbf{r}, \mathbf{v}, t)$  and integrate over  $\mathbf{r}$  and  $\mathbf{v}$ , and subtract the resulting two equations. The integral over  $\mathbf{r}$  is regarded as an integral over some fixed volume containing the system. Taking advantage of the freedom to select an adjoint boundary condition (Morse and Feshbach 1953), we choose

$$\int \int (\mathbf{v}/v) \cdot (\phi_0^+ \nabla \Phi + \Phi \nabla \phi_0^+) d\mathbf{r} d\mathbf{v} = 0,$$

where the double integral represents integration over the six-dimensional phase space.

The integration and subtraction is facilitated by interchanging  $v$  and  $v'$  in certain integrals. After some manipulation, the result is

$$\begin{aligned} & \frac{\partial}{\partial t} \int \int \frac{\phi_0^+ \Phi}{v} d\mathbf{r} d\mathbf{v} = \\ & \frac{k-1}{k} \int \int \int \phi_0^+(\mathbf{r}, \mathbf{v}') [(1-\beta)\chi(v') + \sum_i \beta_i \chi_i(v')] v \Sigma_f \Phi d\mathbf{r} d\mathbf{v} d\mathbf{v}' \\ & - \int \int \int \phi_0^+(\mathbf{r}, \mathbf{v}') [\sum_i \beta_i \chi_i(v')] v \Sigma_f \Phi d\mathbf{r} d\mathbf{v} d\mathbf{v}' \\ & + \sum_i \lambda_i \int \int \phi_0^+ C_i \chi_i(v) d\mathbf{r} d\mathbf{v} + \int \int \phi_0^+ S d\mathbf{r} d\mathbf{v}, \end{aligned} \quad (8-7)$$

where the absence of an argument signifies the appropriate function of  $\mathbf{r}$  and  $\mathbf{v}$  (not  $\mathbf{v}'$ ) and where the time dependence of  $\Sigma_f$  is still present but not explicitly indicated.

Before proceeding, we interpret the last step as a perturbation procedure in which eq. (8-1) is the perturbed system at any instant and eq. (8-6) is the unperturbed system such that  $\phi_0^+$  does not change appreciably in the presence of small changes in  $k$  and the cross-sections. One is thus encouraged to hope for eventual physical significance in all this manipulation.

At this point, we postulate the purely formal identity

$$\Phi(\mathbf{r}, \mathbf{v}, t) = n(t) \phi(\mathbf{r}, \mathbf{v}, t). \quad (8-8)$$

Clearly, eq. (8-8) contains no new assumptions. In practice,  $n(t)$  is called the amplitude function. It may be forced to carry the burden of most of the time dependence, and it may be identified with  $n(t)$  of the preceding chapters if other quantities are interpreted consistently.

The function  $\phi(\mathbf{r}, \mathbf{v}, t)$  is called the shape function, and the general case where  $\phi$  contains  $t$  is called nonseparable. We have

$$\frac{\partial}{\partial t} \iiint \frac{\phi_0^+ \Phi}{v} d\mathbf{r} d\mathbf{v} = \left[ \iiint \frac{\phi_0^+ \phi}{v} d\mathbf{r} d\mathbf{v} \right] \frac{dn}{dt} + n(t) \frac{\partial}{\partial t} \iiint \frac{\phi_0^+ \phi}{v} d\mathbf{r} d\mathbf{v}. \quad (8-9)$$

From eqs. (8-7) through (8-9), we find

$$\begin{aligned} \frac{dn}{dt} &= \frac{k-1}{k} \frac{\iiint \phi_0^+(\mathbf{r}, \mathbf{v}') [(1-\beta)\chi(v') + \Sigma_i \beta_i \chi_i(v')] v \Sigma_f \phi d\mathbf{r} d\mathbf{v} dv'}{\iint (\phi_0^+ \phi/v) d\mathbf{r} d\mathbf{v}} - n \\ &\quad - \frac{\iiint \phi_0^+(\mathbf{r}, \mathbf{v}') [\Sigma_i \beta_i \chi_i(v')] v \Sigma_f \phi d\mathbf{r} d\mathbf{v} dv'}{\iint (\phi_0^+ \phi/v) d\mathbf{r} d\mathbf{v}} \\ &\quad + \Sigma_i \lambda_i \frac{\iint \phi_0^+ C_i \chi_i(v) d\mathbf{r} d\mathbf{v}}{\iint (\phi_0^+ \phi/v) d\mathbf{r} d\mathbf{v}} + \frac{\iint \phi_0^+ S d\mathbf{r} d\mathbf{v}}{\iint (\phi_0^+ \phi/v) d\mathbf{r} d\mathbf{v}} \\ &\quad - n \frac{\partial}{\partial t} \log \iint (\phi_0^+ \phi/v) d\mathbf{r} d\mathbf{v}. \end{aligned} \quad (8-10)$$

Eq. (8-10) is highly suggestive of the familiar point-reactor model. We identify the coefficients of  $n$  as  $\rho/\ell$  and  $\beta_{eff}/\ell$ . The third and fourth terms are  $\Sigma_i \lambda_i c_i$  and  $q$ . There remains the partial derivative term, and the usual procedure is to adopt the form of the point-reactor model, constraining the shape function  $\phi$  such that the partial derivative vanishes.

We have

$$\frac{\rho}{\ell} = \frac{k-1}{k} \frac{\iiint \phi_0^+(\mathbf{r}, \mathbf{v}') [(1-\beta)\chi(v') + \Sigma_i \beta_i \chi_i(v')] v \Sigma_f \phi d\mathbf{r} d\mathbf{v} dv'}{\iint (\phi_0^+ \phi/v) d\mathbf{r} d\mathbf{v}}; \quad (8-11)$$

$$\beta_{\text{eff}} = \frac{\int \int \int \phi_0^+ (\mathbf{r}, \mathbf{v}') [\Sigma_i \beta_i \chi_i(v')] v \Sigma_f \phi \, d\mathbf{r} \, d\mathbf{v} \, dv'}{\int \int (\phi_0^+ \phi/v) \, d\mathbf{r} \, d\mathbf{v}}; \quad (8-12)$$

$$c_i(t) = \frac{\int \int \phi_0^+ C_i(\mathbf{r}, t) \chi_i(v) \, d\mathbf{r} \, d\mathbf{v}}{\int \int (\phi_0^+ \phi/v) \, d\mathbf{r} \, d\mathbf{v}}; \quad (8-13)$$

$$q = \frac{\int \int \phi_0^+ S(\mathbf{r}, \mathbf{v}, t) \, d\mathbf{r} \, d\mathbf{v}}{\int \int (\phi_0^+ \phi/v) \, d\mathbf{r} \, d\mathbf{v}}. \quad (8-14)$$

As pointed out by Henry (1958), the separation of eq. (8-11) into unique factors  $\rho$  and  $\ell$  is arbitrary. One could identify  $\rho$  as  $(k - 1)/k$ , where  $k$  is defined by eq. (8-6), but this is not necessary. As noted in chapter 2, one should regard the parameters  $\rho/\ell$  and  $\beta_{\text{eff}}/\ell$  as more fundamental than  $\rho$ ,  $\beta_{\text{eff}}$ , and  $\ell$ . However, it is common practice to compute  $(k - 1)/k$  by employing eq. (8-6) in a perturbation procedure and to identify the result with  $\rho$  so that eq. (8-11) yields an explicit formula for  $\ell$ . Then, as mentioned in chapter 2, one usually neglects the time dependence of  $\ell$  and  $\beta_{\text{eff}}/\ell$ , though this is not necessary.

The procedure leading to eq. (8-10) is a mathematical formality unless the computations indicated by eqs. (8-11) through (8-14) are practical. The major problem is the computation of the shape function,  $\phi(\mathbf{r}, \mathbf{v}, t)$  in eq. (8-8); this will be examined later in the context of time-dependent diffusion theory.

To find a formula for reactivity, multiply eq. (8-6) by  $\phi(\mathbf{r}, \mathbf{v}, t)$  and integrate over  $\mathbf{r}$  and  $\mathbf{v}$ . Compare this result with a second equation, obtained by setting  $k = 1$  and  $\Sigma_t = \Sigma_{t0}$ , etc. This represents a critical reference system. Make the usual first-order perturbation-theory assumption that  $\phi_0^+$  and  $\phi$  remain unchanged. Subtracting and setting  $\delta\Sigma_t = \Sigma_t - \Sigma_{t0}$ , etc., one finds

$$k - 1 = \frac{\int \int \phi_0^+ \overline{\delta\Sigma} \phi \, d\mathbf{r} \, d\mathbf{v}}{\int \int \int \phi_0^+ (\mathbf{r}, \mathbf{v}') [(1 - \beta)\chi(v') + \Sigma_i \beta_i \chi_i(v')] v \Sigma_f \phi \, d\mathbf{r} \, d\mathbf{v} \, dv'}, \quad (8-15)$$

where

$$\overline{\delta\Sigma} = \delta\Sigma_t - \overline{\delta\Sigma_s} - [(1 - \beta)\chi(v) + \Sigma_i\beta_i\chi_i(v)]v\delta\Sigma_f \quad (8-16)$$

and where bars over terms on the right-hand side of eq. (8-16) signify

$$\overline{x(v)} = \frac{\int x(v')\phi_0^+(r, v') dv'}{\phi_0^+(r, v)}$$

This formula for reactivity, together with whatever approximations are needed to render the computations practical, is useful, but it is a first-order result that is less fundamental than the formula for  $\rho/\ell$ , eq. (8-11). Note that reactivity, like the other parameters in the point-reactor model, is an integral property of the system.

To complete the derivation, multiply eq. (8-2) by  $\phi_0^+(r, v)\chi_i(v)$  and integrate over  $r$  and  $v$ . If eqs. (8-8) and (8-13) together with

$$\left(\frac{\beta_i}{\ell}\right)_{\text{eff}} = \frac{\iiint \phi_0^+(r, v')\beta_i\chi_i(v')v\Sigma_f\phi dr dv dv'}{\iint (\phi_0^+\phi/v) dr dv} \quad (8-17)$$

are used, the result is the familiar precursor equation.

Next, we note that the adjoint function  $\phi_0^+$  may be given a physical interpretation. Consider the impulse

$$S(r, v, t) = \delta(r - r_0)\delta(v - v_0)\delta(t), \quad (8-18)$$

representing a point source of neutrons at  $r_0$  with velocity  $v_0$  at  $t = 0$ . Using eq. (8-14), we obtain

$$q = \frac{\phi_0^+(r_0, v_0)}{\iint (\phi_0^+\phi/v) dr dv} \delta(t). \quad (8-19)$$

The adjoint function is therefore a source-weighting function.

We saw in sec. 2-5 that the impulse response of the point-reactor model asymptotically approaches a constant. For a source  $Q_0\delta(t)$ , the asymptotic neutron population is  $Q_0$ , the number of neutrons injected at  $t = 0$ . Eq. (8-19) shows how each injected neutron is to be weighted according to its position and velocity at  $t = 0$ . The adjoint function is therefore a measure of the number of daughter neutrons that are ultimately contributed by each injected source neutron, and it is therefore called the "neutron importance function."

It is interesting to compare this with the effect of a neutron absorber. Use eqs. (8-15) and (8-16) with  $\bar{\delta\Sigma} = \delta\Sigma_a$ . The reactivity effect of a point absorber at  $\mathbf{r}_0$  and  $\mathbf{v}_0$  is seen to be weighted, not by  $\phi_0^+$ , but by the product  $\phi_0^+ \phi$ , often called the "statistical weight." This means that the integral parameter  $\rho$  is an average over the spatial distribution and velocity dependence of an absorber, weighted by  $\phi_0^+ \phi$ .

These interpretations are somewhat arbitrary in that one may use an arbitrary weighting function in place of  $\phi_0^+$ . This yields new definitions of the reactivity and other parameters. The question is discussed by many writers, e.g., Gross and Marable (1960), Lewins (1961), Gozani (1963), Gyftopoulos (1964b, 1964c), and Deniz (1967). For a discussion of time-dependent importance, see Lewins (1960b) and Becker (1968a). However, the usual procedure is to use  $\phi_0^+$  and to identify eq. (8-10) as the point-reactor model when the steady-state flux is used for the shape function  $\phi$ .

In summary, we have indicated one method of deriving the point-reactor model from neutron transport theory, together with expressions for the integral parameters. To preserve the form of the point model when the shape function  $\phi$  is time dependent, let

$$\frac{\partial}{\partial t} \iint (\phi_0^+ \phi / v) d\mathbf{r} d\mathbf{v} = 0. \quad (8-20)$$

If eq. (8-20) is adopted as a constraint, it is convenient to set

$$\iint (\phi_0^+ \phi / v) d\mathbf{r} d\mathbf{v} = 1.$$

This is equivalent to adopting the definition

$$n(t) = \iint (\phi_0^+ \Phi / v) d\mathbf{r} d\mathbf{v}.$$

Note that this  $n(t)$  may be interpreted as an average neutron density. However, the average fission power would be proportional to

$$\iint \Sigma_f \Phi d\mathbf{r} d\mathbf{v}$$

and would satisfy a different dynamic equation. This is explored in some numerical examples by Yasinsky and Henry (1965).

For further study, the reader is referred to Ussachoff (1955), Cohen (1958), Henry (1958), Weinberg and Wigner (1958), Gyftopoulos and Devooght (1961), Grace (1964), Keepin (1965), Lewins (1965), and Akcasu, Lellouche, and Shotkin (forthcoming).

### 8-2. Multimode Dynamics Equations

Exact solutions of the Boltzmann transport equation are available only in a few special cases, and most of these are not time dependent. Fortunately, neutron transport may frequently be represented by a set of multigroup diffusion equations, in which the energy variable is discretized and the slowing-down process is represented by intergroup transfer cross-sections (Lamarche 1966). Solutions are still difficult to obtain. Even in one space dimension, the direct numerical solution of a time-dependent diffusion problem can be complicated and time-consuming. One way of seeking more practical procedures is the method of eigenfunctions or modal expansions (Kaplan et al. 1964; Stacey 1967a).

The existence of eigenfunctions was postulated in sec 8-1. A general justification in the framework of neutron transport theory does not exist, but there are physical grounds for invoking the concept (Weinberg and Wigner 1958). The procedure has proved to be useful in many practical cases, particularly in diffusion theory. Various types of modes have been constructed, and much progress has been made in studying their properties. We proceed to a general formulation of multigroup diffusion dynamics in terms of the method of weighted residuals, and many of the useful approximate methods are cited as special cases (Fuller 1969).

Write the multigroup diffusion equations in the compact form (Kaplan et al. 1964)

$$V^{-1} \frac{\partial \Psi}{\partial t} = [\nabla \cdot D \nabla - A + (1 - \beta) \chi F^T] \Psi + \Sigma_i \lambda_i \chi_i C_i \quad (8-21)$$

and

$$\frac{\partial C_i}{\partial t} = \beta_i F^T \Psi - \lambda_i C_i, \quad (8-22)$$

where we assume stationary fuel (one isotope) and neglect extraneous sources. The flux  $\Psi$  is a column vector, each component being the scalar flux in an energy group, and  $C_i$  is a scalar (the precursor density for the  $i$ th delayed-neutron group). The neutron speeds are represented in the diagonal matrix

$$V^{-1} = \begin{bmatrix} 1/v_1 & & & \\ & 1/v_2 & & \\ & & \ddots & \\ & & & \ddots \end{bmatrix}$$

having one entry for each group. Similarly, the diffusion constants appear in the diagonal matrix

$$D = \begin{bmatrix} D_1 & & \\ & D_2 & \\ & & \ddots \end{bmatrix}.$$

Absorption and scattering are represented by the matrix

$$A = \begin{bmatrix} \Sigma_1 & & \\ & \Sigma_2 & \\ & & \ddots \end{bmatrix} - \begin{bmatrix} \Sigma_{11} & \Sigma_{12} & & \\ \Sigma_{21} & \Sigma_{22} & & \\ & & \ddots & \\ & & & \ddots \end{bmatrix},$$

where the first part (absorption) is diagonal and the second part (scattering) is a full matrix. The fission cross-sections appear in the column vector

$$F = \begin{bmatrix} v\Sigma_{f1} \\ v\Sigma_{f2} \\ \vdots \\ \vdots \end{bmatrix},$$

and  $F^T$  is the transpose of  $F$ . The emission spectra of prompt and delayed neutrons are also column vectors

$$\chi = \begin{bmatrix} \chi_1 \\ \chi_2 \\ \vdots \\ \vdots \end{bmatrix} \quad \text{and} \quad \chi_i = \begin{bmatrix} \chi_{i1} \\ \chi_{i2} \\ \vdots \\ \vdots \end{bmatrix}.$$

The approximate solution has the general form

$$\Psi(x, y, z, t) = \sum_j \psi_j(x, y, z, t) n_j(t), \quad (8-23)$$

where the  $\psi_j$  are trial functions (a set of functions selected in advance, or modal shape functions to be determined in auxiliary calculations). The undetermined functions  $n_j(t)$  are the amplitude functions, and the goal is to convert eqs. (8-21) and (8-22) into a set of ordinary differential equations for the  $n_j$ . We may write

$$\Psi(x, y, z, t) = \psi(x, y, z, t) n(t), \quad (8-24)$$

where  $\psi$  is a rectangular matrix with elements  $\psi_{kj}$  (kth energy group, jth mode) and  $n$  is a column vector consisting of the  $n_j$ .

Substitute eq. (8-24) into eq. (8-21) to obtain

$$0 = V^{-1} \left( \psi \frac{dn}{dt} + \frac{\partial \psi}{\partial t} n \right) - [\nabla \cdot D \nabla - A + (1 - \beta) \chi F^T] \psi n - \sum_i \lambda_i \chi_i C_i. \quad (8-25)$$

Eq. (8-25) holds if  $\psi n$  is an exact solution. For an approximate solution, we may write, instead,

$$R = V^{-1} \left( \psi \frac{dn}{dt} + \frac{\partial \psi}{\partial t} n \right) - [\nabla \cdot D \nabla - A + (1 - \beta) \chi F^T] \psi n - \sum_i \lambda_i \chi_i C_i, \quad (8-26)$$

where  $R$  is the error or residual (a column vector with one entry for each energy group). The essence of the weighted-residual method is that a weighted integral of  $R$  over some domain shall be made to vanish, thus distributing the error throughout the domain and permitting the determination of unknown parameters or functions in the approximate solution.

Introduce the rectangular matrix of weighting functions

$$W = \begin{bmatrix} W_{11} & W_{12} & \cdots & \cdots \\ W_{21} & W_{22} & & \\ \vdots & & & \\ \vdots & & & \end{bmatrix}, \quad (8-27)$$

where the functions  $W_{kj}$  (kth energy group, jth mode) are as yet unspecified. We multiply all terms in eq. (8-26) from the left by  $W^T$  (the transpose of  $W$ ) and integrate over the space. We set

$$\int W^T R dx = 0, \quad (8-28)$$

where the integral is meant as a volume integral. We further assume

$$\int W^T V^{-1} \frac{\partial \psi}{\partial t} dx = 0, \quad (8-29)$$

which could be satisfied by adopting

$$n(t) = \int W^T V^{-1} \psi dx, \quad (8-30)$$

### 8.2. Spacetime-dependent Neutron Dynamics

in analogy with sec. 8-1. However, it will be more convenient to assume eq. (8-29) without adopting eq. (8-30). Eq. (8-26) becomes

$$\left( \int W^T V^{-1} \psi dx \right) \frac{dn}{dt} = \left[ \int W^T \nabla \cdot D \nabla \psi dx - \int W^T A \psi dx \right. \\ \left. + \int W^T (1 - \beta) F^T \psi dx \right] n + \sum_i \lambda_i \int W^T \chi_i C_i dx. \quad (8-31)$$

Eq. (8-22) may be written as

$$\frac{\partial C_i}{\partial t} = \beta_i F^T \psi n - \lambda_i C_i, \quad (8-32)$$

and residuals could be defined. An alternate procedure would be to integrate eq. (8-22) with respect to time and substitute the result into eq. (8-21). Using residuals, we find

$$\int W^T \chi_i \frac{\partial C_i}{\partial t} dx = \left( \int W^T \beta_i \chi_i F^T \psi dx \right) n - \lambda_i \int W^T \chi_i C_i dx. \quad (8-33)$$

If the emission spectra  $\chi_i$  and the weighting functions  $W_{kj}$  are independent of time, we may write the left-hand side as

$$\frac{d}{dt} \int W^T \chi_i C_i dx,$$

and make the identifications

$$\xi_i = \int W^T \chi_i C_i dx \quad (8-34)$$

and

$$\beta_{i,\text{eff}} = \int W^T \beta_i \chi_i F^T \psi dx. \quad (8-35)$$

Eq. (8-33) becomes

$$\frac{d\xi_i}{dt} = \beta_{i,\text{eff}} n - \lambda_i \xi_i, \quad (8-36)$$

where  $\xi_i$  is a vector analogous to the scalar  $\ell c_i$  of the point-reactor model.

We now return to eq. (8-31). Adding and subtracting  $\beta_{\text{eff}} n$  on the right-hand side, where

$$\beta_{\text{eff}} = \int W^T \Sigma_i \beta_i \chi_i F^T \psi dx, \quad (8-37)$$

we obtain

$$\ell \frac{dn}{dt} = (\rho - \beta_{\text{eff}})n + \sum_i \lambda_i \xi_i, \quad (8-38)$$

where

$$\ell = \int W^T V^{-1} \psi \, dx \quad (8-39)$$

and

$$\rho = \int W^T [\nabla \cdot DV - A + (1 - \beta) \chi F^T + \sum_i \beta_i \chi_i F^T] \psi \, dx \quad (8-40)$$

and where  $\xi_i$  and  $\beta_{\text{eff}}$  are given by eqs. (8-34) and (8-37) respectively. Eqs. (8-36) and (8-38) are vector-matrix equations known as the multimode dynamics equations. The column vectors have one entry for each mode (each trial function  $\psi_j$ ), and the parameters  $\ell$ ,  $\rho$ , and  $\beta_{\text{eff}}$  are square matrices. For practical approximate computations, the number of trial functions is finite, and the multimode equations represent a finite set of ordinary differential equations in time.

The residual  $R$ , as given by eq. (8-26), vanishes identically only for an exact solution. The multimode equations are satisfied by an approximate solution provided the weighted integral of  $R$ , for the weighting  $W(x, y, z)$ , vanishes for all  $t$ . The problem has been reduced to the selection of trial functions and weighting functions, thus permitting the computation of parameters and the time integrations (Fuller 1969; Garabedian 1961; Kaplan 1966; Kaplan et al. 1964; Lewins 1960c; Soodak 1961).

In principle, the choice of trial functions is arbitrary (except that the functions must be linearly independent). Normally, the approximate solution is chosen to satisfy initial conditions and boundary conditions; otherwise, a simple generalization including initial and boundary residuals may be made. The weighting functions are also arbitrary (in principle), though the matrix of weighting functions must be of the same order as the matrix of trial functions, and no two columns of weighting functions may be proportional. If the weighting functions are a set of steady-state adjoint functions, one has a system somewhat analogous to the transport-theory treatment of sec. 8-1.

In one dimension, the method of weighted residuals reduces to the "method of undetermined parameters." It was used for integrating the point-reactor model in sec. 4-6 and has been extended by Fuller to the time integration of the multimode equations (Fuller 1969; Fuller, Meneley, and Hetrick 1969, 1970). Some of the common weighting methods are (Crandall 1956):

## 4.54 Space-dependent Neutron Dynamics

1. Collocation (delta-function weighting;  $R$  vanishes at discrete points)
2. Subdomains (step-function weighting; the integral of  $R$  vanishes over each subdomain)
3. Least squares (the integral of  $R^2$  is minimized with respect to the undetermined parameters)
4. Moments (polynomial weighting; moments of  $R$  are made to vanish)
5. Galerkin method (the weighting functions are the trial functions themselves)
6. Adjoint weighting (closely related to the variational method; the weighting functions are adjoint to the set of trial functions)

The method described in sec. 4-6 (and Fuller's extension of it to the multimode equations) uses subdomain weighting with piecewise polynomials as trial functions.

The variational method, which may be regarded as a special case of the weighted-residual method, is usually derived from a different viewpoint. The criterion

$$\int \psi^\dagger R dx = 0$$

is also the condition that some functional shall be an extremum. The system differential equations (Euler equations) are deduced as a consequence. It is sometimes advantageous to construct a variational functional and obtain additional insight into the behavior of the system, although the procedure can become exceedingly complicated. For reviews, see Becker (1964), Kaplan (1969), and Stacey (1969a). Some basic papers are by Lewins (1962, 1964, 1968), Selengut (1959, 1963), and Stacey (1967b). Other references are given in the next section in connection with the synthesis method. Note that the variational method is equivalent to the Galerkin method for a self-adjoint system.

As suggested earlier, many of the approximate methods of space-dependent reactor dynamics may be regarded as special cases of the weighted-residual method. For example, the point-reactor model for one energy group follows upon selecting a single time-independent mode in eq. (8-23):

$$\Psi(x, y, z, t) = \psi_0(x, y, z)n(t). \quad (8-41)$$

The functions in eq. (8-41) are scalars. The single mode  $\psi_0$  is often taken to be the initial steady-state flux distribution, and the weighting function is usually the steady-state adjoint. Using eqs. (8-34), (8-37),

(8-39), and (8-40), we see that the  $c_i$  and the parameters are scalars whose values depend on the choice of weighting function and mode (trial function); this emphasizes the arbitrariness of the concept of reactivity even in the simplest form of reactor dynamics.

Quasi-static methods represent the first important generalization of this idea. Again using only one mode, we write

$$\Psi(x, y, z, t) = \psi_0(x, y, z, t)n(t). \quad (8-42)$$

The adiabatic method (Henry and Curlee 1958; Curlee 1959) uses for  $\psi_0$  at any instant a fictitious static mode (a lambda mode; see below) corresponding to the instantaneous reactor configuration. The shape function, as it evolves in time, is obtained from a succession of static spatial calculations. This implies that the flux shape responds instantaneously to changes in the reactor properties, certainly a poor assumption for nonuniform changes in a large reactor (Kaplan and Margolis 1960). More sophisticated quasi-static methods (see sec. 8-3) use eq. (8-42) with various realistic computations of the shape function.

Modal expansions, in which the  $\psi_i$  of eq. (8-23) are time independent, have been used by many authors. A review is given by Kaplan et al. (1964). We have already mentioned the lambda modes, which are the eigenfunctions of

$$(-\nabla \cdot D\nabla + A)\psi = \frac{1}{\lambda} [(1 - \beta)\chi F^T + \sum_i \beta_i \chi_i F^T] \psi, \quad (8-43)$$

obtained by constructing a steady-state system from eqs. (8-21) and (8-22). Here  $\lambda$  plays the role of  $k_s$  in eq. (8-3). Eq. (8-43) is essentially the static equation solved by many multigroup-diffusion computer programs. The lambda modes were used by Walter and Henry (1968) in deriving a method for measuring shutdown reactivity.

A second set of modes may be generated by neglecting the delayed-neutron source and using the ansatz

$$\Psi = \psi(x, y, z) \exp(\omega_p t). \quad (8-44)$$

From eq. (8-21), the static eigenvalue problem is

$$[\nabla \cdot D\nabla - A + (1 - \beta)\chi F^T] \psi = \omega_p V^{-1} \psi. \quad (8-45)$$

The eigenfunctions are known as the omega-p modes.

A third set, the omega-d modes or inhour modes, is generated from eqs. (8-21) and (8-22) by writing

$$\Psi = \psi(x, y, z) \exp(\omega_d t) \quad (8-46)$$

and

$$C_i = \zeta_i(x, y, z) \exp(\omega_d t). \quad (8-47)$$

The eigenvalue problem becomes

$$[V \cdot D\nabla - A + (1 - \beta)\chi F^T] \psi + \Sigma_i \lambda_i \chi \zeta_i = \omega_d V^{-1} \psi; \quad (8-48)$$

$$\beta_i F^T \psi - \lambda_i \zeta_i = \omega_d \zeta_i. \quad (8-49)$$

The latter two sets of modes have been called "natural modes" (Kaplan 1961). The omega-d modes have been studied extensively by Henry (1964), who found that these modes occur in clusters of seven. Each cluster has eigenvalues given by a generalized inhour equation, and the spatial shapes within each cluster are similar. When these shapes are assumed identical, orthogonality relations can be derived, and several applications become feasible (especially the analysis of certain experiments in large subcritical reactors). The relationship between the lambda and omega-d modes has been explored by Henry and Kaplan (1965).

Another important method is suggested by the theory of orthogonal functions and Fourier series. It is natural to use as trial functions the complete orthogonal set generated by the Helmholtz equation (see sec. 1-2). The same set is used as weighting functions (Galerkin weighting). Convergence is guaranteed theoretically, but only for linear systems with constant coefficients. The method has been applied by Garabedian and Leffert (1959) and Foderaro and Garabedian (1962). Unfortunately, convergence is quite slow for many practical problems of interest.

The method was applied to the nonlinear problem of reactor excursions with a prompt energy feedback (space-dependent Nordheim-Fuchs model) by Scalettar (1964) and by Garabedian and Lynch (1965). More recent discussions were given by Canosa (1968b) and Shotkin (1969b); the latter paper includes a comparison of the modal-expansion technique with an iterative treatment of the nonlinearity. Other aspects of the space-dependent Nordheim-Fuchs model were studied by Ergen (1965) and Canosa (1967b), who obtained the asymptotic energy distribution following an excursion, and by Ghatak (1968), who compared dynamic formulations of integral parameters with the definitions obtained from static perturbation theory. Other nonlinear problems are treated by Canosa (1969).

Modal expansions using eigenfunctions have been employed to study spatial effects in oscillation experiments (Kylstra and Uhrig 1965; Loewe 1965; Foulke and Gyftopoulos 1967; Saji 1968).

Approximate solutions may be generated as expansions in functions  $\psi_j(x, y, z)$  that are not eigenfunctions. For example, a set of "Green's function modes" were used by Dougherty and Shen (1962). These modes are generated by solving a set of static diffusion problems with neutron sources in various subregions. The time dependence of the amplitude

functions is then determined by means of a semidirect variational method.

Indeed, the functions  $\psi_j(x, y, z)$  may be chosen in quite arbitrary fashion to suit the problem at hand. This is the spirit of the Rayleigh-Ritz, or synthesis, method, which is essentially the weighted-residual method with arbitrary trial functions. This is discussed further in the next section as part of a review of various computing methods.

### 8-3. Calculation Methods

In this section we attempt a review of various calculation methods for space-dependent reactor dynamics. We begin by citing several approaches based essentially on discrete (finite-difference) representations for the space and time derivatives, together with the semidiscrete method of Hansen and his coworkers. This is followed by brief reviews of the synthesis approach and of several quasi-static methods, primarily in the framework of the method of weighted residuals. Nodal methods are cited both in relation to the discrete methods and to synthesis. We conclude by mentioning a few additional methods and by citing studies of the xenon problem and of space-dependent stability. The reader is referred to review articles cited previously and to summary reviews by Kerlin (1965) and Henry (1969).

Finite-difference methods have been used extensively in the solution of many types of diffusion problems (e.g., Crank, 1956; Richtmyer, 1958). A discussion of the many varieties and refinements is outside the scope of this review. We cite only a few of the better-known applications to space-dependent reactor dynamics; other references are given by Kaplan et al. (1964) and Flatt (1968).

A subcritical reactor was studied by Agresta and Borst (1960), using a finite-difference approximation to the time-dependent age-diffusion equation. A highly efficient one-dimensional two-group code, WIGLE, was developed by Cadwell, Henry, and Vigilotti (1964). Other finite-difference applications were made by Nahavandi and von Hollen (1964b), Brickstock, Davies, and Smith (1965), and Perks (1965). An improved version of WIGLE was developed by Henry and Vota (1965). Other codes are STREAK (Smiley 1966), RAUMZEIT (Adams and Stacey 1967), and TWIGL (Yasinsky, Natelson, and Hageman 1968); the latter is a two-dimensional version of WIGLE. A comparison of the implicit time-differencing used in TWIGL with the alternating-direction implicit (ADI) method is reported by Hageman and Yasinsky (1969). A generalized finite-difference method is discussed by Alcouffe and Albrecht (1970).

### 8.1 Space-dependent Neutron Dynamics

These numerical methods are of value in special situations, e.g., analysis of simple reactor systems with a high degree of symmetry, and verification of test cases for approximation methods such as the synthesis or quasi-static techniques. Eventually it may be feasible to calculate any spatially dependent transient by straightforward finite-difference (or Monte Carlo) methods. However, present limitations on computer speed and capacity currently favor the development of approximation techniques such as those to be described.

A space-dependent generalization of Hansen's method (see sec. 4-7) has been highly successful (Andrews and Hansen 1968). This is the basis for the code GAKIN (Hansen and Johnson 1967). The method may be called semidiscrete in that finite differences are used for the space variable, while the time variation is represented by a factor  $\exp(\omega h)$ . In the space-dependent case,  $\omega$  may be a matrix of free parameters determined by a rapidly converging iterative scheme. Extensions to two space dimensions are reported by McCormick and Hansen (1969) and by Reed and Hansen (1969). A comparison of various two-dimensional methods is given by Hansen (1967). See also Reed and Hansen (1970).

Many special methods have been devised for estimating the effect of a reflector on the reactor dynamics (e.g., Rumsey 1954; Gamble 1960; Cohn 1962). Cohn's two-point (two-node) method is closely related to the theory of coupled cores and multiregion reactors (Avery 1958; Garabedian and von Herrmann 1959; Plaza and Köhler 1966; Chezem and Köhler 1967; Komata 1969). Other examples of two-node reactor analysis are given by Baldwin (1959), Hurwitz (1965), and Jeffers and Hall (1968).

These nodal methods may be regarded as extensions of the finite-difference method, using a very coarse spatial mesh and requiring

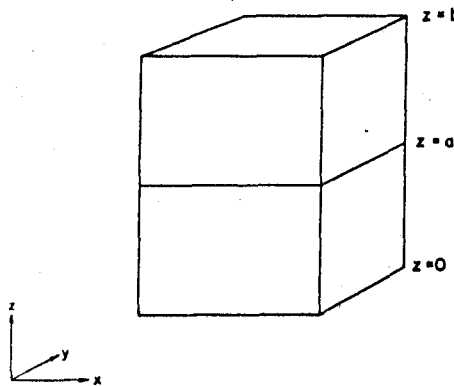


Fig. 8-1. Two-zone reactor illustrating continuous synthesis.

special treatment of the coupling between mesh points. Coupling coefficients, usually obtained from auxiliary diffusion or transport theory calculations, are difficult to derive and verify. The synthesis method has been applied by Yasinsky (1968a), who used one trial function for each subregion; and the weighted-residual treatment of spatial discontinuities provides a systematic method of computing coupling coefficients (Fuller 1969).

We turn now to the method of synthesis (Kaplan 1966; Wachspress 1969; Stacey 1969a). The method was first applied in reactor physics for three-dimensional steady-state flux calculations, and the early work was reviewed by Meyer (1958). For illustration, consider the two-zone reactor in fig. 8-1, where one zone contains partially inserted control rods. Symmetry suggests separability in each zone:

$$\phi(x, y, z) \cong \begin{cases} f_1(x, y)Z(z), & 0 < z < a; \\ f_2(x, y)Z(z), & a < z < b. \end{cases} \quad (8-50)$$

The trial functions  $f_1$  and  $f_2$  are found from two-dimensional calculations typical of reactors with and without control rods. Eq. (8-50) is substituted into the three-dimensional differential equations, which are then integrated over  $x$  and  $y$ . The result is a one-dimensional diffusion equation that may be solved for  $Z$ . The three-dimensional flux shape is then given by eq. (8-50).

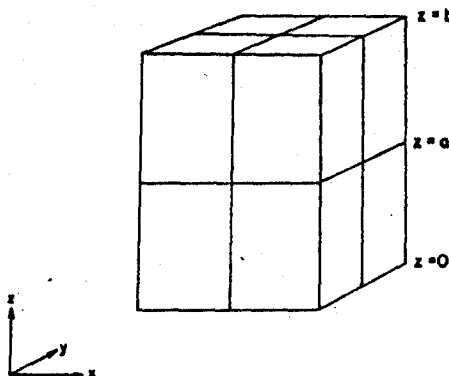


Fig. 8-2. Two-zone reactor illustrating multichannel synthesis.

The method has had wide use in reactor theory. A major shortcoming is the inherent discontinuity at  $z = a$ . An improvement was suggested by Wachspress, Burgess, and Baron (1962). The reactor may be divided into vertical channels, as in fig. 8-2, and eq. (8-50) applied with a

### 4.1(a) Space-dependent Neutron Dynamics

different function  $Z$  for each channel. Integration over each channel yields a differential equation for the function  $Z$  of each channel. This multichannel synthesis reduces the discontinuities in the  $z$ -direction at the expense of introducing discontinuous trial functions and the need for computing coupling between channels.

If one replaces eq. (8-50) by

$$\phi(x, y, z) \cong f_1(x, y)Z_1(z) + f_2(x, y)Z_2(z), \quad (8-51)$$

the flux shape is not required to jump abruptly at  $z = a$  but is instead a smoothly varying mixture of the two shapes  $f_1$  and  $f_2$ . The extension to many axial zones and trial functions may be expressed as

$$\phi(x, y, z) \cong \sum_j f_j(x, y)Z_j(z), \quad (8-52)$$

and the analogy to eq. (8-23) is apparent. The most flexible way to generate equations for the  $Z_j$  is the method of weighted residuals, and excellent practical approximations may be achieved with judicious choices of trial functions and weighting functions. Galerkin weighting and adjoint weighting have proved successful (Kaplan 1966). The former is often more economical because it does not require separate sets of calculations for weighting functions; the latter may be advantageous in that a variational principle may be invoked.<sup>1</sup>

A variational procedure was used by Kaplan (1962a) to derive equations for the  $Z_j$  in eq. (8-52). The variational method was extended by Selengut (Wachspress and Becker 1965) to accommodate discontinuous trial functions and was applied to multichannel flux synthesis by Wachspress (1966b). Since interface conditions may also be derived in the context of weighted residuals, it is again not essential to use a variational approach. Another application of discontinuous trial functions was made by Yasinsky and Kaplan (1967).

Time synthesis proceeds by using, for example (Kaplan 1962b),

$$\Psi(x, y, t) = \psi_1(x, y, t)n_1(t) + \psi_2(x, y, t)n_2(t) + \dots \quad (8-53)$$

Three-dimensional time synthesis may be developed from

$$\Psi(x, y, z, t) = \psi_1(x, y, z, t)n_1(t) + \psi_2(x, y, z, t)n_2(t) + \dots \quad (8-54)$$

or from

$$\Psi(x, y, z, t) = f_1(x, y)Z_1(z, t) + f_2(x, y)Z_2(z, t) + \dots \quad (8-55)$$

1. The variational method can evolve into the variational mystique when adjoint weighting is advocated as superior by virtue of the existence of a variational principle. There seems to be no general evidence favoring such a viewpoint.

The former yields the multimode dynamics equations of sec. 8-2; the latter yields partial differential equations in  $z$  and  $t$ . Time synthesis is discussed by Kaplan, Marlowe, and Bewick (1964) and Becker (1965). Examples of space-time synthesis using a form like eq. (8-55) are reported by Yasinsky (1968b); the Galerkin method was used to derive equations for the  $Z_j(z, t)$ , which were then solved using a one-dimensional code.

As with the  $Z$ -functions in eq. (8-52), whether used in a single channel or in a multichannel formulation, the functions  $n_j(t)$  in time synthesis were originally taken to be continuous. Time-discontinuous functions were introduced by Yasinsky (1967). A variational functional admitting both spatial and temporal discontinuities was subsequently introduced (Stacey 1967b) and extended to multichannel space-time synthesis (Stacey 1968). Both spatial and temporal discontinuities are treated by the method of weighted residuals in the report by Fuller (1969), who includes the possibility of time-discontinuous shape functions. This latter possibility, also noted for the variational method by Becker (1968b), permits the characterization of the quasi-static methods as a special case of multimode weighted-residual dynamics. It was also pointed out by Fuller (1969) that a consistent nodal method may be derived as a special case of multichannel weighted-residual synthesis by using one trial function in each subregion.

Synthesis techniques, now highly developed, are finding wide application. In many transient calculations, the trial functions can be static flux shapes "before and after," thus "bracketing" the shape change. Symmetries can be helpful guides in choosing trial functions. However, the best guides to the selection of trial functions appear to be the ingenuity and experience of the investigator.

Another important class of methods is known collectively as the quasi-static method. The adiabatic method (Henry and Curlee 1958; Curlee 1959) has been discussed in sec. 8-2; it suffers mainly from the assumption that shape changes follow parameter changes without any time lag.

There is one mode, as in eq. (8-42), and the undetermined function  $n(t)$  is the solution of the scalar point-reactor model. The precursor densities and the parameters are given by eqs. (8-34), (8-37), (8-39), and (8-40). Usually, but not necessarily, the weighting functions are the steady-state adjoint functions. The point-reactor model is used until a shape-function recalculation is deemed necessary. The shape function is the solution  $\psi$  of eq. (8-25) written in the form

$$\frac{1}{v} \frac{\partial \psi}{\partial t} = \left[ \nabla \cdot D \nabla - A + (1 - \beta) \chi F^T - \frac{1}{vn} \frac{dn}{dt} \right] \psi + \frac{1}{n} \sum_i \lambda_i C_i \quad (8-56)$$

subject to the constraint

$$\frac{d}{dt} \int (W^T \psi / v) dx = 0. \quad (8-57)$$

In the original adiabatic model, eq. (8-56) is replaced by a steady-state form. In the quasi-static approximation of Ott and Meneley (Ott and Madell 1966; Ott and Meneley 1969; Fuller 1969), eq. (8-56) is used with the term  $\partial\psi/\partial t$  either neglected entirely or approximated by the backward difference

$$\left. \frac{\partial \psi}{\partial t} \right|_{t=t_n} = \frac{\psi(x, t_n) - \psi(x, t_{n-1})}{t_n - t_{n-1}}, \quad (8-58)$$

where the time interval is many times larger than that used in integrating the associated point-reactor equations. The code QX-1 has been developed for calculations that use the first version (Meneley, Ott, and Wiener 1967). A two-dimensional version is being developed. Other quasi-static methods are described by Galati (1969) and by Stacey and Adams (1967).

Other approaches are possible. An analogue computer method was developed by Kelber, Just, and Morehouse (1961). A space-time iteration technique has been proposed by Fuller (1969). Laplace transforms have been applied to a time-dependent age-diffusion problem by Deverall (1958). Störrer et al. (1966) outlined a more general formulation, which uses the Laplace transform with respect to time and the Fourier transform with respect to space. The concept of impulse response was employed by Hoshino, Wakabayashi, and Hayashi (1965), who formulated a multigroup diffusion problem in terms of a spatially dependent transfer function. Spatial effects in forced oscillations are mentioned later in the introduction to neutron waves.

The reader is encouraged to explore the extensive literature on xenon oscillations and stability. A brief sampling of papers before 1964 includes work by Henry and Germann (1957), Randall and St. John (1958, 1962), Gyorey (1962), and Lellouche (1962). Reviews are given by Kaplan et al. (1964) and Shotkin (1964b). More recent work is reported by Kaplan and Yasinsky (1966), Scalettar (1966), Canosa and Brooks (1966), Hooper, Rydin, and Stacey (1968), Shinoda and Mitake (1969), and Stacey (1969c).

The general problem of nonlinear stability in space-dependent reactor dynamics has been studied recently (Hsu 1967; Kastenberg and Chambre 1968; Kastenberg 1969a; Kastenberg and Crawford 1969). A review is given by Kastenberg (1969b). Some of the mathematical methods invoked in these stability studies may yield new practical techniques for calculating space-dependent reactor transients.

#### 8-4. Some Numerical Results

This section contains a selection of numerical results, originally published in the years 1965-69. The purposes are to illustrate some of the important effects that can arise in highly space-dependent dynamic situations and to indicate the value of some of the approximate methods.

A classic numerical experiment was performed by Yasinsky and Henry (1965). Two one-dimensional unreflected cores were subjected to both prompt and delayed supercritical excursions chosen to accentuate spatial effects. Each core, one 240 cm thick and the other 60 cm thick, consisted of three regions, identical except for different transverse bucklings in each region. Two energy groups (fast and thermal) were used.

Each core was made super-prompt critical by step increases of fission cross-sections in only the end quarter (0-60 cm or 0-15 cm), followed by a decreasing ramp of the same cross-sections for 10 millisec such that the original configuration recurred at 5 millisec. Cross-sections were chosen such that perturbation-theory (point-model) reactivities ranged between  $\pm 2$  percent. Delayed neutrons were neglected. Fast-group flux-distributions, computed using the WIGLE code (Cadwell, Henry, and Vigilotti 1964) are shown in figs. 8-3 and 8-4. Note the extreme flux tilt in the larger core.

Time-dependent reactivities are shown in figs. 8-5 and 8-6. The point-kinetics results are monotonically decreasing because fixed spatial shapes are used in computing them. The actual reactivity is greatly different because of the tilting of the flux shape. Reactivity actually increases for a short time, even though the fission cross-sections are decreasing, because of the time-dependent shape function in the defining integral for reactivity. The effect is exaggerated by the adiabatic model (Henry and Curlee 1958) because of the assumption that changes in the flux shape follow the material changes without time lag.

Amplitude functions  $n(t)$  are shown in figs. 8-7 and 8-8. It is very interesting that the point-reactor model underestimates the peak amplitude in fig. 8-7 by more than  $10^4$ . Even in the smaller core (fig. 8-8) the error is a factor of four. The comparison at 10 millisec is also interesting. (The fact that the adiabatic model is an overestimate is consistent with its overestimate of reactivity.)

The extreme response of the 240-cm core is not to be taken as a blanket condemnation of point-reactor dynamics. The example was invented to illustrate an extreme case. It does underscore our earlier remarks (chapter 1) about pitfalls of injudicious application of the point

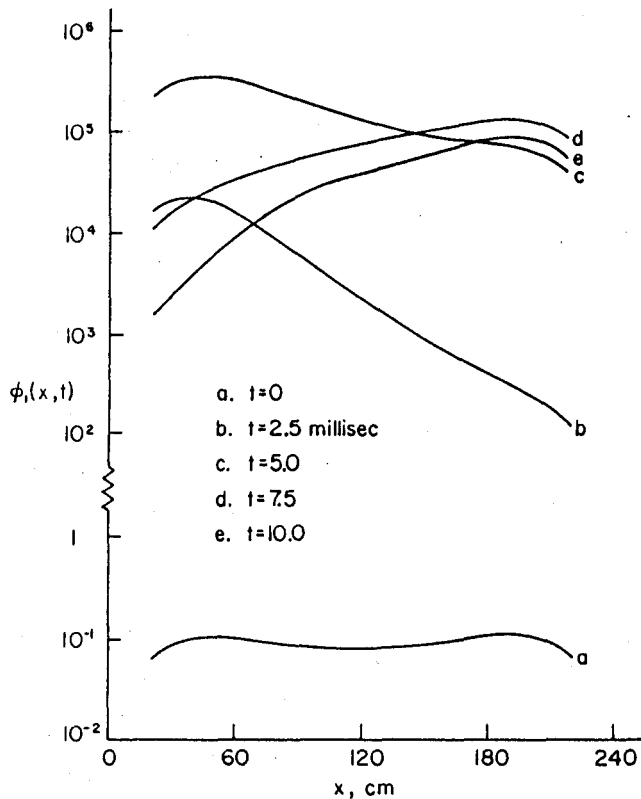


Fig. 8-3. Fast-group flux distributions for a fast excursion in the 240-cm core (Yasinsky and Henry 1965).

model, particularly for highly asymmetric transients in large reactors.

Thermal-group flux distributions are shown in figs. 8-9 and 8-10. Continuous-synthesis computations, using three trial functions in the larger core and two in the smaller, are included for comparison. Two nodal methods were also studied, but the results are not included here; see Yasinsky and Henry (1965) for details. Comparisons of total power and of neutron-detector response with the amplitude function for each excursion are also given by Yasinsky and Henry; the amplitude function is a fair representation of the power but is very poorly correlated with the detector response.

The delayed-critical excursions in the same two cores were induced by ramp increases of fission cross-sections from critical. The ramps were then halted (at 0.8 sec for the larger core and 1.0 sec for the smaller core)

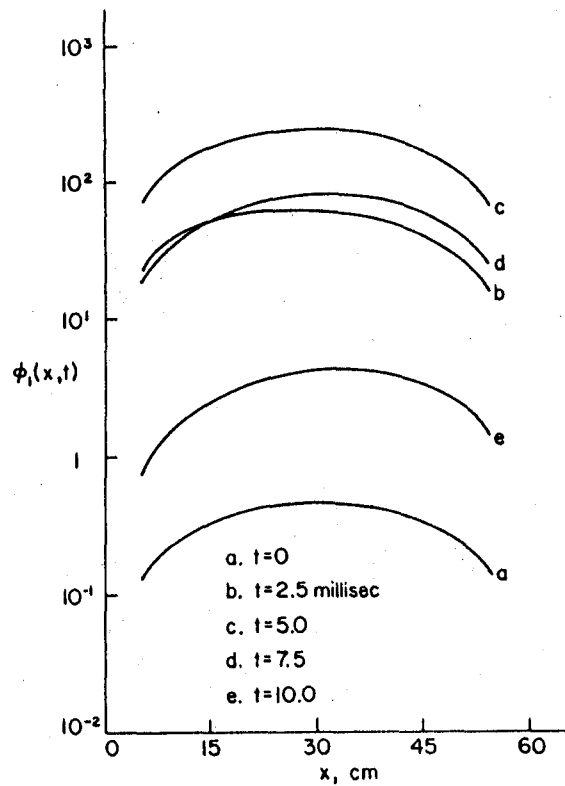


Fig. 8-4. Fast-group flux distributions for a fast excursion in the 60-cm core (Yasinsky and Henry 1965).

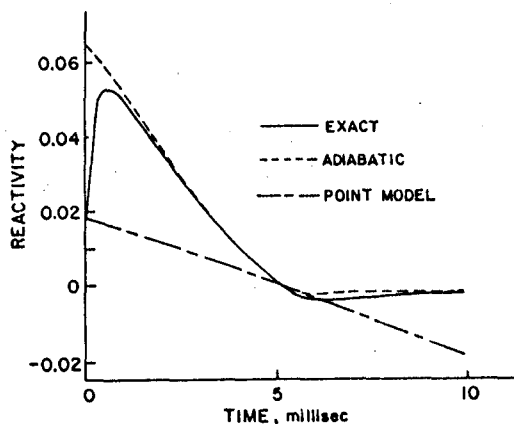


Fig. 8-5. Reactivity vs. time for a fast excursion in the 240-cm core (Yasinsky and Henry 1965).

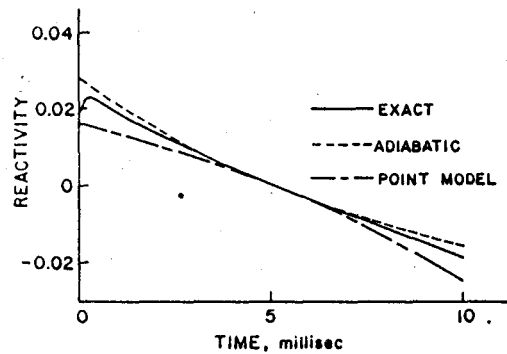


Fig. 8-6. Reactivity vs. time for a fast excursion in the 60-cm core (Yasinsky and Henry 1965).

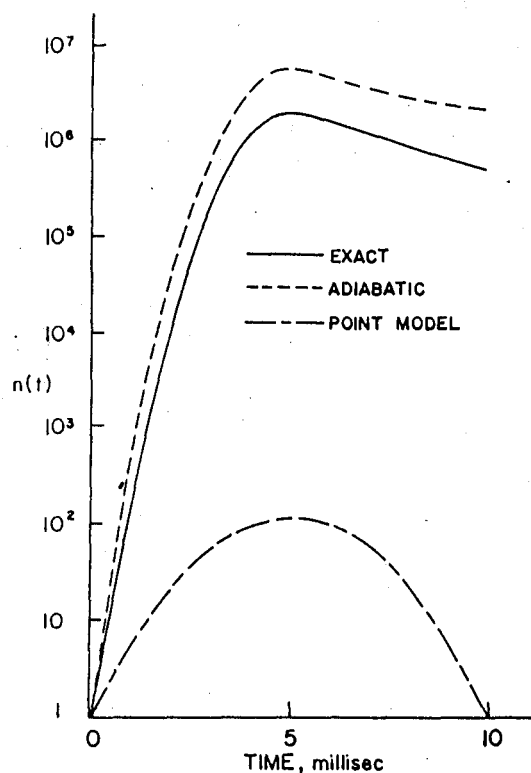


Fig. 8-7. Amplitude function vs. time for a fast excursion in the 240-cm core (Yasinsky and Henry 1965).

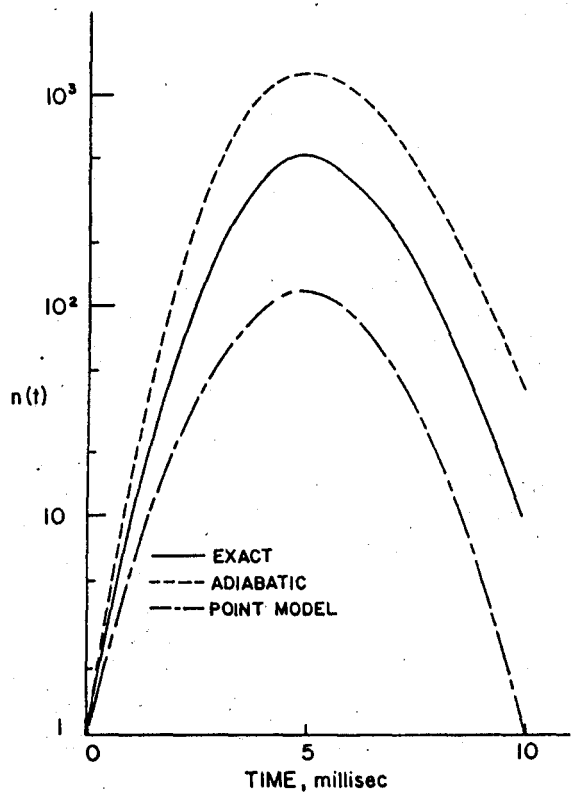


Fig. 8-8. Amplitude function vs. time for a fast excursion in the 60-cm core (Yasinsky and Henry 1965).

and the cross-sections held constant thereafter until  $t = 100$  sec. Reactivities remained below prompt critical at all times, although one could anticipate a case (to be shown later) where the point-model reactivity might be less than prompt critical when the actual reactivity is above prompt critical because of flux tilting.

One group of delayed neutrons was used in these examples. Thermal flux distributions, at the instants when the fission cross-sections stopped increasing, are shown in figs. 8-11 and 8-12. The smaller core is fairly well described by the point model, but the larger core shows that the peak in the flux shape can be underestimated by a factor of three.

These examples show dramatically that spatial effects can be extremely important. Even in the smaller core, the point-reactor model yielded disappointingly poor results for a fast excursion in spite of the lack of extreme flux tilting (see figs. 8-4 and 8-8).

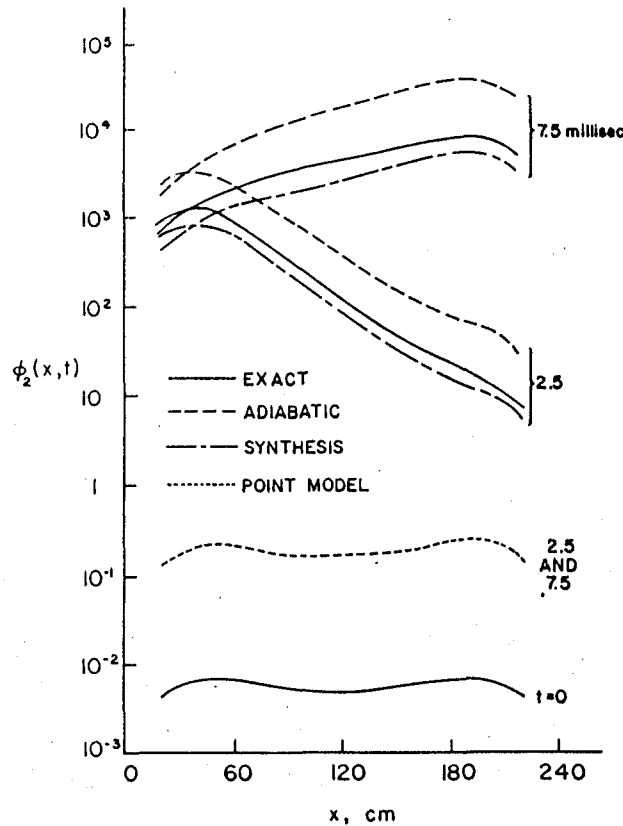


Fig. 8-9. Thermal-group flux distributions for a fast excursion in the 240-cm core (Yasinsky and Henry 1965).

The figures showing thermal-flux distributions indicate the successful use of the continuous-synthesis approximation in these examples. The fast excursion in the 240-cm core was also analyzed by Yasinsky (1967) using time-discontinuous synthesis. Numerical experiments using multichannel space-time synthesis were performed by Stacey (1968). One of these examples, an asymmetric control-rod insertion, is reproduced in figs. 8-13 and 8-14. Single and multichannel synthesis results are compared with an exact solution using the RAUMZEIT code (Adams and Stacey 1967). Note the presence of a large flux tilt, which would be reflected as a large error in the shutdown reactivity and the asymptotic power using the point model.

Examples of the quasi-static method are reproduced from the paper by Ott and Meneley (1969). Fig. 8-15 shows reactivity vs. time, com-

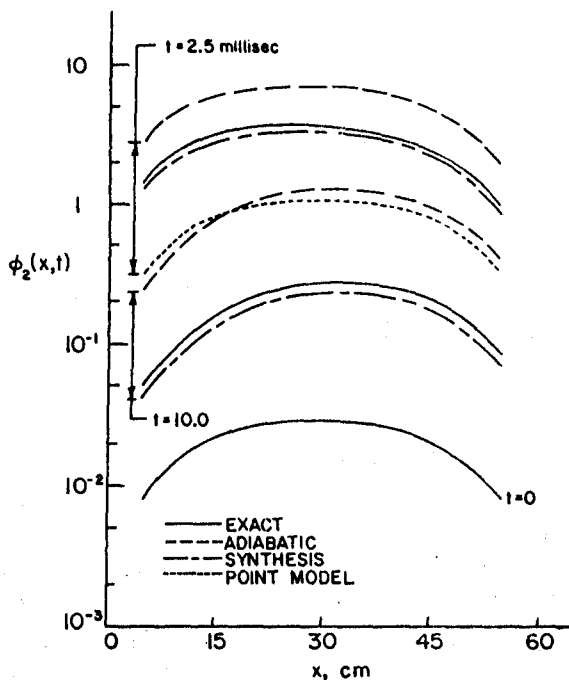


Fig. 8-10. Thermal-group flux distributions for a fast excursion in the 60-cm core (Yasinsky and Henry 1965).

paring the point-model result, an exact calculation, and the result obtained by using the quasi-static code QX-1 (Meneley, Ott, and Wiener 1967). This example is for a rapid ramp increase of  $v$  in one quarter of the 240-cm core used by Yasinsky and Henry (1965). One group of delayed neutrons was used. Note the significant effect of flux tilting on the final reactivity.

A slower excursion is shown in fig. 8-16. At the end of the ramp, the point reactivity is not large, but the exact reactivity is one dollar and is increasing. As noted earlier, the adiabatic result would be expected to overestimate the reactivity during the ramp.

The difference between the final asymptotic shape and the shape at the end of the ramp is shown in fig. 8-17. The precursor distribution at the end of the ramp is also included; it is nearly the same as the initial flux shape, and most of its change occurs after the ramp is terminated.

Numerical comparisons of several multimode methods are reported by Fuller (1969). A one-dimensional reactor 240 cm thick was perturbed by a ramp increase in the fission cross-section, confined to a symmetrical central slab 30 cm thick, and continued for 0.1 sec. The cross-section

was then held constant until  $t = 1$  sec, and the amplitude functions, reciprocal periods, and shape functions were compared at that time. The example quoted here is a super-prompt critical excursion. The WIGLE code was used to obtain the exact solution. Initial and final shapes for the half slab are shown in fig. 8-18.

Table 8-1. Results at  $t = 1$  sec for Space-dependent Reactor Excursion  
Using Various Approximations

	Reciprocal Period (sec <sup>-1</sup> )	Amplitude Function
Exact solution (WIGLE code)	29.51	$3.94 \times 10^{12}$
Point-reactor model	8.84	$4.87 \times 10^4$
Continuous synthesis (good trial functions)	29.51	$3.93 \times 10^{12}$
Two nodes (initial shape as trial function)	12.99	$1.71 \times 10^6$
Five nodes (initial shape as trial function)	17.87	$1.23 \times 10^8$
Eight nodes (initial shape as trial function)	21.55	$3.19 \times 10^9$
Ten nodes (initial shape as trial function)	26.70	$3.17 \times 10^{11}$
One channel (poor trial functions)	9.92	$1.24 \times 10^5$
Two channels (poor trial functions)	20.51	$1.26 \times 10^9$
Three channels (poor trial functions)	24.56	$4.64 \times 10^{10}$
Four channels (poor trial functions)	24.58	$4.72 \times 10^{10}$
Two channels (good trial functions)	29.57	$4.15 \times 10^{12}$

SOURCE: Fuller 1969.

Results are summarized in table 8-1. The slight shape change shown in fig. 8-18 has a profound effect on the ultimate result, as evidenced by the prediction of the point model.

Continuous synthesis was used with two trial functions (the initial and final shapes from fig. 8-18) and Galerkin weighting. Tests using other trial functions and weighting functions showed very little change in the final shape function, with amplitude functions ranging from  $2.45 \times 10^{12}$  to  $5.24 \times 10^{12}$  (reciprocal periods ranging from 28.99 to 29.82). It was noted that the choice of weighting functions is more crucial when the trial functions are less carefully chosen (as might be expected).

A nodal method was tested that uses the initial shape as trial function and weighting function in each region (Galerkin weighting). This is an example of multichannel synthesis, with one mode in each channel. The interface conditions were derived from diffusion theory. Ten nodes yielded a fair representation of the final shape function (Fuller 1969), but more nodes would be needed for a good value of the amplitude function (see table 8-1).

Fuller (1969) also reported a two-mode multichannel synthesis with Galerkin weighting that uses the initial shape and a deliberately poor second trial function (peaking between 15 and 30 cm on either side of

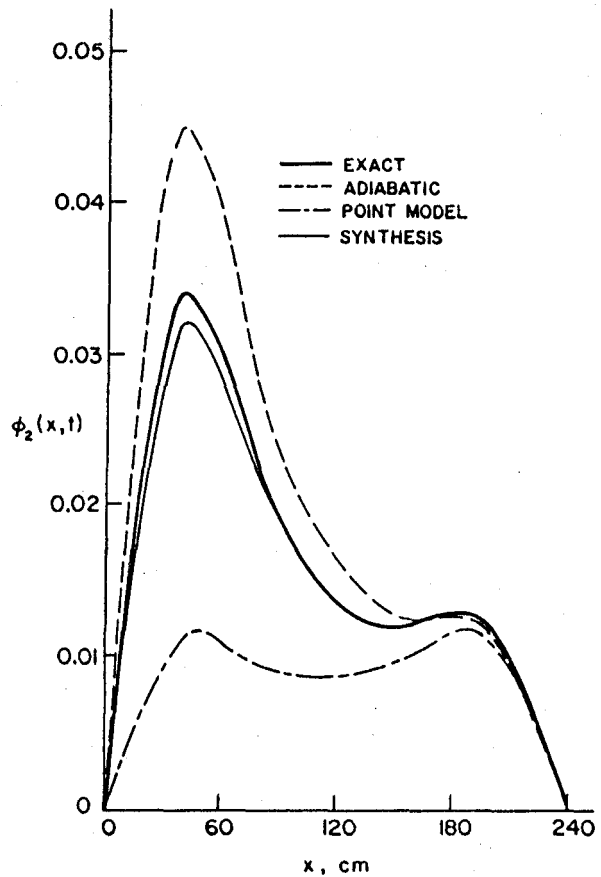


Fig. 8-11. Thermal-group flux distributions for a slow excursion in the 240-cm core (Yasinsky and Henry 1965).

the center). The amplitude functions for these four cases in table 8-1 are not good, although only three channels yielded a fair approximation to the final shape. Finally, a two-channel result using good trial functions is included for comparison.<sup>2</sup>

Other numerical studies using the synthesis method are reported by Kaplan, Marlowe, and Bewick (1964), Rydin (1968), and Yasinsky (1968b). Numerical results for the semidiscrete method are given by Andrews and Hansen (1968). An analysis of rod-ejection accidents that compares point-model results with space-time finite-difference calculations is reported by Yasinsky (1970). Much more work is needed, particularly in comparing different methods using a single fixed set of

2. E. L. Fuller, Argonne National Laboratory, private communication (1970).

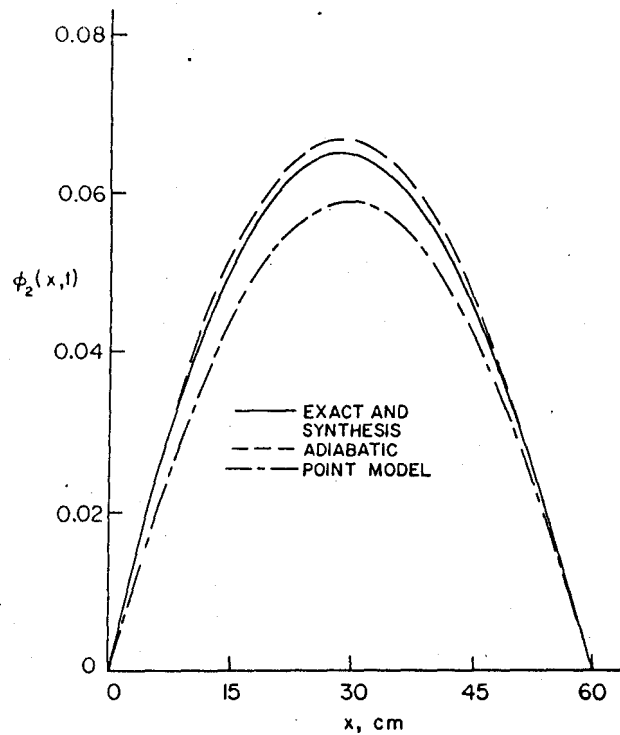


Fig. 8-12. Thermal-group flux distributions for a slow excursion in the 60-cm core (Yasinsky and Henry 1965).

test problems. The comparisons should include not only tests of accuracy but also meaningful comparisons of computer running time, so that reasonable judgements can be made in selecting methods for solving practical problems.

Of course, many practical problems encountered by the engineer will have special complexities. The combination of spatial and spectral effects can be very difficult to predict accurately. Safety calculations in large reactors can be further complicated when coolant voids, fuel motion, or other physical and chemical effects are nonuniformly distributed. The goal in this chapter has been very modest, and we have not attempted to treat these complex phenomena.

#### 8-5. Pulsed Sources

When an intense neutron pulse of brief duration is injected into an assembly (either nonmultiplying or subcritical), the subsequent decay of the neutron distribution may be followed by fast detectors, and the results may be used to infer many properties of the assembly. Thermal

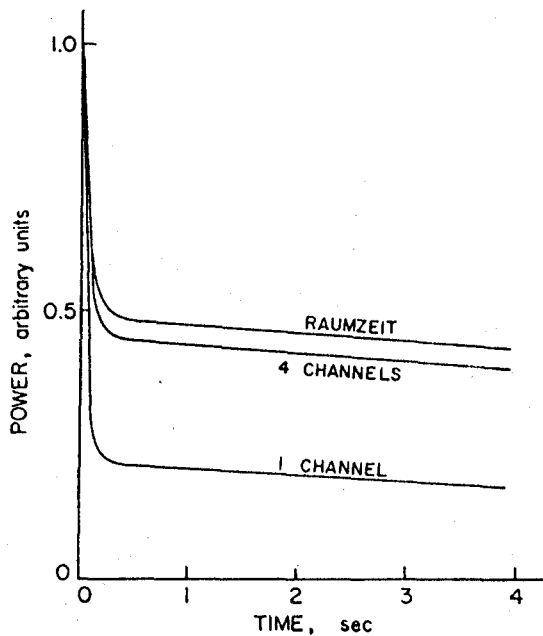


Fig. 8-13. Power vs. time following asymmetric control-rod insertion (Stacey 1968).

diffusion properties may be measured (Beckurts 1957; Lopez and Beyster 1962; Davis, DeJuren, and Reier 1965). Neutron spectra can be observed and the moderation process studied (Beyster et al. 1961; Profio and Eckard 1964; Chen and Lidofsky 1967). Other applications are measurements in fast nonmoderating assemblies (Beghian et al. 1963), studies of heterogeneity effects in lattices (Deniz, Le Ho, and Sagot 1968), and investigations of neutron shielding (Channon and Seale 1967). The reader may also consult the treatise by Beckurts and Wirtz (1964), the proceedings of the symposium at Karlsruhe (IAEA 1965), and the comprehensive review by Cokinos (1966); the latter article has an exhaustive bibliography. The neutron source itself may be a target in the beam of a charged-particle accelerator or it may be a pulsed reactor; see Motz and Keepin (1966) or Stahl, Russell, and Hopkins (1966).

The theory can become quite involved.<sup>3</sup> We present here only a few

3. Some important theoretical papers are by Nelkin (1960), Purohit (1961), Corngold, Michael, and Wollman (1963), Daitch and Ebeoglu (1963), Garelis (1963), Vérites (1963), Clendenin (1964), Cockrell, Perez, and Dalton (1964), Garelis (1964a), Judge and Daitch (1964), Daitch, Lee, and Hobson (1966), Erdmann and Luria (1967), and Devogaught and Machgeels (1968). Other references are cited later in connection with the topics of subcritical reactivity measurements and of continuum eigenvalues.

elementary ideas to introduce the subject. Starting with one-speed diffusion theory, eq. (1-1), we may write

$$\frac{1}{v} \frac{\partial \phi}{\partial t} = D \nabla^2 \phi - \Sigma_a \phi + S_0, \quad (8-59)$$

where  $\phi$  is the neutron flux  $Nv$ . For a nonmultiplying assembly, let  $S_0$  be an impulse in time with an unspecified spatial distribution. Following the neutron burst, we have  $S_0 = 0$  and we seek a solution in the form

$$\phi = A \cos Bx e^{-\lambda t} \quad \text{or} \quad A e^{iBx - \lambda t}, \quad (8-60)$$

where we assume a one-dimensional case for simplicity. This is another example of space and time separability, with the spatial part satisfying a Helmholtz equation as in chapter 1. More properly, we have a separable term for each mode, and the complete solution is a linear superposition that reflects the source distribution.

Substitution in eq. (8-59) with  $S_0 = 0$  yields

$$\lambda = DvB^2 + v\Sigma_a, \quad (8-61)$$

which gives a relation between the decay constant  $\lambda$  and the buckling  $B^2$ . Subscripts on  $\lambda$  and  $B$  could be used to indicate that eq. (8-61) holds separately for each spatial mode. Since  $B^2$  is smallest for the fundamental mode,  $\lambda$  for that mode is smallest and the asymptotic decay is controlled by the fundamental mode. We shall refer to  $\lambda$  as the fundamental-mode decay constant or eigenvalue. Eq. (8-61) is often called a "dispersion law" for reasons that will appear in the section on neutron waves.

Referring to sec. 1-2, we may write eq. (8-61) as

$$\lambda = v\Sigma_a(1 + L^2 B^2) = \frac{1 + L^2 B^2}{\ell_\infty} = \frac{1}{\ell_0}, \quad (8-62)$$

as could have been anticipated from the discussion of neutron lifetime. This viewpoint may help clarify the notion of a particular lifetime associated with each mode in the neutron distribution.

Returning to eq. (8-61), we see how an experiment may be performed. Taking only the asymptotic part of the detector response, we determine the fundamental-mode decay constant  $\lambda$  for each of a set of assemblies of different size. The buckling  $B^2$  may be determined by calculation or by auxiliary measurements with a judiciously located steady source. A graph of  $\lambda$  vs.  $B^2$  should then be a straight line whose slope is  $Dv$  and whose intercepts are  $v\Sigma_a$  (the reciprocal of  $\ell_\infty$ ) and  $-1/L^2$ , as shown in Fig. 8-19.

The dots in fig. 8-19 represent experimental data for graphite (Beckurts 1957). The departure from the straight line for larger  $B^2$

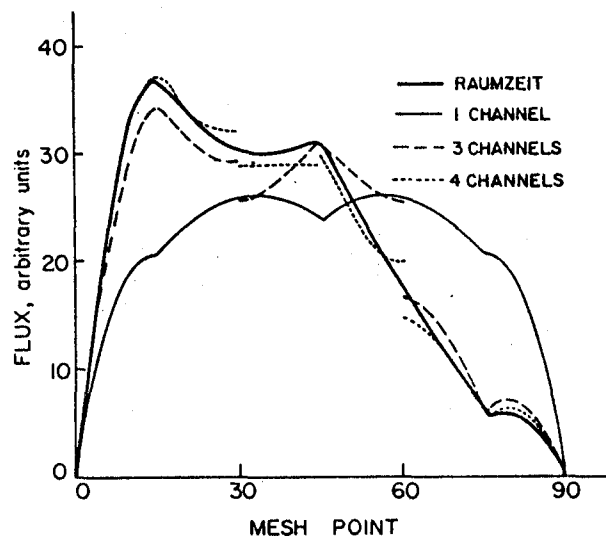


Fig. 8-14. Flux distributions 0.5 sec after asymmetric control-rod insertion (Stacey 1968).

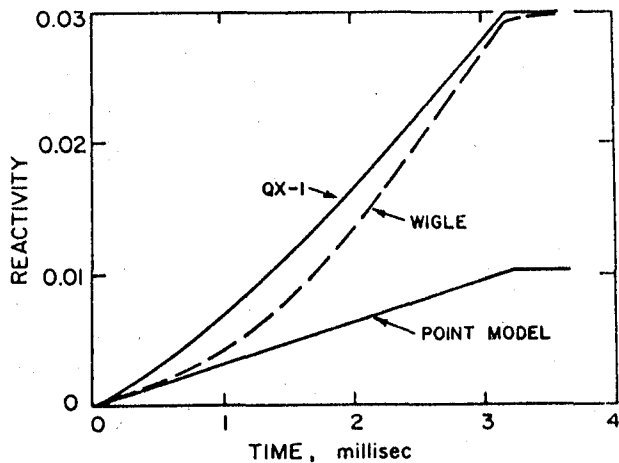
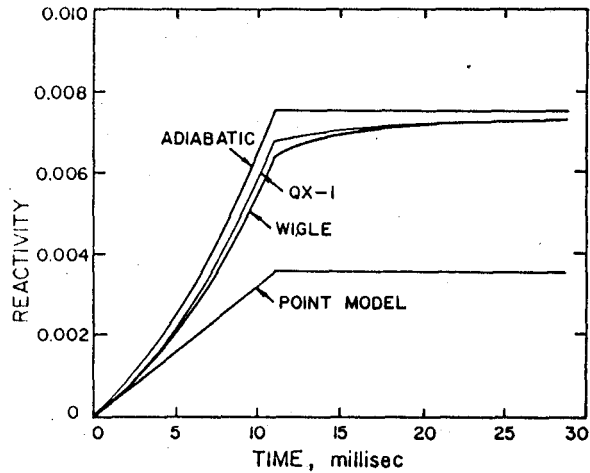
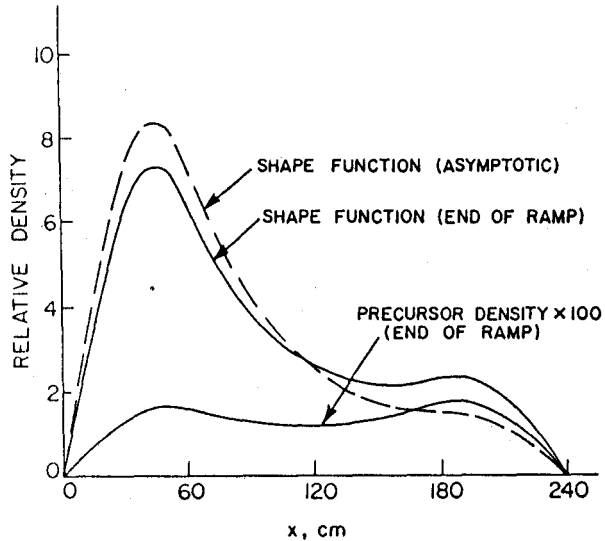


Fig. 8-15. Reactivity vs. time for fast ramp increase of  $v$  (Ott and Meneley 1969).

(smaller systems) is typical and indicates the failure of the simple theory. Such data have often been represented by the formula

$$\lambda = A_0 + A_1 B^2 + A_2 B^4 + \dots, \quad (8-63)$$

where  $A_1$  is  $Dv$  and  $A_2$  is called the diffusion-cooling coefficient (Lamarche 1966).

Fig. 8-16. Reactivity vs. time for limited ramp increase of  $v$  (Ott and Meneley, 1969).Fig. 8-17. Shape functions and precursor distribution for limited ramp increase of  $v$  (Ott and Meneley 1969).

For a multiplying assembly, we may use eq. (1-2). Neglecting the production rate of delayed neutrons, we have

$$S = (1 - \beta)k_{\infty}\Sigma_a\phi + S_0. \quad (8-64)$$

Assume that the pulse decays according to eq. (8-60). We may use

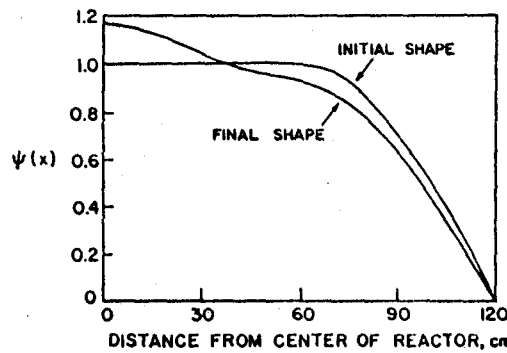


Fig. 8-18. Initial and final shapes for a super-prompt critical excursion (Fuller 1969).

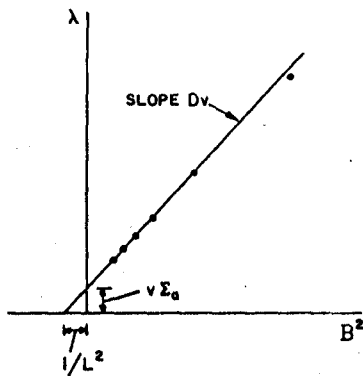


Fig. 8-19. Decay constant vs. buckling for a pulsed-source experiment in graphite (Beckurts 1957).

eq. (8-59) with  $\Sigma_a$  replaced by  $\Sigma_a - (1 - \beta)k_{\infty}\Sigma_a$ . We find

$$\lambda = DvB^2 + [1 - (1 - \beta)k_{\infty}]v\Sigma_a. \quad (8-65)$$

Referring to sec. 1-2, we may write eq. (8-65) as

$$\lambda = \frac{1 - (1 - \beta)k}{\ell_0} \quad (8-66)$$

or as

$$\lambda = \frac{\beta - \rho}{\ell}, \quad (8-67)$$

where  $\ell$  is the neutron generation time. Eq. (8-67) is of course anticipated from the point-reactor model. (The choice of the symbol  $\lambda$  for the decay constant is perhaps unfortunate, but it has become common; the

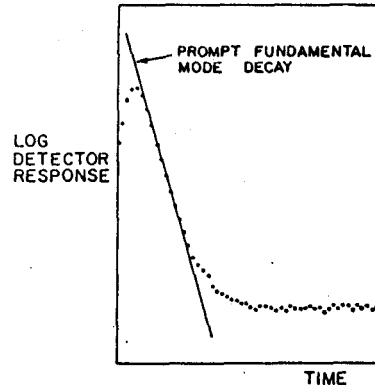


Fig. 8-20. Neutron pulse decay in a subcritical system (Masters and Cady 1967).

symbol  $\alpha$  is also used, but we reserve it for the neutron-wave attenuation factor.)

We conclude that the decay of the fundamental mode in a subcritical assembly is controlled by the largest negative root of the inhour equation, at least until delayed neutrons appear. This prompt decay is followed by a delayed-neutron tail, much like that of the impulse response in fig. 2-10. A typical experimental run, reported by Masters and Cady (1967), is shown in fig. 8-20. The possibility of measuring the reactivity is seen from eq. (8-67).<sup>4</sup>

Extrapolating the delayed-neutron background back to zero time in fig. 8-20 suggests that the background could be subtracted from the total, separating the neutron population into two parts. We use the point-reactor model in the form

$$\frac{dn_p}{dt} = \frac{\rho - \beta}{\ell} n_p + q, \quad (8-68)$$

$$\frac{dn_d}{dt} = \frac{\rho - \beta}{\ell} n_d + \sum_i \lambda_i c_i, \quad (8-69)$$

and

$$\frac{dc_i}{dt} = \frac{\beta_i}{\ell} (n_p + n_d) - \lambda_i c_i, \quad (8-70)$$

4. Pulsed-neutron reactivity measurements are discussed by Sjostrand (1956), Simmons and King (1958), Simmons (1959), Kolar and Kloverstrom (1961), Gozani (1962), Garellis and Russell (1963), Garellis (1964b), Sastre and Weinstock (1964), Wallace (1965), Wallace, Teare, and Green (1966), Mihalczo (1968), and Rotter (1969). Measurements on a critical assembly are reported by Bendt, Karr, and Scott (1958). The theory of pulsed multiplying assemblies is discussed by Fultz (1959), Krieger and Zweifel (1959), Ghatak and Pearlstein (1965), Judge and Daitch (1966), and Jenkins and Daitch (1968). A review is given by Becker and Quisenberry (1966).

where  $n = n_p + n_d$ , the sum of a prompt and a delayed contribution. Let  $q$  be an impulse  $q_0\delta(t)$ , and integrate from  $t = 0$  to  $\infty$ . Assuming that all variables are zero both initially and finally, we find

$$0 = \frac{\rho - \beta}{\ell} A_p + q_0, \quad (8-71)$$

$$0 = \frac{\rho - \beta}{\ell} A_d + \sum_i \lambda_i A_i, \quad (8-72)$$

and

$$0 = \frac{\beta_i}{\ell} (A_p + A_d) - \lambda_i A_i, \quad (8-73)$$

where

$$A_p = \int_0^\infty n_p dt,$$

$$A_d = \int_0^\infty n_d dt,$$

$$A_i = \int_0^\infty c_i dt.$$

We identify  $A_d$  as the area under the delayed-neutron tail, extrapolated back to zero time, and  $A_p$  as the remaining area under the prompt burst. We use eq. (8-73) to eliminate  $A_i$ , with the result

$$\frac{\rho}{\beta} = -\frac{A_p}{A_d}. \quad (8-74)$$

This formula is the key to the area-ratio method of pulsed-neutron reactivity measurements (Sjostrand 1956).

The extrapolated-area method was proposed in an attempt to correct for the presence of higher spatial modes (Gozani 1962). Eq. (8-74) is replaced by

$$\frac{\rho}{\beta} = -e^{\lambda t_w} \frac{\int_{t_w}^\infty n_p dt}{\int_0^\infty n_d dt}, \quad (8-75)$$

where  $t_w$  is a waiting time sufficient for the prompt decay to become asymptotic. The asymptotic prompt-decay curve is thus extrapolated back to zero time, and the higher modes are bypassed.

## Independent Neutron Dynamics

The reactor method is based on eq. (8-67) in the form

$$\frac{\rho}{\beta} = 1 - \lambda \frac{\ell}{\beta}. \quad (8-76)$$

The reactivity can be calculated from the measured decay constant  $\lambda$  if  $\ell/\beta$  is known. The measurement of  $\ell/\beta$  is made by a repetitive pulsing technique.

Suppose the system is pulsed every  $T$  seconds such that  $T$  is large compared to the prompt decay time but small compared to the shortest precursor decay time. The delayed-neutron background will then achieve a quasi-equilibrium. From eqs. (8-69) and (8-70),

$$\bar{n}_d = -\frac{\beta}{\rho} \bar{n}_p, \quad (8-77)$$

where the bar signifies time average. To find  $\bar{n}_p$ , we may average over one cycle. From eq. (8-68) with  $q = q_0 \delta(t)$ ,

$$n_p = q_0 e^{-\lambda t}, \quad 0 < t < T. \quad (8-78)$$

Since  $T \gg 1/\lambda$ , the average is

$$\bar{n}_p = \frac{1}{T} \int_0^T n_p dt \cong \frac{1}{T} \int_0^\infty n_p dt = \frac{q_0}{\lambda T}, \quad (8-79)$$

where the second integral refers to a single pulse. We therefore have

$$\bar{n}_d = -\frac{\beta q_0}{\rho \lambda T}. \quad (8-80)$$

Using eqs. (8-78) and (8-80), we may verify the following identity:

$$\int_0^T n_p e^{(\beta/\ell)t} dt - \int_0^T n_p dt = \bar{n}_d T. \quad (8-81)$$

The parameter  $\beta/\ell$  is chosen such that eq. (8-81) is satisfied by the numerical data. Eq. (8-76) then yields the reactivity.

The success of this method is much greater than indicated in this derivation using the point-reactor model. The technique was proposed and verified by Garellis and Russell (1963), who obtained eq. (8-81) using a modal expansion. The method has come to be known as the  $k\beta/\ell$  method, because the exponent in eq. (8-81) would be  $k\beta/\ell$  if  $\ell$  were the lifetime instead of the generation time.

Using diffusion theory it may be shown that  $-\lambda$  is the algebraically largest member of a set of discrete eigenvalues. However, neutron transport effects become important close to sources and boundaries, and diffusion theory is inadequate for small systems. A complete

solution of a transport-theory problem consists of a sum of eigenfunctions, each corresponding to a discrete eigenvalue, plus an integral over a continuum of singular eigenfunctions corresponding to a continuum of eigenvalues (Case and Zweifel 1967). The discrete functions are closely related to those in diffusion theory, especially when the absorption is not large. The continuum, which is not present in diffusion theory, becomes increasingly important near sources and boundaries, especially when the absorption is large.

The possibility arises in small pulsed systems that the eigenvalue corresponding to the lowest discrete mode may be near the bound of the continuum or even inside the continuum range. The observed decay curve may be difficult to interpret, and the asymptotic decay might not be very close to a pure exponential.

We illustrate with a simple example from one-speed transport theory. Consider the equation

$$\frac{\partial \psi}{\partial t} + \mu v \frac{\partial \psi}{\partial x} + v \Sigma_s \psi = \frac{1}{2} v \Sigma_s \int_{-1}^1 \psi(x, \mu, t) d\mu, \quad (8-82)$$

where  $\psi(x, \mu, t) d\mu$  is the number of neutrons per unit volume having velocity vectors with direction cosines between  $\mu$  and  $\mu + d\mu$ . Eq. (8-82) is a one-dimensional, one-speed special case of eq. (8-1) for isotropic scattering. If we try

$$\psi(x, \mu, t) = A(\mu) e^{jBx - \lambda t}, \quad (8-83)$$

we find

$$(-\lambda + jB\mu v + v\Sigma_s) \psi = \frac{1}{2} v \Sigma_s \int_{-1}^1 \psi d\mu. \quad (8-84)$$

Discrete eigenfunctions generated from eq. (8-84) are similar to those of diffusion theory. However, singular eigenfunctions appear whenever

$$-\lambda + v\Sigma_s + jB\mu v = 0, \quad (8-85)$$

with the right-hand side of eq. (8-84) remaining finite. Eq. (8-85) represents the continuum boundary, and it is seen that complex values of  $\lambda$  must be considered in deriving a complete solution. With more detailed transport-theory models, the structure of the complex  $\lambda$ -plane can be very complicated.<sup>5</sup>

<sup>5</sup> Corngold (1964), Corngold and Michael (1964), Travelli and Culame (1964), Corngold (1965), Ghatak and Honeck (1965), Kothari (1965), Leonard (1965), Corngold (1966), Ghatak and Kothari (1966), Mockel (1966), Williams (1966), Corngold and Durgun (1967), Ritchie and Rainbow (1967), Ahmed and Ghatak (1968), Dorning (1968), Dorning and Thurber (1968a), Conn and Corngold (1969), Dorning, Nicolaenko, and Thurber (1969), Kuscer (1969), and Nguyen (1969).

### *Space-Dependent Neutron Dynamics*

Depending on the representation used, models can be constructed in which the discrete modes are submerged in the continuum or, for small systems, the discrete modes may cease to exist. This latter possibility has been formalized by Corngold (1964), as a theorem which states that in the presence of velocity dependence there exists a maximum  $B^2$  beyond which no discrete eigenvalue exists. However, experiments appear to produce discrete values for  $\lambda$  beyond the Corngold limit. One possible explanation is that the distribution of continuum eigenfunctions is very strongly peaked in a small neighborhood and that this would be very difficult to distinguish from a single discrete mode. On the other hand, it is sometimes possible to recover a discrete eigenvalue by the device of analytic continuation in the  $\lambda$ -plane (Conn and Corngold 1969). The theoretical question may be regarded as not completely resolved. We shall reconsider the continuum briefly in the context of neutron waves.

#### **8-6. Neutron Waves**

The propagation of waves through a neutron population in a diffusing medium was studied theoretically by Cahn, Monk, and Weinberg (1945) and by Weinberg and Schweinler (1948). Experimental observations were made by Raievski and Horowitz (1954, 1955), who measured the "complex diffusion length" using a technique analogous to Angstrom's cyclic method of measuring thermal conductivity (Carslaw and Jaeger 1959). In a diffusion equation, the presence of a first time derivative ensures that attenuation is always present (except at zero frequency). Otherwise, the wave solutions are essentially the same as those for other types of partial differential equations.

The transfer functions that we have derived from the point-reactor model are adiabatic in the sense that the flux is assumed to maintain a fixed shape throughout the reactor, rising and falling in synchronization with the oscillating source or absorber. This picture breaks down at high frequencies and large distances from the source, and the localized fluctuations are propagated as attenuated waves. This may be interpreted in terms of a space-dependent transfer function (Hansson and Foulke 1963; Kylstra and Uhrig 1965; Loewe 1965; Cohn, Johnson, and Macdonald 1966; Saji 1968; Bridges, Clement and Renier 1969). Another viewpoint is that the transfer function is an integral property defined in terms of weighted averages and that the space-dependent dynamic effects are manifestations of the weighting functions. This viewpoint has some theoretical merit, but it tends to obscure the wave propagation.

An experimental research program in neutron waves was initiated in 1962, at the University of Florida, that used a modulated charged-

particle beam, a neutron-producing target, and a thermalizer (Perez and Uhrig 1962; Perez, Booth, and Hartley 1963; Perez and Uhrig 1963; Booth, Hartley, and Perez 1967; Ohanian, Booth, and Perez 1967; Perez and Uhrig 1967). Advances in this area and related fields are reported in the symposium volume edited by Uhrig 1967). The dispersion law for the neutron field was investigated theoretically by Moore (1964, 1965, 1967a). The  $P_1$  approximation has been used by Mortensen and Smith (1965) and by Quddus, Cochran, and Emon (1969).

Transport theory was applied to neutron waves by Moore (1966a), Brehm (1967), Travelli (1967, 1968), and Warner and Erdmann (1969a). Reflection and refraction have been studied by Kladnik (1968) and by Baldonado and Erdmann (1969). Velocity-dependent transport theory has been applied to wave propagation in crystalline moderators by Ahmed, Grover, and Kothari (1968a, 1968b), Duderstadt (1968), Bansal, Ghatak, and Ahmed (1969), Kumar, Ahmed, and Kothari (1969), Tewari and Kothari (1969), Warner and Erdmann (1969b), and Nishina and Akcasu (1970).

The propagation of neutron pulses, which can be analyzed in terms of sinusoidal waves, has been studied by Miley (1965), Cheung and Miley (1966), Moore (1966b), Miley, Tsoulfanidis, and Doshi (1967), Moore (1967b), Booth, Hartley, and Perez (1967), Doshi and Miley (1968, 1970), Takahashi and Sumita (1968), Golay and Cady (1969), and Ohanian and Diaz (1969). The use of pulse-propagation for determining subcritical reactivity is discussed by Ram (1968) and by Ram and Uhrig (1969).

Pulse decay, wave propagation, and pulse propagation are very closely related, as described, for example, in the review by Moore (1967a). The question of external vs. internal sources is also discussed in that paper. Some special experimental advantages are offered by new techniques using internally modulated sources (distributed slowing-down sources produced by entering fast-neutron beams or by accelerator targets inside a medium). For example, decay constants of higher modes can be measured directly (Foley and Seale 1969).

For illustration, consider a one-speed diffusion model of a non-multiplying medium. Let the source be

$$S(x, t) = S_0(x) + S(x) e^{i\omega t}, \quad (8-86)$$

where  $S_0(x)$  represents a steady source that by itself would yield a steady flux  $\phi_0(x)$ . The total flux is represented as  $\phi_0 + \phi$ , where the fluctuating component  $\phi$  satisfies

$$\frac{1}{v} \frac{\partial \phi}{\partial t} = D \nabla^2 \phi - \Sigma_a \phi \quad (8-87)$$

far from the source.

Let the fluctuating part of the flux be represented as

$$\phi = A e^{j(kx + \omega t)}. \quad (8-88)$$

Substitution into eq. (8-87) yields

$$-j\omega = Dv k^2 + v\Sigma_a, \quad (8-89)$$

which is identified as a dispersion law relating the frequency  $\omega$  and the complex propagation constant  $k$ . This may be compared with eq. (8-61) for the decay of a neutron pulse:

$$\lambda = Dv B^2 + v\Sigma_a,$$

which is the same dispersion law with  $\omega$  replaced by  $j\lambda$  and  $k$  replaced by  $B$ . One therefore speaks of "complex decay constants" and "complex bucklings." Note that eq. (8-89) could be written

$$Dv k^2 + v\Sigma_a^c = 0,$$

where  $\Sigma_a^c$  is a "complex absorption cross-section" given by

$$\Sigma_a^c = \Sigma_a + j\omega/v. \quad (8-90)$$

This may also be interpreted in terms of a complex diffusion length (Raievski and Horowitz 1955).

An attenuated plane wave traveling in the positive  $x$ -direction may be represented by

$$\phi = A e^{-\alpha x + j(\omega t - \xi x)}, \quad (8-91)$$

where  $\alpha$  and  $\xi$  are the attenuation and phase constants respectively ( $\alpha$  is the reciprocal of the attenuation length for the envelope of the wave shape, and  $\xi$  is  $2\pi$  divided by the wavelength). Comparing eqs. (8-88) and (8-91) we have

$$k = j\alpha - \xi. \quad (8-92)$$

We substitute eq. (8-92) into eq. (8-89) and equate separately the real and imaginary parts, with the result

$$\alpha^2 - \xi^2 = \frac{\Sigma_a}{D} = \frac{1}{L^2}, \quad (8-93)$$

$$\alpha\xi = \frac{\omega}{2Dv}. \quad (8-94)$$

This suggests that  $L^2$  and  $Dv$  could be experimentally determined from observations of  $\alpha$ ,  $\xi$ , and  $\omega$ .

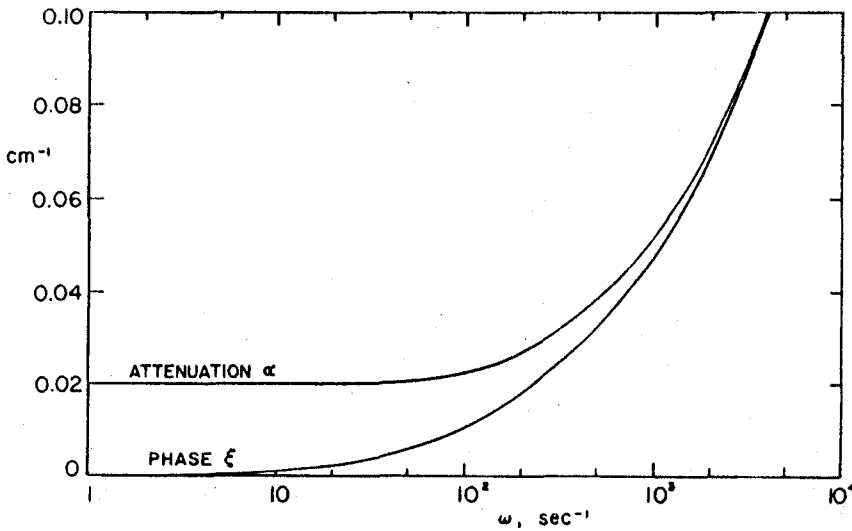


Fig. 8-21. Attenuation and phase constants for a thermal-neutron wave in graphite.

Measurements for thermal neutrons in graphite were reported by Perez, Booth, and Hartley (1963). A linear variation of  $\alpha\xi$  with  $\omega$  was observed. The quantity  $\alpha^2 - \xi^2$  was not a constant, but rather a linear function of  $\omega^2$ , indicating a departure from the simple theory and a means of measuring the diffusion-cooling coefficient.

Eqs. (8-93) and (8-94) may be combined to yield

$$\alpha^2 = \frac{1}{2L^2} + \frac{1}{2} \sqrt{\left(\frac{1}{L^4} + \frac{\omega^2}{D^2v^2}\right)}, \quad (8-95)$$

$$\xi^2 = -\frac{1}{2L^2} + \frac{1}{2} \sqrt{\left(\frac{1}{L^4} + \frac{\omega^2}{D^2v^2}\right)}. \quad (8-96)$$

As  $\omega \rightarrow 0$  we have  $\alpha \rightarrow 1/L$  and  $\xi \rightarrow 0$ , as expected. For small  $\omega$ ,  $\xi$  is approximately  $L\omega/2Dv$ . For large  $\omega$ ,  $\alpha$  and  $\xi$  approach a common value  $(\omega/2Dv)^{\frac{1}{2}}$ . The phase velocity is given by  $\omega/\xi$ , and it is  $2Dv/L$  as  $\omega \rightarrow 0$  and  $(2Dv\omega)^{\frac{1}{2}}$  for large  $\omega$ . Sample calculations are shown in figs. 8-21 and 8-22 for infinite-medium plane waves of thermal neutrons in graphite ( $L = 50$  cm,  $Dv = 2 \times 10^5$  sec $^{-1}$ ). Fig. 8-23 shows the  $\alpha$ ,  $\xi$  plane with  $\omega$  as a parameter (a common way to represent a dispersion law).

A propagating pulse of neutrons may be represented as a superposition

$$f(x, t) = \int_{-\infty}^{\infty} F(x, \omega) e^{i\omega t} d\omega. \quad (8-97)$$

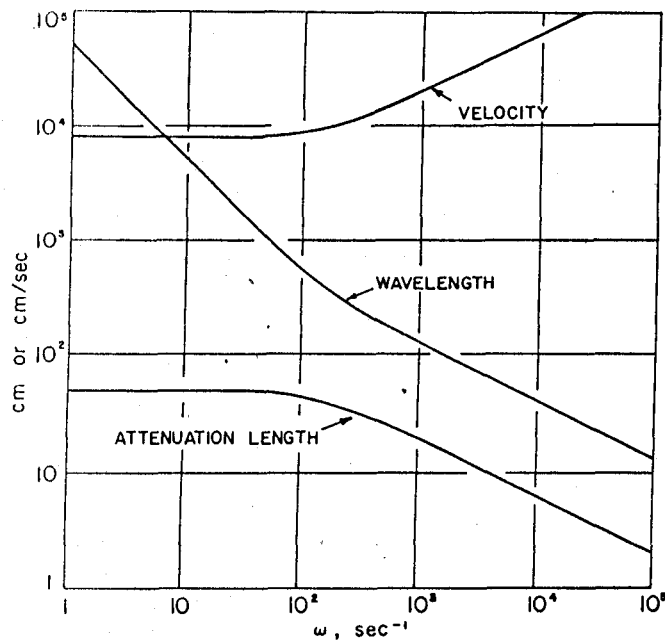


Fig. 8-22. Velocity, wavelength, and attenuation length for a thermal-neutron wave in graphite.

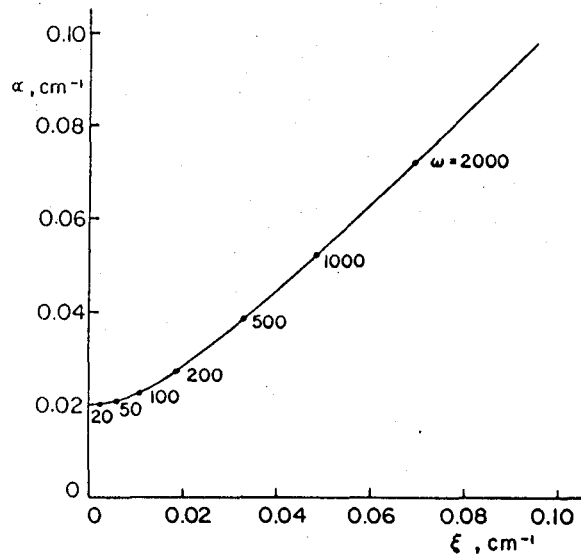


Fig. 8-23. Parametric dispersion law for a thermal-neutron wave in graphite.

A single pulse-propagation experiment contains information about all frequencies, and the information may in principle be recovered by Fourier analysis of the numerical data.

The dispersion law may be generalized to include higher spatial modes. However, as in the case of neutron pulse decay, a complete solution in transport theory contains not only the discrete modes that are closely related to the diffusion-theory modes but also an integral over a continuum of singular eigenfunctions. The significance for neutron waves has been discussed by many authors (e.g., Moore 1966a; Brehm 1967; Travelli 1967; Dorning and Thurber 1968b; Duderstadt 1968; Williams 1968; Warner and Erdmann 1969b).

We illustrate with the one-speed transport-theory model of eq. (8-82). Let

$$\psi(x, \mu, t) = A(\mu) e^{j(kx + \omega t)}. \quad (8-98)$$

The continuum corresponds to the vanishing of the operator on the left-hand side of eq. (8-82). The continuum for wave propagation is therefore

$$j\omega + jk\mu v + v\Sigma_t = 0. \quad (8-99)$$

Using eq. (8-92) and separating into real and imaginary parts, we find

$$\alpha := \frac{1}{\mu} \Sigma_t \quad (8-100)$$

and

$$\xi = \frac{\omega}{\mu v}. \quad (8-101)$$

From eq. (8-100), we see that the continuum corresponds to a neutron beam whose direction cosine is  $\mu$  and whose attenuation is dictated by the total removal cross-section. The wave velocity is

$$\frac{\omega}{\xi} = \mu v, \quad (8-102)$$

which is the  $x$ -component of the neutron velocity. Eqs. (8-100) and (8-101) describe the behavior of the continuum contribution, which is always present to some degree. In the usual terminology these equations are called the continuum conditions, and are regarded as separate from the dispersion law. After all, the continuum wave velocity is independent of the frequency, a characteristic of a nondispersive medium. However, one could regard the continuum conditions as part of the dispersion law in the same sense that the continuum eigenvalues belong to the complex eigenvalue spectrum of the transport operator.

Since  $\mu$  varies from  $-1$  to  $1$ , it is often stated that eqs. (8-100) and (8-101) with  $|\mu| = 1$  represent the boundary of the continuum. This is proper only in the sense that one could indicate the region  $\alpha > \Sigma_i$  in a graph such as that shown in fig. 8-23 as the continuum region. It does not mean that an observed wave having  $\alpha < \Sigma_i$  is purely a discrete mode and one having  $\alpha > \Sigma_i$  is entirely in the continuum. There is no sharp transition, although a wave experiment for sufficiently large  $\omega$  may approach the continuum boundary in the  $\alpha, \xi$  plane with the continuum contribution becoming increasingly important as  $\omega$  increases.

It can be shown that the continuum becomes dominant when the excitation frequency approaches the mean collision frequency  $v\Sigma_i$ , even though the detector is far from sources or boundaries. This is analogous to the situation with neutron-pulse decay in small systems. The wave problem at high frequencies is particularly difficult in small systems, and some mathematical models predict the nonexistence of discrete modes. It is more satisfying physically to think of smooth transitions from primarily asymptotic (discrete) behavior to predominantly continuum-type behavior as the frequency is increased and the size reduced.

Many fascinating possibilities remain to be explored. It seems certain that neutron-wave techniques will become increasingly important both in basic research and in applied reactor analysis. Recent advances in this and other areas of neutron dynamics are described in papers presented at the 1970 University of Arizona symposium (*Dynamics of Nuclear Systems*. [Tucson: University of Arizona Press, forthcoming]).

### Problems

- 8-1. Derive eq. (8-7) from eqs. (8-1) and (8-6).
- 8-2. Derive the perturbation-theory reactivity formula, eq. (8-15).
- 8-3. Show that the neutron generation time is numerically equal to the reactivity change produced by a uniform change in absorption cross-section  

$$\delta\Sigma_a = -1/v.$$
- 8-4. Derive a perturbation-theory formula for reactivity in the multi-mode dynamics formulation.
- 8-5. Explain qualitatively how a spatial xenon instability could be induced by withdrawing control rods from one region of a reactor and simultaneously inserting control rods in another region without changing the total power.

- 8-6. Derive the fundamental formula for the area-ratio method, eq. (8-74).
- 8-7. Derive the Garelis-Russell formula, eq. (8-81).
- 8-8. Derive the neutron-wave attenuation and phase constants, eqs. (8-95) and (8-96).
- 8-9. Using the definition of group velocity in a dispersive medium

$$v_g = \frac{\partial \omega}{\partial \xi},$$

derive a diffusion-theory formula for group velocity of a thermal-neutron wave. Compare with the phase velocity obtained from  $\omega/\xi$ .

- 8-10. Analyze the propagation of thermal-neutron waves in a multiplying medium using diffusion theory.



---

## Bibliography

Entries in the bibliography are arranged alphabetically, with each author's works listed chronologically. Reports issued by national laboratories and federal contractors in the United States are identified by letters and numbers (e.g., ANL-5577, KAPL-3359). These documents are available in libraries designated as Atomic Energy Commission repositories, and they may also be obtained from the Clearinghouse for Federal Scientific and Technical Information, U.S. Department of Commerce, Springfield, Virginia 22151.

Certain conference proceedings are identified as books published by the United States Atomic Energy Commission, Division of Technical Information Extension, Oak Ridge, Tennessee. These are also available from the Clearinghouse in Springfield, Virginia.

Government laboratory reports from countries other than the United States are specifically identified as such (e.g., United Kingdom Atomic Energy Authority report AERE-RP/M-47).

Papers from the three international conferences on the peaceful uses of atomic energy in Geneva, Switzerland (1955, 1958, and 1964) are identified in the same way as journal articles, with the abbreviation *Proc. Geneva Conf.* followed by the volume and page number.

Abramowitz, M., and Stegun, I. A. 1964. *Handbook of mathematical functions*. Washington, D.C.: National Bureau of Standards.

Ackroyd, R. T.; Kinchin, G. H.; Mann, J. E.; and McCullen, J. D. 1958. Stability considerations in the design of fast reactors. *Proc. Geneva Conf.* 12:230.

Adams, C. H., and Stacey, W. M., Jr. 1967. RAUMZEIT: A program to solve coupled time-dependent diffusion equations in one space dimension. KAPL-M-6728.

- Adler, F. T. 1961. Reactor kinetics: Integral equation formulation. *J. Nucl. Energy* 15:81.
- Agresta, J. 1961. Stability studies on fast reactors with delayed reactivity coefficients. NDA 2147-7.
- Agresta, J., and Borst, L. B. 1960. Space-dependent prompt kinetics of a subcritical reactor. *Nucl. Sci. Eng.* 7:64.
- Ahmed, F., and Ghatak, A. K. 1968. On the space-energy separability of the fundamental mode of the neutron transport operator with isotropic scattering. *Nucl. Sci. Eng.* 33:106.
- Ahmed, F.; Grover, P. S.; and Kothari, L. S. 1968a. Neutron-wave propagation through a crystalline moderator. Pt. 1, Beryllium. *Nucl. Sci. Eng.* 31:484.
- . 1968b. Neutron-wave propagation through a crystalline moderator. Pt. 2, Graphite. *Nucl. Sci. Eng.* 34:33.
- Aizerman, M. A. 1958. *Lectures in the theory of automatic control*. (In Russian.) Moscow. English translation, *Theory of automatic control*. Reading, Mass.: Addison-Wesley, 1963.
- Akcasu, A. Z. 1958. General solution of the reactor kinetic equations without feedback. *Nucl. Sci. Eng.* 3:456.
- . 1960. Theoretical feedback analysis in boiling water reactors. ANL-6221.
- . 1966. Local stability in reactors with a linear feedback. *Nucl. Sci. Eng.* 24:88.
- Akcasu, A. Z., and Dalfes, A. 1960. A study of nonlinear reactor dynamics. *Nucl. Sci. Eng.* 8:89.
- Akcasu, A. Z.; Lellouche, G. S.; and Shotkin, L. M. *Mathematical methods in reactor dynamics*. New York: Academic Press, forthcoming.
- Akcasu, A. Z., and Noble, L. D. 1966a. A nonlinear study of reactors with a linear feedback. *Nucl. Sci. Eng.* 25:47.
- . 1966b. Lagrange stability in reactors with a linear feedback. *Nucl. Sci. Eng.* 25:427.
- Akcasu, A. Z., and Shotkin, L. M. 1967. Power oscillations and the describing function in reactors with linear feedback. *Nucl. Sci. Eng.* 28:72.
- . 1968. Approximate zero-power describing function valid at all frequencies. *Nucl. Sci. Eng.* 32:271.
- Albrecht, R. W. 1962. The measurement of dynamic nuclear reactor parameters using the variance of the number of neutrons detected. *Nucl. Sci. Eng.* 14:153.

- Alcouffe, R. E., and Albrecht, R. W. 1970. A generalization of the finite difference approximation method with an application to space-time nuclear reactor kinetics. *Nucl. Sci. Eng.* 39:1.
- Andrews, J. B. II, and Hansen, K. F. 1968. Numerical solution of the time-dependent multigroup diffusion equations. *Nucl. Sci. Eng.* 31:304.
- Argonne National Laboratory. 1963a. Reactor physics constants. ANL-5800.
- . 1963b. Proceedings of the conference on breeding, economics, and safety in large fast power reactors. ANL-6792.
- . 1965. Proceedings of the conference on safety, fuels, and core design in large fast power reactors. ANL-7120.
- . 1966. Proceedings of the international conference on fast critical experiments and their analysis. ANL-7320.
- Ash, M. 1956. Solutions of the reactor kinetics equations for time varying reactivities. *J. Appl. Phys.* 27:1030.
- . 1965. *Nuclear Reactor Kinetics*. New York: McGraw-Hill.
- Atoms International. 1959. Annual technical progress report, AEC unclassified programs, fiscal year 1959. NAA-SR-3850.
- Auerbach, T.; Mennig, J.; and Sarlos, G. 1968. The application of Lie series to time dependent reactor theory. In Proceedings of the Brookhaven conference on industrial needs and academic research in reactor kinetics. BNL 50117 (T-497).
- Austin, A. L. 1964. Thermally induced vibrations of concentric thin spherical shells. *Nucl. Sci. Eng.* 20:45.
- Avery, R. 1958. Theory of coupled reactors. *Proc. Geneva Conf.* 12:182.
- Azzoni, P.; Carpenè, A.; DeCecco, L.; and Randles, J. 1969. A contribution to the theory of uncontrolled prompt critical excursions in liquid metal cooled fast reactors. *J. Nucl. Energy* 23:315.
- Baldonado, O. C., and Erdmann, R. C. 1969. Numerical results of interfacial effects on neutron waves. *Nucl. Sci. Eng.* 37:59.
- Baldwin, G. C. 1959. Kinetics of a reactor composed of two loosely coupled cores. *Nucl. Sci. Eng.* 6:320.
- Bansal, N. K.; Ghatak, A. K.; and Ahmed, F. 1969. Neutron wave propagation through graphite. *J. Nucl. Energy* 23:439.
- Baran, W., and Meyer, K. 1966. Effect of delayed neutrons on the stability of a nuclear power reactor. *Nucl. Sci. Eng.* 24:356.
- Barrett, P. R., and Thompson, J. J. 1969. Stochastic models of power reactor dynamics. *J. Nucl. Energy* 23:147.

- Barton, D. R.; Bennett, G. L.; and Carpenter, W. R. 1965. Power Burst Facility preliminary safety analysis report. IDO-17060.
- Becker, M. 1964. *The principles and applications of variational methods*. Cambridge, Mass.: M.I.T. Press.
- . 1965. On the inclusion of boundary terms in time-dependent synthesis techniques. *Nucl. Sci. Eng.* 22:384.
- . 1968a. A generalized formulation of point nuclear reactor kinetics equations. *Nucl. Sci. Eng.* 31:458.
- . 1968b. Asymmetric discontinuities in synthesis techniques for initial-value problems. *Nucl. Sci. Eng.* 34:343.
- Becker, M., and Quisenberry, K. S. 1966. Spatial dependence of pulsed neutron reactivity measurements. In *Neutron dynamics and control*, ed. D. L. Hetrick and L. E. Weaver, Oak Ridge, Tenn.: USAEC Division of Technical Information Extension.
- Beckjord, E. S. 1958. Dynamic analysis of natural circulation boiling water power reactors. ANL-5799.
- Beckurts, K. H. 1957. Measurements with a pulsed neutron source. *Nucl. Sci. Eng.* 2:516.
- Beckurts, K. H., and Wirtz, K., 1964. *Neutron physics*. German edition, 1958. Berlin: Springer-Verlag.
- Beghian, L. E.; Rasmussen, N. C.; Thews, R.; and Weber, J. 1963. The investigation of neutron kinetics and cross sections in fast non-moderating assemblies by the nanosecond pulsed neutron source technique. *Nucl. Sci. Eng.* 15:375.
- Bell, G. I., and Glasstone, S. 1970. *Nuclear reactor theory: An advanced course*. New York: Van Nostrand Reinhold.
- Belleni-Morante, A. 1963. Solution of the nuclear reactor kinetics equations by a method of successive approximations. *J. Nucl. Energy* 17:439.
- Bendt, P. J.; Karr, H. J.; and Scott, F. R. 1958. Prompt neutron periods of a critical assembly measured with a pulsed source. *Nucl. Sci. Eng.* 4:703.
- Bernstein, S.; Ergen, W. K.; Talbot, F. L.; Leslie, J. K.; and Stanford, C. P. 1956. Yield of photoneutrons from  $U^{235}$  fission products in beryllium and deuterium. *J. Appl. Phys.* 27:18.
- Bernstein, S.; Preston, W. M.; Wolfe, G.; and Slattery, R. E. 1947. Yield of photo-neutrons from  $U^{235}$  fission products in heavy water. *Phys. Rev.* 71:573.
- Bethe, H. A. 1956. Reactor safety and oscillator tests. APDA-117.

- Bethe, H. A., and Tait, J. H. 1956. An estimate of the order of magnitude of the explosion when the core of a fast reactor collapses. (U.S.-U.K. Reactor hazard meeting) United Kingdom Atomic Energy Authority report RHM(56)/113.
- Beyster, J. R., and Russell, J. L. 1965. Repetitively pulsed accelerator boosters. GA-6168.
- Beyster, J. R.; Wood, J. L.; Lopez, W. M.; and Walton, R. B. 1961. Measurements of neutron spectra in water, polyethylene, and zirconium hydride. *Nucl. Sci. Eng.* 9:168.
- Bilharz, H. 1944. Bemerkung zu einem Satz von Hurwitz. *Z. Angew. Math. Mech.* 24:77.
- Birkhoff, G. 1966. Numerical solution of the reactor kinetics equations. In *Numerical solutions of nonlinear differential equations*, ed. D. Greenspan, New York: Wiley.
- Blaesser, G., and Larrimore, J. A. 1969. Discrete kinetics for periodically pulsed fast reactors. *Nucl. Sci. Eng.* 37:186.
- Blaine, R. A., and Berland, R. F. 1965. A reactor system dynamics code: AIROS. In Proceedings of the conference on the application of computing methods to reactor problems, ed. M. Butler, ANL-7050.
- Bodenschatz, C. A.; James, L. R.; Steiner, G. H.; and Wasserman, A. A. 1966. NRX/EST reactor transfer functions. Pt. 1, Power to temperature transfer functions. *Trans. Am. Nucl. Soc.* 9:327.
- Bogoliubov, N. N., and Mitropolsky, Y. A. 1961. *Asymptotic methods in the theory of non-linear oscillations*. New York: Gordon and Breach.
- Bondarenko, I. I., and Staviskii, Yu. Ya. 1961. Pulsed operation of a fast reactor. *Atomnaya Energiya* 7:417 (1959). English translation, *J. Nucl. Energy* 14:55.
- Booth, R. S.; Hartley, R. H.; and Perez, R. B. 1967. On the experimental application of the neutron-wave technique to thermal-neutron systems. *Nucl. Sci. Eng.* 28:404.
- Braess, D.; Küsters, H.; and Thurnay, K. 1967. Improvement in second excursion calculations. In *Proceedings of the international conference on the safety of fast reactors* (Aix-en-Provence, 19–22 September 1967), ed. G. Denielou. Paris: Documentation Française.
- Brehm, R. L. 1967. Analysis of neutron-wave type experiments. In *Neutron Noise, Waves, and Pulse Propagation*, ed. R. E. Uhrig. Oak Ridge, Tenn.: USAEC Division of Technical Information Extension.

- . 1969. Application of the variable gradient method of generating Liapunov functions to problems in reactor stability. *Trans. Am. Nucl. Soc.* 12:737.
- Brehm, R. L., Hetrick, D. L., and Schmidt, T. R. 1969. Stability studies of in-core thermionic reactor concepts. *Nucl. Appl. Tech.* 7:117.
- Brickstock, A.; Davies, A. R.; and Smith, I. C. 1965. A time-dependent multigroup diffusion code with automatic self-shielding of cross sections. In *Proceedings of the conference on the application of computing methods to reactor problems*, ed. M. Butler. ANL-7050.
- Bridges, D. N.; Clement, J. D.; and Renier, J. P. 1969. A method for calculating space-dependent reactor source transfer functions with feedback. *Nucl. Sci. Eng.* 36:122.
- Brittan, R. O. 1956. Some problems in the safety of fast reactors. ANL-5577.
- . 1958. Analysis of the EBR-I core meltdown. *Proc. Geneva Conf.* 12:267.
- Brookhaven National Laboratory. 1968. Proceedings of the Brookhaven conference on industrial needs and academic research in reactor kinetics. BNL 50117 (T-497).
- Brown, H. D. 1957. A general treatment of flux transients. *Nucl. Sci. Eng.* 2:687.
- Burgreen, D. 1967. Thermoelastic dynamics of a pulse reactor. *Nucl. Sci. Eng.* 30:317.
- Bussard, R. W., and DeLauer, R. D. 1958. *Nuclear rocket propulsion*. New York: McGraw-Hill.
- Cadwell, W. R.; Henry, A. F.; and Vigilotti, A. J. 1964. WIGLE: A program for the solution of the two-group space-time diffusion equations in slab geometry. WAPD-TM-416.
- Cahn, A., Jr.; Monk, A. T.; and Weinberg, A. M. 1945. Theory of oscillating absorber in a chain reacting pile. CP-2907.
- Canosa, J. 1964. Dynamics of an adiabatic point reactor. *Nucl. Sci. Eng.* 19:392.
- . 1967a. A new method for nonlinear reactor dynamics problems. *Nukleonik* 9:289.
- . 1967b. Spatial distribution of the energy released in a power excursion. *Trans. Am. Nucl. Soc.* 10:247.
- . 1968a. The effect of delayed neutrons on reactor excursions with ramp reactivity insertion. *Nukleonik* 11:131.

- . 1968b. Comments on two papers on the nonlinear diffusion equation. *Nucl. Sci. Eng.* 32:156.
- . 1969. Diffusion in nonlinear multiplicative media. *J. Math. Phys.* 10:1862.
- Canosa, J., and Brooks, H. 1966. Xenon-induced oscillations. *Nucl. Sci. Eng.* 26:237.
- Carslaw, H. S., and Jaeger, J. C. 1959. *Conduction of heat in solids*. 2d ed. Oxford: Clarendon Press.
- Carter, J. C.; Sparks, D. W.; and Tessier, J. H. 1964. Period effect in reactor dynamics. In *Reactor kinetics and control*, ed. L. E. Weaver. Oak Ridge, Tenn.: USAEC Division of Technical Information Extension.
- Case, K. M., and Zweifel, P. F. 1967. *Linear transport theory*. Reading, Mass.: Addison-Wesley.
- Cesari, L. 1959. *Asymptotic behavior and stability problems in ordinary differential equations*. Berlin: Springer-Verlag.
- Channon, F. R., and Seale, R. L. 1967. The study of thermal neutrons in shields containing ducts by source-separation techniques. *Nucl. Sci. Eng.* 30:242.
- Chapin, D. M. 1969. On the step-response method of determining the zero-power reactor transfer function. *Nucl. Sci. Eng.* 36:113.
- Chen, S., and Lidofsky, L. J. 1967. Spatial dependence of slowing down times for 14.1-Mev neutrons in water. *Nucl. Sci. Eng.* 29:198.
- Chernick, J. 1951. The dependence of reactor kinetics on temperature. BNL 173 (T-30).
- . 1962. A review of nonlinear reactor dynamics problems. BNL 774 (T-291).
- Chestnut, H., and Mayer, R. W. 1951. *Servomechanisms and regulating system design*. New York: Wiley.
- Cheung, K. Y., and Miley, G. H. 1966. On thermal-neutron pulse propagation. *Nucl. Sci. Eng.* 24:216.
- Chezem, C. G., and Köhler, W. H., eds. 1967. *Coupled reactor kinetics*. College Station, Tex.: Texas A. & M. Press.
- Clark, M., Jr., and Hansen, K. F. 1964. *Numerical methods of reactor analysis*. New York: Academic Press.
- Clendenin, W. W. 1964. Temperature dependence of neutron-pulse parameters in  $H_2O$ . *Nucl. Sci. Eng.* 18:351.
- Coats, R. L., and O'Brien, P. D. 1968. Pulse characteristics of Sandia pulsed reactor II. *Trans. Am. Nucl. Soc.* 11:219.

- Cockrell, R. G.; Perez, R. B.; and Dalton, G. R. 1964. One-speed transport study of fast neutron pulses in non-moderating media. *Nucl. Sci. Eng.* 19:423.
- Coddington, E. A., and Levinson, N. 1955. *Theory of ordinary differential equations*. New York : McGraw-Hill.
- Cofler, C. D.; Dee, J. B.; Shoptaugh, J. R., Jr.; West, G. B.; and Whittemore, W. L. 1966. Characteristics of large reactivity insertions in a high-performance TRIGA uranium-zirconium hydride core. In *Neutron dynamics and control*, ed. D. L. Hetrick and L. E. Weaver. Oak Ridge, Tenn: USAEC Division of Technical Information Extension.
- Cohen, E. R. 1958. Some topics in reactor kinetics. *Proc. Geneva Conf.* 11:302.
- Cohn, C. E. 1960. A simplified theory of pile noise. *Nucl. Sci. Eng.* 7:472.
- . 1962. Reflected-reactor kinetics. *Nucl. Sci. Eng.* 13:12.
- Cohn, C. E.; Johnson, R. J.; and Macdonald, R. N. 1966. Calculating space-dependent reactor transfer functions using statics techniques. *Nucl. Sci. Eng.* 26:198.
- Cokinos, D. 1966. The physics of pulsed neutrons. In *Advances in nuclear science and technology*, vol. 3, ed. P. Greebler and E. J. Henley. New York : Academic Press.
- Conn, R., and Corngold, N. 1969. A theory of pulsed neutron experiments in polycrystalline media. *Nucl. Sci. Eng.* 37:85. Analysis of pulsed neutron experiments in polycrystalline media using a model kernel. *Nucl. Sci. Eng.* 37:94.
- Corben, H. C. 1959a. Analysis of the zero power reactor transfer function. *Nucl. Sci. Eng.* 6:461.
- . 1959b. The computation of excess reactivity from power traces. *Nucl. Sci. Eng.* 5:127.
- Corngold, N. 1964. Some transient phenomena in thermalization. Pt. 1, Theory. *Nucl. Sci. Eng.* 19:80.
- . 1965. Decay constant of a neutron pulse. *Nucl. Sci. Eng.* 23:403.
- . 1966. On the maximum absorption theorem. *Nucl. Sci. Eng.* 24:410.
- Corngold, N., and Durgun, K. 1967. Analysis of pulsed neutron experiments in moderators via a simple model. *Nucl. Sci. Eng.* 29:354.
- Corngold, N., and Michael, P. 1964. Some transient phenomena in thermalization. Pt. 2, Implications for experiment. *Nucl. Sci. Eng.* 19:91.

- Corngold, N.; Michael, P.; and Wollman, W. 1963. The time decay constants in neutron thermalization. *Nucl. Sci. Eng.* 15:13.
- Coveyou, R. R., and Mulliken, T. W. 1948. Solution of the equation  $\dot{N} + (a + bt)\dot{N} + (c + dt)N = 0$ . AECD-2407.
- Crandall, S. H. 1956. *Engineering analysis*. New York: McGraw-Hill.
- Crank, J. 1956. *The mathematics of diffusion*. Oxford: Clarendon Press.
- Cunningham, W. J. 1958. *Introduction to nonlinear analysis*. New York: McGraw-Hill.
- \_\_\_\_\_. 1963. The concept of stability. *Amer. Sci.* 51:425.
- Curlee, N. J. 1959. Nonseparable space-time transients resulting from changes in inlet coolant temperature. *Nucl. Sci. Eng.* 6:1.
- Daitch, P. B., and Ebeoglu, D. B. 1963. Asymptotic and transient analysis of pulsed moderators. *Nucl. Sci. Eng.* 17:212.
- Daitch, P. B.; Lee, R. R.; and Hobson, H. L. 1966. Analysis of pulsed neutron experiments in moderating assemblies. In *Neutron dynamics and control*, ed. D. L. Hetrick and L. E. Weaver. Oak Ridge, Tenn.: USAEC Division of Technical Information Extension.
- Davis, S. K.; DeJuren, J. A.; and Reier, M. 1965. Pulsed-decay and extrapolation-length measurements in graphite. *Nucl. Sci. Eng.* 23:74.
- Davison, B. 1957. *Neutron transport theory*. Oxford: Clarendon Press.
- deHoffman, F. 1944. Criticality of the water boiler and effective number of delayed neutrons. AECD-3051.
- Denielou, G., ed. 1967. *Proceedings of the international conference on the safety of fast reactors* (Aix-en-Provence, 19-22 September 1967). Paris: Documentation Française.
- Deniz, V. 1967. Study of the kinetics of thermalized neutron populations in multiplying or nonmultiplying heterogeneous media. *Nucl. Sci. Eng.* 28:397.
- Deniz, V.; Le Ho, J. G.; and Sagot, M. 1968. Study of lattices of graphite with empty channels by means of the pulsed source technique. *Nucl. Sci. Eng.* 32:201.
- DeShong, J. A., Jr. 1969. Dynamic analysis of liquid-metal-cooled fast power reactors. ANL-7529.
- DeShong, J. A., Jr., and Lipinski, W. C. 1958. Analyses of experimental power-reactivity feedback transfer functions for a natural circulation boiling water reactor. ANL-5850.
- Deverall, L. I. 1958. Solution of the time-dependent thermal neutron diffusion problem. *Nucl. Sci. Eng.* 4:495.

500      *Bibliography*

- Devooght, J., and Machgeels, C. 1968. A new synthesis method for pulsed-neutron experiments. *Nucl. Sci. Eng.* 32:82.
- Devooght, J., and Smets, H. B. 1967. Determination of stability domains in point reactor dynamics. *Nucl. Sci. Eng.* 28:226.
- Dickerman, C. E. 1964. Kinetics of the transient reactor test facility (TREAT). In *Reactor kinetics and control*, ed. L. E. Weaver. Oak Ridge, Tenn.: USAEC Division of Technical Information Extension.
- Dickerman, C. E.; Johnson, R. E.; and Gasidlo, J. 1962. Kinetics of TREAT used as a test reactor. ANL-6458.
- Dietrich, J. R. 1964. The reactor core. In *The technology of nuclear reactor safety*, vol. 1, ed. T. J. Thompson and J. G. Beckerley. Cambridge, Mass.: M.I.T. Press.
- Di Pasquantonio, F. 1968. Stability in the first approximation and a critical case relating to nuclear reactor kinetics equations. *Nukleonik* 11:276.
- Di Pasquantonio, F., and Kappel, F. 1970. Comments on theoretical and experimental criteria for reactor stability. *Nucl. Sci. Eng.* 39:133.
- Dorning, J. 1968. Thermal-neutron decay in small systems. *Nucl. Sci. Eng.* 33:65. Time-dependent neutron thermalization in finite light water systems. *Nucl. Sci. Eng.* 33:81.
- Dorning, J.; Nicolaenko, B.; and Thurber, J. K. 1969. The theory of pulse decay in subcritical fast systems with general cross sections. *Trans. Am. Nucl. Soc.* 12:656.
- Dorning, J., and Thurber, J. K. 1968a. An explanation of the apparent violation of the maximum absorption theorem. *Trans. Am. Nucl. Soc.* 11:579.
- . 1968b. Purely discrete neutron wave phenomena in the continuum region. *Trans. Am. Nucl. Soc.* 11:580.
- Doshi, P. K., and Miley, G. H. 1968. Reactor neutron pulse propagation in multiplying media. *Trans. Am. Nucl. Soc.* 11:191.
- . 1970. Neutron pulse propagation in a multiplying medium. *Nucl. Sci. Eng.* 39:182.
- Dougherty, D. E., and Shen, C. N. 1962. The space-time neutron kinetic equations obtained by the semi-direct variational method. *Nucl. Sci. Eng.* 13:141.
- Duderstadt, J. J. 1968. A transport theory of neutron wave propagation in polycrystalline media. *Nucl. Sci. Eng.* 33:119.
- Dunensfeld, M. S. 1961. Analyses of the dynamics of the kinetic experiment water boiler reactor. *Trans. Am. Nucl. Soc.* 4:70.

- , ed. 1962. Kinetic experiments on water boilers: "A" core report. Pt. 2, Analysis of results. NAA-SR-5416.
- Dunensfeld, M. S., and Gamble, D. P. 1959. Analytic solutions to KEWB kinetics equations for short period transients. *Trans. Am. Nucl. Soc.* 2(2):62.
- Dunensfeld, M. S., and Stitt, R. K. 1963. Summary review of the kinetics experiments on water boilers. NAA-SR-7087.
- Erdélyi, A. 1963. Singular perturbations of boundary value problems involving ordinary differential equations. *J. Soc. Ind. Appl. Math.* 11:105.
- Erdmann, R. C., and Lurie, H. 1967. A two-region problem in time-dependent monoenergetic neutron transport theory. *Nucl. Sci. Eng.* 28:190.
- Ergen, W. K. 1954. Kinetics of the circulating fuel reactor. *J. Appl. Phys.* 25:702.
- . 1965. Self-limiting power excursions in large reactors. *Trans. Am. Nucl. Soc.* 8:221.
- Ergen, W. K.; Lipkin, H. J.; and Nohel, J. A. 1957. Applications of Liapunov's second method in reactor dynamics. *J. Math. and Phys.* 36:36.
- Ergen, W. K., and Nohel, J. A. 1959. Stability of a continuous-medium reactor. *J. Nucl. Energy Part A* 10:14.
- Ergen, W. K., and Weinberg, A. M. 1954. Some aspects of non-linear reactor dynamics. *Physica* 20:413.
- Etherington, H., ed. 1958. *Nuclear engineering handbook*. New York: McGraw-Hill.
- Evans, J. W. 1964. A formulation for numerical solution of the inverse problem of the generalized reactor kinetics equations. LA-3045.
- Evans, W. R. 1950. Control system synthesis by root-locus method. *Trans. AIEE* 69:66.
- . 1954. *Control System Dynamics*. New York: McGraw-Hill.
- Farmer, F. R. 1963. Some basic safety considerations in the development of power-producing reactors. *Nucl. Safety* 5:1.
- Feynmann, R. P.; deHoffman, F.; and Serber R. 1956. Dispersion of the neutron emission in  $U^{235}$  fission. *J. Nucl. Energy Part A* 3:64.
- Flatt, H. P. 1962. The numerical solution of the reactor kinetics equations by the method of collocation. *Nucl. Computing Tech. Bull.* no. 5. Los Angeles: IBM Data Processing Div.

502      *Bibliography*

- . 1968. Reactor kinetics calculations. In *Computing methods in reactor physics*, ed. H. Greenspan, C. N. Kelber, and D. Okrent. New York : Gordon and Breach.
- Fleck, J. A., Jr. 1955. The temperature-dependent kinetics of circulating-fuel reactors. BNL-357 (T-65).
- . 1961. The influence of pressure on boiling water reactor dynamic behavior at atmospheric pressure. *Nucl. Sci. Eng.* 9:271.
- Foderaro, A., and Garabedian, H. L. 1962. Two-group reactor kinetics. *Nucl. Sci. Eng.* 14:22.
- Foley, J. E., and Seale, R. L. 1969. Measurement of thermal-neutron decay constants using a sinusoidal neutron source. *Trans. Am. Nucl. Soc.* 12:680.
- Forbes, S. G. 1958. Simple model for reactor shutdown. In Quarterly progress report, January, February, March, 1958, reactor projects branch, ed. G. O. Bright. IDO-16452.
- . 1959. Dependence of the  $k_c(t_m)$  vs  $\alpha$  function on reactor parameters. In Quarterly progress report, January, February, March, 1959, reactor projects branch, ed. J. A. Norberg. IDO-16539.
- Foulke, L. R., and Gyftopoulos, E. P. 1967. Application of the natural mode approximation to space-time reactor problems. *Nucl. Sci. Eng.* 30:419.
- Franz, J. P. 1949. Pile transfer functions. AECD-3260.
- Freund, G. A.; Iskenderian, H. P.; and Okrent, D. 1958. TREAT, A pulsed graphite-moderated reactor for kinetics experiments. *Proc. Geneva Conf.* 10:461.
- Fuchs, K. 1946. Efficiency for very slow assembly. LA-596.
- Fuller, E. L. 1969. Weighted-residual methods in space-dependent reactor dynamics. Ph.D. dissertation, University of Arizona. Published as ANL-7565.
- Fuller, E. L.; Meneley, D. A.; and Hetrick, D. L. 1969. Integration of the multimode kinetics equations by the method of undetermined parameters. *Trans. Am. Nucl. Soc.* 12:710.
- . 1970. Weighted residual methods in space-dependent reactor dynamics. *Nucl. Sci. Eng.* 40:206.
- Fultz, S. C. 1959. The time-dependent thermal neutron flux from a pulsed subcritical assembly. *Nucl. Sci. Eng.* 6:313.
- Galanin, A. D. 1960. *Thermal reactor theory*. New York : Pergamon Press.

- Galati, A. 1969. The metastatic method in nuclear reactor core kinetics calculations. *Nucl. Sci. Eng.* 37:30.
- Gamble, D. P. 1960. The effect of reflector-moderated neutrons on the kinetics of the Kinetic Experiment Water Boiler. *Trans. Am. Nucl. Soc.* 3(1):122.
- Garabedian, H. L. 1961. Core kinetics. In *Nuclear Reactor Theory*, ed. G. Birkhoff and E. P. Wigner. Providence, R.I.: American Mathematical Society.
- Garabedian, H. L., and Leffert, C. B. 1959. A time-dependent analysis of spatial flux distributions. *Nucl. Sci. Eng.* 6:26.
- Garabedian, H. L., and Lynch, R. E. 1965. Nonlinear reactor kinetics analysis. *Nucl. Sci. Eng.* 21:550.
- Garabedian, H. L., and von Herrmann, P. 1959. Reactor kinetics for multi-region multi-fuel reactors. *J. Nucl. Energy* 10:36.
- Garelis, E. 1963. Time-dependent neutron thermalization for a bare multiplying medium. *Nucl. Sci. Eng.* 15:296.
- . 1964a. Theory of pulsing techniques. *Nucl. Sci. Eng.* 18:242.
- . 1964b. On the  $(k\beta/\ell)$  pulsing theory. *Nucl. Sci. Eng.* 19:131.
- Garelis, E., and Russell, J. L., Jr. 1963. Theory of pulsed neutron source measurements. *Nucl. Sci. Eng.* 16:263.
- Garner, R. W. 1962. Review of several models for power behavior and reactivity feedback in reactor excursion studies. IDO-16636.
- General Atomic (Gulf General Atomic). 1958. Technical Foundations of TRIGA. GA-471.
- George, R. E., and Sesonske, A. 1959. Simplified simulation of a boiling water reactor power plant. *Nucl. Sci. Eng.* 6:409.
- Ghatak, A. K. 1968. Space and energy dependent considerations of the Fuchs' model. *J. Nucl. Energy* 22:699.
- Ghatak, A. K., and Honeck, H. C. 1965. On the feasibility of measuring higher time decay constants. *Nucl. Sci. Eng.* 21:227.
- Ghatak, A. K., and Kothari, L. S. 1966. Transient phenomenon in diffusion theory. *Nucl. Sci. Eng.* 26:277.
- Ghatak, A. K., and Pearlstein, S. 1965. Approach to equilibrium of a neutron pulse in a multiplying system. *Nucl. Sci. Eng.* 22:182.
- Glasstone, S., and Edlund, M. C. 1952. *The elements of nuclear reactor theory*. New York: D. Van Nostrand.
- Golay, M. W., and Cady, K. B. 1969. Transform domain analysis of neutron pulse propagation experiments. *Trans. Am. Nucl. Soc.* 12:678.

- Goldstein, R., and Shotkin, L. M. 1969. Use of the prompt-jump approximation in fast-reactor kinetics. *Nucl. Sci. Eng.* 38:94.
- Gozani, T. 1962. A modified procedure for the evaluation of pulsed source experiments in subcritical reactors. *Nukleonik* 4:348.
- . 1963. The concept of reactivity and its application to kinetic measurements. *Nukleonik* 5:55.
- Grace, J. N., ed. 1964. Reactor kinetics. In *Naval reactors physics handbook*, vol. 1, ed. A. Radkowsky. Washington, D.C.: United States Atomic Energy Commission.
- Greenspan, H.; Kelber, C. N.; and Okrent, D., eds. 1968. *Computing methods in reactor physics*. New York: Gordon and Breach.
- Gross, E. E., and Marable, J. H. 1960. Static and dynamic multiplication factors and their relation to the inhour equation. *Nucl. Sci. Eng.* 7:281.
- Gyftopoulos, E. P. 1961. Applications of geometric theory to nonlinear reactor dynamics. *Nucl. Sci. Eng.* 10:254.
- . 1964a. Lagrange stability by Liapunov's direct method. In *Reactor kinetics and control*, ed. L. E. Weaver. Oak Ridge, Tenn.: USAEC Division of Technical Information Extension.
- . 1964b. General reactor dynamics. In *The technology of nuclear reactor safety*, vol. 1, ed. T. J. Thompson and J. G. Beckerley. Cambridge, Mass.: M.I.T. Press.
- . 1964c. Point reactor kinetics and stability criteria. *Proc. Geneva Conf.* 4:3.
- . 1966. Theoretical and experimental criteria for nonlinear reactor stability. *Nucl. Sci. Eng.* 26:26.
- Gyftopoulos, R. P., and Devooght, J. 1961. On the range of validity of nonlinear reactor dynamics. *Nucl. Sci. Eng.* 10:372.
- Gyftopoulos, E. P., and Smets, H. B. 1959. Transfer functions of distributed parameter nuclear reactor systems. *Nucl. Sci. Eng.* 5:405.
- Gyorey, G. L. 1962. The effect of modal interaction in the xenon instability problem. *Nucl. Sci. Eng.* 13:338.
- Hageman, L. A., and Yasinsky, J. B. 1969. Comparison of alternating-direction time-differencing methods with other implicit methods for the solution of the neutron group-diffusion equations. *Nucl. Sci. Eng.* 38:8.
- Hahn, W. 1963. *Theory and application of Liapunov's direct method*. Englewood Cliffs, N.J.: Prentice-Hall.

- Haire, J. C., Jr. 1961. A summary description of the SPERT experimental program. *Nucl. Safety* 2(3):15.
- Hale, J. K., and LaSalle, J. P., eds. 1967. *Differential equations and dynamical systems*. New York : Academic Press.
- Hansen, G. E. 1952. Burst characteristics associated with the slow assembly of fissionable materials. LA-1441.
- . 1960. Assembly of fissionable material in the presence of a weak neutron source. *Nucl. Sci. Eng.* 8:709.
- Hansen, K. F. 1967. A comparative review of two-dimensional kinetics methods. GA-8169.
- Hansen, K. F., and Johnson, S. R. 1967. GAKIN : A program for the solution of the one-dimensional, multigroup, space-time dependent diffusion equations. GA-7543.
- Hansen, K. F.; Kleban, E. R.; and Chang, I. 1969. A new method of integrating the point kinetics equations. *Trans. Am. Nucl. Soc.* 12:617.
- Hansen, K. F.; Koen, B. V.; and Little, W. W., Jr. 1965. Stable numerical solutions of the reactor kinetics equations. *Nucl. Sci. Eng.* 22:51.
- Hansson, P. T., and Foulke, L. R. 1963. Investigations in spatial reactor kinetics. *Nucl. Sci. Eng.* 17:528.
- Harrer, J. M. 1963. *Nuclear reactor control engineering*. New York : D. Van Nostrand.
- Harrer, J. M.; Boyar, R. E.; and Krucoff, D. 1952. Transfer function of Argonne CP-2 reactor. *Nucleonics* 10(8):32 (see also ANL-4373, 1952).
- Harris, D. R., and Prescop, V. 1969. Stability and stationarity of a reactor as a stochastic process with feedback. *Nucl. Sci. Eng.* 37:171.
- Henry, A. F. 1958. The application of reactor kinetics to the analysis of experiments. *Nucl. Sci. Eng.* 3:52.
- . 1964. The application of inhour modes to the description of nonseparable reactor transients. *Nucl. Sci. Eng.* 20:338.
- . 1969. Review of computational methods for space-time kinetics. In *The effective use of computers in the nuclear industry*, ed. B. Maskewitz. Oak Ridge, Tenn.: USAEC Division of Technical Information Extension.
- Henry, A. F., and Curlee, N. J. 1958. Verification of a method of treating neutron space-time problems. *Nucl. Sci. Eng.* 4:727.
- Henry, A. F., and Germann, J. D. 1957. Oscillations in the power distribution within a reactor. *Nucl. Sci. Eng.* 2:469.

506      *Bibliography*

- Henry, A. F., and Kaplan, S. 1965. Some applications of a multimode generalization of the inhour formula. *Nucl. Sci. Eng.* 22:479.
- Henry, A. F., and Vota, A. V. 1965. WIGL 2: A program for the solution of the one-dimensional, two-group, space-time diffusion equations accounting for temperature, xenon, and control feedback. WAPD-TM-532.
- Hermite, C. 1850. Sur le nombre des racines d'une équation algébrique comprises entre des limites données. *J. Reine Angew. Math.* 52:39.
- Hetrick, D. L. 1965a. Application of the prompt-jump approximation to problems in reactor stability. *Trans. Am. Nucl. Soc.* 8:236.
- . 1965b. A Liapunov function for the prompt-jump approximation in reactor dynamics. *Trans. Am. Nucl. Soc.* 8:477.
- . 1967. An illustration of the destabilizing effect of delayed neutrons in the linear two-temperature reactor model. *Trans. Am. Nucl. Soc.* 10:248.
- Hetrick, D. L., and Gamble, D. P. 1958. Transient reactivity during power excursions in a water boiler reactor. *Trans. Am. Nucl. Soc.* 1(2):48.
- Hetrick, D. L., and Schmidt, T. R. 1968. Stability of a fast reactor with in-core thermionic diodes. *Trans. Am. Nucl. Soc.* 11:221.
- Hetrick, D. L., and Weaver, L. E., eds. 1966. *Neutron dynamics and control*. Oak Ridge, Tenn.: USAEC Division of Technical Information Extension.
- . 1968. Some recent advances in reactor dynamics and control. In Proceedings of the Brookhaven conference on industrial needs and academic research in reactor kinetics. BNL 50117 (T-497).
- Hildebrand, F. B. 1956. *Introduction to numerical analysis*. New York: McGraw-Hill.
- Hitchcock, A. 1960. *Nuclear reactor stability*. London: Temple Press.
- Hooper, R. J.; Rydin, R. A.; and Stacey, W. M., Jr. 1968. Verification of a xenon spatial stability criterion. *Nucl. Sci. Eng.* 34:344.
- Hoshino, T.; Wakabayashi, J.; and Hayashi, S. 1965. New approximate solution of space- and energy-dependent reactor kinetics. *Nucl. Sci. Eng.* 23:170.
- Hsu, C. 1967. Control and stability analysis of spatially dependent nuclear reactor systems. ANL-7322.
- Hsu, C., and Sha, W. T. 1969. Determination of stability domain of nonlinear reactor dynamics. *Trans. Am. Nucl. Soc.* 12:295.
- Hughes, D. J.; Dabbs, J.; Cahn, A.; and Hall, D. 1948. Delayed neutrons from fission of U<sup>235</sup>. *Phys. Rev.* 73:111.

- Hurwitz, A. 1895. Über die Bedingungen unter welchen eine Gleichung nur Wurzeln mit negativen reellen Theilen besitzt. *Math. Ann.* 46:273.
- Hurwitz, H., Jr. 1949. Derivation and integration of the pile-kinetic equations. *Nucleonics* 5(1):61.
- \_\_\_\_\_. 1959. Approximate analysis of reactor start-up incidents. *Nucl. Sci. Eng.* 6:11.
- \_\_\_\_\_. 1965. A simplified nonlinear model for qualitative study of reactor power-distribution transients. *Nucl. Sci. Eng.* 23:183.
- Hurwitz, H., Jr.; MacMillan, D. B.; Smith, J. H.; and Storm, M. L. 1963. Kinetics of low source reactor startups. Pt. 1: *Nucl. Sci. Eng.* 15:166. Pt. 2: *Nucl. Sci. Eng.* 15:187.
- IAEA (International Atomic Energy Agency). 1961. *Physics of fast and intermediate reactors*. Seminar proceedings, Vienna. Vienna: International Atomic Energy Agency.
- \_\_\_\_\_. 1962. *Reactor safety and hazard evaluation techniques*. Symposium proceedings, Vienna. Vienna: International Atomic Energy Agency.
- \_\_\_\_\_. 1965. *Pulsed neutron research*. Symposium proceedings, Karlsruhe. Vienna: International Atomic Energy Agency.
- Isbin, H. S. 1963. *Introductory nuclear reactor theory*. New York: Reinhold.
- Jacobowitz, H. J.; Akcasu, A. Z.; and Shotkin, L. M. 1966. Stability considerations with convective time delays. *Trans. Am. Nucl. Soc.* 9:272.
- James, H. M.; Nichols, N. B.; and Phillips, R. S., eds. 1947. *Theory of servomechanisms*. New York: McGraw-Hill.
- Jankus, V. Z. 1962. A theoretical study of destructive nuclear bursts in fast power reactors. ANL-6512.
- Jellers, D. E., and Hall, K. 1968. Flux tilting in a two-zone reactor. *Nucl. Sci. Eng.* 31:358.
- Jenkins, J. F., and Daitch, P. B. 1968. Analysis of pulsed fast-neutron spectra in multiplying assemblies. *Nucl. Sci. Eng.* 31:222.
- Johnson, R. P. 1966. SNAPTRAN 10A/2 kinetics testing and destruct reactor experiments. NAA-SR-11906.
- Judge, F. D., and Daitch, P. B. 1964. Time-dependent flux in small assemblies. *Nucl. Sci. Eng.* 20:428.
- \_\_\_\_\_. 1966. Time-dependent neutron flux in pulsed multiplying assemblies. *Nucl. Sci. Eng.* 26:472.

- Kaganove, J. J. 1960. Numerical solution of the one-group space-independent reactor kinetics equations for neutron density given the excess reactivity. ANL-6132.
- Kalinowski, J. E. 1968. Comments on E. P. Gyftopoulos, "Theoretical and experimental criteria for nonlinear reactor stability." *Nucl. Sci. Eng.* 34:200.
- Kalinowski, J. E., and Bailey, R. E. 1968. A general method for constructing Lyapunov functions employing frequency-domain concepts. *Trans. Am. Nucl. Soc.* 11:573.
- Kalman, R. E. 1963. Liapunov functions for the problem of Lur'e in automatic control. *Proc. Nat. Acad. Sci. U.S.A.* 49:201.
- Kaplan, S. 1961. The property of finality and the analysis of problems in reactor space-time kinetics by various modal expansions. *Nucl. Sci. Eng.* 9:357.
- . 1962a. Some new methods of flux synthesis. *Nucl. Sci. Eng.* 13:22.
- . 1962b. Space and time synthesis by the variational method. *Trans. Am. Nucl. Soc.* 5:412.
- . 1966. Synthesis methods in reactor analysis. In *Advances in nuclear science and technology*, vol. 3, ed. P. Greebler and E. J. Henley. New York: Academic Press.
- . 1969. Variational methods in nuclear engineering. In *Advances in nuclear science and technology*, vol. 5, ed. E. J. Henley and J. Lewins. New York: Academic Press.
- Kaplan, S.; Henry, A. F.; Margolis, S. G.; and Taylor, J. J. 1964. Space-time reactor dynamics. *Proc. Geneva. Conf.* 4:41.
- Kaplan, S., and Margolis, S. G. 1960. Delayed neutron effects during flux tilt transients. *Nucl. Sci. Eng.* 7:276.
- Kaplan, S.; Marlowe, O. J.; and Bewick, J. 1964. Application of synthesis techniques to problems involving time dependence. *Nucl. Sci. Eng.* 18:163.
- Kaplan, S., and Yasinsky, J. B. 1966. Natural modes of the xenon problem with flow feedback: An example. *Nucl. Sci. Eng.* 25:430.
- Kasten, P. R. 1962. Nuclear reactor stability theory. *Nucl. Safety* 3(3):18.
- Kastenberg, W. E. 1969a. A stability criterion for space-dependent nuclear-reactor systems with variable temperature feedback. *Nucl. Sci. Eng.* 37:19.
- . 1969b. Stability analysis of nonlinear space dependent reactor

- kinetics. In *Advances in nuclear science and technology*, vol. 5, ed. E. J. Henley and J. Lewins. New York : Academic Press.
- Kastenberg, W. E., and Chambré, P. L. 1968. On the stability of non-linear space-dependent reactor kinetics. *Nucl. Sci. Eng.* 31:67.
- Kastenberg, W. E., and Crawford, R. M. 1969. Determination of stability domains in space dependent reactor dynamics. *Nucl. Sci. Eng.* 37:311.
- Kazi, A. H.; Tomonto, J. R.; and Cherry, B. H. 1966. Quantitative evaluation of the Nordheim-Fuchs reactor excursion model with nonlinear reactivity feedback. *Nucl. Sci. Eng.* 26:131.
- Keepin, G. R. 1965. *Physics of nuclear kinetics*. Reading, Mass.: Addison-Wesley.
- Keepin, G. R., and Cox, C. W. 1960. General solution of the reactor kinetic equations. *Nucl. Sci. Eng.* 8:670.
- Keepin, G. R.; Wimett, T. F.; and Zeigler, R. K. 1957. Delayed neutrons from fissionable isotopes of uranium, plutonium, and thorium. *Phys. Rev.* 107:1044.
- Kelber, C. N.; Just, L. C.; and Morehouse, N. F., Jr. 1961. The solution of many region reactor kinetics problems on an analog computer. *Nucl. Sci. Eng.* 11:285.
- Kerlin, T. W. 1965. Status of space-time analysis. *Nucl. Safety* 6:395.
- . 1967. Frequency-response testing. *Nucl. Safety* 8:339.
- Kinchin, G. H. 1956. The stability of fast reactors. United Kingdom Atomic Energy Authority report AERE-RP/M-83.
- King, L. P. D. 1965. Description of the KIWI-TNT excursion. *Trans. Am. Nucl. Soc.* 8:126.
- Kistner, G. 1967. Note on the half-width of the neutron pulse of a pulsed reactor. *Nucl. Sci. Eng.* 28:461.
- Kladnik, R. 1968. Reflection and refraction of neutron diffusion waves. *Nucl. Sci. Eng.* 32:370.
- Köhler, W. H. 1969. Reactivity feedback with short delay times. *J. Nucl. Energy* 23:569.
- Kolar, O. C., and Kloverstrom, F. A. 1961. Pulsed neutron measurement of control rod worths. *Nucl. Sci. Eng.* 10:45.
- Komata, M. 1969. On the derivation of Avery's coupled reactor kinetics equations. *Nucl. Sci. Eng.* 38:193.
- Kothari, L. S. 1965. Decay constant of a neutron pulse inside a finite solid moderator assembly. *Nucl. Sci. Eng.* 23:402.

510      *Bibliography*

- Kovanic, P. 1965. A note on the inverse kinetics analysis. *Nucl. Sci. Eng.* 22:118.
- Kramerov, A. Ya., and Shevelev, Ya. V. 1964. *Engineering analysis of nuclear reactors.* (In Russian.) Moscow: Atomizdat.
- Krasovskii, N. N. 1963. *Stability of motion.* Stanford, Calif.: Stanford University Press.
- Krieger, T. J., and Zweifel, P. F. 1959. Theory of pulsed neutron experiments in multiplying media. *Nucl. Sci. Eng.* 5:21.
- Kumar, A.; Ahmed, F.; and Kothari, L. S. 1969. Neutron-wave propagation in crystalline moderators. Pt. 4, A two-group study. *Nucl. Sci. Eng.* 37:358.
- Kurchatov, I. V., et al. 1964. Pulse graphite reactor IGR. (In Russian.) *Proc. Geneva. Conf.* 7:461.
- Kuscer, I. 1969. Complex buckling and complex relaxation times in the decay of neutron pulses. *Nucl. Sci. Eng.* 38:175.
- Kylstra, C. D., and Uhrig, R. E. 1965. Spatially dependent transfer function for nuclear systems. *Nucl. Sci. Eng.* 22:191.
- Lamarsch, J. R. 1966. *Introduction to nuclear reactor theory.* Reading, Mass.: Addison-Wesley.
- Langsdorf, A. S., Jr. 1949. The thermal neutron reactor as an instrument for measuring neutron cross sections. ANL 4342.
- Larrimore, J. A. 1967. Physics of periodically pulsed reactors and boosters: Steady-state conditions, power pulse characteristics, and kinetics. *Nucl. Sci. Eng.* 29:87.
- LaSalle, J. P. 1960. The extent of asymptotic stability. *Proc. Nat. Acad. Sci. U.S.A.* 46:363.
- . 1968. Stability theory for ordinary differential equations. *J. Diff. Eqs.* 4:57.
- LaSalle, J., and Lefschetz, S. 1961. *Stability by Liapunov's direct method.* New York: Academic Press.
- Lass, H. 1950. *Vector and tensor analysis.* New York: McGraw-Hill.
- Lauber, R. 1962. Die Stabilitätsuntersuchung von Reaktor-Regelkreisen unter Berücksichtigung der Nichlinearitäten. D.Sc. Thesis, Technical University, Stuttgart.
- Lazarus, R. B.; Stratton, W. R.; and Hughes, T. H. 1968. Coupled neutronic-dynamic problems. In *Computing methods in reactor physics*, ed. H. Greenspan, C. N. Kelber and D. Okrent. New York: Gordon and Breach.

- Lefschetz, S. 1963. *Differential equations: Geometric Theory*. 2d ed. New York: Wiley.
- . 1965. *Stability of nonlinear control systems*. New York: Academic Press.
- . 1967. Geometric differential equations: Recent past and proximate future. In *Differential equations and dynamical systems*, ed. J. K. Hale and J. P. LaSalle. New York: Academic Press.
- Lehnigk, S. H. 1966. *Stability theorems for linear motions with an introduction to Liapunov's direct method*. Englewood Cliffs, N.J.: Prentice-Hall.
- Lellouche, G. S. 1962. Space dependent xenon oscillations. *Nucl. Sci. Eng.* 12:482.
- . 1966. Reactor kinetics stability criteria. *Nucl. Sci. Eng.* 24:72.
- . 1967a. Effect of spatial shape on stability. *Trans. Am. Nucl. Soc.* 10:204.
- . 1967b. An application of Popov's asymptotic stability criterion. *J. Math. and Phys.* 46:225.
- Leonard, A. 1965. On transient phenomena in thermalization. *Nucl. Sci. Eng.* 22:489.
- Letov, A. M. 1955. *Stability in nonlinear control systems*. (In Russian.) Moscow. English translation, Princeton, N.J.: Princeton University Press, 1961.
- Lewins, J. 1960a. The use of the generation time in reactor kinetics. *Nucl. Sci. Eng.* 7:122.
- . 1960b. The time-dependent importance of neutrons and precursors. *Nucl. Sci. Eng.* 7:268.
- . 1960c. The approximate separation of kinetics problems into time and space functions by a variational principle. *J. Nucl. Energy* 12:108.
- . 1961. The reduction of the time-dependent equations for nuclear reactors to a set of ordinary differential equations. *Nucl. Sci. Eng.* 9:399.
- . 1962. A variational principle for nonlinear systems. *Nucl. Sci. Eng.* 12:10.
- . 1964. Time-dependent variational principles for nonconservative systems. *Nucl. Sci. Eng.* 20:517.
- . 1965. *Importance: The adjoint function*. Oxford: Pergamon Press.
- . 1968. Time-dependent variational theory. *Nucl. Sci. Eng.* 31:160.

512      *Bibliography*

- Liapunov, A. M. 1892. General problem of stability of motion. (In Russian.) *Comm. Soc. Math. Kharkov* (1892). *Problème général de la stabilité du mouvement. Ann. Fac. Sci. Toulouse* 9:203 (1907). Reprinted as *Ann. of Math. Studies*, no. 17. Princeton, N.J.: Princeton University Press, 1949.
- . 1966. *Stability of motion*. New York: Academic Press.
- Lipinski, W. C. 1960. EBWR stability analyses. In *Proceedings of the conference on transfer function measurement and reactor stability analysis*, ed. J. A. DeShong, Jr. ANL-6205.
- Loewe, W. E. 1965. Space-dependent effects in the response of a nuclear reactor to forced oscillations. *Nucl. Sci. Eng.* 21:536.
- Long, R. L. 1966. Operating characteristics of the WSMR fast burst reactor. In *Neutron dynamics and control*, ed. D. L. Hetrick and L. E. Weaver. Oak Ridge, Tenn.: USAEC Division of Technical Information Extension.
- Long, R. L.; McTaggart, M. H.; and Weale, J. W. 1967. VIPER: A versatile pulsed reactor using Doppler and expansion shutdown. *Trans. Am. Nucl. Soc.* 10:608.
- Long, R. L., and O'Brien, P. D., eds. 1969. *Fast burst reactors*. Oak Ridge, Tenn.: USAEC Division of Technical Information Extension.
- Lopez, W. M., and Beyster, J. R. 1962. Measurement of neutron diffusion parameters in water by the pulsed neutron method. *Nucl. Sci. Eng.* 12:190.
- Lur'e, A. I. 1951. *Some nonlinear problems in the theory of automatic regulation*. (In Russian.) Moscow. German translation, Berlin: Akademie Verlag, 1957.
- McCarthy, W. J., Jr.; Nicholson, R. B.; Okrent, D.; and Jankus, V. Z. 1958. Studies of nuclear accidents in fast power reactors. *Proc. Geneva Conf.* 12:207.
- McCarthy, W. J., Jr., and Okrent, D. 1964. Fast reactor kinetics. In *The technology of nuclear reactor safety*, vol. 1, ed. T. J. Thompson and J. G. Beckerley. Cambridge, Mass.: M.I.T. Press.
- McCormick, W. T., Jr., and Hansen, K. F. 1969. Numerical solution of the two-dimensional time-dependent multigroup equations. In *The effective use of computers in the nuclear industry*, ed. B. Maskewitz. Oak Ridge, Tenn.: USAEC Division of Technical Information Extension.
- MacMillan, D. B. 1967. Asymptotic formulas for initial-value problems of non-linear differential equations with a small parameter multiplying the derivative. KAPL-3359.

- MacMillan, D. B., and Storm, M. L. 1963. Kinetics of low source reactor startups. Pt. 3. *Nucl. Sci. Eng.* 16:369.
- MacPhee, J. 1958. The kinetics of circulating fuel reactors. *Nucl. Sci. Eng.* 4:588.
- . 1960. Approximate solutions of the reactor kinetic equations for ramp inputs. *Nucl. Sci. Eng.* 7:33.
- MacPhee, J., and Lumb, R. F. 1965. The transient characteristics of a new pulse research reactor. In *Pulsed neutron research*. Symposium proceedings, Karlsruhe. Vienna: International Atomic Energy Agency.
- Malkin, I. G. 1952. *Theory of stability of motion*. (In Russian.) Moscow: State Publishing House of Technical-Theoretical Literature. German translation, Munich: Oldenbourg, 1959. English translation, AEC-tr-3352, n.d. (This English translation is not recommended.)
- Marable, J. H. 1961. Review of KEWB experimental program. *Nucl. Safety* 3(1):28.
- . 1963. Review of KEWB program. *Nucl. Safety* 5:42.
- Masters, D. F., and Cady, K. B. 1967. A procedure for evaluating modified pulsed-neutron-source experiments in subcritical nuclear reactors. *Nucl. Sci. Eng.* 29:272.
- Meenan, P., and Hetrick, D. 1966. Stability of the two-temperature reactor model with delayed neutrons. *Trans. Am. Nucl. Soc.* 9:458.
- McGhreblian, R. V., and Holmes, D. K. 1960. *Reactor Analysis*. New York: McGraw-Hill.
- Meneley, D. A., Ott, K., and Wiener, E. S. 1967. Space-time kinetics, the QX-1 code. ANL-7310.
- Meyer, J. E. 1958. Synthesis of three-dimensional power shapes. *Proc. Geneva Conf.* 11:519.
- Mihalczo, J. T. 1963. Superprompt-critical behavior of an unmoderated, unreflected uranium-molybdenum alloy reactor. *Nucl. Sci. Eng.* 16:291.
- . 1968. Prompt neutron decay and reactivity measurements in subcritical uranium metal cylinders. *Nucl. Sci. Eng.* 32:292.
- Mihalczo, J. T., Lynn, J. J., and Watson, J. E. 1967. Superprompt critical behavior of a uranium-molybdenum assembly. *Trans. Am. Nucl. Soc.* 10:610.
- Miida, J., and Suda, N. 1961. General stability criteria for nuclear reactor with two feedback paths of single time constant. *Nucl. Sci. Eng.* 11:55.

#### 54-4      *Bibliography*

- Miley, G. H. 1965. Reactor neutron-pulse propagation. *Nucl. Sci. Eng.* 21:357.
- Miley, G. H.; Tsoulfanidis, N.; and Doshi, P. K. 1967. Pulse-propagation experiments with a reactor source. In *Neutron noise, waves, and pulse propagation*, ed. R. E. Uhrig. Oak Ridge, Tenn.: USAEC Division of Technical Information Extension.
- Miller, R. W. 1957. Calculations of reactivity behavior during SPERT-I transients. IDO-16317.
- Minorsky, N. 1962. *Nonlinear oscillations*. Princeton, N.J.: D. Van Nostrand.
- . 1969. *Theory of nonlinear control systems*. New York: McGraw-Hill.
- Mockel, A. 1966. On the disappearance of discrete decay constants in slabs. *Nucl. Sci. Eng.* 26:279.
- Moore, M. N. 1958. The determination of reactor transfer functions from measurements at steady operation. *Nucl. Sci. Eng.* 3:387.
- . 1959. The power noise transfer function of a reactor. *Nucl. Sci. Eng.* 6:448.
- . 1964. The role of the dispersion law in space-dependent kinetics. In *Reactor kinetics and control*, ed. L. E. Weaver. Oak Ridge, Tenn.: USAEC Division of Technical Information Extension.
- . 1965. The determination of reactor dispersion laws from modulated-neutron experiments. *Nucl. Sci. Eng.* 21:565.
- . 1966a. The dispersion law of a moderator. *Nucl. Sci. Eng.* 26:354.
- . 1966b. The dispersion of thermal-neutron pulses in neutronic systems. *Nucl. Sci. Eng.* 25:422.
- . 1967a. The general theory of excitation experiments in space-dependent kinetics. In *Neutron noise, waves, and pulse propagation*, ed. R. E. Uhrig. Oak Ridge, Tenn.: USAEC Division of Technical Information Extension.
- . 1967b. Asymptotic neutron pulse velocity and the system dispersion law. *Nucl. Sci. Eng.* 28:152.
- Morse, P. M., and Feshbach, H. 1953. *Methods of theoretical physics*. New York : McGraw-Hill.
- Mortensen, G. A., and Smith, H. P., Jr. 1965. Neutron-wave propagation using the  $P_1$  approximation. *Nucl. Sci. Eng.* 22:321.
- Moss, L. I., and Buttrey, K. E. 1964. Analytical description of superprompt critical transients in uranium-zirconium hydride fueled reactors. *Trans. Am. Nucl. Soc.* 7:384.

- Moss, L. I., and Rhoades, W. A. 1968. A method for the study of auto-catalysis and/or pressure histories in fast breeder reactors. In Proceedings of the Brookhaven conference on industrial needs and academic research in reactor kinetics. BNL 50117 (T-497).
- Motz, H. T., and Keepin, G. R., eds. 1966. *Intense neutron sources*. Oak Ridge, Tenn.: USAEC Division of Technical Information Extension.
- Murray, H. S., and Schultz, D. G. 1966. Stability of nonlinear coupled-core reactors. In *Neutron dynamics and control*, ed. D. L. Hetrick and L. E. Weaver. Oak Ridge, Tenn.: USAEC Division of Technical Information Extension.
- Murray, R. L.; Bingham, C. R.; and Martin, C. F. 1964. Reactor kinetics analysis by an inverse method. *Nucl. Sci. Eng.* 18:481.
- Nahavandi, A. N., and von Hollen, R. F. 1964a. A space-dependent dynamic analysis of boiling water reactor systems. *Nucl. Sci. Eng.* 20:392.
- . 1964b. A digital computer solution for space-dependent neutron kinetics equations. *Nucl. Sci. Eng.* 18:335.
- Natelson, M.; Osborn, R. K.; and Shure, F. 1966. Space and energy effects in reactor fluctuation measurements. *J. Nucl. Energy* 20:557.
- Nelkin, M. 1955. Appendix to "The effect of temperature coefficients on reactor stability and reactor transfer function," by R. Siegel and H. Hurwitz, Jr. KAPL-1138.
- . 1960. The decay of a thermalized neutron pulse. *Nucl. Sci. Eng.* 7:210.
- Nguyen, D. H. 1969. On the upper bound of the point spectrum for pulsed thermal systems. *Trans. Am. Nucl. Soc.* 12:662.
- Nicholson, R. B. 1960. The Doppler effect in fast neutron reactors. APDA-139.
- . 1964. Methods for determining the energy release in hypothetical fast-reactor meltdown accidents. *Nucl. Sci. Eng.* 18:207.
- Nishina, K., and Akcasu, A. Z. 1970. Neutron wave analysis in finite media. *Nucl. Sci. Eng.* 39:170.
- Nordheim, L. W. 1946. Pile kinetics. MDDC-35.
- . 1964. The Doppler coefficient. In *The technology of nuclear reactor safety*, vol. 1, ed. T. J. Thompson and J. G. Beckerley. Cambridge, Mass.: M.I.T. Press.
- Nyer, W. E. 1958. Ramp-induced bursts. In Quarterly progress report, January, February, March, 1958, reactor projects branch, ed. G. O. Bright. IDO-16452.

516      *Bibliography*

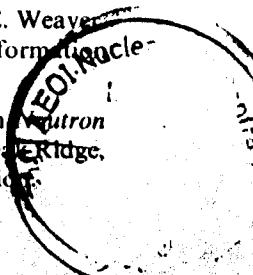
- . 1964. Mathematical models of fast transients. In *The technology of nuclear reactor safety*, vol. 1, ed. T. J. Thompson and J. G. Beckerley. Cambridge, Mass.: M.I.T. Press.
- Nyer, W. E., and Forbes, S. G. 1958. SPERT I reactor safety studies. *Proc. Geneva Conf.* 11:470.
- Nyquist, H. 1932. The regeneration theory. *Bell Syst. Tech. J.* 11:126.
- Oakes, L. C. 1968. The control and safety of pulse reactors. *Nucl. Safety* 9:363.
- Ohanian, M. J.; Booth, R. S.; and Perez, R. B. 1967. Eigenfunction analysis of neutron-wave propagation in moderating media. *Nucl. Sci. Eng.* 30:95.
- Ohanian, M. J., and Diaz, N. J. 1969. The dispersion law of a large, close-to-critical  $H_2O-UO_2$  assembly. *Trans. Am. Nucl. Soc.* 12:257.
- Okrent, D. 1965. A look at fast reactor safety. *Nucl. Safety* 6:317.
- Okrent, D.; Cook, J. M.; Satkus, D.; Lazarus, R. B.; and Wells, M. B. 1959. AX-1: A computing program for coupled neutronic-hydrodynamics calculations. ANL-5977.
- Orndoff, J. D. 1957. Prompt neutron periods of metal critical assemblies. *Nucl. Sci. Eng.* 2:450.
- Ortenberg, L. I. 1967. A comparison of calculated reactivity feedback with recent measurements in NERVA reactors. *Trans. Am. Nucl. Soc.* 10:414.
- Osborn, R. K., and Yip, S. 1967. *The foundations of neutron transport theory*. New York: Gordon and Breach.
- Ott, K., and Madell, J. T. 1966. Quasistatic treatment of spatial phenomena in reactor dynamics. *Nucl. Sci. Eng.* 26:563.
- Ott, K., and Meneley, D. A. 1969. Accuracy of the quasistatic treatment of spatial reactor kinetics. *Nucl. Sci. Eng.* 36:402.
- Oyama, A.; An, S.; and Kondo, S. Analysis of fast reactor core meltdown accidents. In *Proceedings of the international conference on the safety of fast reactors* (Aix-en-Provence, 19–22 September 1967), ed. G. Denielou. Paris: Documentation Française.
- Pacilio, N. 1969. *Reactor-noise analysis in the time domain*. AEC Critical Review Series, no. 7. TID-24512.
- Pai, M. A.; Sastry, V. R.; and Mohan, M. A. 1970. Construction of Lyapunov functions for nonlinear nuclear reactor stability studies. *Nucl. Sci. Eng.* 39:105.
- Parks, P. C. 1962. A new proof of the Routh-Hurwitz stability criterion using the second method of Liapunov. *Proc. Camb. Phil. Soc.* 58:694.

- Perez, R. B.; Booth, R. S.; and Hartley, R. H. 1963. Experimentation with thermal-neutron wave-propagation. *Trans. Am. Nucl. Soc.* 6:287.
- Perez, R. B., and Uhrig, R. E. 1962. Propagation of thermal-neutron waves in moderating media. *Trans. Am. Nucl. Soc.* 5:348.
- . 1963. Propagation of neutron waves in moderating media. *Nucl. Sci. Eng.* 17:90.
- . 1967. Development of techniques of neutron-wave and neutron-pulse propagation. In *Neutron noise, waves, and pulse propagation*, ed. R. E. Uhrig. Oak Ridge, Tenn.: USAEC Division of Technical Information Extension.
- Perks, M. A. 1965. FREAK: A fast reactor multigroup kinetics program. In Proceedings of the conference on the application of computing methods to reactor problems, ed. M. Butler. ANL-7050.
- Plaza, H., and Köhler, W. H. 1966. Coupled-reactors kinetics equations. *Nucl. Sci. Eng.* 26:419.
- Poincaré, H. 1892. *Les méthodes nouvelles de la mécanique céleste*. Paris: Gauthier-Villars.
- Poole, M. J., and Wiblin, E. R. 1958. The design of a high-intensity pulsed source using a neutron booster target. *Proc. Geneva Conf.* 14:266.
- Popov, V. M. 1958. Notes on the inherent stability of nuclear reactors. *Proc. Geneva Conf.* 11:245.
- . 1961. Absolute stability of nonlinear systems of automatic control. (English translation.) *Automation and Remote Control*. 22:857.
- . 1963. A new criterion for the stability of systems containing nuclear reactors. *Rev. Electrotech. Energ.* A8:113.
- Porsching, T. A. 1966. Numerical solution of the reactor kinetics equations by approximate exponentials. *Nucl. Sci. Eng.* 25:183.
- Profio, A. E., and Eckard, J. D. 1964. Investigations of neutron moderation with a pulsed source. *Nucl. Sci. Eng.* 19:321.
- Purohit, S. N. 1961. Neutron thermalization and diffusion in pulsed media. *Nucl. Sci. Eng.* 9:157.
- Quddus, M. A.; Cochran, R. G.; and Emon, D. E. 1969. Axial propagation of neutron waves in heterogeneous media. *Nucl. Sci. Eng.* 35:342.
- Radkowsky, A., ed. 1964. *Naval reactors physics handbook*. Vol. 1. Washington, D.C.: United States Atomic Energy Commission.

518      *Bibliography*

- Raievski, V., and Horowitz, J. 1954. Mesure du libre parcours moyen de transport des neutrons thermiques dans l'eau lourde au moyen d'une source modulée. *Compt. Rend.* 238:193.
- . 1955. Determination of the mean transfer free path of thermal neutrons by measurement of the complex diffusion length. *Proc. Geneva Conf.* 5:42.
- Ram, K. S. 1968. A new approach for determining the reactivity of a subcritical system. *Trans. Am. Nucl. Soc.* 11:191.
- Ram, K. S., and Uhrig, R. E. 1969. Determination of reactivity of a subcritical system. *Nucl. Sci. Eng.* 37:299.
- Randall, D., and St. John, D. S. 1958. Xenon spatial oscillations. *Nucleonics* 16(3):82.
- . 1962. Xenon spatial oscillations. *Nucl. Sci. Eng.* 14:204.
- Randles, J. 1966. Feedback due to elastic waves and Doppler coefficient during the excursions of a pulsed fast reactor. *J. Nucl. Energy* 20:1.
- Reed, W. H., and Hansen, K. F. 1969. Finite difference techniques for the solution of the reactor kinetics equations. MITNE-100.
- . 1970. Alternating direction methods for the reactor kinetics equations. *Nucl. Sci. Eng.* 41:431.
- Remley, M. E.; Flora, J. W.; Hetrick, D. L.; Muller, D. R.; Gardner, E. L.; Wimmer, R. E.; Stitt, R. K.; and Gamble, D. P. 1958. Experimental studies on the kinetic behavior of water boiler type reactors. *Proc. Geneva Conf.* 11:447.
- Renard, A., and Stiévenart, M. 1967. Evaluation of the energy release in case of a severe accident for a fast reactor with important feedbacks. In *Proceedings of the international conference on the safety of fast reactors* (Aix-en-Provence, 19–22 September 1967), ed. G. Denielou. Paris: Documentation Française.
- Reuscher, J. A. 1968. Dynamic mechanical characteristics of the Sandia pulsed reactor II. *Trans. Am. Nucl. Soc.* 11:220.
- Richtmyer, R. D. 1958. *Difference methods for initial-value problems*. New York: Wiley.
- Ritchie, A. I. M., and Rainbow, M. T. 1967. Some measurements of decay constants close to  $(v\Sigma_{\text{inel}})_{\text{min}}$  in pulsed BeO assemblies. *Nucl. Sci. Eng.* 28:306.
- Robinson, L. B. 1954. Concept of stability for nuclear reactors. *J. Appl. Phys.* 25:516.
- . 1955. Effect of delayed fission neutrons on reactor kinetics. *J. Appl. Phys.* 26:52.

- Rosen, J. B. 1961. Stability and bounds for non-linear systems of difference and differential equations. *J. Math. Anal. Appl.* 2:370.
- Rotter, W. 1969. Interpretation of pulsed source measurements by the moments methods. *J. Nucl. Energy.* 23:289.
- Routh, E. J. 1877. *A treatise on the stability of a given state of motion.* London: Macmillan & Co.
- Rumsey, V. H. 1947. The time variation of pile power due to periodic modulation of the effective multiplication constant. CRP-333, PD-217.
- . 1954. Kinetics of piles with reflectors. *J. Appl. Phys.* 25:1395.
- Russell, C. R. 1962. *Reactor safeguards.* New York: Macmillan Co.
- Russell, L. M., and Morris, E. 1965. A computer calculation of the energy yield produced by a hypothetical fast reactor accident. In Proceedings of the conference on the application of computing methods to reactor problems, ed. M. Butler. ANL-7050.
- Rydin, R. A. 1968. Time synthesis: A study of synthesis modes and weighting functions. *Trans. Am. Nucl. Soc.* 10:569.
- Saji, G. 1968. Excitation of higher space modes in reactor transfer function measurement. *Nucl. Sci. Eng.* 32:93.
- Sanathanan, C. K.; Carter, J. C.; Bryant, L. T.; and Amiot, L. W. 1967. The application of a hybrid computer to the analysis of transient phenomena in a fast reactor core. *Nucl. Sci. Eng.* 28:82.
- Sandmeier, H. 1959. Nonlinear treatment of large perturbation in power reactor stability. *Nucl. Sci. Eng.* 6:85.
- Sastre, C. 1964. Reactor transfer functions. In *Advances in nuclear science and technology*, vol. 2, ed. E. J. Henley and H. Kouts. New York: Academic Press.
- Sastre, C., and Weinstock, E. V. 1964. A note on delayed-neutron effects in pulsed-neutron measurements on multiplying assemblies. *Nucl. Sci. Eng.* 20:359.
- Scalettar, R. 1963. The Fuchs-Nordheim model with variable heat capacity. *Nucl. Sci. Eng.* 16:459.
- . 1964. Space- and energy-dependent corrections to the Fuchs-Nordheim model. In *Reactor kinetics and control*, ed. L. E. Weaver. Oak Ridge, Tenn.: USAEC Division of Technical Information Extension.
- . 1966. Adiabatic treatment of the xenon problem. In *Neutron dynamics and control*, ed. D. L. Hetrick and L. E. Weaver. Oak Ridge, Tenn.: USAEC Division of Technical Information Extension.



520      *Bibliography*

- Schmid, P. 1958. Derivation of a basic integral equation of reactor kinetics. *Proc. Geneva Conf.* 11:277.
- Schmidt, T. R. 1969. Nonlinear oscillations and stability of a nuclear reactor with two reactivity feedbacks. Ph.D. dissertation, University of Arizona.
- Schmidt, T. R., and Hetrick, D. L. 1969. Autonomous nonlinear oscillations in nuclear reactors. *Trans. Am. Nucl. Soc.* 12:735.
- \_\_\_\_\_. 1970. Nonlinear oscillations and stability of a nuclear reactor with two reactivity feedbacks. *Nucl. Sci. Eng.* 42:1.
- Schroeder, F.; Forbes, S. G.; Nyer, W. E.; Bentzen, F. L.; and Bright, G. O. 1957. Experimental study of transient behavior in a subcooled, water-moderated reactor. *Nucl. Sci. Eng.* 2:96.
- Schultz, D. G. 1965. The generation of Liapunov functions. In *Advances in control systems*, vol. 2, ed. C. T. Leondes. New York: Academic Press.
- Schultz, D. G., and Melsa, J. L. 1967. *State functions and linear control systems*. New York: McGraw-Hill.
- Schultz, M. A. 1961. *Control of nuclear reactors and power plants*. 2d. ed. New York: McGraw-Hill.
- Secker, P. A., Jr. 1969a. Numerical integration of dynamic nuclear systems equations by optimum integrating factors. Ph.D. dissertation, University of Arizona. Published as LA-4252.
- \_\_\_\_\_. 1969b. Solution of the reactor kinetics equations by optimum integrating factors. *Trans. Am. Nucl. Soc.* 12:618.
- Selengut, D. S. 1959. Variational analysis of multi-dimensional systems. In Nuclear physics research quarterly report, October, November, December, 1958. HW-59126.
- \_\_\_\_\_. 1963. On the derivation of a variational principle for linear systems. *Nucl. Sci. Eng.* 17:310.
- Sha, W. T., and Hsu, C. 1968. Asymptotic stability with positive moderator reactivity coefficients. *Trans. Am. Nucl. Soc.* 11:573.
- Shinoda, W., and Mitake, S. 1969. A three-dimensional analysis of xenon-induced oscillations in boiling water cooled reactors. *Nucl. Sci. Eng.* 36:372.
- Shotkin, L. M. 1963. Nonlinear kinetics of a two-temperature reactor. BNL 815 (T-315).
- \_\_\_\_\_. 1964a. A nonlinear analysis of a reactor with two temperature coefficients. *Nucl. Sci. Eng.* 18:271.

- . 1964b. Reactor stability against xenon oscillations. In *Reactor kinetics and control*, ed. L. E. Weaver. Oak Ridge, Tenn.: USAEC Division of Technical Information Extension.
- . 1969a. Instability bounds in linearly stable systems. *Nucl. Sci. Eng.* 35:211.
- . 1969b. Comparison of modal and iterative approaches to space and space-time nonlinear problems. *Nucl. Sci. Eng.* 36:97.
- Shotkin, L. M.; Hetrick, D. L.; and Schmidt, T. R. 1969. The effect of delayed neutrons on autonomous oscillations in nonlinear reactor systems. *Trans. Am. Nucl. Soc.* 12:294.
- . 1970. Effect of delayed neutrons on autonomous nonlinear power oscillations. *Nucl. Sci. Eng.* 42:10.
- Silberberg, M. 1965. The KEWB program. *Nucl. Safety* 6:386.
- Simmons, B. E. 1959. The dynamic reactivity interpretation of pulsed neutron measurements. *Nucl. Sci. Eng.* 5:254.
- Simmons, B. E., and King, J. S. 1958. A pulsed neutron technique for reactivity determination. *Nucl. Sci. Eng.* 3:595.
- Singer, S. 1962. The period equilibrium effect in reactor dynamics. LA-2654.
- Sjostrand, N. G. 1956. Measurements on a subcritical reactor using a pulsed neutron source. *Arkiv Fysik* 11:233.
- Skinner, R. E., and Cohen, E. R. 1959. Reduced delayed neutron group representations. *Nucl. Sci. Eng.* 5:291.
- Skinner, R. E., and Hetrick, D. L. 1958. The transfer function of a water boiler reactor. *Nucl. Sci. Eng.* 3:573.
- Slivinsky, C. R., and Weaver, L. E. 1969. Reactor control using a new multivariable design technique. *Nucl. Sci. Eng.* 37:163.
- Smets, H. B. 1958. Reactor dynamics at low power. *Proc. Geneva Conf.* 11:237.
- . 1959a. The response of a nuclear power reactor to a linear reactivity variation. *Nukleonik* 1:351.
- . 1959b. On Welton's stability criterion for nuclear reactors. *J. Appl. Phys.* 30:1623.
- . 1960. A general property of boundedness for the power of some stable and unstable nuclear reactors. *Nukleonik* 2:44.
- . 1961. On the stability of homogeneous nuclear reactors with non-linear reactivity dependence on temperature. *Nucl. Sci. Eng.* 11:428.

522      *Bibliography*

- . 1962. *Problems in nuclear power reactor stability*. Brussels: Presses Universitaires de Bruxelles A.S.B.L.
- . 1963. Stability in the large and boundedness of some reactor models. *J. Nucl. Energy* 17:329.
- . 1964. Power oscillations in nuclear reactors. *Revue A, Belgian Society for Automatic Control* 6:137.
- . 1965. Derivation of the describing function for a reactor at power level. *Nukleonik* 7:399.
- . 1966. On the effect of delayed neutrons in reactor dynamics. *Nucl. Sci. Eng.* 25:236.
- . 1967. Propriétés globales des transitoires non linéaires des réacteurs nucléaires. In *Identification, optimisation et stabilité des systèmes automatiques* (Actes du Congrès d'Automatique Théorique, Paris, 1965). Paris: Dunod.
- . 1969. Reply to S. Tan, "On the stabilizing effects of delayed neutrons." *Nucl. Sci. Eng.* 37:326.
- . 1970. Boundedness and stability of some models of nuclear reactors. *Nucl. Sci. Eng.* 39:289.
- Smets, H. B., and Gyftopoulos, E. P. 1959. The application of topological methods to the kinetics of homogeneous reactors. *Nucl. Sci. Eng.* 6:341.
- Smiley, J. W. 1966. STREAK: A numerical solution for space-time neutron diffusion equations. Engineering Research Bulletin B-95. University Park, Penn.: Pennsylvania State University.
- Smith, H. P., Jr. 1962. Closed loop dynamics of nuclear rocket engines with bleed turbine drive. *Nucl. Sci. Eng.* 14:371.
- . 1964. Closed-loop dynamics of nuclear rocket engines with topping turbine drive. *Nucl. Sci. Eng.* 18:508.
- . 1965. Divergence of the mean power level during an oscillation experiment. *Nucl. Sci. Eng.* 22:253.
- Smith, H. P., Jr., and Stenning, A. H. 1961. Open loop stability and response of nuclear rocket engines. *Nucl. Sci. Eng.* 11:76.
- Smith, R. R.; Boland, J. F.; McGinnis, F. D.; Novick, M.; and Thalgott, F. W. 1960. Instability studies with EBR-I, Mark III. ANL-6266.
- Smith, R. R.; Matlock, R. G.; McGinnis, F. D.; Novick, M.; and Thalgott, F. W. 1961. A mechanism explaining the instability of EBR-I, Mark III. ANL-6354.
- Soodak, H. 1961. Problems of reactor kinetics. In *Nuclear reactor theory*,

- ed. G. Birkhoff and E. P. Wigner. Providence, R.I.: American Mathematical Society.
- \_\_\_\_\_, ed. 1962. *Reactor handbook*. 2d ed. Vol. 3, Pt. A. New York: Wiley. (In the edition cited, the list of references for chap. 5, Reactor Dynamics, is incorrect.)
- Spano, A. H. 1963. Self-limiting power excursion tests of a water-moderated low-enrichment UO<sub>2</sub> core. *Nucl. Sci. Eng.* 15:37.
- \_\_\_\_\_. 1964. Analysis of Doppler-limited power excursions in a water-moderated oxide core. *Nucl. Sci. Eng.* 19:172.
- Stacey, W. M., Jr. 1967a. *Modal approximations: Theory and an application to reactor physics*. Cambridge, Mass.: M.I.T. Press.
- \_\_\_\_\_. 1967b. Variational functionals for space-time neutronics. *Nucl. Sci. Eng.* 30:448.
- \_\_\_\_\_. 1968. A variational multichannel space-time synthesis method for nonseparable reactor transients. *Nucl. Sci. Eng.* 34:45.
- \_\_\_\_\_. 1969a. *Space-time nuclear reactor kinetics*. New York: Academic Press.
- \_\_\_\_\_. 1969b. Stochastic kinetic theory for a space- and energy-dependent zero power nuclear reactor model. *Nucl. Sci. Eng.* 36:389.
- \_\_\_\_\_. 1969c. A nonlinear xenon stability criterion for a spatially dependent reactor model. *Nucl. Sci. Eng.* 35:395.
- Stacey, W. M., Jr., and Adams, C. H. 1967. The time-integrated method: A quasistatic neutron space-time approximation. *Trans. Am. Nucl. Soc.* 10:251.
- Stahl, R. H.; Russell, J. L., Jr.; and Hopkins, G. R. 1966. Pulsed neutron sources. In *Advances in nuclear science and technology*, vol. 3, ed. P. Greebler and E. J. Henley. New York: Academic Press.
- Stone, R. S.; Sleeper, H. P., Jr.; Stahl, R. H.; and West, G. B. 1959. Transient behavior of TRIGA, a zirconium-hydride, water-moderated reactor. *Nucl. Sci. Eng.* 6:255.
- Störrer, F. 1960. Analysis of the power feedback relations in fast reactors. In *Proceedings of the conference on transfer function measurement and reactor stability analysis*, ed. J. A. DeShong, Jr. ANL-6205.
- Störrer, F.; Govaerts, P.; Ebersoldt, F.; and Hammer, P. 1966. A method for calculating the flux evolution in a fast-neutron multiplying medium as a function of time, space, and energy. *Nucl. Sci. Eng.* 24:344.

524      *Bibliography*

- Stratton, W. R.; Colvin, T. H.; and Lazarus, R. B. 1958. Analysis of prompt excursions in simple systems and idealized fast reactors. *Proc. Geneva Conf.* 12:196.
- Syrett, J. J. 1954. The variation of power in a fast reactor for a linear increase of reactivity. United Kingdom Atomic Energy Authority report AERE-RP/M-47.
- Szegö, G. P. 1963. A contribution to Liapunov's second method: Nonlinear autonomous systems. In *Nonlinear differential equations and nonlinear mechanics*, ed. J. LaSalle and S. Lefschetz. New York: Academic Press.
- Szeligowski, J., and Hetrick, D. L. 1967. A comparison of some numerical methods for solving the equations of reactor dynamics. In *Proceedings of the international conference on the utilization of research reactors and reactor mathematics and computation*. Mexico, D.F.: Comisión Nacional de Energía Nuclear.
- Tait, J. H. 1964. *Neutron transport theory*. London: Longmans, Green.
- Takahashi, A., and Sumita, K. 1968. Pulse propagation experiments of thermal neutrons in graphite. *J. Nucl. Sci. Technol.* 5(1):7.
- Tan, S. 1966. Solution of reactor kinetics equations by B.W.K. approximation. *Nukleonik* 8:480.
- . 1967. Sinusoidal analysis of a low-power nuclear reactor by the Wentzel-Kramers-Brillouin approach. *Nucl. Sci. Eng.* 30:436.
- . 1969a. On the stabilizing effect of delayed neutrons. *Nucl. Sci. Eng.* 37:323.
- . 1969b. Stability and the degree of stability under the effects of delayed neutrons. *Nucl. Sci. Eng.* 38:167.
- Tewari, S. P., and Kothari, L. S. 1969. Neutron-wave propagation through a crystalline moderator. Pt. 3, Ice. *Nucl. Sci. Eng.* 35:152.
- Thaler, G. J. 1955. *Elements of servomechanism theory*. New York: McGraw-Hill.
- Thalgott, F. W.; Boland, J. F.; Brittan, R. O.; Carter, J. C.; McGinnis, F. D.; Novick, M.; Okrent, D.; Sandmeier, H. A.; Smith, R. R.; and Rice, R. E. 1958. Stability studies on EBR-I. *Proc. Geneva Conf.* 12:242.
- Thie, J. A. 1958. Theoretical reactor statics and kinetics of boiling reactors. *Proc. Geneva Conf.* 11:440.
- . 1959. Dynamic behavior of boiling reactors. ANL-5849.
- . 1963. *Reactor noise*. New York: Rowman and Littlefield.
- . 1964. Water reactor kinetics. In *The technology of nuclear*

- reactor safety*, vol. 1, ed. T. J. Thompson and J. G. Beckerley. Cambridge, Mass.: M.I.T. Press.
- Thompson, T. J. 1964. Accidents and destructive tests. In *The technology of nuclear reactor safety*, vol. 1, ed. T. J. Thompson and J. G. Beckerley. Cambridge, Mass.: M.I.T. Press.
- Thompson, T. J., and Beckerley, J. G., eds. 1964. *The technology of nuclear reactor safety*. Vol. 1. Cambridge, Mass.: M.I.T. Press.
- Titchmarsh, E. C. 1939. *Theory of functions*. New York: Oxford University Press.
- Torlin, B. Z. 1966. Calculation of weak self-oscillation regimes in nuclear reactors. *J. Nucl. Energy* 20:485. Translation from *Atomnaya Energiya* 18:463, 1965.
- Travelli, A. 1967. The complex relaxation length of neutron waves in multigroup transport theory. In *Neutron noise, waves, and pulse propagation*, ed. R. E. Uhrig. Oak Ridge, Tenn.: USAEC Division of Technical Information Extension.
- . 1968. The energy spectra and the dispersion law of neutron waves in fast multiplying media. *Trans. Am. Nucl. Soc.* 11:189.
- Travelli, A., and Calame, G. P. 1964. Thermal-neutron space-time decay constants in various order  $P_N$  approximations. *Nucl. Sci. Eng.* 20:414.
- Truxal, J. G. 1955. *Automatic feedback control system synthesis*. New York: McGraw-Hill.
- Turner, W. J. 1968. Calculation of SPERT transients. *J. Nucl. Energy* 22:397.
- Uhrig, R. E., ed. 1967. *Neutron noise, waves, and pulse propagation*. Oak Ridge, Tenn.: USAEC Division of Technical Information Extension.
- Ussachoff, L. N. 1955. Equation for the importance of neutrons, reactor kinetics and the theory of perturbations. *Proc. Geneva Conf.* 5:503.
- Vasileva, A. B. 1952. On differential equations containing small parameters. (In Russian.) *Mat. Sbornik N.S.* 31(73):587.
- Vaughan, R. A. 1969. Stability of a fast pulsed reactor. *J. Nucl. Energy* 23:299.
- Vaurio, J. K., and Pulkkinen, G. 1970. On the validity of some zero-power describing functions. *Nucl. Sci. Eng.* 39:283.
- Vértes, P. 1963. Some problems concerning the theory of pulsed neutron experiments. *Nucl. Sci. Eng.* 16:363.

526      *Bibliography*

- Vigil, J. C. 1966. Solution of the nonlinear reactor kinetics equations by continuous analytic continuation. Ph.D. dissertation, University of New Mexico, 1966. Published as LA-3518.
- . 1967. Solution of the reactor kinetics equations by analytic continuation. *Nucl. Sci. Eng.* 29:392.
- Wachspress, E. L. 1966a. *Iterative solution of elliptic systems*. Englewood Cliffs, N.J.: Prentice-Hall.
- . 1966b. Numerical studies of multichannel variational synthesis. *Nucl. Sci. Eng.* 26:373.
- . 1969. Variational methods and neutron flux synthesis. In *The effective use of computers in the nuclear industry*, ed. B. Maskewitz. Oak Ridge, Tenn.: USAEC Division of Technical Information Extension.
- Wachspress, E. L., and Becker, M. 1965. Variational synthesis with discontinuous trial functions. In Proceedings of the conference on the application of computing methods to reactor problems, ed. M. Butler. ANL-7050 (see also KAPL-3095, 1965).
- Wachspress, E. L.; Burgess, R. D.; and Baron, S. 1962. Multichannel flux synthesis. *Nucl. Sci. Eng.* 12:381.
- Wallace, S. K. 1965. A note on the analysis of pulsed neutron shutdown measurements. *Nucl. Sci. Eng.* 21:116.
- Wallace, S. K.; Teare, K. R.; and Green, J. B. 1966. Methods for the comparison of pulsed-neutron shutdown measurements with theory. *Nucl. Sci. Eng.* 25:407.
- Wallach, S. 1950. Solutions of the pile kinetic equations when the reactivity is a linear function of the time. WAPD-13.
- Walter, J. F., and Henry, A. F. 1968. The asymmetric source method of measuring reactor shutdown. *Nucl. Sci. Eng.* 32:332.
- Warner, J. H., Jr., and Erdmann, R. C. 1969a. Application of Laguerre polynomials in the analysis of neutron-wave propagation. *Nucl. Sci. Eng.* 35:332.
- . 1969b. Infinite medium neutron wave propagation. Pt. 1, Theory. Pt. 2, Numerical results for water and graphite. *J. Nucl. Energy* 23:117.
- Wasserman, A. A. 1962. Contributions to two problems in space-independent nuclear reactor dynamics. TID-4500.
- Wasow, W. 1944. On the asymptotic solution of boundary value problems for ordinary differential equations containing a parameter. *J. Math. and Phys.* 23:173.

- \_\_\_\_\_. 1963. Singular perturbation problems of systems of two ordinary analytic differential equations. *Arch. Rational Mech. Anal.* 14:61.
- Weaver, L. E. 1963. *System analysis of nuclear reactor dynamics*. New York: Rowman and Littlefield.
- \_\_\_\_\_, ed. 1964. *Reactor kinetics and control*. Oak Ridge, Tenn.: USAEC Division of Technical Information Extension.
- \_\_\_\_\_. 1968. *Reactor dynamics and control: State space techniques*. New York: American Elsevier.
- Weinberg, A. M., and Schweinler, H. C. 1948. Theory of oscillating absorber in a chain reactor. *Phys. Rev.* 74:851.
- Weinberg, A. M., and Wigner, E. P. 1958. *The physical theory of neutron chain reactors*. Chicago: University of Chicago Press.
- Welton, T. A. 1955a. A stability criterion for reactor systems. ORNL-1894.
- \_\_\_\_\_. 1955b. Kinetics of stationary reactor systems. *Proc. Geneva Conf.* 5:377.
- \_\_\_\_\_. 1961. Reactor stability theory. *Nucl. Safety* 3(1):23.
- West, G. B.; Whittemore, W. L.; Shoptaugh, J. R., Jr.; Dee, J. B.; and Coffer, C. O. 1967. Kinetic behavior of TRIGA reactors. GA-7882.
- Westcott, C. H. 1962. Effective cross section values for well-moderated thermal reactor spectra. AECL-1101.
- Whittaker, E. T., and Watson, G. N. 1952. *A course in modern analysis*. 4th ed. New York: Cambridge University Press.
- Wiberg, D. M., and Woyski, J. S. 1968. Stability of nuclear rocket engine dynamics. *Nucl. Appl.* 5:35.
- Widder, D. V. 1946. *The Laplace transform*. Princeton, N.J.: Princeton University Press.
- Wilkins, J. E., Jr. 1959. The behavior of a reactor at prompt critical when the reactivity is a linear function of time. *Nucl. Sci. Eng.* 5:207.
- Williams, M. M. R. 1966. Time and space eigenvalues of the Boltzmann equation with a synthetic thermalization kernel. *Nucl. Sci. Eng.* 26:262.
- \_\_\_\_\_. 1968. The dispersion law of a neutron wave in a finite system. *J. Nucl. Energy* 22:153.
- Wills, L.; Krumbein, A.; Soodak, H.; Certaine, J.; and Guber, W. 1957. A digital computer code for solving the neutron dynamic equations with temperature feedback. Paper read at American Nuclear Society meeting, 28 October 1957, New York.

- Wimett, T. F. 1956. Time behavior of GODIVA through prompt critical. LA-2029.
- Wimett, T. F.; White, R. H.; Stratton, W. R.; and Wood, D. P. 1960. GODIVA II: An unmoderated pulse-irradiation reactor. *Nucl. Sci. Eng.* 8:691.
- Wolfe, B. 1964. The Nordheim-Fuchs excursion model with non-linear reactivity feedback. *Nucl. Sci. Eng.* 20:238.
- . 1969. Fast reactor safety. *Nucl. Safety* 10:19.
- Wylie, C. R., Jr. 1960. *Advanced engineering mathematics*. 2d ed. New York: McGraw-Hill.
- Yasinsky, J. B. 1967. The solution of the space-time neutron group diffusion equations by a time-discontinuous synthesis method. *Nucl. Sci. Eng.* 29:381.
- . 1968a. On the application of time-synthesis techniques to coupled core reactors. *Nucl. Sci. Eng.* 32:425.
- . 1968b. Numerical studies of combined space-time synthesis. *Nucl. Sci. Eng.* 34:158.
- . 1970. On the use of point kinetics for the analysis of rod-ejection accidents. *Nucl. Sci. Eng.* 39:241.
- Yasinsky, J. B., and Henry, A. F. 1965. Some numerical experiments concerning space-time reactor kinetics behavior. *Nucl. Sci. Eng.* 22:171.
- Yasinsky, J. B., and Kaplan, S. 1967. Synthesis of three-dimensional flux shapes using discontinuous sets of trial functions. *Nucl. Sci. Eng.* 28:426.
- Yasinsky, J. B.; Natelson, M.; and Hageman, L. A. 1968. TWIGL: A program to solve the two-dimensional, two-group, space-time neutron diffusion equations with temperature feedback. WAPD-TM-743.
- Yiftah, S., and Okrent, D. 1960. Some physics calculations on the performance of large fast breeder power reactors. ANL-6212.
- Zubov, V. I. 1957. *The methods of Liapunov and their applications*. (In Russian.) Leningrad. English translation, Groningen: P. Noordhoff, 1964.

## Author Index

- Abramowitz, M., 100, 119, 224  
Ackroyd, R. T., 325  
Adams, C. H., 457, 462, 468  
Adler, F. T., 124  
Agresta, J., 299, 457  
Ahmed, F., 481n, 483  
Aizerman, M. A., 380  
Akcasu, A. Z., 3, 77, 78, 107, 328, 342, 372,  
    386, 401, 405, 406, 407, 408, 409, 411,  
    415, 418, 421, 422, 423, 424, 433, 448,  
    483  
Albrecht, R. W., 335, 457  
Alcouffe, R. E., 457  
An, S., 230  
Andrews, J. B., II, 458, 471  
Argonne National Laboratory, 3, 146, 159  
Ash, M., 3, 88, 113, 328, 332  
Atomics International, 148  
Auerbach, T., 119  
Austin, A. L., 222  
Avery, R., 335, 458  
Azzoni, P., 230
- Bailey, R. E., 404, 414  
Baldonado, O. C., 483  
Baldwin, G. C., 458  
Bansal, N. K., 483  
Baran, W., 422  
Baron, S., 459  
Barrett, P. R., 335  
Barton, D. R., 170  
Becker, M., 42, 448, 454, 460, 461, 478n  
Beckerley, J. G., 3, 158, 221, 230  
Beckjord, E. S., 328  
Beckurts, K. H., 473, 474  
Beghian, L. E., 473
- Bell, G. I., 3  
Bellini-Morante, A., 112  
Bendt, P. J., 478n  
Bennett, G. L., 170  
Berland, R. F., 123  
Bernstein, S., 15  
Bethe, H. A., 56, 222, 223, 225, 226, 227,  
    316, 326, 338  
Bewick, J., 461, 471  
Beyster, J. R., 42, 473  
Bilharz, H., 239  
Bingham, C. R., 137, 140  
Birkhoff, G., 57, 136  
Blaesser, G., 38  
Blaine, R. A., 123  
Bodenschatz, C. A., 332  
Bogoliubov, N. N., 413  
Bondarenko, I. I., 38  
Booth, R. S., 483, 485  
Borst, L. B., 457  
Boyar, R. E., 66  
Braess, D., 230  
Brehm, R. L., 317, 404, 483, 487  
Brickstock, A., 457  
Bridges, D. N., 482  
Brittan, R. O., 126, 139, 198, 223, 324, 325  
Brookhaven National Laboratory, 342  
Brooks, H., 462  
Brown, H. D., 119  
Burgess, R. D., 459  
Burgreen, D., 222  
Bussard, R. W., 332  
Buttrey, K. E., 171
- Cadwell, W. R., 457, 463  
Cady, K. B., 478, 483

- Cahn, A., Jr., 482  
 Calame, G. P., 481n  
 Canosa, J., 184, 185, 192, 193, 194, 198, 200, 201, 202, 204, 209, 456, 462  
 Carpenter, W. R., 170  
 Carslaw, H. S., 482  
 Carter, J. C., 76  
 Case, J. M., 3, 481  
 Cesari, L., 342  
 Chambré, P. L., 462  
 Chang, I., 136  
 Channon, F. R., 473  
 Chapin, D. M., 336  
 Chen, S., 473  
 Chernick, J., 342, 360  
 Cherry, B. H., 217n  
 Chestnut, H., 236  
 Cheung, K. Y., 483  
 Chezem, C. G., 335, 458  
 Clark, M., Jr., 3  
 Clement, J. D., 482  
 Clendenin, W. W., 473n  
 Coats, R. J., 171  
 Cochran, R. G., 483  
 Cockrell, R. G., 473n  
 Coddington, E. A., 342  
 Coffer, C. O., 155, 170  
 Cohen, E. R., 29, 30, 56, 61, 105, 123, 124, 134, 174n, 443, 448  
 Cohn, C. E., 335, 458, 482  
 Cokinos, D., 473  
 Colvin, T. H., 222, 226  
 Conn, R., 481n, 482  
 Corben, H. C., 66, 137  
 Corngold, N., 473n, 481n, 482  
 Coveyou, R. R., 79  
 Cox, C. W., 113  
 Crandall, S. H., 126, 453  
 Crank, J., 457  
 Crawford, R. M., 462  
 Cunningham, W. J., 352, 353, 376  
 Curlee, N. J., 455, 461, 463
- Daitch, P. B., 473n, 478n  
 Dalles, A., 415n  
 Dalton, G. R., 473n  
 Davies, A. R., 457  
 Davis, S. K., 473  
 Davison, B., 3  
 deHoffman, E., 8, 335  
 DeJuren, J. A., 473  
 DeLauer, R. D., 332  
 Denielou, G., 230  
 Deniz, V., 448, 473  
 DeShong, J. A., Jr., 327, 328, 329, 330, 331
- Deverall, L. I., 462  
 Devooght, J., 386, 401, 402, 404, 414, 448, 473n  
 Diaz, N. J., 483  
 Dickerman, C. E., 169  
 Dietrich, J. R., 156  
 Di Pasquantonio, F., 422, 438  
 Dorning, J., 481n, 487  
 Doshi, P. K., 483  
 Dougherty, D. E., 456  
 Duderstadt, J. J., 483, 487  
 Dunensfeld, M. S., 137, 171, 219, 220, 221  
 Durgun, K., 481n
- Ebeoglu, D. B., 473n  
 Eckard, J. D., 473  
 Edlund, M. C., 3, 7  
 Emon, D. E., 483  
 Erdélyi, A., 57  
 Erdmann, R. C., 473n, 483, 487  
 Ergen, W. K., 14, 299, 300, 335, 360, 388, 389, 401, 456  
 Etherington, H., 3  
 Evans, J. W., 139  
 Evans, W. R., 236, 275
- Farmer, F. R., 230  
 Feshbach, H., 105, 107, 443, 444  
 Feynman, R. P., 335  
 Flatt, H. P., 126, 457  
 Fleck, J. A., Jr., 328  
 Foderaro, A., 456  
 Foley, J. E., 483  
 Forbes, S. G., 197, 210, 213, 214  
 Foulke, L. R., 456, 482  
 Franz, J. P., 66  
 Fuchs, K., 63, 164, 198, 201  
 Fuller, E. L., 449, 453, 459, 461, 462, 469, 470  
 Fultz, S. C., 478n
- Galanin, A. D., 3  
 Galati, A., 462  
 Gamble, D. P., 197, 219, 220, 458  
 Garabedian, H. L., 453, 456, 458  
 Garelis, E., 42, 473n, 478n, 480  
 Garner, R. W., 214  
 Gasidlo, J., 169  
 General Atomic (Gulf General Atomic), 28  
 George, R. E., 328  
 Germann, J. D., 462  
 Ghatak, A. K., 456, 478n, 481n, 483  
 Glasstone, S., 3, 7

- Golay, M. W., 483  
 Goldstein, R., 136  
 Gozani, T., 42, 448, 478n, 479  
 Grace, J. N., 448  
 Green, J. B., 478n  
 Greenspan, H., 3  
 Gross, E. E., 448  
 Grover, P. S., 483  
 Gyftopoulos, E. P., 174n, 299, 335, 363,  
     388, 411, 422, 448, 456  
 Gyorey, G. L., 462
- Hageman, L. A., 457  
 Hahn, W., 342, 380, 386, 388, 439  
 Haire, J. C., Jr., 210  
 Hale, J. K., 162  
 Hall, K., 458  
 Hansen, G. E., 198, 221, 222, 226, 335  
 Hansen, K. F., 3, 128, 129, 136, 458, 471  
 Hansson, P. T., 482  
 Harrer, J. M., 3, 66, 70, 96, 123, 236, 328  
 Harris, D. R., 335  
 Hartley, R. H., 483, 485  
 Hayashi, S., 462  
 Henry, A. F., 442, 446, 448, 455, 456, 457  
     461, 462, 463, 464, 469  
 Hermite, C., 239  
 Hetrick, D. L., 58, 130, 133, 197, 219, 220,  
     299, 307, 313, 317, 342, 367, 391, 424,  
     430, 431, 453  
 Hildebrand, F. B., 119  
 Hitchcock, A., 3, 335  
 Hobson, H. L., 473n  
 Holmes, D. K., 3  
 Honeck, H. C., 481n  
 Hooper, R. J., 462  
 Hopkins, G. R., 473  
 Horowitz, J., 482, 484  
 Hoshino, T., 462  
 Hsu, O., 396, 404, 405, 414, 462  
 Hughes, D. J., 12  
 Hughes, T. H., 222  
 Hurwitz, A., 239  
 Hurwitz, H., Jr., 102, 104, 335, 458
- IAEA (International Atomic Energy Agency), 159, 222, 230, 473  
 Isbin, H. S., 3
- Jacobowitz, H. J., 405  
 Jaeger, J. C., 482  
 James, H. M., 236  
 Jankus, V. Z., 222, 228  
 Jeffers, D. E., 458
- Jenkins, J. D., 478n  
 Johnson, R. E., 169  
 Johnson, R. J., 482  
 Johnson, R. P., 171, 197  
 Johnson, S. R., 458  
 Judge, F. D., 473n, 478n  
 Just, L. C., 462
- Kaganove, J. J., 126  
 Kalinowski, J. E., 404, 414, 422  
 Kalman, R. E., 421  
 Kaplan, S., 443, 449, 453, 454, 455, 456,  
     457, 459, 460, 461, 462, 471  
 Kappel, F., 422  
 Karr, H. J., 478n  
 Kasten, P. R., 342  
 Kastenberg, W. E., 462  
 Kazi, A. H., 217n  
 Keepin, G. R., 3, 7, 8, 9, 10, 12, 14, 26, 70,  
     71, 74, 76, 96, 102, 110, 113, 115, 134,  
     139, 156, 274, 335, 342, 442, 448, 473  
 Kelber, C. N., 3, 462  
 Kerlin, T. W., 66, 457  
 Kinchin, G. H., 317, 325  
 King, J. S., 478n  
 King, L. P. D., 171  
 Kistner, G., 110  
 Kladnik, R., 483  
 Kleban, E. R., 136  
 Kloverstrom, F. A., 478n  
 Koen, B. V., 128, 129  
 Köhler, W. H., 222, 335, 458  
 Kolar, O. C., 478n  
 Komata, M., 458  
 Kondo, S., 230  
 Kothari, L. S., 481n, 483  
 Kovanic, P., 137  
 Kramerov, A. Ya., 3  
 Krasovskii, N. N., 342, 405  
 Krieger, T. J., 478n  
 Krucoff, D., 66  
 Kumar, A., 483  
 Kurchatov, I. V., 169  
 Kuscer, I., 481n  
 Küsters, H., 230  
 Kylstra, C. D., 456, 482
- Lamarsh, J. R., 3, 7, 142, 144, 145, 146,  
     150, 154, 230, 449, 475  
 Langsdorf, A. S., Jr., 66  
 Larrimore, J. A., 38, 42, 52  
 LaSalle, J. P., 162, 342, 387, 388, 411  
 Lass, H., 382  
 Lauber, R., 424  
 Lazarus, R. B., 222, 226

- Lee, R. R., 473n  
 Leffert, C. B., 456  
 Lefschetz, S., 342, 384, 387, 388, 411, 420, 421  
 Lehnigk, S. H., 239, 241, 370  
 Le Ho, J. G., 473  
 Lelouche, G. S., 3, 299, 300, 320, 335, 342, 386, 401, 406, 415n, 418, 421, 448, 462  
 Leonard, A., 481n  
 Letov, A. M., 384  
 Levinson, N., 342  
 Lewins, J., 7, 448, 453, 454  
 Liapunov, A. M., 342, 373  
 Lidofsky, L. J., 473  
 Lipinski, W. C., 328, 329, 330, 331  
 Lipkin, H. J., 299, 300, 389, 401  
 Little, W. W., Jr., 128, 129  
 Loewe, W. E., 456, 482  
 Long, R. L., 171, 222  
 Lopez, W. M., 473  
 Lumb, R. F., 155, 171  
 Lur'e, A. I., 384, 385  
 Lurie, H., 473n  
 Lynch, R. E., 456
- McCarthy, W. J., Jr., 157, 158, 222, 225, 226, 317  
 McCormick, W. T., Jr., 458  
 Macdonald, R. N., 482  
 Machgels, C., 473n  
 MacMillan, D. B., 58, 136, 335  
 MacPhee, J., 14, 102, 155, 171, 339  
 McTaggart, M. H., 171  
 Madell, J. T., 462  
 Malkin, I. G., 342, 411  
 Marable, J. H., 219, 220, 448  
 Margolis, S. G., 455  
 Marlowe, O. J., 461, 471  
 Martin, C. F., 137, 140  
 Masters, C. F., 478  
 Mayer, R. W., 236  
 Meenan, P., 306  
 Meghrebian, R. V., 3  
 Melsa, J. L., 335  
 Meneley, D. A., 453, 462, 468, 469  
 Mennig, J., 119  
 Meyer, J. E., 459  
 Meyer, K., 422  
 Michael, P., 473n, 481n  
 Mihalezo, J. T., 171, 478n  
 Miida, J., 299, 316  
 Miley, G. H., 483  
 Miller, R. W., 137, 197  
 Minorsky, N., 342, 372, 373, 380, 388  
 Mitake, S., 462  
 Mitropolsky, Y. A., 413
- Mockel, A., 481n  
 Mohan, M. A., 421  
 Monk, A. T., 482  
 Moore, M. N., 335, 483, 487  
 Morehouse, N. F., Jr., 462  
 Morris, E., 230  
 Morse, P. M., 105, 107, 443, 444  
 Mortensen, G. A., 483  
 Moss, L. I., 171, 230  
 Motz, H. T., 473  
 Mulliken, T. W., 79  
 Murray, H. S., 405  
 Murray, R. L., 137, 140
- Nahavandi, A. N., 328, 457  
 Natelson, M., 335, 457  
 Nelkin, M., 423, 473n  
 Nguyen, D. H., 481n  
 Nichols, N. B., 236  
 Nicholson, R. B., 156, 222, 225, 226, 227, 228  
 Nicolaenko, B., 481n  
 Nishina, K., 483  
 Noble, L. D., 372, 407, 408, 409, 422, 433  
 Nohel, J. A., 299, 300, 335, 389, 401  
 Nordheim, L. W., 63, 66, 156, 157, 164  
 Nyer, W. E., 198, 210, 214  
 Nyquist, H., 260
- Oakes, L. C., 170  
 O'Brien, P. D., 171, 222  
 Ohanian, M. J., 483  
 Okrent, D., 3, 157, 158, 222, 225, 226, 230, 317  
 Orndoff, J. D., 335  
 Ortenberg, L. I., 332  
 Osborn, R. K., 3, 335  
 Ott, K., 462, 468, 469  
 Oyama, A., 230
- Pacilio, N., 3, 335  
 Pai, M. A., 421  
 Parks, P. C., 379  
 Pearlstein, S., 478n  
 Perez, R. B., 473n, 483, 485  
 Perks, M. A., 457  
 Phillips, R. S., 236  
 Plaza, H., 458  
 Poincaré, H., 342  
 Poole, M. J., 42  
 Popov, V. M., 385, 396, 405, 420, 421  
 Porschung, T. A., 136  
 Prescop, V., 335  
 Profio, A. E., 473

- Pulkkinen, G., 424  
 Purohit, S. N., 473n
- Quddus, M. A., 483  
 Quisenberry, K. S., 42, 478n
- Radkowsky, A., 3  
 Raievski, V., 482, 484  
 Rainbow, M. T., 481n  
 Ram, K. S., 483  
 Randall, D., 462  
 Randles, J., 222  
 Reed, W. H., 458  
 Reier, M., 473  
 Remley, M. E., 219, 231  
 Renard, A., 230  
 Renier, J. P., 482  
 Reuschler, J. A., 222  
 Rhoades, W. A., 230  
 Richtmyer, R. D., 457  
 Ritchie, A. I. M., 481n  
 Robinson, L. B., 342  
 Rosen, J. B., 386  
 Rotter, W., 478n  
 Routh, E. J., 239  
 Rumsey, V. H., 423, 458  
 Russell, C. R., 230  
 Russell, J. L., Jr., 42, 473, 478n, 480  
 Russell, L. M., 230  
 Rydin, R. A., 462, 471
- Sagot, M., 473  
 St. John, D. S., 462  
 Saji, G., 456, 482  
 Sanathanan, C. K., 335  
 Sandmeier, H., 424  
 Sarlos, G., 119  
 Sastré, C., 66, 478n  
 Sastry, V. R., 421  
 Sealettar, R., 170, 217, 456, 462  
 Schmid, P., 113  
 Schmidt, T. R., 317, 408, 424, 430, 431, 433  
 Schroeder, F., 154, 171, 210  
 Schultz, D. G., 335, 380, 382, 384, 405  
 Schultz, M. A., 3, 33, 70, 96, 100, 102, 123,  
     236, 299, 339  
 Schweinler, H. C., 66, 482  
 Scott, F. R., 478n  
 Seale, R. L., 473, 483  
 Secker, P. A., Jr., 136  
 Selengut, D. S., 454  
 Serber, R., 335  
 Sesonske, A., 328  
 Sha, W. T., 404, 405, 414
- Shen, C. N., 456  
 Shevelev, Ya. V., 3  
 Shinoda, W., 462  
 Shotkin, L. M., 3, 136, 299, 306, 342, 386,  
     401, 404, 405, 406n, 407, 408, 411, 414,  
     415n, 418, 421, 423, 424, 448, 456, 462  
 Shure, F., 335  
 Silberberg, M., 219  
 Simmons, B. E., 478n  
 Singer, S., 76  
 Sjostrand, N. G., 42, 478n, 479  
 Skinner, R. E., 29, 30, 299  
 Slivinsky, C. T., 335  
 Smets, H. B., 3, 79, 88, 113, 115, 174n, 198,  
     297, 299, 335, 342, 361, 363, 386, 388,  
     392, 401, 402, 404, 405, 409, 411n, 414,  
     415, 418, 422n, 424  
 Smiley, J. W., 457  
 Smith, H. P., Jr., 77, 332, 333, 334, 483  
 Smith, I. C., 457  
 Smith, R. R., 260, 317, 326, 327  
 Soodak, H., 3, 9, 33, 37, 56, 102, 230, 453  
 Spano, A. H., 150, 155, 157, 171, 214, 215,  
     217  
 Sparks, D. W., 76  
 Stacey, W. M., Jr., 3, 335, 449, 454, 457,  
     459, 461, 462, 468  
 Stahl, R. H., 473  
 Stavisskii, Yu. Ya., 38  
 Stegun, I. A., 100, 119, 224  
 Stenning, A. H., 332, 333, 334  
 Stiévenart, M., 230  
 Stitt, R. K., 219, 220  
 Stone, R. S., 155, 170  
 Stormi, M. L., 335  
 Störrer, F., 274, 326, 327, 462  
 Stratton, W. R., 222, 226  
 Suda, N., 299, 316  
 Sumita, K., 483  
 Syrett, J. J., 100, 102  
 Szego, G. P., 380  
 Szeligowski, J., 58, 130, 133, 197
- Tait, J. H., 3, 222, 223, 225, 226, 227  
 Takahashi, A., 483  
 Tan, S., 107, 299, 424  
 Teare, K. R., 478n  
 Tessier, J. H., 76  
 Tewari, S. P., 483  
 Thaler, F. J., 236  
 Thalgott, F. W., 325  
 Thie, J. A., 3, 9, 328, 335  
 Thompson, J. J., 335  
 Thompson, T. J., 3, 158, 221, 223, 230, 324  
 Thurber, J. K., 481n, 487  
 Thurnay, K., 230

534 *Author Index*

- Titchmarsh, E. C., 260  
Tomonto, J. R., 217n  
Torlin, B. Z., 424, 430n  
Travelli, A., 481n, 483, 487  
Truxal, J. G., 236  
Tsoullamidis, N., 483  
Turner, W. J., 214
- Uhrig, R. E., 335, 456, 482, 483  
Ussachoff, L. N., 448
- Vasileva, A. B., 58  
Vaughan, R. A., 222  
Vaurio, J. K., 424  
Vértes, P., 473n  
Vigil, J. C., 119, 136  
Vigilotti, A. M., 457, 463  
von Herrmann, P., 458  
von Hollen, R. F., 328, 457  
Vota, A. V., 457
- Wachspress, E. L., 3, 459, 460  
Wakabayashi, J., 462  
Wallace, S. K., 478n  
Wallach, S., 88  
Walter, J. F., 455  
Warner, J. H., Jr., 483, 487  
Wasow, W., 57  
Wasserman, A. A., 424  
Watson, G. N., 81, 260  
Weale, J. W., 171
- Weaver, L. E., 3, 70, 123, 236, 299, 328, 335, 336, 339, 342, 391, 392, 431  
Weinberg, A. M., 3, 7, 66, 144, 360, 388, 448, 449, 482  
Weinstock, E. V., 478n  
Welton, T. A., 342, 415, 418  
West, G. B., 155, 170  
Westcott, C. H., 144  
Whittaker, E. T., 81, 260  
Wiberg, D. M., 332, 333  
Wiblin, E. R., 42  
Widder, D. V., 417  
Wiener, E. S., 462, 469  
Wigner, E. P., 3, 7, 144, 448, 449  
Wilkins, J. E., Jr., 88, 94  
Williams, M. M. R., 481n, 487  
Wills, L., 123  
Wimett, T. F., 10, 170, 172, 222  
Wirtz, K., 473  
Wolfe, B., 217n, 230  
Wollman, W., 473n  
Woyski, J. S., 332, 333  
Wylie, C. R., Jr., 260, 384
- Yasinsky, J. B., 448, 457, 459, 460, 461, 462, 463, 464, 468, 469, 471  
Yiftah, S., 157  
Yip, S., 3, 335
- Zeigler, R. K., 10  
Zubov, V. I., 369n, 386  
Zweifel, P. F., 3, 478n, 481

## Subject Index

- Absorption, 2  
Absorption cross-section, 4; complex, 484; temperature dependence of, 145  
Absorption lifetime, 6  
ADI (alternating-direction implicit) method, 457  
Adiabatic method, 455, 461  
Adiabatic model, 161, 164, 174, 184, 198  
Adjoint boundary condition, 445  
Adjoint function, 443, 447, 454, 461  
Adjoint weighting, 454, 460  
Adler and Cohen, method of, 123-26, 132-36  
AIREK code, 123  
AIROS code, 123  
Amplitude function, 444, 450, 456, 463, 470-71  
Analogue computations, 122-23, 462  
ANCON code, 136  
Angstrom's method, 482  
Area-ratio method, 479  
Argand diagram, 262  
Asymptotic period, 22-23. *See also* Reactor period  
Asymptotic series: for error function, 85; for prompt-jump approximation, 57, 59; for reactor excursions, 190, 194  
Asymptotic stability. *See* Stability  
Autocatalytic effect, 324  
Autonomous oscillations, 429. *See also* Limit cycle  
Autonomous system, 369  
  
Bethe-Tait method, 222-30  
Block diagram, 45, 236-37, 429  
Bode plot, 70, 247  
  
Boiling-water reactors, 155; stability of, 328-32  
Boltzmann transport equation, 441  
Booster, 42, 52; repetitive, 52  
Boundedness, 405-14; Akcasu's criterion for, 406; without delayed neutrons, 409-10; of Laplace-transformable solutions, 407-9; with linear feedback, 417; with two-path feedback, 407-11  
Break frequency, 247-49  
Buckling, 5, 143, 474; complex, 484; temperature coefficient of, 147, 153  
  
Canonical coordinates: dominant, 411-14; for two-path feedback, 319  
Canonical representation: for second-order system, 344-45; for two-path feedback, 300, 318-19  
Canonical variables, 354, 411; for second-order system, 345; for two-path feedback, 301, 319  
Canosa's criterion, 204-7  
Cent, as unit of reactivity, 15, 33  
Center, 350  
Characteristic equation, 20-21; and transfer function, 48, 237-39  
Characteristic polynomial, 238-39  
Circulating-fuel reactor, 5, 14, 339  
Cohen's method, 123, 134  
Collision frequency, 488  
Collocation, 126, 454  
Constant power removal, 161; and linear stability, 286; and nonlinear stability, 360, 366, 389, 391; and ramp excursions, 204

- Constant-source approximation: criteria for, 63; and no delayed neutrons, 64; and prompt-jump approximation, 64-65; ramp-input response for, 85-87; for reactor excursions, 204; step-input response for, 37; transfer function for, 73-74
- Continuum boundary, 481, 488
- Continuum of eigenvalues, 481-82, 487-88
- Corngold limit, 482
- Coupled reactors, 335, 458
- CP-2 reactor, 66
- Criticality: approach to, 19-20; definition of, 19
- Critical power, 293, 325, 421, 430, 433
- Critical reactor, 1
- Critical system, 238, 273, 386, 438
- Decibel, 247
- Delayed-neutron decay function, 113-14
- Delayed-neutron fraction, 4, 12; effective, 8, 13, 446-47
- Delayed-neutron groups, 10-15, 18
- Delayed-neutron precursors, 4, 9, 442, 447; equilibrium, 19; in fast burst, 172; as latent neutrons, 9, 18
- Delayed-neutron probability function, 118, 425
- Delayed neutrons, 2, 4, 10-15; decay constants for, 11-12; energies of, 8; in excursions, 177, 181-84, 204-9, 229; few-group representations for, 14; half-lives for, 11-12; mean decay constants for, 12-13; mean decay times for, 12-13; one-group representations for, 14; origins of, 13-14; photoproduction of, 15; slowing effect of, 23, 34-35; stability effects of, 287-88, 296-99, 308, 313-15, 322-23, 391-92, 416; yields of, 11-12
- Delayed-neutron tail, 40, 44, 172-73, 188, 478-79
- Delta function, 39
- Describing function, 423-24, 428-29
- Diffusion, 3-4
- Diffusion area, 6, 143; for heterogeneous reactor, 152; temperature coefficient of, 146, 152
- Diffusion cooling, 475, 485
- Diffusion constant, 4; temperature dependence of, 146
- Diffusion equation, 3-5, 474; multigroup, 449
- Diffusion length, 5; complex, 482, 484
- Direction field, 186, 357
- Disadvantage factor, 151-52
- Disassembly, 221, 224-25, 227
- Dispersion law, 474, 483-87
- Dollar: in terms of prompt critical, 25; as unit or reactivity, 7, 25
- Domain of attraction, 370-71
- Dominant canonical coordinates, 411-14
- Doppler effect: in fast reactors, 156-58, 222; in SPERT-I reactor, 215; in thermal reactors, 149-50
- Dragon, 38, 51, 110; repetitive, 38, 51
- Dynamic equations: approximate solutions of, 56-65, 102-8; diffusion-theory derivation of, 3-9; integral-equation forms for, 112, 115, 123-24, 127-29; integro-differential form of, 117-19, 425; multimode, 449-57, 461; simplified derivation of, 9-10; transport-theory derivation of, 441-48
- EBR-I reactor, 156, 158n; accident in, 223, 324; stability of, 324-28
- EBR-II reactor, 156, 158
- EBWR reactor, 328, 331. *See also* Boiling-water reactors
- Effective lifetime, 23-24
- Effective-lifetime model: and linear stability, 285-87, 302-6, 318; and no delayed neutrons, 62, 64; and nonlinear oscillations, 432-34; and nonlinear stability, 360-65, 389-94, 401-4; from prompt-jump approximation, 62; transfer function for, 73-74
- Eigenfunctions: in diffusion theory, 5, 449, 455-56, 481; continuum of, 481-82, 487; discrete, 481; singular, 481, 487; in transport theory, 443, 481, 487
- Eigenvalues: continuum of, 481-82, 487-88; for excursion model, 185; of feedback matrix, 300, 334; for omega modes, 456; and reactivity modes, 443; for second-order system, 344-46; in transport theory, 481
- Eigenvectors, 344-45, 357
- Equilibrium, 18-19; for Newton cooling, 160; at zero power, 20, 364
- Equilibrium line, 352
- Equilibrium points, 343-54
- Error function, 81, 85, 224
- Eta ( $\eta$ ), 143; temperature coefficient of, 144, 149
- Euclidean norm, 369
- Excess reactivity, 6n. *See also* Reactivity
- Excursions. *See* Reactor excursions
- Extrapolated-area method, 479
- Fast-burst reactors, 156, 170-71, 197, 222

- Fast fission, 8  
 Fast-fission factor, 143; temperature dependence of, 144, 149  
 Fast reactor, 2; excursions in, 221-30; meltdown, 222; sodium-cooled, 157-58; stability of, 317-28; temperature coefficients for, 155-59  
 Feedback kernel, 162-63, 254  
 Feedback reactivity. *See* Reactivity  
 Feedback transfer function, 163, 236. *See also* Transfer function.  
 Fermi age, 143; for heterogeneous reactor, 153; temperature coefficient of, 146-47, 153  
 Fermi age theory, 7, 143  
 Fermi reactor, 156, 158  
 Fick's law, 4  
 Finite escape time, 341, 372; criteria for, 408-9; and stability, 422, 436  
 Fission, 1; by fast neutrons, 8  
 Fission fragments, 2, 4; as delayed-neutron emitters, 13-14; as heat sources, 148  
 Flux tilt, 8, 463, 468-69  
 Fourier series, 423-30  
 Free neutron, 15  
 Frequency-domain stability criteria, 415-22; of Baran and Meyer, 422; of Gyftopoulos, 422; limitations of, 422; of Popov, 420-22; of Smets, 422n; of Welton, 415-20  
 Frequency response, 44-50; approximations to, 72-74; assumptions in, 46-47; derivation of, 45-46; flat, 74, 248-49; polar plots of, 70-71, 248-56; quadratic factor in, 252-53, 257; for reactivity oscillation, 68-76; representations for, 246-60. *See also* Transfer function  
 Fuchs model, 198-203. *See also* Nordheim-Fuchs model  
  
 Gain margin, 271-72  
 GAKIN code, 458  
 Galerkin method, 461  
 Galerkin weighting, 454, 456, 460, 470  
 Gamma function, 91; incomplete, 100  
 Garelis-Russell method, 480  
 Generation time: definition of, 2, 6; in multigroup theory, 453; and transfer function, 71, 254; in transport theory, 446; values for, 2, 23  
 Generation-time formulation, 6-7, 126  
 GODIVA reactor, 156, 169-70, 222  
 Green's function. *See* Impulse response  
 Green's function modes, 456  
  
 Half node, half saddle, 438  
  
 Hamiltonian function, 388, 391  
 Hansen's method, 128-30, 132-36; space-dependent, 458  
 Harmonic oscillator, 374  
 Helmholtz equation, 5, 443, 456  
 Hermite functions, 81  
 Heterogeneous reactor, 7; temperature coefficients for, 148-55  
 Homogeneous reactor: pulse data for, 169-71; radiolytic gas in, 148, 171, 219; temperature coefficients for, 141-48  
 HPRR reactor, 171  
 Hurwitz approximation, 102-5  
 Hypergeometric functions, 81  
  
 IGR reactor, 169  
 Importance, 447  
 Impulse function, 39  
 Impulse response, 38; characteristic roots for, 41; coefficients for, 41; for critical reactor, 39; graph of, 41; and importance, 447; and inhour equation, 39; Laplace transform of, 39, 48, 50; for one group, 40; for prompt-jump approximation, 52; in space-dependent dynamics, 462; for subcritical reactor, 42; and transfer function, 48  
 Impulse sources, 17, 39, 447, 474  
 Inertial effects: in GODIVA, 170, 222; in KEWB, 221  
 Infinite-bandwidth approximation, 73. *See also* Prompt-jump approximation  
 Infinite-medium lifetime, 6  
 Inhour, as unit of reactivity, 20  
 Inhour equation, 20-26; alternative forms of, 22; approximate, 35; derivation of, 21-22; few-group representations for, 29-30; graphs of, 23, 25-26, 28-29; and impulse response, 39; for no delayed neutrons, 22; one-group representations for, 27-30; near prompt critical, 24-26; for prompt-jump approximation, 24; roots of, 22, 27, 50; and transfer function, 68  
 Inhour modes, 455  
 Integral representation, 88, 91  
 Inverse problem, 137, 39  
 Isoclines, 186, 195, 357; infinite-slope, 357. *See also* ZSI  
  
 Keepin's integral equation, 115; and impulse response, 115; and inhour equation, 116; and numerical computations, 115, 134-35; and transfer functions, 116-17

- KIWB reactor: mathematical models for, 219, 21; pulse data for, 170-71, 197; radiolytic gas in, 148, 171, 219; transient reactivity in, 137.
- Kinetic equations. *See* Dynamic equations
- KIWI reactor, 170-71. *See also* Nuclear rocket
- Lambda modes, 443, 455-56
- Latent neutrons, 9, 18. *See also* Delayed-neutron precursors
- Leakage, 2
- Least squares, 454
- Liapunov: direct method of, 373-88; first method of, 372-73; second method of, 373; theorems of, 372-75, 406
- Liapunov function, 374; with delayed neutrons, 396; as Hamiltonian function, 391; with power coefficient, 402; for simple reactor systems, 389, 391, 394; for two-path feedback, 398
- Lifetime. *See* Effective lifetime; Generation time; Neutron lifetime
- Lifetime formulation, 6, 115, 126
- Limit cycle, 341, 350, 386; Fourier series for, 423, 24, 430; semistable, 423; stable, 370-71, 408, 9, 432-35; unstable, 371, 424, 431, 33, 435-36
- Limiting sets, 387
- Line integral, 382, 83
- Lur'e canonical form, 385-86
- Lur'e Letov function, 384-85, 401
- Mechanical analogy, 390-91
- Meltdown, 222
- Migration area, 6, 147. *See also* Fermi age
- Modal expansion, 443, 449, 455-56, 480
- Moments weighting, 454
- Monte Carlo method, 458
- Multigroup theory, 154, 449
- Multimode dynamics, 449-57, 461, 469
- Multiplication, 19
- Natural modes, 456
- Negative definite function, 374
- Neutron cycle, 9
- Neutron density, 4, 18; and power, 7, 448
- Neutron generation time. *See* Generation time
- Neutron importance, 447
- Neutron lifetime, 6-7, 9, 15, 474. *See also* Generation time
- Neutron number ( $v$ ), 12
- Neutron source: cosmic rays as, 19; extraneous, 4, 7; oscillating, 44, 49-50; pulsed, 42, 472; spontaneous fission as, 19; time-dependent, 38-44; in transport theory, 447
- Neutron spectrum: in fast reactor, 156; Maxwellian, 144, 149
- Neutron temperature, 145
- Neutron waves, 482-88; diffusion theory of, 483-85; dispersion law for, 474, 483-87; transport theory of, 483, 487-88
- Newton cooling, 159-60; and linear stability, 284; and nonlinear stability, 360, 390; and Welton's criterion, 419
- Nodal method, 458-59, 461, 464
- Nonleakage probability, 143; temperature coefficient of, 153
- Nonminimum-phase systems: and finite escape time, 408, 422; illustrations of, 245, 251; and nonlinear oscillations, 432; root locus for, 294
- Nordheim-Fuchs model: as constant-source approximation, 63; and exact solution, 188; for fast excursions, 164-69; limitations of, 169-71, 178; and ramp-input response, 88, 95; as singular perturbation, 63; space-dependent, 456
- Nuclear rocket: delayed neutrons in, 14; destructive test of, 170-71; stability of, 332-35; startup of, 76
- Numerical computations: with backward differences, 121-22; comparison of methods for, 130-36; difficulties in, 119-22; finite-difference, 120-22, 457; with forward differences, 120-21; integral formulations for, 115, 120, 123-24, 127-29; and prompt-jump approximation, 119, 122, 130, 136; space-time, 463-72; step size for, 119, 124, 133, 136
- Nyquist criterion, 260-75
- Omega modes, 455-56
- Oscillating absorber, 50, 66
- Oscillation boundary, 294
- Oscillations: autonomous, 429-36; large-amplitude, 77-78, 423; nonlinear, 423-36; reactivity, 50, 66-78; source, 44, 49-50; subharmonic, 435. *See also* Frequency response; Limit cycle; Transfer function
- Parabolic cylinder functions, 81
- PBF reactor, 169-70
- Period. *See* Reactor period
- Perturbation theory: and fast reactors, 225; and multigroup theory, 456; and reactivity coefficients, 154; in transport theory, 444, 446

- Phase margin, 270-72  
Phase plane, 186, 200, 205, 354-60  
Phase space, in transport theory, 444  
Phase variables, 354-59  
Photoneutrons, 15  
Pile oscillator, 66. *See also* Frequency response; Transfer function  
Pitt's form of Wiener's theorem, 417-18  
Point-reactor model, 6-9; and approximations, 56; energy corrections for, 7-8; and equilibrium, 17-19; generation-time formulation of, 6-7, 126; lifetime formulation of, 6, 115, 126; and multimode dynamics, 452-54, 463-64, 467; and numerical computations, 111; parameters in, 7, 13, 15, 446-47; and quasi-static method, 461; and reactor excursions, 184; and transport theory, 445-48  
Popov's criterion: first, 420; second, 421  
Positive definite function, 374, 384  
Power coefficient, 160, 163; and boundedness, 409; and linear stability, 292-99; and nonlinear stability, 401-4, 414; static, 293, 306  
Power series: in nonlinear systems, 343, 372-73, 411; in small parameters, 56, 107-8  
Precursor density, 4; equilibrium, 19. *See also* Delayed-neutron precursors  
Pressurized-water reactors, 331  
Prompt critical: definition of, 24; as one decay constant, 474; of reactivity, 478-80  
Pulsed neutron source, 42, 472  
Pulsed reactors: booster-type, 42, 52; experimental data for, 169-71; repetitive, 38, 51; as sources, 473. *See also* Reactor excursions  
Pulse propagation, 483, 485, 487  
PULSTAR reactor, 155, 171  
  
Quadratic form, 379, 384  
Quasi-static method, 455, 461-62, 468-69  
QX-1 code, 462, 469  
  
Ramp-input excursions, 198-209  
Ramp-input response, 78-102; asymptotic series for, 85; and constant-source approximation, 85-87; differential equation for, 79; exact, 84-85; integral representation for, 88-91, and Nordheim-Fuchs model, 88, 95; at prompt critical, 93-96; and prompt-jump approximation, 86-88, 94; in reactor startup, 96-102; special functions for, 81, 88  
Rapid-rate approximation, 37. *See also* Constant-source approximation  
RAUMZEIT code, 457, 468  
Rayleigh-Ritz method, 457. *See also* Synthesis

- 181-83; delayed neutrons in, 177, 181-84, 204-9; duration of, 167, 169, 202; experimental data for, 169-71; in fast reactors, 221-30; Fuchs model for, 198-203; Nordheim-Fuchs model for, 164-69; peak power in, 165, 170, 176-77, 179-81, 201, 211, 213, 217-20; near prompt critical, 189-91, 194-98; prompt-jump model for, 174-80; ramp-input, 198-209; reactivity in, 166-68, 176, 178-83, 186, 197, 202-3, 228-29; space-dependent, 456; step-input, 164-98
- Reactor natural frequency, 287
- Reactor noise, 9, 335
- Reactor period, 20, 22; measurement of, 28, 51
- Reactor safety, 230
- Reactor stability: conditional, 293-94, 303-6, 309-12; and delayed neutrons, 287-88, 296-99, 308, 313-15, 322-23, 391-92, 416; effect of source on, 20, 363; frequency-domain criteria for, 415-22; Liapunov method for, 388-405; with power coefficient, 292-99, 401-4, 414; with simple feedback, 284-91, 360-69, 389-96; Störmer's method for, 273-74; with two-path feedback, 299-317, 397-400, 410-11; unconditional, 303-9, 311, 321-22; variable-gradient method for, 392-400. *See also* Stability
- Reflector, 458
- Reproduction factor, 1; as eigenvalue, 443; effective, 6; infinite-medium, 4, 142; in transport theory, 442
- Resonance escape probability, 143; and Doppler effect, 144, 149-50, 156-58; temperature coefficient of, 144, 149-51
- Resonance integral, 150
- RJE-29 code, 126-27
- Rod drop, 44, 52
- Root locus, 275-84; asymptotic, 277-78; and characteristic equation, 275-76; departure points for, 279; and equiphase plots, 275-76
- Rossi-alpha, 335
- Routh criterion, 239-46, 379
- RTS code, 115, 134, 139
- Saddle point, 348
- Separatrix: at node, 365; from saddle point, 353, 357, 365, 414; from shutdown, 364, 432; as stability boundary, 200, 353, 355, 360, 387, 432-33; zero-power, 200
- Shape function, 445-46, 450, 455, 461, 463, 470
- Shutdown power, 19-20
- Shutdown reactivity, 19, 42, 363
- Singular perturbation, 57, 63, 109, 192, 200
- Slowing-down power, 150
- SNAP reactor, 170-71, 197
- Source. *See* Neutron source
- Source insertion, 42-43
- Source jerk, 44
- Source transfer function, 50. *See also* Transfer function
- Space-time iteration, 462
- Space-time separability, 5, 443, 445, 474
- Spectral shift, 8
- SPERT-I reactor: delayed feedback in, 154; Doppler effect in, 215-17; long-delay model for, 212-14; mathematical models for, 210-17; prompt feedback in, 155; pulse data for, 170-71, 197, 212-15; resonance integral for, 150; steam formation in, 154, 171, 210; transient reactivity in, 137; zero-delay model for, 211-12
- Spiral point, 349
- SPR reactor, 171
- Stability, 235, 341; absolute, 371; Aizerman's method for, 381; asymptotic, 238, 370-71, 374-75, 415; of boiling-water reactors, 328-32; conditional, 243; definitions of, 396-71; and describing function, 429; of fast reactors, 317-28; frequency-domain criteria for, 415-22; and frequency response, 47; geometric proof of, 363; global, 370; Lagrange, 370, 405, 407, 411; in the large, 342, 370; Liapunov method for, 372-88; of linear systems, 235-84; of nonlinear systems, 341-60, 369-88, 405-22; of nuclear rocket reactors, 332-35; Nyquist criterion for, 260-75; orbital, 370, 423; quasi-asymptotic, 370; root-locus method for, 275-84; Routh criterion for, 239-46, 379; in the small, 344, 370-71; space-dependent, 462; structural, 371; Szego's method for, 380-82; uniform, 370; variable gradient method for, 382-84, 392-400. *See also* Reactor stability
- Stability boundary: dynamic, 243; infinity, 246; in parameter space, 245-46, 293, 303, 308; in state space, 353, 355, 360, 388, 413-14; static, 243
- Stable focus, 349
- Stable limit cycle, 370-71, 408-9, 432-35
- Stable node, 347
- Stable period, 22, 26. *See also* Reactor period

- Star point, 347, 350  
 Startup accident, 96-102; conditions at critical in, 102; period during, 98-102; and prompt-jump approximation, 97; quasi-static limit for, 100  
 State-variable feedback, 335  
 State variables, 354  
 Statistical weight, 448  
 Step-input excursions, 164-98  
 Step-input response, 30-38; approximate, 35-37; coefficients in, 33-34; equations for, 32; graphs of, 33-34; for one group, 33; and transfer function, 48  
 Stochastic processes, 9, 335  
 STREAK code, 457  
 Subcritical equilibrium, 18  
 Subdomain weighting, 454  
 Sylvester's theorem, 384, 392, 399  
 Synthesis, 457-61; multichannel, 459-61; numerical results for, 464, 468, 470-71; space-time, 461; time, 460-61; variational, 460-61  
 Szego's method, 380-82
- Temperature coefficient: definition of, 142; delayed, 148-56, 317; for fast reactor, 155-59; for heterogeneous reactor, 148-55; for homogeneous reactor, 141-48; isothermal, 142, 148, 158; prompt, 148-56, 317; sign of, 142; temperature dependence of, 147; for thermal reactor, 141-55; and transfer function, 259  
 Thermal reactor, 2; temperature coefficients for, 141-55  
 Thermal utilization, 143; temperature coefficient of, 144-46, 151-52  
 Thermionic reactor, 317  
 Threshold energy, 221, 223, 226-27  
 Transfer function, 44-50, 67-76; approximations to, 72-74; and characteristic equation, 48, 237-39; closed-loop, 237, 255-56; definition of, 45; and differential operators, 47; graphs of, 70-73, 75-76; and impulse response, 48; and inhour equation, 68; and initial conditions, 48; measurements of, 325-26; normalization of, 67; for one group, 69; open-loop, 237; polar plots of, 70-71, 248-56; reactivity, 67; source, 50; space-dependent, 462, 482; and step-input response, 48; for subcritical reactor, 74-75; for supercritical reactor, 74-76; and temperature coefficient, 259; zero-power, 69-72, 253. *See also* Frequency response
- Transfer-function period effect, 76  
 Transport equation, 441  
 Transport theory: for neutron waves, 483, 487-88; for pulsed systems, 481; for reactor dynamics, 441-48  
 Transport time delay, 161-62, 269-71, 325-27, 406, 422  
 TREAT reactor, 169-70, 197  
 Trial functions: for multimode dynamics, 450, 453-56, 460-61, 464, 470-71; for point-reactor dynamics, 126  
 TRIGA reactor: parameters for, 28; prompt feedback in, 155; pulse data for, 170, 197; variable heat capacity, 20, 217-19  
 Turning points: in excursion model, 160; in WKB method, 107  
 TWIGL code, 457  
 Two-energy-group theory, 7, 463
- Undetermined parameters, method of, 453  
 Units: of n, c, and q, 7; of reactivity, 7, 20, 25-26, 33  
 Unstable focus, 349  
 Unstable limit cycle, 371, 424, 431-33, 435-36  
 Unstable node, 347
- Variable gradient method, 382-84, 392-400  
 Variational functional, 454, 461  
 Variational method, 454, 457  
 VIPER reactor, 171  
 Vortex point, 350
- Weber's differential equation, 81  
 Weighted-residual method: for point-reactor dynamics, 126-28, 132-35; for space-dependent dynamics, 449, 451-57, 459-61; and variational method, 454  
 Weighting functions, 451, 453-55, 460-61, 470  
 Welton's criterion, 415-20; Akcasu's derivation of, 415-18; for Newton cooling, 419; Smets' derivation of, 418-19; for two-path feedback, 419-20  
 Westcott's formulation, 146  
 Wiener's theorem, Pitt's form of, 417-18  
 WIGLE code, 457, 463, 470  
 WKB (Wentzel-Kramers-Brillouin) method, 105-8, 128, 424  
 WSMR reactor, 171